

IEEE CONFERENCE RECORD - ABSTRACTS

1999 IEEE International Conference on Plasma Science

June 20 -24, 1999 Monterey, California USA

DISTRIBUTION STATEMENT A

Approved for Public Release Distribution Unlimited

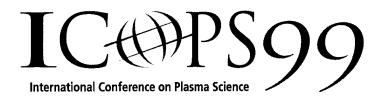
19991014 028

Sponsored by:

The Plasma Science and Applications Committee of The IEEE Nuclear and Plasma Sciences Society

į	REPORT DOCUMENTATION PAG	14	AFRL-SR-BL-TR		
the collection of information. Send comments regarding	estimated to everage 1 hour per response, including the time for in this burden estimate or any other aspect of this collection of in uits 1204, Arlington, VA 22202-4302, and to the Office of Mane	formation, including	0946		and resewing for information
1. AGENCY USE ONLY (Leave blank)	2. REPORT DATE	3. RE.		30 Nov 99 Final	
4. TITLE AND SUBTITLE 26th IEEE International Conf	ference on Plasma Science	J	5. FUND 61102	DING NUMBERS	
20th IEEE michadona Com	etelece on I manua delonce		2301/1		
6. AUTHOR(S) Dr Deeney					
7. PERFORMING ORGANIZATION NAME IEEE Inc.	(S) AND ADDRESS(ES)			ORMING ORGANIZATION RT NUMBER	
445 Hoes Lane P O Box 1331 Piscataway, NJ 08855-1331					
SPONSORING/MONITORING AGENCY	/ NAME(S) AND ADDRESS(ES)		10. SPO	NSORING/MONITORING	
AFOSR/NE 801 North Randolph Street R			AGER	ICY REPORT NUMBER	
Arlington, VA 22203-1977	732			F49620-99-1-0242	
11. SUPPLEMENTARY NOTES					
12a. DISTRIBUTION AVAILABILITY STAT		**** **********		TRIBUTION CODE	
APPROVAL FOR PUBLIC F	RELEASED; DISTRIBUTION U	NLIMITE			
13. ABSTRACT (Maximum 200 words)			<u> </u>		
The ICOPS 1999 Conf California.	ference was successfull	y held	20 - 24 June 19	999 in Monterey,	·
					144
•					
14. SUBJECT TERMS				15. NUMBER OF PAGES	
				16. PRICE CODE	
17. SECURITY CLASSIFICATION OF REPORT	18. SECURITY CLASSIFICATION OF THIS PAGE	19. SECURIT	Y CLASSIFICATION RACT	20. LIMITATION OF ABSTRACT	
UNCLASSIFIED	UNCLASSIFIED	טו	NCLASSIFIED	UL	

Standard Form 298 (Rev. 2-89) (EG) Prescribed by ANSI Std. 239.18 Designed using Perform Pro. WHS/DIOR, Oct 94



IEEE CONFERENCE RECORD - ABSTRACTS

1999 IEEE INTERNATIONAL CONFERENCE ON PLASMA SCIENCE



The 26th IEEE International Conference on Plasma Science

June 20–24, 1999 Monterey California, USA

Sponsored by:
The Plasma Science &
Applications Committee
of the
IEEE Nuclear & Plasma Sciences Society

Co-Sponsors:
Sandia National Laboratories
Los Alamos National Laboratory
Defense Threat Reduction Agency

IEEE CONFERENCE RECORD - ABSTRACTS 1999 IEEE INTERNATIONAL CONFERENCE ON PLASMA SCIENCE

Copyright and Reprint Permission: Abstracting is permitted with credit to the source. Libraries are permitted to photocopy beyond the limit of U.S. Copyright Law for private use of patrons those articles in this volume that carry a code at the bottom of the first page, provided that per-copy fee is indicated in the code is paid through Copyright Clearance Center, 222 Rosewood Drive, Danvers, MA 01923.

For other copying, reprint or reproduction permission write to: IEEE Copyrights Manager, IEEE Service Center, 445 Hoes Lane, PO Box 1331 Piscataway, NJ 08855-1331. All rights reserved. Copyright © 1999 by the Institute of Electrical and Electronics Engineers, Inc.

IEEE Catalog Number:

99CH36297

ISBN

0-7803-5224-6 (Softbound Edition)

ISBN

0-7803-5225-4 (Casebound Edition)

ISBN

0-7803-5226-2 (Softbound Edition)

Library of Congress

81-644315

ISSN:

0730-9244

Additional copies of this Conference Record are available from IEEE Service Center 445 Hoes Lane PO Box 1331 Piscataway, NJ 08855-1331 1-800-678-IEEE

07803-5224-6/99/\$10.00 © 1999 IEEE.

Table of Contents

26th IEEE Conference on Plasma Sciences	
Previous Conferences	04
Invitation to ICOPS 99	05
Conference Organizing Committees	06
National Committee	07
Conference Management	07
Future ICOPS Conferences	07
Conference Sponsors	07
IEEE 1999 Nuclear and Plasma Sciences Society	
NPSS Administrative Committee	07
Plasma Sciences and Applications Committee	07
Women in Plasma Science	07
Session Topics and Organizers	08
Conference Information	10
IEEE Membership Information	12
Placement Center	· ·
Mini Course Offered	14
Hotel and Travel Info	16
Social Events and Companion Program	17
Maps of Hotel and Monterey	18
ICOPS 2000 Conference	20
Technical Sessions	21
Schedule of Technical Sessions.	22
1 Session One Plenary	25
2 Session Two Plenary	32
3 Session Three Plenary	40
4 Session Four Plenary	48
5 Session Five Plenary	57
6 Session Six Plenary	64
7 Session Seven Plenary	72
Conference Record - Abstracts	83
Author Index	33
Conference Schedule (back cover)	

Previous Conferences

1974	University of Tennessee	Knoxville, TN	I. Alexeff
1974	University of Tennessee	Knoxville, TN	I. Alexeff
1975	University of Michigan	Ann Arbor, MI	R. R. Johnson
1976	University of Texas	Austin, TX	E. J. Powers
1977	Rensselaer Polytechnic Institute	Troy, NY	R. L. Hickok
1978	DoubleTree Inn	Monterey, CA	R. Schwirzke
1979	Universite de Montreal	Montreal, Canada	C. Richard
1980	University of Wisconsin	Madison, WI	J. L. Shohet
1981	Sweeney Convention Center	Santa Fe, NM	S. J. Gitomer
1982	Carleton University	Ottawa, Canda	A. J. Alcock
1983	Sheraton Harbor Island Hotel	San Diego, CA	J. L. Luxon
1984	Clarion Hotel	St. Louis, MO	T. J. Menne
1985	Pittsburg Hilton Hotel	Pittsburgh, PA	M. D. Nahemow
1986	Ramada Renaissance Hotel		
	& Bessborough Hotel	Saskatoon, Canada	A. Hirose
1987	Hyatt Regency Crystal City	Arlington, VA	F. C. Young
1988	Seattle Sheraton Hotel	Seattle, WA	L. C. Steinhauer
1989	Hyatt Regnecy	Buffalo, NY	D. M. Benson
1990	Hyatt Regency	Oakland, CA	J. N. Benford
1991	College of William and Mary	Williamsburg, VA	K. H. Schoenbach
1992	Hyatt Regency Westshore	Tampa, FL	N. L. Oleson
1993	Sheraton Landmark Hotel	Vancouver, Canada	A. Ng
1994	Sweeney Convention Center	Santa Fe, NM	A. L. Peratt
1995	University of Wisconsin	Madison, WI	J. E. Scharer
1996	Boston Park Plaza Hotel	Boston, MA	C. Chan
1997	Catamaran Resort Hotel	San Diego, CA	J. Hyman
1998	North Raleigh Hilton	Raleigh, NC	J. Gilligan
1999	DoubleTree Hotel	Monterey, CA	C. Deeney



1999 Program Committee

Dr. Chris Deeney Sandia National Laboratories Albuquerque, NM 87185

Dr. John Gilligan North Carolina State University Raleigh, NC 27695

Dr. Anthony Peratt Department of Energy Gaithersburg, MD 20878

Dr. Kenneth Connor Rensselaer Polytechnic Institute Troy, NY

Dr. Don Cook Sandia National Laboratories Albuquerque, NM

Dr. Art Toor Lawrence Livermore National Laboratories Livermore, CA

Dr. Jack Davis Naval Research Laboratory Washington, DC

Dr. Mark Kushner University of Illinois Urbana, IL

Dr. Paul Ottinger Naval Research Lab Washington, DC

Dr. Gerry Rogoff Plasma Associates Framingham, MA

Dr. Edl Schamiloglu University of New Mexico Albuquerque, NM

Dr. John Thompson Maxwell Technology, Inc. San Diego, CA

Dr. James Trainor Los Alamos National Lab Los Alamos, NM

An Invitation to ICOPS 99 in Monterey, California

We would like to invite you to attend the 1999 ICOPS Conference to be held in Monterey, California, between June 20th and 24th, 1999. The venue will be ideally situated at the DoubleTree Hotel on Fisherman's Wharf, just a stone's throw from the wharf and within a pleasant walking distance from Steinbeck's Cannery Row.

This, our 26th conference, will look both backward at the contributions made by plasma science, and forward to the changing environments and challenges of the next century in our plenary talks. Is our plasma community "millennium ready"? The ICOPS Conference already covers all the diverse areas in plasma science and so is perfectly suited to such discussions. Moreover, the location this year in California further accentuates this diversity since it is close to centers in magnetic fusion, inertial confinement fusion, space plasmas and plasma processing. In 1999, the IEEE Pulsed Power Conference, which follows the ICOPS in the next week, is at the same hotel.

The DoubleTree Hotel gives the attendee an opportunity to ponder the future of plasma science while strolling along the seafront to the sound and sights of seals and otters. The hotel has 370 rooms and the meetings will use the hotel itself and some of the adjoining Monterey Conference Center. The hotel is located at Fisherman's Wharf and is next to downtown Monterey so there are plenty of restaurants within walking distance.

Monterey itself is full of history and major attractions, like the world-famous aquarium. Within a few hours drive of the town there are many other places worth visiting – Point Lobos, the Big Sur, Pebble Beach, Santa Cruz, the Monterey Peninsula wineries and, of course, San Francisco. The weather in late June is excellent, with the temperatures ranging from 55-70 degrees. There will be a Companion Program, and the hotel and the Monterey Visitor's Bureau will have plenty of information on local attractions.

This meeting would not be possible without the support of the organizational committees, the session organizers and the sponsors. Please attend the conference to make this meeting an ICOPS to remember.

Chris Deeney Chair, ICOPS 99

Noah Hershkowitz Chair, Plasma Science and Applications Committee IEEE Nuclear and Plasma Science Society

Co-Sponsors: Sandia National Laboratories Los Alamos National Laboratories Defense Threat Reduction Agency

Organizing Committees

Local

Dr. Jack Agee Air Force Research Lab Albuquerque, NM

Dr. James Benford Publications Chair Microwave Science Lafayette, CA

Mrs. Hillary Benford Companion Program Lafayette, CA

Ms. Deanna Ceballos Sandia National Laboratories Albuquerque, NM

Dr. Chris Deeney Sandia National Laboratories Albuquerque, NM

Ms. Ellen Sandler ESP Meeting Mindes Foster City, CA

Dr. Mary Ann Sweeney Sandia National Laboratories Albuquerque, NM

Program

Dr. Kenneth Connor Rensselaer Polytechnic Institute Troy, NY

Dr. Don Cook Sandia National Laboratories Albuquerque, NM

Dr. Jack Davis Naval Research Laboratory Washington, DC

Dr. John Gilligan North Carolina State University Raleigh, NC 27695

Dr. John Goyer Maxwell Physics International San Leandro, CA

Dr. Mark Kushner University of Illinois 'Urbana, IL

Dr. Paul Ottinger Naval Research Laboratory Washington, DC

Dr. Anthony Peratt Department of Energy Gaithersburg, MD

Dr. Gerry Rogoff Plasma Associates Framingham, MA

Dr. Edl Schamiloglu University of New Mexico Albuquerque, NM Dr. John Thompson Maxwell Technology, Inc. San Diego, CA

Dr. Art Toor Lawrence Livermore National Laboratories Livermore, CA

Dr. James Trainor Los Alamos National Laboratory Los Alamos, NM

International

Professor Koichi Kasuya Tokyo Institute of Technology Yokohama, Kanagawa, Japan

Professor Jae Koo Lee Pohang University of Science & Technology Pohang, Korea

Professor Andrew Ng University of British Columbia Vancouver, Canada

Professor Alan D. R. Phelps University of Strathclyde Glasgow, Scotland

Professor Paul Hiroshi Sakanaka Universidade Estadual de Campinas Campinas, Brazil

Dr. Gerry Yonas Sandia National Laboratories Albuquerque, NM

Conference Management

Dr. Chris Deeney ICOPS 99 Conference Chair Sandia National Laboratories P.O. Box 5800 Albuquerque, NM 87185 USA

Phone: (505) 845-3657 FAX: (505) 845-7864 E-mail: cdeene@sandia.gov

2000

June, New Orleans, LA Chair: M. Mazzola Mississippi State University

2001

May, Las Vegas, NV Chair: Tom Hussey Air Force Research Laboratory

Future ICOPs



The 26th IEEE International Conference on Plasma Science

1999 Nuclear and Plasma Sciences Society Administrative Committee

President Igor Alexeff
Vice President William M. Moses
Secretary Alberta M. Dawson Larsen
Treasurer Edward J. Lampo

Elected Administrative Committee Members

Terms Expiring 1999

Igor Alexeff M. (Kris) Kristiansen George H. Miley William M. Moses

Terms Expiring 2000

Gary T. Alley Jes Asmussen Bruce C. Brown Roy I. Cutler

Terms Expiring 2001

George J. Blanar Mark A. Hopkins Richard T. Kouzes Anthony L. Peratt

Plasma Science and Applications Committee

Chairman Virginia Ayres
Vice Chairman Ricky Faehl
Secretary Tim Grotjohn
Most Recent

Past Chairman Noah Heshowitz

Elected Executive Committee Representative

Term ending 2000

Thomas M. Antonsen, Jr. Melissa Rae Douglas Rickey J. Faehl Steven H. Gold Thomas A. Hargreaves Karl H. Schoenbach

Term ending 2001

Forrest J. Agee Chung Chan Brendan B. Godfrey Valery A. Godyak Robert K. Parker Linda Vahala

Women in Plasma Science

There will be a reception for women in plasma science to be held in the **Portola Room** of the **Doubletree Hotel** on **Monday, June 21 at 6 pm**. This reception will be ideal for networking and the discussion of relevant topics. Come and welcome! (all). For further information, please contact:

Virginia M. Ayres

Associate Professor Department of Electrical & Computer Engineering Michigan State University East Lansing, MI 48824-1226

Tel: 517-355-5236 FAX: 517-353-1980 email: ayresv@egr.msu.edu

List of Topics and Topic/Session Organizers

	TOPIC	ORGANIZER	INSTITUTE	PHONE/E-MAIL	FAX
1.0	Basic Processes in Fully and Partially Ionized Plasma	Mark Kushner	University of Illinois	(217) 244-5137 mjk@uiuc.edu	(217) 244-7097
1.1	Basic Phenomena	Wallace M. Manheimer	Naval Research Laboratory	(202) 767-3128 manheime@ccsalpha2	(202) 767-1607 .nrl.navy.mil
1.2	Space Plasmas	Mark Kushner	University of Illinois	(217) 244-5137 mjk@uiuc.edu	(217) 244-7097
1.3	Partially Ionized Gases	Shahid Rauf	University of Illinois	(217) 244-7094 rauf@uigela.ece.uiuc.e	(217) 244-7097 du
1.4	Computational Plasma Physics	Glenn Joyce	Naval Research Laboratory	(202) 767-6785 joyce@ppd.nrl.navy.mi	(202) 767-0631 !
2.0	Microwave Generation and Microwave Plasma Interaction	Edl Schamiloglu	University of New Mexico	(505) 277-4423 edl@eece.unm.edu	(505) 277-1439
2.1	Intense Beams	Tom Spencer	AFRL/DEHE	(505) 853-3907 spencert@plk.af.mil	(505) 853-3903
2.2	Fast Wave Devices	Bruce G. Danly	Naval Research Laboratory	(202) 767-0032 danly@nrl.navy.mil	(202) 767-1280
2.3	Vacuum Microwaves	Capp Spindt	SFI	(650) 859-2993 capp@unix.sn.com	(650) 859-3090
2.4	Slow Wave Devices	David R. Whaley	Northrop Grumman	(847) 259-9600 ext. 6454 whaley@eiws.esid.nord	(847) 590-3177 hgrum.com
2.5	Microwave Systems	Jeff Calame	Naval Research Laboratory	(202) 404-2799 calame@mmace.nrl.na	(202) 767-1280 vy.mil
2.6	Microwave Plasmas	John Scharer	University of Wisconsin	(608) 263-8142 scharer@tesla.ece.wisc	(608) 262-6707 .edu
3.0	Intense Electron and Ion Beams	Paul Ottinger	Naval Research Laboratory	(202) 404-7567 ottinger@suzie.nrl.navy	(202) 767-0436 v.mil
3.1	Plasma, lon and Electron Sources	lan Brown	University of Berkeley	(510) 486-4174 ibrown@lbl.gov	(510) 486-4374
3.2	Intense Electron and Ion Beams	Bryan V. Oliver	Mission Research Corporation	(505) 768-7706 boliver@mrcabq.com	(505) 768-7601

List of Topics and Topic/Session Organizers

	TOPIC	ORGANIZER	INSTITUTE	PHONE/E-MAIL	FAX	
4.0	High Energy Density Plasmas and their Interactions	Jim Trainor	Los Alamos National Laboratory	(505) 665-0906 trainor@lanl.gov	(505) 667-7684	
4.1	Laser Produced Plasmas	Andrew Mostvich	Naval Research Laboratory	(202) 404-7766 mostovych@this.nrl.nav	(202) 767-0046 vy.mil	
4.2	Inertial Confinement Fusion	David Montgomery	Los Alamos National Laboratory	(505) 665-7994 montgomery@lanl.gov	(505) 665-4409	
4.3	Magnetic Fusion Energy	Ron McKnight	DOE	(301) 903-4597 Ronald.mcknight@mail	(301) 903-1225 gw.er.doe.gov	
4.4	Dense Plasma Focus	Ed Ruden	AFRL/DEHP	(505) 846-0687 ruden@plk.af.mil	(505) 846-9853	
4.5	Fast Z-Pinches and X-Ray Lasers	Bruno Bauer	University of Reno	(702) 784-1363 bbauer@physics.unr.ed	(702) 784-1398 u	
4.6	Spherical Configuration & Ball Lightning	Joe Mack	Los Alamos National	(505) 667-3416 jmmack@lanl.gov	(505) 667-7684	
5.0	Industrial/Commercial Applications of Plasmas	Gerald Rogoff	Plasma Associates	(508) 879-5662 g.rogoff@ieee.org	(508) 879-5662	•
5.1	Non-equilibrium Plasma Processing	Jeff Hopwood	Northeastern University	(617) 373-3006 jhopwood@lynx.neu.ed	(617) 373-8970 lu	
5.2	Thermal Plasma Chemistry and Processing	Don Rej	Los Alamos National Laboratory	(505) 665-1883 drej@lanl.gov	(505) 665-3644	
5.3	Plasma Thrusters and Arcs	Dennis Keefer	University of TN Space Institute	(931) 393-7475 dkeefer@utsi.edu	(931) 454-2271	
5.4	Plasmas for Lighting	Ken Hutcherson	Osram Sylvania	(978) 750-1634 hutcherson@osi.sylvani	(978) 750-1799 a.com	
5.5	Flat Panel Displays	John Verboncoeur	University of California at Berkeley	(510) 642-3477 johnv@eecs.berkeley.ec	(510) 642-6330 Ju	
5.6	Environmental/energy Issues in Plasma Science	Jim Olthoff	National Institute of Standards & Technology	(301) 975-2431 james.olthoff@nist.gov	(301) 948-5796	
6.0	Plasma Diagnostics	Ken Connor	Plasma Dynamics Laboratory	(518) 276-6084 connor@rpi.edu	(518) 276-6261	
7.0	Pulsed Power and Other Plasma Technology Applications	John Thompson	Maxwell Technology	(619) 576-7799 thompson@maxwell.co	(619) 576-7659 om	
7.1	Closing Switches	Mark Savage	Sandia National Laboratories	(505) 845-7462 mesavag@sandia.gov	(505) 845-7864	
7.2	Opening Switches	John Goyer	Maxwell Technology	(510) 278-9523 jgoyer@maxwell.com	(510) 577-7247	
						9

IEEE International Conference on Plasma Science

The 26th IEEE International Conference on Plasma Science will be held Monday through Thursday, June 20–24, 1999, in Monterey, California, USA. The Conference is sponsored by the Plasma Science and Applications Committee of the IEEE Nuclear and Plasma Sciences Society. Learn of conference information updates from our homepage: http://www.sandia.gov/pulspowr/icops99

More information on Monterey can be obtained at html.www.montereynet.com or from the information line at (831) 649-1770.

Conference Location

DoubleTree Hotel At Fisherman's Wharf Two Portola Plaza

Monterey California 93940

See "Hotel Information and Form" on page 10 for reservation information.

Conference Topics

- * Oral and poster sessions reporting research in plasma science and technology
- * Plenary talks by national plasma science leaders
- * Plasma Science and Applications Committee Prize Address by Prize Recipient

Conference Desk and Services

The DoubleTree Hotel will relay incoming calls and faxes to the room of a guest. Conference attendees who are not registered guests of the hotel will have calls and faxes relayed to the conference message desk. A message board will be provided. Outgoing fax and photocopy services will be available for a nominal fee. To contact: phone (408) 649-4511, FAX (408) 649-4115.

Social Events

The Sunday evening Reception will be held at the Monterey Maritime Museum, which is adjacent to the DoubleTree Hotel. A strolling buffet of hors d'oeuvres will be provided. The museum contains many exhibits that cover Monterey's seafaring heritage.

The conference banquet will be held at the DoubleTree Hotel on Tuesday, June 22nd. A nominal co-payment of \$10 will be charged for the banquet for conference registrants and \$20 will be charged for companions. Tickets are limited.

Conference Session Format

The four-day conference will include plenary, oral and poster sessions. Oral sessions will include both invited and contributed papers. Invited papers will be allotted 25 minutes for presentation and 5 minutes for questions. Contributed papers will be allotted 12 minutes for presentation and 3 minutes for questions. Overhead projectors will be available in all oral sessions. Slide projectors (35 mm) and other special equipment such as VCRs should be requested on the enclosed abstract form on page 12. For VCRs, there will be a rental charge that will be passed on to the presenter.

Session Topics and Organizers

The session topics and organizers are listed in the tables on pages 6 & 7 of this book. Contributions (experiment, theory or computation) should fit into one of these topic areas.

IEEE Conference Registration Information

Registration

Early registration is highly recommended. Register in full by Friday, April 30, 1999, to qualify for the lower registration fees. If you pre-register by fax, provide credit card information. Checks or money orders must be in the form of US dollars and drawn on or payable through US banks. American Express, VISA or MasterCard credit cards are also acceptable. Use the enclosed registration form (page 9) or the form available at our Web site (http://www.sandia.gov/pulspowr/icops99) and mail, e-mail, or fax the completed form and your remittance, remembering to include the abstract fee with your abstract to:

ICOPS 99

Yo Dr. Chris Deeney Sandia National Laboratories PO Box 5800 MS1194 Albuquerque NM 87185 Phone: (505) 845-3657 FAX: (505) 845-7864 E-mail: cdeene@sandia.gov

You will be sent an acknowledgement upon receipt of your registration with payment. Registration packets will be available Sunday through Thursday at the DoubleTree Hotel.

Registration at the Conference

All attendees must register. Cash, checks (personal and travelers), money orders and credit cards (American Express, VISA and Master Card) will be accepted. The registration fee includes refreshment breaks, the Sunday reception, conference proceedings and materials.

999

Registration and general information will be available at the DoubleTree Hotel on the following dates and times:

Sunday	June 20	4:00 p.m - 8:00 p.m.
Monday	June 21	7:30 a.m. – 4:30 p.m.
Tuesday	June 22	7:30 a.m. – 4:30 p.m.
Wednesday	June 23	7:30 a.m. – 4:30 p.m.
Thursday	June 24	7:30 a.m. – 12:00 noon

Registration Fees

On or Before April 30, 1999	After April 30, 1
\$320	\$390
\$420	\$500
\$ 70	\$ 90
\$ 70	\$ 90
	April 30, 1999 \$320 \$420 \$ 70

- Registrants in these two categories (Non-Member and Students) are eligible for the free Introductory IEEE membership described in the next section.
- ** No social events are included for these categories. (See "Companion Program and Social Event Registration Form," page11, to order social event tickets.)

Cancellation Policy: If requested in writing, refunds of cancelled Registration will be processed if received by May 22, 1999. There will be a cancellation fee of \$50.00.

Currency Exchange

It is strongly recommended that non-US attendees purchase travelers checks in US dollars, drawn on a US bank, before leaving their home country.

IEEE Membership & Travel Grant Information

Free Introductory IEEE Membership

In order to encourage participation in the activities of the IEEE and the Plasma Science and Application part of the IEEE Nuclear and Plasma Sciences Society, free half-year memberships will be given to all interested non-IEEE members (including students) registering for this conference. This free half-year membership includes a subscription to both the IEEE Spectrum and the Transactions on Plasma Science. The regular cost of a full year's membership can be found on the web site: www.IEEE.org. (Note: varies by region & location. Correct amounts per region are listed on the conference web page under IEEE Membership.) To receive your free membership, fill out the application at the registration desk.

IEEE Membership includes:

- * A subscription to Transactions on Plasma Science, a journal devoted to all aspects of plasma science and technology.
- * A subscription to Spectrum, a magazine covering engineering topics of general technical, economic, political and social interest.
- * A subscription to Society Newsletter with news items about the Conference on Plasma Science, Particle Accelerator Conference and Symposium on Fusion Engineering.
- * Eligibility to participate in a broad range of IEEE activities.
- * Opportunities for IEEE educational services such as video-conferences and individual learning packages.

To join, visit the registration desk at this conference for an application. Membership applications are available anytime by calling 1-800-678-IEEE.

IEEE Student Travel Grant to Conference

A limited number of travel grants, up to \$500, are available to encourage graduate students (IEEE members) to attend the conference. Applicants should submit the following:

- 1) Copy of submitted abstract
- 2) IEEE Membership number
- 3) Social Security number
- 4) Proposed budget for travel to the conference (cost sharing with student's institution is encouraged)
- 5) Two letters of recommendation, one of which is from the student's Adviser, stating the significance of research.

Application information should be sent by March 2,1999, to:

Professor R. M. Gilgenbach Nuclear Engineering Department, Cooley Building University of Michigan 2355 Bonisteel Blvd. Ann Arbor MI 48109-2104

Phone (734) 763-1261 FAX (734) 763-4540 E-mail: rongilg@umich.edu

Placement Center

A placement center will be set up at the conference. Individuals interested in employment opportunities in plasma physics and related areas should send their resumes to:

Dr. Wallace M. Manheimer Naval Research Laboratory 4555 Overlook Ave, SW Washington DC 20375

or

Mr Dan Jobe Sandia National Laboratories PO Box 5800, Albuquerque, NM 87185-1194 (505) 845-7572 FAX (505) 845-7864 E-mail: djobe@sandia.gov

FAX (202) 767-1607

E-mail: manheime@ccalpha2.nrl.navy.mil

The resumes should be marked "ICOPS" in the upper right-hand corner. Those who have positions available should notify Dr. Manheimer or Professor Granatstein.

Information About the Abstract

Abstract Submission Deadline

Interviews will be arranged at the conference. The Placement Center is a free, voluntary service. Abstracts should be submitted as camera-ready by mail, using the attached form or equivalent. The abstract must fit within a rectangle 4.5 in. by 10.5 in. (11.5 cm by 27 cm). For your convenience, an abstract form is enclosed. The single-page abstract must contain the title, author(s) and affiliations as a heading. The abstract must be single spaced with the title centered on one line and author(s) name(s) and affiliation(s) centered under the title. Please use 12 point Times, Times Roman or similar serif font. An abstract form will be available on our Web site. Abstracts will be published in the Conference Record, which will be available at the conference. **Facsimile copies will not be accepted.**

New Abstract Fee

The original and two copies of the abstract must be received no later than **Monday, January 18, 1999,** using the form on the following page. Abstracts will be reviewed by the session organizers and the program committee. Notices will be sent confirming acceptance of all papers. Abstracts received after the **January 18 deadline** will be placed in a post-deadline session, if accepted. The presenter must be one of the authors and a registered conference participant. At least one author should be registered to assure that the abstract appears in the proceedings. In 1999, due to the large number of no shows, we are trying a new system where an abstract fee of \$50 will be charged at the time of submission (see the abstract form). This fee will be deducted from the registration of one of the paper's authors (usually the presenter's). Please mark the abstract form as to whom the deduction will apply, and please indicate on the registration form the title of the abstract being presented. To facilitate the processing and to minimize the registration fee, we encourage early registration, even at the same time as the abstract submission.

Miscellaneous Conference Information

Airfare Discounts

Special discounted airfares to the 1999 ICOPS in Monterey, for 20-25 June, have been negotiated with United (10% off coach fares, 5% off the lowest available super-saver fares) and Continental Airlines (13% off coach fares, 8% off the lowest available super-saver fares). Where super-saver fares or Saturday night stays are not applicable, both airlines are offering zone fares. If, however, you book 60 days in advance of your contracted travel dates, both airlines have an advance booking incentive (United, 15% off coach fares, 10% off super-saver fares; Continental, 18% off coach fares, 13% off super-saver fares). Restrictions apply and airfares are guaranteed to be the lowest available when ticketed. Please note that discounted airfares may also be offered on other airline carriers.

Travel arrangements using the designated air carriers or the carrier of your choice can be made through IEEE Travel Services by calling 800-TRY- IEEE (800-879-4333) within the US. Outside the US, call 732-562-5387 between the hours of 8:30 a.m. and 5:30 p.m. EST Monday through Friday. When calling, please advise the Travel Counselor that you are traveling in connection with the ICOPS 99 Conference. You may also fax requirements to the IEEE Travel Services Department at 732-562-8815. When faxing, please be sure to include your travel dates, departure time, phone and fax numbers. A Travel Counselor will contact you as soon as possible.

Ground Transportation

Car Rental: Special discounted rates have been negotiated with Hertz Rental Car Agency.

Guest Parking: The DoubleTree Monterey is pleased to confirm a \$9.00 self parking rate with in and out privileges and an \$11.00 valet parking rate for each 24 hour stay. These rates are offered to registered hotel guests only. There is lower cost public parking nearby.

Airport Transportation: The Monterey Peninsula Airport is located just four miles from the Hotel. Travel time is ten minutes. Taxi service is approximately \$10 each way.

Monterey is situated 60 miles south of the San Jose International Airport, 120 miles south of downtown San Francisco and 340 miles north of Los Angeles.

Special Mini-Courses Offered

JUNE 24-25, 1999

MC1: Computational Methods in Plasma **Physics**

This two-day course will be organized by Dr. Melissa Douglas, Pulsed Power Division, Sandia National Laboratories and will consist of lectures from various experts in the field of computational modeling of plasmas.

Course Objectives: This course is tailored to scientists who are beginning careers in computational modeling of plasmas and who would like an overview on modeling techniques. The course will also be ideally suited for experimentalists and theorists who would like an improved understanding of modeling techniques.

Lectures: The two-day course will contain lectures in:

- 1) the use of plasma modeling for specific applications
- 2) magnetohydrodynamic codes
- particle-in-cell codes
- 4) hybrid codes
- 5) treating radiation
- 6) basic computational issues.

Course Materials: Notes prepared by the various lecturers.

Dr. Melissa Douglas Sandia National Laboratories Org 9544, MS-1194 PO Box 5800

Phone (505) 845-7472 FAX (505) 845-7864 E-mail: mrdougl@sandia.gov

Albuquerque NM 87185

MC2: Plasma Processes for Thin Film Transistor **Liquid Crystal Displays**

This one-day course will be taught by Professor Yue Kuo of the Thin Film Micro-electronics Research Laboratory of Texas A&M University.

Course Objectives: For those who are familiar with plasmas but not familiar with the thin film transistor (TFT) technology or who are working on TFTs but would like to gain fundamental knowledge on plasma processes or who are eager to learn the up-to-date status of the plasma processes for TFT fabrication. The main emphasis is on liquid crystal displays (LCDs), but non-LCD applications will also be mentioned. This course is designed for engineers, scientists, managers, faculty and graduate students who have a basic background in plasma thin-film technology.

Lectures: To emphasize fundamental and applied topics on various plasma processes in the fabrication of large-area TFT LCDs. The following subjects will be included:

- 1) review of TFT LCD fabrication processes and worldwide activities
- 2) comparison of TFT and VLSI processes and worldwide devices
- plasma deposition for TFTs including specific thin film materials (Si:H, dielectric, etc.) requirements, process influence on TFT characteristics, polysilicon formulation and equipment issues
- plasma etching for TFTs including profile control, etch rate and selectivity of various materials, plasma damages to TFTs, CFC- free processes and equipment design
- advanced plasma processes such as interface modification, ion doping, hydrogenation and novel processes
- 6) future trend in plasma technologies for TFT fabrication.

Course Materials: Notes prepared by Professor Kuo will be distributed in the class.

Conference Registration Form

Conference Fees Conference Registration (please type or print) On or Before After April 30, 1999 April 30, 1999 Affiliation/Company_____ **IEEE Member** \$320 \$390 \$420 \$500 Non-Member Mailing address_____ \$ 70 \$ 90 Student \$ 70 \$ 90 Retired If you have previously submitted an abstract, State/Province please deduct \$50. Country_____Zip code_____ Mini-Course Fees On or Before April 30, 1999 MC1: Computational Methods \$ 500 in Plasma Physics Name to appear on badge_____ MC2: Plasma Processes \$ 350 Transistor Liquid Crystal Displays ☐ I am an IEEE Member **Fee Summary** Membership no.____ Conference Registration ☐ I am not an IEEE Member Mini-Course Fee MC1: \$500 MC2: \$350 Non members must register at the non member rate, Total Amount but if you join during the conference, you will receive a free half-year introductory membership. Abstract Information: If you have previously paid an abstract Fee, please give the paper's Title and Session Number. ☐ I wish to join IEEE Title ___ There will be IEEE Membership material in the Registration Area. Session Number_____ Paper Confirmation Number_____ Note: Early registration discount fees are valid only if **Method of Payment** full payment with registration form are received by April 30, 1999. All payments must be in US dollars. Only checks drawn on or payable through US banks are acceptable. Travelers Checks, Forms received after May 27 will be processed money orders and credit cards listed below are acceptable. at the Conference. Make payable to IEEE ICOPS 99. Mail this form, or a copy, together with your Check or Money Order Enclosed Remittance (payable to IEEE ICOPS 99) VISA MasterCard American Express ICOPS 99 % Chris Deeney Sandia National Laboratories PO Box 5800 MS1194 Cardholder's name (PRINT)_____ Albuquerque NM 87185

Cardholder's signature____

Hotel Information and Form

Rooms have been reserved at the DoubleTree Hotel (designated Conference Hotel). One additional hotel is available at the discounted rate for the period of June 20-24, 1999, only. Please complete hotel arrangements by the date indicated below to obtain the special conference rate. To receive this rate, you must mention you are attending the IEEE International Conference on Plasma Science.

DoubleTree Hotel

At Fisherman's Wharf Two Portola Plaza Monterey CA 93940 (408) 649-4511 FAX: (408) 649-4115 After January: area code (831)

PO Box 1351 Monterey CA 93942-1351 (408) 375-2411 FAX: (408) 375-1365

700 Munras Avenue

After January: area code (831)

Casa Munras Garden Hotel

Hotel Registration Form

For the 1999 IEEE INTERNATIONAL CONFERENCE ON PLASMA SCIENCE.

Please send this form to the hotel of your choice. The form must be received by the early reservation deadline of May 3, 1999.

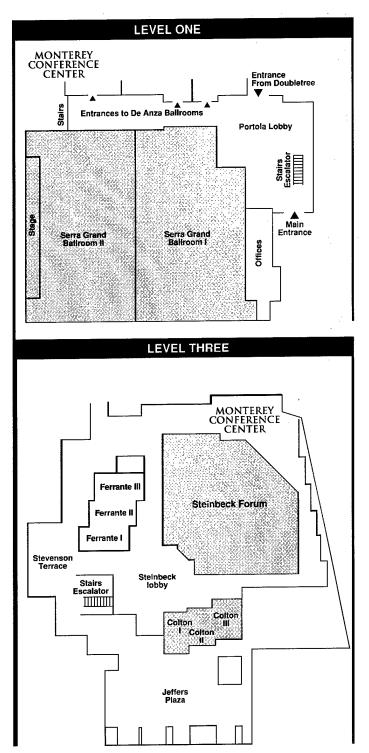
Hotel Name			
Address			
Please make the following	reservations and	d send confirmation	on to:
Name			
Address			
State/Province			·
Country			
Single Room 🚨 Double		_	g 🗖 Smoking 📮
			of Departure
Credit Card # Expiration Date			
Master Card U Visa U	American Expre	ss 🗖	
Cardholder's Name			
	(print)		(signature)
Hotel Room Rate	Single	Double	Group Rate Deadline
DoubleTree Hotel	\$128	\$145	May 3, 1999
Casa Munras Hotel	\$ 94	\$ 94	May 3, 1999
Do you or anyone attendi	ng with you requ	uire special accom	modations or services? No 🚨 Yes 🗀
If yes, please describe:			

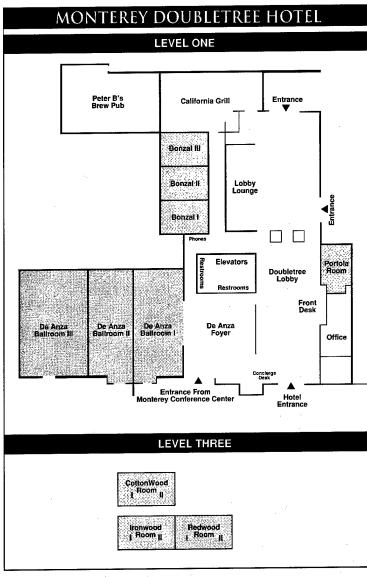
Companion Program & Social Event Ticket Registration Form

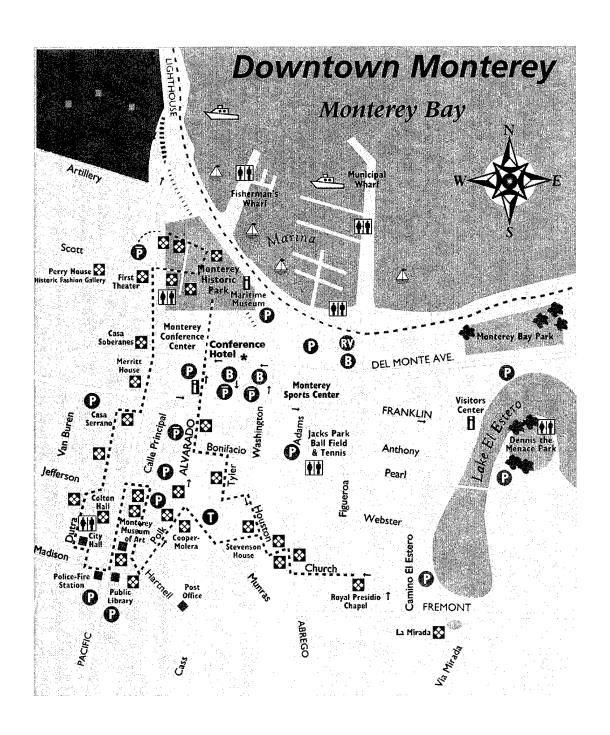
The Companion Program is offered as a focal point for companions to see the wonderful sights of Monterey and to meet friends. To facilitate interactions, there will be a hospitality suite with continental breakfast at the hotel. In addition, three tours of Monterey and its surroundings are being organized. Please sign up for these early since the numbers may be limited for the bus tours. All prices, which are listed on the form, are subject to change.

Name	Method	of Payment:	Make Ch	necks Payable	e to IEEE ICOPS 99
Affiliation/Company	All payme	ents must be i	n U.S. dol	llars. Only che	ecks drawn on or
Mailing address				acceptable. Tra sted below are	avelers Checks,
City					Remittance to:
				dia National La rque NM 871	
State/Province	☐ Chec	k or Money C	order Encl	osed	
CountryZip code		•		American Ex	press
Phone	Card Numbe	er			
Fax					
E-mail	Cardholder's	Name (print)			
		J			
Schedule of Companion Program	Cost				
& Social Events	4051				
	On or Before April 30, 99	After April 30, 99	No. of People	Amount	
Sunday, June 20: Reception at the Maritime Museum Food and cash bar.	\$ 10 🗅	\$ 15 🗅			
Tuesday, June 22: Hotel Banquet	\$ 20 🗅	\$ 20 🗖			
Companion Program					
Monday, June 21: The Monterey Peninsula	\$ 25 🗖	\$ 30 🗖			
Tuesday, June 22: A self-guided tour of Monterey	\$ 10 🗖	\$ 15 🗅			
Wednesday, June 23: Big Sur and Point Lobos There will be a bus tour to Point Lobos for a nature walk, followed by a drive down the Pacific Highway (Route 1) with its breathtaking coastal vistas to Big Sur with lunch at the renowned Nepenthe Restaurant. There will be time to shop for unique gifts and/or hike a little way and take photographs of spectacular	\$ 30 🗖	\$ 40 🗅			
Pacific Ocean views. Transportation and lunch provided.	Totai	\$	·		

Monterey Conference Center Monterey Doubletree Hotel







NEW ORLEANS



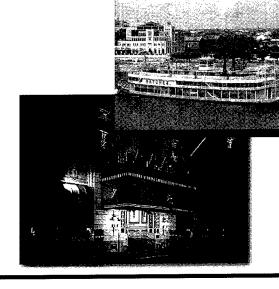


June 4-7 2000 The 27th IEEE International Conference on Plasma Science

Conference Topics:

- Basic Processes in fully & partially ionized plasmas
- Microwave generation & microwave/plasma interactions
- Intense electron & ion beams
- High energy density plasmas
- Industrial & commercial applications of plasma physics
- Plasma diagnostics
- Pulsed power

ICOPS □□□□ will be held at the stately Fairmont Hotel near the historic French **Quarter** in New Orleans.



ICOPS Bar is sponsored by the Plasma Science & Applications Committee of the IEEE Nuclear and Plasma Sciences Society.

Conference Organizer: Dr. Michael S. Mazzola, Box 9571, Department of Electrical & Computer Engineering, Mississippi State University, Mississippi, 39762, USA



Technical Sessions

The 26th IEEE International Conference on Plasma Science

Schedule of Technical Sessions

Monday AM, June 21

Plenary: Laboratory Astrophysics Experiments

1A: Basic Processes in Fully and Partially Ionized Plasmas

1B: Slow Wave Devices

1C: Laser Produced Plamas

1D: Non-Equilibrium Plasma Processing

1P. Space Plasmas, Partially Ionized Gases, Microwave Systems, ICF

Monday PM, June 21

Plenary: The Inexorable Plasma Processing Challenges presented by Moore's law

2A: Space Plasmas and Partially Ionized Gases

2B: Microwave Plasmas

2C: Inertial Confinement Fusion

2D: Plasma Diagnostics

2P: Laser Plasmas, Slow Wave Devices, Basic Phenomena, Computational Plasmas, Environmental Issues

Tuesday AM, June 22

Plenary: Thermal Plasma Processes

3A: Computational Plasma Physics

3B: Microwave Systems

3C: Laser Produced Plasmas and Dense Plasma Focus

3D: Non-equilibrium Plasma Processing

3P: Fast Wave Devices, Diagnostics, Plasma Processing

Tuesday PM, June 22

Plenary: Communicating with Nonscientists and the Media

4A: Intense Electron and Ion Beams

4B: Fast Wave Devices

4C: Spherical Configurations

4D: Thermal Plasma Chemistry and Processing

4P: Microwave Plasmas, Non-equilibrium Plasma Processing, MFE

June 20–24, 1999 Monterey California, USA

Wednesday AM, June 23

PSAC Award Address: Simple Models on Some Nasty Problems in Beams and Plasmas

5A: Plasma, Ion, and Electron Sources

5B: Fast Wave Devices and Intense Beams

5C: Fast Z-Pinches and X-ray Lasers

5D: Plasma Opening Switches

5P: Lighting, Flat Panels, Vacuum Microwaves

Wednesday PM, June 23

Plenary: The Future of High-Power Microwaves

6A: Plasmas for Lighting

6B: Intense Beams

6C: Fast Z-Pinches and X-ray Lasers

6D: Vacuum Microwaves (Microelectronics)

6P: Sources, Beams, Switches

Thursday AM, June 24

Plenary: Z Pinches: Past, Present and Future

7A: Plasmas for Lighting 7B: Magnetic Fusion Energy

7C: Closing Switches and Plasma Opening Switches

7D: Plasma Thrusters and Arcs

7P: Plasma Focus, Z Pinches and X-ray Lasers, Beams,

Postdeadline

Contacts

Dr. Chris Deeney ICOPS99 Conference Chairman email: cdeene@sandia.gov

Lisa S. Waggoner ICOPS99 Conference Coordinator email: lswaggo@sandia.gov De Anza Ballroom 8:30 am, Monday, June 21, 1999

Welcome

Dr. Christopher Deeney 1999 ICOPS Chairperson Sandia National Laboratories

Pienary Talk

Laboratory Astrophysics Experiments High Power Laser and Pulsed Power Facilities

Dr Paul Springer Lawrence Livermore National Laboratory

Chairperson

Dr Christopher Deeney Sandia National Laboratories

De Anza I 10 am, Monday, June 21, 1999

Oral Session 1A Basic Processes in Fully and Partially Ionized Plasmas

Chairperson
Wallace M. Manheimer
Naval Research Laboratory

- 1A01 Neutral Depletion and Transport Mechanisms in Large-Area High Density Plasma Sources
 - G.R. Tynan, University of California, San Diego, La Jolla, CA 92093-0417, USA
- 1A02 Soft X-ray production in spark discharges in hydrogen, nitrogen, air, argon and xenon gases
 - J. Va'vra, P.M. Va'vra and J. Maly, Stanford University, Stanford, CA 94309, USA
- 1A03 High Voltage Subnanosecond Corona Inception
 - J. Mankowski, J. Dickens, M. Kristiansen, J. Lehr, W. Prather and
 - J. Gaudet, Texas Tech University, Lubbock, TX 79409-3102, USA
- **1A04-05 Invited -Resonances and Surface Waves in Bounded Plasmas**Kevin J. Bowers, David W. Qui, H.B. Smith and C.K. Birdsall,
 University of California Berkeley, Berkeley, CA, 94720-1772, USA
- 1A06 Nonlinear Features of Electron Beam-Driven Instabilities in a Magnetized Plasma,

Nagendra Singh and W.C. Leung, University of Alabama, Electrical and Computer Engineering, Huntsville, AL 35899, USA

- 1A07 Electrodynamics of Particle or Dust in Periodic Electric Cusps with Electric Mirrors and Its Applications to Planetary Dust Layers or Rings and Electric Undulators
 - Hiroshi Kikuchi, Nihon University, Chiyoda-ku, Tokoya 101, Japan
- 1A08 Negative Ion Measurements in Electron Cyclotron Resonance Plasmas

Bon-Woong Koo, Noah Hershkowitz and Brent Buhr, Center for Plasma-Aided Manufacture, University of Wisconsin-Madison, Madison, WI 53706, USA

1A09 Negative DC Electrical Corona Interaction with Charged Dust Particles

Deepak K. Gupta, S.V. Kulkarni and P.I. John, Institute for Plasma Research, Gujarat 382428, India De Anza II 10 AM, Monday, June 21, 1999

Oral Session 1B Slow Wave Devices

Chairperson

David R. Whaley

Northrop Grumman

1B01-02 Invited - Numerical Simulation of Backward Wave Excitation in Helix-Traveling Wave Tubes

T.M. Antonsen Jr., D.Chernin, B. Levush, Naval Research Laboratory, Washington, DC 20375, USA

- 1B03 Advances in Plasma-Filled Relativistic Slow Wave Microwave Sources
 Y.Carmel, A. Shkrarunets, S. Kobayashi, J. Rodgers. G.S. Nusinovich, T.M.
 Antonsen Jr. and V.L. Granatstein, University of Maryland, College Park,
 MD 20742-3511, USA
- **1B04** On the Theory of Ion Noise in Microwave Tubes
 Wallace Manheimer, Naval Research Laboratory, Washington, DC 20375-5346, USA
- Three dimensional Simulations of Electron Beams Focused by Periodic Permanent Magnets
 Carol L. Kory, NASA Lewis Research Center, AnaLex/NASA LeRC MS 54-5, Cleveland, OH 44135, USA
- 1B06 Exact Treatment of the Dispersion and Beam Interaction Impedance of a Thin Tape Helix Surrounded by a Radially Stratified Dielectric
 - D. Chernin and C. Kostas, T.M. Antonsen Jr. and B. Levush, Science Applications International Corporation, McLean, VA 22102, USA
- 1B07 Applications of the CTLSS Electromagnetic Eigensolver to Modeling Slow-Wave Devices
 - S.J. Cooke, B. Levush, A. Mondelli, C. Kostas, M. Czarnaski, T.M. Antonsen Jr. D. Chernin and I. Fridman, Naval Research Laboratory Code 6841, Washington, DC 20375, USA
- **Three-dimensional Modeling of Multistage Depressed Collectors**K.R. Vaden and V.O. Heinen, NASA Lewis Reasearch Center, Cleveland, OH 44135, USA
- 1B09 Effects of High Plasma Density on the Electromagnetic Properties of Slow Wave Circuits
 - S. Kobayaski, A. Shkvarunets, Y. Carmel, J. Rodgers, T.M. Antonsen Jr. and V.L. Granatstein, University of Maryland, College Park, MD 20742- 3511, USA
- 1B10 A Novel Ku Band Microwave Source Based on a Complex Extended Interaction Stucture

L.Chen, H.Y. Chen, M.H. Tsao, Y.C. Tsai and K.R. Chu, T.T. Yang, S.S. Chang, C.H. Chang, P.C. Wan and L.C. Chen, National Tsing Hua University, Hsinchu, Taiwan

Session 1C Laser Produced Plasmas

Chairperson

Andrew Mostovych

Naval Research Laboratory

1C01-02 Invited - Laser-produced plasma: A new window for high pressure science

A. Ng, University of British Columbia, Vancouver, BC V6T1Z1, Canada

1C03-04 Invited - Numerical Modeling of ICF Plasmas

J.P. Dahlburg, J.H. Gardner, A. J. Schmitt, D. Colombant, M. Klapisch and L. Phillips, U.S. Naval Research Laboratory, Washington, DC 20375, USA

1C05-06 Invited - Dynamics of Plasma Propagation and Splitting During Pulsed Laser Ablation

R.F. Wood, Oak Ridge National Laboratory, Oak Ridge, TN 37831-6032, USA

1C07 Simulation of Intense Laser Pulse Propagation in Capillary Discharge Plasma Channels

R.F. Hubbard, P. Sprangle, A. Ting and C. Moore, U.S. Naval Research Laboratory, Washington, DC 20375-5346, USA

1C08 Guiding and Triggering of Large-Scale Electrical Discharges using Ultrashort Pulse Lasers

D. Comtois, C.Y. Chien, P. Couture, A. Desparois, T.W. Johnston, Z. Jiang, J.C. Kieffer, B. LaFontaine, F. Martin, R. Mawassi, H.P. Mercure, H. Pepin, C. Potvin, F.A.M Rizk and F. Vidal, INRS Energie et Materiaux, Varennes, Quebec J3X 1S2, Canada

1C09 Electrostatic Measurement of Plasma Plume Dynamics in Pulsed Laser Evaported Graphite

R.M. Mayo, J.W. Newman, A. Sharma, J. Narayan and Y. Yamagata, North Carolina State University, Raleigh, NC 27695, USA

Oral Session 1D Non-Equilibrium Plasma Processing

Chairperson
Jeff Hopwood
Northeastern University

1D01 Control of Ion Energy and Angular Distributions using Voltage Waveform

Shahid Rauf, Motorola, SPS, Austin, TX 78721, USA

- 1D02 A Novel Method of Ion Energy and Ion Energy Distribution Function Control at the Substrate during Plasma Processing Shiang-Bau Want and Amy E. Wendt, University of Wisconsin-Madison, Madison, WI, 53706, USA
- 1D03-04 Invited Review of Ionized-PVD By Hollow Cathode Magnetron Sputtering

K.F. Lai and Q. Lu, Novellus Systems Inc., San Jose, CA 95134, USA

- 1D05 Sputter Heating in Ionized Metal Physical Vapor Deposition
 Junqing lu and Mark J. Kushner, University of Illinois, Urbana, IL 61801,
 USΔ
- 1D06 Irregularities in Electronegative Plasmas Due to Ion-Ion Coupling
 Peter Vitello, LLNL, Livermore, CA 94551, USA
- 1D07 Simulations of Low Field Helicon Discharges Using a Two
 Dimensional Hybrid Plasma Equipment Model
 Ron L. Kinder and Mark J. Kushner, University of Illinois, Urbana, IL
 61801, USA
- 1D08 Space Averaged Kinetic Analysis of Stochastically Heated Electronegative RF Capacitive Discharges

 Zuoding Wang and Allan J. Lichtenberg, University of California Berkeley, Berkeley, CA 94720, USA

Poster Session 1P

Note: Posters should be displayed all day

1P01	Asymptotic modelling of a narrow gap, high pressure glow discharg R. Bektursunova and W.G. Graham, Queen's University of Belfast,
	Northern Ireland, UK
1P02	Experimental Characterization of a Pulsed ICP Discharge
	K.C. Leou, Y.T. Chien, Y.M. Yang, T.L. Lin and C.H. Tsai, National Tsing Hua University, Hisinchu, Taiwan 30043, ROC
1P03	The Dependence of the Decay Time Constant on the Chamber Size
11 05	and Gas Pressure in a Pulsed ICP
	T.L. Lin, Y.T. Chien, K.C. Leou, C.H. Tsai, National Tsing-Hua University,
	Hsinchu, Taiwan 30043, ROC
1P04	Two-Dimensional Modeling of Nonlocal Electron Heating in
	Inductively Coupled Plasma Sources
	Y.Hu, T.L. Lin, and C.W. Chang, National Tsing-Hua University, Hsinchu,
	Taiwan 30043, ROC
1P05	Two-Dimensional Simulation of Electron Cyclotron Resonance
	Discharge
	J.H. Shiau, J.H. Tsai and S.H. Chen
	National Center for High Performance Computing, Hsinchu, Taiwan, ROC
1P06	Susceptibility diagram of multipactor discharge on a dielectric-
	Effects of an external magnetic field and oblique RF electric field
	L.K. Ang, A. Valfells, Y.Y. Lau, and R.M. Gilgenbach, University of
	Michigan, Ann Arbor, MI 48109-2104, USA
1P07	A Theory of RF Window Failure
	A. Valfells, L.K. Ang, Y.Y. Lau, R.M. Gilgenbach, R.A. Kishek, J.
	Verboncoeur, A. Neuber, H. Krompholz and L.L. Hatfield, University of
	Michigan, Ann Arbor, MI 48109-2104, USA
1P08	Design of Quasi-Optical Grills for the Launch of Microwaves into
	Tokamak Plasmas J. Preinhaelter, M.A. Irzak, L. Vahala, G. Vahala, Old Dominion University, Norfolk, VA 23529, USA

Serra I, Conference Centre 10 AM, Monday, June 21, 1999

1P09	Intentionally Unused
1P10	Experimental Investigation of Ion Beam Transport in a Laser
	Initiated High Current Discharge Channel
	A. Tauschwitz, C. Niemann, D. Penache, R. Presura, GSI, Darmstadt, Germany
1P11	Magnetic field generation by periodic helical deformation in RFP Mitsuaki Maeyama, Takanori Miyasita and Eiki Hotta, Saitama University, Saitama 338-8570, Japan
1P12	Magnetohydrodynamic Current Drive for Fusion Confinement G.B. Kirby Meacham and Barbara J. Quill, Meacham & Company, Shaker Ht., OH 44122, USA
1P13	Influence of Triangularity and Ellipticity on the Poloidal Field
	Around a Tokamak Magnetic Surfaces
	P. Martin and J. Puerta, Universidad Simon Bolivar, Caracas 7080A,
	Venezuela
1P14	Preliminary Results from the Flow-Through Z-Pinch Experiment:
	ZaP
	U. Shumlak, B.A. Nelson, R.P. Goilingo, D. Tang and E. Crawford, D.J. Den Hartog and D.J. Holly, University of Washington, Seattle, WA
	98195- 2250. USA
1P15	Magnetized Target Fusion: No Capital Investment Required
5	Irvin R. Lindemuth, Richard E. Siemon, Ronald C. Kirkpatrick, Robert E.
	Reinvosky , Los Alamos National Laboratory, Los Alamos, NM 87545, USA
1P16	Computational Investigation of Plasma-Wall Interaction Issues In
	Magnetized Target Fusion
	Peter Sheehey, Walter Atchison, Rickey Faehl, Ronald Kirkpatrick, Irvin
	Lindemuth and Richard Siemon, Los Alamos National Laboratory,
	Los Alamos, NM 87545, USA

De Anza Ballroom 1: 30 PM, Monday, June 21, 1999

Plenary Talk

"The inexorable plasma processing challenges presented by Moore's law"

Rick Gottscho LAM Inc. De Anza I 3 PM, Monday, June 21, 1999

Oral Session 2A Space Plasmas and Partially Ionized Gases

Chairperson
Shahid Rauf
University of Illinois

2A01-02 Invited - Plasma-Shock Interactions in a Low Pressure Positive Column

B.N. Ganguly, P. Bletzinger and A. Garscadden, U.S. Air Force Research Laboratory, Innovative Scientific Solution Inc., Dayton, OH 45440-3638, USA

- 2A03 Second Harmonic RF Currents in a Cylindrical ICP with a Planar Coil
 V.A. Godyak, R.B. Piejak and B.M. Alexandrovich, Osram Sylvania
 Development Inc, Beverly, MA 01915, USA
- 2A04 A Traveling Wave Driven, Inductively Coupled Large Area Plasma
 Source
 Yaoxi Wu and M.A. Lieberman, University of California-Berkeley, Berkeley,
 CA 94720, USA
- 2A05 Unstable Behavior of Plasma in Inductive Discharges
 A.M. Marakhtanov and M.A. Lieberman, University of California Berkeley, Berkeley, CA 94720, USA
- Nonlinear Stabilization of the Weibel Instability Driven by Counterstreaming Ion Beams
 Nagendra Singh and W. C. Leung, Elect. & Comp. Engr. Dept., University of Alabama, Huntsville, AL 35899, USA
- 2A07 DSCS Satellite Dielectric Charging Correlation with Magnetic Activity
 Shu T. Lai, U.S. Air Force Research Laboratory, Hanscom AFB, MA 01731,
 USA
- 2A08 Ion Energy Distribution in NF3 Based Process Chamber Cleaning Discharges

H.P. Hsueh, B.S. Felker, R.T. McGrath and J.G. Langan, Air Products & Chemicals, Inc, Allentown, PA 18195, USA

Oral Session 2B Microwave Plasmas

Chairperson
John Scharer
University of Wisconsin

2B01-02 Invited - Test Facility for High Pressure Plasmas

Rolf Block, Mounir Laroussi & Karl H. Schoenbach, Old Dominion University, Norfolk, VA 23529, USA

- 2B03 Microhollow Cathode Discharges in Atmospheric Air
 R.H. Stark, U. Ernst, R. Block, M. El-Bandrawy and K.H. Schoenbach, Old
 Dominion University, Norfolk, VA 23529, USA
- 2B04 Further Investigation of P.I.A. (Persistant Ionization in Air) Plasmas
 Using Room Air
 J.F. Kline, J.E. Brandenburg and Vincent DiPietro, Research Support
 Instruments, Lanham, MD 20706, USA
- 2B05 Radio-frequency Sustainment of a Laser-Produced Plasma K.L. Kelly, J. E. Scharer, G. Ding, H. Gui and E. Paller, University of Wisconsin, Madison, WI 53706-1687, USA
- 2B06 Laser and Radio-frequency Wave Creation of Seeded Air Plasmas
 J. Scharer, G.Ding, X. Guo, H. Gui, K. Kelly and E. Paller, University of
 Wisconsin, Madison, WI 53706-1687, USA
- 2B07 Improved Air Filtration and Filter Sterilization Using DC Electric Fields and a One Atmosphere Uniform Glow Discharge Plasma (OAUGDP)

J. Reece Roth, Daniel M. Sherman, Rami B. Gadri, Zhiyu Chen, Fuat Karakaya, Thomas C. Monite, Kimberly Kelly-Wintenberg, and Peter P.Y. Tsai, University of Tennessee, Knoxville, TN 37996-2100, USA

2B08 Sterilization By Plasma Active Species at One Atmosphere Using a Remote Exposure Reactor (RER)

Daniel M. Sherman, Rami B. Gadri, Fuat Karakaya, Zhiyu Che, Thomas C. Montie, Kimberly Kelly-Wintenberg, Peter P.Y. Tsai and J. Reece Roth, University of Tennessee, Knoxville, TN 37996-2100, USA

- 2B09 New Plasma Concepts for Enhanced Microwave Vacuum Electronics
 J.R. Hoffman, P. Muggli, M.A. Gundersen, W.B. Mori, C. Joshi and T.
 Katsouleas, University of Southern California, Los Angeles, CA 900891341, USA
- 2B10 Frequency Transformer: Switched Magnetized Plasma Medium D.K. Kalluri, J.H. Lee, Spencer Kuo, Igor Alexeff, University of Massachusetts-Lowell, Lowell, MA 01854, USA

Session 2C Inertial Confinement Fusion

Chairperson

John Porter

Sandia National Laboratories

2C01-02 Invited - Development of a Z-Pinch-Driven ICF Hohlraum Concept on Z

M.E. Cuneo, J.L. Porter Jr., R.A. Vesey, L.E. Ruggles, W.W. Simpson, M. Vargas, D.L. Hanson, T.Nash, G.A.Chandler, J.R. Asay, C.A. Hall, C. Deeney, R.B. Spielman, J.H. Hammer, A. Toor, O Landen, J. Kock, Sandia National Laboratories, Albuquerque, NM 87185-1193, USA

2C03 Characterization of the Radiation Environment for Capsule Drive in Central and Axial Hohlraums

R.L. Bowers, J.H. Brownell, H.H. Rogers and D.L. Peterson, Los Alamos National Laboratory, Los Alamos, NM 87545, USA

2C04 Radiation History and Energy Coupling to Cylindrical Targets on the Z Machine

J. Aubrey, R.L. Bowers, D.L. Peterson, G.A. Chandler, M.S. Derzon, T.J. Nash and D.L. Fehl, Los Alamos National Laboratory, Los Alamos, NM 87545, USA

- 2C05 Tailoring the Radiation Drive in Dynamic Hohlraums
 M.S. Derzon, T.J. Nash, G.A. Chandler, R.J. Leeper, D.L. Fehl, J. Aubrey, R. Bowers, D. Petersen, D.D. Ryutov and J.J. MacFarlane, Sandia National Laboratories, Albuquerque, NM 87185-1196, USA
- 2C06 Axial Convergent Z-Pinch-Driven Dynamic Hohlraums
 S.A. Slutz, M.R. Douglas and T.J. Nash, Sandia National Laboratories,
 Albuquerque, NM 87185, USA
- 2C07 Two-Dimensional Implosions of Liners onto Spherical Hohlraums I.V. Lisitsyn, S. Katsuki and H. Akiyama, Kumamoto University, Kumamoto 860-8555, Japan
- 2C08 Foot-pulse Radiation Drive Necessary for ICF Ignition Capsule Demonstrated on Z Generator

T.W.L. Sanford, R.E. Olson, G.A. Chandler, D.L. Fehl, J.S. Lash, R.J.Leeper, L. Ruggles, K.W. Struve, R.A. Vesey, M.S. Derzon, T.J. Nash, W.A. Stygar, R.C. Mock, D.E. Hebron, T.L. Gilliland, D.O. Jobe, J.S. McGurn, J.F. Seamen, W. Simpson, J.A. Torres and M.F. Vargars, D.L. Peterson, Sandia National Laboratories, Albuquerque, NM 87185-1196, USA

Two-dimensional Integrated Z-Pinch ICF Design SimulationsJ.S. Lash, Sandia National Laboratories, Albuquerque, NM 87185-1186, USA

Oral Session 2D Plasma Diagnostics

Chairperson	
Ken Connor	
Plasma Dynamics Laborate	ory, RPI

- 2D01 Comparison of Electron Density Measurements in Planar Inductively Coupled Plasmas
 Wei Guo, Richard L.C. Wu, Charles A. DeJoseph, Jr., K Systems Corp., Beavercreek, OH 45432, USA
- 2D02 Emissive Probe Characteristic in an Inductive Plasma Source T.Lho, N. Hershkowitz, G.H. Kim and W. Steer, University of Wisconsin-Madison, Madison, WI 53705, USA
- Elimination of notching and ARDE by simultaneous modulation of source and wafer RF.
 N. Hershkowitz and M.K. Harper, University of Wisconsin, Madison, WI 53706, USA
- 2D04-05 Invited Diagnostics for Plasma Processing

J. Forster, Applied Materials, Santa Clara, CA 95054, USA

- 2D06 Two Color Fiber Optic Interferometer for Gas and Plasma Density
 Measurements

 S.W. Conslor N. Oi. J. Schoin and M. Krichnan, Alameda Applied
 - S.W. Gensler, N. Qi, J. Schein and M. Krishnan, Alameda Applied Sciences Corporation, San Leandro, CA 94577, USA
- 2D07 Diagnosis of Large Volume Pulse Modulated Ar-H2 Plasmas
 K.C. Paul, Y. Tanaka and T. Sakuta, Kanazawa University, Kanazawa 9200944, Japan
- 2D08 Diagnostic Applications of the Most Advanced Theory and Code for Stark Broadening of Hydrogen Lines in Plasmas
 E. Oks, Auburn University, Auburn, AL 36849-5311, USA

Poster Session 2P

Note:	Posters	should	be	displayed	all	day
-------	----------------	--------	----	-----------	-----	-----

- 2P01 Resonant absorption of a short-pulse laser in a doped dielectric L.K. Ang, Y.Y. Lau and R.M. Gilgenbach, University of Michigan, Ann Arbor, MI 48109-2104, USA
- Electromagnetically Induced Transparency and Pulse Propagation in Plasmas
 B. Hafizi, P. Sprangle, R.F. Hubbard and J.R. Penano, Icarus Research, U.S. Naval Research Laboratory, Washington, DC 20375-5346, USA
- **Thermal Filamentation Instability in Laser-Produced Plasma**F. Bouzid and A. Bendib, Laboratoire de Physique des Milieux Ionises, U.S.T.H.B., Algiers, Algeria
- 2P04 Characteristics of Titanium plasma for Ti Vapor Laser
 M.Atta Khedr, H. Sharkaway and TH.M. El Sherbini, Cairo University and University of Wisconsin Madison, Madison, WI 53706, USA
- Electric discharge enhancement of laser produced plasma for thin film deposition
 D.G. Redman, J. Mouillaux, S.Zhe, Y.Y. Tsui and R. Fedosejevs,
 University of Alberta, Edmonton, Alberta T6G2G7, Canada
- 2P06 Ultra-Linear Traveling Wave Tube Development
 D.M. Goebel, R. Liou and W.L. Menninger, Hughes Electron Dynamics,
 Torrance, CA 90509, USA
- 2P07 Full Wave Analysis of Beam Instability of Dense Plasma Wave
 Spectrum in Plasma Filled Periodic Waveguide
 G.I. Zaginaylov, A.A. Rozhkov and J.Y. Raguin, Tech University Hamburg,
 A B Holhfrequenztechmik, Germany
- 2P08 Initial Validation of the CTLSS Eigenmode Solver in Helix Geometry
 D.R. Whaley, C.M. Armstrong, Simon J. Cooke, Northrop Grumman
 Corporation, Rolling Meadows, IL 60008, USA
- The Angular Distribution of Elastically Scattered Electrons, Its
 Modeling and Computed Effect on Collector Performance
 I.L. Krainsky and K.R. Vaden, NASA Lewis Research Center, Cleveland,
 OH 44135, USA
- 2P10 A Simple Theory of Ion Noise in TWT
 Y.Y. Lau, D. Chernin and W. M. Manheimer, U.S. Naval Research
 Laboratory, Washington, DC 20375, USA
- 2P11 Genesis: A 2.5D Nonlinear Simulation Code For Helix Traveling
 Wave Tubes In The Frequency Domain
 H.P. Freund, T.M. Antonsen Jr. and B. LevushY.Y., U.S. Naval Research
 Laboratory, Washington, DC 20375, USA

Serra I, Conference Centre 3 PM, Monday, June 21, 1999

2P12	Localized Growth Rates of Intermodulation Products in a Multiton
	Traveling Wave Tube Amplifier
	J.G. Wohlbier, I. Dodson, J.H. Booske, J.E. Scharer, University of
2242	Wisconsin, Madison, WI 53706, USA
2P13	Analysis of 3-D Phase Space Dynamics of Pencil-to-Sheet Electron Beam Transformation in Highly-Non-Paraxial Quadrupole Lens
	System
	M.J. McNeely, J.H. Booske, J.E. Scharer, & M.A. Basten, University of
	Wisconsin, Madison, WI 53706, USA
2P14	Experimental Validation of CHRISTINE, a 1-D Multi-Frequency
	Helix TWTCode: Drive Curves, Phase, Distortion Products and
	Intermodulation
	D.K. Abe, M.T. Ngo, B. Levush, T.M. Antonsen Jr. and D. Chernin, U.S.
	Naval Research Laboratory, Code 6843, Washington, DC 20375, USA
2P15	Design and Development of a 2-18 GHz MPM TWT
	M.A. Basten, J. Duthie, J. Hutchins and C.M. Armstrong, Northrop
	Grumman Corporation, Rolling Meadows, Il 60008, USA
2P16	Exploiting 2-1/2 D TWT simulations to maximize the efficiency of
	the Hughes 8815HR TWT
	Daniel J. Gregoire, Xiaoling Zhai, HRL Laboratories, Malibu, CA 90265,
	USA
2P17	Resonant Discharge Simulations with Asymmetric Electrodes
	H.B. Smith, K.J. Bowers and C.K. Birdsall, University of California -
2240	Berkeley, Berkeley, CA 94720, USA
2P18	Resonant Discharges: Initiation and Steady State; Comparisons
	with Theory, Simulation and Experiement
	Kevin J. Bowers, David W. Qiu, C.K. Birdsall, University of California -
2040	Berkeley, Berkeley, CA 94720-1772, USA Electrostatic and Electromagnetic Surface Wave Theories
2P19	
	Compared Kevin J. Bowers, University of California - Berkeley, Berkeley, CA 94720-
2020	1772, USA 2D Electromagnetic PIC-MCC Simulation of the Initiation of a Large
2P20	Area Surface Wave Sustained Plasma Source
	Kevin J. Bowers, University of California – Berkeley, Berkeley, CA 94720-
	1772, USA
2024	Vortex formation and transport in 2D magnetized non-neutral
2P21	bounded plasmas
	Hae June Lee, Min Sup Hur, Jin Ho Kang and Jae Koo Lee, Pohang
	University of Science and Technology, Pohang, Kyoungbuk 790-784,
	•
	S. Korea

Serra I, Conference Centre 3 PM, Monday, June 21, 1999

2P22	Self-effect in expanding electron beam plasma
	Manuel Garcia, Lawrence Livermore National Laboratory, Livermore, CA
	94551-0808, USA
2P23	FDTD Simulation of Electromagnetic Wave Transformation in a
	Dynamic Inhomogeneous, Bounded and Magnetized Plasma
	D.K. Kalluri and J.H. Lee, University of Massachusetts - Lowell, Lowell,
	MA 01854, USA
2P24	Nonlinear Trapping Simulations or Helicon Plasma Sources
	H. Gui and J.E. Scharer, University of Wisconsin, Madison, WI 53706-
	1687, USA
2P25	Initial Design for an Experimental Investigation of Strongly
	Coupled Plasma Behavior in the Atlas Facility
	Carter P. Munson, J.F. Benage Jr. A.J. Taylor, R.J. Trainor, Jr. B.P. Wood and
	F. J. Wysocki, Los Alamos National Laboratory, Los Alamos, NM 87545,
2P26	USA Two Species Presheath Measurements In a Multi-dipole Plasma
2F2U	A.M. Hala and N. Hershkowitz, University of Wisconsin-Madison,
	Madison, WI 53705, USA
2P27	Laser Induced Fluorescence Study of NOx in Streamer Discharges
	A. Kharlov, G. Roth, V. Puchkarev and Martin Gundersen, University of
	Southern California, Los Angeles, CA 90089-0424, USA
2P28	Spectroscopic Studies of Emissions from Microhollow Cathode
	Discharges
	P. Kurunczi, K. Becker, Stevens Institute of Technology
	K.H. Schoenbach, A. El-Habachi Old Dominion Universtiy, Stevens
	Institute of Technology, Hoboken, NJ 07030, USA
2P29	Side-Extraction-Type Secondary-Emission Electron Gun Using wire
	Ion Plasma Source
	Masaki Ishikawa, Naoki Kanbe, Akitoshi Okino, Kwang-cheo! Ko and Eik
	Hotta, Tokyo Institute of Technology, Yokohama 226-8502, JAPAN
2P30	Detection of Trivelpiece-Gould Modes in Helicon Discharges
	D.D. Blackwell, T.G. Madziwa, D. Armush, and F.F. Chen, UCLA, Los

Angeles, CA 90095-1594, USA

De Anza Ballroom 8:30 AM, Tuesday, June 22, 1999

Pienary Talk

Thermal plasma PROCESSES: where are they, where do they go?

Prof. P. FAUCHAIS and A. VARDELLE Universite de Limoges

Plasma technology has grown in the last 20 years for many reasons:

- the need for the industrial world to develop more efficient techniques and processes,
- a very attractive electricity power cost in some countries, for example in France and Canada,
- the potential for developing new materials related technologies,
- the enhanced cooperation between manufacters, researchers, industrial ists and electricity producers.

This growth is partly due to the great strides made by the fundamental research in the field allowing a much better understanding of the phenomena involved in thermal plasmas.

We will first recall what is our present knowledge in the production of thermal plasmas, thermodynamic and transport properties, fundamental processes in plasma torches, modeling, measurement techniques and on-line control. However, the number of successful industrial applications is not as important as plasma community would have expected. This is due to the fact that the key plasma parameters are not the only ones controling a process and its reproducibility. The latter will be discussed for four thermal plasma processes:

- plasma cutting,
- plasma spraying,
- ultrafine particle production,
- waste destruction.

The problems linked to the choice of the parameters allowing an on-line control of the process, and not only of the plasma, in industrial conditions will be particularly emphasized.

Chairperson Dr Don Rej Los Alamos National Laboratory De Anza I 10 AM, Tuesday, June 22, 1999

Oral Session 3A Computational Plasma Physics

Chairperson Richard Hubbard Naval Research Laboratory

3A01 A Description Of The New 3D Electron Gun And Collector Modeling Tool: MICHELLE

John Petillo, Alfred Mondelli, Warren Krueger, Kenneth Eppley, Thomas McClure, Paul Blanchard, Simon Cooke, Barauch Levush, Mark Catteloino, Stan Humphries Jr, Jim Burdette, Eric Nelson, Richard True, Norman Dionne, SAIC, Burlington, MA 01803, USA

- 3A02-03 Invited An Improved Jacobi-Davidson Algorithm Applied to Non-Hermitian Electromagnetic Eigenvalue Problems
 - S.J. Cooke, A. Mondelli, E. Nelson and B. Levush, U.S. Naval Research Laboratory, Washington, DC 20375, USA
- 3A04 Two-dimensional Fluid Model for an Inductively Coupled Chemical Vapor Deposition Reactor
 - K. Bera and B. Farouk, Drexel University, Philadelphia, PA 19104, USA
- 3A05 Ion Distribution Functions in an ECR Chlorine Discharge
 Glenn Joyce, Martine Lampe, W.M. Manheimer, Richard Fernsler and S.P.
 Slinker, U.S. Naval Research Laboratory, Washington, DC 20375, USA
- 3A06-07 Invited Modeling The Alignment of Grains in a Dusty Plasma
 D. Winske, J.E. Hammerberg, B.L. Holian, M.S. Murillo and W.R.
 Shanahan, Los Alamos National Laboratory, Los Alamos, NM 87545, USA
- 3A08 Computational Simulation of Magnetic Field Configurations in Helical Magneto-Cumulative Generators
 Michael H. Frese and Sherry D. Frese, NumerEx, Albuquerque, NM 87106, USA
- 3A09 SAMI II: The NRL Low-Latitude Ionosphere Model
 J.D. Huba and G. Joyce, U.S. Naval Research Laboratory, Washington, DC
 20375, USA

De Anza II 10 AM, Tuesday, June 22, 1999

Oral Session 3B Microwave Systems

Chairperson
Jeff Calame
Naval Research Laboratory

- 3B01 Pulsed Testing of a Quasioptical Gyrotron for Materials Processing R.P. Fischer and A.W. Fliflet, U.S. Naval Research Laboratory, Washington, DC 20375, USA
- 3B02 Gyrotron-Powered Millimeter-Wave Beam Facility for Microwave Processing of Materials

 A.W. Fliflet, R.W. Bruce, R.P. Fishcer, A.K. Kinkead and S.H. Gold and S.

Ganguly, U.S. Naval Research Laboratory, Washington, DC 20375, USA 3B03-04 Invited - Microwave Systems for the Processing of Advanced Ceramics

O.Wilson Jr., Y. Carmel, I. Lloyd, T. Olorunyolemi, J. Calame, D. Gershon, E. Pert, G. Xu, M. Walter, A. Jaworski and A. Birnboim, University of Maryland, College Park, MD 20742, USA

- 3B05 Design of a Wide-range Non-contact Temperature Measurement and Control system for a 2.45 GHz Microwave Furnace
 E.Pert, J. Calame, D. Gershon, Y. Carmel, I. Lloyd, O. Wilson,
 T.Olorunyolemi, University of Maryland, College Park, MD 20740, USA
- 3B06 Simulation of Microwave Sintering of Ceramic Bodies with Complex Geometry

A. Birnboim and Y. Carmel, University of Maryland, College Park, MD 20742-3511, USA

De Anza III 10 AM, Tuesday, June 22, 1999

oral Session 3C Laser Produced Plasmas and Dense Plasma Focus

Chairperson
Ed Ruden
Air Force Research Laboratory

3C01-02 Invited - Ultra-high Gradient Acceleration of Electrons by Laser Wakefield Plasma waves

Antonio C. Ting, U.S. Naval Research LaboratoryWashington, DC 20375, USA

3C03-04 Invited - High Gain Table-top Transient Collisional X-ray Lasers James Dunn, Albert L. Osterheld, Yuelin Li, Joseph Nilsen and Vyacheslav N. Shlyaptsev, Lawrence Livermore National

Laboratory, Livermore, CA 94550, USA **Propagation of Short Intense Laser Pulses in Plasma Channels**P. Sprangle, B. Hafizi and R.F. Hubbard, U.S. Naval Research
Laboratory, Washington, DC 20375-5346, USA

3C06-07 Invited - Research on Fast Ion and Electron-Beams from Plasma-Focus Devices

Marek J. Sadowski, Andrzej Soltan Institute for Nuclear Studies, Warsaw, Poland

3C08 Preliminary Peformance of the Charybdis Plasma Focus at Texas A & M University

B.L. Freeman, D.J. Dorsey, T.J. Faleski, T.L. Guy, I.S. Hamilton, T.A. Parish and J.C. Rock, Texas A & M University, College Stations, TX 77843, USA

3C09 Fusion Research in Zimbabwe

3C05

M. Mathuthu, T.G. Zengeni and A.V. Gholap, University of Zimbabwe, Mt. Pleasant, Harare, Zimbabwe

3C10 Study of Hot spot Phenomenon In Z-Pinches

O.G. Semyonov, Brooklyn, NY 11223, USA

Oral Session 3D Non-equilibrium Plasma Processing

Chairperson
Trudy Van Der Stratten
University of Illinois

3D01 Destruction of Isotopically Labeled Nitric Oxide In Air by Corona Discharge: Kinetics and Products Of Destruction

Larisa G. Krishtopa, Lev N. Krasnoperov, New Jersey Institute of Technology, Newark, NJ 07102, USA

3D02-03 Invited - Use of a Remote Plasma Source for CVD Chamber Clean and Exhaust Gas Abatement Applications

William Holber, Xing Chen, Donald Smith and Matt Besen, Applied Science & Technology Inc., Woburn, MA 01801, USA

3D04-05 Invited - Discharge Physics and Chemistry of a Novel Atmospheric Pressure Plasma Source

J. Park, I. Henins, H.W. Herrmann and G.S. Selwyn, Los Alamos National Laboratory, Los Alamos, NM 87545, USA

3D06 2-D Model Of a Large Area Inductively Coupled, Rectangular Plasma Source for CVD

J.L. Guiliani, J.P. Apruzese, A.E. Robson and M. Mulbrandon, V. Shamamiam, R.E. Thomas, R.Rudder and R. Hendry, U.S. Naval Research Laboratory, Washington, DC 20375-5346, USA

3D07 Particle-in-cell and TAMIX simulation of the hydrogen plasma immersion ion implantation ion-cut process

Dixon Tat-Kun Kwok, Paul K. Chu, Blake P. Wood, and Chung Chan, City University of Hong Kong, Hong Kong SAR, China

3D08 Numerical Simulation Versus Experiment On A Long Hollow Target PVD Reactor

P. Bocquet, L. Leylekian and G. Gousset, ONERA, 92322 Chatillon Cedex, France

Serra I, Conference Centre 10 AM, Tuesday, June 22, 1999

Poster Session 3P

	Note: Posters should be displayed all day
3P01	Comprehensive Secondary Electron Emission Modeling For Simulating E-Beam Collection in MICHELLE
	Norman J. Dionne, Raytheon Systems Company, Sudbury, MA 01776, USA
3P02	Progress on a 3d particle-in-cell model of a W-band klystron
	P.J. Mardahl, J.P. Verboncoeur and C. K. Birdsall, University of California - Berkeley, Berkeley, CA 94720, USA
3P03	Design of a 1 MW, 35 GHz, TE02 2nd Harmonic Output
	Gyroklystron
	W. Lawson, M. Walter, K. Nguyen, M. Garven and V. Granatstein,
	University of Maryland IPR, College Park, MD 20742, USA
3P04	Multimegawatt Gyrotrons for Plasma Heating
	R. Advani, D. Denison, K.E. Kreischer, M.A. Shapiro and R.J. Temkin, MIT
3P05	Plasma Science & Fusion Center , Cambridge, MA 02139-4294, USA Design of a Frequency Tripling, Third Harmonic Gyro-TWT
3703	W. Chen, H. Guo, J. Rodgers, V.L. Granatstein, T.M. Antonsen, University
	of Maryland, College Park, MD 20783, USA
3P06	Results from a Ku-Band Second Harmonic Coaxial Gyroklystron
	M.Castle, W. Lawson, B. Hogan, I. Yovchev.V.L. Grantstein and M. Reiser,
	University of Maryland, Institute for Plasma Research, College Park, MD 20742, USA
3P07	Design of High Power Four-Cavity Gyroklystrons for Linear Collider
	Applications
	I. Yovchev, W. Lawson, M. Castle, B. Hogan, V. Granatstein and G.
	Nusinovich, University of Maryland, College Park, MD 20742-3511, USA
3P08	Design of a 50 MW, 34 GHz Second Harmonic Coaxial Gyroklystron
	for Advanced Accelerators
	M.R. Arjona and W. Lawson, University of Maryland, College Park, MD
2000	20742, USA
3P09	Design and Operation of a 70 GHz Second Harmonic four Cavity Gyroklystron for Radar Applications
	M. Walter, W. Lawson, J.P. Calame, M. Garven and V. L. Granatstein,
	University of Maryland, College Park, MD 20742, USA
3P10	Cavity Testing for W-band Gyroklystron Amplifiers
••	D.E. Pershing, A.H. McCurdy, B.G. Danly, J.M. Cameron and M. Blank,
	Mission Research Corporation, Newington, VA 22122, USA

Serra I, Conference Centre 10 AM, Tuesday, June 22, 1999

3P11	Harmonic Gyrotrons at 94 GHz
	R.C. Stutzman, D.B. McDermott, D.A. Gallagher, C.M. Armstron, T.A.
	Spencer and N.C. Luhmann, Jr., University of California, Davis,
	Department of Applied Science, Davis, CA 95616, USA
3P12	UCD Gyro-TWT Program: 94-GHz TE01 Gyro-TWT and 44-GHz
	Third- Harmonic Slotted Gyro-TWT
	D.B. McDermott, Y. Hirata, S.B. Harriet, A.T. Lin, D.A. Gallagher, C.M.
	Armstrong, Q.S. Wang, C.K. Chong, K.C. Leou, H.E. Huey and N.C.
	Luhmann, Jr., Department of Applied Science, Davis, CA 95616, USA
3P13	W-Band Harmonic Gyro-TWT Amplifier
	Q.S. Wang, H.E. Huer, D.B. McDermott, and N.C. Luhmann, Jr.,
	Micramics, Inc., Santa Clara, CA 95051, USA
3P14	Simulation Study of Fast and Slow Wave Cyclotron Instabilities
	S.H. Chen, Y.C. Lan, J. H. Tsai, National Center for High-Performance
	Computing, Hsinchu, Taiwan, ROC
3P15	Results of a Wideband 2nd Harmonic Gyro-Amplifier (phigtron)
	Experiment
	H.Guo, J. Rodgers, J. Zhao and B.L. Granatstein, University of Maryland,
	Institute for Plasma Research, College Park, MD 20742, USA
3P16	Analyzer for Profile Measurement of a Beam from a Magnicon
	Electron Gun
	S.H. Gold, A.K.Kinkead, A.W. Fliflet, R. True, R.J. Hansen and J.L
	Hirshfield, U.S. Naval Research Laboratory, Code 6793, Washington, DC
	20375, USA
3P17	Nonlinear Electron Interaction with TM Modes in a Low-Voltage
	Waveguide FEL
	X.H. Zhong and M.G. Kong, University of Liverpool, Liverpool L69 3GT, UK
3P18	Experiments on a 28GHz, 200kW Gyroklystron Amplifier for Plasma
	Heating#
	J.J. Choi, S.W. Baik, W.K. Han, D.M. Park, J.H. Oh, S. H. Lee, J.G. Yang
	and S.M. Hwang, Kwangwoon University, Seoul 139-701, KOREA
3P19	A broad band (4-25 GHz) calorimeter for diagnosing high power
	microwave sources
	A. Shkvarunets, S. Kobayashi, Y. Carmel, J. Rodger, T. Antonsen, Jr and V.
	Granatstein, University of Maryland, Institute for Plasma Research,
	College Park, MD 20742-3511, USA
3P20	Spherically curved crystals for x-ray plasma diagnostics
	Y. Aglitskiy and T. Lehecka, S. Obenschain, C. Pawley, C.M. Brown, J.
	Seely, U.S. Naval Research Laboratory, Washington, DC 20375-5352, USA

Serra I, Conference Centre 10 AM, Tuesday, June 22, 1999

3P21	Flash X-ray diagnostics of argon jets: X-ray induced fluorescence imaging and radiography
	L. Hure, E. Robert, C. Cachoncinlle, R. Viladrosa and J.M. Pouvesle, GREMI, 45067 Orleans Cedex 2, France
3P22	Secondary electron energy profiles as a diagnostic tool for RF
	plasma sheaths
	D.M. Shaw, M. Watanabe, H. Uchiyama, and G. J. Collins, Colorado State
	University, Fort Collins, CO 80523, USA
3P23	Langmuir Probe Diagnostics of Electronegative Radio Frequency
	Inductively Coupled Plasma
	T.H. Chung, D.C. Seo, S.W. Chung and H.J. Yoon, Dong-A University,
	Pusan 604-714, Korea
3P24	Laser Induced Fluorscence of Argon Ion in Plasma Presheaths
	M. Atta Khedr, A.M. Hala, L. Oksuz and N. Hershkowitz, University of
2025	Wisconsin-Madison, Madison, WI 53706, USA
3P25	Use of Mach probes and Langmuir probes in a drifting
	un-magnetized non-uniform plasma
	L. Oksuz, N. Hershkowitz, University of Wisconsin-Madison, Madison, WI
2026	52705, USA
3P26	Time Evolution of Ion Energy Distributions and Optical Emissions
	in Pulsed Radio Frequency Plasmas Martin Misakian, Eric Benck, Yicheng Wang, James Olthoff and James
	Roberts, NIST, Gaithersburg, MD 20899-8113, USA
3P27	Installation of the Madison Symmetric Torus Heavy Ion Beam
3727	Probe
	K.A. Connor, T. P. Crowley, D.R. Demers, J. Lei, J.G. Schatz, P.M. Schoch,
	U. Shah, Rensselaer Ploytechnic Institute, Troy, NY 12180-3590, USA
3P28	The Los Alamos Penning Fusion experiment-lons
31 20	Karl R. Umstadter, Martin M. Schauer, Dan C. Barnes, Fred L. Ribe, Lou S.
	Schrank, Los Alamos National Laboratory, Los Alamos, NM 87545, USA
3P29	Neutron emission profiles measurements from the FTU Tokamak
3.23	neutron collimator diagnostic
	L. Bertalot and B. Esposito, P. Batistoni, Associazione EURATOM-ENEA,
	00044 Frascati, Italy
3P30	Measurement of Plasma Flow Parameters and Microparticle
	Velocity in Pulsed Electrothermal Launcher
	E.Ya. Shcolnikov, M. Yu. Guzeyev, S.P. Maslennikov, A.V. Melnik, A.V.
	Chebotarev, M.I. Khaimovitch, Moscow State Engineering Physics
	Institute, Moscow 115409, Russia

De Anza Ballroom 1:30 PM, Tuesday, June 22, 1999

Special Panel Plenary Session

Communicating With Nonscientists and the Media

Chairperson
Gerry Rogoff
The Coalition for Plasma Science

Moderator
Rick Borchelt
Lecturer in Technology Policy and Communication
Vanderbilt University

This session will provide an unusual opportunity to hear from and question representatives of various media who deal regularly with communicating science to nonscientists. This should be a valuable learning opportunity for plasma researchers who must communicate the importance of their ongoing and proposed work to funding agency representatives, government policy-makers, the general public, and younger students who may be potential graduate students. Brief presentations by the panelists will be followed by an audience/panel discussion period. The scheduled panelists include:

Greg Lefevre, San Francisco Bureau Chief, CNN; Gregory Favre, Vice President, News, of the newspaper company The McClatchy Company and former Executive Editor of The Sacramento Bee; and Charles Petit, Science Writer, U.S. News & World Report.

Sponsored by The Coalition for Plasma Science

De Anza I 3 PM, Tuesday, June 22, 1999

Oral Session 4A Intense Electron and Ion Beams

Chairperson

Bryan Oliver

Mission Research Corporation

4A01-02 Invited - Intense Beam-Target Interactions in Linear Induction Accelerator Radiography Systems

G.J. Caporaso, Y.J Chen, T. Houck and S. Sampayan, T. Hughes, B. Oliver and D. Welch, C. Christ, Lawrence Livermore National Laboratory, Livermore, CA 94551, USA

4A03 Plasma Suppression and Spot Size Stabilization in Single and Multiple Pulse Flash X-ray Radiography

Thomas J.T. Kwan and Charles M. Snell, Los Alamos National Laboratory, Los Alamos, NM 87544, USA

4A04 The TriMeV Accelerator for Pulsed Power Driven Radiography Experiments

E.Hunt, G. MacLeod, L.Woo, D. Droemer, S. Cordova, J. Gustwiller, D. Johnson, J. Maenchen, P.Menge, I. Molina, C. Olson, S. Rosenthal and D. Rovang, B.Oliver and D. Welch, C. Eichenberger, P.Spence, I Smith and V. Bailey, Bechtel Nevada, DOE, Las Vegas, NV 89193, USA

- **4A05** Optimization of Radiographic Spot for the TriMeV Accelerator
 D.R. Welch, B.V. Oliver, S.E. Rosenthal and C.L. Olson, Mission Research
 Corporation, Albuquerque, NM 87106, USA
- **4A06** Particle In Cell Simulations of High Power Electron Beam Diodes S.B. Swanekamp, R.J. Commisso, G. Cooperstein, U.S. Naval Research Laboratory, Washington, DC 20375, USA

4A07-08 Invited - Self-Pinched Transport of Intense Ion Beams

P.F. Ottinger, J.M. Neri, S.J. Stephanakis, D.V. Rose, F.C. Young, B.V. Weber, M. Myers, D.D. Hinshelwood and D. Mosher, D.R. Welch and C.L. Olson, U.S. Naval Research Laboratory, Washington, DC 20375, USA

4A09 Simulation and Modeling of the Gamble II Self-Pinched Ion Beam Transport Experiment

D.V. Rose, P.F. Ottinger, D.D. Hinshelwood, D. Mosher, M.C. Myers, J.M. Neri, S.J. Stephanakis, B.V. Weber and F.C. Young, D.R. Welch, U.S. Naval Research Laboratory, Washington, DC 20375, USA

4A10 Direct Measurement of Electrons Co-Moving in Vacuum with a 100-kA, MeV-Proton Beam

B.V. Weber, D. D. Hinshelwood, J. M Neri, P.F. Ottinger, D.V. Rose, S. J. Stephanakis and F.C. Young, U.S. Naval Research Laboratory, Washington, DC 20375, USA

De Anza II 3 PM, Tuesday, June 22, 1999

Oral Session 4B Fast Wave Devices

Chairperson

David McDermott

University of California, Davis

4B01-02 Invited - Demonstration of a High Power W-Band Gyroklystron Amplifier for Radar Applications

M. Blank, B.G. Danly, B. Levush, J.P. Calame, K.T. Nguyen, D.E. Pershing, J. Petillo, T.A. Hargreaves, R.B. True, A.J. Theiss, G.R. Good, K. Felch, B. James P. Borchard, T.S. Chu, H. Jory, W. Lawson and T.M. Antonsen Jr., U.S. Naval Research Laboratory, Code 6843, Washington, DC 20375, USA

- 4B03 Decoherence in a Chirped-Pulsed Free-Electron Maser
 F.V. Hartemann, E.C. Landahl. A.L. Troha, J.P. Heritage, H.A. Baldis and
 N.C. Luhmann Jr., LLNL-Institute for Laser Science & Applications,
 Livermore, CA 94550, USA
- Development of a Mutliple Stage Depressed Collector System for 2 MW
 CW Gyrotrons, Lawrence Ives, Max Mizuhara, Jeff Nielson, Richard Schumacher, Amarjit Singh, Victor Granatstein, Calabazas Creek Research Inst., Saratoga, CA 95070-3753, USA
- **Design of a Single-Stage, Depressed Collector for a 1 MW**CW Gyrotron, G.P. Saraph, K. Felch, S. Cauffman, T.S. Chu and H. Jory,
 Communications Power Industries, Palo Alto, CA 94304, USA
- 4B06 Stimulated Electromagnetic Interactions in Spatio-temporally
 Gyrating Relativistic Electron Beams
 John A. Davies and Chiping Chen, Clark University, Worcester, MA
 01610, USA
- 4B07 Intrinsic Noise Measurements in Gyroklystrons
 J.P. Calame, B.G. Danly and M. Garven, U.S. Naval Research Laboratory,
 Code 6843, Washington, DC 20375, USA
- 4B08 Experimental Study of Intrinsic and Technical Phase Noise in a Second Harmonic Gyrotron Amplifier (Phigtron)
 J. Rodgers, H. Guo, G.S. Nusinovich and V.L. Granatstein, University of Maryland, College Park, MD 20742-3511, USA

Session 4C Spherical Configurations and Ball Lightning

Chairperson
Stanley Singer
Athenex Research Associates

4C01-02 Invited - Ball lightning as a free-force magnetic knot with linked streamers

A.F. Ranada, M. Soler and J.L Trueba, Fisica Universidad Complutense, Madrid 28040, Spain

- **4C03 James L. Tuck Los Alamos Ball Lightning Pioneer**D.A. Baker, Los Alamos National Laboratory, Los Alamos, NM 87544, USA
- 4C04 Production of Spherical Plasmoid or Ball Lightning by Rocket-Triggered Lightning
 Hiroshi Kikuchi, Nihon University, 1-chome, Chiyaoda-ku Tokyo 101,
- **4C05** Electro-Nuclear Reactions in Micro Ball Lighting
 Takaaki Matsumoto, Hokkaido University, Sapporo 060-0813, Japan
- Some Results of Artificially Produced Ball Lightning Formation in Atmospheric Air
 Paul M. Koloc, Neoteric Research Inc., College Park, MD 20741-1037, USA
- 4C07 A Review of the Performance of the Vacuum Spark (VSX) and the Spherical Pinch (SPX) X-Ray/EUV Point Sources
 F.Wu, W. Tang, K.W. Wirpszo and E. Panarella, ALFT, Inc., Hull, PQ
 J8Z157, Canada
- **4C08 Ball Lightning as A Shell of Water Molecules**A.I. Mesenyashin, Box 126, St. Petersburg, 192283, Russia
- 4C09 High Energy Long Living Non-equilibrium Plasmoids in a gas Flow and Atmosphere

A.I. Klimov, Russian Academy of Science, Moscow 127412, Russia

Oral Session 4D

Thermal Plasma Chemisty and Processing And Environmental Issues in Plasma Science

Chairperson

Joachim Heberlein

University of Minnesota

4D01-02 invited - Study of the LTE Departure in a Low Pressure Supersonic Plasma Jet in AR-H2 and in AR-N2-H2 Mixtures

M. Rajabian, S. Vacquie and D.V. Gravelle, Universite Paul Sabatier, Toulouse, France

4D03 Low-Rate Reactive and Non-Reactive Low Pressure Plasma Spraying

W.S. Crawford, H. Hamatani, M.A. Cappelli, F.B. Prinz, Stanford University, Stanford, CA 94305-3032, USA

4D04 Mass Spectrometric Investigations of a Plasma Jet Chemical Vapor Deposition Reactor

Alan E. Kull and Mark A. Cappelli, Stanford University, Stanford, CA 94305-3032, USA

4D05 Arc Voltage Behavior as Indication of Different Operating Modes in a Plasma Torch

Z. Duan, K. Wittmann, J. Heberlein, J.F. Coudert and P. Fauchais, University of Minnesota, Minneapolis, MN 55455, USA

4D06-07 Invited - NOx Removal in Jet-Engine Exhaust: Proposed Non-Thermal Plasma Systems and Economic Considerations

L.A. Rosocha, J.S. Chang, K. Urashima, S.J. Kim, A.W. Miziolek, M.J. Nusca and R.G. Daniel, R.F. Huie and J.T. Herron, Los Alamos National Laboratory, Los Alamos, NM 87545, USA

4D08 A comparative study of remote plasma sources for environmentally-friendly CVD chambers cleaning.

S.Raux, K.C. Lai, H. Nguyen, M. Sarfaty, S.T. Li, J.Davidow and T.F. Huang, Applied Materials, Santa Clara, CA 95054, USA

4D09 Coal Combustion Mercury Control by Means of Corona Discharge Dennis J. Helfritch and Paul L. Feldman, Environmental Elements

Corporation, Baltimore, MD 21227, USA

4D10 Properties of Corona Discharge in a Hot Chamber

Han S. Uhm, Ajou University, Suwon 442-749, Korea

Poster Session 4P

Note: Posters should be di	isplayed all day
----------------------------	------------------

\$P01	Pulsed Operation of Microhollow Cathode Discharges in
	Atmospheric Air
	Uwe Ernst, Robert H. Stark, Karl. H. Schoenbach, Klaus Frand and Werner
	Hartmann, University of Erlangen-Nuremberg, Erlangen, Germany
1P02	Microhollow Cathode Discharges as Plasma Cathodes for
	Atmospheric Pressure Glow Discharges in Air
	Robert H. Stark and Karl H. Schoenbach, Old Dominion University,
	Norfolk, VA 23529, USA

- 4P03 Nitrogen Influences On A Laser Produced TMAE Plasma
 G. Ding, J.E. Scharer and K.L. Kelly, University of Wisconsin, Madison, WI 53706-1687, USA
- **4P04** A Laser-Produced Plasma Sustained by a Radiofrequency Source K.L. Kelly, J.E. Scharer and G. Ding, University of Wisconsin, Madison, WI 53706-1687, USA
- 4P05 High Pressure N2, O2 and Air Mixture Plasmas Produced by a Radiofrequency Helicon Plasma Source
 J.E. Scharer, X.M. Guo, K.L. Kelly and H.Gui, University of Wisconsin, Madison, WI 53706-1687, USA
- Temporal and Spatial Evolution of Gas Discharges Induced by High-Power, Pulsed Microwaves
 M. Onoi, T. Hayashida, K. Azuma, E. Fujiwara and M. Yatsuzuka, Himeji Institute of Technology, Himeji, Hyogo 671-2201, Japan
- 4P07 Experiments of New Plasma Concepts for Enhanced Microwave Vacuum Electronics
 P. Muggli, J.R. Hoffman, J. Yampolsky, J.F. Cordell, M.A. Gundersen, C. Joshi and T. Katsouleas, University of Southern California, Los Angeles, CA 90095, USA
- 4P08 The One Atmosphere Uniform Glow discharge Plasma (OAUGDP)
 As A Classical Normal Glow Discharge
 Rami B. Gadri, Daniel M. Sherman, Zhiyu Chen, Fuat Karakaya and J.
 Reece Roth, University of Tennessee, Knoxville, TN 37996-2100, USA
- 4P09 Mechanism of Killing Microorganizms by a One Atmosphere
 Uniform Glow Discharge Plasma
 Kimberly Kelly-Wintenberg, Tom Monite, Amanda Hodge, John Gaskins,
 J. Reece Roth, and Zhiuy Chen, University of Tennessee, Knoxville, TN
 37996, USA

Serra I, Conference Center 3 PM, Tuesday, June 22, 1999

4P10	Sterilization and Decontamination of Surfaces Using Atmospheric
	Pressure Plasma Discharges
	Eusebio Garate, Olga Gornostaeva, Igor Alexeff, Applied Pulsed Power
	Technologies, Corona Del Mar, CA 92625, USA
4P11	Investigation Of Unmagnetized Plasma Heating In a Low Pressure
	Microwave Discharge
	M. Perrin, T. Grotjohn and J. Asmussen, Michigan State University, East
	Lansing, MI 48824, USA
4P12	The Electrodeless Discharge at Atmospheric Pressure
	Mounir Laroussi, Old Dominion University, Newport News, VA 23606,
	USA
4P13	Modes of Operation of the Glow Discharge at Atmospheric
	Pressure (GDAP)
	Mounir Laroussi and Igor Alexeff, Old Dominion University, Newport
	News, VA 23606, USA
4P14	Plasma diagnostics in ECRIN- a prototype microwave plasma reac
	tor for thin film deposition
	Carmen Ciubotariu, University of Lethbridge, Lethbridge (AB) T4K3MY,
	Canada
4P15	High Voltage Ionization during Plasma Immersion Ion Implantation
	X.B. Tian, Z. M. Zeng, T. K. Kwok, B.Y. Tang and P.K. Chu, City University
	of Hong Kong, Hong Kong, SAR, China
4P16	Influence of Sample Placement on Dose Uniformity in Plasma
	Immersion Ion Implantation of Industrial Bearings
	Z.M Zeng, X.B. Tian, T.K. Kwok, B.Y. Tank and P.K. Chu, City University o
	Hong Kong, Hong Kong, SAR, China
4P17	Comparison of Hot Cathode and Inductively Coupled Discharges
	for Application in Plasma Immersed Ion Implantation and
	Deposition
	G.H. Kim, S.A. Nikiforov, Y. Kan, C.H. Cho, Y.W. Choi, H.S. Lee, G.H. Lim
	Korean Electrotechnology Research Institute Changwon 641-600, Korea
4P18	Plasma Drift and Non-Uniformity Effects in Plasma Immersion Ion
	Implantation
	M. Keidar, O.R. Monteiro and I.G. Brown, Lawrence Berkeley National
	Laboratory, Berkeley, CA 94720, USA
4P19	Ion Sheath Dynamics in a Plasma for Plasma-based Ion
	Implantation
	M. Yatsuzuka, S. Miki, K. Azuma, E. Fujiwara and O. Ishihara, Himeji
	Institute of Technology, Himeji, Hyogo 6712201, Japan

Serra I, Conference Center 3 PM, Tuesday, June 22, 1999

IP20	Electron Beam Ablated Plasma Plumes and Deposited Thin Films of
	fused Silica
	S.D. Kovaleski, R.M. Gilgenbach, L.K. Ang, Y. Y. Lau, University of
	Michigan, Ann Arbor, MI 48109-2104, USA
IP21	A Steady-State One Atmosphere Uniform DC Glow Discharge
	Plasma
	Igor Alexeff, Mounir Laroussi, Weng Lock Kang and Ali Alikafesh,
	University of Tennessee, Knoxville, TN 37996-2100, USA
1P22	Effects of Non-Equilibrium Plasmas on Microorganisms
	Mounir Laroussi, Igor Alexeff, Old Dominion UniversityNewport News, V.
	23606, USA
1P23	Characteristics of a barrier discharge in monatomic gases
	R. Sankaranarayanan, B. Pashaie and S. K. Dhali, Southern Illinois
	University, Carbondale, IL 62901, USA
1P24	Diagnostic of hydroxyl radical concentration in high pulse voltage
	triggered dielectric barrier discharges
	C. Hibert, I. Gaurand, O. Motret, M. Nikravech, R. Viladrosa and J. M.
	Pouvesle, University of Orleans, BP 6759 45007 Orleans Cedex 2, France
1P25	A Low Frequency Impedance Matching Circuit for a one
	Atmosphere Uniform Glow Discharge Plasma (OAUGDP) Reactor
	Zhiyu Chen, Dnaiel M. Sherman, Rami B. Gadri, Fuat Karakaya and J.
	Reece Roth, University of Tennessee, Knoxville, TN 37996-2100, USA
4P26	Atmospheric Pressure Plasma for Decontamination of Chem/Bio
	Warfare Agents
	H.W. Herrmann, G.S. Selwyn, I. Henins, J. Park, Los Alamos National
1007	Laboratory, Los Alamos, NM 87545, USA A New Electrothermal-Chemical Method for Metals Carbides and
4P27	Ceramics Hard Coating: Experiment and Theory
	D. Zoler, C. Bruma, S. Cuperman, Tel-Aviv University, Tel-Aviv, 69978, Israel
4P28	Constrained Evolutionary Optimization of the Signal Growth rate
+ Γ20	in an RKO with an Axially Varying Waveguide Diameter
	Laurence D. Merkle and John W. Luginsland, U.S. Air Force Research
	Laboratory, Kirtland AFB, NM 87117, USA
4P29	Comparisons of Particle Tracking and Charge Deposition
TI 2.5	Schemes for a Finite Element Gun Code
	E.M. Nelson, K.R. Eppley, J.J. Petillo and S. Humphries Jr., SAIC,
	Burlington, MA 01803, USA
4P30	Comparison of Electrostatic Wave Energy Levels in Models of
	Electron Beam-Plasma Interactions
	D.V. Rose, J.U. Guillory, J.H. Beall, Jaycor, Alexandria, VA 22303, USA
	, y, ,y , , , , , , , , , , , , , ,

Serra I, Conference Center 3 PM, Tuesday, June 22, 1999

4P31	Implementation of the FRED 2-D Electromagnetic PIC Code on a
	Distributed Memory Parallel Computer with Application to the
	Modeling of the Long Conduction time POS
	Paul Steen and Eduardo Waisman, Maxwell Technologies, San Diego, CA
	92123, USA
4P32	Preliminary Implementation of Piecewise Linear Conformal
	Boundaries in ICEPIC

Boundaries in ICEPICJoseph D. Blahovec, Jr., Gerald E. Sasser, John W. Luginsland, U.S. Air

Force Research Laboratory, KAFB, NM 87118-5776, USA

Progress Toward a Parallel MAGIC

4P33 Progress Toward a Parallel MAGIC
 M.H. Bettenhausen, L. Ludeking, D. Smithe, S. Hayes, Mission Research
 Corporation, Newington, VA 22122-8560, USA

4P34 Analysis of Self-Force Error In Relativistic PIC Simulations
K.L. Cartwright, J.P. Verboncoeur and C.K. Birdsall, University of
California, Berkeley, Cory Hall, Berkeley, CA 94720, USA

 4P35 Accurate, Finite-Volume Methods for Three Dimensional Magneto-Hydrodynamics on Lagrangian Meshes
 C.L. Rousculp and D. C. Barnes, Los Alamos National Laboratories, Los Alamos, NM 87545, USA

4P36 A Numerical Method for the Solution Of The Magnetic Convection-Diffusion Equation For High Magnetic Reynolds Numbers C.A. Borghi and A. Cristofolini, University of Bologna, I-40136 Bologna, Italy

4P37 A Fully Implicit Method for the Numerical Solution of the MGD
Problem in an SF6 Discharge
C.A. Borqhi and A. Cristofolini, University of Bologna, I-40146 Bologna, Italy

4P38 Trace Hazardous Metals Detection with an Atmospheric Microwave- Generated Plasma Kamal Hadidi, Paul Woskov, Karyn Green, Guadalupe Flores III and Paul Thomas, Massachusetts Institute of Technology, Cambridge, MA 02139, USA

4P39 Radiation Power of Ar Torch Short Plasma as Function of Length near 100A

Toru Iwao, Takayuki Ishida, Tatsuya Hayashi, Takahiro Hirano, Masao Endo and Tsuginori Inaba, Chuo University, Tokyo 112-8551, Japan

4P40 The Effect of Carbonaceous Deposit for NOx Dissociation by Barrier Discharge

Kazue Fujiwara, Kagehiro Itoyama, Takeshi Yanobe, Nagasaki University, Nagasaki 852-8521, Japan

4P41 Study of pulsed HF discharge in N2/O2/NO for gas cleaning M. Baeva, H. Gier, A. Pott, J. Uhlenbusch, University of Dusseldorf, Dusseldorf, Germany De Anza Ballroom 8:30 AM, Wednesday, June 23, 1999

Plenary Talk Plasma Science and Applications Committee Award Address

Simple models on some nasty problems in beams and plasmas

Prof. Y.Y. Lau University of Michigan

Chairperson Prof. Igor Alexeff University of Tennessee De Anza I 10 AM, Wednesday, June 23, 1999

Oral Session 5A Plasma, Ion and Electron Sources

Chairperson

Paul Chu

City University of Hong Kong

5A01-02 Invited - Large-Area Plasma Processing System

R.F. Fernsler, W.M. Manheimer, R.A. Meger, D.P. Murphy, D. Leonhardt, R.E. Pechacek, S.G. Walton and M. Lampe, U.S. Naval Research Laboratory, Washington, DC 20375-5346, USA

- 5A03 Development of Hollow-Cathode Plasma Electron Gun for Operation at Forepump Gas Pressure Viktor Burdovitsin, Alexey Mytnikov and Efim Oks, State University of Control Systems and Radioelectronics, TUSUR, Tomsk 634055, Russia
- 5A04 Carbon Shunting Arc and Its Induced Plasma and DLC Film Deposition Ken Yukimura, Ryoto Isono and Kenji Yoshioka, Doshisha University, Kyotanabe Kyoto, Japan
- Recent Advances in Plasma-based Ion Sources for Commercial Ion Implantation of Semiconductors
 T.N. Horsky and B.H. Vanderberg, Eaton Corporation SEO, Beverly, MA 01915, USA
- TiN coating to Three Dimensional Materials by PBII Using Vacuum
 Titanium Arc Plasma
 Masanori Sano and Ken Yukimura, Toshiro Maruyama, Akiyoshi
 Chayahara and Yuji Horino, Doshisha University, Kyotamake, Kyoto, Japan
- 5A07 High Current Vacuum Arc Ion Source for Heavy Ion Fusion
 N.Qi, J. Schein, S. Gensler, R. R. Prasad, M. Krishnan, I. Brown, Alameda
 Applied Sciences Corporation, San Leandro, CA 94577, USA
- 5A08 Hydrogen and Hydrogegn-Argon Discharge Measurements and Models of a Compact Microwave ECR Plasma Source
 M.H. Tsai and T. A. Grotjohn, Michigan State University, East Lansing, MI 48824, USA

De Anza II 10 AM, Wednesday, June 23, 1999

Oral Session 5B Fast Wave Devices and Intense Beams

Chairperson
Steve Gold
Naval Research Laboratory

5B01-02 Invited - Analytical Theory of Multi-State Gyro-Amplifiers G.S. Nusinovich and B. Levush, University of Maryland, College Park, MD 20742-3511, USAA

- 5B03 Dynamic Simulation of Mode Selective Extended Interaction Cavity for Wideband, High Power Gyrotron Applications A.T. Lin, H. Guo and V. Granatstein, University of California, Department of Physics, Los Angeles, CA 90095-1547, USA
- **A Smith-Purcell Free Electron Laser Based on an X-Band Photoinjector**E. Schamiloglu, S.R.J. Brueck and F. Hegeler, R.V. Hartemann, E.C.
 Landahl, A.L. Troha, C.H. Ho, J.P. Heritage, H.A. Baldis and N.C. Luhmann
 Jr., University of New Mexico, Albuquerque, NM 87131, USA.
- 5B05 Initial Operation of a High Power Cusp Gun
 D. Gallagher, M. Barsanti, J. Richards, F. Scafuri, C. Armstrong, Northrop
 Grumman ESSS-DSD, Rolling Meadows, IL 60008, USA
- 5B06 Linear Theory of the Multi-Stage Gyro-TWT
 G. Nusinovich, M. Walter, University of Maryland IPR, College Park, MD 20742, USA
- 5B07 Experimental Studies of a Four-Cavity, 35 GHz Gyroklystron Amplifier M. Garven, J.P. Calame, B.G. Danly, B. Levush and F. Wood, U.S. Naval Research Laboratory, Code 6843, Washington, DC 20375, USA
- Spontaneous Emission of an Electron Beam in a Quasiperiodic
 Wiggler Magnet Configuration
 M.G. Kong and A. Vourdas, University of Liverpool, Liverpool L69 3GT, UK
- Influence of the Microwave Magnetic Field on High Power
 Microwave Window Breakdown
 D. Hemmert, A. Neuber, J. Dickens, H. Krompholz, L.L. Hatfield and M. Kristiansen, Texas Tech University, Lubbock, TX 79409-3102, USA
- 5B12 A Long Pulse (>1 µsec) Field Emission Electron Gun With Stable Cross Secrion for HPM Sources

O. Loza, P. Strelkov, I. Ivanov, Y. Carmel, J. Rodgers, T. Antonsen, Jr, V.L. Granatstein, University of Maryland, Institute for Plasma Research, College Park, MD 20742-3511, USA

Session 5C

Fast Z-pinches and X-ray Lasers

Chairperson

Bruno Bauer

University of Nevada, Reno

5C01-02 Invited – Long Implosion experiments and simulations on the Saturn and Z machines

M.R. Douglas, C. Deeney, R.B. Spielman, N. Roderick, & M.G. Haines, Sandia National Laboratories, Albuquerque, NM 87185-1194, USA

- 5C03-04 Invited New X-ray Backlighting Results on Small-Scale Structure Formation, Including Liquid-vapor Foam-like Appearance, in Exploding wire Z-pinches and X-pinches
 S.A. Pikuz. T.A. Shelkovenko, D.A. Hammer, D.B. Sinars, Y.S. Dimant and
 - S.A. Pikuz, T.A. Shelkovenko, D.A. Hammer, D.B. Sinars, Y.S. Dimant and J.B. Greenly, Cornell University, Ithaca, NY 14853, USA
- 5C05 Dynamic Hohlraum and ICF Pellet Implosion Experiments on Z T.J. Nash, M.S. Derzon, G.A. Chandler, R. Leeper, D. Fehl, J. Lash, C. Ruiz, S. Slutz, G. Cooper J.F. Seaman, J. McGurn, S. Lazier, J. Torres, D. Jobe, T. Gilliland, R. Mock, P. Ryan, D. Nielsen, J. Armijo, J. McKenney, R. Hawn and D. Hebron, D. Petersen, R. Bowers and W. Matuska, Sandia National Laboratories, Albuquerque, NM 87185-1196, USA
- 5C06 Issues in the 2-D Simulation Physics of High-Performance Z-Pinch
 Experiments

 D. L. Peterson, J. Aubrey, R. L. Bowers, W. Matuska, K.D. McLenithan, G.

D.L. Peterson, J. Aubrey, R.L. Bowers, W. Matuska, K.D. McLenithan, G. Chandler, C. Deeney, M. Derzon, M. Douglas, T. Nash, M.K. Matzen, R.B. Spielman, Los Alamos National Laboratory, Los Alamos, NM 87545, USA

- 5C07 Long Implosion Wire Array Implosions on the Saturn and Z Accelerators C. Deeney, M.R. Douglas, C.A. Coverdale, R.B. Spielman, K. Struve, D.L. Peterson and M.G. Haines, Sandia National Laboratories, Albuquerque, NM 87185, USA
- 5C08 Two Dimensional and Three Dimensional MHD Simulations of Wire Array Z-pinch Experiments
 J.P. Chittenden, S.V. Lebedev, R. Aliaga-Rossel, A.R. Bell, S.N. Bland, S.G. Lucek and M.G. Haines, Imperial College, London SW72BZ, UK
- 5C09 A study of Rayleigh-Taylor instability growth in wire array z-pinch experiments
 S.V. Lebedev.R. Aliaga-Rossel, S.N. Bland, J.P. Chittenden, A.E. Dangor, M.G. Haines and O. Willi, Imperial College, Imperial College, London SW72BZ, UK
- 5C10 Time-resolved optical spectroscopy measurements of pre-pulse plasma formation on Z

J.E. Bailey, A.L. Carlson, M.E. Cuneo, C. Deeney, P. Lake, R.B. Spielman, K.W. Struve and W.A. Stygar, Sandia National Laboratories, Albuquerque, NM 87185-1196, USA

Oral Session 5D Plasma Opening Switches

Chairperson
Ralph Schneider
Defense Threat Reduction Agency

- 5D01 Spectroscopic Characterization of Impurity Ions on the Hawk POS J.J. Moschella, C.C. Klepper, C. Viodoli, R.C. Commisso, D.C. Black, B. Moosmann, Y. Maron, HY-Tech Research Corporation, Radford, VA 24141, USA
- 5D02-03 Invited --Magnetic Field and Electron Density evolutions in a POS

 R. Arad, K. Tsigutkin and Y. Maron, A. Fruchtman, Weizmann Institute of Science, 78100 Rehovot, Israel
- 5D04 Effect of Plasma Flow Direction on the Performance of
 Microsecond Plasma Opening Switch
 I.V. Lisitsyn, S. Kohno, Y. Teramoto, S. Katsuki, H. Akiyama, Kumamoto
 University, Kumamoto 860-8555, Japan
- Electron Angular Distribution in an Opening Switch Driven Coaxial Diode
 V.J. Harper-Slaboszewicz and C. Martinez, Sandia National Laboratories, Albuquerque, NM 87185-1159, USA
- 5D06 High Energy Electron Production in Plasma Opening Switches
 John R. Goyer, David Kortbawi, John E. Rauch, William Rix and John R.
 Thompson, Mark A. Babineau, Maxwell Technologies, San Diego, CA
 92123, USA
- **5D07** MACH2 Simulations of the DECADE Plasma Opening Switch
 Dennis Keefer and Robert Rhodes, University of Tennessee Space Institute,
 Tullahoma, TN 37388, USA
- 5D08-09 Invited POS-Load Coupling Performance On Ace 4

 J.R. Thompson, P.L. Coleman, R.J. Crumley, P.J. Goodrich, J.R. Goyer and
 J.E. Rauch, Maxwell Technologies Inc., San Diego, CA 92123, USA
- 5D10 Electron Energy Balance and MHD Modeling of the Conduction
 Phase in a Plasma Opening Switch

 LW Schumer D. Mosher S.R. Swanekamp P.F. Ottinger R. L. Commiss
 - J.W. Schumer, D. Mosher, S.B. Swanekamp, P.F. Ottinger, R.J. Commisso, U.S. Naval Research Laboratory, Washington, DC 20375, USA

Poster Session 5P

	Note: Posters should be displayed all day
5P01	Cathode Fall Measurements in a High Pressure Low Current Argon Arc Using Langmuir Probes
	Jens Luhmann, Daniel Nandelstadt, Jurgen Mentel, Ruhr University
	Bochum, 44780 Bochum, Germany
5P02	Determination of the Cathode Fall in a High Pressure Argon Model
	Using Pyrometric and Temperature Measurements
	Daniel Nandelstadt, Jens Luhmann, Jurgen Mentel, Ruhr University
	Bochum, 44780 Bochum, Germany
5P03	Two-temperature, two-dimensional modeling of cathode hot spot
	formation including sheath effects application to high pressure
	xenon arc lamps
	J. Wendelstorf, H. Wohlfahrt and G. Simon, Technische Universitat
	Braunschweig, D-38023 Braunschweig, Germany
5P04	Modeling and Measurements of Tungsten Sputtering in High
	Intensity Discharge Lamps During Starting
	Alan Lenef, Osram Sylvania, Beverly, MA 01915, USA
5P05	Measurement of barium emitted from thermionic electrodes in
	steady-state Hg-rare gas discharges
- D0 <i>C</i>	R.C. Garner, Osram Sylvania, Beverly, MA, 01915, USA Ionization Wave Propagation In Long Tube Discharges
5P06	R. Kenneth Hutcherson, Osram Sylvania, Beverly, MA 01915, USA
5P07	Atomic transition probabilities for Dy I and Dy II
JPU/	G. Nave, M.E. Wichliffe and J.E. Lawler, NIST, Gaithersburg, MD 20899-
	8421, USA
5P08	The geometry effects of the ditched dielectric in AC-PDP cell
JI 00	Y.K. Shin, C.H. Shon, W. Kim and J.K. Lee, Pohang University of Science
	and Technology, Pohang, Kyoungbuk 790-784, S. Korea
5P09	Simulation of Magnetron Sputter with Three-Dimensional
	Magnetic Field
	C.H. Shon, J.S. Park and J.K. Lee, Pohang University of Science and
	Technology, Pohang, Kyoungbuk 790-784, S Korea

Serra I, Conference Centre 10 AM, Wednesday, June 23, 1999

5P10 Structure Y.C. Lan, S.H. Chen, J.H. Tsai, T.L. Lin, Y.Hu, J.T. Lai, C.M. Lin, C.H. Wan, W.C. Wang, National Center for High-Performance Computing, Hsinchu, Taiwan 300, ROC 5P11 Measurement of plasma parameters by electric probes in a simulated PDP K.S. Chung, Y.S. Choi, D.H. Chang, Y.H. Jung, K.C. Ko, G.H. Kim, Hanyang University, Seoul, Korea 5P12 Study of High Power, Two-Stage, TWT X-Band Amplifier P.Wang, Cz. Golkowski, Y. Hayashi, J.D. Ivers, J.A. Nation, Cornell University, Ithaca, NY 14853, USA 5P13 High Power Microwave Generation using a Repetitive Electron gun with a Ferroelectric Cathode Y. Hayashi, J.D. Ivers, J.A. Nation, P. Wang, Cz. Golkowski, D. Flechtner, Cornell University, Ithaca, NY 14850, USA 5P14 High Power Ka band TWT Amplifier Cz. Golkowski, J. D. Ivers, J.A. Nation, P. Wang, Cornell University, Ithaca, NY 14850, USA

Computer Simulation of Field Emission Devices with Focusing

De Anza Ballroom 1:30 PM, Wednesday, June 23, 1999

Plenary Talk The Future of High-Power Microwaves

James N. Benford Microwave Sciences, Inc., Lafayette, CA USA and John A. Swegle Lawrence Livermore National Laboratory, Livermore CA USA

The field of High-Power Microwaves [>100 MW] has matured considerably in the quarter century since the initial development of relativistic backward wave oscillators and other source types by researchers in Russia and in the US. In this talk, we discuss the future in relation to the general development of electromagnetic technology, review some of the signs of the maturity of the field, including changes such as an observed narrowing in the number of source types under development, an increase in commercial suppliers, and a growing internationalization of the research field. In addition, within the context of historical trends in the field, we discuss the development of high peak power systems and the abandonment of the pursuit of ever-higher power in favor of the development of gigawatt-level systems with manageable weight and volume, repetitive operation, and tunability. Such systems offer scientific and engineering users flexibility for a range of applications.

Chairperson

Dr Jack Agee

Air Force Office of Science and Research

De Anza I 3 PM, Wednesday, June 23 1999

Oral Session 6A Plasmas for Lighting

Chairperson
Ken Hutcherson
Osram Sylvania

- 6A01 Microhollow Cathode Discharge Excimer Light Sources

 A.El-Habachi, M. Moselhy, A. El-Dakroury and K.H. Schoenbach, Old
 Dominion University, Norfolk, VA 23529, USA
- 6A02 Investigation of a Moly-Oxide Electrodeless Discharge For Lighting Applications

 J.L. Giuliani, R.A. Meger, R.E. Pechacek and D.D. Hinshelwood,

V. Shamamian and J.E. Butler, U.S. Naval Research Laboratory, Washington, DC 20375-5346, USA

- 6A03-04 Invited Atomic physics in plasma modeling for lighting
 R.E.H. Clark, G. Csanak and J. Abdallah, Los Alamos National Laboratory,
 Los Alamos, NM 87545, USA
- 6A05 Modeling of Ba low pressure discharges
 G.G. Lister, Osram Sylvania Inc., Beverly, MA 01915, USA
- **6A06 Modelling the Spectrum of a S2 High Pressure Discharge**Achim Korber, Philips Research Laboratories, D52085 Aachen, Germany
- 6A07 Application of Vane-type Resonator to Microwave Powered Electrodeless HID Lamp Akira Hochi, and Mamoru Takeda, Matsushita Electric Industrial Co. Ltd, Soraku, Kyoto 619-0237, Japan
- 6A08 High Luminance Metal Halide Lamp Containing ScBr3 for LCD
 Projectors

 Kiyoski Takahashi, Makoto Horiuchi, Mamoru Takeda, Matsushita Electric
 Industrial Co., Soraku, Kyoto 619-0237, Japan
- **6A09** Non-equilibrium plasma formation as a lighting source
 Dr. Pankova M., State Research Institute for Aviation Systems, 121248
 Moscow, Russia

De Anza II 3 PM, Wednesday, June 23, 1999

Oral Session 6B Intense Beams

Chairperson
Tom spencer
AFRL/DEHE

6B01 Characterization of the Power Handling Capability of an S-Band and Double Disc Gas Cooled Microwave Window

A. Neuber, P. Ferguson, K. Hendricks, D. Hemmert, H. Krompholz, L.L. Hatfield, M. Kristiansen, Texas Tech University, Lubbock, TX 79409-3102,

6B02-03 Invited - 3D PIC Simulation Study of a Relativistic, Rising Sun Magnetron

R.W. Lemke, T.C. Genoini and T.A. Spencer, Sandia National Laboratories, Albuquerque, NM 87185-1186, USA

6B04 Development of a High Power Klystron For the Spallation Neutron Source

T.A. Hargreaves, M.F. Kirshner, R. J. Hansen, Y. Misaki, R.B. True, G.R. Good, Litton Electron Devices, San Carlos, CA 94070, USA

6B05 Electrodynamic Pulse Shortening Mechanism Due to a Novel Beam/Cavity Interaction

J.W. Luginsland, K. J. Hendricks, D.A. Shiffler and Y.Y. Lau, U.S. Air Force Research Laboratory, Kirtland AFB, NM 87117, USA

6B06 Halo Formation In High-Power Klystrons

Renato Pakter & Chiping Chen, MIT Plasma Science & Fusion Center PSFC/NW16-164, Cambridge, MA 02139, USA

6B07 High Efficiency Milo

M. Joseph Arman, Air Force Research Lab, Kirland AFB, NM 87117-5776, USA

6B08 Initial Studies of an Annular Cesium Iodide Cathode

R. Umstadtt, M. Lacour, K. Hendricks, D. Shiffler, T. Spencer and D. Voss, U.S. Air Force Research Laboratory, AFRL/DEHE, Kirtland, NM 87117, USA

Session 6C

Fast Z-pinches and X-ray Lasers

Chairperson
Bruno Bauer
University of Nevada, Reno

6C01-02 Invited - Review of Electrical Resistivity Measurements of Dense Aluminum

John F. Benage Jr., William R. Shanahan, Michael S. Murillo, Los Alamos National Laboratory, Los Alamos, NM 87545, USA

- **Examination of Resistivity Issues In Solid Liner Z-Pinches**W.L. Atchison, R.J. Faehl and R.E. Reinovsky, Los Alamos National Laboratory, Los Alamos, NM 87545, USA
- 6C04 Radius Scaling of Titanium Wire Arrays on the Z Accelerator
 C.A. Coverdale, C. Deeney, R.B. Spielman, M.R. Douglas, T.J. Nash, K.G.
 Whitney, J.W. Thornhill, J. P. Apruzeses, R.C. Clark, J. Davis, D.L. Peterson,
 F.N. Beg, J. Ruiz-Comacho, R.Schneider, Sandia National Laboratories,
 Albuquerque, NM 87185-1159, USA
- 6CO5 Long Implosion PRS Experiments On Double Eagle J.S. Levine, P.L. Coleman, B.H. Failor, J.C. Riordan, Y. Song, H.M. Sze, E.M. Waisman, C.Deeney, J.S. McGurn, J.P. Apruzese, J.Davis, A. Fisher, B. Moosman, S. Stephanakis, J.W. Thornhill, B.V.Weber, K.G. Whitney, S. Gensler, N.Qi and R.F. Schneider, Maxwell Physics International, San Leandro, CA 94577, USA
- X-Ray Spectroscopy on Double Eagle and DM-2
 E.J. Yadlowsky, E.P. Carlson, J.Niemel, F. Barakat, R.C.Hazelton, C.C.
 Klepper, J.Riordan, B. Failor, P.Coleman, J. Levine, Y.Song, B. Whitton, J. Apruzese, J. Davis, F. Cochran, K. Whitney, HY-Tech Research Corporation, Radford, VA 24141, USA
- **72-pixel, diamond soft x-ray camera**R.R. Prasad, A.C. Crisman, N.Qi, S.W. Gensler and M. Krishnan, Alameda Applied Sciences Corp., San Leandro, CA 94577, USA
- 6C08 Model of enhanced energy deposition in a RT unstable strongly radiating Z-pinch plasma due to fast penetration of magnetic bubbles to the axis

L. I. Rudakov, J. Davis and A. L. Velikovich, Advanced Power Techologies, Springfield, VA 22150, USA

- Time Resolved Detection of the XUV-Laser Activity in a Fast Z-Pinch Plasma
 B. Bayerlein, A. Tauschwitz and R. Presura, Universitat Erlangen-
 - Nurnberg, GSI, 64294 Darmstadt, Germany

 Payloich Toylor Stability Criteria for Magnetically Imploded Soli
- 6C10 Rayleigh-Taylor Stability Criteria for Magnetically Imploded Solid Liners Edward L. Ruden, Air Force Research Laboratory, KAFB, NM 87117, USA

Oral Session 6 Vacuum Microwaves (Microelectronics)

Chairperson
Capp Spindt
SRI

6D01-02 Invited - PPM Focused TWT Using a Field Emitter Array Cold Cathode

D.R. Whaley, C.M. Armstrong, B. Gammon, Northrop Grumman Corporation, Rolling Meadows, IL 60008, USA

6D03-04 Invited - Performance of Field Emission Cathodes in Xenon Environments

C.M. Marrese, J.E. Polk, K.L. Jensen, A.D. Gallimore, C. Spindt, R.L. Fink and Z.L. Tolt W.D. Palmer, U.S. Naval Research Laboratory, Washington, DC 20375-5347, USA

6D05 High Current dc and Pulsed Field Emission From Single Cyrstal ZrC(100) emitters mounted in apertures

W.A. Mackie, Tianbao Xie, Kristin Lee, and P.R. Davis, Linfield Research Institute, McMinnville, OR 97128, USA

6D06 Migration and Escape of Barium Atoms in a Thermionic Cathode and Their Contribution to Noise

K.L. Jensen, Y.Y. Lau, B. Levush, Naval Research Laboratory, Washington, DC 20375-5347, USA

6D07 Electron Migration Across Transverse Kicker Magnet In Beam Collector/RF Waveguide System

K.T. Nguyen, N.J. Dionne, M. Blank, B.D. Danly and B. Levush, Naval Research Laboratory, Washington, DC 20375, USA

Poster Session 6P

	Note: Posters should be displayed all day
6P01	Diagnostics and Experiments on LAPPS
	D. Leonhardt, D.P. Murphy, S.G. Walton, R.A. Meger, R.F. Fernsler and
	R.E. Pechacek, U.S. Naval Research Laboratory, Washington, DC 20375, USA
6P02	Generation of High Density Plasma with Large Volume Using
	Pulsed Glow Discharge
	K. Takaki, D. Kitamura and T. Fujiwara, Iwate University, Morioka/Iwate 020-8551, Japan
6P03	On the Theory of a Low Pressure Magnetron Glow Discharge
	L. Pekker, S.I. Krasheninnikov, DSI, Santa Rosa, CA, 95401, USA
6P04	Discharge Regimes and Density Jumps in a Helicon Plasma Source
	S. Shinohara and K. Yonekura, Kyushu University, Kasuga, Fukuoka 816-
	8580, Japan
6P05	RF Wave Propagation in Large Diameter Plasma under the Various
	Magnetic Field Configurations
	S. Shinohara, S. Takechi and A. Fukuyama, Kysushu University, Kasuga,
	Fukuoka 816-8580, Japan
6P06	Evanescent Electromagnetic Field Structures in Inductively Coupled
	Plasma S. Shinohara and S. Takechi, Kyushu University, Kasuga, Fukuoka 816-
	8580, Japan
6P07	Electrostatic probe measurements of electron temperature and
	number density in helium ICP-MS interface region
	Hironobu Yabuta, Akitoshi Okino and Eiki Hotta, Tokyo University of
	Technology, Yokohama 226-8502, Japan
6P08	Experimental and Simulation Study of Spherically Convergent
	Beam Fusion
	Yasushi Takeuchi, Kunihito Yamauchi, Yutaka Ogina, Masato Watanabe, Akitoshi Okino, Kwang-cheol Ko and Eiki Hotta, Tokyo Institute of
	Technology, Yokohama 226-8502, Japan
6P09	Particle-in-cell modeling of electron oscillation inside a vacuum arc
51 05	plasma source duct
	T.K. Kwok, T.Zhang, P.K. Chu, M.M.M. Bilek and I.G. Brown, City
	University of Hong Kong, Hong Kong SAR, China
6P10	Generation of High Charge State Ions in Vacuum Arc Ion Sources
	by a "Current Jump" Method
	A.S. Bugaev, E.M. Oks, G. Yu. Yushkov and I.G. Brown, High Current
	Electronics Institute, Tomsk 634055, Russia

Serra I, Conference Center 3 PM, Wednesday, June 23, 1999

6P11 Importance of repeller voltage on ion current generation in an arc ion source B.H. Vanderberg and T.N. Horsky, Eaton Corporation SEO, Beverly, MA 01915, USA 6P12 Laser Heated LaB6 Thermionic Cathode on a MV Electron Beam Accelerator R.M. Gilgenbach, D. Vollers, R. Jaynes, J. Rintamaki, M. Johnston, W. Cohen, W.D. Getty, Y.Y. Lau and T.A. Spencer, University of Michigan,

- Ann Arbor, MI 48109-2104, USA

 6P13 Electron Emission from Photo-cathodes for FEL

 T.Inoue, S. Miyamoto, M. Yatsuzuka and T. Mochizuki, Himeji Institute of Technology, Himeji Hyogo 6712201, Japan
- 6P14 The Effect of the surface microstructures on the Emission
 Characteristics of Ferroelectric Cathode
 Koichi Yasuoka, Kenji Suzuki, Masatoshi Miyake and Shozo Ishii, Tokyo
 Institute of Technology, Tokyo 152-8552, Japan
- **6P15 Electron Emission from Ferroelectric Thin Film Cathodes**F.Liu and C.B. Fleddermann, University of New Mexico, Albuquerque, NM 87131, USA
- **6P16** Penetration of a Plasma by a Beam in Multipulse Radiography
 A.G. Sgro and T.J.T. Dwan, Los Alamos National Laboratory, Los Alamos,
 NM 87545, USA
- Focusing Methods for Drifting Relativistic Electron Beams for Radiography at AWE
 C.L. Olson, S.E. Rosenthal, B.V. Oliver and D.R. Welch, A. Birrell, R. Edwards, D. Forster, T.J. Goldsack and M. Sinclair, Sandia National Laboratories, Albuquerque, NM 87185, USA
- Theory and Simulation of Electron Beam Dynamics in the AWE Superswarf Magnetically Immersed Diode
 B.V. Oliver, D.R. Welch, C.L. Olson, S.E. Rosenthal and D.C. Rovang, Mission Research Corporation, Albuquerque, NM 87106, USA
- 6P19 Experimental Study of Ion-Beam Self Pinched Transport for MeV
 Protons

 J.M Neri, F.C. Young, S.J. Stephanakis, P.F. Ottinger, D.V. Rose, D.D.
- Hinshelwood and B.V. Weber, U.S. Naval Research Laboratory,
 Washington, DC 20375, USA

 6P20 Electron Density Measurements During Ion Beam Transport on

Gamble II

B.V. Weber, D. D. Hinshelwood, J.M. Neri, P.F. Ottinger, D.V. Rose, S.J. Stephanankis and F.C. Young, U.S. Naval Research Laboratory, Washington, DC 20375, USA

Serra I, Conference Center 3 PM, Wednesday, June 23, 1999

48109-2104, USA

6P21 Advanced Diagnostics and Applications of Pulsed Ion Beams and Lasers

K.Kasuya, T. Yamashita, Y. Kishi, S. Tamamura, C.Wu, T. Kamiya, M. Funatsu, S. Saitoh, H. Koinuma T. Renk, D. Hanson, K. Lamppa, J. Torres, B.Turman, T. Mehrhorn, R. Leeper, J.Quintenz and M. Thompson, Tokyo Institute of Technology, Midori-ku Yokohama 226-8502, Japan

6P22 SABRE Extraction Ion Diode Results and the Prospects for Light Ion Inertial Fusion Energy Drivers

M.E. Cuneo, R.G. Adams, J.E. Bailey, M.P. Desjarlais, A.B. Filuk, W.E. Fowler, D.L. Hanson, D.J. Johnson, T.A. Mehlhorn, P.R. Menge, C.L. Olson, T.D. Pointon, S.A. Slutz, R.A. Vesey, D.F. Wenger and D.R. Welch, Sandia National Laboratories, Albuquerque, NM 87185-1193, USA

Effects of RF Plasma Processing on the Impedance and Electron Emission Characteristics of a MV Beam Diode J.I. Rintamaki, R.M. Gilgenbach, W.E. Cohen, R.L. Jaynes, L.K. Ang, Y.Y. Lau, M.E. Cuneo and P.R. Menge, University of Michigan, Ann Arbor, MI

- 6P24 Ultra-Violet Triggered Vacuum Flashover of a Water-Vacuum Interface as a Low-Inductance Closing Switch
 L. Courtois, B. Cassany, G. Avrillaud, L. Frescaline, SCA ITHPP, Thegra 46500, France
- Evaluating the Residual Inductance of a Ranchero Coaxial Flux-Compression Generator as Storage Inductance for Powering Imploding Hydrodynamic Liner Loads
 J.H. Goforth, W.L. Atchison, C.M. Fowler, E.A. Lopex, H. Oona, R.E. Reinovsky, J.L. Stokes, D.G. Tasker, I.R. Lindemuth, J.V. Parker, Los Alamos National Laboratory, Los Alamos, NM 87545, USA
- **6P26** Operation of a Heated POS IN DM1

 N.R. Pereira, J.R. Goyer, D. Kortbawi, J.R. Thompson and S.E. Davis, Ecopulse, Springfield, VA 22150, USA
- A POS with a Two-Ion-Species Plasma
 N. Chakrabarti, A. Fruchtman, Weizmann Institute of Science, 76100
 Rehovot, Israel
- **6P28** Mass Separation in a 100-ns Plasma Opening Switch
 A. Weingarten, C. Grabowski, N. Chakrabarti, and Y. Maron, A.
 Fruchtman, Weizmann Institute of Science, Rehovot 76100, Israel
- 6P29 Compact Pulsed Power Generator Using a Marx Circuit and a Exploding Wire

 Naoyuki Shimomura, Masayoshi Nagata, Hidenori Akiyama,

Naoyuki Shimomura, Masayoshi Nagata, Hidehori Akiyama, University of Tokushima, Tokushima 770-8506, Japan De Anza Baliroom 8: 30 AM, Thursday, June 24, 1999

Plenary Talk

Z-Pinches: Past, Present and Future

Prof. Malcom Haines Imperial College

Chairperson

Dr Keith Matzen Sandia National Laboratories De Anza I 10 AM, Thursday, June 24, 1999

Oral Session 7A Plasmas for Lighting Lighting Consortium (EPRI/ALITE) Overview

Chairperson Voitek Byszewski Osram Sylvania

- **7A01-02 Invited Radiation Trapping of the Hg 185 nm Resonance Line**J.E. Lawler, J.J. Curry, K.L.Mennigen, Madison, University of Wisconsin Madison, Madison, WI 53706, USA
- 7A03 On The Radiation Trapping Calculation on Discharge Lamps Hasnaa Sarroukh, Michel Aubes, Georges Zissis and Jean Jacques Damelincourt, CAPAT Univ. P. Sabatier, Toulouse 31062, France
- 7A04 Chemi-ionization of Excited Mercury
 R.L. Martin, J.S. Cohen and L.A. Collins, Los Alamos National Laboratory,
 Los Alamos, NM 87545, USA
- **7A05** Chemi-ionization in mercury and neon discharges
 Valery Sheverev, Lorcan Folan, Vadim Stephaniuk, Polytechnic University,
 Brooklyn, NY 11201, USA
- 7A06 Chemo-lonization in Decaying Neon Plasma
 D. Loffhagen, S. Pfau and R. Winkler, INP Greifswald, 17489 Greifswald, Germany
- 7A07 Modeling of Highly Loaded Fluorescent Lamps
 G.G. Lister, J.E. Lawler and J.J. Curry, Osram Sylvania, Inc., Beverly, MA
 01915, USA

Oral Session 7B Magnetic Fusion Energy

Chairperson
Irv Lindermuth
Los Alamos National Laboratory

7B01-02 Invited - Magnetic pressure driven implosion of solid liner suitable for compression of Field Reversed Configurations

J.H. Degnan, R. Bartlett, T. Cavazos, D. Clark, S.K. Coffey, R.J. Faehl, M. Frese, D. Fulton, D.Gale, T.W. Hussey, T. P. Intrator, R. Kirkpatrick, G.F. Kiuttu, F.M. Lehr, I. Lindemuth, W. McCullough, R. Moses, R.E. Perterkin, R.E. Reinovsky, N.F. Roderick, E.L. Ruden, J. Schlacter, K. Schoenbert, D. Scudder, R.E. Siemon, W. Sommars, P.J. Turchi, G. Wurden, F. Wysocki, U.S. Air Force Research Laboratory, Albuquerque, NM 87117-5776, USA

- 7B03 Proton Ring Formation Studies on the Cornell Field-reversed Ion Ring Experiment FIREX
 - W.J. Podulka, J.B. Greenly, A.Gretchikha and Y. Tang, Cornell University, Ithaca, NY 14853, USA
- 7B04 Numerical Simulations of Plasma Working Fluid Compression of a Cylindrical Copper Target Liner

 Norman F. Roderick and Robert E. Peterkin Jr., U.S. Air Force Research
- Laboratory, Kirtland AFB, NM 87117, USA

 7B05 Solid Liner Inner Surface Phenomena During Compression Of A
 Field Reversed Configuration Plasma For A Magetized Target
 Fusion Proof Of Principle Demonstration
 G.F. Kiuttu, P.J. Turchi, R.J. Faehl, U.S. Air Force Research Laboratory,
- **7B06** Numerical Studies of Liners for Magnetized Target Fusion (MTF)
 R.J. Faehl, W.L. Atchison, P.T. Sheehey and I.R. Lindemuth, Los Alamos
 National Laboratory, Los Alamos, NM 87545, USA

Kirtland AFB, NM 87117-5776, USA

7B07 Measurement of MTF Target Plasma Temperature Using Filtered Photodiodes

J.M. Taccetti, F.J. Wysocki, G. Idzorek, H. Oona, R.C. Kirkpatrick, I.R. Lindemuth, P.T. Sheehey, F.Y. Thio, Los Alamos National Laboratory, Los Alamos, NM 87545, USA

7B08 Analysis of Data From X-Pinch MTF Target Plasma Experiments F.J. Wysocki, J.M Taccetti, J.F. Benage, G. Idzorek, H. Oona, R.C. Kirkpatrick, I.R. Lindemuth and P.T. Sheehey, Los Alamos National Laboratory, Los Alamos, NM 87544, USA De Anza III 10 AM, Thursday, June 24, 1999

Session 7C Closing Switches and Plasma Opening Switches

Chairperson

Mark Savage

Sandia National Laboratories

7C01-02 Invited - Hobetron Current Regulating Switch TubeR.B. True, R.J. Hansen, D.N. Deb, G.R. Good and W.A. Reass, Litton Systems Inc., San Carlos, CA 94070, USA

- 7C03 Geometric Considerations for UltraFast Spark Gap Switching Jane M. Lehr and Carl E. Baum, U.S. Air Force Research Laboratory, KAFB, NM 87117-5776, USA
- Rise Time Considerations For Photoconductive Switch Materials
 Used in High Power UWB Microwave Applications
 N.E. Islan, E. Schamiloglu, C.B. Fleddermann, J.S. H Schoenberg, R. P. Joshi, University of New Mexico, Albuquerque, NM 87131, USA
- 7C05 Explosively Formed Fuses for High Voltage Systems
 D.G. Tasker, J.H. Goforth, C.M. Fowler, D.H. Herrera, J.C. King, E.A.
 Lopez, E.C. Martinez, H. Oona, S.P. Marsh, R.E. Reinovsky, J.L. Stokes, L.J.
 Tabaka, D.T. Torres, F.C Sena G. Kiuttu and J. Degnan, Los Alamos
 National Laboratory, Los Alamos, NM 87545, USA
- 7C06 Experimental Study of the Decade Cableguns
 Dennis Keefer, L. Montgomery Smith and Newton Wright, University of
 Tennessee Space Institute, Tullahoma, TN 37388, USA
- 7C07 Testing of the MITL and POS for the Decade Quad D. Kortbawi, F.K. Childers, H.D. Price, Maxwell Physics International, San Leandro, CA 94577, USA
- 7C08 Analysis of Power Flow in a Plasma Opening Swith Coupled to an Electron-Beam Diode
 D.C. Black, R.J. Commisso, B.V. Weber, U.S. Naval Research Laboratory, Washington, DC 20375, USA

Bonsai I/II 10 AM, Thursday, June 24, 1999

Oral Session 7D Plasma Thrusters and Arcs

Chairperson
Mark Capelli
Stanford University

7D01-02 Invited - Electron Transport and Electron Energy Dissipation in Hall Thruster Discharges

M.A. Cappelli, N.B. Meezan and D. Schmidt, Stanford University, Stanford, CA 94305-3032, USA

7D03 Abrupt sonic transition in the Hall thruster

A. Fruchtman, N.J. Fisch, Center for Technological Education, Holan, Holan 58102, Israel

7D04 LIF Measurements of a low-power Helium Arcjet

Q.E. Walker and M.A. Cappelli, Stanford University, Stanford, CA 94305, USA

7D05 Ablation and Erosion Measurements in an Electrothermal Plasma

G.E. Dale and M.A. Bourham, North Carolina State University, Raleigh, NC 27695-7909, USA

Poster Session 7P

- 7P01 Time correlation of plasma focus X-ray emission in various energy ranges
 - I. Paraschiv, V. Zoita, R. Presura, University of Nevada Reno, Reno, NV 89557, USA
- 7P02 Transition in x-ray yield, mass scaling observed in the high-wirenumber, plasma-shell regime

K.G. Whitney, P.E. Pulsifer, J.P. Apruzese, J.W. Thornhill and J. Davis, T.W.L. Sanford, R.C. Mock and T.J. Nash, U.S. Naval Research Laboratory, Washington, DC 20375, USA

7P03 Zero Dimensional Scaling of Ar K-shell Radiation in Long Implosion Z-Pinch Experiments

Eduardo Waisman, Philip Coleman and Charlie Gilbert, Maxwell Technologies, San Diego, CA 92123, USA

7P04 Robust Gas Preionization System For Double Eagle PRS Experiments

Y.Song, P.L. Coleman, B.H. Failor, D. Kortbawi, J.S. Levine, J.C. Riordan, H.M. Sze, J.R. Thompson, R.J. Commisso, B. Moosman, S.J. Stephanakis, B.V. Weber, A. Fisher and R.F. Schneider, Maxwell Physics International, San Leandro, CA 94577-0599, USA

7P05 Correlation of the Time History of Argon Z-Pinch K-Shell Emission and Initial Gas Distribution

Philip Coleman and J. Levine, Maxwell Technologies, San Diego, CA 92123, USA

7P06 Results of structured load implosion experiments and its comparison with simulation

A.V. Shishlov, R.B. Baksht, A.V. Fedunin, B.M. Kovalchuk, V.A. Kokshenev, A. Yu. Labetsky, V.I. Oreshkin, A.G. Russkikh, High Current Electronics Institute, Tomsk 634055, Russia

7P07 Simulation of imploding Z-pinch loads with quasi two-dimensional models

V.I. Oreshkin, A.V. Shishlov, High Current Electronics Institute, Tomsk 634055, Russia

7P08 Gas Puff Z-Pinch Plasmas driven by Inductive Voltage Adder ASO-X modified by POS

Sunao Katsuki, Koichi Murayama, Susumu Kohno, Igor V. Lisitsyn and Hidenori Akiyama, Kumamoto University, Kumamoto 860-8555, Japan

7P09 X-ray spectrometers with cylindrical, spherical and toroidal dispersive elements

E.O. Baronova, V.V. Lider, M.M. Stepanenko, V.V. Vikhrev and N.R. Pereira, Eco Pulse Inc., Springfield, VA, USA

7P10 Calculations of Capillary Z-Pinch At 100 MA Scale Currents Yu V. Afanas'ev, V.N. Shlyaptsev, A.L. Osterheld, Lebedev Physical Institute, Moscow, Russia

7P11 Study of capillary discharges for soft x-ray lasers D. Hong, R. Dussart, W. Rosenfeld, S. Gotze, C. Cachoncinlle, R. Viladrosa, C. Fleurier and J.M. Pouvesle, Universite d'Orleans, 45067 Orleans Cedex 2, France

7P12 Characterisation of a 10 A/s Micro Capillary Discharge as an Ion and Soft X-rays Source

A. Engel, P. Choi, C. Dumitrescu, I. Krisch, J. Larour, J. Rous, T.N. Hansen, J.G. Lunney, LPMI, Palaiseau 91128, France

7P13 Dynamic Properties of Ultra-fast Pulsed Capillary Discharge Devices

I. Krisch, P. Choi, C. Dumitrescu, A. Engel, J. Larour, J. Rous, L. Juschkin, H-J. Kunze, LPMI, Palaiseau 91128, France

7P14 Scaling Calculations of Optimal Liner Performance to Determine the Voltage Design Configuration in Atlas

Huan Lee, Los Alamos National Laboratory, Los Alamos, NM, 87545, USA

7P15 Simulations of the Formation of Strongly Coupled Plasmas Using Pulsed Power

R.K. Keinigs, Blake Wood, Carter Munson and R.J. Trainor, Los Alamos National Laboratory, Los Alamos, NM 87545, USA

7P16 Computational Modeling of Z-Pinch-Driven Hohlraum Experiments

R.A. Vesey, J.L Porter Jr., M.E. Cuneo, C.A. Hall, T.A.Mehlhorn, L.E. Ruggles, W.W. Simpson, M.F. Vargas, J.H. Hammer, O. Landen, J. Koch, Sandia National Laboratories, Albuquerque, NM 87185, USA

7P17 Time and space resolved measurements of soft x-ray emission viewed from the z axis at Z

S. Lazier, J. McKenney, D. Jobe, M. Derzon, T. Nash and G. Chandler, Sandia National Laboratories, Albuquerque, NM 87185-1196, USA

7P18 Investigating Differences between Calculated and Observed X-ray Images, of Z-Pinches

W. Matuska, R. Bowers, D. Peterson, C. Deeney, M. Derzon, Los Alamos National Laboratory, Los Alamos, NM 87545, USA

7P19 Optimization of the inner array in a nested array Z-Pinch

Kyle Cochrane, Melissa Douglas, Norman F. Roderick, Sandia National Laboratories, Albuquerque, NM 87185-1106, USA

7P20-21 Multi-Dimensional Z-Pinch Calculations With Alegra

Allen C. Robinson, Chris J. Garasi, Thomas A. Haill, Richard L. Morse, Peter H. Stolz, Sandia National Laboratories, Albuquerque, NM 87185-0819, USA

7P22 Dense Z-Pinch Research at the Nevada Terawatt Facility

B.S. Bauer, V.L. Kantsyrev, N. LeGalloudec, R.C. Mancini, G.S. Sarkisov, A.S. Shlyaptseva, F. Winterberg, S. Batie, W. Brinsmead, H. Faretto, B. LeGalloudec, A. Oxner, M.Al-Shorman, D.A. Fedin, I. Golovkin, I. Paraschiv, M. Sherrill, N. Ammons, S. Hansen, D. McCrorey, J.W. Farley and J.S. DeGroot, University of Nevada - Reno, Reno, NV 89557-0058, USA

7P23 X-ray and EUV Diagnostics for the Nevada Terawatt Facility: Plasma Imaging, Spectroscopy and Polarimetry

V.L. Kantsyre, B.S. Bauer, R.C. Mancini, A.S. Shlyaptseva, D.A. Fedin, A. Golovkin, P. Hakel, I. Paraschiv, N. Ammons, S. Hansen, University of Nevada - Reno, Reno, NV 89557-0058, USA

Serra I, Conference Centre 10 AM, Thursday, June 24, 1999

7P24	Studies of the Initial Phases of Exploding W and Al Wire and Wire array Plasma Formation Using X-ray Backlighting
	D.B. Sinars, J.B. Greenly, S.A. Pikuz, T.A. Shelkovenko, D.A. Hammer and
	B.R. Kusse, Cornell University, Ithaca, NY 14853, USA
7P25	Studies of Late Time Behavior of Exploding Wires Using X-ray
	Backlighting
	J.B. Greenly, T.A. Shelkovenko, S.A. Pikuz, D.B. Sinars and D.A. Hammer,
	Cornell University, Ithaca, NY 14853, USA
7P26	Formation of Highly Structured Dense Cores from Exploding Wires
	with 1-5 kAper Wire
	Y.S. Dimant, S.A. Pikuz, T.A. Shelkovenko, D. B. Sinars, J.B. Greenly and D. A. Hammer, Cornell University, Ithaca, NY 14853, USA
7P27	X-ray Backlighting Density Measurements of Tungsten and
	Aluminum Wire and Wire Array Z-pinches,
	D.A. Hammer, S.A. Pikuz, T.A. Shelkovenko, J.B. Greenly, D.B. Sinars and
	A.R. Mingaleev, Cornell University, Ithaca, NY 14853, USA
7P28	X-pinch Dynamics Close to the Time of X-ray Burst Emission and X
	pinch Bright Spot Location Using X-ray Backlighting
	T.A.Shelkovenko, S.A. Pikuz, D.B. Sinars, D.A. Hammer, V. Serlin, Cornell
	University, Ithaca, NY 14853, USA
7P29	The effect of wire material on plasma formation in wire array
	z-pinches
	S.V. Lebedev, R. Aliaga-Rossel, S.N. Bland, J.P. Chittenden, A.E. Dangor
7000	and M.G. Haines, Imperial College, London, SW72BZ, UK
7P30	Investigation of magnetic field effects on the mitigation of the
	magneto hydrodynamic Raleigh-Taylor instability in fast z-pinch
	implosions Melissa Douglas, Christopher Deeney, Norm Roderick,
	Sandia National Laboratories, Albuquerque, NM 87185-1194, USA
7P31	Material Field Strength Studies at Microsecond Pulsed Voltages
	D. Shiffler, M. Lacour, K. Hendricks, R. Umstattd, T. Spencer, M. Haworth
	D. Vozz and A. Lovesee, U.S. Air Force Research Laboratory, AFRL/DEHE,
	Kirtland AFB, NM 87117, USA
7P32	Progress In The Control of a Smart Tube High Power Backward
,	Wave Oscillator
	G.T. Park, V.S. Soualian, C.T. Abdallah, E. Schamiloglu and F. Hegeler,
	University of New Mexico, Albuquerque, NM 87131, USA
7P33	Progress on Pulse Lengthening of a Realativistic Backward Wave
	Oscillator
	F. Hebeler & E. Schamiloglu, S.D. Korovin and V.V. Rostov, University of
	New Mexico, Albuquerque, NM 87131, USA
7P34	Comparison of Theory and Simulation for a Radially Symmetric
	Transit-Time Oscillator,
	Robert L. Wright, Edl Schamiloglu, John W. Luginsland, M. Joseph Armar
	University of New Mexico, Albuquerque, NM 87131, USA
7P35	Comparison of Simulation and Experimental Results for a Radially
	Symmetric Transit-Time Oscillator
	Robert L. Wright, Edl Schamiloglu, M. Joseph Arman, Walter R. Fayne,
	Kyle J. Hendricks, Diana L. Loree, John W. Luginsland, Thomas A.
	Spencer Thomas C. Cavazos, Kenneth E. Golby, University of New

Mexico, Albuquerque, NM 87131, USA

Serra I, Conference Centre 10 AM, Thursday, June 24, 1999

7P36 Development and Application of a Parallel Two-Dimensional Particle-in-Cell code Based on an Existing Three-Dimensional Parallel PIC Code

John J. Watrous, Gerald E. Sasser, John W. Luginsland, Shari C. Collela, Numer Ex, Albuquerque, NM 87106, USA

7P37 3-D PIC Investigation of an Output Circuit for the Relativistic Klystron Oscillator

L.A. Bowers, J.W. Luginsland, G.E. Sasser, J.J. Watrous, K.J. Hendricks and M.J. Arman, U.S. Air Force Research Laboratory, Albuquerque, NM 87117, USA

7P38 Magnetron Structure Design Using 2-and 3-D EM Codes Thomas A. Spencer, John W. Luginsland, and Ray W. Lemke, U.S. Air

Force Research Laboratory, Kirtland AFB, NM 87117, USA

7P39 Optical Spectroscopy of Plasma and Plasma Processing in High Power Microwave Pulse Shortening Experiments

W.E. Cohen, R.M. Gilgenbach, R.L. Jaynes, J.I. Rintamaki, C.W. Peters, Y.Y. Lau, T.A. Spencer, G.P. Scheitrum and L.L. Laurent, University of Michigan, Ann Arbor, MI 48109-2104, USA

7P40 Microwave Production and Beam Transport in a Multi-MW Large-Orbit, Axis Encircling, Coaxial Gyrotron Oscillator

R.L. Jaynes, R.M. Gilgenbach, C.W. Peters, W.E. Cohen, J.I. Rintamaki, J.M. Hochman, Y.Y. Lau and T.A. Spencer, University of Michigan, Ann Arbor, MI 48109-2104, USA

7P41 Modeling of Space Charge Effects in Intense Electron Beams Using Two and Three Dimensional Green's Functions

M. Hess, R. Pakter, C. Chen, MIT-Plasma Science & Fusion Center PSFC/NW16-168, Cambridge, MA 02139-4294, USA

7P42 3-D PIC Simulations of the Convolute and inner MITL on the Z Accelerator,

T.D. Pointon, Sandia National Laboratories, Albuquerque, NM 87185-1186, USA

7P43 Proton and Neutron Irradiation Effects of Ti: Sapphires

Guangean Wang, Jin Zhang and Jingjing Yang, Yunnan University, Kumming Yunnan 655091, China

7P44 Fluorescence Increasing Effects In Electron and Proton Irradiated BaF2:Sr Crystals

Jin Zhang, Guangcan Wang and Jingjing Yang, Yunan University, Kumming, Yunnan 650091, China

7P47 Steam Plasma ARC Cutting

H. Pauser, J. Laimer, H. Stori, Fronius Schweissmaschinen, Wels A-4600, Austria

7P48 Density and Velocity Measurements of a Sheath Plasma from MPD Thruster

J.J. Ko, T.S. Cho, M.C. Choi, E. H. Choi, G.S. Cho, Kwangwoon University, Ajou University, Paidal-Gu Suwon 448-749, Korea

7P49 X-Ray Spot Measurement and Modulation Transfer Function for the 12MeV LIA

Shi Jinshui, Li Jing, Li Qing, Luo Dashi, CAEP, Institite of Fluid Physics, Chengdu 610003, ROC

Serra I, Conference Centre 10 AM, Thursday, June 24, 1999

7P50	High Power Microwave Generation from the Axially-Extracted
	Virtual Cathode Oscillator
	E.H. Choi, G.S. Cho, J.J. Ko, Y. Jung, M.C. Choi, Kwangwoon University,
	Dept. of Physics, Ajou University, Suwon 442-749, Korea
7P51	Plasma Surface Modification of Aluminum Alloy Samples Treated
	with Argon Discharge Conditioning
	S.J. Karandikar, Chetan C. Samant, S.V. Gogawale, University of Mumbai, Vidyanagari Mumbai 400098, India
7P52	Dynamics of Plasma Bunch in Weakly Inhomogeneous Magnetic
	Field
	D.S. Dorozhkina, V.E. Semenov, Institute of Applied Physics RA S, Nizhny
	Novgorod 603600, Russia
7P53	Initial Experimental Results of a 35 GHz Efficient Harmonic
7P54	Amplifier
	Jose E. Velazco, Peter H. Ceperley & Doug M. Menz, Microwave
	Technologies Inc., Fairfax, VA 22030, USA
	Improved Transition Probabilities for Mnll
	Rainer Kling and Ulf Greismann, National Institute of Standards and
	Technology, Gaithersburg, MD 20899, USA
7P55	Self-oscillations of positive corona current in nitrogen
7733	Y.S. Akishev, M.E. Grushin, A. A. Deryugin, A.P. Napartovich, M.V.
	Pan'kin, N.I. Trushkin, Troitsk Institute for Innovation & Fusion Research,
	Triniti, Russia
7P56	Nonlinear Interaction of Microwave and Magnetoactive Plasma:
	Hysteresis Phenomena and Application
	Dr. Andrei B. Petrin, Russian Academy of Sciences, Moscow 127412,
	Russia
7P57	Modelling the Spectrum of a S2 High Pressure Discharge
, 731	Achim Korber, Philips Research Laboratory, D-52085 Aachen, Germany
7P58	Experimental and Theoretical Researches of Energy Exhcange
/ i JU	Between the Electrical Circuits, Containing Plasma Active Elements
	and Environment
	R.F. Avramenko, V.A. Grishin, V. I. Nikolaeva, A.S. Paschina, L.P.
	Poskacheeva, International Institute of Experimental Physics, Moscow,
	Russia
7P59	Cathode Development for the Hard-Tube MILO
7735	M. Haworth, K.Hendricks, D. Vozz, R. Guarnieri, M. Sena, M. LaCour, D.
	Ralph and T. Cavazos, Air Force Research Laboratory, Kirtland AFB, NM
	87117, USA
7060	Plasma Coaxial Discharge Efficiency
7P60	E. A. Mehanna, Military Technical College, Nasr City, Cairo, Egypt
	The Generation and Application of Micro Discharge Plasmas
7P61	Masatoshi Miyake, Hikaru Takahaski, Koichi Yasuoka and Shozo Ishii,
	Tokyo Institute of Technology, O-okayama, Meguro-k 152-8552, Tokyo
	Japan
	Japan

Serra i, Conference Centre 10 AM, Thursday, June 24, 1999

A Capsule Review of Three Years of Progress in the Sandia Z-Pinch **7P62** Program, M.A. Sweeney, Sandia National Laboratories, Albuquerque, NM 87185-1186, USA Lagrangian Approach in the Analysis of Plasma-filled Diodes **7P63** X. Chen, P.A. Lindsay, J. Watkins and J. Zhang, King's College London, Strand, London, WC2R 2LS, UK Laser-Cooled Non-Neutral Plasma Experiments at NIST **7P64** L.B. King, J.J. Bollinger, B.M. Jelenkovic, T.B. Mitchell, W. M. Itano, D.J. Wineland, NIST, Boulder, CO 80303, USA Optimization of Microwave Generation by Coaxial Vircator **7P65** W. Jiang, K. Woolverton, J. Dickens and M. Kristiansen, Texas Tech University, Lubbock, TX 79409-3102, USA 3D PIC simulations of the Relativistic Klystron Oscillator **7P66** G.E. Sasser, L. Bowers, J.W. Luginsland, J.J. Watrous, Air Force Research Laboratory, AFRL, Kirtland AFB, NM 87117, USA Control of Mechanisms for Pulse Shortening in the Reltron **7P67** J. Golden, Berkeley Research Associates, Springfield, VA 22150, USA **Photocell Enhanced Technique For Measuring Electrode Starting** 7P68 **Temperature In Fluorescent Lamps** E.E. Hammer, FIEEE, FIES.LC, FIEEE, FIES, LC

Conference Record - Abstracts

De Anza Ballroom 8:30 am, Monday, June 21, 1999

Welcome

Dr. Christopher Deeney 1999 ICOPS Chairperson Sandia National Laboratories

Plenary Talk

Laboratory Astrophysics
Experiments High Power Laser
and Pulsed Power Facilities

Dr Paul Springer Lawrence Livermore National Laboratory

Chairperson

Dr Christopher Deeney Sandia National Laboratories

1ADe Anza I 10 AM, Monday, June 21, 1999

Oral Session 1A

Basic Processes in Fully and Partially Ionized Plasmas

Chairperson
Wallace M. Manheimer
Naval Research Laboratory

1A01

Neutral Depletion and Transport Mechanisms in Large-Area High Density Plasma Sources

G.R. Tynan, University of California, San Diego, La Jolla, CA 92093-0417, USA

Neutral Depletion and Transport Mechanisms in Large-Area High Density Plasma Sources G.R. Tynan, Department of Mechanical and Aerospace Engineering, University of California, San Diego Plasma uniformity has been recognized as a significant parameter in large sized high density plasma processing tools. In this paper we show experimental and modeling results which indicate that significant neutral uniformity variations can also occur in high density plasma processing tools. The experiments are carried out in both inductively coupled plasma (ICP) and helicon plasma sources. A movable static pressure gauge is used to obtain the static radial and axial neutral pressure distribution both with and without a discharge present. Without a wafer present in the reactor, significant (~20-40%) reductions in neutral pressure are observed in these sources during steady-state plasma operations. This spatially averaged neutral depletion is accompanied by hollow neutral pressure profile. The degree of on-axis neutral depletion is found to be determined by both plasma density and neutral fill pressure. We attribute these variations to the "plasma pumping" effect, wherein electron impact ionization of neutral particles is followed by their rapid removal from the plasma by the presheath electric field. A one-dimensional neutral diffusion model that incorporates this mechanism provides reasonable agreement with our results. This net loss of neutral particles can result in a large (~50%) neutral density variation across 300mm wafers. Neutral recycling from the wafer can create a new particle source in the center region and partially mitigate these effects. Results which demonstrate this effect, along with associated modeling results will also be shown.

1A02

Soft X-ray production in spark discharges in hydrogen, nitrogen, air, argon and xenon gases

J. Va'vra, P.M. Va'vra and J. Maly, Stanford University, Stanford, CA 94309, USA

Soft X-ray production in spark discharges in hydrogen, nitrogen, air, argon and xenon gases

J.Va'vra¹, P.M. Va'vra² and J. Maly³

1 - S.L.A.C., Stanford University, Stanford, CA94309, USA

2-67 Pine Lane, Los Altos, CA 94022, USA

3 - Applied Science Consultants, 5819 Ettersburg Dr., San Jose, CA95123, USA

We describe a production of soft X-rays of energy 2-10keV by sparking in gases at low pressure with sparking voltages as low as 0.8kV. The sparking device operates with the peak spark currents 0.2-0.5kA, the total spark charge $4x10^{14}$ electrons/spark, and the spark stored energy 0.024-0.17J/pulse. In addition, we measured a profile of V(t), I(t) and dI/dt during the spark and their relationship to the X-ray production.

The X-rays were detected using several gaseous detectors, a Geiger counter, and YAP and CsI crystals. We also monitored the associated production of positive ions using a small ion drift chamber, which extracted the ions directly from the sparking gap. The experimental aim was to measure the following parameters of the X-ray production: (a) multiplicity distribution per single spark, (b) angular distribution relative to spark axis, (c) production rate as a function of sparking voltage and Z of the gas, (d) production relative to the dI/dt curve, (e) energy distribution using the range method, wire chamber charge, and the YAP and CsI crystals.

So far, we have determined the X-rays are produced with a distribution resembling a power law distribution between 2 and 10keV, with average energy of 4keV based on the range measurement, and with no large energy total deposit in a 4-pi CsI crystal detector surrounding the spark gap. Furthermore, the X-rays are produced in clusters, their production threshold increases with Z of the gas, and their production threshold coincides with the production of the positive ions. We calculate a probability to produce an X-ray event per one electron in a given spark to be less than 5×10^{-16} . Several other experiments are in progress.

The sparks in our tests are relatively large by a typical standard, however, compared to the spark energies used in typical plasma pinch experiments, they are considerably smaller, by at least a factor of $-4x10^4$. If our results are due to the pinch effect, we are then observing the pinch effect phenomenon at the smallest spark energy reported so far in the literature, i.e., we are investigating its threshold behavior. However, at present, we do not have yet a sufficient experimental information to allow a firm explanation of the X-ray production in our tests based on the pinch effect.

Some results of this work were reported recently in Nuclear Instruments and Methods, A418 (1998) 405-419. Additional results will be presented at this conference.

1A03

High Voltage Subnanosecond Corona Inception

J. Mankowski, J. Dickens, M. Kristiansen, J. Lehr, W. Prather and J. Gaudet, Texas Tech University, Lubbock, TX 79409-3102, USA

HIGH VOLTAGE SUBNANOSECOND CORONA INCEPTION

J. Mankowski, J. Dickens, and M. Kristiansen
Texas Tech University
Pulsed Power Laboratory
Departments of Electrical Engineering and Physics
Lubbock, TX 79409-3102

J. Lehr, W. Prather, and J. Gaudet Air Force Research Lab/Directed Energy Site 3550 Aberdeen Avenue Kirtland AFB, Albuquerque, NM 87117-5776

Corona discharges caused by ultra-fast pulses are of concern in systems that create and radiate these pulses. Corona discharge in these systems can have adverse effects such as pulse reflection, phase dispersion, and significant power losses.

We have experimentally observed corona development and discharge in this type of environment under several conditions. E-field, gas pressure and pulse repetition rates have all been varied and the resultant corona observed. Several gas dielectrics, including air, SF₆, and admixtures of SF₆ and N₂ have been used. Applied pulse characteristics vary from 10 to 300 kV, 0.3 to 1.5 nsec risetimes, 1 to 100 nsec FWHM, and rep-rates from single shot to 5 kHz.

Both coaxial and point-plane geometries are used in the test gap. Observations of the corona inception are made with a streak camera and an image intensifying CCD framing camera. The streak camera provides information on corona development of a single pulse, while the CCD framing camera provides an integrated image of the ionized region during a series of pulses.

This work was primarily funded by the High Energy Microwave Device MURI program funded by the Director of Defense Research & Engineering (DDR&E) and managed by the Air Force Office of Scientific Research (AFOSR).

1A04-5

Invited -

Resonances and Surface Waves in Bounded Plasmas

Kevin J. Bowers, David W. Qui, H.B. Smith and C.K. Birdsall, University of California - Berkeley, Berkeley, CA, 94720-1772, USA

Resonances and Surface Waves in Bounded Plasmas

Kevin J. Bowers, David W. Qiu, H.B. Smith and C.K. Birdsall EECS Department, University of California at Berkeley, Berkeley, CA 94720-1770

In the 1930s it was observed in scattering experiments off a bounded unmagnetized plasma column that the plasma exhibited many resonances between the series resonance frequency (the frequency at which the capacitive sheath resonates with the bulk plasma) and the plasma frequency, now known as Tonks - Dattner resonances. These resonances were first explained in [1], modeling the plasma with a density gradient and isotropic scalar pressure. This description of a bounded plasma has been extended; for example, in [2], the Tonks - Dattner and series resonances are treated as cutoffs of surface waves modes. These surface waves are Bohm-Gross waves at the local plasma frequency trapped in the sheath by the density gradient.

Surface waves provide a promising means of creating large area plasmas. These waves can uniformly distribute the excitation energy and while presenting a small resistance and zero reactance to the driving source. Experimentally and in our simulations, the electron temperature is low (like 1 - 3 eV) as is the plasma potential (like 10 Te). The use of surface waves experimentally, and now industrially, to sustain large area plasma sources with device size is comparable to free space wavelength have motivated us to refine the theories of [1] and [2] to be fully electromagnetic. The wave dispersion predicted by the electromagnetic theory differs from the predictions of the prior theories and the results illuminate limitations of the electrostatic model. The use of surface waves have also motivated us to explore the mechanisms by which surface waves heat the plasma. In our 1d electrostatic simulations (which model a resonant discharge experiment performed in [3]), high velocity electron bunches are formed in the sheaths and are alternatively accelerated from each sheath into the bulk plasma each RF cycle. We speculate similar mechanisms provide the ionization in surface wave discharges. We also see in these simulations the plasma makes an abrupt transition from capacitively coupled to resistively coupled and the series resonance "locks" onto the drive frequency; these abrupt transitions resemble "mode-jumping" seen experimentally in large area sources. Furthermore, the density profile of the plasma tracks the drive frequency while in the resonant mode giving a new mechanism by which the plasma parameters can be controlled. We are currently investigating the effect the driving electrode shape has on these resonances and conducting 2d simulations of a large area surface wave source to explore the ignition of surface wave devices and how the plasma fills in the device.

[1] J.V. Parker, J.C. Nickel, R.W. Gould. "Resonance Oscillations in a Hot Nonuniform Plasma." The Physics of Fluids. Vol. 7. No. 9. September 1964.

[2] D.J. Cooperberg. "Electron Surface Waves in a Nonuniform Plasma Slab." Physics of Plasmas. Vol. 5. No. 4. April 1998.

[3] V.A. Godyak, et. al. Paper 3C9. IEEE ICOPS. Santa Fe, NM. 6-8 June 1994.

This work is supported by DOE contract DOE-FG03-97ER54446, AFOSR contract FDF 49620-96-1-0154, ONR contracts N00173-98-1-G001 and N00014-97-1-0241 and the Hertz Foundation Fellowship Program

1A06

Nonlinear Features of Electron Beam-Driven Instabilities in a Magnetized Plasma,

Nagendra Singh and W.C. Leung, University of Alabama, Electrical and Computer Engineering, Huntsville, AL 35899, USA

Nonlinear Features of Electron Beam-Driven Instabilities in a Magnetized Plasma

Nagendra Singh and W. C. Leung

Department of Electrical and Computer Engineering
University of Alabama in Huntsville
Huntsville, Alabama 35899

Abstract. Using a fully 3-dimensional parallel particle-incell (PPIC) code, we have studied the excitation and nonlinear evolution of plasma waves driven by an electron beam in a magnetized plasma. The transverse dimensions of the beam is varied. The early stage of the beam-driven instability shows excitation of high frequency waves near the plasma frequency. These waves quickly evolve into electron holes, which are vortexes in the phase space. This leads to nearly complete plateauing of the electron beam. At later times, a broad spectrum of waves is excited ranging form the lower hybrid to the electron plasma frequency. In time domain the waves appear as an amplitude modulated signal. An analysis of such results and the fully 3-dimensional structures of the waves will be discussed.

1A07

Electrodynamics of Particle or Dust in Periodic Electric Cusps with Electric Mirrors and Its Applications to Planetary Dust Layers or Rings and Electric Undulators

Hiroshi Kikuchi, Nihon University, Chiyoda-ku, Tokoya 101, Japan

Electrodynamics of Particle or Dust in Periodic Electric Cusps with Electric Mirrors and Its Applications to Planetary Dust Layers or Rings and Electric Undulators

Hiroshi Kikuchi

Nihon University, College of Science and Technology 8, Kanda Surugadai, 1-chome, Chiyoda-ku, Tokyo 101, Japan

Electrodynamics of particle or dust in an electric cusp [1] is extended to the case of a longitudinal sequence of horizontal dipoles or double layers with vertically periodic electric-cusps formed by a cascade of quadrupoles. When a particle, uncharged or charged, is entering the first quadrupole-domain, it will be decelerated until it reaches the cusp centre. As soon as the particle passes through the cusp centre, it will be rapidly accelerated until it enters the next quadrupole-domain, repeating deceleration and acceleration alternately as its sequence lasts, finally being decelerated after going out of the last one.

The motion of a particle, neutral (uncharged) or charged, in such an electric configuration is described on the basis of nonlinear electrodynamics of particle in such an electric configuration with a new physical concept of 'electric reconnection' [2]. Actually, such a whole system with periodic cusps constitutes 'electric mirrors' analogous to magnetic ones, making particle trapping possible between conjugate mirrors for particles below a certain energy threshold or below the escape velocity at the mirror point. The particle receives an energy from the electric field produced by quadrupoles and returns it back to the field during its journey through the periodic cusps, maintaining its total energy, namely the sum of its kinetic and potential energy, constant, ignoring its radiation loss. The particle trajectory depends on the initial conditions and whether it is uncharged or charged. An uncharged particle entering the first quadrupole-domain along the vertical centre-line will keep going straight on due to the symmetry left and right but an uncharged particle apart from the centre-line will proceed, undulating across the center-line, both repeating deceleration and acceleration alternately as mentioned above. A charged (positively or negatively) particle is essentially the same as the uncharged particle on the off-centre-line, undulating across the centre-line, repeating deceleration and acceleration.

If an external electric field is applied vertically along the centre-line, the uncharged particle will gain energy from it continuously, moving straight on the centre-line or undulating across the center-line, resulting in overall acceleration. This is also true for a charged particle, negative for a downward electric field and positive for an upward electric field, and its vertical motion is essentially unchanged, undulating horizontally across the center-line, and gaining energy from the field and overall acceleration like an 'electric undulator'.

Particle trajectory and velocity for various cases above are obtained analytically and numerically with particular reference to 'electric undulators' and 'planetary dust layer and ring formation', taking into account gravity and horizontal electrification of planetary clouds.

- [1] H. Kikuchi, Eletrodynamics in an Electric Cusp and a New Type of Particle Acceleration by Electric Reconnection, ICOPS98, IEEE Conference Record - Abstracts, 1A06, 1998, p.118.
- [2] H. Kikuchi, Electric Reconnection in Dusty Plasmas, in Dusty and Dirty Plasmas, Noise, and Chaos in Space and in the Laboratory, ed. by H. Kikuchi, Plenum, New York, 1994, pp.535-544.

1A08

Negative Ion Measurements in Electron Cyclotron Resonance Plasmas

Bon-Woong Koo, Noah Hershkowitz and Brent Buhr, Center for Plasma- Aided Manufacture, University of Wisconsin-Madison, Madison, WI 53706, USA

Negative Ion Measurements in Electron Cyclotron Resonance Plasmas *

Bon-Woong Koo, Noah Hershkowitz, and Brent Buhr.
University of Wisconsin-Madison, Center for Plasma-Aided
Manufacturing

Electrically confined negative ions are known as the precursors of particle formation in low pressure processing plasmas. The presence of negative ions can cause various negative aspects during the process: contamination of wafers, limitation of the manufacturing productivity and device reliability in microelectronics production. Various negative ions were detected in low-pressure, high-density Electron Cyclotron Resonance plasmas $(H_2, O_2, CF_4, \text{ and } Cl_2)$ by an Omegatron mass spectrometer. Preliminary results show H^- and H_2^- in H_2 plasmas, O^- in O_2 plasmas, F^- and CF^- in CF_4 Two other techniques were employed for the verifications of the observed negative ions: photo-detachment and a Langmuir probe in magnetized plasmas. (1) For photodetachment, a pulsed Nitrogen laser (~4 mJ, 50 nsec) was used to detach the electrons from H^- and Cl^- , and a cylindrical probe, positively biased above the plasma potential, was used to collect the additional electrons. (2) A Langmuir probe theory was developed and employed for various ECR plasmas (H_2 , He, N_2 , O_2 , Ar, and CF_4). The theory, adapted to magnetized, partially ionized, low temperature processing plasmas, was based on radial diffusion into the depleted flux tube unlike earlier work by Stangeby in fusion plasmas where Bohm diffusion dominates.

* This work was supported by U.S. NSF Grant No. EEC-8721545.

1A09

Negative DC Electrical Corona Interaction with Charged Dust Particles

Deepak K. Gupta, S.V. Kulkarni and P.I. John, Institute for Plasma Research, Gujarat 382428, India

Negative DC Electrical Corona Interaction with Charged Dust Particles

Deepak K Gupta, SV Kulkarni and PI John Institute for Plasma Research, Bhat, Gandhinagar, India

Presence of dust particles is ubiquitous in many electrical corona applications. In order to study the dust-corona interaction, negative dc corona current pulse shape is studied in presence of fine dust particles. Some of the observed current pulses show multiple avalanches in single corona current pulse when dust particles are present very near to high voltage active electrode. Phenomenon of space charge disturbance, due to charged dust, is explored for its possible explanation.

Photographic methods are used for simultaneous measurement of the location and charge of the dust particles, when multiple avalanches occur. Dust charges is estimated from the deflected dust trajectory, due to the influence of electrical, gravitational and gas drag force.

For better insight numerical simulation of corona current pulse shape with charged dust particle is also carried out, without and with charge dust. One dimensional, time dependent continuity equations are solved for electron, positive ions and negative ions, in point- plane geometry. Effects of space charge along with ionization, attachment, recombination and secondary emission from electrodes are taken into account. Usual corona pulses without dust and modified corona pulses with charged dust particles are observed.

1B

De Anza II 10 am, Monday, June 21, 1999

Oral Session 1B Slow Wave Devices

Chairperson

David R. Whaley

Northrop Grumman

1B01-2

Invited -

Numerical Simulation of Backward Wave Excitation in Helix-Traveling Wave Tubes

T.M. Antonsen Jr., D.Chernin, B. Levush, Naval Research Laboratory, Washington, DC 20375, USA

Numerical Simulation of Backward Wave Excitation in Helix-Travelling Wave Tubes*

T. M. Antonsen Jr^{†*}, D. Chernin*, and B. Levush

Vacuum Electronic Branch Naval Research Laboratory Washington DC 20375

The maximum achievable gain in individual sections of helix type traveling wave amplifiers is limited by the requirement that the device be stable with respect to the excitation of backward waves. Generally, there is critical length above which the backward wave is absolutely unstable. Whether this length is exceeded in a specific device depends on a number of details that must be computed numerically. We will present a model, based on the TWT simulation code CHRISTINE, in which BWO stability is determined including a number of important effects. These are: the placement of severs, their reflection and transmission coefficients, the profile of attenuation along the interaction length, the presence of a driven signal, and the coupling of forward and backward waves due to asymmetries in the helix support structure. Specifically our model calculates the gain for the coupled forward and backward waves in a specified frequency band. Asymmetries result in a stop band near the pi point formed by the coupling of the forward and backward waves. Here the beam interacts with a composite mode formed by the fundamental spatial harmonic of the forward wave and first spatial harmonic of the backward wave. These modes will have differing coupling coefficients with the beam which we calculate using an improved solution of the tape-helix dispersion equations.

1B03

Advances in Plasma-Filled Relativistic Slow Wave Microwave Sources

Y.Carmel, A. Shkrarunets, S. Kobayashi, J. Rodgers. G.S. Nusinovich, T.M. Antonsen Jr. and V.L. Granatstein, University of Maryland, College Park, MD 20742-3511, USA

ADVANCES IN PLASMA-FILLED, RELATIVISTIC, SLOW WAVE MICROWAVE SOURCES*

Y. Carmel, A. Shkvarunets, S. Kobayashi, J. Rodgers, G. S. Nusinovich, T.M. Antonsen, Jr., and V.L. Granatstein, University of Maryland, College Park, MD.

Significant improvements in the performance of microwave sources, both nonrelativistic⁽¹⁾ and relativistic⁽²⁾, have been achieved in recent years by introducing a controlled amount of background plasma. Recent advances in plasma-filled relativistic devices-both experimental and theoretical-are reviewed. In particular, plasma filling has been credited with increasing the electron beam current and frequency tunability (~300%). The formation of hybrid waves in plasma-filled corrugated slow wave structures and the role of these modes in improving the beam/wave coupling will also be discussed. We review those issues as well as recent experimental results of plasma-loaded backward wave oscillators (BWO) operating over wide range of beam currents (0.8-4 kA) and plasma densities (10¹⁰ -10¹³ cm⁻³).

- 1) Dan M. Goebel, "Advances in Plasma-Filled Microwave Sources", invited talk, 40th Annual Meeting of American Physical Society, New Orleans, Nov. 1998 (paper Q7I1 6).
 2) A. Shkvarunets, S. Kobayashi, Y. Carmel, J. Rodgers, T.M. Antonsen, Jr., L. Duan and V. Granatstein, "Operation of a Relativistic Backward Wave Oscillator Filled With Preionized, High Density, Radially Inhomogeneous Plasma", IEEE Trans. Plasma Science, 26, 3, 1998.
- * Work supported by AFOSR, MURI program on High Power Microwaves.

^{*}Also Science Application International Corporation and †University of Maryland

^{*}Work supported by ONR

On the Theory of Ion Noise in Microwave Tubes

Wallace Manheimer,

Naval Research Laboratory, Washington, DC 20375-5346, USA

On the Theory of Ion Noise in Microwave Tubes, Wallace Manheimer, Code 6707, Plasma Physics Division, NRL, Washington, DC 20375

Microwave tubes have been plagued by what has been called 'ion noise' for decades now. This is a slow phase modulation of the output signal in time with a period that typically depends on the background pressure. Recently there has been an extensive study of the ion noise phenomena at NSWC, Crane, Indiana on a CW X-band tube called the continuous wave illuminator (CWI)1. These measurements attempt to ascertain properties of the ion noise with microwave measurements. Earlier, there had been an analogous study of ion effects in a high power klystron, this time by studying the ion current to the cathode². These measurements are in many ways complementary. This work discusses initial theoretical interpretations of these measurements. Some things analyzed are the effect of the beam ripples and ions on the microwave phase shift³, the effect of ionization by the secondary electrons, steady state ion current to the cathode in a beam with no ripples, ion relaxation oscillations in a beam with ripples, and the effect of a depressed collector and its role as a Penning trap for the secondary electrons. Finally, the possible role of different types of particle in cell numerical simulations is discussed.

This work was supported by ONR

- 1. D. Thelan, private communication
- 2. J. Smith, Ph.D thesis, Cambridge University, 1972
- 3. YY Lau, D. Chernin, and W. Manheimer, submitted to IEEE Trans. Electron Devices

1B05

Three dimensional Simulations of Electron Beams Focused by Periodic Permanent Magnets

Carol L. Kory, NASA Lewis Research Center, AnaLex/NASA LeRC MS 54-5, Cleveland, OH 44135, USA

Three-dimensional Simulations of Electron Beams Focused by Periodic Permanent Magnets

Carol L. Kory
Analex Corporation
NASA Lewis Research Center
21000 Brookpark Road, MS 54-5
Cleveland, OH 44135
(216) 433-3512 Phone
(216) 433-8705 Fax
Carol.L.Kory@lerc.nasa.gov

A fully three-dimensional (3D) model of an electron beam focused by a periodic permanent magnet (PPM) stack has been developed. First, the simulation code MAFIA was used to model a PPM stack using the magnetostatic solver. The exact geometry of the magnetic focusing structure was modeled; thus, no approximations were made regarding the off-axis fields. The fields from the static solver were loaded into the 3D particle-in-cell (PIC) solver of MAFIA where fully 3D behavior of the beam was simulated in the magnetic focusing field. The PIC solver computes the time-integration of electromagnetic fields simultaneously with the time integration of the equations of motion of charged particles that move under the influence of those fields. Fields caused by those moving charges are also taken into account; thus, effects like space charge and magnetic forces between particles are fully simulated [1]. The electron beam is simulated by a number of macro-particles. These macro-particles represent a given charge Q amounting to that of several million electrons in order to conserve computational time and memory. Particle motion is unrestricted, so particle trajectories can cross paths and move in three dimensions under the influence of 3D electric and magnetic fields. Correspondingly, there is no limit on the initial current density distribution of the electron beam, nor its density distribution at any time during the simulation.

Simulation results including beam current density, percent ripple and percent transmission will be presented, and the effects current, magnetic focusing strength and thermal velocities have on beam behavior will be demonstrated using 3D movies showing the evolution of beam characteristics in time and space. Unlike typical beam optics models, this 3D model allows simulation of asymmetric designs such as non-circularly symmetric electrostatic or magnetic focusing as well as the inclusion of input/output couplers.

¹ The MAFIA Collaboration, MAFIA TS3 the 3D-PIC Solver, December, 1996.

Exact Treatment of the Dispersion and Beam Interaction Impedance of a Thin Tape Helix Surrounded by a Radially Stratified Dielectric D. Chernin and C. Kostas, T.M. Antonsen Jr. and F.

D. Chernin and C. Kostas, T.M. Antonsen Jr. and B. Levush, Science Applications International Corporation, McLean, VA 22102, USA

Exact Treatment of the Dispersion and Beam Interaction Impedance of a Thin Tape Helix Surrounded by a Radially Stratified Dielectric*

D. Chernin and C. Kostas Science Applications International Corporation McLean, VA 22102

T.M. Antonsen, Jr.[†]
University of Maryland
College Park, MD 20742

B. Levush Naval Research Laboratory Washington, DC 20875

An exact dispersion relation has been obtained 1 for electromagnetic waves propagating on a thin metallic tape helix of arbitrary width, surrounded by a radially stratified dielectric layer and enclosed by a metallic shell. By expanding the surface currents on the tape in a series of Chebyshev polynomials, the unquantifiable assumptions made in all previously published analyses of the tape helix regarding the forms of the surface current on the tape, or the electric fields at the radius of the tape, have been avoided. The power flow and interaction impedance have also been exactly computed. This new formulation of tape helix dispersion and impedance has been included in the CHRISTINE large signal, multi-frequency TWT simulation code².

Examples will be presented in which the dispersion relation is solved numerically for slow waves and the resulting phase velocity and interaction impedance are compared to those computed using (1) the frequently made analytical assumptions of constant current along the tape and zero current across the tape and (2) results from a finite difference, frequency domain EM code. These examples will include both single and multiple dielectric supporting layers. It is found that for wide tapes significant errors are made in both the phase velocity and interaction impedance when neglecting the transverse variation of the longitudinal current and neglecting the transverse current. An example will be given showing the existence of an optimum tape width, at which the on-axis interaction impedance is maximized.

*Work supported by the Office of Naval Research

[†]Also with Science Applications International Corp., McLean, VA

1B07

Applications of the CTLSS Electromagnetic Eigensolver to Modeling Slow-Wave Devices

S.J. Cooke, B. Levush, A. Mondelli, C. Kostas, M. Czarnaski, T.M. Antonsen Jr. D. Chernin and I. Fridman, Naval Research Laboratory Code 6841, Washington, DC 20375, USA

Applications of the CTLSS Electromagnetic Eigensolver to Modeling Slow-Wave Devices *

S.J. Cooke[‡], B. Levush, A. Mondelli[‡], C. Kostas[‡], M. Czarnaski[‡], T.M. Antonsen, Jr[†], D. Chernin[‡], and I. Fridman[†]

Naval Research Laboratory

Washington, DC 20375

The Cold-Test and Large-Signal Simulator (CTLSS) code is a three-dimensional simulation tool developed specifically for the modeling of vacuum electron devices. It is a three-dimensional resonant electromagnetic frequency-domain code coupled to the CHRISTINE¹ large-signal model. This paper will describe new results in the application of CTLSS to design calculations for slow-wave devices. Current directions for CTLSS development will also be described.

Simulations of helix TWTs are presented that demonstrate a methodology consisting of using CHRISTINE for parametric optimization, followed by CTLSS cold-test calculations of the CHRISTINE optimum to capture the effects of real geometry and real materials on the dispersion and impedance of the helix device with support rods. As a final step, CHRISTINE is exercised using the cold-test parameters from CTLSS to compute the consequences of materials and geometry for device performance.

¹ D. Chernin, T.M. Antonsen, Jr., and B. Levush, to appear in IEEE Trans. Electron Devices.

² T.M. Antonsen, Jr. and B. Levush, "CHRISTINE: A Multifrequency Parametric Simulation Code for Traveling Wave Tube Amplifiers," NRL Memo report NRL/FR/6840-97-9845 (1997).

^{*}Work supported by the Office of Naval Research.

[‡]Science Applications International Corp., McLean, VA 22102.

[†]University of Maryland, College Park, MD 20742

¹ T.M. Antonsen, Jr. and B. Levush, CHRISTINE: A Multifrequency Parametric Simulation Code for Traveling Wave Tube Amplifiers, NRL/FR/6840—97-9845 (1997).

Three-dimensional Modeling of Multistage Depressed Collectors

K.R. Vaden and V.O. Heinen, NASA Lewis Reasearch Center, Cleveland, OH 44135, USA

Three-dimensional Modeling of Multistage Depressed Collectors

K. R. Vaden and V. O. Heinen NASA Lewis Research Center 21000 Brookpark Road M.S. 54-5 Cleveland OH 44135

The results of the computer modeling of instantaneous currents within three-dimensional multistage depressed collectors (MDCs) will be presented. The classic method for the analysis and design of collectors, which has been used for more than 20 years at NASA Lewis Research Center, uses two types of twodimensional codes. First, a large signal analysis code produces the spatial and energetic distributions of the spent electron beam. An electron trajectory code then uses those distributions to perform the actual collector analysis. While this computational procedure is successful in the analysis of circularly symmetric collectors, it can only be applied as an approximation to the analysis of asymmetric collectors which many manufacturers produce. In addition, most electron trajectory codes use a steady state solver that must disregard any phase space information associated with the spent beam model.

The computational procedure reported uses the Detweiler code to produce the spent beam model and MAFIA a threedimensional particle-in-cell (PIC) code available from CST, to perform the collector analysis. MAFIA can calculate the time dependency of collector currents and the energy dissipated by the incident beam on the collector electrodes. While MAFIA is a powerful code, it was not originally written to easily model the complexities of a modulated electron beam; and being a time dependent analysis, a large number of RF cycles were required to approach steady state conditions. dimensional, time dependent analysis of an MDC was found to be a large and computationally demanding procedure. While the computational intensity of the procedure is a disadvantage, excellent results have been obtained and unique insights into collector operation have been provided by means of animated displays. The results of a MAFIA analysis of the 10 Watt, 32 GHz TWT developed for the Cassini mission demonstrate excellent agreement with experimental measurements and with the classical method of analysis.

1B09

Effects of High Plasma Density on the Electromagnetic Properties of Slow Wave Circuits

S. Kobayaski, A. Shkvarunets, Y. Carmel, J. Rodgers, T.M. Antonsen Jr. and V.L. Granatstein, University of Maryland, College Park, MD 20742-3511, USA

EFFECTS OF HIGH PLASMA DENSITY ON THE ELECTROMAGNETIC PROPERTIES OF SLOW WAVE CIRCUITS *

S. Kobayashi, A. Shkvarunets, Y. Carmel, J. Rodgers, T. M. Antonsen, Jr. and V.L. Granatstein. Institute for Plasma Research, University of Maryland College Park, MD 20742-3511 USA

The presence of background plasma in a slow wave circuit can change its electromagnetic properties and affect the interaction of an electron beam with the circuit. In particular, loading of a slow wave structure with a radially nonuniform background plasma of high density ($\omega_{plasma} \ge \omega_{radiation}$) can dramatically change the nature of the waves in the structure, leading to the formation of hybrid modes. These modes are hybrids of the plasma and the empty structure modes, with no analog in an evacuated system. Two C-band coupled cavity TWT (CCTWT) circuits and an X-band corrugated wall cavity were studied over a wide plasma density range. The radial profile and the absolute density of the background plasma were measured using a combination of a newly developed Langmuir-like probe and a small resonant cavity that measured the frequency shifts due to the plasma. For the corrugated cavity, resonant frequencies of both the TM₀₁ and TM₀₂ modes were measured over the density range $10^{10} < N_p < 10^{13}$ cm⁻³. As a plasma density was increased, flattening of the dispersion (o-k) diagram was observed up to N_p= 2x10¹² cm³. At still higher densities, strong frequency upshifts were measured. Our calculation showed that both the flattening of the dispersion curves and the large frequency upshifts are associated with the formation of hybrid plasmastructure waves in the corrugated cavity.

* Work supported by AFOSR, MURI program on HPM

A Novel Ku Band Microwave Source Based on a Complex Extended Interaction Stucture

L.Chen, H.Y. Chen, M.H. Tsao, Y.C. Tsai and K.R. Chu, T.T. Yang, S.S. Chang, C.H. Chang, P.C. Wan and L.C. Chen, National Tsing Hua University, Hsinchu, Taiwan

A Novel Ku Band Microwave Source
Based on a Complex Extended Interaction Structure*

L. Chen, H.Y. Chen, M.H. Tsao, Y.C. Tsai and K.R. Chu Department of Physics, National Tsing Hua University, Hsinchu 300, Taiwan

T.T. Yang, S.S. Chang
RF Group, Synchrotron Radiation Research Center,
Hsinchu 300, Taiwan

C.H. Chang, P.C. Wan, and L.C. Chen
Electronic Research and Service Organization,
Industrial Technology Research Institute,
Chutung 310, Hsinchu, Taiwan

We report experimental investigation of a novel scheme for efficient interaction between a linear electron beam and the electromagnetic wave in a complex extended interaction cavity. The proposed structure consists of a high R/Q five-gap extended interaction cavity which incorporates a coaxial section of a quarter plasma wavelength, placed between the first and second gaps, for the dual function of frequency tuning and efficiency enhancement. In the coaxial section, beam and wave propagate in separate channels. Frequency tuning is achieved by a ceramic plunger inserted into the wave channel of the coaxial section, hence causing minimum disturbance to the gap fields. An inner channel running through the center conductor of the coaxial section provides a cutoff drift space for ballistic bunching of electrons, an effect that can significantly enhance the interaction efficiency. Oscillation power of 1.35 kW at 16.8 GHz was demonstrated with an interaction efficiency of 31.0 %. The total efficiency was further increased to 46 % by a two-stage depressed collector.

In addition, a helix section is added between the cathode and the complex cavity. This provided phase locking of the oscillator with 50 db demonstrated gain as well as allowing the device to function as a normal and frequency doubling amplifier.

1C

Monday AM, June 21 De Anza III

Session 1C Laser Produced Plasmas

Chairperson
Andrew Mostovych
Naval Research Laboratory

^{*}Work supported by the National Science Council, ROC

1C01-02

Invited - Laser-produced plasma: A new window for high pressure science

A. Ng, University of British Columbia, Vancouver, BC V6T1Z1, Canada

Laser-produced plasma: A new window for high pressure science

A. Ng
Department of Physics & Astronomy
University of British Columbia, Vancouver, B.C., Canada

High-energy-density laser-produced plasmas offer an unique window for the investigation of high pressure phenomena. From observations of the intensity of optical emission from and the reflectivity of a plasma generated by a laser-driven shock wave, one learns about not only the rate of thermal equilibriation between electrons and ions in a strongly coupled plasma but also the state of two-temperature non-equilibrium that exists in a shock wave. Or, one may use the K-shell photoabsorption spectrum in similar plasmas to test our understanding of pressure ionization processes. Alternatively, a plasma produced by the isochoric heating of an ultrathin foil using an ultrashort pulse laser can be used to assess the equation of state at high pressure. An overview of these examples will be presented.

1C03-4

Invited -

Numerical Modeling of ICF Plasmas

J.P. Dahlburg, J.H. Gardner, A. J. Schmitt, D. Colombant, M. Klapisch and L. Phillips, U.S. Naval Research Laboratory, Washington, DC 20375, USA

Numerical Modeling of ICF Plasmas.

J. P. Dahlburg, J. H. Gardner, A. J. Schmitt, D. Colombant, M. Klapisch, and L. Phillips Plasma Physics Division; LCP&FD; ARTEP Naval Research Laboratory, Washington, DC 20375

Radiation transport hydrodynamics codes play an important role in the design and development of ignition-regime and high-gain direct drive Inertial Confinement Fusion (ICF) pellets. In this concept, laser light is used to symmetrically implode a spherical pellet to sufficiently high densities and temperatures to achieve thermonuclear fusion. This requires a very symmetric illumination and a stable hydrodynamic implosion. Simulations of the dynamics of both planar and spherical targets are being performed to provide better understanding of how to control the Rayleigh-Taylor (RT) instability, using the 1-, 2- and 3-dimensional laser matter interaction (LMI) code FAST. To benchmark FAST, and the Super Transition Array2 material opacities used in the pellet design simulations, comparisons are being made with experimental data obtained in planar LMI experiments on the Naval Research Laboratory Nike KrF laser. One of the major efforts is to understand the behavior of the RT instability in planar laseraccelerated targets. Since this is one of the primary obstacles to successful ICF, experimental comparison is not only providing for code benchmarking, but will also lead to a better understanding of how to control this basic instability. Code benchmarking is also being performed using data from Nike opacity experiments, and from equation of state experiments in ICF-relevant regimes. In this talk we present an overview of FAST and a comparison of simulation results with data from ongoing laboratory experi-

- *Work supported by US DOE and ONR.
- ¹M. H. Emery et al., Appl.Phys.Lett., 41, 808 (1982); J. H. Gardner et al., Phys.Plas., 5 (May, 1998).
- ²A. Bar-Shalom et al., Phys. Rev. A, 40, 3183 (1989); A. Bar-Shalom & J. Oreg Phys. Rev. E, 54, 1850 (1996).

1C05-6

Invited - Dynamics of Plasma Propagation and Splitting During Pulsed Laser Ablation

R.F. Wood, Oak Ridge National Laboratory, Oak Ridge, TN 37831-6032, USA

Dynamics of Plasma Propagation and Splitting During Pulsed-Laser Ablation

> R. F. Wood Solid State Division Oak Ridge National Laboratory

Pulsed laser ablation has become a well-established technique for depositing thin films of many different types of technologically important materials. Deposition is usually carried out in a lowpressure ambient background gas to aid in control of the process or to promote interactions in the gas phase. Consequently, the theoretical analysis of the dynamics of the laser-generated plasma plume in the presence of a background gas has generated widespread interest. Experimentally, it is found that the plume frequently splits into two components, one traveling at nearvacuum velocity and the other greatly slowed by interaction with the background gas. Purely hyrodynamic descriptions of the plume-background system have been unable to describe this "plume splitting". A new approach to the problem, based on a combination of multiple scattering and hydrodynamic formulations has been developed. Although relatively simple in structure, the model gives excellent fits to various experimental data for Si in background gases of He and Ar, including the previously unexplained splitting of the ablated plume. It allows the plume to be broken up into scattering order, for which particles undergo 0, 1, 2,.... collisions with the background. Particles can only be transferred from one order to the next higher order by collisions. The densities in the individual orders propagate according to the usual conservation equations to give the overall plume expansion. When Ar is the background gas, there is a non-negligible probability that Si plume atoms will reach the detector without undergoing any collisions. This gives rise to a flux component that is undisplaced from that obtained when no background gas is present in addition to the delayed peak from the scattered flux. In Ar only a few orders are necessary for convergence. The behavior in He is more complex because of the relatively small effect of any one scattering event and the calculations must be carried out to higher orders. A brief review of the experimental situation and previous modeling efforts will be given, after which the new approach and results obtained with it will be discussed.

1C07

Simulation of Intense Laser Pulse Propagation in Capillary Discharge Plasma Channels

R.F. Hubbard, P. Sprangle, A. Ting and C. Moore, U.S. Naval Research Laboratory, Washington, DC 20375-5346, USA

SIMULATION OF INTENSE LASER PULSE PROPAGATION IN CAPILLARY DISCHARGE PLASMA CHANNELS*

R. F. Hubbard, P. Sprangle, A. Ting, and C. Moore Beam Physics Branch, Plasma Physics Division Naval Research Laboratory, Washington, DC 20375-5346

D. Kaganovich and A. Zigler Racah Institute of Physics Hebrew University, Jerusalem, Israel 91904

B. Hafizi Icarus Research, Inc., Bethesda, MD 20824-0780

Many applications of ultra intense laser pulses require propagation in plasmas over distances of many Rayleigh lengths. Hollow plasma channels such as those produced by a capillary discharge have successfully guided pulses with small spot size $(r_s \sim 30 \,\mu\text{m})$ over distances as long as 6 cm. Recent experiments have extended the capillary discharge technique to laser intensities of 10¹⁷ W/cm³. These experiments use a double capillary design that allows more control over plasma parameters. Simulations of laser propagation in these channels show that the laser pulse radius undergoes oscillations about the expected matched radius r_M at the expected frequency. The pulse may be distorted by several effects, including lasergenerated ionization and plasma motion in the intense laser fields. In addition, finite pulse length corrections to the wave equation cause initially the oscillations in the laser beam size to damp in the front of the beam and grow in the back. Eventually, the oscillations are damped by phase mixing effects. Experiments to date have been at relatively high densities $(\sim 10^{19} \text{ cm}^{-3}).$ For standard laser wakefield accelerator applications, the on-axis channel density is likely to be substantially lower. As expected, simulations in this lower density regime show lower accelerating gradients, larger laser spot sizes, and higher wakefield phase velocities. dephasing limit on single stage final electron beam energy is thus also much higher. Possible methods for producing lower density plasma channels will also be discussed.

*Supported by the Office of Naval Research, the Department of Energy, and the U.S.-Israeli Binational Science Foundation

1C08

Guiding and Triggering of Large-Scale Electrical Discharges using Ultrashort Pulse Lasers

D. Comtois, C.Y. Chien, P. Couture, A. Desparois, T.W. Johnston, Z. Jiang, J.C. Kieffer, B. LaFontaine, F. Martin, R. Mawassi, H.P. Mercure, H. Pepin, C. Potvin, F.A.M Rizk and F. Vidal, INRS Energie et Materiaux, Varennes, Quebec J3X 1S2, Canada

Guiding and Triggering of Large-Scale Electrical Discharges using Ultrashort Pulse Lasers[‡]

D. Comtois, C.Y. Chien, P. Couture[†], A. Desparois, T.W. Johnston, Z. Jiang, J.-C. Kieffer, B. La Fontaine, F. Martin, R. Mawassi, H.P. Mercure[†], H. Pépin, C. Potvin[†], F.A.M. Rizk and F. Vidal

INRS-Énergie et Matériaux, 1650 Lionel-Boulet, Varennes, Québec, Canada J3X 1S2 † IREQ, Hydro-Québec, 1800 Lionel-Boulet, Varennes, Ouébec, Canada J3X 1S1

The possibility of channeling lightning discharges is of enormous scientific and economic value but presents great technical challenges.

The use of lasers to trigger and guide such discharges is an area of intense international research. Recent advances in ultra-short pulse lasers have opened new possibilities of achieving this goal. We have demonstrated the propagation of high intensity laser filaments over distances in excess of 200 meters, which could be used to guide lightning.

We have studied the basic processes involved in the initiation and propagation of long-gap discharges using ultra-short pulse lasers, both experimentally and via numerical simulations.

We will report on experiments performed with air gaps of up to 5 meters where the electrodes are charged with voltage pulses of up to 1.5MV. The influence of the laser-created plasma on the discharge process is investigated using time-resolved optical diagnostics as well as with electric field and current probes. Experiments performed on this scale will provide fundamental knowledge on the transition from pure streamer-discharges to the formation of leaders, and the phenomenon of breakdown at the levels of electric fields characteristic of thunderstorms.

We will also present results from smaller-scale discharges initiated by laser (gaps of 30 cm) together with numerical simulations of the streamer inception process and results on the characterization of the plasma using interferometry and spectroscopy.

1C09

Electrostatic Measurement of Plasma Plume Dynamics in Pulsed Laser Evaported Graphite

R.M. Mayo, J.W. Newman, A. Sharma, J. Narayan and Y. Yamagata, North Carolina State University, Raleigh, NC 27695, USA

Electrostatic Measurement of Plasma Plume Dynamics in Pulsed Laser Evaporated Graphite

R. M. MAYO, J. W. NEWMAN
Department of Nuclear Engineering
North Carolina State University, Raleigh, NC 27695

A. SHARMA, J. NARAYAN

Department of Materials Science and Engineering

North Carolina State University, Raleigh, NC 27695

Y. YAMAGATA

Department of Electrical and Computer Engineering Kumamoto University, Kumamoto 869, Japan

Thin films of Diamond-Like-Carbon (DLC) are routinely produced by pulsed laser evaporation (PLE) of graphite targets. The optical, electrical, and mechanical properties of such films make them rather attractive for applications from wear resistant coatings for optical components to substrate material for advanced semiconductor devices. Pulsed laser deposition (PLD) has numerous advantages, particularly, the presence of energetic species in the plasma results in a large fraction of sp³ bonded carbon. This study concentrates on electrostatic (Langmuir) probe measurements in the carbon PLE plume to investigate plume dynamics and, in future work, correlate against film properties.

The experimental facility for PLE at NCSU (J. Appl. Phys., 73 (1993) 316) consists of a spherical vacuum chamber ($\lesssim 10^{-7}$ Torr), a Lambda Physik KrF (248 nm) excimer laser with ~ 45 ns pulse width (25 ns FWHM) delivering typically 2-3.5 J/cm² to a rotated graphite target at 45° incidence, and a substrate mounted 5-10 cm from the target. Normal to the target, on a sliding vacuum seal, is installed a triple Langmuir probe for the studies discussed herein. The probe consists of three cylindrical Tungsten tips (10 mil dia., and 5 mm in length) and is biased to -7 to -10 V to reach ion saturation. Time resolved (currently at 5Ms/s) measurements of n_e , T_e , and floating potential are recorded at probe-target separation of 1, 3, and 5 cm. Beyond this separation, ion saturation signal strength is greatly diminished.

Preliminary results indicate electron densities on the order of 10^{12} - 10^{15} cm⁻³ and electron temperatures ~ 0.25 -0.5 eV at 1 cm from the target surface. Plasma density is often observed to increase initially with probe-target separation distance before decreasing, a result thus-far attributed to slightly off-center probe tip occulting by the highly forward directed plume. Plume front energy is estimated to be in excess of 100 eV, by peak density signal arrival time at several probe-target separations, and is constant with distance although an increasing function of laser energy and decreasing with fill gas pressure, as will be presented. Increased fill gas density delays ion saturation signal arrival time and reduces magnitude as expected. In the presence of intermediate background Ar and N_2 fill (100-300 mTorr) a second, long delayed feature in the n_e signal is observed. This is a possible signature of heavy cluster formation, although formation and ionization mechanisms are currently under investigated.

^{*} Work supported in part by the Natural Science and Engineering Research Council of Canada.

Bonsai I/II 10 AM, Monday, June 21, 1999

Oral Session 1D Non-Equilibrium Plasma Processing

Chairperson

Jeff Hopwood

Northeastern University

1D01

Control of Ion Energy and Angular Distributions using Voltage Waveform

Shahid Rauf, Motorola, SPS, Austin, TX 78721, USA

Control of Ion Energy and Angular Distributions using Voltage Waveform

Shahid Rauf Motorola SPS, 3501 Ed. Bluestein Blvd., Austin, TX 78721

A number of plasma-aided microelectronics manufacturing processes sensitively depend on the ion characteristics at the substrate, in particular the ion energy (IEDF) and angular (IADF) distribution functions. outcome of these processes can be much more precisely controlled if one has direct control over the IEDFs and IADFs. Past studies have explored the influence of rf bias voltage amplitude and frequency, inductive power deposition and gas pressure on the ion characteristics at the substrate. The factor that influences the ion dynamics most is however the timedependent sheath voltage and, as demonstrated in this paper, sheath voltage can be accurately controlled using the rf bias voltage waveform. In this paper, we computationally examine the influence of the rf bias voltage waveform on the IEDFs and IADFs at the substrate in an inductively coupled plasma (ICP) reactor.

This study has been conducted using a coupled set of the Hybrid Plasma Equipment Model (HPEM) and a circuit model, and the Plasma Chemistry Monte Carlo Simulation (PCMCS). The HPEM is a 2-dimensional hybrid simulation of the plasma dynamics. The circuit model uses HPEM results in conjunction with the Riley's sheath model to estimate dc bias, sheath voltages and electrode currents. Once steady-state plasma and circuit quantities have been computed, a Monte Carlo simulation (PCMCS) is used to determine the IEDFs and IADFs at the substrate.

The model has been used to simulate a generic ICP reactor geometry with Ar and Ar/Cl₂ gases. It is demonstrated that the sheath voltage at the substrate closely follows the applied rf bias voltage waveform. Since displacement current increases with rf bias frequency, voltage waveforms which have sharp gradients (e.g. square wave) lead to large electrode currents. IEDFs and IADFs are also strongly influenced by the voltage waveform, specially under circumstances where the ion transit time through the sheath is smaller than the rf time period.

¹S. Rauf and M. J. Kushner, J. Appl. Phys. **83**, 5087 (1998) ²R. J. Hoekstra and M. J. Kushner, J. Appl. Phys. **77**, 3668 (1995).

Novel Method of Ion Energy and Ion Energy Distribution Function Control at the Substrate during Plasma Processing

hiang-Bau Want and Amy E. Wendt, University of Wisconsin-Madison, Madison, WI, 53706, USA

Control of Ion Energy and Angular Distributions using Voltage Waveform

Shahid Rauf Motorola SPS, 3501 Ed. Bluestein Blvd., Austin, TX 78721

A number of plasma-aided microelectronics manufacturing processes sensitively depend on the ion characteristics at the substrate, in particular the ion energy (IEDF) and angular (IADF) distribution functions. outcome of these processes can be much more precisely controlled if one has direct control over the IEDFs and IADFs. Past studies have explored the influence of rf bias voltage amplitude and frequency, inductive power deposition and gas pressure on the ion characteristics at the substrate. The factor that influences the ion dynamics most is however the timedependent sheath voltage and, as demonstrated in this paper, sheath voltage can be accurately controlled using the rf bias voltage waveform. In this paper, we computationally examine the influence of the rf bias voltage waveform on the IEDFs and IADFs at the substrate in an inductively coupled plasma (ICP) reactor.

This study has been conducted using a coupled set of the Hybrid Plasma Equipment Model (HPEM) and a circuit model, and the Plasma Chemistry Monte Carlo Simulation (PCMCS). The HPEM is a 2-dimensional hybrid simulation of the plasma dynamics. The circuit model uses HPEM results in conjunction with the Riley's sheath model to estimate dc bias, sheath voltages and electrode currents. Once steady-state plasma and circuit quantities have been computed, a Monte Carlo simulation (PCMCS) is used to determine the IEDFs and IADFs at the substrate.

The model has been used to simulate a generic ICP reactor geometry with Ar and Ar/Cl₂ gases. It is demonstrated that the sheath voltage at the substrate closely follows the applied rf bias voltage waveform. Since displacement current increases with rf bias frequency, voltage waveforms which have sharp gradients (e.g. square wave) lead to large electrode currents. IEDFs and IADFs are also strongly influenced by the voltage waveform, specially under circumstances where the ion transit time through the sheath is smaller than the rf time period.

¹S. Rauf and M. J. Kushner, J. Appl. Phys. **83**, 5087 (1998) ²R. J. Hoekstra and M. J. Kushner, J. Appl. Phys. **77**, 3668 (1995).

1D03-4

Invited -

Review of Ionized-PVD By Hollow Cathode Magnetron Sputtering

K.F. Lai and Q. Lu, Novellus Systems Inc., San Jose, CA 95134, USA

Review of Ionized-PVD By Hollow Cathode Magnetron Sputtering

K.F. Lai and Q. Lu

Novellus Systems, 3970 N. First St., San Jose, CA 95134

The Hollow Cathode Magnetron (HCM) is a new type of high density plasma device developed for ionized physical vapor deposition (I-PVD). Unlike other I-PVD approaches where post-ionization of sputtered or evaporated metal atoms by either radiofrequency (rf) or microwave generated high density plasma is necessary, the HCM uses only a single dc power supply to both sputter and ionize the target material. A novel magnetic geometry provides the confining magnetic field to sustain a magnetron discharge within a cup-shaped hollow cathode and the means of ion extraction to allow the metal plasma to stream to the substrate.

In conjunction with efficient water cooling, the HCM is capable of operating at more than ten times the power density of conventional planar magnetrons. High power density, together with efficient confinement allow the HCM to achieve extremely high plasma density (~10¹³cm⁻³). Compared to I-PVD using rf inductively coupled plasma (RFiPVD) which has a plasma density of 10¹¹cm⁻³ to 10¹²cm⁻³ and operates best above tens of millitorr, the HCM achieves high degrees of ionization at only a few millitorr, primarily due to its extremely high plasma density and efficient neutral confinement.

The HCM can be used for the deposition of a large variety of conductive materials simply by a change of the sputtering target. Pulsed dc or rf can be used for the deposition of non-conductive materials. By use of a mixture of inert and reactive gases such as nitrogen or oxygen, many different kinds of binary compounds can be deposited using reactive sputtering. Because of its extremely high plasma density and sputtering rate, the HCM is capable of maintaining the target surface in the non-poisoned (i.e. the metallic) mode avoiding problems commonly encountered in reactive sputtering. The characteristics of HCM deposited film can be dramatically different from those by conventional PVD. The physics of metal ion deposition under high flux, low energy ion bombardment and its effect on film properties will be discussed.

The HCM can generate an adjustable self-bias of -10 to -60 volts on a floating substrate which has proven to be adequate to impart a high degree of directionality for most metalization applications. The use of a separate power supply to independently bias the substrate can further improve step coverage and process capability for future generations of ULSI devices. The recent process results for Ti/TiN liner, Cu seed layer, and Ta/TaN diffusion barrier using a commercial HCM source will be reported.

Sputter Heating in Ionized Metal Physical Vapor Deposition

Junging lu and Mark J. Kushner, University of Illinois, Urbana, IL 61801, USA

Sputter Heating in Ionized Metal Physical Vapor Deposition*

Junqing Lu and Mark J. Kushner

University of Illinois, Dept. of Electrical and Computer Engineering, 1406 W. Green St., Urbana, IL 61801 USA

Ionized metal physical vapor deposition (IMPVD) is a process whereby metal fluxes with a high ionization fraction can be deposited for microelectronics fabrication. IMPVD reactors augment a magnetron sputter source, which produces the metal vapor, with an auxiliary plasma source, typically an inductively coupled plasma, to ionize the metal atoms during their transit from the target to the substrate. Recent experimental observations suggest that gas heating resulting from the slowing of sputtered atoms from the target produces sufficient rarefaction that deposition properties, such as the ionization fraction of the metal atom flux, may be affected.

In this paper, sputter heating and subsequent rarefaction in IMPVD reactors is investigated using a plasma equipment model. The Hybrid Plasma Equipment Model has been improved to include processes relevant to sputter heating. Specifically, the algorithms for yields and sputtered atom energies have been improved to account for the ion identity and energy as a function of position on the target. The transport and slowing of sputtered atoms is addressed using a Monte Carlo simulation. By collecting statistics on the energy and momenta of slowing sputtered atoms before and after a collision, rates of momentum transfer and random heating of the gas are computed. These quantities are then used in the momenta and energy equations for neutral and ion species.

Parametric studies have been performed for sputter heating in aluminum and copper IMPVD systems operating at low to high powers (\leq 1200 W ICP, \leq 2500 W magnetron) in 10s mTorr Ar. When operating with ICP excitation only, gas temperatures of 800 K are typically obtained with powers of > 1 kW. Additional temperature rises of 500 -1500 K from sputter. heating can be obtained, depending on the magnetron power and accommodation coefficient of the gas on the walls.

* Work supported by the Semiconductor Research Corp.

1D06

Irregularities in Electronegative Plasmas Due to Ion-Ion Coupling

Peter Vitello, LLNL, Livermore, CA 94551, USA

Irregularities in Electronegative Plasmas Due to Ion-Ion Coupling

Peter Vitello
Chemical Science Division
Lawrence Livermore National Laboratory

In partially ionized electronegative plasmas at low neutral pressure and high plasma density, coupling between positive and negative ions through space charge effects and through Coulomb scattering can lead to turbulence and irregularities in the ion density and flux. In this regime, the force on ions due to ion-ion Coulomb scattering may dominate that from ion scattering with neutrals. This can lead to the formation of a, possibly turbulent, negative ion boundary layer containing the bulk of the negative ions. Commercial Inductively Coupled Plasma reactors used in the semiconductor industry typically operate at low pressure and high plasma density. Simulations are presented for a Chlorine discharge in the GEC reactor modified for Inductively Coupled operation. Results show that ion-ion coupling can induce large variations in the plasma density, and that accurate modeling of spatial plasma structure should include these effects.

Simulations of Low Field Helicon Discharges Using a Two Dimensional Hybrid Plasma Equipment Model

Ron L. Kinder and Mark J. Kushner, University of Illinois, Urbana, IL 61801, USA

Simulations of Low Field Helicon Discharges Using a Two Dimensional Hybrid Plasma Equipment Model*

Ron L. Kinder and Mark J. Kushner University of Illinois, Dept. of Electrical and Computer Engineering, 1406 W. Green St., Urbana, IL 61801 USA

As the semiconductor industry moves towards larger wafers, a greater degree of process uniformity than is currently available with conventional inductively coupled plasma reactors will be necessary. Due to their high ionization efficiency, high flux density and their ability to deposit power within the volume of the plasma, helicon reactors are being developed for downstream etching and deposition. The power coupling of the antenna radiation to the plasma is of concern due to issues related to process uniformity. Furthermore, operation of helicon discharges at low magnetic fields (5 - 20 G) is not only economically attractive, but lower fields provide greater ion flux uniformity to the substrate.

At low magnetic fields, it has been observed that there is a resonant peak in the power deposition and plasma density [1]. This has been attributed to the occurrence of an electron cyclotron wave, or Trivelpiece-Gould (TG) mode, when ω/ω is of order unity. To investigate these issues, we have improved the electromagnetics module of the HPEM [2] to resolve the helicon wave structure of a m = 0 mode. The electrostatic component of the wave equation has been neglected, so this work focuses on the effects of the Helicon mode. Plasma dynamics are coupled to the electromagnetic fields through a tensor form of Ohm's law and an effective collision frequency for Landau damping has been incorporated. Using a solenoidal magnetic field and an antenna operating at 13.65 MHz, studies show a shift in the power deposition towards the center of the reactor as the magnetic field is decreased below 30 G. Furthermore, peak values and wave structure is sensitive to the magnetic field configuration. Results for process relevant gas mixtures are examined and the dependence on magnetic field strength, field configuration and power are discussed.

*Work supported by DARPA/NSCU, SRC, and NSF

- [1] F.F. Chen, X. Jiang, J. D. Evans, G. Tynan, and D. Arnush, PPG 1564, UCLA, Sept. 1996.
- [2] S. Rauf and M. J. Kushner, J. Appl. Phys. 81, 5966, (1997).

1D08

Space Averaged Kinetic Analysis of Stochastically Heated Electronegative RF Capacitive Discharges Zuoding Wang and Allan J. Lichtenberg, University of California - Berkeley, Berkeley, CA 94720, USA

Space Averaged Kinetic Analysis of Stochastically Heated Electronegative Rf Capacitive Discharges

Zuoding Wang[†], Allan J. Lichtenberg[†] and Ronald H. Cohen[‡]

University of California, Berkeley, CA 94720

[‡]Lawrence Livermore National Laboratory Livermore, CA 94550

Abstract

In low pressure capacitive rf plasma discharges, stochastic sheath heating, combined with potentials that exclude low energy electrons from reaching the sheath, produce an electron energy probability function (EEPF) which approximates a two-temperature Maxwellian, as seen in both experiments and numerical simulations. We have used the fundamental kinetic equation to drive a space- and time-averaged kinetic equation to analytically calculate this EEPF. We improve over our model for stochastic heating by allowing the stochastic heating to be gradually turned on over a range of electron energy, instead of abruptly. A complete set of equilibrium conditions are used so that all the unknown parameters can be solved self-consistently. The theory is applied to oxygen discharges, for which the equilibrium equations for the two ion species are coupled with the electron kinetic equation. The spatial diffusion profiles and the EEPF both agree well with PIC simulations.

Serra I, Conference Centre 10 AM, Monday, June 21, 1999

Poster Session 1P

1P01

Asymptotic modelling of a narrow gap, high pressure glow discharge

R. Bektursunova and W.G. Graham, Queen's University of Belfast, Northern Ireland, UK

Asymptotic modelling of a narrow gap, high pressure glow discharge*

R.Bektursunova and W.G.Graham
Pure and Applied Physics Dept., The Queen's University of
Belfast, BT7 1NN, Northern Ireland

Atmospheric pressure non-thermal plasmas are now being used for various applications such as pollution control, light sources, medical and waste. Here a self-consistent continuum model is presented for a narrow gap plane-parallel dc glow discharge. The set of governing equations consisting of continuity and momentum equations for positive ions, fast (emitted by the cathode) and slow electrons (generated by fast electron impact ionization) coupled with Poisson's equation is treated by the technique of matched asymptotic expansions [1]. This analytic procedure reduces the unnecessary computational effort associated with Monte-Carlo approach with acceptable accuracy. In addition it is more physically transparent. Explicit results are obtained in the asymptotic limit: pL >> 1, $(\chi \delta) << 1$, where p is the gas pressure, L is the gap length, χ is the normalised applied voltage, and $\delta = \left(\frac{r_D}{L}\right)^2$, where r_D is the Debye radius. In the limit of large

pL the electron energy relaxation length is much smaller than gap length and local field approximation is valid. The discharge space divides naturally into a cathode fall sheath, a quasineutral plasma region and an anode fall sheath. The length of each region is derived. The electric field and charge density distribution obtained for each region (in a (semi)-analytical form) is asymptotically matched to the adjoining one in the region of overlap. The effects of the gas pressure, gap length and applied voltage on the discharge properties are investigated. The cathode fall parameters predicted by the asymptotic model are in reasonable agreement with available experimental data [2]. Work underway to apply this method for the calculation of dielectric barrier discharge characteristics.

*This work was partly funded by The Islamic Development
Rank

1.A.Nayfeh, Perturbation Methods, John Viley, New York, NY, (1973)

2.J.P.Novak, R.Bartnikas, J.Appl.Phys.62, p.479, (1987)

Experimental Characterization of a Pulsed ICP Discharge

K.C. Leou, Y.T. Chien, Y.M. Yang, T.L. Lin and C.H. Tsai, National Tsing Hua University, Hisinchu, Taiwan 30043, ROC

Experimental Characterization of a pulsed ICP discharge

K.C. Leou, Y.T. Chien, Y.M Yang, T.L.Lin and C.H. Tsai Engineering and System Science Department National Tsing Hua University Hsinchu, Taiwan, ROC

Pulsed low-pressure high-density plasmas attracted a great deal of attention recently owing to their applications in ULSI processing[1]. It has been demonstrated that processing with pulsed plasma can reduce charge-induced damage, such as notching effect. It has been shown that this feature is related to the effect of a reduced electron temperature and an increase of negative ion density during the off period of the pulse. purpose of this work is to characterize basic properties of a pulsed ICP discharge by employing various diagnostic tools, including a Langmuir probe, a 36 GHz interferometer, an ion energy analyzer, a plasma impedance probe, as well as a monochromator. These tools have been modified from existing ones^[2] to measure timeresolved signals associated with a pulsed discharge. Preliminary measurement results show that, in an Ar plasma, electron temperature drops much faster than plasma density. The plasma potential also decreases during the off period because the plasma becomes cooler. The result from the interferometer measurement exhibits a different time dependence of the plasma density from the Langmuir probe data. This is mainly because the former measures the line-averaged values while the latter extracts local properties. In a time-modulated plasma with a typical frequency around 10 - 100 kHz, there will be a time-delay on the plasma properties, such as density and temperature, at different location in a plasma chamber. As it is averaged spatially, the time dependence is smeared out and exhibits a totally different behavior from the local ones. Further study is being conducted to investigate this issue. Detailed experimental results will be presented.

(Work supported by NSC grant No. 87-WFA04J0010018 and 86-2622-E-007-007R, ROC)

T. H. Ahn, K. Nakamura and H. Sugai, Jpn. J. Appl. Phys. 34, 1405(1995).
 K. C. Leou, et al, IEEE Conference Record - ICOP 1997, P141.

1P03

The Dependence of the Decay Time Constant on the Chamber Size and Gas Pressure in a Pulsed ICP

T.L. Lin, Y.T. Chien, K.C. Leou, C.H. Tsai, National Tsing-Hua University, Hsinchu, Taiwan 30043, ROC

The Dependence of the Decay Time Constant on the Chamber Size and Gas Pressure in a Pulsed ICP

T.-L. Lin, Y.-T. Chien, K.-C. Leou, C.-H. Tsai Department of Engineering and System Science National Tsing-Hua University, Hsinchu 30043, Taiwan, ROC

The electron temperature in inductively coupled plasma (ICP) can be significantly lowered when it is operated in a puled mode. Lower electron temperature, in together with the increase in negative ions, was found to be able to reduce notching effects in etching processes.

The local plasma properties in a pulsed ICP can be measured by Langmuir probes. The probe current can be measured as a function of delay time for each pule cycle at different but fixed bias voltages. The current versus delay time data for different bias voltages can then be used to reconstruct the typical I-V curves for each delay time. The plasma density and electron temperature as a function of delay time can then be determined from these I-V curves. For an Ar plasma with a chamber height of 40 cm and diameter of 40 cm, operated at 30 mtorr gas pressure, 13.56 MHz RF, and 10 kHz pulse rate at 50% duty cycle (50 μ s on and 50 μ s off), both the temperature and the plasma density were found to decay initially very fast and then much slower in the power off period. The decay time constants are expected to depend on the gas pressure which affects the ionization rate and diffusion coefficient, and also on the chamber size which affects the loss rate of the plasma. Experiments will be carried out for various gas pressures and chamber heights to see how the decay time constants vary with these two parameters. (Work supported by the NSC grant No. 87-2622-E-007-006, ROC)

Two-Dimensional Modeling of Nonlocal Electron Heating in Inductively Coupled Plasma Sources

Y.Hu, T.L. Lin, and C.W. Chang, National Tsing-Hua University, Hsinchu, Taiwan 30043, ROC

Two-Dimensional Modeling of Nonlocal Electron Heating in Inductively Coupled Plasma Sources

Y. Hu, T. L. Lin, and C. W. Chang Dept. of Engineering and System Science National Tsing Hua University, Hsinchu 30043, Taiwan, ROC

Nonlocal (collisionless) electron heating can be important in low-pressure inductively coupled rf discharges. We have developed a two-dimensional, electromagnetic, PIC-MCC code to study power deposition in an inductively coupled plasma source. Simulation results for the collisionless heating power are found to be significantly higher than that predicted by the analytic model of Vahedi et al [1]. This discrepancy can be attributed to the fact that they consider only the axial motion of the electrons to determine the collisionless heating. In this work we present an analytic model to consider the nonlocal heating of the electrons during their radial motion as well as their axial motion. Here we consider electrons moving both axially and radially. The azimuthal electric field decays exponentially into the plasma along the axial direction and has a nonuniform radial profile typical of ICPs. In addition to being reflected by the sheath potential while moving axially toward the dielectric window, an electron can be reflected by the sheath potential at the cylindrical chamber wall during its of the system to be finite. Adopting the similar approach outlined in Ref. [1], we arrive at an expression for the collisionless heating power. This two-dimensional analytic model gives good agreement with the results of particle simulations.

Work supported by NSC grant No. 87-2622-E-007-006, ROC.

[1] V. Vahedi, M. A. Lieberman, G. DiPeso, T. D. Rognlien, and D. Hewett, J. Appl. Phys. 78, 1446(1995).

1P05

Two-Dimensional Simulation of Electron Cyclotron Resonance Discharge

J.H. Shiau, J.H. Tsai and S.H. Chen National Center for High Performance Computing, Hsinchu, Taiwan, ROC

Two-Dimensional Simulation of Electron Cyclotron Resonance Discharge

J. H. Shiau, J. H. Tsai and S. H. Chen National Center for High-performance Computing, Hsinchu, Taiwan, R.O.C.

J. Y. Yang and C. J. Chiou Institute of Applied Mechanics, National Taiwan University, Taipei, Taiwan, R.O.C.

A two-dimensional three-moment simulation code was developed and performed for the study of the electron cyclotron resonance (ECR) plasma sources based on the self-consistent fluid model which determines the dynamics of the plasma as well as its interactions with the microwave. In particular, the ECR discharges can be characterized by two major parameters, one is the selection of the microwave mode [1], and the other is the magnetic field configuration [2]. In this study, two different waveguide modes, i.e. TE₀₁ and TM₀₁, with the same frequency 2.45 GHz, are applied to induce the ECR discharges in the different magnetic field configurations with uniform, diverging, and mirror profiles [2]. The input power and the background argon pressure are scanned in the range of 0.3-1.2 kW and 1-20 mTorr, respectively. In order to examine their effects on the ECR discharges, we diagnose the plasma density profile, plasma generation rate, spatial temperature distribution, and the spatial deposition of the wave power, By investigating these plasma distributions, appropriate operating conditions for the ECR discharge will be suggested.

- 1. R. L. Kinder and M. J. Kushner, TECHCON '98, Las Vegas, Nevada, September 1998.
- W. Cronrath, N. Mayumi, M. D. Bowden, K. Uchino, K. Muraoka, and M. Yoshida. J. Appl. Phys. Vol. 82, No. 3, pp. 1036-1041, 1997.

Susceptibility diagram of multipactor discharge on a dielectric- Effects of an external magnetic field and oblique RF electric field

L.K. Ang, A. Valfells, Y.Y. Lau, and R.M. Gilgenbach, University of Michigan, Ann Arbor, MI 48109-2104, USA

Susceptibility diagram of multipactor discharge on a dielectric – Effects of an external magnetic field and oblique RF electric field.

L.K. Ang, A. Valfells, Y.Y. Lau, and R.M. GilgenbachNuclear Engineering & Radiological Sciences Dept.U of Michigan, Ann Arbor, MI 48109-2104

Monte-Carlo simulations have recently been used to construct the susceptibility diagram of multipactor discharge on a dielectric, under the assumption that the RF electric field is parallel to the dielectric surface [1]. This diagram, constructed from kinematic considerations, turns out to be extremely useful in the prediction of the saturation level [2]. Here, we generalize the susceptibility diagram in two aspects: inclusion of an external magnetic field and the effects of an oblique RF electric field.

It is found that the presence of an external magnetic field does not qualitatively change the susceptibility diagram, regardless of the orientation of the magnetic field. This statement holds for all magnetic fields simulated, up to those values whose cyclotron frequency is on the order of the RF frequency.

The effects of an oblique RF electric field show a more significant change on the susceptibility diagram. In general, the lower bound (in RF electric field) of the susceptibility diagram [1] does not suffer a qualitative change as ϕ increases from zero, where ϕ is the angle between the RF electric field and the dielectric surface. However, the upper bound changes markedly once of exceeds about 10 degrees. The overall effect is that nonzero o narrows the range of RF electric field in which multipactor can occur. However, since the saturation of multipactor is determined from the lower boundary of the susceptibility diagram [2], the present study then shows that oblique RF electric field and external magnetic field do not qualitatively affect the existence or the saturation level. More important, then, is the effect of outgassing that is considered elsewhere [3] in this Conference.

Supported by DoE, MURI/AFOSR, and Northrop Grumman Corp.

- [1] Kishek and Lau, Phys. Rev. Lett. 80, 193 (1998).
- [2] Ang et al., IEEE Trans. Plasma Sci. 26, 290 (1998).
- [3] Valfells et al., in this Conference.

1P07

A Theory of RF Window Failure

A. Valfells, L.K. Ang, Y.Y. Lau, R.M. Gilgenbach, R.A. Kishek, J. Verboncoeur, A. Neuber, H. Krompholz and L.L. Hatfield, University of Michigan, Ann Arbor, MI 48109-2104, USA

A Theory of RF Window Failure

A. Valfells, L.K. Ang, Y.Y. Lau, R.M. Gilgenbach,
R.A. Kishek*, J. Verboncoeur**, A. Neuber***,
H. Krompholz***, and L.L. Hatfield***
Nuclear Engineering & Radiological Sciences Dept.
U. Michigan, Ann Arbor, MI 48109-2104

We have recently developed a novel theory of multipactor discharge on a dielectric. The main results include the susceptibility diagram [1] and the prediction that about one percent of the RF power is deposited to the dielectric surface over a wide range of conditions [2]. In this paper, we extend the analysis to include the effects of outgassing and the subsequent ionization by the multipactoring electrons. This is an attempt to understand the final stage of dielectric failure that is initiated by multipactor. Similarities and differences in such failures, under RF and DC conditions, are explored. Analytic theory and simulation results will be presented and compared with experiments.

Supported by MURI/AFOSR, DoE, and Northrop Grumman Corp.

- *U of Maryland, College Park, MD
- **U of California, Berkeley, CA
- ***Texas Tech. U, Lubbock, TX
- [1] Kishek and Lau, Phys. Rev. Lett. 80, 193 (1998).
- [2] Ang et al., IEEE Trans. Plasma Sci. 26, 290 (1998).

Design of Quasi-Optical Grills for the Launch of Microwaves into Tokamak Plasmas

J. Preinhaelter, M.A. Irzak, L. Vahala, G. Vahala, Old Dominion University, Norfolk, VA 23529, USA

Design of Quasi-Optical Grills for the Launch of Microwaves into Tokamak Plasmas

J. Preinhaelter, Czech Academy of Sciences
 M. A. Irzak, Ioffe Institute, St. Petersburg
 L. Vahala, Old Dominion University
 G. Vahala, William & Mary

While lower hybrid (LH) waves are very efficient in controlling the current profiles in the outer edges of a plasma, it is very difficult to design standard multijunction grills to launch waves in the 5-8 GHz range because of cooling and structural stability. However, if one turns to the Quasi-Optical Grill (QOG), one can design microwave launchers that are relatively simple and robust.

To minimize the effects of poloidal inhomogeneity of the plasma in front of the grill, one can design the QOG in modular form. Each module will have its own klystron feeding structure. The power from each klystron is divided into a row of standard rectangular waveguides which are flared. Several of these waveguides are then joined into an active hyperguide with an appropriate LSE_{mn} mode, together with an auxiliary passive hyperguide (for the absorption of reflected power from the plasma). For incident power of 3 MW, the electric field in the feeding structures can reach 7 kV/cm in a standard waveguide. However, this is reduced to 3 kV/cm in flared waveguides and only 1.75 kV/cm in the auxiliary hyperguide. The plane wave in the main hyperguide then irradiates a row of rods obliquely. If neutron shielding is required then, from diffraction theory, one would elongate the cross-section of the rod by integer multiples of half-wavelength in the direction of propagation. Thus the rods become more like plates, with the gaps between the rods so narrow that evanescent waves are very effectively damped. In this way the diffraction properties of the rods are independent of the shape of the gaps in the central region and hence can be bent sufficiently so as to prevent neutron streaming.

A box limiter must be placed at the grill mouth in order to achieve good directivity. In this way, the plasma density in front of the QOG will be less than the critical density. The maximum electric field in the structure determines the maximum power that can be transmitted with out electrical breakdown. While it is hard not to exceed a maximum of 3 kV/cm for a QOG operating at 5 GHz, this can be achieved for operation at 8 GHz. There are two causes of large electric fields at the grill mouth: (a) the amplitudes of the incident and reflected Te_{n0} modes and which give rise to standing waves in the gaps between the rods, and (b) the amplitudes of the higher evanescent modes at the waveguides or rod corners - since these fields have driven runaway electrons in LHCD experiments with resultant holes in the vacuum chamber. Here we study the effects of rounding of the rods to reduce these amplitudes.

Applications are made to design of QOG for ITER-like plasmas as well as EBW for NSTX plasmas

J. Preinhaelter, Nucl. Fusion 36 (1996) 593.

J. Preinahelter et. al. 25th EPS Conf., Prague (1998), Vol. 22C (1998) 1426.

1P10

Experimental Investigation of Ion Beam Transport in a Laser Initiated High Current Discharge Channel

A. Tauschwitz, C. Niemann, D. Penache, R. Presura, GSI, Darmstadt, Germany

Experimental Investigation of Ion Beam Transport in a Laser Initiated High Current Discharge Channel

A. Tauschwitz¹, C. Niemann², D. Penache², R. Presura²,

¹Gesellschaft für Schwerionenforschung GSI, Darmstadt, Germany ²Technical University Darmstadt, Germany

The transport of space charge dominated ion beams is of interest to many applications using high power particle beams. The most challenging demands are found in the field of ion beam driven inertial confinement fusion. Motivated by this application the space charge and current neutralized beam focusing and transport in gas discharge plasmas is under investigation since a number of years. Paralleled by engineering design work of a modified HILIFE II reactor with discharge channel based final beam transport, and by experimental investigations of laser initiated high current discharges at the Lawrence Berkeley National Laboratory (LBNL) the ion optical properties of such a channel will be studied for the first time with a heavy ion beam at GSI.

The experiment uses the heavy ion beam of the GSI-UNILAC linear accelerator with a typical ion energy of 11.4 MeV/amu. First experiments will use a carbon ion beam, heavier ions are planned for the near future. A parallel ion beam of one centimeter diameter is injected into a discharge channel of 50 cm length and is diagnosed behind the channel with the help of a combination from fast camera systems and scintillators. The current in the discharge channel can be increased up to 50 kA, which is the same current range as investigated in Berkeley and required by the engineering design study. The discharge is ignited in ammonia gas of low pressure. To initiate and stabilize the channel, the gas will be heated by a CO₂ laser along the path of the desired breakdown.

First experimental results from a beam time early in 1999 will be compared with ion optical simulations of the beam transport process.

This work is partially funded by the German ministry for education and research (BMBF)

Magnetic field generation by periodic helical deformation in RFP

Mitsuaki Maeyama, Takanori Miyasita and Eiki Hotta, Saitama University, Saitama 338-8570, Japan

Magnetic field generation by periodic helical deformation in RFP

Mitsuaki Maeyama ,Takanori Miyasita and Eiki Hotta*
Saitama University, Urawa, Saitama 338-8570, Japan
*Tokyo Institute of Technology,
Nagatsuda, Midori-ku, Yokohama, 226-8502, Japan

Effects of periodic helical deformations on the dynamo mechanism in RFP are examined using a simple electric circuit model. Modeling the plasma to toroidal and poloidal current channels, we use the method which switches mutual inductance matrices discontinuously on the condition conserving magnetic flux to simulate periodic onset and extinction of helical deformations.

Modeling the plasma to toroidal and poloidal current channels, circuit parameters of mutual inductance matrices in case of symmetric and asymmetric(helical) plasma are derived. To simulate periodic onset and extinction of helical deformations, we use the method of switching these two mutual inductance matrices on the condition conserving magnetic flux of each circuits.

And even if helical deformations occur periodically, phenomena of continuous energy transports from a toroidal external power source to a poloidal circuit and toroidal flux sustainment with appropriate Θ value are shown to be demonstrated with sufficient accuracy using the proposed circuit model.

References

- [1] R.B.Howell, et al., Phys. Fluids 30, 1828(1987)
- [2] K. Sugisaki, J. Phys. Soc.Jpn 56, 3176(1987)
- [3] Y.Ohta, et al., T.IEE Japan, 107-A, 255(1987)

1P12

Magnetohydrodynamic Current Drive for Fusion Confinement

G.B. Kirby Meacham and Barbara J. Quill, Meacham & Company, Shaker Ht., OH 44122, USA

Magnetohydrodynamic Current Drive for Fusion Confinement

G. B. Kirby Meacham and Barbara J. Quill Meacham & Company

A closed current loop in a plasma is an effective means of confining plasma for fusion reactions, and is widely used in the tokamac and a variety of other toroidal systems. The problem is that the current loops are typically formed by induction, and therefore limited to pulsed operation. Methods such as helicity injection or the bootstrap effect to achieve steady state operation have been investigated with the tokamac, but tend to be complex.

Magnetohydrodynamic current drive, in contrast, offers a simple means of forming and maintaining steady-state current loops in fusion reactors. Plasma flow through an axially symmetric converging magnetic stator field acts as an internally shorted magnetohydrodynamic generator that forms a freestanding stationary current loop in the plasma stream. The current loop is sustained by flow energy, and remains at steady state as long as the flow continues. Further, refueling is automatic. The through flow of plasma brings in fresh fuel and removes reaction products.

Influence of Triangularity and Ellipticity on the Poloidal Field Around a Tokamak Magnetic Surfaces

P. Martin and J. Puerta, Universidad Simon Bolivar, Caracas 7080A, Venezuela

INFLUENCE OF TRIANGULARITY AND ELLIPTICITY ON THE POLOIDAL FIELD AROUND A TOKAMAK MAGNETIC SURFACES

P. Martin and J.Puerta

January 7, 1999

Departamento de Física, Universidad Simón Bolívar Apdo. 89000, Caracas-Venezuela e-mail: pmartin@usb.ve, jpuerta@usb.ve

Abstract

In previous paper an equation for the poloidal magnetic field around a tokamak surface was described [1]. We analyze here the effect of the tringularity and ellipticity [2] on that poloidal field. An expansion in the triangularity parameter is carried out and compared with the case when no triangularity is present. Numerical computation for different values of the ellipticity and triangularity have been also performed.

References

- 1.- P. Martin and M.G. Haines *Phys. Plasmas*, **5**, 410 (1998).
- C.M. Roach, J. W. Connor and S. Janjua, Plasma Phys. Control Fusion, 37, 679 (1995).

1P14

Preliminary Results from the Flow-Through Z-Pinch Experiment: ZaP

U. Shumlak, B.A. Nelson, R.P. Goilingo, D. Tang and E. Crawford, D.J. Den Hartog and D.J. Holly, University of Washington, Seattle, WA 98195- 2250, USA

Preliminary Results from the Flow-Through Z-Pinch Experiment: ZaP*

U. Shumlak, B.A. Nelson, R.P. Golingo, D. Tang, and E. Crawford

Aerospace and Energetics Research Program
University of Washington
Seattle, Washington

D.J. Den Hartog, and D.J. Holly
 Sterling Scientific, Inc.
 Madison, Wisconsin

The stabilizing effect of an axial flow on the m=1 kink instability in z-pinches has been studied numerically by reducing the linearized ideal MHD equations to a one-dimensional eigenvalue equation for the radial displacement. A diffuse z-pinch equilibrium is chosen that is made marginally stable to the m=0 sausage mode by tailoring the pressure profile. The principal result reveals that a sheared axial flow does stabilize the kink mode when the shear exceeds a threshold value which is inversely proportional to the wavelength of the mode. This threshold value can be satisfied with a peak flow which is less than the Alfven speed for certain wavelengths. Additionally, the m=0 sausage mode is driven from marginal stability into the stable regime which suggests that the equilibrium pressure profile control can be relaxed. The flow stabilization agrees with experimental observations. The details of the theoretical development will be presented.

The implications of this stabilizing effect are to be investigated with a flow-through Z-pinch experiment, ZaP. The experiment will produce a Zpinch plasma which is 50 cm in length by initiating the plasma with a one meter coaxial gun. The design of the experiment will be presented in this paper. Velocity profile measurements will be made using a spectrometer. The spectrometer will have 20 cords through the pinch. Multicord, time-dependent density measurements will be made using interferometry. A two-dimensional mapping of the density will be generated with a holography system to produce a zebra-stripe interferogram. Other diagnostics include surface and insertable B-dot probes and a fast framing camera.

^{*} This work is supported by a grant from the Department of Energy.

Magnetized Target Fusion: No Capital Investment Required

Irvin R. Lindemuth, Richard E. Siemon, Ronald C. Kirkpatrick, Robert E. Reinvosky , Los Alamos National Laboratory, Los Alamos, NM 87545, USA

MAGNETIZED TARGET FUSION: NO CAPITAL INVESTMENT REQUIRED!!!

Irvin R. Lindemuth, Richard E. Siemon, Ronald C. Kirkpatrick, Robert E. Reinovsky Los Alamos National Laboratory, Los Alamos NM

The constraints of steady-state operation for magnetic confinement and of no magnetic field for inertial confinement have forced fusion research into two extreme corners separated by more than ten orders of magnitude in time and density scales and requiring multi-billion dollar capital investments for the next steps. Simple analysis shows that combining the compressional heating of inertial confinement with the thermal insulating properties of magnetic confinement and operating in a density and time space intermediate between the two conventional fusion approaches leads to a path to fusion that can be accessed by pulsed power facilities that either already exist or are under construction in non-fusion contexts.

1P16

Computational Investigation of Plasma-Wall Interaction Issues In Magnetized Target Fusion

Peter Sheehey, Walter Atchison, Rickey Faehl, Ronald Kirkpatrick, Irvin Lindemuth and Richard Siemon, Los Alamos National Laboratory, Los Alamos, NM 87545, USA

COMPUTATIONAL INVESTIGATION OF PLASMA-WALL INTERACTION ISSUES IN MAGNETIZED TARGET FUSION

Peter Sheehey, Walter Atchison, Rickey Faehl, Ronald Kirkpatrick, Irvin Lindemuth, and Richard Siemon Los Alamos National Laboratory, Los Alamos, NM 87545 USA

In the concept known as Magnetized Target Fusion (MTF) in the United States and Magnitnoye Obzhatiye (MAGO) in Russia, a preheated and magnetized target plasma is hydrodynamically compressed to fusion conditions. Because the magnetic field suppresses losses by electron thermal conduction in the fuel during the target implosion heating process, the implosion velocity may be much smaller than in traditional inertial confinement fusion. Hence "liner-onplasma" compressions, magnetically driven using relatively inexpensive electrical pulsed power, may be practical. The relatively dense, hot target plasma, with starting conditions O(10¹⁸ cm⁻³, 100 eV, 100 kG), may spend 10 or more microseconds in contact with a metal wall during formation and compression. Influx of a significant amount of high-Z wall material during this time could lead to excessive cooling by dilution and radiation that would prevent the desired nearadiabatic compression heating of the plasma to fusion conditions. Magnetohydrodynamic (MHD) calculations including detailed effects of radiation, heat conduction, and resistive field diffusion are being done, using several different computer codes, to investigate such plasma-wall interaction issues in ongoing MTF target plasma experiments and in proposed liner-on-plasma MTF experiments.

Ana; ysis of Magnetic Surface Functions using Experimentally Measured Data

T. Yamaguchi, M. Macyama Saitama University, Japan

Analysis of Magnetic Surface Functions using Experimentally

Measured Data

T.Yamaguchi, M.Maeyama Saitama University, Japan

A reversed field pinch (RFP) has a property that plasma itself makes magnetic fields which are necessary to confine plasma. The self organization phenomenon is explained by Taylor's relaxation theory. From the artificial or theoretical considerations of relaxation processes, forms of the magnetic surface function I=rB_t and P, where B_t is a toroidal magnetic field and P is a kinetic pressure, are derived and used for equilibrium, stability and transport analyses.

For axi-symmetric plasma which are Tokamak or RFP, we are developing a code to interpolate these surface functions from experimentally measured data.

The merits of this code are as follows:

- •We identify a more realistic surface function and compare those with theoretical ones.
 - · We can analyze realistic equilibrium configurations.
- •We can obtain the time history of the helicity which is a crucial parameter of the relaxation theory.

As for measured data, we use poloidal flux at some points of vacuum vessel surface, toroidal flux, F-value, θ -value and β -value at a plasma center. As the results, we could develop the code which derives surface functions I, P from those data. And effects of measurement error on those functions are examined

2

De Anza Ballroom 1: 30 PM, Monday, June 21, 1999

Plenary Talk

"The inexorable plasma processing challenges presented by Moore's law"

Rick Gottscho LAM Inc.

De Anza I 3 PM, Monday, June 21, 1999

Oral Session 2A

Space Plasmas and Partially Ionized Gases

Chairperson

Shahid Rauf

University of Illinois

2A01-02

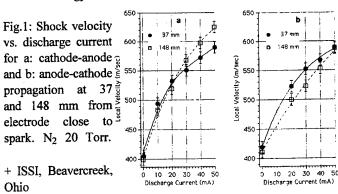
Invited -

Plasma-Shock Interactions in a Low Pressure Positive Column

B.N. Ganguly, P. Bletzinger and A. Garscadden, U.S. Air Force Research Laboratory, Innovative Scientific Solution Inc., Dayton, OH 45440-3638, USA

Plasma - Shock Interactions in a Low Pressure Positive Column

B.N.Ganguly, P,Bletzinger+ and A.Garscadden Air Force Research Laboratory, WPAFB, Ohio 45433 We have investigated the effect of interactions of weak acoustic shock (<Mach 2) propagation on the shock velocity, shock dispersion, current-voltage modulation and spatially-temporally resolved plasma induced emission in low pressure (5-20 Torr), low current (2 to 10 mA/cm²) N₂ positive column discharges. The acoustic shock impulse was produced by a 40 - 140 Joule stored energy electric spark discharge. Simultaneous multipoint laser photodeflection measurements of shock propagation local velocity change versus axial distance in the positive column showed that the shock velocity increased with increasing path length. The increase is not only depending on the discharge current density but also on the polarity of the applied electric field (fig.1). These observations suggest the shock speed increase may involve relatively long range shock - electrostatic - thermal energy exchange through screened Coulomb interactions. Furthermore, the shock wave dispersion and damping for a given gas pressure and discharge current is dependent on the shock amplitude. Similarly, for a given discharge condition, the observed recovery of the shock dispersion in the post discharge region is also dependent on shock amplitude. All these observations can not entirely be explained by axial and radial temperature gradients. The shock induced discharge current-voltage and N₂ C - B emission modulation show that the electric field perturbation ahead of the shock is dependent on the applied electric field direction and correlates with the shock speed increase in the plasma. The plasma-shock interaction is strong enough to extinguish the C-B plasma emission behind the shock wave. The measurements suggest shock induced local E/N modification ahead of the shock front is relevant to the observed shock velocity and dispersion change. The requirement of current continuity possibly is a mechanism for the shock to electrostatic to kinetic energy transfer.



Second Harmonic RF Currents in a Cylindrical ICP with a Planar Coil

V.A. Godyak, R.B. Piejak and B.M. Alexandrovich, Osram Sylvania Development Inc, Beverly, MA 01915, USA

Second Harmonic RF Currents in a Cylindrical ICP with a Planar Coil

V. A. Godyak, R. B. Piejak and B. M. Alexandrovich OSRAM SYLVANIA Development Inc. Beverly, MA 01915

The possibility of non-linear effects in inductively coupled plasma (ICP) associated with rf components of the magnetic field is a subject of discussion in the current literature. It has been shown that the rf magnetic field changes the direction of electron acceleration and may modulate the plasma density and generate an rf field at the second harmonic in the skin layer of an ICP. Here we report on experimental observations of rf currents at the second harmonic $J_{2\omega}$ directed orthogonal to the main azimuthal (θ) discharge current at the fundamental frequency $J_{\theta\omega}$. resolved measurement of the axial $J_{z2\omega}(r)$ and radial $J_{r2\omega}(z)$ components of the rf current density at the second harmonic have been performed with a magnetic (dB/dt) probe in an ICP driven at 3.39; 6.78 and 13.56 MHz in argon gas at 1, 10 and 100 mTorr. An independent measurement of $J_{z2\omega}(r)$ has also been made with a flat differential Langmuir probe maintained at the plasma potential. The measurements show that the second harmonic current is nearly proportional to the discharge power, inversely proportional to the square of the driving frequency and is falling with gas pressure. The spatial dependencies of the phase of $J_{z2\omega}(r)$ and $J_{r2\omega}(z)$ suggest a circular (poloidal) structure of the second harmonic current forming a closed path with a corresponding azimuthal (toroidal) rf magnetic field at the second harmonic. Integration of $J_{z2\omega}(r)$ over the discharge cross-section has shown that the total axial rf current at the second harmonic is nearly zero. This supports the notion of a closed current path at the second harmonic and is a consequence of the multi-dimensional ICP structure and the presence of a weakly conductive sheath on the plasma boundaries. The second harmonic currents $J_{z2\omega}(r)$ and $J_{r2\omega}(z)$ found in this work originate from Lorentz force $\propto [JxB] \propto \cos^2(\omega t + \phi)$, produced by the interaction between current density $J_{\theta\omega}$ and components of the rf magnetic field $B_{r\omega}$ and $B_{z\omega}$. This essentially non-linear effect occurs in both collisional and stochastic heating regimes and is most pronounced at the lowest gas pressure and the lowest driving frequency where the electron drift velocity and the rf magnetic field maintaining the ICP are greatest.

2A04

A Traveling Wave Driven, Inductively Coupled Large Area Plasma Source

Yaoxi Wu and M.A. Lieberman, University of California-Berkeley, Berkeley, CA 94720, USA

A Traveling Wave Driven, Inductively Coupled Large Area Plasma Source*

Yaoxi Wu and M. A. Lieberman University of California, Berkeley CA 94720

A large area inductive plasma source driven by a 13.56 MHz traveling wave has been investigated. Launching a traveling wave eliminates standing wave effects to obtain a uniformly excited processing plasma. The plasma source is rectangular in shape with a processing area of 71cm × 61cm, and contains a substrate holder large enough to study processing of 300 mm diameter silicon wafers and 360 mm × 465 mm glass substrates. The antenna coil consists of a series (serpentine) connection of eight parallel rods embedded in the plasma inside thin quartz tubes. The antenna coil configuration and the circuit used to launch a traveling wave are described. The plasma properties, including plasma potential, ion density profile, and electron temperature were measured as a function of discharge power (up to 2000 W) and gas pressure (1-100 mTorr), with a capacitive probe and a Langmuir probe. The Langmuir probe is driven by two stepper motors to provide a two-dimensional density profile. Both motor motion and data acquisition and processing are controlled by a computer in real time through a data acquisition board. We find that it is possible to tune the system to launch a traveling wave for a wide range of powers and pressures. The measured plasma densities ranged up to 3×10^{11} cm⁻³, indicating an inductive coupling mode. The efficiency of delivery of the rf power to the plasma is 77% at 500 watts and 18 mTorr. The measurements are compared to analytical and numerical simulation models of the coupled circuit-antenna-plasma system.

^{*} Work supported by the UC-SMART Program No. SM-97-01 and the NFS Grant No. ECS-95-29658

Unstable Behavior of Plasma in Inductive Discharges

A.M. Marakhtanov and M.A. Lieberman, University of California - Berkeley, Berkeley, CA 94720, USA

Unstable Behavior of Plasma in Inductive Discharges*

A.M. Marakhtanov and M.A. Lieberman
Department of Electrical Engineering and Computer
Sciences
University of California, Berkeley, CA 94720

Instabilities in a transformer coupled plasma (TCP) source have been studied. An inductive discharge has been created by a 13.56 MHz rf-driven planar inductive coil mounted on the top of an aluminum cylindrical vacuum chamber. Electronegative gases such as O₂ and SF₆ and their mixtures with Ar have been used as operating gases.

To detect plasma instabilities, time-resolved diagnostics have been used including optical emission spectroscopy and Langmuir probe measurements of the ion current. Instabilities have been observed in a transition region where the discharge changes its mode from capacitive (E-mode) to inductive (H-mode). Frequencies of plasma fluctuations (fluctuations of the ion current or intensity of the light emitted from the plasma) were in the range of 1 Hz –0.9 MHz for operating gas pressures of 2.5-20 mTorr and an absorbed power of 150-600 W. These plasma instabilities may be related to a hysteresis-like behavior of the inductive discharge in the E-H transition region and associated with the balance of power absorbed and lost by electrons.

2A06

Nonlinear Stabilization of the Weibel Instability Driven by Counterstreaming Ion Beams

Nagendra Singh and W. C. Leung, Elect. & Comp. Engr. Dept., University of Alabama, Huntsville, AL 35899, USA

Nonlinear Stabilization of the Weibel Instability Driven by Counterstreaming Ion Beams

Nagendra Singh and W. C. Leung

Department of Electrical and Computer Engineering
University of Alabama in Huntsville
Huntsville, Alabama 35899

Counterstreaming ion beams are a common feature of the Earth's magnetosphere. Such ion beams occur in the outer regions of the plasmasphere, the plasma sheet and the lobes. Weibel showed that when fast ion beams counterstream they drive purely growing modes. We have studied the excitation and nonlinear evolution of the ion-beam driven instabilities by means of a 2.5-D particle-in-cell code. It is shown that in the electrostatic regime, the instability is not effective in slowing down the beams; it is stabilized by perpendicular heating of the beam ions. The driven waves interact with the beam ions through the anomalous cyclotron resonance, which converts a small fraction of the parallel drift energy of the beam ions into their perpendicular energy. As the ions' perpendicular energy increases, the increase in the ion Larmor radius ρ_i makes $J_n(k_\perp \rho_i) \rightarrow 0$, where J_n is the Bessel function of order n, k_{\perp} is the wavelength perpendicular to the ambient magnetic filed. This stops the perpendicular ion energization and the instability is quenched. Since for the electrostatic ion cyclotron modes $k_1 \rho_i \sim 1$; the perpendicular ion acceleration by the electrostatic Weibel instability is only modest. The perpendicular acceleration of ions leads to change in the ions' pitch angle. This leads to the trapping of the ions in a magnetic mirror. Incorporation of these results into large-scale refilling model of the plasmashpere will be discussed.

^{*}Work supported by the UC-SMART Program No. SM-97-01 and the NSF Grant No. ECS-95-29658

DSCS Satellite Dielectric Charging Correlation with Magnetic Activity

Shu T. Lai, U.S. Air Force Research Laboratory, Hanscom AFB, MA 01731, USA

DSCS Satellite Dielectric Charging Correlation with Magnetic Activity

Shu T. Lai Air Force Research Laboratory Hanscom AFB, MA 01731

Spacecraft charging is a result of spacecraft-plasma interaction in space. The onset of spacecraft charging depends not only on the surface material properties but also on the density and temperature of the ambient plasma. While the surface material properties are practically constant, the space plasma condition varies in time everyday. The variable space plasma condition is now commonly called space weather. In recent years, it has been established that the Sun controls significantly the Earth's space weather. The Sun sends out plasma clouds propagating through and interacting with the interplanetary magnetic field. When a significant plasma cloud reaches the Earth's geomagnetic environment, the Earth's magnetic field and plasma conditions are disturbed. Compression and stretching of the magnetic field lines can result in plasma energization. Energetic plasma can cause the onset of negative charging of spacecraft surface materials. Extremely energetic (MeVs) electrons and ions can even cause deep (or bulk) charging in materials of low conductivity. We present the statistical results of three years of charging events of the dielectric surface samples on a DSCS satellite at geosynchronous altitudes and confirm a high correlation of the events with the level of geomagnetic activity.

2A08

Ion Energy Distribution in NF₃ Based Process Chamber Cleaning Discharges

H.P. Hsueh, B.S. Felker, R.T. McGrath and J.G. Langan, Air Products & Chemicals, Inc, Allentown, PA 18195, USA

Ion Energy Distribution in NF₃ Based Process Chamber Cleaning Discharges

H.P. Hsueh, B.S. Felker⁺, R.T. McGrath, and J.G. Langan⁺

Electronic Materials & Processing Research Laboratory Engineering Science & Mechanics Department 227 Hammond Building The Pennsylvania State University State College, PA 16802

*Air Products & Chemicals, Inc. 7201 Hamilton Boulevard Allentown, PA 18195-1501

Abstract

NF₃ based discharges are commonly used for cleaning residual silicon dioxide and nitride from plasma enhanced chemical vapor deposition (PECVD) process chambers. In order to find a balance between fast chamber cleans and overly aggressive cleaning chemistries, which can lead to premature hardware failure, a fundamental understanding of the physical and chemical characteristics of the discharge is required. For this reason, we have measured the ion energy distribution functions (IEDFs) and the relative concentration of the ionic and neutral species present within capacitively coupled parallel plate discharges operated with NF, diluted with either argon, helium, neon or oxygen. For reactor operation at a fixed power of 1.35 W/cm² and fixed NF₃ mole fraction of 25%, we found that when argon was used as the diluent, the principal ion present was Ar+ for all pressures investigated (0.5-1.5 Torr). In contrast, for similar reactor operating conditions using helium dilution, He⁺ concentration was relatively low, with NF₂⁺, N₂F⁺, F^+ , F_2^+ , and N_2^+ all having larger concentrations.

Under all operating conditions studied, double peaked IEDFs were observed. These result when ion transit times across the plasma sheath are faster than the rf power cycle. Incident ion energies for argon diluted plasmas had mean energies near 20 eV and peak energies often in excess of 40 eV. Helium, neon and oxygen diluted discharges had mean ion energies of 10 eV with peak energies near 20 eV. For each diluent studied, the IEDFs shifted toward lower energies with increasing discharge electronegativity and increasing pressure, reflecting increased collisionality within the discharge. For example, NF₃/O₂ discharges at 0.75 Torr have mean ion energies near 4 eV and peak ion energies below 10 eV.

De Anza II 3 PM, Monday, June 21, 1999

Oral Session 2B Microwave Plasmas

Chairperson

John Scharer

University of Wisconsin

2B01-2

Invited -

Test Facility for High Pressure Plasmas

Rolf Block, Mounir Laroussi & Karl H. Schoenbach, Old Dominion University, Norfolk, VA 23529, USA

Test Facility for High Pressure Plasmas*

Rolf Block, Mounir Laroussi, and Karl H. Schoenbach Physical Electronics Research Institute/ Appl. Research Center Old Dominion University, Norfolk/ Newport News, VA

High pressure nonthermal plasmas are gaining increasing importance because of their wide range of applications, e.g. in air plasma ramparts, gas processing, surface treatment, thin film deposition, and chemical and biological decontamination. In order to compare various methods of plasma generation with respect to efficiency, development of instabilities, homogeneity, lifetime etc., a central test facility for high pressure plasmas is being established.

The facility will allow us to study large volume (> 100 cm³), nonthermal (gas temperature: < 2000 K) plasmas over a large pressure range (10⁻⁶ Torr up to more than 1 atmosphere) in a standardized discharge cell. The setup was designed to generate plasmas in air as well as in gas mixtures. The available voltage range extends to 25 kV dc (10 kW power). The electrodes can be water cooled.

Electrical diagnostics include a 400 MHz, 2 GS/s 4channel oscilloscope for current and voltage measurements and the detection of the onset of instabilities.

For optical diagnostics, a CCD video camera is used to record the appearance of dc discharges. A high-speed light intensified CCD-camera (25 mm MCP with photocathode, gating speed: 200 ps, adjustable in 10 ps steps) allows to study the development of instabilities and can also be utilized in temporally resolved spectroscopic measurements.

Optical emission spectroscopy allows us to determine plasma parameters such as electron density (through Stark broadening measurements) and gas temperature measurements. We have particularly concentrated our efforts on gas temperature diagnostics. The rotational structure of the second positive system of nitrogen contains information on the neutral gas temperature, which is identical with the rotational temperature [1]. Taking the apparatus profile into account, the temperature of the rotational excited molecules is determined by a comparison of simulated and measured data. A spectrograph with an instrument profile of FWHM=0.1Å is available.

Interferometry is well suited for electron density measurements especially in weakly ionized plasmas. A 4 mm microwave interferometer will be used for this diagnostics. Number densities up to $7\cdot10^{13}$ cm⁻³ can be measured in this wavelength range. For higher densities we plan to use an IR interferometer with a CO₂ laser as source.

- * Funded by the Air Force Office of Scientific Research in Cooperation with the DDR&E Air Plasma MURI Program.
- [1] Rolf Block, Olaf Toedter and Karl H. Schoenbach, "Temperature Measurement in Microhollow Cathode Discharges in Atmospheric Air", Bull. APS 43, No. 6, NW1 2, p. 1478, 1998.

Microhollow Cathode Discharges in Atmospheric Air

R.H. Stark, U. Ernst, R. Block, M. El-Bandrawy and K.H. Schoenbach, Old Dominion University, Norfolk, VA 23529, USA

Microhollow Cathode Discharges in Atmospheric Air

R. H. Stark, U. Ernst¹, R. Block, M. El-Bandrawy, and K. H. Schoenbach Physical Electronics Research Institute, Old Dominion University, Norfolk, VA 23529

Microhollow electrode discharges (MHCD) [1] are gas discharges between closely spaced (submillimeter) electrodes containing openings with diameter, D, on the same order as the electrode gap. In previous experiments the reduction of the size of the cathode opening to 100 µm has allowed us to generate stable, direct current discharges in air up to atmospheric pressure [2]. The microhollow cathode discharges were operated at currents of up to 20 mA, corresponding to current densities of 250 A/cm² and at average electric fields of 16 kV/cm. The gas temperature of the MHCD was determined by spectroscopic measurements of the excited vibrational states of the nitrogen molecules. First results indicate that the gas temperature at atmospheric pressure and currents of 20 mA is close to 2000 °K. Parallel operation of MHCDs can be achieved by ballasting each discharge resistively [3]. Without resistive ballast, the discharge itself needs to be resistive, that means the current voltage characteristic of the discharge must have a positive slope. Results of modeling [4] show an increase of the forward voltage with current at high current values. However, overheating of the electrodes prevents de operation of parallel discharges in atmospheric air in this current range. In order to extend the range of operation into the high current mode, were the discharge becomes resistive, it needs to be pulsed. In pulsed operation, with pulse duration in the range from 1 to 100 microseconds, the current range could be extended to 80 mA. At higher current, glow-to-arc transition was observed. The results show, that pulsed operation at high current might allow to operate discharges in parallel without individual ballast.

[1] K. H. Schoenbach, A. El-Habachi, W. Shi, and M. Ciocca, "High Pressure Hollow Cathode Discharges," Plasma Sources Science and Technology 6, 468 (1997).

[2] R. Block, O. Toedter, and K. H. Schoenbach, "Temperature Measurements in Microhollow Cathode Discharges in Atmospheric Air", Bull. APS 43, 1478 (1998).

[3] W. Shi, R. H. Stark and K. H. Schoenbach, "Parallel Operation of Microhollow Cathode Discharges", to appear in IEEE Trans. Plasma Science.

[4] A. Fiala, L. C. Pitchford, and J. P. Boeuf, Proc. XXII Conf. Phenomena in Ionized Gases, Hoboken, NJ, 1995, Contr. Papers 4, p.191.

This work was solely funded by the Air Force Office of Scientific Research (AFOSR) in cooperation with the DDR&E Air Plasma Ramparts MURI program.

2B04

Further Investigation of P.I.A. (Persistant Ionization in Air) Plasmas Using Room Air

J.F. Kline, J.E. Brandenburg and Vincent DiPietro, Research Support Instruments, Lanham, MD 20706, USA

Further Investigation of PIA(Persistant Ionization in Air) Plasmas Using Room Air

J.F.Kline, J.E. Brandenburg, and Vincent DiPietro 4325-B Forbes Blvd. Research Support Instruments Lanham Maryland

Further research on PIA (Brandenburg and Kline 1998) plasmas, glow discharge-type plasmas created in room air, is reported. These plasmas can be made in a modified 1kW microwave oven (2.45 GHz) and can be sustained for an indefinite period by the microwaves. They have now been made in a much larger size using 915MHz industrial microwaves at 30-75kW of microwave power. These new plasmas range from roughly spherical and approximately 50cm in diameter to highly irregular and dynamic shapes of larger size. Thus it is demonstrated that the PIA phenomenon can be scaled upward in size and power. The properties of the 915MHz PIA plasmas appear similar to that made with 2.45GHz, except that visible spectra appear to display more bright bands. The plasma also appears to seek microwave sources, like a classic breakdown, rather than retreat from it, as is the behavior of the PIA at 2.45GHz. This suggests that the 915MHz plasmas may be more strongly driven and closer to a classical arc discharge in properties. Further measurements on PIA plasmas will be reported. We believe these plasmas are a new and unusual plasma state first reported by Manwaring and Powell and Finklestein (1970) whom used 30kW at 75 MHz. Recent research results will be shown. Work supported by AFOSR.

J.R. Powelland D. Finkelstein (1970) American Scientist 58,1970, p. 262.

Brandenburg J. E. and Kline J. F. (1998) IEEE Transactions on Plasma Science, 26, 2, p145.

Radio-frequency Sustainment of a Laser-Produced Plasma

K.L. Kelly, J. E. Scharer, G. Ding, H. Gui and E. Paller, University of Wisconsin, Madison, WI 53706-1687, USA

Radiofrequency Sustainment of a Laser-Produced Plasma

K. L. Kelly, J. E. Scharer, G. Ding, H. Gui and E. Paller

Department of Electrical and Computer Engineering University of Wisconsin, Madison 53706

The plasma is generated by photoionization of the organic seed molecule tetrakis(dimethylamino)ethylene (TMAE) and is sustained by RF coupling through the use of an antenna. Both highly collisional ohmic heating, and collisionless Landau wave absorption are studied as various neutral gas pressures are varied over several orders of magnitude. A multiple turn helical coil is utilized to maintain the discharge and a strong magnetic field is introduced to enhance field penetration. A strong magnetic field gradiants is used to help initiate the discharge. Plasma densities of the order 10¹³ cm⁻³ are obtained in a 2.5 cm radius tube. The computer codes^a ANTENA2 and MAXEB are used to help model the results. Non linear effects of collisionless damping and plasma creation are investigated. TMAE gas is being investigated as a possible seed gas for initiating atmospheric air plasmas because the plasma can be initiated with such a high initial condition^b.

Acknowledgments

Air Force Office of Scientific research grants (Grant F49620-97-1-0262) Defense Department Research and Engineering Air Plasma Ramparts Multi-University Research Initiative and in part by NSF grant ECS-9632377.

2B06

Laser and Radio-frequency Wave Creation of Seeded Air Plasmas

J. Scharer, G.Ding, X. Guo, H. Gui, K. Kelly and E. Paller, University of Wisconsin, Madison, WI 53706-1687, USA

Laser and Radiofrequency Wave Creation of Seeded Air Plasmas

J. Scharer, G. Ding, X. Guo, H. Gui, K. Kelly and E. Paller

Department of Electrical and Computer Engineering University of Wisconsin, Madison 53706

We are examining 193 nm laser ionization of an organic seed gas TMAE(tetrakis-dimethyl-amino-ethylene) in air plasma constituants including nitrogen and oxygen. The peak plasma density($n \ge 10^{13}~{\rm cm}^{-3}$, temperature($T_e = 0.2~{\rm eV}$) and lifetimes are measured for pure TMAE and with the air constituants added at pressures from 100 mTorr to atmospheric. The role of superexcited states, metastable states and the seed gas character is discussed. The effect of the wave frequency, magnetic field and antenna design for radiofrequency created plasmas in seed gases(argon and TMAE) and added air constituants are discussed. We examine laser and high voltage spark initiated plasmas at higher pressures and their radiofrequency sustainment. Modelling utilizing the ANTENAII^a and MAXEB^b codes are used to describe the wave penetration and absorption for different antennas.

Acknowledgments

Air Force Office of Scientific research grants (Grants F49620-94-1-0054 and F49620-97-1-0262) Defense Department Research and Engineering Air Plasma Ramparts Multi-University Research Initiative and in part by NSF grant ECS-9632377.

^aY. Mouzouris and J. E. Scharer. *Phys. Plasmas*. **5**(12): 4253-61, 1998.

^bK. Kelly, et. al. Journ. App. Phys. **85**(1): 63-68 1998

^aY. Mouzouris and J. E. Scharer. *IEEE Trans. Plasma Sci.*. **24**(1): 152-160, 1996.

^bY. Mouzouris and J. E. Scharer. *Phys. Plasmas.* **5**(12): 4253-61, 1998.

Improved Air Filtration and Filter Sterilization Using DC Electric Fields and a One Atmosphere Uniform Glow Discharge Plasma (OAUGDP)

J. Reece Roth, Daniel M. Sherman, Rami B. Gadri, Zhiyu Chen, Fuat Karakaya, Thomas C. Monite, Kimberly Kelly-Wintenberg, and Peter P.Y. Tsai, University of Tennessee, Knoxville, TN

IMPROVED AIR FILTRATION AND FILTER STERILIZATION USING DC ELECTRIC FIELDS AND A ONE ATMOSPHERE UNIFORM GLOW DISCHARGE PLASMA (OAUGDP)*

<u>Dennis J. Helfritch</u> and Paul Feldman Environmental Elements Corporation, Baltimore, MD

J. Reece Roth¹, Daniel M. Sherman¹, Rami B. Gadri¹, Zhiyu Chen¹, Fuat Karakaya¹, Thomas C. Montie², Kimberly Kelly-Wintenberg², and Peter P.-Y. Tsai³ The University of Tennessee, Knoxville, TN

ABSTRACT

The filtration of bacteria and viruses from indoor air is hindered by two characteristics of the organisms - their extremely small size and the ability to reproduce. The effective filtration of particles the size of microorganisms - tens of nanometers to a few microns - is difficult, and the organisms captured by the filter can reproduce in situ and be released into the airstream, giving rise to the "sick building syndrome". The application of DC electric fields and atmospheric plasmas such as the One Atmosphere Uniform Glow Discharge Plasma^[1] (OAUGDP) to a filter can address both of these challenges. Enhancement of filter capture efficiency through the application of DC electrostatic fields is well established. Electrophoretic effects induced by a strong electric field produce an attractive force between particles and filter fibers, resulting in significantly enhanced filter efficiency, especially for small particles. The sterilization of surfaces through exposure to the One Atmosphere UniforM Gas Discharge Plasma has been demonstrated to be very effective^[2]. At UTK we have recently developed the "Volfilter" (TM), a. planar version of the OAUGDP produced by attaching insulated rod electrodes to both sides of a sheet of dielectric filter material and energizing the electrodes with a high voltage, low frequency RF source. Thus the mode of operation is that when the filter material captures microorganisms by DC fieldenhanced filtration, the captured microorganisms are killed by periodic plasma sterilization by the Volfilter. The combination of these effects results in effective capture and sterilization of even the smallest microorganisms and requires minimum maintenance. This paper will describe results obtained during the operation of a laboratory-scale DC enhanced filter and a Volfilter challenged by two kinds of microorganisms, Staphylococcus aureus and the bacterial virus Phi X 174. We will present data showing that the Volfilter is capable of more than a 100,000-fold reduction in the number of captured S. aureus.

- *This work was supported in part by EPA contract 68-D-98-118.
- ¹.) Department of Electrical Engineering ².) Department of Microbiology ³.) UTK Textiles and Nonwovens Development Center (TANDEC)
- 1.) Roth, J. R. (1995): Industrial <u>Plasma Engineering: Volume 1 Principles</u>. Institute of Physics Press, Bristol, UK ISBN 0-7503-0318-2. See Section 12.5.2.

 2.) Kelly-Wintenberg, K; Montie, T. C.; Brickman, C; Roth, J. R.; Carr, A. K.; Sorge, K.; Wadsworth, L.; and Tsai, P. P.-Y. (1998): "Room Temperature Sterilization of Surfaces and Fabrics with a One-Atmosphere Uniform Glow Discharge Plasma". Journal of Industrial Microbiology & Biotechnology Vol. 20, PP 69-74.

2B08

Sterilization By Plasma Active Species at One Atmosphere Using a Remote Exposure Reactor (RER)

Daniel M. Sherman, Rami B. Gadri, Fuat Karakaya, Zhiyu Che, Thomas C. Montie, Kimberly Kelly-Wintenberg, Peter P.Y. Tsai and J. Reece Roth,

STERILIZATION BY PLASMA ACTIVE SPECIES AT ONE ATMOSPHERE USING A REMOTE EXPOSURE REACTOR (RER)*

Daniel M. Sherman¹, Rami B. Gadri¹, Fuat Karakaya¹, Zhiyu Chen¹, Thomas C. Montie², Kimberly Kelly-Wintenberg², Peter P.-Y. Tsai³, and J. Reece Roth¹ The University of Tennessee, Knoxville, TN

Dennis J. Helfritch and Paul Feldman Environmental Elements Corporation, Baltimore, MD

ABSTRACT

In the past few years, intensive efforts have been made to develop for plasma processing such atmospheric plasmas as corona discharges, dielectric barrier discharges, filamentary discharges, atmospheric arcs, and the One Atmosphere Uniform Glow Discharge Plasma^[1] (OAUGDP) to avoid the consequences of operating in vacuum systems. In many plasma processing applications at one atmosphere, the requirement that the workpiece be immersed in the plasma or located at the plasma surface can lead to damage by high electric fields, overheating of the workpiece, etching or erosion by active species other than those which produce the desired effect, exposure to ultraviolet radiation, etc. In addition, large or irregularly shaped workpieces cannot fit between the electrodes of many of these atmospheric plasma reactors, limiting their use to flat workpieces, fabrics, or webs.

At the UTK Plasma Sciences Laboratory we developed a Remote Exposure Reactor (RER) based on the OAUGDP^[1] which generates a plasma in an array of flat panels^[2] using air or other gases at one atmosphere. The RER convects the active species responsible for sterilization and increasing the surface energy of materials to a remote chamber in which the workpiece is located. This arrangement allows workpieces of any size or shape to be exposed to active species in the remote chamber, and does not make it necessary to expose them to the detrimental effects of being in direct contact with the plasma. The RER has closed return air recirculation, which convects active species at least once around the pneumatic loop, thus building up their concentration above that characteristic of a single pass of the active-species laden airflow past the workpiece. The active species of most relevance to sterilization and increasing surface energy appear to be atomic oxygen and possibly ozone. We have demonstrated the ability of the RER to increase the surface energy of workpieces in the remote exposure chamber, and to reduce the number of microorganisms on test samples by several powers of ten. Specific examples of the performance of the RER will be reported at the conference.

- *This work was supported in part by a subcontract with the Environmental Elements Co. of Baltimore, MD under AFOSR contract 98-C-0069.
- ¹.) Department of Electrical Engineering ².) Department of Microbiology ³.) UTK Textiles and Nonwovens Development Center (TANDEC)
- 1.) Roth, J. R. (1995): Industrial <u>Plasma Engineering: Volume I. Principles</u>. Institute of Physics Press, Bristol, UK ISBN 0-7503-0318-2. See Section 12.5.2.
 2.) Roth, J. R. (1997): Method and Apparatus for Covering Bodies with a Uniform Glow Discharge Plasma and Applications Thereof. U. S. Patent #5,669,583, Issued September 23, 1997.

New Plasma Concepts for Enhanced Microwave Vacuum Electronics

J.R. Hoffman, P. Muggli, M.A. Gundersen, W.B. Mori, C. Joshi and T.Katsouleas, University of Southern California, Los Angeles, CA 90089-1341, USA

"New Plasma Concepts for Enhanced Microwave Vacuum Electronics"

J.R.Hoffman, P. Muggli, M.A. Gundersen, W.B.Mori*, C. Joshi*, and T. Katsouleas

Electrical Engineering- Electrophysics Department, University of Southern California, Los Angeles CA 90089, USA

*Electrical Engineering Department, University of California, Los Angeles CA 90095, USA

Recently, new concepts in the field of microwave radiation generation have led to the possibly of major advances on the frontier of microwave vacuum devices. These concepts include the emerging technology of dc to ac radiation converters, or DARC sources, ionization fronts for frequency upshifting and conversion of extremely large plasma wakes into a Cherenkov radiation source. In the DARC source, alternatively biased "capacitors" produce a static electric field, which upon passing through a moving relativistic, underdense ionization front, is converted into a short pulse of electromagnetic (em) radiation. The frequency of this em wave is tunable by varying either the plasma density or the spacing between capacitors. We will discuss the technology involved in going from the proof of principle design which produced only a few tens of milliwatts of microwave power, to current devices at the 100W range, to future devices at the kilowatt and megawatt levels of output power. In the planned Cherenkov source, a fraction of the energy stored in the large amplitude electrostatic wave (wake) generated in plasma based accelerators is converted into em radiation by applying a static magnetic field perpendicularly to the driving laser beam. The laser beam couples to the L branch of the XO mode of the magnetized plasma through Cherenkov radiation. This radiation is emitted predominantly in the forward direction at the plasma frequency (THz range). The output power is expected to scale with the square of the applied magnetic field strength. For applied fields of 6 to 180kG, megawatt to gigawatt power level, are achievable.

This work is supported by NSF grant No ECS-9632735, DOE grant No DE-FG03-92ER-40745, and AFOSR grant No F49620-95-1-0248.

2B10

Frequency Transformer: Switched Magnetized Plasma Medium

D.K. Kalluri, J.H. Lee, Spencer Kuo, Igor Alexeff, University of Massachusetts-Lowell, Lowell, MA 01854, USA

Frequency Transformer: Switched Magnetized Plasma
Medium

D. K. Kalluri & J. H. Lee
Electromagnetics and Complex Media Research Laboratory
University of Massachusetts Lowell
Lowell, MA 01854
Spencer Kuo

Electrical Engineering Department Polytechnic University New York Farmingdale, New York 11735 Igor Alexeff

Electrical and Computer Engineering Department University of Tennessee Knoxville Knoxville, TN 37996-2100

The frequency of a source wave is changed by a timevarying electromagnetic medium. A magnetoplasma is a suitable electromagnetic medium for frequency transformation since its dielectric constant can be changed by orders of magnitude by changing the plasma density or the direction and strength of the static magnetic field. Two such effects were recently described [1]:

- (1) Frequency Upshifting with Power Intensification of a Whistler Wave by a Collapsing Plasma Medium
- (2) Conversion of a Whistler Wave into a Controllable Helical Wiggler Magnetic Field

Frequency transformation of a signal is of great significance in high frequency electrical engineering. It is cost effective to construct high frequency generators in certain frequency bands and very difficult and expensive to do the same in certain other frequency bands. A frequency transformer is thus a potentially useful device. Moreover, by controlling the static magnetic field parameters and the level of ionization, the frequency shift ratio can be changed and the frequency transformer becomes tunable.

The authors of this abstract have recently mounted a collaborative effort to further develop the theory, numerical simulation and experimental work on this topic. Some of the remarkable effects that can be obtained by modifying plasmas in space and time will be presented.

[1] D. K. Kalluri, Electromagnetics of Complex Media: Frequency Shifting by a Transient Magnetoplasma Medium, CRC Press, Boca Raton, August 1998

De Anza III 3 PM, Monday, June 21, 1999

Session 2C Inertial Confinement Fusion

Chairperson

John Porter

Sandia National Laboratories

2C01-02

Invited - Development of a Z-Pinch-Driven ICF Hohlraum Concept on Z

M.E. Cuneo, J.L. Porter Jr., R.A. Vesey, L.E. Ruggles, W.W. Simpson, M. Vargas, D.L. Hanson, T.Nash, G.A.Chandler, J.R. Asay, C.A. Hall, C.Deeney, R.B. Spielman, J.H. Hammer, A. Toor, O Landen, J. Kock, Sandia National Laboratories, Albuquerque, NM 87185-1193, USA

Development of a Z-Pinch-Driven ICF Hohlraum Concept on Z*

M. E. Cuneo, J. L. Porter, Jr., R. A. Vesey, L. E. Ruggles, W. W. Simpson, M. Vargas, D. L. Hanson, T. Nash, G. A. Chandler, J. R. Asay, C. A. Hall, C. Deeney, R. B. Spielman Sandia National Laboratories

J. H. Hammer, A. Toor, O. Landen, J. Koch Lawrence Livermore National Laboratory

Recent development of high power Z-pinches (>150 TW) on the Z driver [1] has permitted the study of high-temperature, radiation-driven hohlraums. Three complementary, Z-pinch source-hohlraum-ICF capsule configurations are being developed to harness the x-ray output of these Z-pinch's [2]. These are the dynamic-hohlraum, static-wall hohlraum, and Z-pinch-driven hohlraum concepts. Each has different potential strengths and concerns. In this paper, we report on the first experiments with the Z-pinch-driven hohlraum (ZPDH) concept. A high-yield ICF capsule design for this concept appears feasible, when driven by Z-pinches from a 60 MA-class driver [3].

In the ZPDH system, the Z-pinch x-ray source resides in a primary hohlraum, the capsule in a secondary hohlraum. Radiation transport is primarily in vacuum, where the wall absorbs and re-emits the radiation, smoothing x-ray drive non-uniformity to a level compatible with capsule implosions [3]. The primary and secondary are separated by a radial spoke array which carries the Z-pinch drive current and allows radiation transport to the secondary. Potential strengths for the ZPDH are minimal emphasis on Z-pinch uniformity and stability, and therefore minimal reliance on control of the high-energy-density plasma physics of the Z-pinch. De-coupling the Z-pinch from the capsule physics promises an approach that is more readily modeled with available 2-D codes, and therefore has improved predictability to scale the system. The principal concern is that the driver requirement is the largest of the three approaches.

Initial experiments characterize the behavior of the spoke array on Z-pinch performance and x-ray transmission, and the uniformity of radiation flux incident on a foam capsule in the secondary, for a single-sided drive. Measurements of x-ray wall re-emission power and spectrum, radiation temperatures, spoke-plasma location, and drive uniformity will be presented and compared with 0-D energetics, 2-D Lasnex rad-hydro, and 3-D radiosity calculations of energy transport and drive uniformity.

R. B. Spielman, et al., Phys. Plasmas, 5, 2105(1998).
 R. J. Leeper, et al., IAEA-F1-CN-69/OV3/4 in Proceedings of the 17th IAEA Fusion Energy Conference (Yokohama, Japan), 1998.
 J. H. Hammer et al., IAEA-F1-CN-69/IFP/18, ibid.
 *Sandia is a multi-program laboratory operated by Sandia Corporation, a Lockheed Martin Company, for the U. S. Department of Energy under Contract No. DE-AC04-94AL85000.

Characterization of the Radiation Environment for Capsule Drive in Central and Axial Hohlraums R.L. Bowers, J.H. Brownell, H.H. Rogers and D.L. Peterson, Los Alamos National Laboratory, Los Alamos, NM 87545, USA

Axial Convergent Z-pinch Driven Dynamic Hohlraums

S. A. Slutz, M. R. Douglas and T. J. Nash Sandia National Laboratories, Albuquerque, N.M. 87185

Axial convergence during the implosion of an initially cylindrical z pinch plasma increases the radiation temperature produced within a dynamic hohlraum. Quasi-spherical z pinch implosions have been demonstrated with thick liners initially in a spherical shape 1. However, wire arrays have been demonstrated to be superior to liners for generating radiation. We shall present numerical simulations demonstrating two methods of obtaining axial convergence with z pinch driven wire arrays. Our simulations show that appropriate profiling of the mass per unit length of the wires can result in an almost spherical shaped to the wire array plasma just before stagnation. Simulations also show that proper mass profiling and shaping of material surrounding the fusion capsule can result in a nearly spherical dynamic hohlraum. Comparisons between cylindrical and axially convergent dynamic hohlraum conditions will be presented.

2C04

Radiation History and Energy Coupling to Cylindrical Targets on the Z Machine

J. Aubrey, R.L. Bowers, D.L. Peterson, G.A. Chandler, M.S. Derzon, T.J. Nash and D.L. Fehl, Los Alamos National Laboratory, Los Alamos, NM 87545, USA

Radiation History and Energy Coupling to Cylindrical Targets on the Z Machine

J. Aubrey, R. L. Bowers, D. L. Peterson Los Alamos National Laboratory Los Alamos, New Mexico 87545

G. A. Chandler, M. S. Derzon, T. J. Nash and D. L. Fehl Sandia National Laboratories Albuquerque, New Mexico 87185

A series of experiments have been designed and fielded on the Sandia Z machine to characterize the radiation history and energy coupling to cylindrical targets embedded in a central cushion. The implosion of a nested wire array, which has produced temperatures of 230 eV in a central cushion (Flying Radiation Case/Dynamic Hohlraum), is used as a source, in the calculations, to drive ablative shocks in cylindrical shells. These shells have initial radii of 1 mm, wall thickness of 20 to 50 μm and are embedded in low density foam. Simulations of the radiation environment in the cushion, including the radiation prepulse associated with the run-in of the load plasma and the energy coupling to the target will be presented. The dynamics of the imploding plasma, its evolution near the axial aperture and its effects on diagnostic access will also be considered.

Tailoring the Radiation Drive in Dynamic Hohlraums

M.S. Derzon, T.J. Nash, G.A. Chandler, R.J. Leeper, D.L. Fehl, J. Aubrey, R. Bowers, D. Petersen, D.D. Ryutov and J.J. MacFarlane, Sandia National Laboratories, Albuquerque, NM 87185-1196, USA

Tailoring the Radiation Drive in Dynamic Hohlraums*

M.S. Derzon, T.J. Nash, G.A Chandler, R.J. Leeper, D.L. Fehl, Sandia National Laboratories

J. Aubrey, R. Bowers, D. Petersen Los Alamos National Laboratory

D.D. Ryutov Lawrence Livermore National Laboratory

J.J. MacFarlane
Prism Computational Sciences

At the Sandia Z-facility, we have created a condition where the imploding pinch interacting with an inner target creates an intense radiation field or Dynamic Hohlraum environment. By tailoring the characteristics of this inner target the time-dependent temperature of the Dynamic Hohlraum can be varied. This control over the temperature history is necessary for performing Inertial Confinement Fusion experiments near the Fermi degenerate isentrope. In this presentation we will show the effect of target Z and density profile on the radiation history produced. We will compare the experimental results with modeling of the temperature histories.

*Sandia is a multiprogram laboratory operated by Sandia Corporation, a Lockheed Martin Company, for the United States Department of Energy under Contract DE-AC04-94AL85000.

2C06

Axial Convergent Z-Pinch-Driven Dynamic Hohlraums

S.A. Slutz, M.R. Douglas and T.J. Nash, Sandia National Laboratories, Albuquerque, NM 87185, USA

Axial Convergent Z-pinch Driven Dynamic Hohlraums

S. A. Slutz, M. R. Douglas and T. J. Nash Sandia National Laboratories, Albuquerque, N.M. 87185

Axial convergence during the implosion of an initially cylindrical z pinch plasma increases the radiation temperature produced within a dynamic hohlraum. Quasi-spherical z pinch implosions have been demonstrated with thick liners initially in a spherical shape 1. However, wire arrays have been demonstrated to be superior to liners for generating radiation. We shall present numerical simulations demonstrating two methods of obtaining axial convergence with z pinch driven wire arrays. Our simulations show that appropriate profiling of the mass per unit length of the wires can result in an almost spherical shaped to the wire array plasma just before stagnation. Simulations also show that proper mass profiling and shaping of material surrounding the fusion capsule can result in a nearly spherical dynamic hohlraum. Comparisons between cylindrical and axially convergent dynamic hohlraum conditions will be presented.

Two-Dimensional Implosions of Liners onto Spherical Hohlraums

I.V. Lisitsyn, S. Katsuki and H. Akiyama, Kumamoto University, Kumamoto 860-8555, Japan

TWO-DIMENSIONAL IMPLOSION OF LINER ONTO A SPHERICAL HOHLRAUM

I. V. Lisitsyn, S. Katsuki and H. Akiyama

Department of Electrical and Computer Engineering,
Kumamoto University,
2-39-1 Kurokami, Kumamoto 860, Japan.

A two-dimensional implosion of liners is studied. This is instead of the conventional one-dimensional cylindrical implosion of Z pinches where a wire array or a gas-puff liner, which has a cylindrical shape and an uniform mass distribution along the z-axis. Two-dimensional Z-pinch compression can be realized utilizing either a spherically shaped wire array or a double gas-puff single-shell liner with a special mass distribution along the z-axis.

The results obtained from computer simulations show that both kinds of liners can be compressed in both the z and the r directions. This leads to a uniform and a high-power heating of the spherical dynamic hohlraum placed inside the liner. The spherical, two-dimensional liner implosion increases the power density at the hohlraum surface, improves the symmetry of the capsule irradiation and helps partially in quenching of the Rayleigh-Taylor instability.

The spherical liner implosions can have some advantages in the hohlraum experiments over those conducted with conventional cylindrical liners. These advantages are: a higher power density due to 2-D liner implosion and a possibility to operate with spherical or quasi-spherical hohlraums instead of cylindrical by selecting the initial shape of the liner from a variety of geometries. It becomes possible to optimize the implosion with one more degree of freedom compared to recent studies.

2C08

Foot-pulse Radiation Drive Necessary for ICF Ignition Capsule Demonstrated on Z Generator T.W.L. Sanford, R.E. Olson, G.A. Chandler, D.L. Fehl, J.S. Lash, R.J.Leeper, L. Ruggles, K.W. Struve, R.A. Vesey, M.S. Derzon, T.J. Nash, W.A. Stygar, R.C. Mock, D.E. Hebron, T.L. Gilliland, D.O. Jobe, J.S.

McGurn, J.F. Seamen, W. Simpson, J.A. Torres and M.F. Vargars, D.L. Peterson, Sandia National Laboratories, Albuquerque, NM 87185-1196, USA

Foot-pulse Radiation Drive Necessary for ICF Ignition Capsule Demonstrated on Z Generator

T. W. L. Sanford, R. E. Olson, G. A. Chandler, D. L. Fehl. J. S. Lash, R. J. Leeper, L. Ruggles, K. W. Struve, R. A. Vesey, M. S. Derzon, T. J. Nash, W. A. Stygar, R. C. Mock, D. E. Hebron, T. L. Gilliland, D. O. Jobe, J. S. McGurn, J. F. Seamen,

> W. Simpson, J. A. Torres, and M. F. Vargas Sandia National Laboratories

D. L. Peterson

Los Alamos National Laboratory

Implosion and ignition of an indirectly-driven ICF capsule operating near a Fermi-degenerate isentrope requires initial Planckian-radiation-drive temperatures of 70-to-90 eV to be present for a duration of 10-to-15 ns prior to the main drive pulse [1]. Such capsules are being designed for high pulsed-power generators such as X1 [2, 3]. This *foot-pulse* drive capability has been recently demonstrated in a NIF-sized ($\phi = 6$ -mm 1 = 7-mm), gold hohlraum, using a one-sided *static-wall* hohlraum geometry [1-3] on the Z generator [4].

The general arrangement utilized nested tungsten-wire arrays of radii (mass) 20 mm (2 mg) and 10 mm (1 mg) that had an axial length of ~10 mm. The arrays were driven by a peak current of ~21 MA and were made to implode on a 2- μ m-thick Cu annulus (mass = 4.5 mg), which had a radius of 4 mm and was filled with a lowdensity CH foam, all centered about the z-axis. The gold hohlraum was mounted on axis and above the Cu/foam target. A 2.9-mm-radius axial hole between the top of the target and hohlraum permitted the xrays generated from the implosion to enter the hohlraum. The radiation within the hohlraum was monitored by viewing the hohlraum through a 3-mm diameter hole on the lateral side of the hohlraum with a suite of diagnostics. The radiation entering the hohlraum was estimated by an additional suite of on-axis diagnostics [3], in a limited number of separate shots, when the hohlraum was not present. Additionally, the radiation generated outside the Cu annulus was monitored, for all shots, through a 3-mm diameter aperture located on the outside of the current return can.

In the full paper, the characteristics of the radiation measured from these diagnostic sets, including the Planckian temperature of the hohlraum and radiation images, will be discussed as a function of the incident wire-array geometry (single vs nested array and array mass), target length (10, or 20 mm), annulus material (Cu, Au, or nothing), and CH-foam-fill density (10, 6, 2.5, or 0 mg/cc). Comparisons of a limited number of these variations with 1-D and 2-D rad-hydro and 3-D radiosity simulations will also be reviewed. Lastly, hole closure in the on- and off-axis apertures will be discussed.

[1] R. E. Olson, et al., Phys. Plasmas, 4, 1818 (1997).

[2] R. E. Olson, et al., to be published in Fusion Tech. (March 1999)
[3] R. J. Leeper, et al., in Proceedings of 17th IAEA Fusion Energy

Conference (Yokohama, Japan, 19-24 October 1998).

[4] R. B. Spielman, et al., *Phys. Plasmas*, **5**, 2105 (1998). *Sandia is a multiprogram laboratory operated by the Sandia Corporation, a Lockheed Martin Company, for the U.S. Department of Energy under Contract No. DE-AC04-94AL85000.

Two-dimensional Integrated Z-Pinch ICF Design Simulations

J.S. Lash, Sandia National Laboratories, Albuquerque, NM 87185-1186, USA

Two-dimensional Integrated Z-Pinch ICF Design Simulations

J. S. Lash

Sandia National Laboratories, Albuquerque, NM 87185

The dynamic hohlraum ICF concept for a Z-pinch driver utilizes the imploding wire array collision with a "target" to produce a radiation history suitable for driving an embedded inertial confinement fusion (ICF) capsule. This "target" may consist of various shaped layers of low-density foams or solid-density materials. The use of detailed radiation magneto-hydrodynamic (RMHD) modeling is required for understanding and designing these complex systems. Critical to producing credible simulations and designs is inclusion of the Rayleigh-Taylor unstable wire-array dynamics; the "bubble and spike" structure of the collapsing sheath may yield regions of low-opacity enhancing radiation loss as well as introduce non-uniformities in the capsule's radiation drive. Recent improvements in LASNEX have allowed significant progress to be made in the modeling of unstable z-pinch implosions. Combining this with the proven ICF capsule design capabilities of LASNEX, we now have the modeling tools to produce credible, fully-integrated ICF dynamic hohlraum simulations. We present detailed two-dimensional RMHD simulations of recent ICF dynamic hohlraum experiments on the Sandia Z-machine as well as design simulations for the next-generation Z-pinch facility and future high-yield facility.

2D

Bonsai I/II 3 PM, Monday, June 21, 1999

Oral Session 2D Plasma Diagnostics

Chairperson
Ken Connor
Plasma Dynamics Laboratory, RPI

Comparison of Electron Density Measurements in Planar Inductively Coupled Plasmas

Wei Guo, Richard L.C. Wu, Charles A. DeJoseph, Jr., K Systems Corp., Beavercreek, OH 45432, USA

Comparison of Electron Density Measurements in Planar Inductively Coupled Plasmas by Microwave Interferometer and Langmuir Probe

Wei Guo, Richard L. C. Wu, Charles A. DeJoseph, Jr.*

K Systems Corp., 1522 Marsetta Dr., Beavercreek, OH 45432-2733. Tel. (937) 429-5151; FAX (937)429-1122 * Air Force Research Laboratory, Aero Propulsion and Power Directorate, Wright-Patterson Airforce Base, OH 45433-7919. Tel. (937)255-5179; FAX (937)656-4095

Abstract

A Langmuir probe and a heterodyne microwave interferometer have been used to characterize a planar inductively coupled ion source operated in one of two configurations. In the normal configuration, moly extraction grids are used to form a beam of ions with energy over the range 50-500 eV. Alternately, the source is operated without grids resulting in a diffuse plasma which can be probed just outside the source. We have investigated probe tip orientations parallel and perpendicular to the plasma flow under both configurations. In the experiments, spatially resolved electron densities measured by Langmuir probe are fitted to a polynomial, spatially integrated, and compared with the line-integrated plasma density measured with the microwave interferometer. Results indicate that the two density measurements, extended over a broad range of input rf power, differ in the range of a few percent to approximately 30%. In addition to presenting measured data under various plasma conditions, the effects of probe tip orientation and other factors contributing to the total measurement errors will be discussed.

2D02

Emissive Probe Characteristic in an Inductive Plasma Source

T.Lho, N. Hershkowitz, G.H. Kim and W. Steer, University of Wisconsin-Madison, Madison, WI 53705, USA

Emissive Probe Characteristic in an Inductive Plasma Source

T. Lho, N. Hershkowitz, G.H. Kim¹, and W. Steer

Dept. of Engineering Physics, University of Wisconsin, 1500 Engineering Dr., Madison, WI 53705, U.S.A.

Abstract

Two new features of a time averaged emissive probe characteristic have been studied in an inductive source. One is the effect of harmonics of the rf fluctuation. Without the higher harmonics, the derivative of the time averaged emissive probe I-V characteristic has two peaks whose separation approximately indicates the peak to peak rf amplitude. When higher harmonics of the rf fluctuation are present, the derivative has more than two peaks. Experimental I-V characteristics involving the first and second harmonics, and the resulting differentiated curve containing three peaks, has been measured in E-mode operation.

The other effect is an additional heating of the emissive probe by collected electrons. When the ICP is operated in H-mode, it can be characterized by a high rf fluctuation and high density mode. Under these circumstances, the time averaged input power to the probe by collected electrons becomes larger than the external heating and induces additional emission current from the probe. This additional emission current appears as a current distortion in the I-V characteristic curve. The total emission current, including the additional emission, is limited by the probe temperature when $V_b \ll V_p$ and by space charge effects when $V_b \leq \widetilde{V_p}$, where V_b is a probe bias voltage and $\widetilde{V_p}$ is a time varying plasma potential. The total emission current ceases when V_b is several orders of T_w/e higher than the plasma potential, where T_w is the probe wire temperature. This assumption with temperature and space charge limited emission current is consistent with the experimental data.

¹Now at Dept. of Physics, University of Hanyang-Ansan, Guynggi-Do, Ansan-Si, Korea

Elimination of notching and ARDE by simultaneous modulation of source and wafer RF.

N. Hershkowitz and M.K. Harper, University of Wisconsin, Madison, WI 53706, USA

Elimination of notching and ARDE by simultaneous modulation of source and wafer RF.

N. Hershkowitz and M.K. Harper*, University of Wisconsin, Madison.

Notch formation and Aspect Ratio Dependent Etching (ARDE) are becoming serious problems in the over-etching of line and space structures in poly-Si on SiO₂. Experimental results for Cl2 plasma etching of poly-Si and C₂H₂F₄ in SiO₂ in a helicon etch tool are presented which are modeled by differential charging and ion assisted etching. It is shown that modulation of the 13.56 MHz RF source can eliminate both of these effects in the absence of RF wafer bias but fails in the presence of CW wafer bias. It is also shown that simultaneous source and wafer modulation eliminates both notch formation and ARDE. On/off modulation with a 50% duty cycle and period ranging from 0 to 200 μs are investigated and optimum notch and ARDE reduction are found at 40 to 200 µs.

This work was supported by National Science Foundation Grant #EEC-8721545.

* present address Intel Corporation, Hillsboro, Oregon

2D04-05

Invited - Diagnostics for Plasma Processing

Applied Materials, Santa Clara, CA 95054, USA

Diagnostics for Plasma Processing - An Overview J.Forster - Applied Materials, Santa Clara, CA

The use of plasmas in the production of integrated circuits has rurred the development of a variety of diagnostic tools. The goal plasma diagnostics in this application is twofold. The diagnostic tools are used to aid in understanding of plasma physics and chemistry, so that processes and hardware may be optimized. For this goal the diagnostic tools are used in an R+D setting. Plasma diagnostic methods are also sought after to serve as sensors for process control. For this application the diagnostic techniques must be low cost, non-invasive, robust, and repeatable. Much understanding has been obtained by applying the "classic" plasma diagnostic techniques, such as Langmuir probes, optical spectroscopy, and microwave interferometry, to processing plasmas. More detailed information has come from advanced diagnostics such as energy analysis of charged particles, laser induced flourescence, and mass spectrometry. The demands of process control have been met by non-invasive techniques that require minimal access to the plasma, such as optical emission spectroscopy, RF measurements outside the plasma source, and to some extent by residual gas analysis. An overview of these diagnostics will be given, along with their contribution to the understanding of plasma physics and plasma chemistry.

Two Color Fiber Optic Interferometer for Gas and Plasma Density Measurements

S.W. Gensler, N. Qi, J. Schein and M. Krishnan, Alameda Applied Sciences Corporation, San Leandro, CA 94577, USA

Two Color Fiber Optic Interferometer for Gas and Plasma Density Measurements*

S. W. Gensler, N. Qi, J. Schein and M. Krishnan

Alameda Applied Sciences Corporation San Leandro, CA 94577

A 2-color, 4-beam Fiber Optic Interferometer (FOI) with ~10⁻⁴ wave sensitivity when sampled at 1 µs intervals is being built to measure gas and plasma densities. The final instrument will be completed under a 2 year SBIR contract; initial results from one beam of the instrument will be presented. The FOI uses 1310 nm and 1550 nm CW diode lasers and is contained in a ~6" x 17" x 17" volume, which makes the system compact and portable. The two colors enable the FOI to measure neutral gas and plasma densities simultaneously [1], so that partially ionized plasmas can be characterized. The multiple beams in the complete instrument will allow rapid characterization of gases and plasmas, including the measurement of correlated density variations.

Neutral gas and electron density profile measurements have been taken as a function of time from a supersonic nozzle designed for z-pinch loads and a cable gun. The project goal sensitivity of $\sim 10^{-4}$ wave will allow simultaneous measurement of neutral and electron density-length integrals down to $\approx 6 \times 10^{15}$ Ar atoms/cm² and $\approx 7 \times 10^{13}$ electrons/cm². For a typical path length of 10 cm in nozzles or opening switch plasmas, these numbers correspond to densities of 6×10^{14} Ar atoms/cm³ and 7×10^{12} electrons/cm³. A description of the FOI and initial density measurements with sensitivity of $< 10^{-3}$ of a wave will be presented.

1. B.W. Weber and S. Fulghum, Rev. Sci. Instrum. **68** (2) 1227 (1997).

*Work supported by the Defense Threat Reduction Agency under contract DSWA01-98-C-0173.

2D07

Diagnosis of Large Volume Pulse Modulated Ar-H2 Plasmas

K.C. Paul, Y. Tanaka and T. Sakuta, Kanazawa University, Kanazawa 920-0944, Japan

Diagnosis of Large Volume Pulse Modulated Ar-H₂ Plasmas

¹K.C. Paul, Y.Tanaka and T. Sakuta

Electrical & Computer Engineering, Kanazawa University 2-40-20 Kodatsuno, Kanazawa 920-8667, JAPAN.

¹E-mail: khokan@kenroku.kanazawa-u.ac.jp

Atmospheric pressure plasma in pre-mixed Ar/H₂ (Ar: 84% molar concentration) flow was generated experimentally at pulse-modulated approach. The plasma torch has a special kind of feature; the length of coil region is extremely large, 158 mm. Ratio of the coil length to coil diameter is about 3:2, which is usually opposite in the ordinary torch. This huge coil length should have caused high plasma region and thus, should be more suitable for materials processing. Pulse modulation of plasma helps to understand the changes of plasma responses with time, and thus, this technique is likely to be helpful to control the plasma energy and species concentration in time domain for better application of radio-frequency (rf) inductively coupled plasma (ICP). The numerical model [1], which used 2-dimensional field variations and was for optically thin and local thermodynamic equilibrium (LTE) considerations, revealed many characteristic properties of plasma for sudden change in active power of plasma. The model was found effective to predict different response times of plasma. Experimentally generated pulse-modulated plasma [2] reported on-time and pressure effects upon the atomic argon line intensity at 751 nm wavelength. Both works were for same torch configuration.

Our present work is to reveal spectroscopically measured results of the new ICP torch with large coil length. In addition, the ICP code of Ref.1 was changed for current pulsation and used in predicting ICP responses for the same operating conditions of experiment. Experimentally, the source side power was 30 kW before pulsation and thus, the plasma power would had around 25.6 kW considering 85% matching efficiency. Please note that the change of plasma power during pulsing period was not measured due to lack of facility. The rf power was pulse modulated by imposing an external pulsed signal to switch a MOSFET. The other operating conditions were: 760 Torr pressure, 85 slpm total gas flow rate, 0.45 MHz nominal frequency of the supply, 67% duty factor (10 ms on-time and 5 ms off-time), and 100 to 61.7% shimmer current level (SCL). Monochromated emission of atomic argon at 751 nm was detected and stored to see the pulse effect. The time constants for rising and falling time, measured with the help of current intensity after pulsation, were 0.114 and 0.054 ms respectively. Please note that these time constants are the measure of times required to reach the intensity from 10% to 90% and 90% to 10% of its final or steady-state value after the pulse-on and pulse-off, respectively. The same time constants, measured by atomic argon line intensity at 751 nm, were 4.6 and 3.6 ms respectively; and numerically these values were found as 4.99 ms and 4.44 ms respectively. The power level varied between 33 to 7 kW theoretically during the pulsing period and the coil current between 210 to 120 A. The coil current needed to produce the 25.6-kW plasma at steady-state before pulsation was 189.4 A.

[1] J. Mostaghimi, K.C. Paul and T. Sakuta, *J.Appl. Phys.*, **83**, 1898-1908 (1998).

[2] T. Sakuta, K.C. Paul, M. Katsuki and T. Ishigaki, J. Appl. Phys. [will be published in Feb. issue. 1999]

Diagnostic Applications of the Most Advanced Theory and Code for Stark Broadening of Hydrogen Lines in Plasmas

E. Oks, Auburn University, Auburn, AL 36849-5311, USA

Diagnostic Applications of the Most Advanced Theory and Code for Stark Broadening of Hydrogen Lines in Plasmas

E. Oks

Physics Department, 206 Allison Lab. Auburn University, AL 36849-5311

The theory combines two new phenomena in broadening with an electron treatment of the ion dynamics. The first new phenomenon is a strong <u>Indirect Coupling</u> (IC) between the electron and ion broadenings carried out via the radiating atom acting as an intermediary. The higher the plasma density and/or the principal quantum number of the radiator, the more important the IC becomes. For most hydrogen lines, the IC results in a significant decrease of the linewidth, except few lines, such as the L_{α} line, where the IC decreases the width.

The second new phenomenon is a strong <u>Direct Coupling</u> (DC) between the electron and ion broadenings, represented by the acceleration of the perturbing electron by the ion nearest to the radiator. The DC results in a narrowing of the lines, which becomes quite dramatic as the temperature decreases and/or the density increases.

The improved treatment of the ion dynamics is based on the first <u>analytical solution</u> for this problem, obtained using the generalized broadening theory published by us earlier. This analytical result supersedes the existing approximate simulation models for the ion dynamics.

The unique combination of the above three novel features is incorporated into a code, making it the most advanced in the world. Several diagnostic applications of the code are presented. They cover a broad range of electron densities (from 10¹³ cm⁻³ to 10¹⁹ cm⁻³) and resolve dramatic discrepancies between the conventional theory and a number of experiments.

2D09

Spherically curved crystals for x-ray plasma diagnostics

Y. Aglitskiy, T. Lechecka, S. Obenschain, C. Pawley, C.M. Brown, J. Seely, Space Science Division, Naval Research Laboratory, Washington DC 20375-5352, USA

Spherically curved crystals for x-ray plasma diagnostics

Y. Aglitskiy and T. Lehecka
Science Applications International Corp., McLean VA 22102
S. Obenschain, C. Pawley
Plasma Physics Division, Naval Research Laboratory, Washington
DC 20375

C. M. Brown, J. Seely Space Science Division, Naval Research Laboratory, Washington DC 20375

We report on our continued development of the x-ray plasma diagnostics based on spherically curved crystals. The diagnostics include x-ray spectroscopy with 1D spatial resolution and 2D monochromatic self-imaging and backlighting. The system is currently used, but not limited to diagnostics of the targets ablatively accelerated by the NRL Nike KrF laser.

A spherically curved quartz crystal (2d=6.68703 Å, R=200 mm) has been used to produce monochromatic backlit images with the He-like Si resonance line (1865 eV) as the source of radiation. The spatial resolution of the X-ray optical system is 1.7 μ m in selected places and 2-3 μ m over a larger area. Time resolution has been obtained with the help of four-strip x-ray framing camera. Time resolved, 20x magnified, backlit monochromatic images of CH planar targets driven by the Nike facility have been obtained with spatial resolution of 2.5 μ m in selected places and 5 μ m over the focal spot of the Nike laser. Another quartz crystal (2d=8.5099 Å, R=200mm) with the H-like Mg resonance line (1473 eV) has been used for backlit imaging with higher contrast. Spherically curved mica (2d=9.969 Å in the second order of reflection, R=200mm) has been used for backlighting of the low density foam targets with the backlighter energy of 1.26 keV.

A second crystal with a separate backlighter was added to the imaging system. This makes it possible to use of all four strips of the framing camera. As a result we have four monochromatic "snapshots" of developing instabilities.

We are currently exploring the enhancement of this technique to the higher and lower x-ray energies.

Serra I, Conference Centre 3 PM, Monday, June 21, 1999

Poster Session 2P

2P01

Resonant absorption of a short-pulse laser in a doped dielectric

L.K. Ang, Y.Y. Lau and R.M. Gilgenbach, University of Michigan, Ann Arbor, MI 48109-2104, USA

Resonant absorption of a short-pulse laser in a doped dielectric

L.K. Ang, Y.Y. Lau, and R.M. Gilgenbach, Nuclear Engineering & Radiological Sciences Dept. U. Michigan, Ann Arbor, MI 48109-2104

A simple model is used to calculate the efficiency of energy absorption when a laser of short pulselength impinges on a dielectric slab that is doped with an impurity with a resonant line at the laser frequency. The impurity is assumed to have a finite linewidth. Dimensionless parameters are constructed that combine the dopant concentration, the dopant resonant linewidth, laser pulselength, separation between the laser frequency and the dopant transition frequency, and the width of the dielectric slab. This allows calculation with one set of normalized parameters be used to infer the results expected for other sets of parameters. It is found that the energy absorption efficiency is maximized for a certain degree of doping concentration (at a given pulselength), and also for a certain pulselength (at a given dopant concentration). Typically, tens of percent of the laser energy can be resonantly absorbed with only a modest amount of impurities.

Supported by NSF, DoE and AFOSR/MURI.

2P02

Electromagnetically Induced Transparency and Pulse Propagation in Plasmas

B. Hafizi, P. Sprangle, R.F. Hubbard and J.R. Penano, Icarus Research, U.S. Naval Research Laboratory, Washington, DC 20375-5346, USA

Electromagnetically Induced Transparency and Pulse Propagation in Plasmas

B. Hafizi¹, P. Sprangle², R.F. Hubbard² and J.R. Peñano²

¹Icarus Research, Inc., PO Box 30780, Bethesda, MD 20824-0780

²Plasma Physics Division, Naval Research Laboratory, Washington, DC 20375

Electromagnetically induced transparency (EIT) is a process in which a low frequency electromagnetic wave (below the plasma frequency $\omega_{_{p}}$) propagates essentially unattenuated in the presence of a high frequency wave (above ω_p) [1]. In EIT the nonlinear plasma current that arises from the beating of the waves cancels the linear plasma current. A narrow bandpass region, below ω_p , exists when the frequency difference between the wave is close to ω_p . The bandpass region consists of nonlinear modes having positive and negative group velocities. We present a general analysis of EIT that is based on the interaction of three EM waves, representing the pump, the Stokes and the anti-Stokes waves. along with a plasma wave. Based on the nonlinear dispersion relation we discuss the propagation characteristics of the waves inside the plasma. Numerical solutions are presented that illustrate the conditions under which propagation of the Stokes wave in the plasma is possible.

*Supported by ONR

*NRC-NRL Research Associate
[1] S.E. Harris, Phys. Rev. Lett. 77, 5357 (1996)

Thermal Filamentation Instability in Laser-Produced Plasma

F. Bouzid and A. Bendib, Laboratoire de Physique des Milieux Ionises, U.S.T.H.B., Algiers, Algeria

Thermal Filamentation Instability in Laser-Produced Plasmas

F. Bouzid and A. Bendib

Laboratoire de Physique des Milieux Ionisés, Institut de Physique, U. S. T. H. B, El Alia, B. P. 32, Bab Ezzouar, Algeria

Abstract

The theoretical study of the thermal filamentation instability in fully ionized plasmas is presented.

The collisionless fluid model equations used, take into account the off-diagonal terms of the generalized stress tensor and the generalized heat flux corresponding mainly to the temperature anisotropy and convective thermal energy respectively.

The non-stationary description of the thermal filamentation instability is carried out and the dispersion relation of the unstable light filaments is explicitly established. The numerical stability analysis of the electromagnetic modes shows that these additional terms decrease the growth rate of this instability in comparison with the previous results of the literature¹.

The convective e-folding rate in inhomogeneous plasmas is derived by using the W. K. B. method and the results obtained are then compared to those of current experiments.

¹ T. B. Kaiser, B. I. Cohen, R. L. Berger, B. F. Lasinski, A. B. Langdon, and E. A. Williams, Phys. Plasmas 1 (5) (1994).

2P04

Characteristics of Titanium plasma for Ti Vapor Laser

M.Atta Khedr, H. Sharkaway and TH.M. El Sherbini, Cairo University and University of Wisconsin -Madison, Madison, WI 53706, USA

Characteristics of Titanium plasma for Ti vapor laser

M.Atta Khedr*, H.Sharkawy and TH.M.El.Sherbini, Physics Department Faculty of science and National Institute of laser Enhanced Sciences (NILES), Cairo university, Giza, Egypt

*) Now: Dep. of Engineering Physics, university of Wisconsin -Madison, 1500 Engineering Dr., Madison WI 53706, USA

The application of direct laser vaporization is a useful technique to obtain a metal vapor in metal - vapor lasers, especially for high melting metals [1].

Characteristics of laser produced titanium plasma have been investigated using spectroscopic methods and CCD camera. The plasma was produced using pure Ti target irradiated with a pulsed switched Nd: YAG laser of 350 mJ/pulse at 1064 nm, pulse duration of 7 ns & repetition rate of 5 Hz).

The electron temperature Te was found to be 8153 K with Ar background gas up to a pressure of 3 mbar. The electron density was found to be 1.4 10¹⁶ cm⁻³ and increases with the Ar pressure up to 3 mbar. Two spectral lines at 551.4 nm and 625.8 nm were observed in the Ti spectra and were identified correspond to (3D01 - 3F2) and (3G04 - 3F3) transitions respectively.

The intensities of these lines show remarkable increase with the Ar gas pressure up to a maximum value of about 8 mbar.

The two lines are very promising for optically pumped Ti vapor lasers with Ar gas as a background.

^[1] K.Hirata, S.Yoshino, and H.Ninomiya, J.Appl. Phys. 66 (4) (1990) 1460.

Electric discharge enhancement of laser produced plasma for thin film deposition

D.G. Redman, J. Mouillaux, S.Zhe, Y.Y. Tsui and R. Fedosejevs, University of Alberta, Edmonton, Alberta T6G2G7, Canada

Electric discharge enhancement of laser produced plasma for thin film deposition

D.G. Redman, J. Mouillaux, S. Zhe, Y.Y. Tsui and R. Fedosejevs Department of Electrical and Computer Engineering, University of Alberta, Canada T6G 2G7

Plasma produced by focusing a KrF laser (248nm, 15ns) onto a solid target can be captured and guided by a curved solenoidal magnetic field to yield a debris free, controlled deposition source for the fabrication of thin films [1,2]. In our magnetic field guiding process only the ionized component of the laser ablated material contributes to the deposition source. With the aim of increasing the coating rate, we have investigated the use of a fast-switched capacitor discharge through a plume of laser ablated material which increases significantly the plasma content. The angular distribution of the flux of the additional plasma generated by the electric discharge enhancement of laser produced plasma was observed to be more isotropic in comparison to that of the non-enhanced laser produced plasma. The angular distribution of the flux of electric discharge enhanced laser produced plasma has been measured in detail with an array of Faraday cups for both C and Al plasmas. During the experiment, laser intensities were ranged from 109 W/cm² to 10¹¹ W/cm², both a C and a W pair of discharge electrodes were used, and the time delay between the laser plasma formation and the triggering of the electric discharge was varied. Experimental results indicating an increase in the plasma component of the plume of the laser ablated material will be presented.

- [1] Y.Y. Tsui, D.G. Redman, R. Rankin, C.E. Capjack, D. Vick, and R. Fedosejevs, *International Conference on Plasma Science*, Raleigh, North Carolina, June 1-4, 1998.
- [2] Y.Y. Tsui, D. Vick, R. Fedosejevs, Appl. Phys. Lett. 70, 1953 (1997)

2P06

Ultra-Linear Traveling Wave Tube Development D.M. Goebel, R. Liou and W.L. Menninger, Hughes Electron Dynamics, Torrance, CA 90509, USA

Ultra-Linear Traveling Wave Tube Development

D. M. Goebel, R. Liou, and W. L. Menninger Hughes Electron Dynamics, Torrance, CA 90509

Traveling wave tubes (TWT) intended for telecommunications applications are increasingly required to have high linearity and good intermodulation performance, especially for use as modern multi-carrier power amplifiers (MCPA) and in systems that use digital signal encryption. The linearity of a TWT can be improved by optimization of the taper of the helix circuit to reduce the gain compression and phase shift of the output signal as the drive level is increased, and by operation of the tube significantly backed off from saturation in the linear region of the AM/AM and AM/PM transfer curves. However, backed off operation at a given output power level requires increased beam current and power handling capabilities compared to a design operating at saturation, and also results in a greatly reduced efficiency of the TWT. At Hughes, we have developed L-band and S-band TWTs for telecommunication applications that provide good intermodulation performance and high efficiency compared to solid-state amplifiers of similar power levels. To date, the TWTs have produced up to 150 W of continuous output power with an 8-tone continuous-random-phase signal intermodulation level of about -30 dBc and an efficiency of over 20%. At similar power levels, a comparable solid state MCPA has an efficiency well below 10% and nearly twice the cost. These low-frequency communications tubes are normally operated 9 to 10 dB backed off from saturation, and they utilize an optimized helix taper and multi-stage depressed collector design to increase the overall TWT performance and efficiency. The characteristics and intermodulation performance of several TWTs that operate in the 1.5 to 2.4 GHz frequency range will be presented.

Full Wave Analysis of Beam Instability of Dense Plasma Wave Spectrum in Plasma Filled Periodic Waveguide

G.I. Zaginaylov, A.A. Rozhkov and J.Y. Raguin, Tech University Hamburg, A B Holhfrequenztechmik, Germany

Full Wave Analysis of Beam Instability of Dense Plasma Wave Spectrum in Plasma-Filled Periodic Waveguide

G.I. Zaginaylov¹, A.A. Rozhkov² and J.-Y. Raguin³

¹ Presently with Tech. Univ. Hamburg-Harburg Arbeitsbereich Hochfrequenztechnik D-21071 Hamburg, Germany on leave from Kharkov State University Svobody Sq.4, Kharkov, 310077, Ukraine

² Scientific Center of Physical Technologies Novgorodskaya 1, Kharkov, 310145, Ukraine

³ Tech. Univ. Hamburg-Harburg Arbeitsbereich Hochfrequenztechnik D-21071 Hamburg, Germany

The influence of plasma on dispersion properties of periodic waveguides is under extensive experimental, theoretical and numerical investigations¹. Nevertheless, one of the major theoretical problems, namely, a rigorous analysis of the beam instability of plasma waves which originate the so-called "dense" spectrum², is left open. Such spectral behaviour can hardly be treated by the conventional approach based on the expansion of the fields into the spatial harmonic series, since the resulting dispersion relation in the form of an infinite determinant diverges when the number of spatial harmonics is increased³.

To clarify this issue, a new approach, based on an integral equation (IE) method, has been developed. For planar periodic waveguide filled with homogeneous longitudinally magnetized plasma and driven by a thin electron beam, an IE with a singular kernel has been obtained for the field on the waveguide axis. It has been regularized by extracting the statical part of the kernel. Spectral properties of the resulting Volterra integral equation of the first type were analysed in the quasistatic approximation. The periodical "cold" solutions for the fields have been obtained in closed analytical form. The periodicity of the "cold" dispersion relation with respect to the wavenumber is qualitatively satisfied over several periods. The dispersion relation with the beam has unstable solutions, which can be interpreted as Cherenkov instabilities of the spatial plasma harmonics.

For low plasma densities, the spatial growth rate of the first backward harmonic of the plasma wave is shown to be remarkably larger compared with that obtained by the conventional technique which consists in truncating an infinite matrix⁴. This discrepancy can be attributed to the principal role of the interaction between highest plasma and beam spatial harmonics which form the quasistatical part of fields. The relative estimations for plasma wave energy in the saturation regime predict a beam-wave energy transfer much more efficient compared with the conventional ones.

- 1. G.S.Nusinovich et al., IEEE Trans. PS-26, 628, (1998)
- 2. W.R.Lou et.al., Phys. Rev. Lett., <u>67</u>, 2481 (1991).
- 3. K.Ogura, J. Phys. Soc. Jpn., 61, 4022 (1992).
- 4. V.I.Kurilko et al., Sov. Phys. Tech. Phys., 26, 812 (1981).

2P08

Initial Validation of the CTLSS Eigenmode Solver in Helix Geometry

D.R. Whaley, C.M. Armstrong, Simon J. Cooke, Northrop Grumman Corporation, Rolling Meadows, IL 60008, USA

Initial Validation of the CTLSS Eigenmode Solver in Helix Geometry*

D. R. Whaley, C. M. Armstrong Northrop Grumman Corporation, 600 Hicks Rd., M/S H6402, Rolling Meadows, IL 60008

Simon J. Cooke Science Applications International Corporation 1710 Goodridge Dr., McLean, VA 22102

The Cold Test and Large Signal Simulation (CTLSS) eigenmode solver, developed by SAIC, has been used to model the dispersion and impedance characteristics of a Northrop Grumman X-Band helix TWT. Helix geometry complicates the solution for solvers of this type due to the fact that the objects being modeled, circular backwall and helix as well as rectangular dielectric rods, do not easily lend themselves to accurate representation by any one coordinate system. This is further complicated by the fact that helix geometry is axially periodic and therefore solution times can become quite long since an entire pitch period must be modeled to allow for the correct periodicity of the helical system. Measured dispersion and impedance data from a Northrop Grumman X-Band TWT is being used to benchmark the results generated by CTLSS for helix geometry.

A GUI is included with the CTLSS distribution which generates a CTLSS input file for any type of geometry desired. Several templates are available for common structures including helix TWTs, coupled-cavity TWTs, and klystron cavities. The GUI allows one to easily modify the size and shape of individual components as well as set or modify numerical parameters necessary for solution. A visualization toolkit is also provided with the CTLSS distribution which allows one to view the resulting CTLSS structure. This allows for verification of the physical layout of the structure being modeled. A separate option displays the computed eigenmode fields in 3D contour format. Comments on use of both the CTLSS GUI and visualization toolkit will be presented.

CTLSS can be run on both UNIX and PC platforms. Both platforms have been used for this study and will be compared. Information on setup times will be included as well as solution times. Proper gridding is always important when setting up problems of this type. Many different approaches can be used to determine the optimum grid features to allow for the most accurate representation of the physical structures involved. A discussion of some of these approaches as well as the features of the helical system which most strongly affect the computed results will be given.

Interaction impedance is an important input parameter for modeling of the beam/RF interaction of any helix TWT and determines the coupling of the individual electron macroparticles, rings, or discs to the RF wave traveling on the surrounding helix. Once the eigenmodes have been computed, this interaction impedance can be determined by integrating the axial electric field along the axis of the helical system. This quantity has been experimentally determined for the X-Band TWT using a perturbation method and an automated phase measurement system. The results of the comparison of measurement and CTLSS calculation will be presented.

^{*}Supported by the Office of Naval Research.

The Angular Distribution of Elastically Scattered Electrons, Its Modeling and Computed Effect on Collector Performance

I.L. Krainsky and K.R. Vaden, NASA Lewis Research Center, Cleveland, OH 44135, USA

The Angular Distribution of Elastically Scattered Electrons, Its Modeling and Computed Effect on Collector Performance

I. L. Krainsky and K. R. Vaden NASA Lewis Research Center Cleveland, OH 44135

It is known that the suppression of secondary electron emission significantly improves the performance of electron beam collectors. However, a complete analysis of the effects of secondary emission on collector performance has not been possible because of the lack of quantitative data on secondary electrons. The measurements of the angular distribution of elastically scattered secondary electrons from surfaces of polished copper, ion-textured copper, and isotropic (POCO) graphite will be presented.

An electron source, with an energy ranging from 100 to 3000 eV and a spot size of less than 1 mm, was directed the target. The angle of incident for the source was varied from normal to grazing incidence in 2 or 3 degree increments. At each angle of incidence, secondary electrons within 2 to 20% of the energy of the incident beam were measured throughout the half-sphere above the target surface in 1 degree increments.

Elastically scattered electrons have a complex angular distribution that is strongly dependent on the energy and angle of incidence of the electron beam, as well as the atomic number and surface morphology of the target material. At low energies and normal incidence, elastically scattered electrons from polished copper are primarily directed back towards the electron source (back-scattered). Forward scattering increases with incident angle. Forward scattering also increases with primary energy until, at high energies, forward scattering can dominate the angular distributions as the incident angle Although back-scattered secondary approaches grazing. electrons dominate the distributions of the ion-textured copper surface, the yield is substantially lower. POCO graphite has a distribution similar to polished copper; however, it has a much lower yield. The results of angular distribution measurements and the application of that data to collector design will be presented.

2P10

A Simple Theory of Ion Noise in TWT

Y.Y. Lau, D. Chernin and W. M. Manheimer, U.S. Naval Research Laboratory, Washington, DC 20375, USA

A Simple Theory of Ion Noise in TWT

Y. Y. Lau*, D. Chernin**, and W. M. Manheimer Naval Research Laboratory, Washington, DC 20375

Phase noise in traveling wave tubes, of amplitude 1 degree or less, is of concern in certain radar applications, and has been extensively characterized [1]. The noise is of low frequency, ranging from ten's of Hz to kHz, and is found to be extremely sensitive to minor adjustments of the confining magnetic field that is used for beam focusing [1]. For example, a one-percent change in the confining magnetic field may turn on or off such noise.

The physical mechanism for the generation of the phase noise is not well understood, although it has been widely conjectured to be due to the ions that are trapped in the electrostatic potential well that is formed by the scalloping motion of the electron beam [2]. Consequently, such noise has been called ion noise. Tubes manufactured under nominally identical conditions can exhibit vastly different ion noise behavior. This tube-to-tube variability is one of the central puzzles of ion noise.

In this paper, we present a simple theory to explain some key features of ion noise observed in experiments. It is shown that, in the event that beam scalloping due to mismatch cannot be avoided, the most effective way to suppress ion noise is adjustment of the magnetic field so that the interaction length is an integral multiple of the scalloping wavelength. The theory, which isolates the largely uncharacterized ionic processes, is able to account for the experimental observations [1]: (1) the extreme sensitivity of ion noise levels to the strength of the magnetic focussing field and cathode voltage, (2) the marginal sensitivity of ion noise to cathode heater filament voltage, and (3) the insensitivity of ion noise to rf drive level and collector voltage.

This work was supported by ONR, NRL, and NSWC/Crane.

- *U. Michigan, Ann Arbor, MI
- **SAIC, McLean, VA
- [1] R. English and W. Funk (1998; unpublished).
- [2] A. S. Gilmour, Jr. (1998; unpublished).

Genesis: A 2.5D Nonlinear Simulation Code For Helix Traveling Wave Tubes In The Frequency Domain

H.P. Freund, T.M. Antonsen Jr. and B. LevushY.Y., U.S. Naval Research Laboratory, Washington, DC 20375, USA

GENESIS: A 2.5D NONLINEAR SIMULATION CODE FOR HELIX TRAVELING WAVE TUBES IN THE FRE-QUENCY DOMAIN*

H.P. Freund,[†] T.M. Antonsen, Jr.,[†] and B. Levush Code 6840, Naval Research Laboratory Washington, DC 20375

A nonlinear analysis of the helix traveling wave tube (TWT) in the frequency domain is presented for a configuration where an electron beam propagates through a sheath helix surrounded by a conducting wall. Dielectric- and vane-loading of the helix are included as is circuit tapering and external focusing by means of either a solenoidal magnetic field or a periodic field produced by a periodic permanent magnet (PPM) stack. These field models permit the treatment of tapered solenoidal and PPM fields. The electromagnetic field is treated as a superposition of waves in the sheath helix approximation in which the amplitudes and phases are assumed to vary slowly in z. The dynamical equations for the field are solved in conjunction with the three-dimensional Lorentz force equations for an ensemble of electrons. Collective effects from the fluctuating RF beam space-charge waves are included by means of a superposition of solutions of the Helmholtz equation. The DC self-fields due to the bulk charge and current densities of the beam are also included. The simulation is compared with a linear theory of the interaction as well as a time-domain simulation model, each of which is applied to an example corresponding to a tube built at Northrop-Grumman Corp. The frequency- and time-domain simulations are in substantial agreement for the case under consideration. The advantages of the frequency-domain formulation derive from the fact that the run time is substantially shorter than for the time-domain simulation. Because of this, the frequency-domain simulation can more easily treat such effects as beam thermal effects and multiple waves with closely spaced frequencies. GENESIS has also been applied to study the use of tapered solenoidal or PPM fields to improve the linearity of helix TWTs. The basic concept here is to use a tapered focusing field to modify the beam size which, in turn, alters the local interaction impedance. We study whether the effect of this local variation in the interaction impedance can extend the linearity of the amplification process. Finally, analysis has begun to include a fully 3D tape helix model into GENESIS.

2P12

Localized Growth Rates of Intermodulation Products in a Multitone Traveling Wave Tube Amplifier

J.G. Wohlbier, I. Dodson, J.H. Booske, J.E. Scharer, University of Wisconsin, Madison, WI 53706, USA

Localized Growth Rates of Intermodulation Products in a Multitone Traveling Wave Tube Amplifier

J. G. Wöhlbier, I. Dobson, J. H. Booske, J. E. Scharer

Department of Electrical and Computer Engineering University of Wisconsin, Madison 53706

Recently developed ultrawideband (UWB) TWTAs (bandwidth exceeds one octave) present new possibilities for simultaneous amplification of multiple carrier signals (multitone operation). However, additional aspects of nonlinearity (giving rise to unwanted intermodulation products or IMPs) are also introduced, due to the fact that carrier harmonics and IMPs are now included within the broader gain bandwidth of the amplifier. By modifying a perturbational technique previously developed for FELs and Gyrotrons [1,2] we are able to predict local growth rates of these deleterious signals in the presence of two driving tones, and hence estimate their levels at the tube output. The technique represents an IMP or harmonic as a perturbation about a nonlinear numerical solution of a Hamiltonian TWTA model with two driving tones. A dispersion relation and hence growth rate as a function of frequency and distance along the tube is attained. The technique allows us to examine the dependence of the IMP growth rate on the frequencies and amplitudes of the drive signals.

Acknowledgments

Supported in part by a Northrop Grumman Industrial Associates grant.

References

- T. M. Antonsen, Jr., B. Levush. Phys. Fluids B. 1(5), 1097. 1989.
- [2] B. Levush, T. M. Antonsen, Jr. IEEE Trans. Plasma. Sci. Vol. 18. No. 3. June 1990.

^{*}Work supported by the Office of Naval Research.
†Permanent Address: Science Applications International Corp.,
McLean, VA 22102.

Analysis of 3-D Phase Space Dynamics of Pencilto-Sheet Electron Beam Transformation in Highly-Non-Paraxial Quadrupole Lens System M.J. McNeely, J.H. Booske, J.E. Scharer, &

M.A. Basten,

University of Wisconsin, Madison, WI 53706, USA

Analysis of 3-D Phase Space Dynamics of Pencil-to-Sheet-Electron-Beam Transformation in Highly-Non-Paraxial Quadrupole Lens System*

M. J. McNeely, J. H. Booske, J. E. Scharer, M. A. Basten**

Department of Electrical and Computer Engineering University of Wisconsin, Madison 53706

Sheet electron beams have the potential to make possible higher power sources of microwave radiation due to their ability to transport high currents, at reduced current densities, through a single narrow RF interaction structure. Previous investigations have indicated the feasibility for laboratory formation of an elliptical sheet beam using magnetic quadrupoles and a Pierce gun pencilbeam source [1,2]. The configuration exhibits several unique physical features of phase space evolution not observed in more conventional, paraxial beam transport systems. Previous numerical simulations using MAGIC3-D indicate the r.m.s. phase space volume occupied by the sheetbeam increased longitudinally, which contradicts the principle of phase space conservation for a conservative system (Liouville's theorem). The explanation is that is Liouville's theorem does not strictly apply to r.m.s. emittance calculations and some alternative phase space measure might provide closer agreement with Liouville's theorem. The developed phase space measure is non-statistical and uses principles from mathematical morphology. We discuss and compare the results of numerical simulations using the TRACE3-D and MAGIC3-D codes. In addition, we discuss the morphological algorithm for computing phase space area and compare its results with that of the r.m.s. formalism for calculating phase space area.

Acknowledgments

*supported in part by ONR, administered by NRL; also by a Northrop Grumman Industrial Affiliates grant

**current address, Northrop Grumman Corp, Rolling Meadows, IL 60008

References

- M.A. Basten, J.H. Booske, and J. Anderson, IEEE Trans. Plasma Sci. 22[5], 960. 1994.
- [2] M.A. Basten, J.H. Booske, L.J. Louis, J. Joe, and J.E. Scharer, Proc. IEEE ICOPS, paper 5HP20, 1996.

2P14

Experimental Validation of CHRISTINE, a 1-D Multi-Frequency Helix TWTCode: Drive Curves, Phase, Distortion Products and Intermodulation D.K. Abe, M.T. Ngo, B. Levush, T.M. Antonsen Jr. and D. Chernin, U.S. Naval Research Laboratory, Code 6843, Washington, DC 20375, USA

Experimental Validation of CHRISTINE, a 1-D, Multi-Frequency Helix TWT Code: Drive Curves, Phase, Distortion Products, and Intermodulation*

D.K. Abe, M.T. Ngo[§], B. Levush, T.M. Antonsen, Jr[†], and D. Chernin[‡] Naval Research Laboratory Washington, DC 20375

Experimental measurements of a Hughes 8537H 80 W CW helix TWTA operated from 1.4 to 1.75 GHz are compared with predictions made by CHRISTINE, a 1-D multifrequency helix TWT simulation code. The simulations utilize a recently implemented tape helix model.² Extensive experimental measurements were carried out to validate the code in both linear and saturated regimes using both single and multiple driven tones. In general, the model has shown excellent agreement with experimental measurements over a broad range of frequencies. Predicted TWT gain versus frequency characteristics agree to better than 3% of measured data with deviations in agreement explained by strong reflections at the output window that are not modeled by the code. Single tone experimental and predicted drive curves agree to better than 3% in the linear regime and to better than 1% near saturation; phase shift and AM-PM conversion predictions agree to within experimental measurement accuracies. Two-tone experimental and predicted data exhibit similarly good agreement, including third- and fifth-order intermodulation product data. Second harmonic measurements were also carried out and compared to CHRISTINE simulations with good agreement.

^{*}Work supported by the Office of Naval Research.

[§]Mission Research Corp., Newington, VA 22122.

[†]Institute for Plasma Research, University of Maryland, College Park, MD 20742 and Science Applications International Corp., McLean, VA 22102.

[‡]Science Applications International Corp., McLean, VA 22102.

¹ T.M. Antonsen, Jr. and B. Levush, NRL Report 97-9845, 1997.

² D. Chernin, et al., IEEE Trans. Electron Dev., to be published.

Design and Development of a 2-18 GHz MPM TWT

M.A. Basten, J. Duthie, J. Hutchins and C.M. Armstrong, Northrop Grumman Corporation, Rolling Meadows, Il 60008, USA

Design and Development of a 2-18 GHz MPM TWT¹
M. A. Basten, J. Duthie, J. Hutchins, and C. M. Armstrong
Northrop Grumman ESSS-DSD
Rolling Meadows, IL 60008-1098

Northrop Grumman Corporation, ESSS-DSD, is actively developing a 2-18 GHz, 125 W CW WideBand Microwave Power Module (WB-MPM) for use in decoy, remote transmitter, and other applications. The basic design philosophy of the WB-MPM is to incorporate a two-and-one-half octave, 3-18 GHz, 125 CW W vacuum power booster traveling wave tube (TWT), with a solid-state harmonic injection circuit and signal conditioner integrated within the MPM architecture, in order to meet the full performance objective of 125 W of fundamental power in excess of 3 octaves of bandwidth.

The work described here concentrates primarily on the design and development of the 3-18 GHz vacuum power booster TWT. This TWT development effort builds on the success of the Northrop Grumman 4.5-18 GHz, 125 W CW UltraBand MPM TWT. Bandwidth extension to 3 GHz will be realized through circuit design modifications and optimization for low-end fundamental power. A number of TWT design codes, including the CHRISTINE² and GATOR³ codes, are being utilized in this effort. Additionally, optimizer routines for power-bandwidth performance have been incorporated in the 1-D CHRISTINE code for circuit design optimization. A comparison of the performance predicted by these routines with actual measured performance will be provided.

A related effort is also underway to characterize the performance of the existing 2-octave UltraBand TWT under conditions of controlled harmonic drive. A breadboard harmonic generator and injection circuit has been designed, built, and tested with the TWT. Experimental data showing the fundamental power increase and reduced harmonic output from the TWT with optimized harmonic phase and amplitude down to 2 GHz will be presented. Comparisons will also be made to the predictions of the 1-D CHRISTINE code and, where possible, to the power and helix intercept predictions of the 2-D GATOR code.

2P16

Exploiting 2-1/2 D TWT simulations to maximize the efficiency of the Hughes 8815HR TWT

Daniel J. Gregoire, Xiaoling Zhai, HRL Laboratories, Malibu, CA 90265, USA

Exploiting 2-1/2 D TWT simulations to maximize the efficiency of the Hughes 8815HR TWT

Daniel J. Gregoire djGregoire@hrl.com HRL Laboratories Malibu, CA 90265 Xiaoling Zhai William L. Menninger Hughes Electron Dynamics Division Torrance, CA 90505

Beam efficiency, the RF output power divided by the electron beam power, is a critical parameter for the commercial success of a traveling-wave tube (TWT). Over the past thirty years, TWT designs have consistently established higher efficiency levels by developing advanced design techniques for analyzing parametric changes to the electron gun, helix geometry, and especially, the electron-beam collector. Advanced TWT simulation codes have emerged in recent years that offer the capability to simulate the electron-RF interactions with enhanced dimensionality on desktop computers. The Naval Research Laboratory has developed one such code, known as GATOR and another was developed by the NASA Lewis Research Center. These codes track the electron beam in two spatial and three momenta coordinates, and provide the TWT designer with more information on the electron beam dynamics than has traditionally been available.

In this paper, we present the results of our effort to design a collector for the Hughes 8815HR TWT based on the results of the 2-1/2 D simulations performed by GATOR and the NASA Lewis code. The simulation results will be compared to experimental measurements of the RF performance and the spent beam distribution. We also present experimental results of the performance comparisons between the old collector design and the new design based on the 2-1/2 D simulations.

¹ Research sponsored in part by the Office of Naval Research under Naval Research Laboratory Contract No. N00173-98-C-2038.

² T.M. Antonsen and B. Levush, "CHRISTINE: A multi-frequency parametric simulation code for traveling wave tube amplifiers", Naval Research Laboratory Memorandum Report NRL/FR/6840-97-9845, May, 1997.

³ H. Freund and E. Zaidman, "Nonlinear theory of collective effects in helix traveling wave tubes", *Phys. Plasmas*, 4, p. 2292 (1997).

Resonant Discharge Simulations with Asymmetric Electrodes

H.B. Smith, K.J. Bowers and C.K. Birdsall, University of California - Berkeley, Berkeley, CA 94720, USA

Resonant Discharge Simulations with Asymmetric Electrodes

H.B. Smith, K. J. Bowers and C.K. Birdsall EECS Department, University of California at Berkeley, Berkeley, CA 94720-1770

Bounded plasmas exhibit two basic natural resonances - the plasma frequency and the series resonance frequency. The latter is associated with the edge of the plasma, and involves density perturbations in the sheath; it is also the cut-off frequency for waves propagating along the wall.

Series resonant discharges have been previously simulated in planar 1d3v (one spatial dimension, 3 velocity dimensions) models. Results from these simulations are found to compare well with experimental measurements [1]. In this paper we will look at 1d3v simulations of series resonant discharges between concentric cylinders and concentric spheres, also 1d3v. First, the natural series resonant frequency is determined by simulating an undriven plasma between short-circuited electrodes, looking for the resonance in the current; this frequency will be checked with simple circuit modeling. Second, we drive the same model near this resonance, in order to obtain a selfsustained discharge. We will report in detail on the differences between the driven symmetric and asymmetric discharges with respect to start-up, lock-on and steady state behavior, as well as on scaling laws.

[1] C.K. Birdsall and K. J. Bowers, Paper OWP5 2, Gaseous Electronics Conference, October 1998, Maui, Hawaii.

Support is from DOE contract DE-FG03-97ER54446, ONR contract N00014-97-1-0241, and the Hertz Foundation Fellowship Program.

2P18

Resonant Discharges: Initiation and Steady State; Comparisons with Theory, Simulation and Experiement

Kevin J. Bowers, David W. Qiu, C.K. Birdsall, University of California - Berkeley, Berkeley, CA 94720-1772, USA

Resonant Discharges: Initiation and Steady State; Comparisons with Theory, Simulation and Experiment

Kevin J. Bowers, David W. Qiu, C.K. Birdsall EECS Department, University of California at Berkeley, Berkeley, CA 94720-1770

Discharges driven at the series resonance frequency have many desirable properties. The input resistance is small, and the voltage and current are in phase. The voltage drive is small (~ Te) and the average plasma potential is low (~10 Te). Such is observed experimentally in [1] and in our PIC-MCC simulations. Scaling laws at fixed pressure derived in [2] show peak electron density proportional to the cube of the drive frequency (capacitive discharge is as the square), permitting the density to be controlled. Simulation results show at low pressure, the ion energy distribution at the target has a sharp peak at the plasma potential with narrow angular spread about the normal. The V-I phase angle versus I curve is measured in simulation and compared with experimental results and the theoretical scaling laws are compared with simulation results and the transition of a capacitively coupled plasma to a resonantly sustained plasma is discussed. During this transition or "lock-on" (which occurs in a few RF cycles, a time scale much faster then ion related frequencies), the plasma changes dramatically: the electron kinetic energy and the plasma potential more than doubles; the circuit impedance of the discharge goes from capacitive to resistive; the motion of bulk plasma changes from nearly in phase to nearly out of phase with the voltage drive; and the characteristic heating pattern of these discharges takes shape. In these discharges, the formation of high velocity electron bunches in the sheath regions is seen. During an RF cycle, these bunches are alternately accelerated from each sheath into the bulk plasma. We speculate these bunches provide the ionization in resonantly sustained discharges. We also speculate that the lock-on process is similar to the mode-jumping seen in other resonantly and surface wave sustained discharges.

[1] V. A. Godyak, "Paper 3C9," IEEE ICOPS, Sante Fe, NM, June 1994.

[2] V. A. Godyak, "Steady-State Low-Pressure RF Discharges," Soviet J. Plasma Physics, Vol. 2, No. 1, January-February 1976.

This work is supported by DOE contract DE-FG03-97ER54446, AFOSR contract FDF 49620-96-1-0154, ONR contract N00173-98-1-G001 and the Hertz Foundation Fellowship Program.

Electrostatic and Electromagnetic Surface Wave Theories Compared

Kevin J. Bowers, University of California - Berkeley, Berkeley, CA 94720-1772, USA

Electrostatic and Electromagnetic Surface Wave Theories Compared

Kevin J. Bowers
EECS Department, University of California at Berkeley,
Berkeley, CA 94720-1770

The theory of resonance oscillations in a non-uniform thermal plasma given in [1] and the electrostatic surface wave theory given in [2] is extended. The new theory is fully electromagnetic. The theory is being used to investigate large area plasma sources and sheath phenomena. For a planar plasma loaded waveguide, the theory predicts two classes of waves. Modes with TE (transverse electric) like field components can be found by solving Maxwell's equations with a non-uniform dielectric given by the local cold plasma dielectric. These modes are unaffected by thermal effects in the limit of this theory. Modes with TM (transverse magnetic) like field components are more complicated - electron inertial and thermal effects allow new quasi-electrostatic (QES) modes to propagate below the peak electron plasma frequency similar to Tonk-Dattner resonances. The wave dispersion predicted by the electromagnetic theory differ from the electrostatic theories for long wavelength surface waves though. This discrepancy is explored. The results illuminate limitations of the electrostatic theories when used to predict phenomena in large area plasma sources.

J. V. Parker, J. C. Nickel, and R. W. Gould, "Resonance Oscillations in a Hot Nonuniform Plasma," Physics of Fluids, Vol. 7, No. 9, September 1964.
 D. J. Cooperberg, "Electron Surface Waves in a Nonuniform Plasma Slab," Physics of Plasmas, Vol. 5, No. 4, April 1998.

This work is supported by DOE contract DE-FG03-97ER54446 and the Hertz Foundation Fellowship Program.

2P20

2D Electromagnetic PIC-MCC Simulation of the Initiation of a Large Area Surface Wave Sustained Plasma Source

Kevin J. Bowers, University of California – Berkeley, Berkeley, CA 94720-1772, USA

2D Electromagnetic PIC-MCC Simulation of the Initiation of a Large Area Surface Wave Sustained Plasma Source

Kevin J. Bowers EECS Department, University of California at Berkeley, Berkeley, CA 94720-1770

A 2-D electromagnetic PIC-MCC simulation of a large area plasma source is being performed. In this simulation, the plasma is contained in a metal bound cylindrical region. In one version, the plasma is excited by a ring slot on top of the chamber by oscillatory radial electric fields across the slot. The simulation demonstrates the initiation and fill-in process of a slot excited surface wave sustained plasma source. The steady state density is compared with the predictions of a simple model of the diffusion of the plasma from the source. In the diffusion model, plasma undergoes ambipolar diffusion and is only lost at the walls. Also, the role of electromagnetic effects, such as ponderomotive forces, in the initiation and fill-in are explored.

This work is supported by the DOE contract DE-FG03-97ER54446 and the Hertz Foundation Fellowship Program.

Vortex formation and transport in 2D magnetized non-neutral bounded plasmas

Hae June Lee, Min Sup Hur, Jin Ho Kang and Jae Koo Lee, Pohang University of Science and Technology, Pohang, Kyoungbuk 790-784, S. Korea

Vortex formation and transport in 2D magnetized nonneutral bounded plasmas

Hae June Lee, Min Sup Hur, Jin Ho Kang, and Jae Koo Lee Dept. of Phys., Pohang University of Science and Technology, Pohang 790-784, S. Korea

The nonlinear behaviors of the magnetized nonneutral plasmas in two-dimensional cylindrical and Cartesian geometries are studied with particle-in-cell codes. In the (r, θ) cylindrical geometry, the self-induced radial electric field E_r due to charge nonneutrality causes $E \times B$ velocity shear, which induces some instabilities to form various vortex patterns and changes the transport behaviors. The effects of control parameters such as the applied magnetic field B, the electron-ion charge nonneutrality, and a external drive voltage on the vortex formation and the radial particle fluxes are investigated. In the (x, y) rectangular geometry, the dust oscillation due to induced space-charge field and the large inertia of dust is shown under slowly turning magnetic field even in the charge neutral plasma. The charge to mass ratio of the dust and the differences of charge densities among electrons, ions, and dusts play important roles of the oscillation. The flux changes and the pattern formation of dusts for various control parameter are examined.

2P22

Self-effect in expanding electron beam plasma

Manuel Garcia, Lawrence Livermore National Laboratory, Livermore, CA 94551-0808, USA

Self-effect in expanding electron beam plasma

Manuel Garcia

Lawrence Livermore National Laboratory, L-153, PO box 808, Livermore, CA 94550. garcia22@llnl.gov, (925) 422-6017

An analytical model of plasma flow from metal plates hit by intense, pulsed, electron beams aims to bridge the gap between radiation-hydrodynamics simulations and experiments, and to quantify the self-effect of the electron beam penetrating the flow. Does the flow disrupt the tight focus of the initial electron bunch, or later pulses in a train? This work aims to model the spatial distribution of plasma speed, density, degree of ionization, and magnetization to inquire. The initial solid density, several eV plasma expands to 1 cm and 10⁻⁴ relative density by 2 µs, beyond which numerical simulations are imprecise. Yet, a Faraday cup detector at the ETA-II facility is at 25 cm from the target and observes the flow after 50 µs. The model helps bridge this gap. The expansion of the target plasma into vacuum is so rapid that the ionized portion of the flow departs from local thermodynamic equilibrium. When the temperature (in eV) in a parcel of fluid drops below $V_I \times [(2\gamma - 2)/(9\gamma + 15)]$, where V_I is the ionization potential of the target metal (7.8 eV for tantalum), and y is the ratio of specific heats (5/3 for atoms), then the fractional ionization and electron temperature in that parcel remain fixed during subsequent expansion. The freezing temperature as defined here is $V_I/22.5$. The balance between the self-pinching force and the space charge repulsion of an electron beam changes on penetrating a flow: 1) the target plasma cancels the space-charge field, 2) internal eddy currents arise to counter the magnetization of relativistic electrons, 3) electron beam heating alters the flow magnetization by changing the plasma density gradient and conductivity magnitude. This causes beam expansion (besides scattering). The evolution of the total magnetic induction B (beam-in-target) is given by

$$\frac{\partial \mathbf{B}}{\partial t} = \left[\frac{\nabla^2 \mathbf{B}}{\sigma \mu} + \operatorname{curl}(\mathbf{v} \times \mathbf{B}) + \frac{\nabla \sigma}{\sigma} \times \frac{\operatorname{curl}(\mathbf{B})}{\sigma \mu} \right] + \left[\frac{\nabla \mathbf{k} T_e \times \nabla N_e}{e N_e} - \frac{\nabla^2 \mathbf{B}_0}{\sigma \mu} - \frac{\nabla \sigma}{\sigma} \times \frac{\operatorname{curl}(\mathbf{B}_0)}{\sigma \mu} \right]$$

where B_0 is the beam magnetic induction. The generated magnetic field has the opposite polarity to the self-field of the electron beam. Large local values arise where the density gradients are large: at the leading edge of the cloud, and at the exit of the plate. The second square bracket includes the thermal source term powered by beam heating, and the internal eddy current terms powered by the beam magnetization. Heating raises σ when a beam enters a cloud, which slows the diffusive loss of **B** and diminishes the first B-dot bracket. The second B-dot bracket appears because significant ∇T_e and \mathbf{B}_0 arise. When a beam pulse ends, expansion cooling dissipates ∇T_e , and both \mathbf{B}_0 and the second B-dot bracket disappear. The diminution of σ raises the first B-dot bracket and gives rise to a large $\partial \mathbf{B}/\partial t$, possibly observable as a "surface flashover" across the front of the cloud. This work was performed under the auspices of the U.S. DOE by LLNL under contract no. W-7405-Eng-48.

FDTD Simulation of Electromagnetic Wave Transformation in a Dynamic Inhomogeneous, Bounded and Magnetized Plasma

D.K. Kalluri and J.H. Lee, University of Massachusetts - Lowell, Lowell, MA 01854, USA

FDTD Simulation of Electromagnetic Wave Transformation in a Dynamic, Inhomogeneous, Bounded, and Magnetized Plasma

D. K. Kalluri & J. H. Lee Electromagnetics and Complex Media Research Laboratory University of Massachusetts Lowell Lowell, MA 01854

The electromagnetic wave transformations in a dynamic, inhomogeneous, bounded, and magnetized plasma medium are studied by using the Finite-Difference Time-Domain method (FDTD). A Lorentz plasma model is used and the source frequency of the waves is considered high enough that ion motions are neglected. The frequency shifting characteristics are extensively studied. The successive reduction method is developed to find frequencies and amplitudes of the fields from the time series generated by the FDTD simulation. The method is superior to the conventional FFT method.

In one-dimensional problems, time-only formulation is used for unbounded problems and for the periodic problems, one unit cell space formulation is used. For the plasma slab, total field/scattered field formulation and PML absorption boundary condition are used to implement compact size FDTD code. The FDTD method is compared with approximate analytical methods (perturbation method and WKB method) and the validity ranges of those analytical methods are obtained.

It is shown that the source wave is modified when the change of plasma density is slow while new modes are generated when the change of the plasma density is fast. It is also verified that when the source wave is a whistler wave, collapsing of the plasma medium generates frequency upshifting with power intensification and the switching off the external magnetic field generates a wiggler wave.

The modes generated by switched periodic magnetoplasma layers are studied. The characteristics of additional downshifted modes due to the presence of the static magnetic field are discussed.

For the case of the three-dimensional anisotropic problem, a new FDTD formulation is implemented by positioning the current density vector at the center of the Yee's cube. Appropriate time stepping algorithm is used to obtain accurate solution for arbitrary values of the collision frequency and the electron cyclotron frequency.

The technique is illustrated by calculating the frequency shifts in a cavity due to a switched magnetoplasma medium with a time-varying and space-varying electron density profile.

The algorithms developed make it possible to simulate many of the complex problems associated with using a laboratory generated practical switched magnetoplasma as a frequency transformer.

2P24

Nonlinear Trapping Simulations or Helicon Plasma Sources

H. Gui and J.E. Scharer, University of Wisconsin, Madison, WI 53706-1687, USA

Nonlinear Trapping Simulations for Helicon Plasma Sources*

H. Gui and J. E. Scharer

Department of Electrical and Computer Engineering University of Wisconsin, Madison 53706

The nonlinear trapping process is an important effect which may contribute to the extraordinary high wave damping rate of helicon sources. We are developing a numerical simulation method and code to study nonlinear phenomena in plasmas with complex wave structure. An open system with a steady-state initial distribution function is considered. In the case of low density(n<10¹¹/cm³) where collision effects can be neglected, the distribution function as a function of time and space is obtained by solving the motion equation and tracing particle trajectories back to the starting point. Our simulation results for a sinusoidal wave field show that trapped electrons with wave-particle phase confined within a range of phase less than 2π appear as the wave field intensity increases, and the distribution function shows bunching of fast particles around 40 eV at an Ez field intensity of 100V/m. We are studying the effects of a wave number spectrum, a frequency spectrum, and field components including $\mu \nabla_z B_z$ and \mathbf{E}_\perp in addition to the electrostatic Ez on the nonlinear trapping process. The modelling of wave fields are based on the simulation results from our ANTENA IIa and MAXEB codes. We will also carry out the simulation utilizing MAGIC Particle-In-Cell code and comparison between these two approaches will be discussed. We will at the same time compare our simulation results with current experiments being carried out on our helicon experimental facility.

Acknowledgments

*This work was supported by NSF Grant No. ECS-9632377.

 b Y´. Mouzouris and J. E. Scharer; *Phys. Plasmas.* 5(12): 4253. 1998.

[°]Y. Mouzouris and J. Scharer; IEEE Trans. Plasma Science. 24(1): 152. 1996.

Initial Design for an Experimental Investigation of Strongly Coupled Plasma Behavior in the Atlas Facility

Carter P. Munson, J.F. Benage Jr. A.J. Taylor, R.J. Trainor, Jr. B.P. Wood and F. J. Wysocki, Los Alamos National Laboratory, Los Alamos, NM 87545, USA

Initial Design for an Experimental Investigation of Strongly Coupled Plasma Behavior in the Atlas Facility

Carter P. Munson, J.F. Benage, Jr., A. J. Taylor, R. J. Trainor, Jr B.P. Wood, and F.J. Wysocki Los Alamos National Laboratory, Los Alamos, NM 87545

Atlas is a high current (~30 MA peak, with a current risetime ~ 4.5 μ sec), high energy (E_{stored} = 24 MJ, E_{load} = 3-6 MJ), pulsed power facility which is being constructed at Los Alamos National Laboratory with a scheduled completion date in the year 2000. When operational, this facility will provide a platform for experiments in high pressure shocks (> 20 Mbar), adiabatic compression (p/p₀ >5, P>10 Mbar), high magnetic fields (~2000 T), high strain and strain rates (ε> 200%, dε/dt ~ 10⁴ to 10⁶ s⁻¹), hydrodynamic instabilities of materials in turbulent regimes, magnetized target fusion, equation of state, and strongly coupled plasmas. For the strongly coupled plasma experiments, an auxiliary capacitor bank will be used to generate a moderate density (< 0.1 solid), relatively cold (~ 1 eV) plasma by ohmic heating of a conducting material of interest such as titanium. This target plasma will be compressed against a central column containing diagnostic instrumentation by a cylindrical conducting liner that is driven radially inward by current from the main Atlas capacitor bank. The plasma is predicted (by 1-D numerical simulations using the RAVEN1 and CRUNCH² codes) to reach densities of ~1.1 times solid, achieve ion and electron temperatures of ~10 eV, and pressures of ~ 4-5 Mbar. This is a density/temperature regime which is expected to experience strong coupling ($\Gamma \sim 14$), but only partial degeneracy ($\Theta \sim 0.7$). X-ray radiography is planned for measurements of the material density at discrete times during the experiments; diamond Raman measurements are anticipated for determination of the pressure. In addition, a neutron resonance spectroscopic technique is being evaluated for possible determination of the temperature (through low percentage doping of the titanium with a suitable resonant material). Initial target plasma formation experiments are being planned on an existing pulsed power facility at LANL (the COLT³ facility), and will be completed before the start of operation of Atlas.

Details of the expected experimental configuration and results of the numerical simulations performed will be presented.

¹RAVEN—a 1-D, Lagrangian, radiative, MHD code developed by C.M. Lund, T.A. Oliphant, and K.H. Witte, Los Alamos National Laboratory

²CRUNCH – Stanley Humphries, Jr., Field Precision, PO Box 3595, Albuquerque, New Mexico 87192 USA

³ F.J. Wysocki et al., Digest of Technical Papers for the 11th IEEE International Pulsed Power Conference, Baltimore, Maryland, June 29 to July 2, 1997, G. Cooperstein and I. Vitkovitsky eds., pg. 1393.

2P26

Two Species Presheath Measurements In a Multidipole Plasma

A.M. Hala and N. Hershkowitz, University of Wisconsin-Madison, Madison, WI 53705, USA

Two Species Presheath Measurements In a Multi-dipole Plasma

A. M. Hala and N. Hershkowitz University of Wisconsin-Madison

Emissive probe measurements of plasma presheath potential profiles were made in a DC hot filament multidipole plasma discharge. The measurements were done with Argon, Xenon and a combination of the two gases. The presheath plasma potential near a negatively biased plate was mapped in two dimensions. The inflection point method in the limit of zero emission was used. The presheath was found to be a region of constant electric field with characteristic length the order of the ion-neutral collision length. The results show contraction of the presheath in the direction perpendicular to the plate as the pressure increases (between 0.5 and 3 mtorr). Two competing processes affect the presheath. These are ionization and collisions with ionization becoming more important at lower pressures. Experimental results are compared to various presheath models.

^{*} Supported by DOE grant DE-FG0297ER54437.

^{*} Smith et al. (1979). Rev. Sci. Instrum. 50, 210.

Laser Induced Fluorescence Study of NOx in Streamer Discharges

A. Kharlov, G. Roth, V. Puchkarev and Martin Gundersen, University of Southern California, Los Angeles, CA 90089-0424, USA

Laser Induced Fluorescence Study of NOx in **Streamer Discharges**

A. Kharlov, G. Roth[†], V. Puchkarev and Martin Gundersen

University of Southern California Los Angeles, CA 90089-0484

A study of temporal and spatial dependence of NO and NO₂ in a transient plasma, using laserinduced fluorescence, is reported. Reactors including coaxial corona-type were studied under flowing conditions. The laser is used to study processes occurring during the time of streamer formation and propagation, the decomposition of NO in close proximity to the streamer channel. The chemistry of NO and NO2 in pure N2, occurring several milliseconds following pulsed excitation was studied and spatially resolved concentration profiles were Initial simulations of chemical obtained. kinetics will also be presented. Energy costs associated with single streamers for NO destruction will be reported, and the role of streamers in generating plasma chemistry will be discussed.

Work support in part by the U.S. Army Research Office under contract # DAAG55-98-1-0408, the U.S. Office of Naval Research under grant # N00014-94-1-0650 and the National Science Foundation under grant # CTS-9713275.

[†]Now with Litex Corporation, Detroit, MI

2P28

Spectroscopic Studies of Emissions from Microhollow Cathode Discharges

P. Kurunczi, K. Becker, Stevens Institute of Technology K.H. Schoenbach, A. El-Habachi Old Dominion Universtiy, Stevens Institute of Technology, Hoboken, NJ 07030, USA

Spectroscopic Studies of Emissions from Microhollow Cathode Discharges

P. Kurunczi, K. Becker, Stevens Institute of Technology K.H. Schoenbach, A. El-Habachi Old Dominion University

Conventional hollow cathode discharges are typically operated at pressures ranging from mTorr to Torr. Operation at higher pressures (up to atmospheric pressure) is possible, if the hole diameter is reduced to dimensions of about 100 µm with a corresponding reduction in the cathode-anode gap (microhollow cathode discharge). A microhollow cathode discharge (MHCD) operated at high (atmospheric) pressure is a simple, compact, and efficient sources of radiation such as rare gas excimer emissions [1]. The conditions in a MHCD satisfy the two criteria necessary for excimer formation, (i) a sufficiently large number of energetic electrons and (ii) pressures high enough that three-body collisions occur with sufficient frequency.

We have started a series of spectroscopic studies of emissions from MHCDs in the rare gases Xe, Ar, and Ne as well as in molecular nitrogen and air aimed (i) at elucidating the basic collision and relaxation processes in a MHCD and (ii) at obtaining a rudimentary understanding of the electron, neutral and ion temperatures in MHCDs under various operating conditions (pressure, current, electrode geometry, and hole size). We use a set-up in which the MHCD is mounted directly on the entrance slit of either a high resolution visible/UV monochromator (Δλ=0.01 nm, fwhm) or a medium resolution VUV monochromator (Δλ=0.1 nm, fwhm) equipped with appropriately chosen photon detectors. The MHCD can be operated either sealed with a LiF window or "open" with a small pin hole to allow detection at wavelengths below the LiF cut-off near 106 nm. Measurements include

- (i) high resolution emission spectroscopy of a dc MHCD in the visible (line shape analysis, line broadening studies, and intensity ratio measurements)
- (ii) time-resolved emission spectroscopic and fluorescence decay studies of a pulsed MHCD using gated photon detection and/or time-to-amplitude conversion techniques. Selected emissions include vacuum ultraviolet as well as visible

emissions of appropriately chosen species (rare gas ion and excimer emissions in the VUV, atomic and ionic N and O emissions in the VUV, and molecular nitrogen and nitrogen ion emissions in the visible).

First results will be presented and discussed at the Conference.

[1] A. El-Habachi, K.H. Schoenbach, Applied Physics Letters 72, 22 (1998)

Work supported by the NSF and the AFOSR.

Side-Extraction-Type Secondary-Emission Electron Gun Using wire Ion Plasma Source

Masaki Ishikawa, Naoki Kanbe, Akitoshi Okino, Kwang-cheol Ko and Eiki Hotta, Tokyo Institute of Technology, Yokohama 226-8502, JAPAN

Side-Extraction-Type Secondary-Emission Electron Gun Using Wire Ion Plasma Source

Masaki ISHIKAWA, *Naoki KANBE, *Akitoshi OKINO, **Kwang-cheol Ko and Eiki HOTTA

Department of Energy Sciences, Tokyo Institute of Technology,
Nagatsuta, Midori-ku, Yokohama, 226-8502, Japan.
*Department of Electrical and Electronic Engineering,
Tokyo Institute of Technology,
O-okayama, Meguro-ku, Tokyo, 152-8552, Japan.
**Department of Electrical and Computer Engineering,
Hanyang University,
Seongdong-ku, Seoul, 133-791, Korea.

A wire ion plasma source (WIPS) is a compact ion source, which consists of a central thin wire anode and a grounded coaxial cathode. The cathode also acts as a vacuum chamber. The configuration allows the initiation of low-pressure gas discharge only by applying voltage of several hundreds on the anode by virtue of the geometrical electron confinement.

A secondary emission electron gun is set beside the WIPS. The electrode set in the gun is highly negative-biased. Ions extracted from the WISP through a grid are accelerated toward the electrode and they collide on its surface with high kinetic energy, which corresponds to the electrode bias voltage. By collision of ions, secondary electrons are emitted from the electrode surface. The emitted electrons are then accelerated toward the extraction window and form a very wide electron beam. The extraction window is set on the side orthogonal to the ion extraction grid and is on earth potential. In this configuration, the accelerating potential distribution is considerably different from that of the plane parallel electrode configuration and it affects the extraction of electron beam. Therefore, the loci of electrons and the current distribution of beam at the extraction window are computed and compared with the experimental results.

This work is supported by the Ministry of Education, Science, Sports and Culture, Japan under Grant-in-Aid for Scientific Research (No.10555088).

2P30

Detection of Trivelpiece-Gould Modes in Helicon Discharges

D.D. Blackwell, T.G. Madziwa, D. Armush, and F.F. Chen, UCLA, Los Angeles, CA 90095-1594, USA

Detection of Trivelpiece-Gould Modes in Helicon Discharges

D.D. Blackwell, T.G. Madziwa, D. Armish, and F.F. Chen, UCLA

That helicon discharges produce higher plasma densities than unmagnetized inductively coupled plasmas (ICPs) is well known in the plasma processing community. A reason for the high RF coupling efficiency in these discharges has been suggested by Shamrai et al.¹; namely, that helicon waves, though weakly damped themselves, can transfer their energy at the boundary to electrostatic electron cyclotron waves [called Trivelpiece-Gould (TG) modes in confined cylinders], and these, in turn, are rapidly damped as they propagate inward toward the axis. To test this hypothesis, we have performed an experiment to detect the TG waves directly.

At high magnetic fields B_0 , TG waves are localized to a thin surface layer and are not easily detected, though they can cause most of the RF absorption. They are most easily seen at low magnetic fields, where their radial wavelengths are comparable to those of the helicon (H) waves. The radial profiles of the wave magnetic field B can then be differentiated from those of pure H waves. Typical operating conditions in the 10-cm diam chamber are $B_0 = 30$ G, $n = 10^{12}$ cm⁻³, p = 3 mTorr of argon, and $P_{\rm nf} = 1.2$ kW at 11 MHz. To remove possible azimuthal asymmetries, a single-turn m = 0 antenna was used; to eliminate capacitive coupling, a slotted Faraday shield was inserted between the antenna and the vacuum chamber.

Since theory predicts that the RF current j follows $j \approx k_{\perp}B/\mu_0$, and $k_{\perp}(TG) >> k_{\perp}(H)$, existence of the TG mode would be even more obvious in the j profiles. A new diagnostic was therefore developed to measure j. This is a small current transformer (essentially an RF Rogowski coil) inserted in the plasma and carefully wound and shielded to eliminate pickup of both B and E fields. The signal was taken out with a twisted pair into a balun transformer. The RF response was tested by inserting the j-probe into a pool of mercury, and the pickup level was measured in situ in the discharge.

Theoretical B- and j-profiles were computed with the code developed by Arnush and Chen², which includes the exact antenna geometry, the density profile, damping by neutral and Coulomb collisions, and the coupling between H and TG modes. The results show profiles which agree fairly well with the predictions and are distinct from what is expected from pure H modes.

¹K.P. Shamrai, V.P. Pavlenko, and V.B. Taranov, Plasma Phys. Control. Fusion **39**, 505 (1997).

²D. Arnush and F.F. Chen, Phys. Plasmas 5, 1239 (1998).

De Anza Ballroom 8:30 AM, Tuesday, June 22, 1999

Plenary Talk

Thermal plasma Processes: where are they, where do they go?

Prof. P. FAUCHAIS and A. VARDELLE Universite de Limoges

Plasma technology has grown in the last 30 years for many reasons:

- the need for the industrial world to develop more efficient techniques and processes,
- a very attractive electricity power cost in some countries, for example in France and Canada,
- the potential for developing new materials related technologies,
- the enhanced cooperation between manufacters, researchers, industrialists and electricity producers.

This growth is partly due to the great strides made by the fundamental research in the field allowing a much better understanding of the phenomena involved in thermal plasmas.

We will first recall what is our present knowledge in the production of thermal plasmas, thermodynamic and transport properties, fundamental processes in plasma torches, modeling, measurement techniques and on-line control. However, the number of successful industrial applications is not as important as plasma community would have expected. This is due to the fact that the key plasma parameters are not the only ones controling a process and its reproducibility. The latter will be discussed for four thermal plasma processes:

- plasma cutting,
- plasma spraying,
- ultrafine particle production,
- waste destruction.

The problems linked to the choice of the parameters allowing an on-line control of the process, and not only of the plasma, in industrial conditions will be particularly emphasized.

Chairperson Dr Don Rej Los Alamos National Laboratory

3A

De Anza Ballroom 8:30 AM, Tuesday, June 22, 1999

Oral Session 3A

Computational Plasma Physics

Chairperson
Richard Hubbard
Naval Research Laboratory

3A01

A Description Of The New 3D Electron Gun And Collector Modeling Tool: MICHELLE

John Petillo, Alfred Mondelli, Warren Krueger, Kenneth Eppley, Thomas McClure, Paul Blanchard, Simon Cooke, Barauch Levush, Mark Catteloino, Stan Humphries Jr, Jim Burdette, Eric Nelson, Richard True, Norman Dionne, SAIC, Burlington, MA 01803, USA

A Description Of The New 3D Electron Gun And
Collector Modeling Tool: MICHELLE*

John Petillo, Alfred Mondelli, Warren Krueger, Kenneth Eppley,
Thomas McClure, Paul Blanchard Simon Cooke, SAIC, Baruch
Levush, NRL, Mark Cattelino, CPI, Stan Humphries Jr., Field
Precision, Jim Burdette, Hughes, Eric Nelson, LANL, Richard
True, Litton, and Norm Dionne, Raytheon

A new 3D finite element gun and collector modeling code is under development at SAIC in collaboration with industrial partners and national laboratories. This development program has been designed specifically to address the shortcomings of current simulation and modeling tools. In particular, although there are 3D gun codes that exist today, their ability to address fine scale features is somewhat limited in 3D due to disparate length scales of certain classes of devices. Additionally, features like advanced emission rules, including thermionic Child's law and comprehensive secondary emission models also need attention. The program specifically targets problems classes including gridded-guns, sheet-beam guns, multi-beam devices, and anisotropic collectors.

The presentation will provide an overview of the program objectives, the approach to be taken by the development team, and a status of the project.

* Work supported by DOE, contract W-7405-ENG-36, and ONR, NRL contract N00014-97-C-2076.

3A02-3

Invited -

An Improved Jacobi-Davidson Algorithm Applied to Non-Hermitian Electromagnetic Eigenvalue **Problems**

S.J. Cooke, A. Mondelli, E. Nelson and B. Levush, U.S. Naval Research Laboratory, Washington, DC 20375, USA

An Improved Jacobi-Davidson Algorithm Applied to Non-Hermitian Electromagnetic Eigenvalue Problems

S.J. Cooke[‡], A. Mondelli[‡], E. Nelson[#], and B. Levush

Naval Research Laboratory Washington, DC 20375

An implementation of the Jacobi-Davidson method for solving non-Hermitian eigenproblems in electromagnetics will be presented. The standard Jacobi-Davidson algorithm has been extended to reduce memory requirements and to improve computational speed through the use of a multigrid approach. Algorithmic details particular to the types of problem typically encountered in design applications will be described, including the capability to handle highly lossy materials and the need for many degrees of freedom to accurately represent an electromagnetic field.

The classes of eigenproblem to which this method has been applied include periodic and lossy structures, discretized on both structured and unstructured meshes. Each class of problem will be described, with reference to the particular difficulties that it presents, and examples will be used to demonstrate the effectiveness of this technique as a general eigenfrequency solver.

3A04

Two-dimensional Fluid Model for an Inductively **Coupled Chemical Vapor Deposition Reactor**

K. Bera and B. Farouk, Drexel University, Philadelphia, PA 19104, USA

Two-dimensional Fluid Model for an Inductively Coupled **Chemical Vapor Deposition Reactor**

K. Bera and B. Farouk

Department of Mechanical Engineering and Mechanics Drexel University Philadelphia, Pennsylvania 19104, USA

self-consistent ABSTRACT two disconnections two-dimensional radio-frequency inductively coupled glow discharge model has been developed in cylindrical coordinates using a fluid model. The objective of the study is to provide insights to charged species dynamics and investigate their effects on plasma process for a non-reacting Ar and depositing methane discharges. The model includes continuity, momentum and energy equations for electron and ions. An electromagnetic model that considers electric field due to space charge within the plasma and due to inductive power coupling, is also incorporated. For methane discharge we expect to find higher flux to the cathode, and hence higher deposition rate. The independent control of ion energy to the cathode in an inductive discharge will facilitate a control of quality of the deposited film. Swarm data as a function of electron energy are provided as input to the model. The model predicts electron density, ion density, and their fluxes and energies to the cathode. The role of electrons, and dominating ions in high density discharge will be investigated. The neutral and radical densities in the discharge are calculated using a global model.

The advantages of capacitively coupled discharges are simplicity of design, initial cost and ease of operations. The limiting factor of capacitively coupled discharge is that the ion-bombarding flux and bombarding energy cannot be varied independently. An inductively coupled reactor can be used to obtain higher ion flux and hence higher deposition rate for a given power with separate control of ion-flux and ion energy. An inductively coupled reactor with planar configuration (as shown in Figure 1) has been considered in this study.

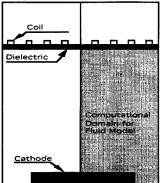


Figure 1. Computational domains for the inductively coupled reactor

The numerical model for inductively coupled rf discharge considers a reactor with planar configuration with four coils at the top of the reactor separated by a dielectric window. The fluid model equations are solved in the interior of the discharge chamber. The electromagnetic model equations are solved over a domain that includes the discharge chamber, quartz insulator, and a vacuum region that includes the coils. We have carried out parametric studies to study the effects of operating conditions of the reactor on deposition characteritics.

^{*}Work supported by the Office of Naval Research.

^{*}Science Applications International Corp., McLean, VA 22102.

Los Alamos National Laboratory, Los Alamos, NM

¹G.L.G. Sleijpen and H.A.van der Vorst, "A Jacobi-Davidson method for linear eigenvalue problems", SIAM J. Matrix Anal. Appl., vol.17, no.2, pp401-425 (1996)

3A05

Ion Distribution Functions in an ECR Chlorine Discharge

Glenn Joyce, Martine Lampe, W.M. Manheimer, Richard Fernsler and S.P. Slinker, U.S. Naval Research Laboratory, Washington, DC 20375, USA

Ion Distribution Functions in an ECR Chlorine Discharge*

Glenn Joyce, Martin Lampe, W. M. Manheimer, Richard Fernsler, and S. P. Slinker

> Plasma Physics Division Naval Research Laboratory Washington, DC 20375

We have developed an axisymmetric quasi-neutral particle simulation code, QUASI-rz, to study heating and transport of plasma in an ECR reactor configuration. All species are treated as particles. The code contains a kinetic formulation for ECR heating that includes Doppler shifts and selfconsistent wave attenuation. The plasma is high density and weakly collisional, with mean free paths on the order of a few centimeters. We will present the results of simulating a chlorine-argon gas mixture with pressures on the order of a few milliTorr. Charged particles collide with the neutral gas and with other charged particles. We include ion-ion, and electron-electron scattering. In chlorine, ions can be either positively, or negatively charged. Negative ions, unlike electrons are not constrained to a single field line, and may contribute to the cross field particle flux. We present results from the simulation showing the densities of the various species. We also show the velocity distribution functions of the ions at various locations in the system. The relative importance of ion-ion and ion-neutral scattering in the presheath region will be examined.

3A06-7

Invited -

Modeling The Alignment of Grains in a Dusty Plasma

D. Winske, J.E. Hammerberg, B.L. Holian, M.S. Murillo and W.R. Shanahan, Los Alamos National Laboratory, Los Alamos, NM

87545, USA

MODELING THE ALIGNMENT OF GRAINS IN A DUSTY PLASMA

D. Winske, J. E. Hammerberg, B. L. Holian, M. S. Murillo and W. R. Shanahan

Los Alamos National Laboratory Los Alamos, NM 87545 USA

Dusty plasmas provide new challenges for traditional computational plasma physics methods. For example, in the last few years it has been shown that dust grains in a plasma tend to form into regular crystalline arrays, known as "plasma crystals". The grains are trapped in the sheath region of rf discharges and tend to become aligned in the direction of ion flow toward the electrode, which can lead to crystal structures different from those predicted by the theory of strongly coupled plasmas. The alignment process has been studied with molecular dynamics simulations that treat the dust grains as discrete charged particles interacting via screened potentials. An asymmetric addition to the interaction is included through a dipole force. The addition of a very weak dipole is sufficient to modify the structure of the crystal, making it more consistent with experiments, and phase transitions to different configurations occur as the dipole contribution is increased. Experiments at Los Alamos have studied the particle spacing in chains of dust grains as a function of the discharge parameters and suggest that wake effects from the flowing ions can provide a dipole of correct magnitude to explain the observations. The detailed properties of the wake potential surrounding a single grain or a linear array of grains are studied with particle-in-cell simulations that treat both dust grains and the flowing plasma ions as discrete particles that are collisionally coupled to the background neutral gas. The simulations address the dipole approximation, nonlinear modifications to the standard test particle approach, shielding from ions orbiting the dust grains, and wake damping due to phase-mixing and collisional effects.

^{*}Supported by Office of Naval Research

3A08

Computational Simulation of Magnetic Field Configurations in Helical Magneto-Cumulative Generators

Michael H. Frese and Sherry D. Frese, NumerEx, Albuquerque, NM 87106, USA

Computational Simulation of Magnetic Field Configurations in Helical Magneto-Cumulative Generators
Michael H. Frese and Sherry D. Frese, NumerEx.

Helical magneto-cumulative generators (MCGs) driven by high explosive can be used to generate a few microseconds of mega-ampere current for pulsed power applications. They usually consist of a helically wound cylindrical coil surrounding a cylindrical armature. The armature is driven radially outward by the detonation of explosive inside it, reducing the inductance in the device, and creating an electromotive force on a load.

Engineering design of MCGs has depended on few-zone or one-dimensional numerical models that segment the stator and armature into rings and solve circuit equations for the currents in those rings to compute the magnetic flux between them. While often satisfactory, these models have some weaknesses. They usually employ simplifying assumptions about the armature currents, rather than solving selfconsistently for them. These approximations can result in significant errors, particularly as the contact point nears a change in coil pitch, a common design feature. Furthermore, they do not provide detailed pictures of the magnetic field configurations that occur during the generator run. This information can be crucial for understanding the performance of actual generators. Self-consistent two-dimensional calculation of the magnetic field created in the gap by the currents imposed in the stator and induced in the armature thus offer significant advantages.

Modifications to the 2-1/2 dimensional MHD code MACH2 have been made that enable it to simultaneously solve for the near-solenoidal magnetic field in the air and its diffusion into the armature. This technique has been applied to configurations of armature and stator produced by a self-consistent hydrodynamic calculation of modest resolution. In these simulations — each requiring a few hours on a 450 MHz Pentium-II computer running NT — a coupled external circuit driven by the variation of the generator inductance self-consistently determines the changing current. The generator inductance is determined at every computational time by integration of the flux linked to the stator current. The technique will be described and results will be shown from simulations that incorporate such common MCG design techniques as varying coil pitch.

3A09

SAMI II: The NRL Low-Latitude Ionosphere Model J.D. Huba and G. Joyce, U.S. Naval Research Laboratory, Washington, DC 20375, USA

SAMI II: The NRL Low-Latitude Ionosphere Model

J.D. Huba and G. Joyce Plasma Physics Division Naval Research Laboratory Washington, DC 20375

A new low-latitude ionosphere model is has been developed at the Naval Research Laboratory. The model solves the continuity, momentum, and energy equations for ions along a field line from hemisphere to hemisphere. The electron energy equation is also solved. Two models have been developed: collisional and inertial. The collisional model neglects inertial effects in the momentum and energy equations. The inertial model includes these effects so that the model is self-consistent at high altitudes (above 800 km). Seven ion species are considered: H⁺, He⁺, N⁺, O⁺, N⁺₂, NO⁺, and O⁺₂. The corresponding neutral species are also considered; the MSIS86 and HWM93 models are used to obtain neutal densities and winds. The daytime photodeposition is based upon the solar EUV model of Richards et al. (1994) and the nighttime photodeposition is based upon that of Strobel et al. (1980). The new code is similar in scope to the Field Line Interhemispheric Plasma model (FLIP) developed by Richards and Torr but uses different numerical schemes. We will contrast the results from the collisional and inertial models to demonstrate at what altitudes inertial effects become important and how they affect the ionospheric morphology. To our knowledge this is the first global low-latitude ionospheric model that includes ion inertia and the full ion temperature equation. We will discuss the numerical schemes that have been developed to address these issues.

Richards et al., J. Geophys. Res. 99, 8981 (1994). Strobel et al., Planet. Space Sci. 28, 1027 (1980). Research supported by ONR and a grant from the DoD HPC Shared Resource Centers CEWES and NAVO.

3B

De Anza II 10 AM, Tuesday, June 22, 1999

Oral Session 3B Microwave Systems

Chairperson

Jeff Calame

Naval Research Laboratory

3B01

Pulsed Testing of a Quasioptical Gyrotron for Materials Processing

R.P. Fischer and A.W. Fliflet, U.S. Naval Research Laboratory, Washington, DC 20375, USA

Pulsed Testing of a Quasioptical Gyrotron for Materials Processing*

R.P. Fischer and A.W. Fliffet
Beam Physics Branch
Plasma Physics Division
U.S. Naval Research Laboratory
Washington, D.C. 20375-5000

The quasioptical gyrotron (QOG) is under development at the Naval Research Laboratory as a high power source of millimeter-wave radiation. Recent experimental results include the production of up to 150 kW output power with 20% efficiency in 13 μ sec pulses [1].

A new application of the QOG is the processing of ceramics and other non-metallic materials. High power millimeterwave radiation offers unique capabilities for the application of coatings, sintering, brazing and soldering, and treatment of polymers. The new experiment is designed to produce 4 kW average power from 75-95 GHz using a 20 kV, 1.5 A dc electron beam. Initial pulsed testing has been performed at 20-60 kV cathode voltage, 0-6 A in 13 μ sec pulses. A pair of capacitive probes in the drift region are used to measure the average pitch ratio ($\alpha = v_{\perp}/v_{\parallel}$) of the gyrating electron beam. The pitch ratio is varied by adjusting the magnetic field at the gun or the intermediate anode voltage. Measurements indicate that the average α of the beam is less than simulation values for low cathode voltages. However, increasing the cathode voltage to $55~\mathrm{kV}$ greatly improves the beam quality. Initial efficiencies in the untilted resonator are unexpectedly low ($\eta = 5\%$), as is the maximum frequency detuning ($\Delta\omega/\omega=2\%$). Tilting the resonator by 2° relative to the plane perpendicular to the electron beam is predicted to increase the achievable frequency detuning and single-mode output efficiency. An asymmetric tilted resonator has been installed in the gyrotron and cold tested at 94 GHz. Pulsed measurements will be performed on gyrotron output power, efficiency, mode spectrum, and output radiation pattern. This tunable QOG will complement existing processing experiments at 2.45, 35, and 83 GHz.

[1] R.P. Fischer *et al.*, "Phase locking, amplification, and mode selection in an 85 GHz quasioptical gyroklystron," *Phys. Rev. Lett.*, vol. 72, no. 15, pp. 2395-2398, 11 Apr. 1994.

*This work is supported by the Office of Naval Research.

3B02

Gyrotron-Powered Millimeter-Wave Beam Facility for Microwave Processing of Materials

A.W. Fliflet, R.W. Bruce, R.P. Fishcer, A.K. Kinkead and S.H. Gold and S. Ganguly, U.S. Naval Research Laboratory, Washington, DC 20375, USA

Gyrotron-Powered Millimeter-Wave Beam Facility for Microwave Processing of Materials*

A. W. Fliflet, R.W. Bruce, R.P. Fischer, A.K. Kinkead, and S.H. Gold

Beam Physics Branch

Plasma Physics Division,

Naval Research Laboratory

Washington, DC 20375

and

S. Ganguly

Center for Remote Sensing,

Fairfax, VA 22030

The high intensity millimeter-wave beams (10³-10⁵ W/cm²) that can be generated by powerful gyrotron oscillators have unique capabilities for rapid, selective heating of nonmetallic materials [1]. A new CW gyrotron-based system is being set up at the Naval Research Laboratory (NRL) to investigate such beams. The facility is being operated jointly by NRL and the Center for Remote Sensing (CRS) and will be applied to important areas of material processing including: coating of materials, soldering and brazing, and treatment of ceramics and polymers. The heart of the system is a Gycom, Ltd. industrial 83 GHz gyrotron operating at 27 kV and 1.9 A, and producing 15 kW of power in a Gaussian beam. This paper will describe the new facility, including the gyrotron, work chamber, and control system. Available results of initial beam characterization and material heating experiments will also be presented.

3B03-4

Invited -

Microwave Systems for the Processing of Advanced Ceramics

O.Wilson Jr., Y. Carmel, I. Lloyd, T. Olorunyolemi, J. Calame, D. Gershon, E. Pert, G. Xu, M. Walter, A. Jaworski and A. Birnboim, University of Maryland, College Park, MD 20742,

Microwave Systems for the Processing of Advanced Ceramics

O. Wilson, Jr., Y. Carmel, I. Lloyd, T. Olorunyolemi, J. Calame*, D. Gershon, E. Pert, G. Xu, M. Walter, A. Jaworski, and A. Birnboim

University of Maryland, College Park, MD 20742 *Naval Research Laboratory, Washington, DC 20375

Microwave processing systems are continually evolving to incorporate more unique capabilities and design features. These new developments are instrumental in expanding the scope of microwave systems for studying complex phenomena in materials synthesis and processing. On a more fundamental level, questions concerning the nature of interactions between microwaves and ceramic materials systems can be addressed to provide direct impact on processing strategies for advanced ceramic materials. A novel microwave processing system is being developed to study fundamental issues in the sintering of advanced ceramic materials with enhanced dielectric, thermal, optical, and mechanical properties for applications in microelectronics, biomaterials, and structural applications. The system consists of a single and dual frequency microwave furnace that operates at 2.45 and 28 GHz, an optical pyrometric temperature measuring system, and an optical, non-invasive, non-contact, extensometer for measuring sintering shrinkage and kinetics. The additional ability to process at 28 GHz provides opportunities to sinter a wider range of ceramic materials by direct coupling. An even more exciting benefit of the dual frequency system is the potential to process ceramics at two frequencies simultaneously. This capability can provide a unique way to tailor the microstructure of advanced ceramics by controlling the extent of both volumetric and surface heating. Experimental results for microwave sintering studies involving ZnO, hydroxyapatite, AIN-SiC composites, and alumina composites will be presented, with an emphasis on the processing of nanograin ceramics. In particular, the role of surface modification and microwave field intensification effects (Figure 1) will be discussed. (The authors acknowledge the support of the AFOSR Ceramic Materials Program and NRL)

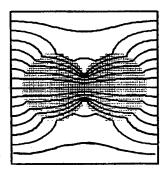


Figure 1. Electric field lines in the vicinity of two adjoining ceramic particles.

^{*} Work supported by the Office of Naval Research (ONR). A portion of this work was also supported by an ONR Small Business Innovative Research (SBIR) Grant to CRS.

[†] Icarus Research, Inc. † Sachs Freeman Assoc.

^[1] B. E. Paton, V. E. Sklyarevich, and M. M. G. Slusarczuk, "Gyrotron Processing of Materials," MRS Bulletin 18, 58-63 (November 1993)

3B05

Design of a Wide-range Non-contact Temperature Measurement and Control system for a 2.45 GHz Microwave Furnace

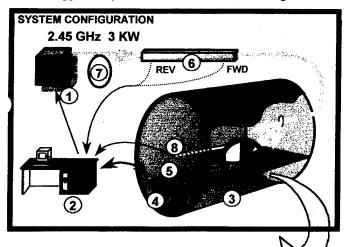
E.Pert, J. Calame, D. Gershon, Y. Carmel, I. Lloyd, O. Wilson, T.Olorunyolemi, University of Maryland, College Park, MD 20740, USA

Design of a Wide-range Non-contact Temperature Measurement and Control System for a 2.45 GHz Microwave Furnace*

E. Pert, J. Calame[†], D. Gershon, Y. Carmel, I. Lloyd, O. Wilson, T.Olorunyolemi University of Maryland, College Park, MD, 20742 [†]Naval Research Laboratory, Washington DC, 20375

The design of a pyrometric non-contact temperature measurement and control system for a 3kW 2.45 GHz microwave processing furnace is presented. Design considerations specifically relevant to implementing non-contact temperature measurement and control over the wide range of 25 to 2500°C are discussed. The completed system, in use as a research tool for microwave processing studies, provides versatile and contiguous control of sample heating from room temperature to the process temperature, with real-time access to parameters of the power control algorithm.

* Work supported by AFOSR, Ceramic Materials Program.



(14)

- 1. Magnetron Unit
- 2. Control Cart
- 3. Process Cavity
- 4. Pyrometer Array
- 5. Barium Fluoride Lens
- 6. Bi-Directional Coupler
- 7. Circulator (Isolator)
- 8. Thermocouple
- 9. Gold Mirror
- 10. Black Phenolic Mask
- 11. Table Thermocouple
- '2. Stainless Steel Table
- 13. Sample
- 14. Sample Powder
- 15. Low Loss Insulation

3B06

Simulation of Microwave Sintering of Ceramic Bodies with Complex Geometry

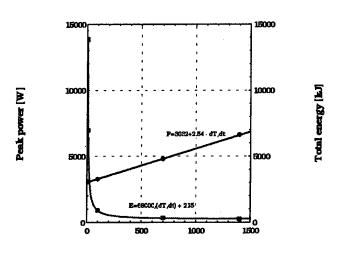
A. Birnboim and Y. Carmel, University of Maryland, College Park, MD 20742-3511, USA

Simulation of Microwave Sintering of Ceramic Bodies with Complex Geometry *

A. Birnboim and Y. Carmel, Inst. for Plasma Research, Univ. of Maryland, College Park, MD.

Microwave sintering is an emerging technology in which the energy is directly applied to the material, enabling fast sintering with a potential for synthesis of advanced ceramic materials with superior properties. A dynamic balance between the rate of electromagnetic energy absorbed within the bulk of the sample and the rate of energy loss from its surface generally give rise to temperature gradients. These temperature gradients may be especially important during microwave sintering of bodies having a complex geometry since both the diffusion distance and the electromagnetic penetration depth do not scale with sample dimensions. The gradients generated in a zinc-oxide green body of a complex geometry were studied theoretically using various microwave sintering approaches. It was found that: (a) dual frequency (2.45 GHz and 30 GHz) microwave processing leads to reduction in the duration of the temperature gradients, and (b) an increase in the heating rate from 5 °C/min to 1400 °C/min at 2.45 GHz reduces the total required microwave energy by a factor of 55 (see figure below), while at the same time the internal temperature gradients are maintained over a substantially shorter time.

* Work supported by AFOSR, Ceramic Materials Program, grant number F496209710270.



Heating rate dT/dit [°C/min]

3C

De Anza III 10 AM, Tuesday, June 22, 1999

Oral Session 3C Laser Produced Plasmas and Dense Plasma Focus

Chairperson

Ed Ruden

Air Force Research Laboratory

3C01-2

Invited -

Ultra-high Gradient Acceleration of Electrons by Laser Wakefield Plasma waves

Antonio C. Ting, U.S. Naval Research Laboratory, Washington, DC 20375, USA

Ultra-high Gradient Acceleration of Electrons by Laser Wakefield Plasma Waves¹

ANTONIO C. TING,² Plasma Physics Division, Naval Research Laboratory, Washington, DC 20375

Short, intense laser pulses can be produced by table top laser systems utilizing the chirped-pulse-amplification (CPA) technique to have femto-second pulse lengths and terawatt power levels. These laser pulses have very good beam qualities which allow them to be focused to intensities in excess of 10¹⁸ W/cm². At such intensities, the wiggling motion caused by the laser field of the electrons in a plasma reaches relativistic velocities. The electrons can experience a tremendous ponderomotive force from the radiation pressure and be expelled from the vicinity of the laser pulse. When the intense laser pulse propagates through a plasma with the appropriate density, the expelled electrons can resonantly excite a large amplitude plasma wave in the wake of the laser pulse, the Laser Wakefield Accelerator (LWFA). This wakefield plasma wave has phase velocity close to the speed of light and longitudinal electric field strength of tens of GV/m. Self-trapped plasma electrons or externally injected electrons can be accelerated by the wakefield to multi-MeV energies in distances of mm's. The LWFA mechanism and other laser driven plasma acceleration schemes will be reviewed. Recent experimental results of electron acceleration to 100 MeV, efforts to extend acceleration distances to beyond Rayleigh diffraction lengths, and the Laser Ionization and Ponderomotive Acceleration (LIPA) electron injection scheme will be presented. Supported by DoE and ONR

Supported by Both and Grad
 In collaboration with C.I. Moore, D. Kaganovich, T. Jones, K. Krushelnick, J. Qiu, R. Fischer, R. Hubbard, P. Sprangle, and B. Hafizi.

3C03-4

Invited -

High Gain Table-top Transient Collisional X-ray Lasers

James Dunn, Albert L. Osterheld, Yuelin Li, Joseph Nilsen and Vyacheslav N. Shlyaptsev, Lawrence Livermore National Laboratory, Livermore, CA 94550, USA

High Gain Table-top Transient Collisional X-ray Lasers

James Dunn, Albert L. Osterheld, Yuelin Li¹, Joseph Nilsen, and Vyacheslav N. Shlyaptsev²

Lawrence Livermore National Laboratory, Livermore, CA 94550, USA

ILSA, Lawrence Livermore National Laboratory, Livermore, CA 94550, USA

Dept. of Applied Science, University of California Davis-Livermore, Livermore, CA 94550, USA

In the last few years, there has been rapid progress in the development of higher efficiency laser-pumped x-ray lasers which has led to a significant reduction in the energy required to produce a population inversion. At LLNL, we are continuing research on table-top transient collisional excitation schemes generated by high power (15 TW), 500 fs pulses from the COMET laser. Strong lasing has been demonstrated on various Ne-like and Nilike ion x-ray lasers operating in the 130 - 320 Å range using typically 5 - 10 J of laser energy on target. Ultra high gains up to 55/cm have been observed allowing the possibility of achieving gain saturation and x-ray laser output energy of 1 - 10 uJ with target lengths of a few millimeters. Recent experiments show enhanced output of the x-ray laser when the short laser pulse irradiates the target in a traveling wave geometry. The high gain region in the plasma has been determined using multi-layer coated optics imaging and is compared with simulations to better understand the generation of the transient x-ray laser.

This work was performed under the auspices of the US Department of Energy by the Lawrence Livermore National Laboratory under Contract No. W-7405-Eng-48.

3C05

Propagation of Short Intense Laser Pulses in Plasma Channels

P. Sprangle, B. Hafizi and R.F. Hubbard, U.S. Naval Research Laboratory, Washington, DC 20375-5346, USA

Propagation of Short Intense Laser Pulses in Plasma Channels*

P. Sprangle, B. Hafizi⁺ and R. F. Hubbard

Beam Physics Branch, Plasma Physics Division, Washington DC 20375

⁺ Icarus Research, Inc., P.O. Box 30780, Bethesda, MD 20824-0780

Finite pulse length effects play a major role in the propagation of intense laser beams in a preformed plasma channel. An envelope equation is derived which describes the dynamics of short laser pulses in plasma channels including nonlinear effects[1]. The nonlinear terms arise from relativistic and atomic (bound) electron effects. The laser field is shown to be significantly modified for pulses less than a few tens of wavelengths long. Short laser pulses in plasma channels are found to undergo an envelope oscillation in which the front of the pulse is always damped while the back initially grows. The envelope modulation on the pulse eventually damps due to frequency spread phase mixing. In addition, finite pulse length effects are shown to significantly modify nonlinear focusing processes.

*Supported by ONR & DoE

[1] P. Sprangle, B. Hafizi and P. Serafim, Physical Review Letters, February 1999, accepted for publication; Phys. Rev. E, March 1999.

3C06-07

Invited -

Research on Fast Ion and Electron-Beams from Plasma-Focus Devices

Marek J. Sadowski, Andrzej Soltan Institute for Nuclear Studies, Warsaw, Poland

Research on Fast Ion- and Electron-Beams from Plasma-Focus Devices

Marek J. Sadowski

The Andrzej Soltan Institute for Nuclear Studies (IPJ) 05-400 Otwock-Swierk by Warsaw, Poland e-mail: msadowski@ipi.gov.pl

This invited talk concerns studies of pulsed ion streams emitted from outlets of Plasma-Focus (PF) machines. Also presented are investigations of fast electron beams emitted in the upstream direction. Results obtained with different PF facilities of energy ranging from several kJ to about 500 kJ, are summarized. Attention is brought to PF experiments performed at two Polish laboratories: the Andrzej Soltan Institute for Nuclear Studies (IPJ) in Swierk by Warsaw, and the Institute of Plasma Physics and Laser Microfusion (IFPiLM) in Warsaw.

In Swierk the MAJA-PF machine, run up to 60 kJ, at 35 kV, has been used for fast e-beam and X-ray studies. X-rays were measured with scintillation detectors, pinhole cameras and crystal spectrometers. E-beams, escaping through an axial hole in the central electrode, were measured by means of a miniature magnetic spectrometer and special Cerenkov-type detectors. Attention has been paid to non-linear phenomena within a pinch column, and particularly to the formation of hot-spots. The X-ray spectroscopic measurements, as performed for D₂+Ar discharges, revealed some differences in the polarization of X-ray lines emitted by highly-ionized Ar ions. It was explained by a difference in the polarization of the investigated lines, due to interactions of fast e-beams with dense plasma and local magnetic fields. Recent studies demonstrated good correlation of the X-ray pulses from hot-spots and fast e-beams escaping through the axial channel.

The PF-360 machine in Swierk, operated up to 240 kJ, at 35 kV, was used mainly for the optimization of the neutron yield and for studies of charged particle beams. E-beam energy spectrum, as measured behind the main collector plate, ranges from about 60 keV to above 600 keV. An ion energy spectrum extends even to about 3.5 MeV. An angular distribution of fast primary deuterons, showing a local minimum close to the z-axis, has been explained by computations of ion trajectories, taking into account a filamentary structure and curvature of the current sheath. Recent measurements have been concentrated on temporal correlation of X-ray and charged-particle pulses.

Some ion measurements were also performed at IFPiLM within a megajoule PF-1000 facility. The electrodes used (330 mm in length, 100 mm and 150 mm in diameter) were too small to optimize the driver-load coupling, but preliminary studies of current sheath dynamics, as well as X-rays and ions, were performed successfully up to 400 kJ. Recent experiments have been devoted mainly to studies of X-ray spectra and to preliminary measurements of high-energy ion beams. An angular distribution of fast primary protons, emitted from H₂ shots, has also showed the local minimum close to the discharge axis.

3C08

Preliminary Peformance of the Charybdis Plasma Focus at Texas A & M University

B.L. Freeman, D.J. Dorsey, T.J. Faleski, T.L. Guy, I.S. Hamilton, T.A. Parish and J.C. Rock, Texas A & M University, College Stations, TX 77843, USA

Preliminary Performance of the Charybdis Plasma Focus at Texas A&M University†

B.L. Freeman, D.J. Dorsey, T.J. Faleski, T.L. Guy, I.S. Hamilton, T.A. Parish, and J.C. Rock Texas A&M University College Station, Texas 77843-3133

A new plasma focus machine, CHARYBDIS, is being assembled at Texas A&M University on its Riverside Research Campus. This system will be a 60kV capacitor bank with a maximum energy storage of ~475kJ. The capacitor bank will be assembled using 144 of the 1.85µF, 60kV capacitors from the original SHIVA machine, donated from the Air Force Research Laboratory in Albuquerque. The power supply for this machine will be a salvaged, ANTARES, ±80kV unit from the Los Alamos National Laboratory. Six rail-gap switches, from the ATLAS program, will switch the bank into its load. The plasma focus device and its supporting equipment was originally used at Los Alamos on a number of capacitor configurations. When fully operational, this machine should provide peak currents of 3 to 4MA to the plasma focus, with a rise time of about 5µs. From experience with a modular machine at LANL that stored, 260kJ, 580kJ, or 780kJ at 120kV, we expect this system to exceed the performance of the LASL, DPF6.5 machine, abstracted in the 1973 APS Plasma Conference. Preliminary operational characteristics of CHARYBDIS will be reported at the conference.

†Work supported by Texas A&M University

3C09

Fusion Research in Zimbabwe

M. Mathuthu, T.G. Zengeni and A.V. Gholap, University of Zimbabwe, Mt. Pleasant, Harare, Zimbabwe

FUSION RESEARCH N ZIMBABWE

M. MATHUTHU, T. G. ZENGENI and A. V. GHOLAP UNIVERSITY OF ZIMBABWE, DEPT. OF PHYSICS P. O. BOX MP 167, MT PLEASANT HARARE, ZIMBABWE

Abstract

This work describes in part the results of a simplified three stage model of a plasma focus device in terms of the dimensions, filling gas pressure and charging voltage. An optimum pinch radius ratio of 0.03 to 0.4 was realised. The model showed that final axial velocity determines the initial inward radial velocity. The second part is the design, fabrication and characterisation of a plasma focus device which has the inner electrode negatively charged (-12 kV). The optimum operating conditions of this plasma focus device were found to be in the pressure range between 0.5 and 2.0 mbar, for all the gases tested and for an inner electrode length of 40~mm. The experimental results obtained with the device are presented.

3C10

Study of Hot spot Phenomenon In Z-Pinches

O.G. Semyonov, Brooklyn, NY 11223, USA

STUDY OF HOT SPOT PHENOMENON IN Z-PINCH

O.G.SEMYONOV*

Vacuum spark discharge was studied experimentally with a set of X-ray diagnostics including dosimetry, pin-holes cameras, time resolved X-ray spectrometry and X-ray line polarization measurements, as well as laser interferometry, shadowgraphy and Faradey rotation diagnostics.

Consecutive phases of the discharge with iron electrodes are discussed. In ignition phase the electrons extracted from the trigger plasma are concentrated on the anode tip providing vaporization and pressure rising in anode-cathode gap. In starting phase collision ionization prevails and arc discharge begins. During MHD phase anode and cathode necks are formed due to initial inhomogeneities of discharge plasma radius and linear concentration along z-axis. As a result Bennet pinch $\varnothing 0.2 \times 1$ mm is formed with $n_e \sim 10^{21}$ cm⁻³ and $T \approx 50$ eV. Hot spots (micropinches) having the dimensions $\varnothing 40 \times 150$ μ in spectral region near 1 keV and decaying on z - 3 smaller micropinches $\varnothing 3 \times 10$ μ in spectral band hv > 3 keV are formed mainly in the anode neck. The plasma parameters in the micropinch: $n_e \geq 10^{22}$ cm⁻³ and $T \sim 1$ keV. The micropinches emit up to 10 J of X-ray radiation within the band 0.5 - 1.5 keV and $\sim 10^{-3}$ J in hv > 3 keV in the pulse $\tau \leq 2$ ns.

The experimental data are compared with the computer simulation of iron plasma pinch evolution (zero- and one-dimensional models with radiative losses). Bennet pinch evolution could be described as

losses). Bethiet pinch evolution count of the described as $\frac{f/r}{f'} = (c^2/l^2) Q_j \ (1-Q_{loss}/Q_j), \ \text{where } r-\text{micropinch radius, } I-\text{current, } Q_j-\text{Joule heating per unit of length and } Q_{loss} = (5/2)(1+Z)N_i \ T/\tau_b + Q_i + Q_r \approx Q_r, \text{where } N_i-\text{linear ion density, } \tau_b-\text{characteristic time of plasma axial blow-loff, } Q_i-\text{ionization losses and } Q_r-\text{radiative losses which prevail significantly } (\text{line radiation}) \ \text{other losses. According to the model radiative compression down to } r \sim 1 \ \mu, n_e \sim 10^{24} \ \text{cm}^{-3}, T \sim 1 \ \text{keV occurs if } I > 70 \ \text{kA} \ \text{within } 10^{15} < N_i < 10^{16} \ \text{cm}^{-1} \ \text{where the neck evolves due to axial plasma blow-off. It is shown that theoretical model of hot spot dynamics and calculated plasma parameters that the experimental data.}$

There are experimental evidences inconsistent with the model: 1) measured current in the neck doesn't exceed 20 kA and 2) X-ray line polarization data showed that the line radiation of high-Z ions is produced by nonthermal electrons moving chiefly across the discharge axis. Trajectories of high energy (> 10 keV) electrons in Bennet micropinch were considered: $\vec{E} \times \vec{B}$ drift leads to axisymmetric orbit of electrons elongated along r direction with $r_{max} \approx$ 1.6ωa, ω ≈ $(va/2)^{1/2}$, where $a = eB_0/mcr_p = 2eI/mc^2r_p^2$, $v = (2E_e/m)^{1/2}$. Electrons oscillate along r and drift along z direction to the anode with $\Delta z(\pi/\omega) \approx 0.9 r_{max}$ and $\vec{v}_z \sim \bar{v}/2$ gaining energy from inductive electric field E: $E_n \approx \Delta z e E$ (modified run-away). For $I \sim 10 \text{ kA } r_{max} \approx r_p$. On average the period of time when these electrons move perpendicular to z-axis ≈ 2 times more than along z-axis hence statistically they excite ions more often when $v_r > v_z$ resulting in appropriate polarization of X-ray lines. Taking into account the experimental concentration of nonthermal electrons $n_n \sim .01n_e$ evaluation of energy losses Qn due to ran-away gives Qn >> Qr so run-away process would control compression of the micropinch with current I < 70kA. According to polarization measurements and Bennet relation plasma temperature and density in hot spot are smaller then it was considered earlier^{1,2}.

¹Vikhrev V.V. et al., Sov. Plasma Phys., 1982, 8, 1211.

²Sidelnikov Yu.V. Ph.D. Thesis, 1982, Institute of Spectroscopy, Russia.

^{*}The experimental work was performed at P.N.Lebedev Institute of Physics.

3D

Bonsai I/II 10 AM, Tuesday, June 22, 1999

Oral Session 3D Non-equilibrium Plasma Processing

Chairperson
Trudy Van Der Stratten
University of Illinois

3D01

Destruction of Isotopically Labeled Nitric Oxide In Air by Corona Discharge: Kinetics and Products Of Destruction

Larisa G. Krishtopa, Lev N. Krasnoperov, New Jersey Institute of Technology, Newark, NJ 07102, USA

DESTRUCTION OF ISOTOPICALLY LABELED NITRIC OXIDE (15N18O) IN AIR BY CORONA DISCHARGE: KINETICS AND PRODUCTS OF DESTRUCTION.

Larisa G. Krishtopa, Lev N. Krasnoperov

New Jersey Institute of Technology,
Department of Chemical Engineering, Chemistry, and
Environmental Science,
University Heights, Newark, NJ 07102

Destruction of isotopically labeled nitric oxide (¹⁵N¹⁸O) in air by corona discharge was studied using tubular-flow, coaxial wire, AC-powered dielectric barrier corona discharge reactor coupled with on-line quadrupole mass spectrometer. The kinetics and products of the destruction were determined as functions of specific discharge energy.

There has been no direct confirmation of molecular nitrogen production in the process of NO destruction in air by corona discharge due to the overwhelming excess of these molecules in the bath gas. Use of ¹⁵N and ¹⁸O labeled NO allowed to overcome this difficulty. Reduction of NO to molecular nitrogen was clearly demonstrated (Fig.1). The concentration profiles of all nitrogen oxides were measured and compared with model calculations.

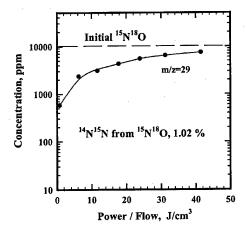


Fig.1. Molecular nitrogen production: formation of ¹⁴N¹⁵N (m/z=29) from ¹⁵N¹⁸O (m/z=33).

3D02-3

Invited -

Use of a Remote Plasma Source for CVD Chamber Clean and Exhaust Gas Abatement Applications

William Holber, Xing Chen, Donald Smith and Matt Besen, Applied Science & Technology Inc., Woburn, MA 01801, USA

Use of a Remote Plasma Source for CVD Chamber Clean and Exhaust Gas Abatement Applications William Holber, Xing Chen, Donald Smith, and Matt Besen Applied Science and Technology, Inc., 35 Cabot Road, Woburn, MA, 01801

Remote plasma sources have traditionally been used in semiconductor processing applications such as dry removal of photoresist, where the capability of delivering a large flux of atomic oxygen into a semiconductor process chamber, with little of the associated plasma used to dissociate the oxygen, has made them attractive. With the development of fluorine-compatible remote plasma sources, a range of new application opportunities has opened up. In remote cleaning of CVD chambers, the remote plasma source is positioned before the process chamber, and a stream of atomic fluorine from the source is flowed into the chamber, where it can effectively clean a wide variety of materials such as SiO₂, Si_3N_4 , and W. The cleaning process is purely chemical, with no associated in-situ plasma which can cause degradation of the process chamber. In exhaust gas abatement, the remote plasma source is located between the outlet of the etch or deposition process chamber and the mechanical pump. By adding appropriate gases, the exhaust stream from the chamber can be converted to a form which can be managed more readily. Using an robust toroidal plasma source design, the ASTRONTM remote plasma source has been used to address both of these areas. As an atomic fluorine source, over the typical operating range of 2-10 Torr several SLM of gases such as NF3 can be fully dissociated. As an exhaust gas abatement device, with operating pressure in the 0.1-1.0 Torr regime, abatement of perfluorocompounds (PFC's) at greater than 95% levels has been demonstrated. Using a variety of techniques - FTIR, RGA, and sample etching - the operation of this source technology and issues such as transport of atomic fluorine over substantial distances has been investigated.

3D04-5

Invited -

Discharge Physics and Chemistry of a Novel Atmospheric Pressure Plasma Source

J. Park, I. Henins, H.W. Herrmann and G.S. Selwyn, Los Alamos National Laboratory, Los Alamos, NM 87545, USA

Discharge Physics and Chemistry of a Novel Atmospheric Pressure Plasma Source

J. Park, I. Henins, H.W. Herrmann and G.S. Selwyn Los Alamos National Laboratory J. Y. Jeong and R. Hicks, UCLA

The atmospheric pressure plasma jet (APPJ) is a unique plasma source operating at atmospheric pressure. The APPJ operates with RF power and produces a stable non-thermal discharge in capacitively-coupled configuration. The discharge is spatially and temporally homogeneous and provides a unique gas phase chemistry that is well suited for various applications including etching, film deposition, surface treatment and decontamination of chemical and biological warfare (CBW) agents. A theoretical model shows electron densities of 0.2-2x10¹¹ cm⁻³ for a helium discharge at a power level of 3-30 W cm⁻³. The APPJ also produces a large flux, equivalent of up to 10,000 monolayer s⁻¹, of chemically-active, atomic and metastable molecular species which can impinge surfaces several cm downstream of the confined source. In addition, the efforts are in progress to measure the electron density using microwave diagnostics and to benchmark the gas phase chemical model by using LIF and titration.

3D06

2-D Model Of a Large Area Inductively Coupled, Rectangular Plasma Source for CVD

J.L. Guiliani, J.P. Apruzese, A.E. Robson and M. Mulbrandon, V. Shamamiam, R.E. Thomas, R.Rudder and R. Hendry, U.S. Naval Research Laboratory, Washington, DC 20375-5346, USA

2-D MODEL OF A LARGE AREA, INDUCTIVELY COUPLED, RECTANGULAR PLASMA SOURCE FOR CVD*

J.L. Giuliani, J.P. Apruzese, A.E. Robson[†], and M. Mulbrandon Plasma Physics Division, Naval Research Laboratory Washington, DC 20375

V. Shamamian

Chemistry Division, Naval Research Laboratory Washington, DC 20375

R.E. Thomas, R. Rudder, and R. Hendry Center for Semiconductor Research, Research Triangle Institute Research Triangle Park, NC 27709

A novel design for an inductively coupled, rectangular plasma source is described. The design encompasses several key issues of large area thin film growth by CVD: structural integrity; electrostatic screening; substrate temperature control; and maximal growth surface. A test reactor has been utilized to grow diamond films over $\sim 1800~\rm cm^2$ at 13 MHz and ~ 1 Torr pressure with 45 kW coupled power. The design is readily scalable to larger areas. To analyze the axial plasma uniformity, a 2-D simulation model is presented. The electromagnetic coupling, non-equilibrium plasma chemistry, and multi-species diffusion are self-consistently treated. In this 2-D approach, the slotted Faraday screen behaves as a diamagnetic medium in transmitting the magnetic field. Results are compared with experimental data for the hydrogen plasma extent, electron, and gas temperatures. Neutral gas thermal conduction and hydrogen recombination dominate the energy deposition to the wall, and in turn govern the plasma length. A tradeoff between quality and growth area is predicted for the reactor as the pressure is decreased.

* Work supported by BMDO/TO and DARPA.

† BRA, Springfield, VA 22150

3D07

Particle-in-cell and TAMIX simulation of the hydrogen plasma immersion ion implantation ion-cut process

Dixon Tat-Kun Kwok, Paul K. Chu, Blake P. Wood, and Chung Chan, City University of Hong Kong, Hong Kong SAR, China

Particle-in-cell and TAMIX simulation of the hydrogen plasma immersion ion implantation ion-cut process

Dixon Tat-Kun Kwok¹, Paul K. Chu¹, Blake P. Wood², and Chung Chan³

¹ Department of Physics & Materials Science, City University of Hong Kong, 83 Tat Chee Avenue, Kowloon, Hong Kong

² Los Alamos National Lab., PO Box 1663 MSE526, Los Alamos, NM 87545

³ Department of Electrical and Computer Engineering, Northeastern University, Boston, MA 02115

Silicon-on insulator (SOI) is an attractive material compared with bulk silicon substrate for high speed, low power, low voltage complementary metal oxide semiconductor (CMOS) integrated circuits. A bond-cut process, commercially referred to as Smart-CutTM developed by SOITEC, has provided excellent SOI wafers. One of the critical steps of Smart-Cut is to implant a fairly high dose of hydrogen into the wafer to form a plane along which the wafer can crack. Conventional beam-line ion implantation can be replaced by plasma immersion ion implantation (PIII) to achieve a higher throughput and lower cost. For hydrogen PIII/bond-cut, the coexistence of H⁺, H₂⁺, and H₃⁺ in the plasma tends to spread the implanted hydrogen profile that cracking may not occur uniformly. Hydrogen plasma immersion ion implantation (PIII) into a 200 mm diameter silicon wafer placed on top of a cylindrical stage has been numerically simulated by the particle-in-cell (PIC) method. The plasma consists of three hydrogen species H^{\dagger} , H_2^{\dagger} , and H_3^{\dagger} in different ratio. The retained dose and sputtering loss are calculated by TAMIX. The highest retained dose is found for the H⁺ ion whereas half of the hydrogen atoms are not retained when H₃⁺ is implanted. The combined effect of the three species show a maximum non-uniformity in the retained dose of 11.5% along the radial distance. The depth profile is shallower at the edge, but within a 6.375 cm radius, the depth profile is fairly uniform with the difference less than 5%.

3D08

Numerical Simulation Versus Experiment On A Long Hollow Target PVD Reactor

P. Bocquet, L. Leylekian and G. Gousset, ONERA, 92322 Chatillon Cedex, France

3P

Serra I, Conference Centre 10 AM, Tuesday, June 22, 1999

NUMERICAL SIMULATION VERSUS EXPERIMENT ON A LONG HOLLOW TARGET PVD REACTOR

P. Bocquet⁽¹⁾, <u>L. Leylekian⁽¹⁾</u> and G. Gousset⁽²⁾
1- Materials Systems & Composites Department
ONERA, 29 av. de la division Leclerc, 92322 Chatillon, France
2 - Laboratoire de Physique des gaz et des plasmas - Bat 210
Université Paris-Sud Orsay, 91405 Orsay cedex, France

The work described hereafter has been performed in the general framework of a pre-industrial PVD reactor development. This device is devoted to the online coating of ceramic fibers for aerospace industries and, to achieve this task, the fiber passes axially through an hollow cylindrical target which is sputtered by the confined plasma.

This unusual geometry has been chosen to maximize the flux of sputtered atoms on the fiber although the ratio between facing surfaces remains very low (~10⁻³), and to produce a columnar plasma which should ideally stand close to the inner surface of the target. It should also be noted that the ratio between the length and the radius of the confining target is high (~30), and can be suspected to generate instabilities.

The plasma is at the moment obtained with argon gas and is sustained by a electron gun which provides it a feeding DC current. The electromagnetic configuration of the reactor chamber is initially defined by the electron gun potential located at the top of the cylindrical target, by the anode potential located at the bottom and by the potential of the target itself. Moreover, the running fiber can be polarized if necessary. On the other hand a mainly longitudinal magnetic field is supposed to play the double role of magnetic bottle (the field closes up near both the gun and the anode) and ionization booster (a magnetron effect should occur in the sheath).

The key-feature experimentally observed on a steady fiber is the following: the coating is longitudinally inhomogeneous and shows two sharp maximums located at the edges of the target whereas its center is characterized by a very tiny sputtered film. This reproducible experimental evidence can hardly be linked to standard probe measurements which seem to reveal an history-dependent plasma configuration. Moreover, probe measurements cannot be performed in the same conditions that the coating and are not necessarily reliable.

We recently started Monte Carlo simulations to reproduce, understand and fix this phenomenon. First computations show that electrons are accelerated from the gun, following the magnetic field lines (as it is classically expected) but loose their energy in the first collisions which occur at the top of the target. Then, they are probably not able to recover this lost energy in the constant plasma potential. Further numerical results should confirm this hypothesis. In this case, post-accelerating strategies will be implemented to enhance the sputtering and the coating processes.

Comprehensive Secondary Electron Emission Modeling For Simulating E-Beam Collection in MICHELLE

Norman J. Dionne, Raytheon Systems Company, Sudbury, MA 01776, USA

Comprehensive Secondary Electron Emission Modeling For Simulating E-Beam Collection in MICHELLE *

Norman J. Dionne Raytheon Systems Company Sudbury, Massachusetts 01776

Electron beam collection systems variously employed in O-type fast-wave and slow-wave devices such as gyrotrons, gyroklystrons, klystrons, and TWTs must often be carefully designed to avoid potentially undesirable consequences of secondary electron production at the electrode surface(s). Some high performance device applications may experience added noise power resulting from secondary electron current refocused into the RF interaction space. In high average-power slow-wave devices, this returning current may contribute intolerable additional thermal dissipation power on RF circuit structures, already thermally stressed. For more efficient operation of the amplifier system, multiple electrode geometries, set at prescribed "depressed" voltages, are often used to recover energy from "spent" beams exiting from the RF interaction space. However, the emission of secondary particle currents can alter the expected efficiency improvements by refocusing and redistributing the collected currents toward electrodes with the higher potential values, producing additional thermal stress in the process.

An advanced, three-dimensional electron beam design tool, called MICHELLE, is currently undergoing development by a team lead by SAIC under ONR sponsorship. As part of this new effort, an algorithmic representation of a comprehensive model of secondary emission is being developed for this computational tool in order to achieve an accurate beam collection design capability.

The secondary emission model separates the emission problem into two macroparticle species; 1) true secondary electrons (SSE) and 2) rediffused (or backscattered) primary electrons (BSE). Each emitted particle species is assigned empirically-based, discrete angular and energy distributions in normalized form, which in turn are dependent upon both the incident particle energy and angle of incidence. Also, provisions for material-specific surface roughness contributions are included in approximate fashion. Algorithms used to capture the secondary emission model will be detailed.

* Work supported by the Office of Naval Research under Contract Number N00014-97-C-2076

3P02

Progress on a 3d particle-in-cell model of a W-band klystron

P.J. Mardahl, J.P. Verboncoeur and C. K. Birdsall, University of California - Berkeley, Berkeley, CA 94720, USA

Progress on a 3d particle-in-cell model of a W-band klystron ¹

P. J. Mardahl, J. P. Verboncoeur, and C. K.Birdsall Electronics Research Laboratory University of California, Berkeley, CA 94720

For a significant class of microwave-beam devices, including multibeam tubes and devices with azimuthally asymmetric interaction circuits, two-dimensional models do not provide a description of the key physical phenomena. A fully three-dimensional computational model which captures the kinetic and nonlinear aspects of such devices is required.

XOOPIC ² is in the process of being extended from a 2d electromagnetic PIC code into a 3d parallel code. The 3d code will be applied to modeling a klystron operating in the W-band ³.

The XOOPIC code is presently a 2d particle-in-cell code in r-z and x-y coordinates written in C++. XOOPIC presently runs on Unix platforms ranging from Linux PCs to workstations to MPI-capable parallel computers. Design and initial implementation of an extension from two to three dimensions (x-y-z and r- θ -z) is described for the XOOPIC code.

The klystron of interest is to operate at 91GHz, with a 125kW peak power, 120kV, 2.5A, 1us pulse, and 0.8mm drift tube diameter. The device uses periodic permanent magnetic focusing to contain the beam within the drift tube. A 3d model is required because the drift tube is circular, while the cavities are rectangular. The circular drift tube will be modeled using stair-stepped boundaries.

 $^{^1\}mathrm{Work}$ supported by AFOSR grants FDF 49620-96-1-0154, and F49620-95-1-0253

²J. P. Verboncoeur, A. B. Langdon, and N. T. Gladd, "An object-oriented electromagnetic PIC code." Computer Physics Communications 87 (1995) 199-211.

³G. Caryotakis, E. Jongewaard, G. Schietrum, A. Vlieks, R.L. Kustom, N.C. Luhmann, M.I. Petelin, "W-Band Micro-fabricated Modular Klystrons." –Private communication

Design of a 1 MW, 35 GHz, TE02 2nd Harmonic Output Gyroklystron

W. Lawson, M. Walter, K. Nguyen, M. Garven and V. Granatstein, University of Maryland IPR, College Park, MD 20742, USA

Design of a 1 MW, 35 GHz, TE₀₂, 2nd Harmonic Output Gyroklystron

W. Lawson, M. Walter, K. Nguyen*, M. Garven, and V. Granatstein IPR, University of Maryland, College Park, MD 20742 *KN Research Silver Spring, MD 20905

Abstract:

Work has begun on the next generation of gyroklystrons in a cooperative effort between the University of Maryland-IPR and NRL. The primary design goals are to achieve 1 MW of output power at 35 GHz with a bandwidth of approximately 1% without using superconducting magnets.

The design will incorporate a first harmonic, TE_{011} , 17.5 GHz input cavity followed by 2^{nd} harmonic, TE_{021} , 35 GHz buncher cavities to improve the gain. The output cavity will also operate at the 2^{nd} harmonic, TE_{021} , at 35 GHz.

Codes used in the design include the MAGYKL suite, a modified version of MAGY II to allow simulation of both harmonics, and HFSS. The electron gun was designed using Egun with gun parameters fixed at a voltage, V_b =70 kV, a beam current, I_b =40 A, a perpendicular to axial velocity ratio, α =1.5, and an axial velocity spread, Δv_z <6%.

Manufacturing is scheduled to begin in the spring of 1999 followed by cold tests and full power operation. The design process, considerations, and experimental results will be presented.

This work is supported by Naval Research Laboratories under grant N00173981G000.

3P04

Multimegawatt Gyrotrons for Plasma Heating R. Advani, D. Denison, K.E. Kreischer, M.A. Shapiro and R.J. Temkin, MIT Plasma Science & Fusion Center, Cambridge, MA 02139-4294, USA

Multimegawatt Gyrotrons for Plasma Heating

R. Advani, D. Denison, K. E. Kreischer, M. A. Shapiro and R. J. Temkin,

Plasma Science and Fusion Center Massachusetts Institute of Technology Cambridge, MA 02139

The gyrotron is under development as a high power source for plasma heating at electron cyclotron resonance. For heating large scale plasmas, such as the DIII-D machine at General Atomics, it is advantageous to have high unit power heating sources to reduce the cost and complexity of the system. We will present preliminary designs of 1.5 and 2 MW gyrotrons at a frequency of 110 GHz. The gyrotron designs are based on previous successful results at the 1 MW level at frequencies from 110 to 170 GHz. The baseline design is for a TE_{28,8} mode cavity with an electron beam of 80 to 110 kV and a current of up to 80A. The expected efficiency exceeds 30% but it should increase to over 50% with a depressed collector. The output beam will be a Gaussian TEM₀₀ mode in free space. The gyrotron will be investigated experimentally in short pulse operation (~3 microseconds) at MIT and, if successful, will be developed in a 10s pulsed or CW version by industry.

There are two competing approaches for the design of multimegawatt gyrotrons: conventional, cylindrical cavity gyrotrons and coaxial cavity gyrotrons. The conventional cavity approach is being considered as an extension of present day gyrotron research at 110 GHz. The coaxial cavity gyrotron is under investigation at MIT with the goal of output powers of 3 MW at 140 GHz. Recent experimental results from the coaxial cavity gyrotron at power levels in excess of 1 MW will be presented.

Research supported by the Department of Energy, Office of Fusion Energy Sciences

Design of a Frequency Tripling, Third Harmonic Gyro-TWT

W. Chen, H. Guo, J. Rodgers, V.L. Granatstein, T.M. Antonsen, University of Maryland, College Park, MD 20783, USA

Design of a Frequency Tripling, Third Harmonic Gyro-TWT

W. Chen, H. Guo, J. Rodgers, V. L. Granatstein, T. M. Antonsen Institute for Plasma Research, University of Maryland College Park, MD20742, USA

A two-stage gyro-traveling-wave-tube(gyro-TWT) separated by a radiation-free drift section is being designed. The rf input and output sections of gyro-TWT operate at 11.5 GHz fundamental harmonic and 34.5 GHz third harmonic respectively. By choosing a proper drift section length, the third harmonic of the modulated electron beam current at the entrance to the output waveguide may be comparable to the fundamental harmonic due to the ballistic bunching of the beam in the drift section. The well prebunched beam makes beam-wave interaction in the output waveguide more efficient. The magnetic field B_0 is about $4.4\,kG$ so that permanent magnetic packaging is possible. This type Gyro-TWT features subharmonic injection, compact volume and superior stability.

Mode selective circuits are used in both the input and the output gyro-TWT sections to suppress spurious oscillation and mode competition. The interaction structure of the output gyro-TWT, which realizes the mode conversion of $TE_{03} \rightarrow TE_{04} \rightarrow TE_{05}$ over a wide frequency range in the simulation, ensures the operation stability and promotes the power capability of gyro-TWT. Matching loads are introduced in all ends of the interaction sections to avoid the reflection of the amplified wave. A large-signal code is currently being used to simulate the beam-wave interaction in the gyro-TWT and the results will be presented.

The design parameters of this gyro-TWT are as follows: a 80kV, 50A beam, $\alpha = 1.5$, $\eta \ge 25\%$, output power of 1MW, gain of 40dB, bandwidth of 6%. Testing of a prototype two-stage gyro-TWT, which is also based on the concept of harmonic multiplying, is in preparation in the University of Maryland. Preliminary experiment results will also be presented.

This work has been supported by the DoD MURI program on high-power microwave under AFOSR grant F4962001528306.

3P06

Results from a Ku-Band Second Harmonic Coaxial Gyroklystron

M.Castle, W. Lawson, B. Hogan, I. Yovchev, V. L. Grantstein and M. Reiser, University of Maryland, Institute for Plasma Research, College Park, MD 20742, USA

Results from a Ku-Band Second Harmonic Coaxial Gyroklystron

M. Castle, W. Lawson, B. Hogan, I. Yovchev, V. L. Granatstein, and M. Reiser

Electrical Engineering Department Institute for Plasma Research University of Maryland College Park, MD 20742 USA

Investigations into the performance of high-powered gyroklystrons have been pursued for over 14 years at the University of Maryland. Recent results culminated in an 80 MW TE $_{01}$ output signal at 8.57 GHz for 1.3 μ s. The efficiency of this tube was 32% and the saturated gain was 31 dB. This was the first of a proposed series of coaxial circuits whose powers are to be on the order of 100 MW.

Testing of a second harmonic circuit is currently being undertaken. The designed output is a TE_{02} signal at 17.11 GHz (detuned from ideal second harmonic to optimize efficiency) driven by a 500-700 A, 460 kV beam. An X-Band coaxial magnetron (8.5 – 9.6 GHz, 2 μ s) provides an input signal of up to 150 kW. The circuit consists of three cavities, an input, which operates at the fundamental, and a bunching and output, which operate at the second harmonic. The theoretical gain and efficiency are 49 dB and 40 % respectively.

This presentation will describe in detail the experimental results and the outcome of this work. It will also detail any planned and completed efforts to improve performance from this initial second harmonic tube. In addition, experimental work intended on customizing the system to power a small accelerator will be presented.

This work was supported by the US Department of Energy.

¹ W. Lawson, et. al., "High-Power Operation of a Three-Cavity X-Band Coaxial Gyroklystron", *Phys. Rev. Lett.*, vol. 81 n. 14, 5 Oct 1998

Design of High Power Four-Cavity Gyroklystrons for Linear Collider Applications

I. Yovchev, W. Lawson, M. Castle, B. Hogan, V. Granatstein and G. Nusinovich, University of Maryland, College Park, MD 20742-3511, USA

Design of High Power Four-Cavity Gyroklystrons for Linear Collider Applications

I. Yovchev, W. Lawson, M. Castle, B. Hogan, V. Granatstein, and G. Nusinovich

Institute for Plasma Research and Electrical Engineering
Department,
University of Maryland, College Park, MD 20742

The future development of linear electron-positron colliders depends to a great extent on two very important characteristics of the microwave amplifiers used to drive the colliders – efficiency and cost. The cost is related to the number of required amplifiers which is approximately inversely proportional to the parameter $A=P\tau/\lambda^2$, where P and τ are, respectively, the power and duration of the amplifier output pulse and λ is the wavelength. In order to increase A it is beneficial to develop microwave devices with higher operating frequency.

This article reports the results from a theoretical design of a four-cavity 17.1 GHz gyroklystron. The X-band input cavity operates in the TE₀₁₁ mode, while the remaining three cavities (buncher, penultimate and output) operate in the TE₀₂₁ mode, doubling the frequency of the input signal. The simulations show that both very high efficiency and gain of over 43 % and 70 dB, respectively, can be realized, using an electron beam with 500 kV voltage, 700 A current, perpendicular-to-parallel velocity ratio of 1.5 and parallel velocity spread of 6.4 %. The attained gain at an output power of more than 100 MW (which seems to be experimentally possible, taking into account the above mentioned values of efficiency and electron beam power) would probably permit the application of solid state microwave generators as input signal sources. These generators are cheaper and more stable than the magnetrons used to drive the present gyroklystrons.

In a view of the tendency to increase the frequency of sources for driving future linear colliders, we have begun a design of a frequency quadrupling gyroklystron, preliminary results of which are also reported. In this design the input cavity operates at the fundamental electron cyclotron frequency in the X-band, a buncher 17.1 GHz cavity operates at the second harmonic and the last two (penultimate and output) 34.3 GHz cavities operate at the fourth harmonic frequency.

3P08

Design of a 50 MW, 34 GHz Second Harmonic Coaxial Gyroklystron for Advanced Accelerators M.R. Arjona and W. Lawson, University of Maryland, College Park, MD 20742, USA

Design of a 50 MW, 34 GHz Second Harmonic Coaxial Gyroklystron for Advanced Accelerators*

M. R Arjona and W. Lawson

Electrical Engineering Department and Institute for Plasma Research University of Maryland College Park, MD 20742

At the University of Maryland, we have been investigating the feasibility of using gyroklystrons and gyrotwystrons as drivers for linear colliders and advanced accelerators for a number of years. Our most recent experimental tube achieved a peak power of about 80 MW at 8.57 GHz with 32% efficiency and over 30 dB gain with a three-cavity first harmonic circuit. The current experimental effort is devoted to producing about 100 MW of peak power at 17.14 GHz with a second-harmonic three-cavity tube. Some schemes for advanced linear colliders with center-of-mass energies of 5 TeV or more expect to require higher frequency sources, perhaps near 35 GHz or 91 GHz. A design study at 95 GHz indicated that peak powers near 7 MW were possible.

In this design study, we present the simulated operating characteristics of a four cavity 34 GHz second-harmonic gyroklystron tube which is capable of producing about 60 MW of peak power with an efficiency of about 40% and a gain above 50 dB. The electron gun is a single-anode magnetron injection gun. The input cavity is a TE_{011} cavity which is driven at 17 GHz. The remainder of the cavities are TE_{021} cavities which interact near the second harmonic of the cyclotron frequency. The gain cavity and the output cavities are at twice the drive frequency, but the penultimate cavity is detuned to enhance efficiency. All cavities are abrupt-transition cavities. Both systems are derived from scaled versions of our 17 GHz tube. In this paper, we present detailed designs and performance predictions for both the electron gun and the microwave circuit.

- 1. V. L. Granatstein and W. Lawson, "Gyro-Amplifiers as RF Drivers for Multi-TeV Linear Colliders," *IEEE Trans. Plasma Sci.* 24 (1996) 648.
- 2. W. Lawson, et al., "High Power Operation of a Three-Cavity X-Band Coaxial Gyroklystron," *Phys. Rev. Lett.*, **81** (1998) 3030-3033.
- 3. M. R. Arjona and W. Lawson, "Design of a 7 MW, 95 GHz, Three-Cavity Gyroklystron," *IEEE Trans. Plasma Sci.*, (in press).

^{*}This work is supported by the US Department of Energy.

Design and Operation of a 70 GHz Second Harmonic four Cavity Gyroklystron for Radar **Applications**

M. Walter, W. Lawson, J.P. Calame, M. Garven and V. L. Granatstein, University of Maryland, College Park, MD 20742, USA

Design and Operation of a 70 GHz Second Harmonic Four Cavity Gyroklystron for Radar Applications*

M. Walter, W. Lawson, J. P. Calame[†], M. Garven, and V. L. Granatstein

> Electrical Engineering Department and Institute for Plasma Research University of Maryland College Park, MD 20742

At the University of Maryland, we have been investigating the feasibility of using gyroklystrons and gyrotwystrons as drivers for linear colliders and advanced accelerators for a number of years. With a two-cavity second harmonic tube, we produced over 32 MW of peak power at 19.76 GHz with nearly 30% efficiency via the interaction with a 450 kV, 240 A beam. The first cavity was driven at 9.88 GHz in the TE₀₁₁ mode. The second harmonic output cavity resonated in the TE₀₂₁ mode at 19.76

In this paper, we present the application of this frequencydoubling technology to an existing first harmonic gyroklystron which has been under investigation at the Naval Research Laboratory.2 This system has been successfully operated with from 2-5 cavities. In a two cavity system, a peak power of 210 kW was achieved near 35 GHz with 37% efficiency and a gain near 24 dB. The bandwidth was approximately 0.36%. The nominal beam parameters include a voltage of 70 kV, a current of 8 A, and a perpendicular to parallel velocity ratio of about 1.35.

In our experiment, we utilize the first harmonic input and gain cavities, but replace the penultimate and output cavities with ones that are designed to operate in the TE₀₂₁ mode near 70 GHz. About 140 kW of power with an efficiency near 25% is predicted via MAGYKL simulations. The complete design simulations and cold test results for this system will be presented. If viable, the experimental hot test results will also be described.

- 1. V. L. Granatstein and W. Lawson, "Gyro-Amplifiers as RF Drivers for Multi-TeV Linear Colliders," IEEE Trans. Plasma Sci. 24 (1996) 648.
- 2. J. J. Choi, et al., "Experimental Investigation of a High Power, Two-Cavity, 35 GHz Gyroklystron Amplifier, IEEE Trans. Plasma Sci. 26 (1998) 416.
- *This work is supported by the Naval Research Laboratory under grant N00173981G000.

3P10

Cavity Testing for W-band Gyroklystron **Amplifiers**

D.E. Pershing, A.H. McCurdy, B.G. Danly, J.M. Cameron and M. Blank, Mission Research Corporation, Newington, VA 22122, USA

Cavity Testing for W-band Gyroklystron Amplifiers

D. E. Pershing, A. H. McCurdy#, B. G. Danly*, J. M. Cameron+, and M. Blank*

Mission Research Corporation, Newington, VA 22122 #Lucent Technologies, Norcross, GA 30071 +Dyn Meridian, Rockville, MD 20852 *Naval Research Laboratory, Vacuum Electronics Branch, Washington, DC 20375

The Naval Research Laboratory has undertaken a 94 GHz gyroklystron amplifier development program for radar applications. This program comprises both in-house development as well as cooperative development between NRL, Communication and Power Industries, Litton Electron Devices, and the University of Maryland.

These devices utilize multiple cavities tuned to different frequencies, typically in the range of 93 to 95 GHz to achieve the desired gain, power, and bandwidth requirements. The cavities operate in the TE₀₁ mode with Q's in the range of 100 - 200. Due to the sensitivity of cavity performance characteristics to tolerances, it is essential that the cavity manufacturing be measured after assembly. For the characteristics NRL/industrial amplifier, space considerations preclude usage of apertures in cavities for diagnostics, so we rely on TE01 axial transmission evanescently coupled through cavity irises to determine the resonant frequency and Q. Specifics of the measurement depend on the cavity type to be measured; input, intermediate, or output.

Transmission or reflection data are taken using an HP 8510 vector network analyzer with a W - band test set. Marie converters are used to convert from the TE10 in WR10 rectangular waveguide to the TE₀₁ mode in 0.2" dia. circular guide. To allow propagation of the TE01 mode in waveguide diameters below air-loaded cutoff, diagnostic probes were fabricated using a dielectric loaded circular waveguide with approximately the same diameter as the cavity iris. Each waveguide is connected to a nonlinear transition region to couple a TE₀₁ wave in 0.2" air loaded waveguide to a TE₀₁ wave in 0.109" diameter Rexolite loaded waveguide with miminal reflection and mode conversion.

Measurements are found to be highly sensitive to mismatches at the -20 dB level. With precision manufacture of the dielectric probes, careful alignment, and TRL calibration at the probe tips to minimize mismatch effects, consistent and reliable results have been obtained. Details of dielectric probe development, testing methodology and typical data will be

presented.

This work was supported by the Office of Naval Research.

[†]Naval Research Laboratory, Washington, D. C. 20375

Harmonic Gyrotrons at 94 GHz

R.C. Stutzman, D.B. McDermott, D.A. Gallagher, C.M. Armstron, T.A. Spencer and N.C. Luhmann, Jr., University of California, Davis, Department of Applied Science, Davis, CA 95616, USA

Harmonic Gyrotrons at 94 GHz

R.C. Stutzman, D.B. McDermott, D.A. Gallagher¹, C.M. Armstrong¹, T.A. Spencer² and N.C. Luhmann, Jr.

Department. of Applied Science, University of California, Davis

1 Northrop Grumman Corp., Rolling Meadows, IL

2 Air Force Research Lab, Directed Energy Directorate, NM

20-100 kW, 94 GHz, s=2-8 harmonic gyrotrons utilizing both MIG and Cusp electron guns are being developed at a new facility at UCD. The initial experiment will test a 50 kW, sixth-harmonic slotted gyrotron with a predicted efficiency of 20% that is driven by a 70 kV, 3.5 A, v_⊥/v_z=1.5, axis-encircling electron beam from a Cusp gun on order from Northrop Grumman. For a fixed ratio of Larmor radius to inner vane radius, slotted gyrotrons are fairly insensitive to the electron energy. The operating voltage was chosen for favorable beam propagation. Designs will also be presented for other planned 94-GHz high-harmonic gyrotrons with axis-encircling electron beams:

a 4th-harmonic, 35 kW, 14% efficient, smooth-bore TE41 gyrotron; a 4th-harmonic, 75 kW, 30% efficient, slotted gyrotron;

and an 8th-harmonic, 22 kW, 9% efficient, slotted gyrotron.

The 8th-harmonic device is of considerable interest because its magnetic field can be supplied by a lightweight permanent magnet. In addition, the high- T_C superconducting magnet and predicted characteristics will be described for a 25 kW, second-harmonic TE₀₂ gyrotron using a 25 kV, 4 A, v_{\perp}/v_{z} =1.5, MIG electron beam with a predicted device efficiency of 25%.

This work has been supported by AFOSR under Grant F49620-95-1-0253 (MURI) and Contract F30602-94-2-0001 (ATRI).

3P12

UCD Gyro-TWT Program: 94-GHz TE01 Gyro-TWT and 44-GHz Third- Harmonic Slotted Gyro-TWT D.B. McDermott, Y. Hirata, S.B. Harriet, A.T. Lin, D.A. Gallagher, C.M. Armstrong, Q.S. Wang, C.K. Chong, K.C. Leou, H.E. Huey and N.C. Luhmann, Jr., Department of Applied Science, Davis, CA 95616,

UCD Gyro-TWT Program: 94-GHz TE₀₁ Gyro-TWT and 44-GHz Third-Harmonic Slotted Gyro-TWT

D.B. McDermott, Y. Hirata, S.B. Harriet, A.T. Lin¹, D.A. Gallagher², C.M. Armstrong², Q.S. Wang³, C.K. Chong⁴, K.C. Leou⁵, H.E. Huey³ and N.C. Luhmann, Jr.

Department of Applied Science, University of California, Davis

- 1 Department of Physics, UCLA, Los Angeles, CA
- ² Northrop Grumman Corp., Rolling Meadows, IL
- ³ Micramics, Inc., Santa Clara, CA
- 4 Hughes Electron Dynamics Division, Torrance, CA
- 5 Engineering, National Tsing Hua University, Taiwan

Two high performance gyro-TWT amplifiers are being constructed at UCD. A high power CW-capable gyro-TWT operating in the low-loss TE01 mode will be driven by a 100 kV, 5 A, $v_{\perp}/v_z=1.0$ MIG electron beam with $\Delta v_z/v_z=5\%$. The three-stage amplifier is predicted by our large-signal simulation code to generate 105 kW at 94 GHz with 21% efficiency, 45 dB saturated gain and 5% constant-drive bandwidth. Linear theory has been used to determine the threshold start-oscillation beam current for absolute instability and the critical section lengths for the potential harmonic gyro-BWO interactions. A novel, lossy mode-selective circuit is being considered for increasing the section lengths in order to remove one sever and further increase the efficiency.

In addition, a third-harmonic gyro-TWT amplifier will be tested at 44 GHz. A slotted interaction circuit is utilized to achieve strong amplification near the third cyclotron harmonic frequency. The start-oscillation conditions were determined by linear theory. The dominant threat to the amplifier's stability is from a third-harmonic peniotron backward-wave interaction. Our large-signal simulation code predicts the three-section, slotted third-harmonic gyro-TWT will yield an output power of 20 kW with an efficiency of 20%, a saturated gain of 40 dB and a constant-drive bandwidth of 2%. The $50 \, \text{kV}$, $2 \, \text{A}$, $v_{\perp}/v_z = 1.4$, $\Delta v_z/v_z = 6\%$, axis-encircling electron beam will be produced by a $70 \, \text{kV}$, $3.5 \, \text{A}$ Cusp gun on order from Northrop Grumman.

This work has been supported by AFOSR under Grant F49620-95-1-0253 (MURI) and Contract F30602-94-2-0001 (ATRI).

W-Band Harmonic Gyro-TWT Amplifier

Q.S. Wang, H.E. Huer, D.B. McDermott, and N.C. Luhmann, Jr., Micramics, Inc., Santa Clara, CA 95051, USA

W-Band Harmonic Gyro-TWT Amplifier

Q.S. Wang, H.E. Huey, D.B. McDermott* and N.C. Luhmann, Jr.* Micramics, Inc., Santa Clara, CA 95051, U.S.A.

Considerable interest exists in developing high power microwave amplifiers at W-band for both commercial industrial and military applications. A multi-purpose harmonic gyrotron traveling wave tube (gyro-TWT) amplifier that can stably deliver moderately high peak and high average power in W-band has been designed and will be presented.

The designed 400 kW peak and 400 W average power harmonic gyro-TWT amplifier will be powered by a 2.5 MW electron beam emitted from a magnetron injection gun (MIG). The TE_{02} overmoded interaction waveguide will be sufficiently large to handle the RF power generated and provide appropriate clearance for the high current electron beam. Operating in the second harmonic of the electron cyclotron frequency, high RF output power can be generated. An innovative mode selective interaction circuit will further prevent the amplifier from oscillating in undesired modes. Also included in the design to be presented are details of the MIG and RF input coupler.

This program is supposed by an SBIR grant from U.S. Department of Energy with grant No. DE-FG03-98ER82619.

* Department of Applied Science, University of California, Davis, California 94619, U.S.A.

3P14

Simulation Study of Fast and Slow Wave Cyclotron Instabilities

S.H. Chen, Y.C. Lan, J. H. Tsai, National Center for High-Performance Computing, Hsinchu, Taiwan, ROC

Simulation Study of Fast and Slow Wave Cyclotron
Instabilities*

S. H. Chen, Y. C. Lan, J. H. Tsai National Center for High-Performance Computing, Hsinchu, Taiwan K. R. Chu

Dept. of Physics, National Tsing Hua University, Hsinchu, Taiwan

The fast-wave and slow-wave cyclotron instabilities have been studied in both an infinite plasma [1] and waveguiding structures. In the later case, the fastwave instability forms the basis for the gyro-TWT and CARM, while the slow-wave instability was exploited in a device called the slow wave cyclotron amplifier Most linear theories and simulation (SWCA) [2]. codes model the gyro-TWT, CARM, and SWCA by a perturbation approach, namely, the electron beam is treated as a perturbation to the waveguide mode whose transverse profile is prescribed to be that of an empty waveguide. This approach is rigorous only when the electron beam and the electromagnetic wave are in When this condition is cyclotron resonance. apparently violated, the perturbation theory still predicts a growth rate for the fast wave and even generates a new branch of slow-wave mode with broad band growth in a fast wave structure. In this study, we examine the validity of the cyclotron instabilities in these non-resonant regimes with the MAGIC code [3] which evaluates the transverse as well as longitudinal field structure self-consistently in the presence of the electron beam. Cases under study include the CARM amplifier where the beam resonance line intersects the waveguide dispersion curve at two points. behavior at frequencies between the two intersections will be examined and results compared with those obtained with a particle tracing code whose validity in this regime is in question. The other case concerns the slow-wave branch of modes predicted by the perturbation theory. Its existence and properties will be clarified with fully consistent particle simulations.

* work supported by National Science Council, ROC.

1. K. R. Chu and J. L. Hirshfield, Phys. Fluids 21, 461(1978).
2. H. Guo, L. Chen, H. Keren, J. L. Hirshfield, S. Y. Park, and K. R. Chu, Phys. Rev. Lett. 49, 730(1982).
3. B. Goplen, L. Ludeking, D. Smithe, and G. Warren, MAGIC User's Manual, Mission Research Corp., MRC/WDC-R-409, 1997.

Results of a Wideband 2nd Harmonic Gyro-Amplifier (phigtron) Experiment

H.Guo, J. Rodgers, J. Zhao and V.L. Granatstein, University of Maryland, Institute for Plasma Research, College Park, MD 20742, USA

Results of a Wideband 2nd Harmonic Gyro-Amplifier (Phigtron) Experiment

H. Guo, J. Rodgers, J. Zhao, and V. L. Granatstein institute for Plasma Research, University of Maryland, MD20742, USA

A new member of gyrotron family, a "phase coherent, harmonic-multiplying, inverted gyrotwystron" (phigtron) has been experimentally characterized operating as a high performance, powerful millimeter wave amplifier. This novel device consists of a gyro-TWT as the prebunching input section operating at the fundamental cyclotron resonance and a two cavity, second harmonic output section. Operating parameters were optimized. Frequency doubled peak power of 430 KW was achieved in the TE

mode with an ≈0.85% bandwidth, 35 dB gain, 0.026 degree per volt phase fluctuation (due to beam voltage variation), and 32% efficiency at center frequency of 33.4 GHz. This measured performance considerably advance the state-of-the-art for millimeter wave gyrotron amplifiers.

A upgraded design of the phigtron using a new extended interaction cavity (EIC) as an output section is also presented. Fig.1 shows the configuration of the EIC and the simulated mode structure (TE02 \rightarrow TE03 \rightarrow TE04) at one of the cavity resonant frequencies corresponding to those points with minimum D value shown in Fig.2. Due to these resonance's, which can overlap each other and cover the amplification range provided by the input gyro-TWT section, the operating bandwidth of the tube is expanded to more than 2%.

This new amplifier has demonstrated high efficiency, high gain, good phase stability, potentially high average power, and wide bandwidth. At the same time, operation is advantageously characterized by the harmonic- multiplying feature which results in a low magnetic field requirement, low drive frequency and small phase fluctuation.

This work has been supported by the DoD MURI program under AFOSR grant F4962001528306 .



Fig. 1. Mode structure in the Extended Interaction Cavity (EIC).

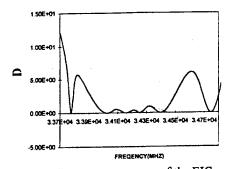


Fig. 2. Frequency response of the EIC.

3P16

Analyzer for Profile Measurement of a Beam from a Magnicon Electron Gun

S.H. Gold, A.K.Kinkead, A.W. Fliflet, R. True, R.J. Hansen and J.L. Hirshfield, U.S. Naval Research Laboratory, Code 6793, Washington, DC 20375, USA

Analyzer for Profile Measurement of a Beam from a Magnicon Electron Gun*

S.H. Gold, A.K. Kinkead, A.W. Fliflet, R. True, R.J. Hansen, and J.L. Hirshfield

 ¹Beam Physics Branch, Plasma Physics Division, Naval Research Laboratory, Washington DC 20375
 ²Sachs-Freeman Associates, Inc., Landover, MD 20785
 ³Litton Systems, Inc., San Carlos, CA 94070
 ⁴Omega-P, Inc., 345 Whitney Ave., New Haven, CT 06511

A key parameter in determining the efficiency of a magnicon amplifier is the quality of the electron beam used to drive the device, and in particular the diameter of the electron beam and its matching into the axial magnetic field. The electron gun for the 11.4 GHz magnicon amplifier experiment at NRL is an ultrahighconvergence Pierce-type gun designed to produce a 480-kV, 210-A electron beam of diameter less than 2 mm.^{1,2} A novel beam analyzer has been built to characterize this beam, with a design based on a similar analyzer used for measuring the beam of an earlier magnicon.³ The analyzer allows the beam profile to be monitored as changes are made in the magnetic flux linking the cathode, and with changes in the bias on the cathode focus electrode. The analyzer makes use of ten graphite apertures that are mounted at 30° intervals on an off-axis rotating drum, so that only a single aperture will intercept beam current at one time. The drum is rotated by a stepper motor, and its precise rotation is read out to an accuracy of better than 0.1° using a digital shaft encoder, permitting spatial measurements with an accuracy of better than 60 microns. The apertures are spaced at 1-cm intervals along the beam axis, a spacing that permits resolution of beam scalloping and centroid displacement effects. These apertures are designed to measure only the position of the beam edges, since interception of the maximum current density of up to 12 kA/cm² would destroy the graphite apertures. The analyzer also includes two ten-cm graphite tubes, of 4 and 8 mm inner diameter, at the remaining two angular stations, for use in measuring the net transmitted and intercepted current.

This paper will describe the calibration of the beam analyzer, and its application to the measurement of the magnicon electron beam.

*This work is supported by the US Department of Energy, by the Office of Naval Research, and by a Small Business Innovation Research (SBIR) grant to from the US Department of Energy to Omega-P, Inc.

¹S.H. Gold, et al., Phys. Plasmas, vol. 4, pp. 1900–1906, 1997. ²V.P. Yakovlev, O.A. Nezhevenko, and R.B. True, in Proc. 1997 Particle Accelerator Conf. (IEEE, Piscataway, NJ, 1998), vol. 3, pp. 3186–3188.

³Yu.V. Baryshev, et al., Nucl. Instrum. Methods Phys. Res., vol. A340, pp. 241–258, 1994.

Nonlinear Electron Interaction with TM Modes in a Low-Voltage Waveguide FEL

X.H. Zhong and M.G. Kong, University of Liverpool, Liverpool L69 3GT, UK

Nonlinear Electron Interaction with TM Modes in a Low-Voltage Waveguide FEL

X. H. Zhong and M. G. Kong

Department of Electrical Engineering and Electronics University of Liverpool, Liverpool L69 3GJ, UK

Compact free electron lasers (FELs) operating in the spectrum from microwave to the far infrared have recently command much attention due to their many potential applications in industry and medicine[1][2]. These FEL devices employ low current electron beams to reduce the size and cost of the required electron source, and hence the output power is only modest. To increase the output power, many gain and efficient enhancement techniques have been suggested, for instance the employment of prebunched electron beams[2] and the waveguide optical klystron arrangement[3].

A parallel approach to reduce the size of these compact waveguide FEL systems is to minimize the electron beam voltage required to generate a strong radiation at a given frequency. In a recent work, we have demonstrated that the electron interaction with the longitudinal electric field component of TM modes leads to an electron velocity component oscillating at a period half as long as the wiggler period, λ_w in the longitudinal direction[4]. Therefore the electron beam experiences an effective wiggler magnet of λ_w . For a waveguide FEL based on such a longitudinal interaction mechanism, the required electron voltage for a strong radiation at a given frequency is therefore less than that for a waveguide FEL based on the conventional transverse interaction mechanism. In this contribution, we extend our previous results and consider the nonlinear behaviour of the electron-wave interaction. Since the space charge effects are negligible for these low power waveguide FELs, the electron interaction with TM modes are simulated in the Compton regime. It is shown that a previously ignored nonresonant term in the energy conservation equation could be significant in the FEL interaction, and under certain operation conditions its contribution may be adjusted to enhance the interaction gain. This new interaction feature may be unique to low voltage waveguide FELs for which the wavelength of the radiation field is in the same order as the wiggler period. Numerical simulation is then extended to the nonlinear interaction regime and similar saturation behaviours to those in a conventional waveguide FEL are found although their saturation onsets are different. The numerical work reported in this contribution may be used as a design base for TM mode based low voltage waveguide FEL systems.

References:

- [1] Y. U. Jeong et al, Phys. Rev. Letts. 68 (1992) 1140.
- [2] F. Ciocci et al, Phys. Rev. Letts. 70 (1993) 928.
- [3] M. G. Kong, Optics Comm. 132 (1996) 464.
- [4] M. G. Kong, Optics Comm. 141 (1997) 48.

3P18

Experiments on a 28GHz, 200kW Gyroklystron Amplifier for Plasma Heating#

J.J. Choi, S.W. Baik, W.K. Han, D.M. Park, J.H. Oh, S. H. Lee, J.G. Yang and S.M. Hwang, Kwangwoon University, Seoul 139-701, KOREA

A high-resolution (100-ps, 100-µm) microchannel plate gated pinhole camera to study fast Z-pinch implosions

S. Breeze, L. Ruggles, L. Anderson, C. Deeney, R.B. Spielman, and J.L. Porter Sandia National Laboratories P.O. Box 5800 Albuquerque, NM 87185-1194

Fast, high current Z-pinch implosions are used to produce intense x-ray pulses for various applications. For high-energy photon production and for inertial fusion applications, the imploding Z pinch can achieve velocities between 50 and 100 cm/µs. To image such implosions, a high time resolution is needed. Furthermore, the final pinches formed can be only 1 to 1.5 mm in diameter but 20 mm long. Given a basic microchannel plate resolution of 80 μm , then a high magnification (>1.5) is required to maintain good spatial resolution. To satisfy these requirements, we have designed and fielded a nine-frame, gated-MCP pinhole camera on the 20-MA Z accelerator. Each MCP frame is 6 cm by 2 cm, and is gated with a 100 ps duration pulse. We will describe the design and operation of this camera, in addition to showing data from Z-pinch and hohlraum experiments using this camera.

A broad band (4-25 GHz) calorimeter for diagnosing high power microwave sources

A. Shkvarunets, S. Kobayashi, Y. Carmel, J. Rodger, T. Antonsen, Jr and V. Granatstein, University of Maryland, Institute for Plasma Research, College Park, MD 20742-3511, USA

Intrinsic Resitivity Nickel and Gold Thin Film Bolometers for Pulsed X-ray Measurements

J. McGurn, J. McKenney, C. Deeney, C.A. Coverdale, R.B. Spielman, D. Fehl, P. Ryan, and G. Chandler Sandia National Laboratories P.O. Box 5800 Albuquerque, NM 87185-1194

The accurate measurements of the emitted x-ray powers and yields from high-current Z pinches are essential in applying Zpinches to Inertial Fusion energy research, and to studying radiationmaterial interactions. On the 20-MA Z and the 10-MA Saturn accelerators, 1-µm thick nickel and gold bolometers have been employed to measure the total yields and the 1 to 5 keV radiated x-rays from wire arrays and gas puff Z-pinch configurations. By careful deposition processes, these elements can be fabricated on pyrex substrates with resistivities that are near (within a few percent) of the intrinsic (bulk material) values. Moreover, oven calibrations have shown that the measured rate of change of resistivity with temperature also agrees with the bulk material value. Due to the quality of the thin film parameters, we have found good agreement between the bolometer calculated x-ray yields and those determined from calorimeters and diamond photoconductive detectors. In this paper, we will review the fabrication and calibration processes and we will discuss the comparison of bolometer measurements to other diagnostics.

3P20 Moved to 2D09

Spherically curved crystals for x-ray plasma diagnostics

Y. Aglitskiy and T. Lehecka, S. Obenschain, C. Pawley, C.M. Brown, J. Seely, U.S. Naval Research Laboratory, Washington, DC 20375-5352, USA

Flash X-ray diagnostics of argon jets: X-ray induced fluorescence imaging and radiography

L. Hure, E. Robert, C. Cachoncinlle, R. Viladrosa and J.M. Pouvesle, GREMI, 45067 Orleans Cedex 2, France

Flash X-ray diagnostics of argon jets: X-ray induced fluorescence imaging and radiography

L. Huré, E. Robert, C. Cachoncinlle, R. Viladrosa and J.M. Pouvesle GREMI, CNRS/Université d'Orléans, BP 6759, 45067 Orléans Cedex 2, France

In this work we report on the development and application of two flash x-ray diagnostic techniques. A compact x-ray source specially designed for these studies was used to characterize argon flows at atmospheric pressure in ambient air.

The table-top x-ray source emits strong doses of x-ray photons of about 10 keV in pulses of 20 ns FWHM with an x-ray emission zone smaller than 300 μ m. Single shot radiography of two converging argon flows expanding through rectangular nozzles (1mm x 20 mm) was achieved with the use of Polaroid films. This experiment, that confirms some previous studies on soft x-ray radiography¹, has been performed to allow a straight comparison of the radiograph with the results from the imaging technique described below.

The fluorescence spectrum resulting from the flash Xray excitation of argon jets in ambient air has been recorded from 185 to 800 nm. The deposition of a part of the x-ray incident flux in argon induces the formation of molecular ionic species and the excitation, through transfer reactions, of N₂ and OH radiative molecules. We performed the imaging of this X-ray Induced Fluorescence (XIF) on an intensified multichannel analyzer synchronized with the flash X-ray source. The use of different optical filters indicate that the main fluorescence detected by the CCD sensor originates from N₂* second positive system. The XIF imaging enables us to follow the trajectory of the same two argon jets previously characterize with radiography. This result indicates that in our experimental conditions, i.e. pulsed X-ray excitation and atmospheric pressure, argon flows could be characterized by recording the nitrogen emissions which have a very short lifetime (~200 ns) thus allowing to neglect diffusion.

The agreement between the results obtained by the two methods clearly validate the XIF diagnostics. XIF imaging and radiography, could be performed simultaneously, as presented in this study, or independently in other potential applications. Work is in progress to apply these techniques for characterization of turbulent, polyphasic, high temperature or high pressure flows.

This work is supported by MENRT and La Société de Secours des Amis des Sciences

¹ J. Geiswiller, E. Robert, L. Huré, C. Cachoncinlle, R. Viladrosa and J.M. Pouvesle, *Meas. Sci. Technol.*, 9, 1537 (1998).

3P22

Secondary electron energy profiles as a diagnostic tool for RF plasma sheaths

D.M. Shaw, M. Watanabe, H. Uchiyama, and G. J. Collins, Colorado State University, Fort Collins, CO 80523, USA

Secondary electron energy profiles as a diagnostic tool for rf plasma sheaths

D. M. Shaw, M. Watanabe, H. Uchiyama, and G. J. Collins Dept. of Electrical Engineering, Colorado State University, Fort Collins, Colorado, 80523.

Ion-induced secondary electron energy profiles from a radio frequency biased (13.56 MHz) electrically insulating (Al₂O₃) electrode placed adjacent to an inductively coupled plasma (ICP) discharge are studied both experimentally and theoretically. Plasma feedstock gases include Ar, He, H₂, and N₂ over the pressure range of 2 – 20 mTorr. Radio frequency electrode bias voltages of 140, 285, and 425 V (peak to ground) are employed and the complete electron energy spectrum is measured 14 cm from the rf biased electrode using a differentially pumped retarding potential analyzer. The experimental measurements are compared to a collisionless Child-Langmuir rf sheath model, indicating that this technique is a useful *in-situ* diagnostic method to check the validity of rf sheath theories.

Langmuir Probe Diagnostics of Electronegative Radio Frequency Inductively Coupled Plasma

T.H. Chung, D.C. Seo, S.W. Chung and H.J. Yoon, Dong-A University, Pusan 604-714, Korea

Langmuir Probe Diagnostics of Electronegative Radio Frequency Inductively Coupled Plasma

T. H. Chung, D. C. Seo, S. W. Chung and H. J. Yoon

Department of Physics, Dong-A University, Pusan 604-714, KOREA

Langmuir probe diagnostics are performed on a electronegative radio frequency inductively coupled oxygen plasma. With a simultaneous use of single probe and double probe, an approximate ratio of the electron temperature to the negative ion temperature can be determined, and then particle densities of charged species are properly estimated. The plasma parameters including electron energy distribution function are measured as a function of the gas pressure and the power. According to the prevailing particle loss mechanism, the parameter space can be divided into a volume recombinationloss-dominated region and an ion-flux-loss-dominated region. Based on the global model equations, the scaling laws of plasma variables with the control parameters for the ion-fluxloss-dominated region are estimated and compared with experimental results. In addition, the experimentally obtained spatial profiles of plasma parameters are compared with the results of two-dimensional fluid simulation.

3P24

Laser Induced Fluorscence of Argon Ion in Plasma Presheaths

M. Atta Khedr, A.M. Hala, L. Oksuz and N. Hershkowitz, University of Wisconsin-Madison, Madison, WI 53706, USA

Laser Induced Fluorscence of Argon Ion in Plasma Presheaths

M. Atta Khedr, A.M. Hala, L. Oksuz, and N. Hershkowitz Dept. of Engineering Physics, University of Wisconsin, 1500 Engineering Dr., Madison, WI 53706, USA

A tunable diode laser system has been used to measure ion velocity distribution functions of ArII in plasma presheaths using laser - induced fluorscence (LIF). The diode laser system can examine the velocity distribution function with marginally greater resolution than the dye laser owing to their smaller line width (0.001 nm) [1].

LIF of ArII requires excitation at 668.61 nm. The diode laser is centered at that wavelength with a tuning range of 0.15 nm and the optical amplifier (MOPA) is at 10 nm. LIF measurements of presheaths as a function of pressure (0.5 - 3 mTorr) were made in a DC hot - filament produced multidipole plasma discharge near a negatively biased plate. The ion velocity has range of 10³cm/s - 10⁵cm/s for presheaths thickness 0.5 cm - 5cm.

These measurements are compared with results obtained by using a double sided Langmuir probe (Mach probe) and an emissive probe.

Reference

[1] G.D. Severn, D.A.Edrich, and R.Mc Williams, Rev. Sci., Instrum. 69(1), p.10-15, January (1998).

Work is supported by DOE grant no. DE-FG02-97ER54437.

Use of Mach probes and Langmuir probes in a drifting un-magnetized non-uniform plasma

L. Oksuz, N. Hershkowitz, University of Wisconsin-Madison, Madison, WI 52705, USA

Use of Mach probes and Langmuir probes in a drifting unmagnetized nonuniform plasma

L. Oksuz, N. Hershkowitz
Engineering Physics Dept. University of Wisconsin-Madison
Abstract

Although Mach probes have been used to measure the ion drift velocities in fusion plasma applications, their operation in unmagnetized plasma is less well understood. The effects of nonuniform drifting plasma on Langmuir probes and Mach probes have been investigated in a multi-dipole plasma. A circular conducting plate was mounted into the multi-dipole chamber. A Mach probe consists of two single sided Langmuir probes back to back. Mach probe theory^{1,2} was used to determine the ion drift

velocity from $\frac{J_U}{J_D} = \exp(ku_m)$ where J_U, J_D are the upstream

and downstream currents, k is constant, u_m is the Mach number. The Mach probe data were collected for different probe sizes and for different noncollecting part biases. Controlling the voltage of the noncollecting part of the Mach probe makes the collecting part of the I-V traces less noisy. While different biases applied to the noncollecting part perturbed the collected data, the current ratios didn't change if the applied bias voltage was comparable to the plasma potential. Using Mach probes, diameters 0.125" and 0.375", (smaller than the ion collision length ~3cm at 1mTorr) didn't change the current ratios. The total current from both sides of the Mach probe was equal to the current collected by a two sided Langmuir probe. The calculated plasma potential from the Langmuir probe was found to be the average of the plasma potentials calculated from each side of the Mach probe. Mach probe theory was found to be consistent with the experimental results. Using this Mach probe theory, the ion drift velocity profile was obtained in nonuniform drifting plasma and the plasma characteristics were determined. The density gradient, electric field and collisions play a role in determining the plasma drift. The ions start to drift at the center of the plasma and at the presheath entrance they drift at 5-6% of the ion sound velocity. Up to the presheath, ambipolar diffusion plays a role. The Mach probes data and fluid theories were compared. Comparison shows ionization is important in the presheath. With the fluid theory one can also use a Langmuir probe to find the drift velocity profile at the presheath.

Work is supported by DOE grant no.DE-FG02-97ER54437

3P26

Time Evolution of Ion Energy Distributions and Optical Emissions in Pulsed Radio Frequency Plasmas

Martin Misakian, Eric Benck, Yicheng Wang, James Olthoff and James Roberts, NIST, Gaithersburg, MD 20899-8113, USA

Time Evolution of Ion Energy Distributions and Optical Emissions in Pulsed Radio Frequency Plasmas

Martin Misakian, Eric Benck, Yicheng Wang, James Olthoff, and James Roberts National Institute of Standards and Technology Gaithersburg, MD 20899

Pulsed inductively coupled plasmas have recently received considerable attention because of their possible advantages over continuous plasma discharges in industrial applications.¹⁻³ We report the results of time-resolved measurements of ion energy distributions, relative ion densities, as well as optical emissions and electrical characteristics in such plasmas for the simple gas mixture of argon and oxygen (50% Ar/50% O2). Comparisons with pure argon are also presented. An inductively coupled version of the Gaseous Electronics Conference rf reference cell is used to produce the pulsed plasmas and the ions are sampled though a 10 µm diameter hole in the center of a grounded plate electrode. Ions exiting through the hole are characterized with a 45° electrostatic energy analyzer connected in series with a quadrupole mass spectrometer. Optical emission measurements have been made at several different wavelengths to monitor the time evolution of excited species of argon and oxygen.

Examination of the time evolution of the ion energy distributions over the pulse cycle indicates that when the plasma is energized, the plasma begins in the dim (E) mode. The E mode is characterized by a steadily increasing average plasma potential and a decreasing energy distribution width, before a sudden transition to the bright (H) mode. Throughout most of the pulse cycle, the ions Ar^+ , O_2^+ , and O^+ maintain the relation O_2^+ O_2^+ O_2^+ .

Optical emission measurements display a dramatic difference between the light output of the E mode and the H mode. Depending on the pulsing conditions, it is possible for the plasma to remain in the E mode for several milliseconds before the transition into the H mode.

For a pulsed discharge in pure argon, the E mode is very brief when compared to the O₂/Ar mixture at the same gas pressure and power. For lower pressures and power, the duration of the E mode for the pure gas is extended.

References:

- 1. S. Samukawa, Jpn. J. Appl. Phys. Pt. 1 33, 2133 (1994).
- S. Samukawa and H. Ohtake, J. Vac. Sci. Technol. A 14, 3049 (1996).
- G.A Hebner and C.B. Fleddermann, J. Appl. Phys. 82, 2814 (1997).

M. Hudis L.M.Lidsky J.Applied Physics V41 No12 November 1970
 Kyu-Sun Chung J. Applied Physics 69 1991

Installation of the Madison Symmetric Torus Heavy Ion Beam Probe

K.A. Connor, T. P. Crowley, D.R. Demers, J. Lei, J.G. Schatz, P.M. Schoch, U. Shah, Rensselaer Ploytechnic Institute, Troy, NY 12180-3590, USA

Installation of the Madison Symmetric Torus-Heavy Ion Beam Probe*

K. A. Connor, T. P. Crowley, D. R. Demers, J. Lei, J. G. Schatz, P. M. Schoch, U. Shah Plasma Dynamics Laboratory Rensselaer Polytechnic Institute, Troy, NY, 12180.

A heavy ion beam probe has been designed for application on the Madison Symmetric Torus with final construction and installation occurring in early 1999. The HIBP will be capable of making measurements of the plasma space potential $\Phi(r)$, simultaneous density and potential fluctuations, and magnetic measurements (both equilibrium fields and fluctuations). On MST, measurements of ne(t) and Φ(t) will take priority once the system is fully functional, with some effort also dedicated to equilibrium measurements, particularly of the confining magnetic field. The latter measurements will not be standard direct heavy ion beam probe measurements based on the detection of secondary ions produced by collisions between the probing beam and plasma electrons. Rather, information on the magnetic field will be inferred from overall ion trajectory characterization. While this basic set of measurements is being made, we will also be collecting information to determine the next plasma parameter to address. The prospects for these HIBP measurements are very exciting, since the information to be obtained has not previously been available from the core of a hot Reversed Field Pinch.

The main components of this HIBP system are a 200 kV accelerator and a 100 kV electrostatic energy analyzer. Unique to MST-HIBP are cross-over sweep systems which make it possible to obtain a large angular range for the ion beam trajectories through MST's small ports. The relatively low confining magnetic field strength of MST permits a variety of probing ions (lithium, sodium, and potassium) to be used to obtain the measurements listed above at essentially all plasma radii. This rich choice of probing conditions and the excellent reproducibility of MST plasmas will permit us to study instrumental issues to an extent never before possible on a beam probe. This is indeed fortunate since MST also presents us with several new challenges. The level of plasma and UV flux is quite high so we have designed and implemented magnetic apertures to protect the elaborate cross-over sweep systems. These apertures can also incorporate electrical screens if necessary. Since the magnetic field structure is largely produced by the plasma, one can only predict a range of possible probing ion trajectories. Thus, it has been necessary to produce a large number of trajectories to be sure all possibilities are considered and to build in some flexibility in the system support structure.

*Work Supported by USDOE

3P28

The Los Alamos Penning Fusion experiment-lons

Karl R. Umstadter, Martin M. Schauer, Dan C. Barnes, Fred L. Ribe, Lou S.Schrank,

Los Alamos National Laboratory, Los Alamos, NM 87545, USA

The Los Alamos Penning Fusion eXperiment – Ions Karl R. Umstadter, Martin M. Schauer, Dan C. Barnes,

Jmstadter, Martin M. Schauer, Dan C. Barnes Fred L. Ribe, Lou S. Schrank

Los Alamos National Laboratory, Los Alamos, New Mexico 87545

Virtual cathode machines (usually called Penning Fusion or PF machines) have achieved the required physics goals of maintaining required nonthermal electron distributions, spherical focussing, and excellent electron energy confinement, and are poised to study ion physics. PF systems attempt to tailor the electron cloud to produce a spherical ion well, while maintaining desired electron confinement. In addition to the steady ion convergent mode of IEC machines (Spherically Convergent Ion Focus or SCIF), PF systems potentially may access a recently discovered oscillating ion mode (Periodically Oscillating Plasma Sphere or POPS), if a uniform density electron cloud is formed with appropriate electrostatic boundary conditions.

The Penning Fusion experiment - Ions (PFX-I), part of the Innovative Concepts Initiative of the Office of Fusion Energy (OFE) is a unique magnetic confinement concept based upon the traditional nonneutral-plasma Penning trap. It is an electron/ion trap comprised of a small magnetic flux-shaper, an electron emitter, and gas supply. The trap itself has an ID of less than 40mm, with access to the center restricted through ports less than 15mm in diameter.

The small trap size and relatively low electron density discounts several diagnostics. The initial diagnostic we are developing is based upon the Stark broadening of the Hydrogen alpha (λ =6563Å) and beta (λ =4861Å) lines when neutral H₂ gas is added to the electron cloud confined in the trap. For our experimental conditions (n_e -10¹⁰cm⁻³), calculations indicate that ~10¹³photons/sec•cm³ should be emitted from the plasma and the H_{α} line should be broadened by ~1Å.

In the previous experiment¹, PFX demonstrated super-Brillouin spherical electron focus. More recently we have trapped over 3 billion electrons (figure 1) in a simplified penning trap. Near term R&D goals are:

- Ion well depth of 50 kV
- $< n > of 10^{18} m^{-3}$
- Convergence of 100:1
- Applied voltage > 100 kV
- Mean neutron rate of > 10¹¹/s
- Lifetime of > 1000 hrs.
- Q > 0.01
- Reactivity 1000 Brillouin
- Study POPS

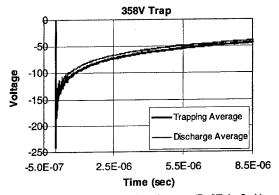


Figure 1. Electron Trapping Signature (B=2T, i_T =2 μ A)

A possible limitation is that the Q of the device may be limited by ionion collisions. Engineering challenges include the limited access for diagnostics and high-voltage breakdown. The advantages of this approach include a compact, cheap, simple, and incremental R & D path and range of near- and medium-term applications. Furthermore, the "arbitrarily small" fusion power reactor embodiment and advanced fuel operation possibilities are excellent.

References: 1. D. C. Barnes, T. B. Mitchell, and M. M. Schauer, Phys. Plasmas, 4, 1745 (1997)

Neutron emission profiles measurements from the FTU Tokamak neutron collimator diagnostic

L. Bertalot and B. Esposito, P. Batistoni, Associazione EURATOM-ENEA, 00044 Frascati, Italy

Neutron emission profiles measurements from the FTU tokamak neutron collimator diagnostic

L. Bertalot and B. Esposito, P.Batistoni

Associazione EURATOM-ENEA sulla Fusione, CR Frascati, CP 65, 00044 Frascati, Rome, Italy

An overview of the neutron emission profiles measured in the Frascati Tokamak Upgrade (FTU) during the 1998 experimental campaign is presented. FTU is a high magnetic field compact device and takes part to the European tokamak project. The major and minor plasma radii are 93.5 and 30cm, respectively. Different auxiliary heating systems are available on FTU: Lower Hybrid (2 MW at 8 GHz), Electron Cyclotron (800 KW at 140 Chz) and Ion Bernstein (300 kW at 433 MHz).

The neutron emission profiles are obtained by means of a 6-channel collimator equipped with NE213 organic neutron/gamma pulse scintillators and discrimination circuitry. Particular care has been given to the construction of the multicollimator and it shielding components, due to the material. The use of lithium is necessary to suppress the production of y-rays from thermal neutron capture reactions in the shield structure. An additional shield has been recently installed to reduce the neutron and gamma background in some of the channels. The lines of sight view the plasma radially and the spatial resolution is about 3 cm. The typical measured neutron count rate is 200 c/s at a total neutron rate of 2x10¹² n/s in the central channel, and the interfering breakthrough of gamma events in the neutron channels is less than 0.2%. Typically, the count rate of y-ray events is 5-10 times higher than that of neutron events. Technical details of the electronics and detectors' set up are illustrated.

Both ohmic and additional heated deuterium discharges at various density and plasma current values are considered. The FTU neutron profile monitor is found to operate well and free from unwanted background radiation. The results show that the diagnostic is capable of resolving profile features arising both from the use of different heating systems and from changes in the plasma position. The application of these data is the physical analysis of the plasma discharges is discussed.

3P30

Measurement of Plasma Flow Parameters and Microparticle Velocity in Pulsed Electrothermal Launcher

E.Ya. Shcolnikov, M. Yu. Guzeyev, S.P. Maslennikov, A.V. Melnik, A.V. Chebotarev, M.I. Khaimovitch, Moscow State Engineering Physics

Measurement of Plasma Flow Parameters and Microparticle Velocity in Pulsed Electrothermal Launcher

E. Ya. Shcolnikov, M. Yu. Guzeyev, S.P. Maslennikov, A.V. Melnik, A.V. Chebotarev, M.I. Khaimovitch*.

Moscow State Engineering Physics Institute (technical university) - MEPhI, Kashirskoye shosse 31, Moscow, 115409, Russia.

*All-Russian Research and Development Institute of Experimental Physics - VNIIEF, Prospect Mira 37, Sarov-city, Nizhny Novgorod region, 607190, Russia.

The high velocity pulsed plasma flows may be used for the powder materials microparticles acceleration and obtaining coatings with super quality parameters. In this respect the experimental study of parameters of flows, generated in discharge gaps of the electrothermal launcher, has been carried out. The following parameters were to be measured: velocities and extension of various parts of the pulsed flows, i.e. the shockly compressed gas region and the high temperature region. Pressure piezosensors, photodiodes, photomultipliers were used in measurements as well as the shadowy photography techniques on the basis of a pulse laser. The flows visualization was carried out. In obtained pictures, in particular, the shockly compressed gas region shrinkage due to shock-waves interaction was observed as well as this region backward boundary diffusion due to various nonstabilities.

For the flow temperature measurement the method of relative intensities of the plasma radiation spectrum lines was used. For this purpose the corresponding copper lines were chosen. The velocity of various powder materials (corundum, tungsten, titanium etc.) microparticles with typical dimensions 3÷40 μm , which are accelerated by the plasma flow, was measured with use of the pulsed laser with the pulse duration 10 ns, the pulse energy 0,02 J and the wave length 543 nm. To diminish the effect of the plasma flow radiation the interference light-sensitive filters were used.

Microparticles images were obtained either by means of registration of the laser beam reflected from their surface or by obtaining shadowy photographies. The conducted measurements permitted to analyze the microparticle dynamics, in particular, their capture by the shockly compressed gas region which follows the head shock-wave. The measurement results have also demonstrated strong dependence of the microparticles velocity on their concentration in the flow.

A high-resolution (100-ps, 100-µm) microchannel plate gated pinhole camera to study fast Z-pinch implosions

S. Breeze, L. Ruggles, L.Anderrson, C. Deeney, R.B. Spielman and J.L.Porter, Sandia National Laboratories, Albuquerque, NM 87185-1194, USA

The Effect of Cathode Geometry on Stability of an Atmospheric Pressure Arc.

MAX KARASIK, L. E. ZAKHAROV, S. J. ZWEBEN, Princeton Plasma Physics Lab

Atmospheric plasma arcs are used extensively in material processing applications such as welding and metallurgy. An experimental arc furnace operating in air with graphite cathode and steel anode at 100-250 A exhibits large (~ 10% rms) voltage and current fluctuations for certain cathode geometries, with the arc assuming a rotating helical shape persistent for many cycles. The instability occurs for cathode tip diameters of 1.5 to 3 times the cathode spot diameter, with the amplitude strongly dependent on current. A model for the instability is developed in which ordered cathode spot motion and the cathode jet give rise to the observed arc shape. Previous experiments on arc dynamics in applied AC magnetic field* are used as a diagnostic for jet velocity. The model gives a good description of arc shape for low amplitudes. Possible mechanisms for spot motion on the cathode and its dependence on geometry will be proposed. Cathode shape is seen as an important means of controlling arc stability and broadening effective arc volume.

3P32

Intrinsic Resitivity Nickel and Gold Thin Film Bolometers for Pulsed X-ray Measurements

J. McGurn, J. McKenney, C. Deeney, C.A. Coverdale, R.B. Spielman, D. Fehl, P. Ryan and G. Chandler, Sandia National Laboratories, Albuquerque, NM 87185-1194, USA

Anode voltage drops of the DC discharge in air

V.A. Lisovskiy, S.D. Yakovin

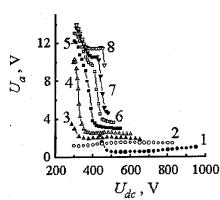
Kharkov State University, pl. Svobody 4, Kharkov, 310077, Ukraine

*Scientific Center of Physical Technologies, Novgorodskaya Str. 1, Kharkov, 310145, Ukraine

In the present work the anode voltage drops are determined in the low pressure glow discharge in air in a wide discharge tube. The experiments were carried out with in pressure range of air $p = 10^{-2}$ - 10 Torr and with in the range of constant voltage on the electrodes $U_{dc} < 10^3 \ \mathrm{V}$ and discharge currents I_{dc} < 100 mA. Distance between the cathode and anode was equal to L = 33 mm. The diameters of discharge tube and anode were equal to 100 mm. Figure shows the anode voltage drop, measured by us, on the anode layer U_a . At low pressure with growth of U_{dc} the anode voltage drop Ua at first slightly decreases, reaches a minimum and then weakly increases. Thus the value of anode voltage drop is $U_a \le 2 - 3$ V. With growth of air pressure the anode voltage drop increases (with the fixed value of voltage U_{dc}). With occurrence of an anode glow the anode voltage drop sharply grows, at that $U_a \sim 10$ V. With increase of voltage U_{dc} the anode voltage drop decreases; at U_{dc} , when the boundary of a negative glow reaches an anode layer boundary, the anode glow disappears, U_a sharply decreases up to value $U_a \sim 3$ - 5 V and with the further growth of U_{dc} the anode voltage drop remains practically constant. With increase of air pressure the boundary of a negative glow reaches an anode layer at higher voltage U_{dc} , and the reduction of U_a with disappearance of an anode glow has almost a step behavior.

Figure.

Dependence of the anode voltage drop on value of a voltage on electrodes with *L* = 33 mm and air pressures: 1 - 0.05 Torr, 2 - 0.2 Torr, 3 - 0.4 Torr, 4 - 0.5 Torr, 5 - 0.6 Torr, 6 - 0.7 Torr, 7 - 0.8 Torr, 8 - 1 Torr.



^{*}ICOPS'98 3P32

The Effect of Cathode Geometry on Stability of an Atmospheric Pressure Arc

Max Karasik, L.E. Zakharov, S. J. Zweben, Princeton Plasma Physics Laboratory, Princeton, NJ 08543, USA

A POLYPHASE LOW FREQUENCY RF POWER SUPPLY FOR A ONE ATMOSPHERE UNIFORM GLOW DISCHARGE PLASMA (OAUGDP)

Fuat Karakaya, Daniel M. Sherman, and J. Reece Roth

UTK Plasma Sciences Laboratory Department of Electrical Engineering The University of Tennessee Knoxville, TN 37996-2100

ABSTRACT

A flexible, reliable, and robust RF power supply capable of delivering the frequency and voltage required to energize the One Atmosphere Uniform Glow Discharge Plasma OAUGDP is needed, but off-the-shelf availability of such a RF power supply is quite limited. Using one or more insulated electrodes, the critical parameters required to generate the OAUGD plasma were identified as the gap distance between electrodes, the RF driving frequency, and the rms. voltage. For basic research, the desired frequency range ranges between 0.6 kHz to 10 kHz and the output rms. voltage between 2.2kV to 20 kV. For wide a range of applications, a minimum of 1.5 kW of power with impedance matching^[2] is required, whereas 4 kW to 6 kW is necessary for the generation of the OAUGDP without impedance matching or to create the OAUGD plasma in large volumes. These parameter ranges are suitable for research and prototype development of a variety of industrial applications, including surface cleaning and modification, microbiological chemical sterilization, decontamination. aerodynamic flow control, and plasma deposition.

A RF power supply designed to generate the OAUGDP is composed of a frequency generator, amplifiers, and a transformer. If the power supply is built from several smaller subunits (amplifier and transformer) that combine to supply the RF electrical power rather than just one larger unit, a component failure only implies a partial loss in power, rather than a complete shutdown. By properly choosing the components of the RF power supply, the additional capability to generate a polyphase voltage output and electric field gradients across an array of electrodes is also gained. Our previous OAUGDP aerodynamic research^[3] explored only the aerodynamic effects created by the generation of the OAUGD plasma. However another method of OAUGDP plasma formation - polyphase peristaltic acceleration - uses the electric field gradient generated by this RF power supply. [4]

*Supported in part by a DoD-AFOSR STTR subcontract from Environmental Elements Corporation of Baltimore, MD and a Research Agreement with March Instruments, Inc. of Concord, CA

- 1.)
- Roth, J. R. (1995): Industrial <u>Plasma Engineering: Volume 1 Principles</u>. Institute of Physics Press, Bristol, UK ISBN 0-7503-0318-2. See Section 12.5.2. Impedance matching an OAUGDP RF power supply will be covered in another poster paper by Z. Chen et al.

 Roth J. R., Sherman D. M., Wilkinson S. P., (1998): "Boundary Layer Flow Control with a One Atmosphere Uniform Glow Discharge Surface Plasma", AIAA Paper 98-0328, 36th AIAA Aerospace Sciences Meeting and Exhibit, Reno NV, January 13, 1998.

 Roth, J. R. (1997): "Method and Apparatus for Covering Bodies with a Uniform Glow Discharge Plasma and Applications Thereof", U.S. Patent #5,669,583, Issued September 23, 1997.

3P34

Anode voltage drops of the DC discharge in air V.A. Lisovskiy, S.D. Yakovin,

Kharkov State University, Kharkov 310077, Ukraine

Anode voltage drops of the DC discharge in air

V.A. Lisovskiy, S.D. Yakovin*

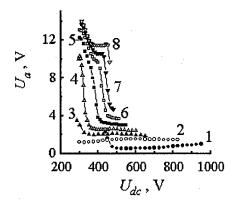
Kharkov State University, pl. Svobody 4, Kharkov, 310077, Ukraine

"Scientific Center of Physical Technologies, Novgorodskaya Str. 1, Kharkov, 310145, Ukraine

In the present work the anode voltage drops are determined in the low pressure glow discharge in air in a wide discharge tube. The experiments were carried out with in pressure range of air $p = 10^{-2}$ - 10 Torr and with in the range of constant voltage on the electrodes $U_{dc} < 10^3$ V and discharge currents $I_{dc} < 100$ mA. Distance between the cathode and anode was equal to L = 33 mm. The diameters of discharge tube and anode were equal to 100 mm. Figure shows the anode voltage drop, measured by us, on the anode layer U_a . At low pressure with growth of U_{dc} the anode voltage drop U_a at first slightly decreases, reaches a minimum and then weakly increases. Thus the value of anode voltage drop is $U_a \le 2 - 3 \text{ V}$. With growth of air pressure the anode voltage drop increases (with the fixed value of voltage U_{dc}). With occurrence of an anode glow the anode voltage drop sharply grows, at that $U_a \sim 10$ V. With increase of voltage U_{dc} the anode voltage drop decreases; at U_{dc} , when the boundary of a negative glow reaches an anode layer boundary, the anode glow disappears, U_a sharply decreases up to value $U_a \sim 3$ - 5 V and with the further growth of U_{dc} the anode voltage drop remains practically constant. With increase of air pressure the boundary of a negative glow reaches an anode layer at higher voltage U_{dc} , and the reduction of U_a with disappearance of an anode glow has almost a step behavior.

Figure.

Dependence of anode voltage drop on value of a voltage on electrodes with 33 mm and air pressures: 1 - 0.05 Torr, 2 -0.2 Torr, 3 - 0.4 Torr, 4 - 0.5 Torr, 5 - 0.6 Torr, 6 - 0.7 Torr, 7 - 0.8 Torr, 8 - 1 Torr.



A Polyphase Low Frequency RF Power for a one Atmosphere Uniform Glow Discharge Plasma (OAUGDP)

Faut Karakaya, Daniel M. Sherman and J. Reece Roth, University of Tennessee, Knoxville, TN 37996-2100, USA

A POLYPHASE LOW FREQUENCY RF POWER SUPPLY FOR A ONE ATMOSPHERE UNIFORM GLOW DISCHARGE PLASMA (OAUGDP)

Fuat Karakaya, Daniel M. Sherman, and J. Reece Roth

UTK Plasma Sciences Laboratory Department of Electrical Engineering The University of Tennessee Knoxville, TN 37996-2100

ABSTRACT

A flexible, reliable, and robust RF power supply capable of delivering the frequency and voltage required to energize the One Atmosphere Uniform Glow Discharge Plasma OAUGDP is needed, but off-the-shelf availability of such a RF power supply is quite limited. Using one or more insulated electrodes, the critical parameters required to generate the OAUGD plasma were identified as the gap distance between electrodes, the RF driving frequency, and the rms. voltage. [1] For basic research, the desired frequency range ranges between 0.6 kHz to 10 kHz and the output rms. voltage between 2.2kV to 20 kV. For wide a range of applications, a minimum of 1.5 kW of power with impedance matching[2] is required, whereas 4 kW to 6 kW is necessary for the generation of the OAUGDP without impedance matching or to create the OAUGD plasma in large volumes. These parameter ranges are suitable for research and prototype development of a variety of industrial applications, including surface cleaning and modification, applications, including surface cleaning microbiological sterilization, chemical decontamination, aerodynamic flow control, and plasma deposition.

A RF power supply designed to generate the OAUGDP is composed of a frequency generator, amplifiers, and a transformer. If the power supply is built from several smaller subunits (amplifier and transformer) that combine to supply the RF electrical power rather than just one larger unit, a component failure only implies a partial loss in power, rather than a complete shutdown. By properly choosing the components of the RF power supply, the additional capability to generate a polyphase voltage output and electric field gradients across an array of electrodes is also gained. Our previous OAUGDP aerodynamic research^[3] explored only the aerodynamic effects created by the generation of the OAUGD plasma. However another method of OAUGDP plasma formation - polyphase peristaltic acceleration - uses the electric field gradient generated by this RF power supply. [4]

- *Supported in part by a DoD-AFOSR STTR subcontract from Environmental Elements Corporation of Baltimore, MD and a Research Agreement with March Instruments, Inc. of Concord, CA
- Roth, J. R. (1995): Industrial <u>Plasma Engineering: Volume 1 Principles.</u> Institute of Physics Press, Bristol, UK ISBN 0-7503-0318-2. See Section 12.5.2. Impedance matching an OAUGDP RF power supply will be covered in another poster paper by X. Chen et al.
- by J. Chen et al.

 Roth J R., Sherman D. M., Wilkinson S. P., (1998): "Boundary Layer Flow Control with a One Atmosphere Uniform Glow Discharge Surface Plasma", AIAA Paper 98-0328, 36th AIAA Aerospace Sciences Meeting and Exhibit, Reno NV, January 13, 1998.

 Roth, J. R. (1997): "Method and Apparatus for Covering Bodies with a Uniform Glow Discharge Plasma and Applications Thereof", U.S. Patent #5,669,583, Issued September 23, 1007

De Anza Ballroom 1:30 PM, Tuesday, June 22, 1999

Plenary Talk

Special Panel Plenary Session

Communicating With Nonscientists and the Media

Chairperson
Gerry Rogoff
The Coalition for Plasma Science

Moderator
Rick Borchelt
Lecturer in Technology Policy and Communication
Vanderbilt University

This session will provide an unusual opportunity to hear from and question representatives of various media who deal regularly with communicating science to nonscientists. This should be a valuable learning opportunity for plasma researchers who must communicate the importance of their ongoing and proposed work to funding agency representatives, government policy-makers, the general public, and younger students who may be potential graduate students. Brief presentations by the panelists will be followed by an audience/panel discussion period. The scheduled panelists include:

Greg Lefevre, San Francisco Bureau Chief, CNN; Gregory Favre, Vice President, News, of the newspaper company The McClatchy Company and former Executive Editor of The Sacramento Bee; and Charles Petit, Science Writer, U.S. News & World Report.

Sponsored by The Coalition for Plasma Science

De Anza Ballroom 1:30 PM, Tuesday, June 22, 1999

Oral Session 4A
Intense Electron and Ion Beams

Chairperson

Bryan Oliver

Mission Research Corporation

4A01-2

Invited -

Intense Beam-Target Interactions in Linear Induction Accelerator Radiography Systems

G.J. Caporaso, Y.J Chen, T. Houck and S. Sampayan, T. Hughes, B. Oliver and D. Welch, C. Christ, Lawrence Livermore National Laboratory, Livermore, CA 94551, USA

Intense Beam-Target Interactions in Linear Induction Accelerator Radiography Systems

G. J. Caporaso, Y.-J. Chen, T. Houck and S. Sampayan Lawrence Livermore National Laboratory

> T. Hughes, B. Oliver and D. Welch Mission Research Corporation

> > C. Christ Sandia National Laboratory

Abstract

Modern flash x-ray systems employing electron linear induction accelerators require focal spot sizes of order 1 mm diameter incident on high-Z Bremsstrahlung targets. Typical beam parameters are in the range of several kiloamperes, tens of MeV with pulse lengths of order 50 ns. A single pulse with these parameters is so intense that it converts the target material into a hot plasma with velocities on the order of several centimeters per microsecond. Intense axial electric fields will exist on the target surface which may lead to the extraction of light contaminant ions. These ions can travel upstream where they will act as an electrostatic lens which can cause a time varying disruption of the focal spot. Experimental and theoretical work on this backstreaming ion mechanism will be presented along with issues for multiple pulse operation.

Plasma Suppression and Spot Size Stabilization in Single and Multiple Pulse Flash X-ray Radiography

Thomas J.T. Kwan and Charles M. Snell, Los Alamos National Laboratory, Los Alamos, NM 87544, USA

Plasma Suppression and Spot Size Stabilization in Single and Multiple Pulse Flash X-ray Radiography

> Thomas J. T. Kwan and Charles M. Snell Los Alamos National Laboratory Los Alamos, NM USA 87545

Next generation x-ray radiography machines must use high electron beam current to provide the necessary dose and very small spot size to achieve the desired optical resolution. However, this combination of high current in a small area leads to undesirable side effects that were not important in old machines. Specifically, the intense local energy deposition from the high intensity electron beam causes vaporization of the bremsstrahlung target. The hot plasma thus generated provides a copious source of positive ions that are rapidly accelerated into the negative potential well of the incoming electron beam. As the ions propagate upstream, they partially charge neutralize the electron beam, causing its spot size to increase.[1,2] We have studied the electron beam spot stabilization for the Dual Axis Radiographic Hydrotest Facility (DARHT). In 1997 the concept of an electrically self-biased target was developed to limit the length of the charge neutralizing ion column through the use of the electron beam to charge the target negatively.[3] Shortly thereafter, a target chamber based on the self-biased target concept was designed and fielded on the Los Alamos Integrated Test Stand for DARHT. The experiments clearly confirmed the validity of the theoretical concept and the utility of the design to achieve a stable radiographic spot throughout the electron beam pulse.[4] The negatively charged target creates a bias potential large enough to trap the ions in a small spatial region near the target, resulting in a stable radiographic spot. The self-bias target has obvious application for single pulse radiography. However, for multiple pulses, one has to contain the plasma plume evolving from the target. This can be best achieved through the use of a mechanical barrier constructed of low atomic weight, high temperature material, such as beryllium, special alloys, or carbides. This thin barrier is placed about 1-cm upstream from the converter target and allows the electron beam to pass through with minimal scattering and energy degradation. The plasma plume is confined between the target and the barrier. Computer simulation has shown stability of the electron beam spot throughout the pulse. The plasma plume expansion is spatially confined by this design to retain stable spot size for subsequent pulses. Detailed simulation results with experimental validation will be presented.

- (1) Thomas J. T. Kwan, John C. Goldstein, and Barbara G. DeVolder, "Influence of Ions on Electron Beam Spot Xize in ITS/DARHT," Los Alamos National Laboratory Research Note, XPA-RN(U)97-021 (June 1997).
- (2) Dale R. Welch and Thomas P. Hughes, "Effect of Target-Emitted Ions on the Focal Spot of an Intense Electron Beam," Laser and Particle Beams, Vol. 16, no. 2, pp.285-294, 1998.
- (3) T. J. T. Kwan and C. M. Snell, "Stabilization of Radiographic Spot Size via Self-Biasing Targets," Los Alamos National Laboratory Research Note, XPA-RN(U)97-048 (November 1997).
- (4) Thomas J. T. Kwan, "Electron Beam-Target Interaction in X-Ray Radiography," Los Alamos National Laboratory Report LA-UR-98-4802, 1998, submitted to the Physics of Plasmas.

4A04

The TriMeV Accelerator for Pulsed Power Driven Radiography Experiments

E.Hunt, G. MacLeod, L.Woo, D. Droemer, S. Cordova, J. Gustwiller, D. Johnson, J. Maenchen, P.Menge, I. Molina, C. Olson, S. Rosenthal and D. Rovang, B.Oliver and D. Welch, C. Eichenberger, P.Spence, I Smith and V. Bailey, Bechtel Nevada, DOE, Las Vegas, NV 89193, USA

The TriMeV Accelerator for Pulsed Power Driven Radiography Experiments*

E. Hunt, G. MacLeod, L. Woo, D. Droemer, Bechtel Nevada, Las Vegas, NV 89193

S. Cordova, J. Gustwiller, D. Johnson, J. Maenchen, P. Menge, I. Molina, C. Olson, S. Rosenthal, and D. Rovang Sandia National Laboratories, Albuquerque, NM 87185

B. Oliver and D. Welch Mission Research Corporation, Albuquerque, NM 87106

C. Eichenberger, P. Spence, I. Smith, and V. Bailey Pulsed Sciences Incorporated, San Leandro, CA, 94577

TriMeV is a compact 3 MeV, 30 kA electron beam accelerator driving an x-ray radiographic source. It was previously operated by French researchers and has recently been purchased by Bechtel Nevada for experiments in Las Vegas. In normal operating mode the accelerator emits an e-beam from a flat cathode which focuses in a ~ 10 Torr Nitrogen gas cell onto a flat bremsstrahlung target.

The extremely fast \sim 3ns rise-time of the TriMeV voltage pulse is ideal for studying beam transport issues. A series of radiographic source optimization experiments planned in collaboration with Sandia National Laboratories will investigate different diode configurations to reduce the radiographic spot size. Both ballistic propagation and nonneutralized transport, where the self-fields pinch the beam, will be studied. A magnetically-immersed diode, where a mm-diameter electron beam is launched from a needle cathode and confined in a \sim 12 T solenoidal magnetic field during acceleration to the target in vacuum, will also be studied. This immersed diode previously demonstrated < 2-mm spots on the Hermes III accelerator. It is anticipated that similar results will be attained on TriMeV.

A review of the operating parameters, geometry, and electrical characteristics will be presented along with an outline of the experimental program and a description of the diode and transport configurations studied. The most recent shot data will also be presented with an emphasis on the results from the immersed diode experiments.

^{*}Supported by Sandia Labs. Sandia is a multiprogram laboratory operated by Sandia Corporation, a Lockheed Martin Company, for the United States Department of Energy under Contract DE-ACO4-94AL85000

Optimization of Radiographic Spot for the TriMeV Accelerator

D.R. Welch, B.V. Oliver, S.E. Rosenthal and C.L. Olson, Mission Research Corporation, Albuquerque, NM 87106, USA

Optimization of Radiographic Spot for the TriMeV Accelerator*

D. R. Welch, B. V. Oliver Mission Research Corporation, Albuquerque, NM 87106 S. E. Rosenthal and C. L Olson Sandia National Laboratory, Albuquerque, NM 87185

We are examining diode configurations for the 3-MeV, 30-kA TriMeV electron-beam accelerator at Bechtel Nevada. These include a flat-cathode diode with focusing into a gas cell¹ and a magnetically-immersed diode similar to that used on HERMES III at Sandia National Laboratories. We are in the process of optimizing the diode designs using the hybrid kinetic-fluid simulation code IPROP² which models both vacuum flow and gas breakdown. These configurations will be fielded on TriMeV this year.

The TriMeV voltage pulse is somewhat unique in that it has a 3-ns rise and fall time with a 14-ns flat top. This sharp rise and fall in voltage make it ideal for studying beam focusing. The flat-cathode diode uses a 3.5-cm radius velvet electron emitter and a 4-cm anode-cathode gap that has produced a 23 kA beam self-focused in vacuum into a gas cell of 2.8-cm radius. The time-integrated beam spot has been optimized experimentally with 10 Torr nitrogen in the ballistic focusing regime where self fields are minimal. Net currents < 5 kA were measured at the gas cell wall for 5-15 Torr nitrogen.1 Below 2 Torr, the net current increases rapidly to the full beam current. IPROP has simulated this behavior in reasonable agreement with experiment. The code predicts that, due to finite plasma current decay, the time-integrated spot is increased as the beam focus moves upstream of the target. If the diode voltage is sufficiently stable, IPROP predicts a rootmean-square (RMS) radius < 2 mm in the runaway regime

In an immersed TriMeV diode, a 10–15 kA electron beam is emitted from a sub-millimeter needle cathode into a strong 12–18 Tesla solenoidal field. The remaining current is lost to the outer wall. The large fields are necessary to limit growth of the magnetized ion-hose instability. With careful design of the cathode structure, we can minimize the current flowing into the diode from large radius. IPROP calculates an RMS radius < 1 mm. With close collaboration of theory and experiment, we hope to reduce of the beam spot size and better understand the impedance behavior of these diodes.

*Work supported by Sandia National Laboratories.

- J. P. Lidestri, et al., IEEE Trans. On Plasma Science, 19, 855-859, 1991.
- D. R. Welch, C. L. Olson, and T. W. L. Sanford, Phys. Plasmas 1, 764-773, 1994.

4A06

Particle In Cell Simulations of High Power Electron Beam Diodes

S.B. Swanekamp, R.J. Commisso, G. Cooperstein, P.F. Ottinger and J.W. Schumer U.S. Naval Research Laboratory, Washington, DC 20375, USA

Particle-In-Cell Simulations of High-Power Electron Beam Diodes*

S.B. Swanekamp^a), R.J. Commisso. G. Cooperstein, P.F. Ottinger, and J.W. Schumer^b) Plasma Physics Division, Naval Research Laboratory Washington, DC 20375

High-power electron beams have a wide variety of applications including electron beam welding, electron-beam-pumped KrF lasers, and the production of bremsstrahlung radiation for radiography and weapons effects studies. One of the present research areas of high-power electron beam diodes is to develop an intense radiographic source with a sub-millimeter-diameter spot size with an endpoint energy of a few hundred keV. At the heart of this technology is the electron-beam diode where electrons are accelerated by strong diode electric and magnetic fields.

If the discharge current is small compared to the critical current, then the electron flow is space-charge-limited (SCL) and the current increases as V^{3/2}. If the discharge current is large compared to the critical current, then the electron flow is magnetically limited and the current increases as $(V^2+V)^{1/2}$. When the discharge current is comparable to the critical current there is currently no analytic formula that accurately predicts the I-V characteristic. We have used particle-in-cell (PIC) simulations to develop a universal curve that accurately predicts the I-V characteristic over a wide range of voltages and diode geometries. This universal curve is parameterized by the voltage, V[†], at which the SCL current is equal to the critical current and contains all the information about geometry and whether or not ions are present. For voltages much larger and much smaller than V[†], the simulations show that the electron flow is stable. However, for weakly pinched beams that have voltages close to V[†] the simulations show that an interaction between the space-charge and the self-magnetic field causes the electron flow to be unstable.

To make an intense x-ray radiographic source with a sub-millimeter-diameter spot size, it is desirable to operate in a pinched-beam mode. To do this, it is necessary for the diode to draw enough current at, or below, the desired endpoint voltage so that the beam will be strongly pinched (i.e. V>>V[†]). Since the SCL current is a strong function of the diode geometry and the critical current is a very weak function of the diode geometry, choosing the appropriate diode geometry is an ideal way to achieve this goal. Some preliminary designs that theoretically achieve this goal and available experimental data will be presented.

*Work supported by DOE through SNL and LANL.

^{a)}JAYCOR, McLean, VA 22012.

^bNational Research Council Research Associate at NRL.

4A07-8

Invited - Self-Pinched Transport of Intense Ion Beams

P.F. Ottinger, J.M. Neri, S.J. Stephanakis, D.V. Rose, F.C. Young, B.V. Weber, M. Myers, D.D. Hinshelwood and D. Mosher, D.R. Welch and C.L. Olson, U.S. Naval Research Laboratory, Washington, DC 20375,

Self-Pinched Transport of Intense Ion Beams*

P.F. Ottinger, J.M. Neri, S.J. Stephanakis, D.V. Rose¹, F.C. Young¹, B.V. Weber, M. Myers, D.D. Hinshelwood, and D. Mosher

Plasma Physics Division, Naval Research Laboratory Washington, DC 20375

D.R. Welch

Mission Research Corporation, Albuquerque, NM 87106

C.L. Olson

Sandia National Laboratory, Albuquerque, NM 87185

Electron beams with substantial net currents have been routinely propagated in the self-pinched mode for the past two decades. However, as the physics of gas breakdown and beam neutralization is different for ion beams, previous predictions indicated insufficient net current for pinching so that ion beam selfpinched transport (SPT) was assumed impossible. Nevertheless, recent numerical simulations using the IPROP code have suggested that ion SPT is possible. These results have prompted initial experiments to investigate SPT of ion beams. A 100-kA, 1.2-MeV. 3-cm-radius proton beam, generated on the Gamble II pulsed-power accelerator at NRL, has been injected into helium in the 30- to 250-mTorr regime to study this phenomenon. Evidence of self-pinched ion beam transport was observed in the 35- to 80-mTorr SPT pressure window predicted by IPROP. Measured signals from a time- and space-resolved scattered proton diagnostic and a time-integrated Li(Cu) nuclear activation diagnostic, both of which measure protons striking a 10-cm diameter target 50 cm into the transport region, are significantly larger in this pressure window than expected for ballistic transport. These results are consistent with significant self-magnetic fields and self-pinching of the ion beam. On the other hand, time-integrated signals from these same two diagnostics are consistent with ballistic transport at pressures above and below the SPT window. Interferometric electron line-density measurements, acquired during beam injection into the helium gas, show insignificant ionization below 35 mTorr, a rapidly rising ionization fraction with pressure in the SPT window, and a plateau in ionization fraction at about 2% for pressures above 80 mTorr. These and other results are consistent with the physical picture for SPT. IPROP simulations, which closely model the Gamble II experimental conditions, produce results that are in qualitative agreement with the experimental results. advantages of SPT for beam transport in the reactor chamber of a heavy-ion-driven inertial-confinement-fusion energy system will also be discussed.

4A09

Simulation and Modeling of the Gamble II Self-Pinched Ion Beam Transport Experiment

D.V. Rose, P.F. Ottinger, D.D. Hinshelwood, D. Mosher, M.C. Myers, J.M. Neri, S.J. Stephanakis, B.V. Weber and F.C. Young, D.R. Welch, U.S. Naval Research Laboratory, Washington, DC 20375, USA

Simulation and Modeling of the Gamble II Self-Pinched Ion Beam Transport Experiment

D. V. Rose[†], P. F. Ottinger, D. D. Hinshelwood, D. Mosher, M. C. Myers, J. M. Neri, S. J. Stephanakis, B. V. Weber, and F. C. Young[†] Plasma Physics Division, Naval Research Laboratory Washington, DC 20375

D. R. Welch

Mission Research Corporation, Albuquerque, NM 87106

Progress in numerical simulations and modeling of the self-pinched ion beam transport experiment at the Naval Research Laboratory (NRL) is reviewed. In the experiment, a 1.2-MeV, 100-kA proton beam enters a 1-m long, transport region filled with a low pressure gas (30 -250 mTorr helium, or 1 Torr air). The time-dependent velocity distribution function of the injected ion beam is determined from an orbit code that uses a pinch-reflex ion diode model and the measured voltage and current from this diode on the Gamble II generator at NRL. This distribution function is used as the beam input condition for numerical simulations carried out using the hybrid particlein-cell code IPROP. Results of the simulations will be described, and detailed comparisons will be made with various measurements, including line-integrated electrondensity, proton-fluence, and beam radial-profile measurements. As observed in the experiment, the simulations show evidence of self-pinching for helium pressures between 35 and 80 mTorr. Simulations and measurements in 1 Torr air show ballistic transport. The relevance of these results to ion-driven inertial confinement fusion will be discussed.

*Work supported by US DOE. *Jaycor, McLean, VA 22102.

^{*} Work supported by US DOE.

¹ JAYCOR, McLean, VA 22102.

Direct Measurement of Electrons Co-Moving in Vacuum with a 100-kA, MeV-Proton Beam B.V. Weber, D. D. Hinshelwood, J. M Neri, P.F. Ottinger, D.V. Rose, S. J. Stephanakis and F.C. Young, U.S. Naval Research Laboratory, Washington, DC 20375, USA

Direct Measurement of Electrons Co-Moving in Vacuum with a 100-kA, MeV-Proton Beam*

B. V. Weber, D. D. Hinshelwood, J. M. Neri, P. F. Ottinger, D. V. Rose, S. J. Stephanakis, and F. C. Young

Plasma Physics Division, Naval Research Laboratory Washington, DC 20375

Propagation of intense ion beams in vacuum can be shown to be physically impossible without a significant degree of charge- and current-neutralization from comoving electrons. High-sensitivity laser interferometry was used to measure the electron density co-moving in vacuum with an intense proton beam (100 kA, 1 MeV, 50 ns) from the Gamble II generator. This measurement is nonperturbing and sufficiently quantitative to allow benchmarking of codes (particularly IPROP) used to model beam-gas interaction and ion-beam transport. Very high phase sensitivity is required for this measurement. For example, a 100-kA, 1-MeV, 10-cm-radius proton beam with uniform current density has a line-integrated proton density equal to $n_p L = 3 \times 10^{13}$ cm⁻². An equal electron line-density, $n_e L = n_p L$, (expected for transport in vacuum) will be detected as a phase shift of the 1.064 µm laser beam of only 0.05° , or an optical path change of 1.4×10^{-4} waves (about the size of a hydrogen atom!). The line-integrated electron density, measured across a diameter of the transport chamber at 43 cm from the input aperture, has the same time dependence and magnitude as the proton density ($n_eL \sim$ n_pL), where n_pL is estimated from ion beam diagnostics. The measurements will be compared with theoretical predictions from the IPROP code.

4B

De Anza II 10 AM, Tuesday, June 22, 1999

Oral Session 4B Fast Wave Devices

Chairperson

David McDermott

University of California, Davis

^{*} Work supported by US DOE.

<sup>Jaycor, McLean, VA 22102.
1. B. V. Weber and S. F. Fulghum, Rev. Sci. Instrum. 68, 1227 (1997).</sup>

4B01-2

Invited -

Demonstration of a High Power W-Band Gyroklystron Amplifier for Radar Applications

M. Blank, B.G. Danly, B. Levush, J.P. Calame, K.T. Nguyen, D.E. Pershing, J. Petillo, T.A. Hargreaves, R.B. True, A.J. Theiss, G.R. Good, K. Felch, B. James P. Borchard, T.S. Chu, H. Jory, W. Lawson and T.M. Antonsen Jr., U.S. Naval Research Laboratory, Code 6843, Washington, DC 20375, USA

Demonstration of a High Power W-Band Gyroklystron Amplifier for Radar Applications*

M. Blank, B.G. Danly, B. Levush, J.P. Calame, K.T. Nguyen¹, D.E. Pershing², J. Petillo³
Naval Research Laboratory, Washington, D.C. 20375

T.A. Hargreaves, R.B. True, A.J. Theiss, G.R. Good Litton Electron Devices Division, San Carlos, CA 94070

K. Felch, B. James, P. Borchard, T.S. Chu, H. Jory Communications and Power Industries, Palo Alto, CA 94304

W. Lawson and T.M. Antonsen, Jr. University of Maryland, College Park, MD 20742

There is currently a need for high-power, W-band amplifiers for millimeter wave radars. In response to this need, a four cavity, 94 GHz gyroklystron amplifier has been designed and constructed in a collaborative effort between the Naval Research Laboratory, Litton Electron Devices, Communications and Power Industries, and the University of Maryland. The amplifier was designed to produce 80 kW peak output power and 10 kW average output power at 20% efficiency with a bandwidth in excess of 600 MHz.

The amplifier was constructed and low duty tests are underway. The gyroklystron has produced peak output powers up to 115 kW and 29% efficiency with -3 dB bandwidths exceeding 600 MHz. Experimental parametric studies and the results of upcoming high duty tests will be presented.

*This work was supported by the Office of Naval Research. The computational work was supported in part by a grant of HPC time from the DoD HPC Centers NAVO and ARL.

- 1. K-N Research, Silver Spring, MD 20906
- 2. Mission Research Corp., Newington, VA 22122
- 3. Science Applications International Corp., Burlington, MA

4B03

Decoherence in a Chirped-Pulsed Free-Electron Maser

F.V. Hartemann, E.C. Landahl. A.L. Troha, J.P. Heritage, H.A. Baldis and N.C. Luhmann Jr., LLNL-Institute for Laser Science & Applications, Livermore, CA 94550, USA

Decoherence in a Chirped-Pulse Free-Electron Maser

F.V. Hartemann, E.C. Landahl, A.L. Troha, J.P. Heritage, H.A. Baldis, and N.C. Luhmann, Jr. Institute for Laser Science and Applications, LLNL Department of Applied Science, UC Davis

Theoretical studies [1-3] have shown that the relativistic subpicosecond electron bunches produced by highbrightness of photoinjectors can be used to generate coherent synchrotron radiation in a free-electron maser (FEM). Furthermore, in a waveguide structure, the group velocity of the radiation can be matched to the axial bunch velocity in the helical wiggler, thus minimizing slippage in the device and yielding extremely short pulse of coherent millimeter-wave radiation, with instantaneous bandwidths exceeding 50%. Because of group velocity dispersion, the output pulses are chirped. The transition from coherent to incoherent synchrotron radiation in the FEM has first been studied within the context of a relativistic fluid model [2-3]; we will discuss the limitations of such a model, and propose a new hybrid model capable of describing the electron bunch behavior both in the electron fluid and stochastic gas limits. In particular, there is a continuous transition from the exponential coherence factor of the fluid model, $N_e^2 \exp \left[- \left(\frac{\omega \Delta z}{2\beta_{H}c} \right)^2 \right]$, to the incoherent radiation scaling, N_{θ} . Here, N_{θ} is the number of electrons in the bunch, ω is the Doppler-shifted radiation frequency, Δz is the bunch duration, and $\beta_{\prime\prime}$ is its axial velocity. This will be discussed both in the context of fast-wave FEMs, and for short wavelength, laser-driven Compton sources.

- [1] A. Gover et al., Phys. Rev. Lett. 72, 1192 (1994).
- [2] F.V. Hartemann, et al., Phys. Plasmas 1, 1306 (1994).
- [3] F.V. Hartemann, et al., Phys. Plasmas 3, 2446 (1996).

This work was partially supported under the auspices of the US DoE by LLNL under contract No. W-7405-ENG-48 through ILSA, and by DoD/AFOSR (MURI) F49620-95-1-0253, AFOSR (ATRI) F30602-94-2-001, and ARO DAAHO4-95-1-0336.

4B04

Development of a Mutliple Stage Depressed Collector System for 2 MW

CW Gyrotrons, Lawrence Ives, Max Mizuhara, Jeff Nielson, Richard Schumacher, Amarjit Singh, Victor Granatstein, Calabazas Creek Research Inst., Saratoga, CA 95070-3753, USA

Development of a Multiple Stage Depressed Collector System for 2 MW CW Gyrotrons

by
Lawrence Ives, Max Mizuhara,
Jeff Neilson, Richard Schumacher
Calabazas Creek Research, Inc.

&

Amarjit Singh, Victor Granatstein Institute for Plasma Research, University of Maryland

Calabazas Creek Research, Inc. is developing a multiple stage depressed collector system that includes the depressed collector, power supplies, and computer control system for 2 MW CW gyrotrons. The goal of the program, funded by the Department of Energy's Small Business Innovation Research program, is to develop a single system that will be applicable to all Gaussian mode gyrotrons operating between 100 GHz and 170 GHz. The Phase II program is funded, and the design is being finalized using a variety of simulation and analysis codes.

Previous research showed that secondary and reflected electrons can significantly impact depressed collector performance. Current research is focused on understanding this issue and developing techniques to minimize the impact on collector efficiency. Recent experiments in Germany indicated that location of the body - collector gap can significantly impact the effect of secondary electrons. Simulations are in progress to study this effect by varying the location of the collector-body gap and modeling the trajectories of secondary and backscattered electron.

The program is also examining techniques for minimizing the generation of reflected and secondary electrons. Research at NASA/Lewis demonstrated that ion texturing can dramatically reduce these electrons by trapping them within the textured surface. A system is being designed to facilitate texturing of the large components of the proposed collector.

Work is also in progress to develop the optimization software to control gyrotron operation and maximize efficiency under all operating conditions. The software will be integrated into a finite element particle simulation code for testing. Once developed, the technique will be used to control the gyrotron power supplies during actual operation.

This presentation will describe these efforts and present thermomechanical analysis results for 2 MW CW operation. The schedule for parts acquisition, construction, and testing will also be presented.

- 1. Bernhard Piosczyk, private communication, September 1998.
- 2. NASA Tech Briefs, pp 86-88, November 1995.

4B05

Design of a Single-Stage, Depressed Collector for a 1 MW

CW Gyrotron, G.P. Saraph, K. Felch, S. Cauffman, T.S. Chu and H. Jory, Communications Power Industries, Palo Alto, CA 94304, USA

Design of a Single-Stage, Depressed Collector for a 1 MW, CW Gyrotron

G. P. Saraph, K. Felch, S. Cauffman, T. S. Chu and H. Jory Communications Power Industries (CPI) Palo Alto, CA 94304

1 MW, CW millimeter-wave gyrotron oscillators are being developed for electron cyclotron resonance heating (ECRH) of plasma in fusion experiments. These gyrotrons have to operate at very high order operating modes due to high frequencies and high power levels. The electron beam in such a gyrotron is very thin compared to the beam radius and carries about 2.5-3.0 MW of DC beam power. The tight helical trajectories of the electrons have to be unwound and spread out in the collector region to get peak power density on the collector wall below 1000 W/cm². High power density in the incoming electron beam makes it a challenging task to design a collector under such operating conditions.

With a single-stage, depressed collector the overall efficiency of the gyrotron is increased and power deposited by the beam on collector walls is lowered. We have analyzed different operating schemes for a single-stage depressed collector for a 1 MW, CW gyrotron. Iron shield and collector coils are used to steer the electron trajectories in the collector region. However, a fixed magnetic field configuration requires a rather large collector size since the trajectories are not well spread out. We have also analyzed varying the current through collector coils to sweep the beam on the collector surface. In this scheme the time-averaged power density has a more uniform distribution over the collector surface. The electron beam sweeping can be done using an axial or transverse magnetic coil making it a 2-D or a 3-D magnetic problem. Results from the 2-D and 3-D simulations will be presented along with the final depressed collector design.

4B06

Stimulated Electromagnetic Interactions in Spatio-temporally Gyrating Relativistic Electron Beams

John A. Davies and Chiping Chen, Clark University, Worcester, MA 01610, USA

Stimulated Electromagentic Interactions in
Spatiotemporally Gyrating Relativistic Electron Beams
John A. Davies and Chiping Chen
Plasma Science and Fusion Center
Massachusetts Institute of Technology

One possible method to significantly widen the bandwidths of present gyroklystron amplifiers is to utilize extended interaction structures in the input sections, the buncher sections and the output sections, in conjunction with stagger tuning. Through extended interactions, however, electron beams can undergo stimulated electromagnetic interactions, causing multimode excitations. In this paper, we investigate stimulated electromagnetic interactions in relativistic electron beams gyrating in an externally applied uniform magnetic field. The electron gyrophases are assumed to have strong spatiotemporal correlations. By applying Vlasov-Maxwell equations together with Lorentz transformations, we obtain the general dispersion relation for electromagnetic and electrostatic wave perturbations on the electron beam for this system. The dispersion relation is used to analyze a variety of stimulated electromagnetic interactions on such electron beams. Results of these analyses are discussed. This work was supported by AFOSR.

4B07

Intrinsic Noise Measurements in Gyroklystrons

J.P. Calame, B.G. Danly and M. Garven, U.S. Naval Research Laboratory, Code 6843, Washington, DC 20375, USA

Intrinsic Noise Measurements in Gyroklystrons*

J.P. Calame, B.G. Danly, and M. Garven[†]
Naval Research Laboratory
Washington, DC 20375

Measurements of intrinsic shot noise in a 35 GHz, threecavity gyroklystron have been obtained over a wide range of operating parameters. The noise emissions from both the input and output cavities were measured under carrier-free (zerodrive power) conditions. The spectrum of noise emitted by the input cavity is found to have a Lorentzian shape, with the peak frequency and spectral width in good agreement with the beam loaded frequency and Q predicted by simulation codes. At the nominal operating parameters of the gyroklystron, which were 70 kV, 10A, $\alpha = 1.27$, and a magnetic field of 13.07 kG, we find the peak temperature of the input cavity noise to be 4.4×10^8 K (6.3×10⁻¹⁵ W/Hz), with a FWHM of 160 MHz. The peak noise temperature was found to exhibit complex variations with respect to beam current, beam velocity ratio, and magnetic field. Detailed data sets which illustrate these trends will be presented. Compared to theoretical predictions of bare shot noise in gyroklystrons [1], the experimental noise levels are 0 to 5 dB lower than theory, with the greatest reductions appearing at high currents. We also do not observe any evidence for excess noise generation from electrostatic cyclotron instabilities. The output cavity noise spectrum is found to be essentially equal to the product of the linear gyroklystron frequency response with the input cavity noise spectrum. This allows a noise-to-carrier ratio to be estimated based on the measured input cavity noise levels and the typical 200 W of drive power applied to the input cavity during nonlinear amplifier operation. Noise-to-carrier ratios are found to be in the range of -90 to -80 dBc, with noise-density-tocarrier ratios of -175 to -165 dBc/Hz. These values reflect only the contribution from shot noise, since lower frequency noise sources such as flicker noise that will be multiplied up into Ka-band by the carrier are not accounted for. Systematic studies of the noise-to-carrier ratio indicate that it is a strong function of magnetic field and operating voltage. Results of these parametric studies will be presented, and the impact of noise-to-carrier considerations on higher gain, four-cavity gyroklystron operation will be discussed. Ongoing work involving directly measuring the intrinsic phase noise in the presence of a full power carrier will be described.

- * Work supported by the Office of Naval Research
- [†] University of Maryland, College Park, MD 20742
- [1] T.M. Antonsen, Jr. and W.M. Manheimer, IEEE Trans. Plasma Sci 26, 444 (1998).

4B08

Experimental Study of Intrinsic and Technical Phase Noise in a Second Harmonic Gyrotron Amplifier (Phigtron)

J. Rodgers, H. Guo, G.S. Nusinovich and V.L. Granatstein, University of Maryland, College Park, MD 20742-3511, USA

Experimental Study of Intrinsic and Technical Phase Noise in a Second Harmonic Gyrotron Amplifier (Phigtron)

J. Rodgers, H. Guo, G. S. Nusinovich and V. L. Granatstein Institute for Plasma Research, University of Maryland College Park, MD 20742

The phigtron is a millimeter wave, frequency-doubling amplifier that has been demonstrated to produce 360 kW peak power with frequency centered at 33.7 GHz, a bandwidth of 0.6%, saturated gain of 30 dB and electronic efficiency of greater than 35%. The input signal, injected into a Ku-band fundamental gyro-TWT input section, modulated a 60 kV, 25 A electron beam produced by a MIG-type gun. After transit through a drift section, prebunching in the electron beam excited the TE03 mode at twice the input frequency in an output cavity with a measured total quality factor of ~600. A substantial range of magnetic field profiles was surveyed using a computer-controlled system in order to optimize operating parameters with respect to output power, bandwidth and efficiency. A set of operating conditions was established and the phase noise performance was measured for both the saturated (360 kW output power) and linear gain (100 kW output power) cases. The phase noise at 100 Hz from the carrier was observed to be as low as -40 dBc/Hz. Furthermore, a high degree of correlation was established between sources of technical noise (e.g. fluctuations in beam voltage, current and magnetic field) and this value. The intrinsic phase noise was estimated to be at least 10 dB/Hz lower at the same frequency offset.

The significance of distinguishing correlated from uncorrelated sources of noise is that the former comes from sources that can be addressed technically, whereas the latter is related to the intrinsic physical processes in the phigtron.

The phigtron design will be presented along with the experimental results and a comparison of the measured phase noise with a theoretical prediction of both the technical and intrinsic quantities.

This work is supported by the DoD MURI program on high power microwaves under grant F4962001528306.

4CSession 4C
De Anza III

10 AM, Tuesday, June 22, 1999 Spherical Configurations and Ball Lightning

Chairperson

Stanley Singer

Athenex Research Associates

4C01-2

Invited - Ball lightning as a free-force magnetic knot with linked streamers

A.F. Ranada, M. Soler and J.L Trueba, Fisica Universidad Complutense, Madrid 28040, Spain

Ball lightning as a free-force magnetic knot with linked streamers

A.F. Rañada¹, M. Soler² and J.L. Trueba³,

¹ Dept. Física Teórica, Universidad Complutense, 28040

Madrid, Spain; ² Dept. Física Atómica y Nuclear, Universidad

Complutense, 28040 Madrid, Spain; ³ ESCET, Universidad Rey

Juan Carlos, 28933 Móstoles, Spain.

We consider a recently proposed model of ball lightning¹, based on the ideas of magnetic knot (a magnetic field with linked force lines) and free-force magnetic field (a magnetic field such that $\mathbf{B} \times (\nabla \times \mathbf{B}) = 0$). The fireball is assumed to consist in an air ball coupled to a magnetic knot in such a way that the current flow along some streamers, separated from one another and also linked, so that the system is very tangled indeed. It turns out that the linking of the lines, which can be measured by the helicity integral (the integral of the scalar product $\mathbf{A} \cdot \mathbf{B}$), has a stabilizing effect on the system. The streamers are hot, in the range 16,000 K-19,000 K, where the curve of the power density emitted by the plasma has a shoulder in which the emission is approximately constant, this explaining why the ball loses energy by radiation without decreasing its radiance.

Near an ordinary lightning discharge, many streamers are formed in a very rapid process. In some special cases, some streamers short-circuit, and form closed loops which are also linked, so that the helicity is non vanishing. As proved by Chandrasekhar and Woltjer, under general conditions a closed system tends to decay to a force-free field, which represent the final energy state which it can attain, in such a way that the helicity is conserved in the process.

A ball lightning would proceed as follows. Once the magnetic knot is formed near a lightning discharge, a rapid relaxation process would take place following the Taylor mechanism, leading to a force-free configuration, during which the total helicity is conserved. In the MHD approximation, this would lead to a stationary linked solution. However, the system must expand and cool, since it radiates away energy. The stabilizing effect of the helicity conservation (i.e. of the linking) is to impede the expansion along most of the channels (which are not consistent with that conservation), leaving only a slow channel along which the ball expands slowly.

Although we have no analytical solutions for force-free fields with discrete streamers, the analysis of a near solution indicates that the lifetime of a linked ball would be of the order of seconds while the expansion of unlinked balls would be instantaneous. The model explains also why some witnesses are burnt by ball lightnings, while others do not feel warmth.

4C03

James L. Tuck Los Alamos Ball Lightning Pioneer D.A. Baker, Los Alamos National Laboratory, Los Alamos, NM 87544, USA

James L. Tuck Los Alamos Ball Lightning Pioneer*

D.A. Baker

Los Alamos National Laboratory Group P-24, MS E526 Los Alamos, NM 87545

James Tuck was well known for starting the Project Sherwood group at Los Alamos Scientific Laboratory in 1952. This group was formed to study and develop concepts for controlled fusion energy. In his later years after retiring from Controlled Fusion Division, he continued research at Los Alamos on the topic of ball lightning. He traveled widely giving lectures on both observations of others and his own experimental efforts. He collected anecdotal observations obtained from those in his lecture audiences during his travels and from responses from newspaper articles where he asked for specific information from ball lightning observers. He finally cut off this collection of data when the number of responses became overwhelming. Tuck's primary publication on ball lightning was a short laboratory report [1]. He planned on publishing a book on the subject but this was never completed before his death.

Tuck focused his experimental effort on attempting to duplicate the production of plasma balls claimed to be observed in US. Navy submarines when a switch was opened under overload conditions with battery power. During lunch breaks he made use of a Los Alamos N-division battery bank facility to mock up a submarine power pack and switch gear. This non-funded effort was abruptly terminated when an explosion occured in the facility.

An overview of Tuck's research and views will be given. The flavor Jim's personality as well as a ball produced with his experimental apparatus will be shown using video clips.

 * Supported in part by USDOE.
 [1] J.L. Tuck, "Ball Lightning; A Status Summary to November 1971", Los Alamos Scientific Laboratory Report, LA-4847-MS, Issued December 1971.

4C04

Production of Spherical Plasmoid or Ball Lightning by Rocket-Triggered Lightning

Hiroshi Kikuchi,

Nihon University, 1-chome, Chiyaoda-ku Tokyo 101, Japan

Production of Spherical Plasmoid or Ball Lightning by Rocket-Triggered Lightning

Hiroshi Kikuchi

Nihon University, College of Science and Technology 8, Kanda Surugadai, 1-chome, Chiyoda-ku, Tokyo 101, Japan

A possibility of ball lightning formation by rocket-triggered lightning with a trailing inductive coil grounded has been suggested in my paper, 7E05: 'EHD and MHD Models of Fireballs and Their Relevance to Natural and Artificial Ball Lightning for the Oral Session 7E: 4.6 Spherical Configuration/Ball Lightning at the ICOPS 97 [1]. The present paper proceeds in more detail along this line.

One of places capable for energy conversion from electrostatic energy accumulated by thunderclouds to ionization and discharge current energy would be an electric cusp where X-type electric reconnection could occur by any perturbation exerted on it, typically an sharp object. In other words, an electric cusp initially formed plays an important role in energy conversion mentioned above as a result of electric reconnection via an object invading an electric cusp [2]. Based on this principle, it can be stated that a most favorable condition for triggering lightning discharge is to launch a rocket into an electric cusp.

In addition, the idea is to utilize electrostatic energy accumulated in thunderclouds to produce ball lightning by converting it partly to plasma energy for ball lightning and mainly to magnetic energy for plasmoid confinement. To effect this, it is necessary to insert some inductance in a rocket trailing-wire grounded which constitute a circuit with a cloud capacitance parallel to it after a discharge or leader channel will be formed. Then we have three cases in general in terms of a circuit, namely (i) $R^2 > 4L/C$ (logarithmic case); (ii) $R^2 < 4L/C$ (oscillatory case); (iii) $R^2 = 4L/C$ (critical case), where R is the resistance of a trailing wire, L the inductance of the coil inserted, and C is the cloud capacitance.

For example, take a rocket-triggered lightning event with a trailing wire grounded but without coil on December 12, 1981 in Japan [2]. Then, electrostatic energy released by the first stroke is estimated to be $W_E = (1/2)QV = 90$ MJ from cloud charge, $Q \sim 50$ C, cloud voltage, $V \sim 3.6$ MV, and cloud capacitance, $C \sim 13.9$ µF. Let's imagine that the rocket had a trailing wire with an inductive coil grounded, rather than just a straight wire that was the case so far, under critical or oscillatory circuit conditions: $R^2 \le 4L/C$, where $R \sim 1.3$ k Ω . Thus, the required inductance for the coil can be estimated as $L \ge 5.87$ H. Then the angular frequency of free oscillations is written as $\omega = [(1/LC) - (R^2/4L^2)]^{1/2}$. Choose L = 10 H, C = 13.9 µF, and R = 1.3 k Ω for an oscillating case. Then we have f = 8.67 Hz for the frequency of free oscillations.

Further, assume that most of the electrostatic energy estimated above were converted to magnetic energy by the inductive coil loaded within a volume of, say, (5 cm)³, where a fireball or plasmoid could be produced. Then, its magnetic energy density is estimated to be 1.2 MJ/cm³ which may be considered much larger than the plasma energy density of typical lightning balls, say 1 kJ/cm³.

- H. Kikuchi, EHD and MHD Models of Fireballs and Their Relevance to Natural and Artificial Ball Lightning, ICOPS97, IEEE
 Conference Record Abstracts, 7E05, 1997, p.319.
- [2] H. Kikuchi, Electric Reconnection, Critical Velocity, and Triggered Lightning, in *Laboratory and Space Plasmas*, ed. by H. Kikuchi, Springer-Verlag, New York (1989), pp.331-344.

4C05

Electro-Nuclear Reactions in Micro Ball Lighting Takaaki Matsumoto, Hokkaido University, Sapporo 060-0813, Japan

Electro-Nuclear Reactions in Micro Ball Lighting

Takaaki MATSUMOTO Department of Nuclear Engineering Hokkaido University(Sapporo 060-0813, JAPAN)

Abstract

The artificial generation of micro Ball Lightning(BL) during underwater spark discharges(USD) will be presented. An atomic cluster in a special state was generated, called an "itonic" cluster, which could exist for a moment as a stable body and run around underwater as well as in air. Curious behavior of the cluster very well resembled BL in the natural environment(1). It was amazing that several new kinds of nuclear reactions("Electro-Nuclear Reactions(ENRs)") took place in the cluster(2). The most significant of ENRs among them was nuclear collapse, "Electro-Nuclear Collapse(ENC)." Since the electromagnetic force is 40 orders stronger than the gravitational force, ENC was very easy to induce even in laboratory. Nuclear transmutation(ENT) was also stimulated in the cluster(2). Many experimental evidence for ENRs will be shown(3). The mechanisms of ENRs will be explained by The Nattoh Model(2).

References

- T. Matsumoto, "Ball Lightning during Underwater Spark Discharges and the Matsumae Earthquakes," Proc. of Int. Symp. of Ball Lightning(ISBL'97), Tsugawa, p 193 (1997).
- (2) T. Matsumoto, "Mechanisms of Electro-Nuclear Collapse: Comprehensive Explanation by The Nattoh Model," Review, distributed at ICCF-7, Vancouver (1998) and to be distributed at ICOPS99(1999).
- (3) T. Matsumoto, "Photographs of Electro-Nuclear Collapse," distributed at ICCF-7, Vancouver (1998) and to be distributed at ICOPS99(1999).

4C06

Some Results of Artificially Produced Ball Lightning Formation in Atmospheric Air

Paul M. Koloc, Neoteric Research Inc., College Park, MD 20741-1037, USA

Some Results of Artificially Produced Ball Lightning Formation in Atmospheric Air

> Paul M. Koloc Neoteric Research, Inc.

Artificial ball lightning has been produced in atmospheric air using input energies from 20 Joules to 4 kiloJoules, resulting in lifetimes of a few milliseconds to many tens of milliseconds. This work was the result of attempts to form encapsulated all-plasma Spheromaks (PMKs) at atmospheric pressure, based on speculations about the PLASMAK™ model. Representative frames showing a variety of features of the formed plasmoids will be displayed and discussed. One set of frames shows the formation, disruption, and fluorescence from the recontracted air. Energetic beams released by the disruption generated an x-ray signature in lead. Frames of PMKs are shown translated from their plasma blow-off clouds and the formation apparatus. Production of a formed and hyperaccelerated PMK is included. Frames of the step-by-step decay of the residual plasma (magnetized Hill's vortex) are depicted. The PLASMAK™ model will be briefly discussed.

4C07

A Review of the Performance of the Vacuum Spark (VSX) and the Spherical Pinch (SPX) X-Ray/EUV Point Sources

F.Wu, W. Tang, K.W. Wirpszo and E. Panarella, ALFT, Inc., Hull, PQ J8Z157, Canada

A REVIEW OF THE PERFORMANCE OF THE VACUUM SPARK (VSX) AND THE SPHERICAL PINCH (SPX) X-RAY/EUV POINT SOURCES

F. Wu, W. Tang, K. W. Wirpszo, and E. Panarella Advanced Laser and Fusion Technology, Inc. 189 Deveault St., Unit 7, Hull, P.Q., J8Z 1S7 Canada

The technology of X-ray/EUV point plasma sources is competing with the multiple beam synchrotrons as radiation sources for submicron lithography. The company ALFT has been doing research and development on two plasma point sources for several years now. They are the vacuum spark (VSX) and spherical pinch (SPX) technologies. Both have a long history of previous research to support the contention that are well qualified to be converted into technological tools for the manufacturing of the next generation of chips.

The VSX is essentially a miniature discharge capable of emitting soft x-ray radiation. Because the radiation is emitted in small dose in each spark, it is necessary to repeat the phenomenon at high frequency in order to have a quasi-continuous wave. Over a long time, the soft X-ray power distribution will be nearly uniform, thus meeting the requirement for microlithography. The SPX is mainly a strong source of EUV radiation that operates at a frequency of one hertz or more.

The two machines are complementary in their specifications, as well as in their technological challenges. The vacuum spark challenges lie in the high repetition rate, and the extraction of heat from the minute volume surrounding the radiation emitting region. The spherical pinch challenge lies in the optimization of the energy conversion efficiency from electrical into radiative.

A progress report will be presented on both machines in relation to their status for microlithography applications.

4C08

Ball Lightning as A Shell of Water Molecules

A.I. Mesenyashin, Box 126, St. Petersburg, 192283, Russia

Ball Lightning as a Shell of Water Molecules

A.I.Mesenyashin Box 126,PO283, St. Petersburg 192283, Russia

A theory is developed in this paper where the ball lightning (BL) is regarded as an electrostatically charged shell of water molecules with opposite sign charges arranged about opposite shell poles in accordance with cosinusoid law, the thickness of the shell being of the order of (0.004-100)·10⁻⁶ m. Such array of the charges is sure to generate an electrostatic field which makes water molecules distribute in ordered pattern imparting the shell properties not unlike those of crystals.

There was noted a striking correlation between BL shell and that of a soap bubble. The difference lies in that BL shell is a multi-layer one whereas the soap bubble features only two ordered layers of surface molecules.

BL shell is made stable owing to free energy caused by ordered orientation of dipole water molecules and hydrogen bond. The magnitude of this free energy may be as high as 4 eV. The potential of free energy may be stored from some external electric field such as that generated by common forked lightning.

BL shell is made stable also due to electrostriction pressure within it. Electric charges within the thin shell layer gradually discharge onto each other so that the life of the shell is extended for some seconds. Both the calculations and the observation give evidence that the larger is the diameter of BL the longer is its life period. An electrostatically charged body can get discharged with explosion or just fade away quietly. Prior to discharge such a body is neither destructive nor dangerous for human beings, it generates no heat and no air whirls have been detected around such bodies.

It is to be emphasized that above mentioned shell thickness is responsible for both life duration and magnitude of energy stored. Besides, this provides possibility for BL to soar in air. Owing to zero potential of circumferential line established on the shell BL can be attached to power transmission lines and move along them. As for luminescence, or glow of BL, this can be ascribed to crystalline structure of the shell and high surface field intensity which is apt to generate streamer corona effect.

4C09

High Energy Long Living Non-equilibrium Plasmoids in a gas Flow and Atmosphere

A.I. Klimov,

Russian Academy of Science, Moscow 127412, Russia

High Energy Long Living Non Equilibrium Plasmoids in a Gas Flow and Atmosphere

Klimov A.I.

Institute for High Temperatures Russian Academy of Science (IVTAN RAS), Izhorskaya 13/19, Moscow 127412 Russia Phone: (095)-413-1212, E-mail: aklim@orc.ru

High energy long living structural non equilibrium plasma formation (further named plasmoids, P) were created by means of pulse plasma gun (erosive discharge), HF and microwave discharge generators. It was discovered very complex filamentary structure of these plasma objects. Following anomalous properties of these objects were revealed in flow and in atmosphere:

High non equilibrium level of plasma (Ne>1015 cm³, Te~1eV>>Tg~ 1000K),
High sound velocity inside P, Vs~ 2000 mps,
Surface tension,
Super penetration of the P throw supersonic flow,

Super penetration of the P throw supersonic now, Selective interaction of the P with metals and dielectrics, Penetration of the P throw narrow channels, Distraction of these objects by additional heating, And others.

Specific plasma energy of these objects could reach up to 10-100 eV/ atom. There were revealed two different types of decay of these objects: with explosion and without explosion We used these plasmoids for drag reduction of body in supersonic flow.

Bonsai I/II 3 PM, Tuesday, June 22, 1999

Oral Session 4D
Thermal Plasma Chemisty and Processing
And
Environmental Issues in Plasma Science

4D01

nvited -

Study of the LTE Departure in a Low Pressure Supersonic Plasma Jet in AR-H2 and in AR-N2-H2 Mixtures

M. Rajabian, S. Vacquie and D.V. Gravelle, Universite Paul Sabatier, Toulouse, France

STUDY OF THE LTE DEPARTURE IN A LOW PRESSURE SUPERSONIC PLASMA JET IN AR- H_2 AND IN AR- N_2 - H_2 MIXTURE.

M.Rajabian¹, S. Vacquie² and D.V. Gravelle¹
¹ CRTP, Universite de Sherbrooke, Sherbrooke, Quebec, Canada.
² CPAT, Universite Paul Sabatier, Toulouse, France.

Plasma torches at low pressure and controlled atmosphere are used in major applications for the production and processing of materials due to their potential for high performance, and low contamination. A good knowledge of the plasma parameters is necessary, particularly for the design of high-performance mathematical models that avoid the building of expensive prototypes for performance assessment.

The present work is undertaken on a DC plasma torch operating over a wide pressure range (8 kPa to 100 kPa) at an arc power fixed at 17.5 kW. Emission spectroscopy diagnostics was carried out for determining temperature, electron and particle density profiles in two gas mixtures: Ar-N2-H2 with flow rates of 40, 10, and 1 slpm respectively, and Ar-H2 with input flow rates of 35 and 7 slpm respectively. The electron temperature was determined by using a Boltzmann diagram of Ar spectral lines. The absolute values of the intensity of these lines, of the molecular bands and of the continuum was obtained by using a standard tungsten filament lamp. Local values were obtained by Abel transform. For the rotational temperature measurement, the first negative system of N2⁺ was used using a method that consists in comparing the experimental spectra and the simulated molecular bands. The N2⁺ population density was calculated by using the band head intensity (the integrated 1-26 P-branch lines). To measure the electron density, we used the broadening of the Ha line of hydrogen by the Stark effect. The local profile of Ha was obtained by Abel inversion of the integrated profiles for 25 wavelengths on either side of the peak.

For the gas mixtures used, the supersonic shock occurs at a distance from the nozzle exit growing when the pressure decreases (8,10, and 13 mm for pressures of 13, 20 and 26 kPa). For pressures of 100 kPa and 53 kPa, we observe a good agreement between the values of electron density Ne experimentally measured independently of local thermodynamic equilibrium (LTE) and the values obtained by calculation using the temperature obtained with Boltzmann diagram. Local thermodynamic equilibrium conditions prevail at these values of pressure. For the lower values of the pressure, the experimental value of N₂ ion density are higher than the calculated values, using the rotational temperature T_h , or the Boltzmann temperature T_e. The discrepancy is lower with the use of T_e. That shows the importance of the collisions between electrons and heavy particles, due to the high values of the electron density (4.10¹⁶ cm⁻³ in the supersonic shock wave for 13 kPa). For pressure lower than 26 kPa important deviation from LTE conditions are observed.

Low-Rate Reactive and Non-Reactive Low Pressure Plasma Spraying

W.S. Crawford, H. Hamatani, M.A. Cappelli, F.B. Prinz, Stanford University, Stanford, CA 94305-3032, USA

Low-Rate Reactive and Non-Reactive Low Pressure
Plasma Spraying
W.S. Crawford, H. Hamatani, M.A. Cappelli, F.B. Prinz
Mechanical Engineering Department, Stanford University,
Stanford, CA 94305-3032

A low pressure plasma spray (LPPS) process has been developed to operate at 3-4 kW and to deposit metals or ceramic compounds at rates of 0.1-10 g/min, with a coating spot diameter of 1-1.5 cm. The two novel features of this facility are the low power and deposition rate, 10 to 100 times below those of conventional plasma spray processes, and the capacity for reactive plasma spraying. These spray parameters lend themselves to applications in mesoscale (dimensions on order 0.1-1 mm) devices, including substrates for microelectronics. Low-rate spraying may facilitate the construction of mesoscale parts in a layered technique similar to VLSI fabrication. Traditional VLSI fabrication processes are ill-suited to build parts with thickness on the millimeter scale.

In the case of non-reactive spraying, solid metal powders with particle sizes from 2 to 44 µm are injected into the plume of a 3-4 kW DC arcjet operating on a combination of argon, hydrogen and nitrogen. The plasma jet melts and convects the powder toward a cooled substrate where it solidifies to form a coating. Reactive spraying is similar except that the plasma gases include a component which reacts with the solid powder to form a compound coating. Results will be presented for the reactive spraying of AIN and the non-reactive spraying of Cu, in terms of density, mechanical strength, bond strength and thermal conductivity. In the case of pure Cu, for example, these coatings have achieved densities of 92-96% with shear strength exceeding that of pure rolled and annealed copper. These properties will be studied as functions of substrate temperature, particle size, and plasma parameters such as arc power and plasma temperature.

4D04

Mass Spectrometric Investigations of a Plasma Jet Chemical Vapor Deposition Reactor

Alan E. Kull and Mark A. Cappelli, Stanford University, Stanford, CA 94305-3032, USA

Mass Spectrometric Investigations of a
Plasma Jet Chemical Vapor Deposition Reactor
Alan E. Kull and Mark A. Cappelli
Thermosciences Division,
Mechanical Engineering Department, Stanford University

High density plasma-enhanced chemical vapor deposition is a technology of growing importance in the deposition of materials for the semiconductor and optoelectronics industries. Direct current (DC) plasma jets (also known as arcjets) are a particular form of high density plasma source that produce a high velocity (5-10 km/sec) plasma stream (20-30% dissociation fraction, $n_e \sim 10^{13}$ cm⁻³). The plasma jet provides large convective fluxes of chemically reactive radical species, in super-equilibrium concentrations, that are stagnated on a substrate on which film growth occurs. High quality films of materials such as diamond, cubic boron nitride, aluminum nitride, and gallium nitride have been grown by this method at growth rates that are high compared with other deposition methods.

The radical species are key to the growth of these materials. To determine the concentrations of the important gas phase species and thus elucidate the growth kinetics of the deposited films, mass spectrometry is employed. A small amount of the plasma is passed through a hole in the substrate; the hole is sized to be comparable with the collisional mean free path. The sampled plasma is expanded into a nearly collisionless environment provided by differential pumping. Such effusive sampling guarantees that the plasma sampled will be representative of the chemistry within a few mean free paths of the film growth surface. This effusive beam is analyzed by a mass spectrometer to determine the constituency of the plasma and by an ion energy analyzer to determine the energy distribution of the ions present. The roles of different species in film growth mechanisms can then be compared.

Arc Voltage Behavior as Indication of Different Operating Modes in a Plasma Torch

Z. Duan, K. Wittmann, J. Heberlein, J.F. Coudert and P. Fauchais,

University of Minnesota, Minneapolis, MN 55455, USA

Arc Voltage Behavior as Indication of Different Operating Modes in a Plasma Torch

Z. Duan, ¹ K. Wittmann, ² J. Heberlein, ¹
J.F. Coudert, ² and P. Fauchais ²
¹University of Minnesota, Minneapolis, MN/USA
²University of Limoges, Limoges/France

An uncontrolled plasma instability is a phenomenon that most processes try to avoid. In plasma spraying, such an instability can lead to a deterioration of the coating quality. In our investigation, the voltage fluctuations of a subsonic DC plasma torch have been analyzed and correlated with appearance of plasma jet instabilities. The torch has a straight bore anode nozzle and a button shape cathode. The arc gas can be injected forming either a straight flow or a swirling flow.

Three arc operating modes have been found: the "restrike" mode which is characterized by a saw-tooth shape voltage waveform and a large fluctuating amplitude, the "take-over" mode which is represented with a more or less sinusoidal or triangle shape waveform with a varying amplitude, and the "steady" mode which shows a nearly flat voltage profile with a low mean voltage. In addition to the analysis of the voltage waveform, analysis of high speed video images obtained from end-on observation of the arc in the anode nozzle has been used as diagnostics.

The occurrence of these different operating modes can be related to the changes in the thickness of the cold gas boundary layer between the arc column and the anode surface. A thick boundary layer will require a higher voltage drop and is associated with the "restrike" mode. A thin boundary layer will reduce the breakdown voltage and randomize the attachment resulting in the "take-over" mode. A very thin boundary layer would reduce the insulating properties of the cold gas boundary layer to an extent that no breakdown is required and the arc assumes an attachment close to the anode channel entrance with little movement, and the "steady" mode is the consequence. This mode, although stable, leads to poor gas heating efficiencies and rapid anode erosion. The regions in the operating parameter space in which the different modes are dominant are presented.

This work has been supported in part by NSF through the ERC for Plasma-Aided Manufacturing grant EEC-8721545 and through an international collaboration grant NSF/INT-9415715.

4D06-7

Invited - NOx Removal in Jet-Engine Exhaust: Proposed Non-Thermal Plasma Systems and Economic Considerations

L.A. Rosocha, J.S. Chang, K. Urashima, S.J. Kim, A.W. Miziolek, M.JNusca and R.G. Daniel, R.F. Huie and J.T. Herron, Los Alamos National Laboratory, Los Alamos, NM 87545, USA

NO_x Removal in Jet-Engine Exhaust: Proposed Non-Thermal Plasma Systems and Economic Considerations *

L. A. Rosocha Los Alamos National Laboratory

J.-S. Chang, K. Urashima, and S.J. Kim McMaster University

A.W. Miziolek, M.J. Nusca, and R.G. Daniel Army Research Laboratory

R.F. Huie and J.T. Herron National Institute for Standards and Technology

Incentives for implementing new pollution-control technologies are both regulatory and economic. Given considerable regulatory pressure, e.g., the promulgation of a NESHAPS (National Emissions Standard for Hazardous Air Pollutants) for NOv emissions in CY 2000, new de-NO_x technologies are being explored. One major reason for this is that conventional de-NO_x methods (like wet scrubbers plus Selective Catalytic Reduction -SCR) will not work effectively for the low NO concentrations (e.g., < 50 ppm), high exhaust-gas flow rates ($\sim 10^6$ Nm³/h), and low gas temperatures (near ambient) characteristic of Jet Engine Test Cells (JETCs). Our project is currently evaluating nonthermal plasma (NTP) technologies for treating jet-engine exhaust and other hazardous air pollutants. In this paper, we will present our initial design options for NTP reactor systems for a field-pilot demonstration on small jet engines (e.g., F107 or F112; flow rates $\sim 10^4$ Nm³/h). The field-pilot demonstration is necessary to provide further data and operating experience to more fully evaluate economic and performance projections for NTP de-NO_x technology and to design larger systems with confidence. We are presently considering five candidate NTP reactor systems: pulsed corona, dielectric barrier (silent discharge), hybrid NTP reactor-adsorber, plasma-catalytic hybrid, and corona radical shower. Because of the cost and logistics of using an electron-beam NTP reactor (for which some economic data will be given), we have limited our candidate systems to those based on electric-discharge-driven NTP reactors. This paper will discuss the exhaust stream to be addressed, the test setup, candidate reactor systems, and projected operating parameters and specifications for the field-pilot units - as well as initial cost comparisons of three NTP-based de-NO_x systems with two SCR-based systems based on published small scale test results and our bench-scale experiments.

^{*} This work supported in whole or in part by the U.S. Strategic Environmental Research and Development Program (SERDP).

A comparative study of remote plasma sources for environmentally-friendly CVD chambers cleaning.

S.Raux, K.C. Lai, H. Nguyen, M. Sarfaty, S.T. Li, J.Davidow and T.F. Huang, Applied Materials, Santa Clara, CA 95054, USA

A comparative study of remote plasma sources for environmentally-friendly CVD chambers cleaning.

S. Raoux, K.C. Lai, H. Nguyen, M. Sarfaty, S.T. Li, J. Davidow and T.F. Huang.
Applied Materials Inc., 3050 Bowers Ave., Santa Clara, California 95054.

CVD chamber cleaning is the main source of perfluorocompound (PFC) emission from semiconductor fabrication plants. Over the past years, several attempts have been made to optimize chamber cleaning efficiency and reduce its environmental impact. A new cleaning technology has been introduced that improves the overall tool productivity while virtually eliminating PFC emission concerns. A remote high-density plasma source dissociates NF3 molecules, and the reactive byproducts are injected in the CVD chamber to etch the deposition residues. Due to near-complete utilization of the source gas, the technology provides reduced clean time, and the MMTCE (Million Metric Ton Carbon Equivalent) of the process can be reduced by two orders of magnitude, compared to classical in-situ RF plasma cleans.

In this study, we compare the characteristics of a microwave-driven and a magnetically-enhanced inductively coupled NF₃ discharge. Optical Emission Spectroscopy, Quadrupole Mass Spectroscopy, Fourrier Transform Infra Red and etch rate measurements were used to characterize the different sources and assess the environmental impact of the clean processes.

A comparative analysis of the two types of plasma sources is made with respect to implementation of this cleaning technology in an industrial environment.

4D09

Coal Combustion Mercury Control by Means of Corona Discharge

Dennis J. Helfritch and Paul L. Feldman, Environmental Elements Corporation, Baltimore, MD 21227, USA

Coal Combustion Mercury Control by Means of Corona Discharge

by

Dennis J. Helfritch and Paul L. Feldman Environmental Elements Corporation

More than 39 states currently have health advisories concerning the consumption of fish caught in lakes and rivers because of elevated levels of mercury. Every one of Michigan's more than 11,000 lakes have mercury advisories. Because of the enormous volume of coal that they burn, power plants represent a major source of mercury emissions.

The work reported here describes the testing of a novel corona discharge flue gas reactor designed to oxidize mercury vapor at the low concentrations found in coal-fired power plant flue gas. An insoluble gas at these temperatures, elemental mercury is not captured by conventional air pollution controls. The oxidation of elementary mercury vapor to the more soluble mercuric oxide allows it to be captured in an existing downstream wet scrubber control device used for sulfur dioxide control.

A corona discharge in flue gas produces oxidizing radicals, such as OH and atomic oxygen, which then react to oxidize elemental mercury and other flue gas constituents. A unique corona reactor in which an intense and uniform corona is generated has been designed. The evaluation of the corona reactor took place in the laboratory and at pilot scale at Alabama Power's Plant Miller power station. The results showed that the spatially distributed corona discharge produced by the corona reactor operating at short residence times will yield a high level of mercury vapor oxidation at moderate power consumption.

Properties of Corona Discharge in a Hot Chamber Han S. Uhm, Ajou University, Suwon 442-749, Korea

4P

Serra I, Conference Center 3 PM, Tuesday, June 22, 1999

Poster Session 4P

Properties of Corona Discharge in a Hot Chamber

Han S. Uhm
Department of Physics, Ajou University
Suwon 442-749, Korea

The corona discharge system has been studied lately for its potential application to reduce NO_x and SO_x gas emission, where high electrical voltage (typically 50 kV) is applied to electrodes, inducing electrical breakdown in an atmospheric pressure and generating a plasma volume. One of the important issues in the corona discharge system is an effective generation of plasmas in the system. The electrical power needed for the plasma generation is one of the main operating costs of the corona discharge system. Less power consumption for plasma generation makes the corona discharge system more economical. Air pollutants are very often emitted from hot chambers such as municipal incinerators or electric power plants. It is therefore necessary to investigate influence of the chamber temperature on properties of the corona discharge system. From present work, we found that the critical voltage V_c required for the corona-discharge breakdown is inversely proportional to the chamber temperature T. The electrical energy w_c required for corona-discharge breakdown is inversely proportional to the square of the chamber temperature T. Thus, the electrical energy consumption for corona-discharge system decreases significantly as the temperature increases. The plasma generation by corona discharge in a hot chamber is much more efficient than that in a cold chamber.

Pulsed Operation of Microhollow Cathode Discharges in Atmospheric Air

Uwe Ernst, Robert H. Stark, Karl. H. Schoenbach, Klaus Frand and Werner Hartmann, University of Erlangen-Nuremberg, Erlangen, Germany

Pulsed Operation of Microhollow Cathode Discharges in Atmospheric Air

Uwe Ernst¹, Robert H. Stark², Karl H. Schoenbach², Klaus Frank¹ und Werner Hartmann³

- 1) Department of Physics, University of Erlangen-Nuremberg, Germany
- 2) Physical Electronics Research Institute, Old Dominion University, Norfolk, VA 23529, USA
- 3) Siemens AG Erlangen, Germany

Reducing the diameter of the cathode opening to values on the order of 100 micrometer allowed us to operate stable dc hollow cathode glow discharges in air at atmospheric pressure. Discharge currents of up to 30 mA with forward voltages around 400 V have been realized. In order to generate arrays of microhollow discharges without cathode resistive ballast, the current voltage characteristic of the discharge needs to have a positive slope. Results of modeling show the required increase of the forward voltage with current at high current values. However, overheating of the electrodes prevents dc operation of parallel discharges in atmospheric air in this current range. In order to extend the range of operation into the high current mode, the discharge has been operated pulsed with pulse duration from 1 to 100 microsecond. First experimental results confirm the modeling results. The electrical characteristic and the optical appearance of the discharge plasma in pulsed microhollow cathode discharges and its applications will be discussed.

This work was supported by the National Science Foundation (NSF), the Air Force Office of Scientific Research (AFOSR) and Siemens Germany

4P02

Microhollow Cathode Discharges as Plasma Cathodes for Atmospheric Pressure Glow Discharges in Air

Robert H. Stark and Karl H. Schoenbach, Old Dominion University, Norfolk, VA 23529, USA

Microhollow Cathode Discharges as Plasma Cathodes for Atmospheric Pressure Glow Discharges in Air

Robert H. Stark and Karl H. Schoenbach Physical Electronics Research Institute, Old Dominion University, Norfolk, VA 23529

One of the main obstacles for dc operation of high-pressure glow discharges is the glow-to-arc transition, an instability that originates in the high field region of the discharge: the cathode fall. Reduction or even elimination of the cathode fall is possible by using a plasma cathode. A microhollow cathode discharge (MHCD) [1] has been used as plasma cathode for a glow discharge in air, sustained between the hollow anode of the MHCD and a third electrode which was positively biased with respect to the MHCD anode [2]. With this method we were able to obtain stable dc operation in air up to atmospheric pressure without reaching the threshold for glow-to-arc transition. Current and voltage characteristics, axial electric field distribution and the visual appearance of this glow discharge and the MHCD were studied in air at atmospheric pressure [3]. In order to obtain the stable air discharge the current in the MHCD needs to exceed a threshold value. Typical threshold currents for a 100 µm diameter hollow cathode are 5-10 mA. Above the threshold, the current in the glow discharge is identical with the MHCD current and can be controlled by varying the MHCD voltage. The glow discharges were operated at currents of up to 22 mA, corresponding to current densities of 3.8 A/cm² and at average electric fields of 1.2 kV/cm. Electron densities in the glow were estimated to be on the order of 10¹³ cm⁻³. Temperature measurements in one MHCD indicated that the temperature in the glow discharge is below 2000 °K [4]. Parallel operation of these glow discharges by using arrays of MHCDs offers the possibility for large volume high pressure operation [5].

- [1] K. H. Schoenbach, A. El-Habachi, W. Shi, and M. Ciocca, Plasma Sources Sci. Techn. 6, 468 (1997).
- [2] R. H. Stark and K. H. Schoenbach, "Direct Current High Pressure Glow Discharges", to appear in J. Appl. Phys.
- [3] R. H. Stark and K. H. Schoenbach, "Direct Current Glow Discharges in Atmospheric Air", submitted to Appl. Phys. Lett.
- [4] R. H. Stark, U. Ernst, R. Block, and K. H. Schoenbach, "Microhollow Cathode Discharges in Atmospheric Air", this conference.
- [5] W. Shi, R. H. Stark and K. H. Schoenbach, "Parallel Operation of Microhollow Cathode Discharges", to appear in IEEE Trans. Plasma Science".

This work was solely funded by the Air Force Office of Scientific Research (AFOSR) in cooperation with the DDR&E Air Plasma Ramparts MURI program.

Nitrogen Influences On A Laser Produced TMAE Plasma

G. Ding, J.E. Scharer and K.L. Kelly, University of Wisconsin, Madison, WI 53706-1687, USA

NITROGEN INFLUENCES ON A LASER PRODUCED TMAE PLASMA

G. Ding, J. E. Scharer and K. L. Kelly

Department of Electrical and Computer Engineering University of Wisconsin, Madison 53706

TMAE is a readily ionized organic gas, tetrakis(dimethylamino)ethylene, which can be single photon ionized by a 193 nm laser, so that a large volume (hundreds of cm³), high initial plasma density (> 10^{13} cm⁻³) plasma can be created. Additional high pressure nitrogen admixture effects in this plasma are studied by measuring planar Langmuir probe electron saturation currents, which provide more reliable electron density measurements than those from ion saturation current, because the former is not dependent on ion species but the latter is. The former is much more difficult in the experiment due to the difficulty of accurately identifying the electron saturation current, but we have got very flat curves of the electron saturation current vs. the bias voltage so that the electron saturation currents can be accurately identified. The technique of these fast probe measurements which include a detailed considerations of probe structure, probe surface cleaning, shielding, probe perturbation, frequency response, temporal and spatial resolutions, dummy probe corrections as well as noise analysis will be shown. The electron densities and temperatures vs. time at different TMAE pressures, nitrogen pressures and laser powers will be present. The experimental results show that the nitrogen is helpful to sustain a TMAE plasma. The comparison of helium admixture effects in this TMAE plasma is also shown, which has a negligible effect on TMAE plasma. This comparison experiment implies that nitrogen is special for TMAE plasma. The admixture effect is believed to involve complex processes. We will discuss when nitrogen is introduced to TMAE plasma, (1) TMAE+ ions can be changed into other molecule or radical ions, which can have significantly different plasma decay processes comparing to the pure TMAE plasma. (2) Many metastable atoms, molecules or radicals can be created, and they can be involved in many new ionization processes.

Acknowledgments

This work is primarily supported by Air Force Office of Scientific Research grant (Grant: F49620-97-1-0262) in cooperation with the Defense Department Research and Engineering Air Plasma Ramparts Multi-University Research Initiative program.

4P04

A Laser-Produced Plasma Sustained by a Radiofrequency Source

K.L. Kelly, J.E. Scharer and G. Ding, University of Wisconsin, Madison, WI 53706-1687, USA

A Laser-Produced Plasma Sustained by a Radiofrequency Source

K. L. Kelly, J. E. Scharer, and G. Ding

Department of Electrical and Computer Engineering University of Wisconsin, Madison 53706

The creation a high density plasma in atmospheric air is studied. The plasma is generated by photoionization of the organic seed molecule tetrakis(dimethylamino)ethylene (TMAE) and is sustained by RF coupling through the use of an antenna. The coupled power is a function of antenna configuration, plasma density, working gas, and applied magnetic field. Previous studies have utilized these antennas to couple power to the plasma through the inductive mode of operation. The inductive source operates by coupling power to the plasma through collisional ohmic heating of the wave energy. Helicons have shown to be very efficient sources in the low pressure argon regime with densities of the order 4×10^{12} cm⁻³ with only 600 W of power in a 5 cm radius tube. The VUV laser in this experimenta has created plasmas of order 10¹⁴ cm⁻³. The high density gives an initial condition which allows higher radiation resistance and more power to couple to the plasma. The computer codes^b ANTENA2 and MAXEB are used to optimize the experiment and interpret results. The effects of adding seperate air constituants will be studies as a function of neutral pressure, and will be compared to the effects of adding inert gases. Both highly collisional power absorption and noncollisional Landau effects will be investigated.

Acknowledgments

Air Force Office of Scientific research grants (Grant F49620-97-1-0262) Defense Department Research and Engineering Air Plasma Ramparts Multi-University Research Initiative and in part by NSF grant ECS-9632377.

^aK. Kelly, et. al. Journ. App. Phys. **85**(1): 63-68 1998 ^bY. Mouzouris and J. E. Scharer. Phys. Plasmas. **5**(12): 4253-61, 1998.

High Pressure N2, O2 and Air Mixture Plasmas Produced by a Radiofrequency Helicon Plasma Source

J.E. Scharer, X.M. Guo, K.L. Kelly and H.Gui, University of Wisconsin, Madison, WI 53706-1687, USA

High Pressure N_2 , O_2 and Air Mixture Plasmas Produced by a Radiofrequency Helicon Plasma Source

J. E. Scharer, X. M. Guo, K. L. Kelly, and H. Gui

Dept. of Electrical and Computer Engineering University of Wisconsin, Madison 53706

High pressure (10-760 Torr) plasmas of N2, O2 and air gas mixture are investigated in this work by using a radiofrequency helicon plasma source. Langmuir probe theory and collisional helicon wave propagation characteristics at high pressure are utilized to obtain plasma density and electron temperature. The wave modelling results show that higher rf wave frequency and applied magnetic field will enhance electromagnetic wave penetration and absorption profiles for these highly collisional plasmas. The higher rf frequency on plasma properties will be carried out by means of a broadband (2-200 MHz) amplifier. A balanced driven matching circuit will be developed to efficiently couple rf power to plasmas at higher rf frequency regimes. Different kinds of rf antennas including multiple turn helices are studied to obtain efficient coupling at high pressures. Seed gases including Ar and TMAE and high voltage spark initiation will also be examined to reduce the power requirment to create high pressure plasmas. Wave B_z field profiles and antenna input impedances are measured and compared to the 2-D MAXEB code^a. We will utilize a nonuniform magnetic field with a cyclotron resonance zone to assist starting these high pressure plasmas.

Acknowledgments

This work is primarily supported by Air Force Office of Scientific Research grant (Grant: F49620-97-1-0262) in cooperation with the Defense Department Research and Engineering Air Plasma Ramparts Multi-University Research Initiative program. It is also supported in part by NSF Grant ECS-9632377 and by the University of Wisconsin-Madison.

4P06

Temporal and Spatial Evolution of Gas Discharges Induced by High-Power, Pulsed Microwaves

M. Onoi, T. Hayashida, K. Azuma, E. Fujiwara and M. Yatsuzuka, Himeji Institute of Technology, Himeji, Hyogo 671-2201, Japan

Temporal and Spatial Evolutions of Gas Discharge Induced by a High-Power, Pulse Microwave

M. Onoi, T. Hayashida, K. Azuma, E. Fujiwara and M. Yatsuzuka
Himeji Institute of Technology
Himeji, Hyogo 671-2201, Japan

High-power, short-pulse microwave with the peak power of 20 MW, frequency of 13 GHz and pulse duration of 14 ns, which is generated from a virtual cathode oscillator, is irradiated on a gap space between a spherical and a spherical electrodes to induce gas discharge. The electrode is being biased at a constant dc voltage less than that for breakdown at the moment of microwave pulse injection. The gap separation is 15 mm. Gas pressure is changed from 760 Torr to 50 Torr. A high-speed image converter camera observes temporal and spatial evolutions of gas discharge luminescence.

Streak pictures show that microwave-induced discharge begins at several spots between the gap at the higher-pressure region than 300 Torr. Each luminescence of the discharge grows in time to link together, and then the gap breakdown occurs. The gap breakdowns are delayed by about 30 - 300 ns depending on the pressure and the applied dc voltage which determine the electron drift time between the gap. At the lower pressure region than 300 Torr, two-stage breakdowns occur. In the first stage, a single large discharge luminescence (#1 luminescence) appears in the gap center at the almost same time with the injection of microwave pulse and disappears after about 50 ns. Just before disappear of #1 luminescence other luminescences (#2 luminescence) are observed in both sides between the #1 luminescence and the electrodes. The #2 luminescences are continued for a few 100 ns. After a few microsecond of the first stage discharge, the second stage discharge followed by the gap breakdown discharge suddenly appears.

^eY. Mouzouris and J. E. Scharer; *Phys. Plasmas.* 5(12): 4253. 1998.

Experiments of New Plasma Concepts for Enhanced Microwave Vacuum Electronics

P. Muggli, J.R. Hoffman, J. Yampolsky, J.F. Cordell, M.A. Gundersen, C. Joshi and T. Katsouleas, University of Southern California, Los Angeles, CA 90095, USA

Experiments on New Plasma Concepts for Enhanced Microwave Vacuum Electronics

P. Muggli, J.R. Hoffman, J. Yampolsky, J.F Cordell, M.A. Gundersen, C. Joshi*, and T. Katsouleas

Electrical Engineering- Electrophysics Department, University of Southern California, Los Angeles CA 90089, USA

*Electrical Engineering Department, University of California, Los Angeles CA 90095, USA

Recently new schemes have been proposed for plasma based microwave sources that could lead to output power increases by orders of magnitude, as well as offer new possibilities such as broad band tuning and frequency chirping, ultra-short pulse generation, pulse design, etc. In the first scheme, the static field of an alternatively biased capacitor is directly converted into short pulses of tunable electromagnetic (em) radiation upon transmission through a relativistic, underdense ionization front. The structure presently under investigation consist of pin pairs (capacitors) inserted into an X-band waveguide through its narrow side wall and separated by 1.134 cm. The generated frequency is in the Xband frequency range (8.4-12.4 GHz) when operated with plasma densities between 10¹¹ and 10¹² cm⁻³. The output power is in the 100 W range with an applied voltage of 6 kV and is limited by high voltage (HV) breakdown inside the structure. Much higher output power levels are expected with the new, shorter pulse, HV pulser, since the output power is proportional to the square of the applied voltage. At larger plasma densities, generation of a higher order mode traveling in the backward direction is also observed. In the second scheme, a fraction of the large amplitude electrostatic (es) wave generated in a plasma beat wave acceleration (PBWA) experiment (up to 3 GeV/m) is converted into em radiation by applying a static magnetic field perpendicularly to the driving laser beam. The two-frequency CO_2 laser beam resonantly drives the es wave, and couples to the L branch of the XO mode of the magnetized plasma through Cherenkov radiation. The radiation is emitted predominantly in the forward direction (direction of the laser beam), and is at the plasma frequency ($n_e \approx 10^{16}$ cm⁻³, $f \approx 1$ THz). With an applied magnetic field of 6 kG the output power is calculated to be in the megawatt range (for a sharp plasma/vacuum boundary). The parameters of the emitted radiation will also be used as a diagnostic for the plasma wave of a PBWA experiment, measuring its amplitude, phase, life time, etc. Design and experimental results are presented.

Work supported by NSF grant No ECS-9632735, DOE grant No DE-FG03-92ER-40745, and AFOSR grant No F49620-95-1-0248.

4P08

The One Atmosphere Uniform Glow discharge Plasma (OAUGDP) As A Classical Normal Glow Discharge

Rami B. Gadri, Daniel M. Sherman, Zhiyu Chen, Fuat Karakaya and J. Reece Roth, University of Tennessee, Knoxville, TN 37996-2100, USA

THE ONE ATMOSPHERE UNIFORM GLOW DISCHARGE PLASMA (OAUGDP) AS A CLASSICAL NORMAL GLOW DISCHARGE

Rami B. Gadri, Daniel M. Sherman, Zhiyu Chen, Fuat Karakaya, and J. Reece Roth

> UTK Plasma Sciences Laboratory Department of Electrical Engineering The University of Tennessee Knoxville, TN 37996-2100

ABSTRACT

The One Atmosphere Uniform Glow Discharge Plasma (OAUGDP) operating in air and other gases, has been recently developed at the UTK Plasma Sciences Laboratory and is proprietary to the University of Tennessee^[1,2]. The plasma is driven at low RF frequency, on the order of a few kilohertz, and is formed in a relatively large gap (several mm in air), between plane parallel insulated metal electrodes. For the proper values of gap distance, RF driving frequency, and rms voltage^[3], the OAUGDP operates uniformly, without producing filamentary microdischarges, and its physical characteristics are, in spite of the high pressure, surprisingly analogous to those observed in a normal DC glow discharge [4,5]. Numerical simulations and experimental timeresolved photographs [4,5] show that all the features of the classical normal glow discharge are present between the instantaneous cathode and anode: the cathode dark space, a linear electric field in the cathode region obeying Aston's law, the negative glow, the Faraday dark space, and the positive column. The glow discharge nature of the OAUGDP is significant because normal glow discharges operate very efficiently as plasma sources at or near the Stoletow point^[3] where the energy cost of generating an ion-electron pair in air is only 81 eV. In other atmospheric plasmas, such as arcs, this energy cost can be at least 10 KeV per ion-electron pair. We have developed a variety of configurations for the electrodes which permits both large and small processing volumes and allows a large range of applications to be accommodated. The electrical and physical characteristics of the OAUGDP will be presented.

- * This work was supported in part under a subcontract with the Environmental Elements Corporation of Baltimore (MD), the Air Force Office of Scientific Research contract number 98-C-OO69, and the Environmental Protection Administration contract number 68-D-98-118.
- 1.) Roth, J. R.; Tsai, P. P.; and Liu, C. (1995): Steady State, Glow Discharge Plasma, U.S. Patent #5,387,842, Issued February 7, 1995.
- 2.) Roth, J. R.; Tsai, P. P.; Liu, C.; Laroussi, M.; and Spence, P. D. (1995): One Atmosphere, Uniform Glow Discharge Plasma. U. S Patent 5,414,324, Issued May 9, 1995.
- 3.) Roth, J. R. (1995): Industrial <u>Plasma Engineering: Volume 1 Principles</u>. Institute of Physics Press, Bristol, UK ISBN 0-7503-0318-2. See Section 12.5.2.
- 4.) R. Ben Gadri, "One Atmosphere Glow Discharge Structure Revealed by Computer Modeling". IEEE Transactions on Plasma Science, February 1999.
- 5.) F. Massines, A. Rabehi, Ph. Decomps, R. Ben Gadri, P. Ségur, and Ch. Mayoux, "Experimental and Theoretical Study of a glow discharge at atmospheric pressure controlled by dielectric barrier". Journal of Applied Physics, Vol. 83, N 6, pp 2950-2957, March 1998.

Mechanism of Killing Microorganizms by a One Atmosphere Uniform Glow Discharge Plasma

Kimberly Kelly-Wintenberg, Tom Monite, Amanda Hodge, John Gaskins, J. Reece Roth, and Zhiuy Chen, University of Tennessee, Knoxville, TN 37996, USA

Mechanism of Killing of Microorganisms by a One Atmosphere Uniform Glow Discharge Plasma*

<u>Kimberly Kelly-Wintenberg</u>¹, Tom. Montie¹, Amanda Hodge¹, John Gaskins¹, J. Reece Roth², and Zhiyu Chen² The University of Tennessee, Knoxville, TN

There is an urgent need for the development of new disinfection/ for sterilization or technologies decontamination in the fields of healthcare, industrial and food processing. Researchers continue to develop and evaluate new and innovative means of inhibiting, destroying, and controlling pathogenic microorganisms which is safe and cost effective and does not result in the deleterious effects of the treated material. We have previously demonstrated the efficacy of a One Atmosphere Uniform Glow Discharge Plasma (OAUGDP) in killing bacteria and spores in seconds to minutes. The OAUGDP operates in air and produces a uniform plasma without filamentary discharges at room temperature, which is advantageous for sterilization of heat sensitive materials. The OAUGDP operates in a frequency band determined by the ion trapping mechanism provided that, for air, the electric field is above 8.5kV/cm. The OAUGDP efficiently generates plasma reactive oxygen species (ROS) including atomic oxygen and oxygen free radicals without the requirement of a vacuum system. Recent experiments using this OAUGDP technology have been applied to understanding the mechanism of killing of various microorganisms. Experiments using ultraviolet adsorption to measure macromolecular leakage from treated bacterial cells indicate rapid destruction of membranes. Results from electron microscopy studies show that bacteria with an outer membrane are more susceptible to fragmentation than those without an outer membrane, probably due to the sensitivity of lipids to ROS. Consistent with these findings are results that show the relative resistance of non-enveloped viruses to the plasma. Further results will be presented describing these mechanisms including attempts to characterize altered macromolecules.

4P10

Sterilization and Decontamination of Surfaces Using Atmospheric Pressure Plasma Discharges Eusebio Garate, Olga Gornostaeva, Igor Alexeff, Applied Pulsed Power Technologies, Corona Del Mar, CA 92625, USA

Sterilization and Decontamination of Surfaces Using Atmospheric Pressure Plasma Discharges*

Eusebio Garate, Olga Gornostaeva Applied Pulsed Power Technologies, Corona del Mar, CA

Igor Alexeff, Weng Lock Kang E. E. Department, University of Tennessee, Knoxville

The goal of the program is to demonstrate that an atmospheric pressure plasma discharge can rapidly and effectively sterilize or decontaminate surfaces that are contaminated with model biological and chemical warfare agents. The plasma is produced by corona discharge from an array of pins and a ground plane. The array is constructed so that various gases, like argon or helium, can be flowed past the pins where the discharge is initiated. The pin array can be biased using either DC. AC or pulsed discharges. The work done to date has focused on the sterilization of aluminum, polished steel and tantalum foil metal coupons, about 2 cm on a side and 2 mm thick, which have been innoculated with up to 10⁶ spores per coupon of Bacillus subtilis var niger or Bacillus stearothermophilus. Results indicate that 5 minute exposures to the atmospheric pressure plasma discharge can reduce the viable spore count by 4 orders of magnitude. The atmospheric pressure discharge is also effective in decomposing organic phosphate compounds that are simulants for chemical warfare agents. Details of the decomposition chemistry, by-product formation, and electrical energy consumption of the system will be discussed.

* This work is supported by a DARPA STTR under contract # DAAH01-98-C-R174.

^{*}This work was supported in part under a subcontract with the Environmental Elements Corporation of Baltimore, MD, the AFOSR contract number 98-C-0069.

¹Department of Microbiology, ²Department of Electrical Engineering

Investigation Of Unmagnetized Plasma Heating In a Low Pressure Microwave Discharge

M. Perrin, T. Grotjohn and J. Asmussen, Michigan State University, East Lansing, MI 48824, USA

INVESTIGATION OF UNMAGNETIZED PLASMA HEATING IN A LOW PRESSURE MICROWAVE DISCHARGE

M. Perrin, T. Grotjohn, and J. Asmussen Michigan State University, East Lansing, MI 48824

In this investigation an argon plasma is excited in a cylindrical cavity applicator with inner diameter of 17.78 cm. Power is coupled into the cavity with a variable length (0-6 cm) coaxial probe antenna placed in the center of a variable height (5-15 cm) sliding short. The power input is 100-400 W at a microwave frequency of 2.45 GHz. The discharge pressure is varied from 1-60 mTorr and the argon flow rates range from 2-50 sccm. The discharge chamber is 12.5 cm in diameter and 8 cm tall. No permanent or electro-magnets are used in this experiment.

Microcoaxial electric field probes are used to measure the magnitude and spatial variation of the electromagnetic (EM) fields normal to the walls of the cavity applicator at several pressures. The circumferential and axial variation of the impressed EM field is measured, and special attention is given to the impressed EM fields measured adjacent to the cylindrical discharge chamber. The electron density and electron temperature of the discharge are measured using both double and single Langmuir probe techniques (LPT) and electron energy distribution functions (EEDF). Average electron neutral collision frequencies are determined using experimentally measured EEDF and argon collision cross-section data. Experimental measurements are summarized vs. pressure, input power and gas flow rates.

A self-consistent two dimensional electromagnetic field and plasma discharge model is used to simulate the discharge. The discharge models considered include both cold and warm plasma models. The experimental input variables for the model include: incident microwave power, cavity geometry, pressure, and gas type. The output of the simulation provides the strength and spatial distribution of the impressed EM field, plasma density and electron temperature, in the cavity applicator and the discharge. A comparison is made between the measured EM fields and plasma properties and the simulated values.

The contribution of various heating mechanisms/phenomenon including: ohmic heating, space charge resonances, surface wave effects, microwave electric field skin depth, and other non-ohmic heating mechanism are assessed versus reactor operating conditions including pressure and input microwave power. The microwave coupling efficiency is determined from the simulated and measured impressed EM fields.

4P12

The Electrodeless Discharge at Atmospheric Pressure

Mounir Laroussi, Old Dominion University, Newport News, VA 23606, USA

The Elecrodeless Discharge at Atmospheric Pressure*

Mounir Laroussi Applied Research Center Old Dominion University 12050 Jefferson Ave. Newport News, VA 23606

Abstract

Recently the generation and applications of atmospheric pressure plasmas received increased interest in the plasma research community. Applications such as the surface modification of materials [1], and the decontamination of matter [2] have been under investigation. In this context, we introduce a new means of generating an atmospheric pressure discharge, which is suitable for use in the above-mentioned applications, and in the treatment of undesirable or polluting gases, such as VOC's. This device is a capacitively coupled discharge. It is basically made of a nonconducting tube with two independent loops of wire wrapped around it, and separated by a distance d. A stable discharge is generated inside the tube when an AC voltage of few hundred volts to few kilovolts, at a frequency of few kilohertz, is applied between the loops. One end of the tube is completely open to the outside air, and a seed gas (generally a noble gas such as Helium) is introduced in the tube. The plasma generated with this method is weakly ionized, cold, and is maintained by a relatively low input power (few tens of watts, depending on the size of the tube). In this paper, the discharge electrical characteristics, its radiation emission characteristics, and the measurement of relevant plasma parameters will be presented.

- [1] F. Massines, C. Mayoux, R. Messaoudi, A Rabehi, and P. Segur, "Experimental Study of an Atmospheric Pressure Glow Discharge: Application to Polymers Surface Treatment", in Proc. 1992 Int. Conf. Gas Discharges & their Applications, pp. 730-733.
- [2] M. Laroussi "Sterilization of Contaminated Matter with an Atmospheric Pressure Plasma", IEEE Trans. Plasma Sci., Vol. 24, No. 3, pp. 1188-1191, 1996.
- * Work supported in part by AFOSR STTR Contract F49620-97-C-0074 in cooperation with DDR&E Air Plasma Ramparts MURI program.

Modes of Operation of the Glow Discharge at Atmospheric Pressure (GDAP)

Mounir Laroussi and Igor Alexeff, Old Dominion University, Newport News, VA 23606, USA

Modes of Operation of the Glow Discharge at Atmospheric Pressure (GDAP)*

Mounir Laroussi Applied Research Center Old Dominion University 12050 Jefferson Ave. Newport News, VA 23606

Igor Alexeff
Microwave & Plasma Laboratory
The University of Tennessee
Knoxville, TN 37996-2100

Abstract

In this paper, we present a simple model of the Glow Discharge at Atmospheric Pressure (GDAP), based on its electrical characteristics. The GDAP is a capacitively coupled device, which uses the dielectric barrier discharge configuration. It is capable of generating a steady-state uniform glow, when driven by an AC voltage in the kHz range [1], [2]. Taking into account the rate of production and loss of particles, two nonlinear differential equations relating the applied voltage, the discharge current, and the number density are derived. Solutions of these equations reveal that two modes of operation of the discharge exist. For frequencies below about 20 kHz, the discharge current is a pulse each half cycle. For higher frequencies (f > 20 kHz). the current changes its form to a distorted sine-wave. It is also found that in the "higher frequency" mode of operation, less applied power is required to maintain a plasma number density comparable to the "lower frequency" mode. Therefore, it is more efficient to run the GDAP at driving frequencies higher than about 20 kHz.

- [1] S. Kanazawa, M. Kogoma, T. Moriwaki, and S. Okazaki, "Stable Glow Plasma at Atmospheric Pressure", J. Phys. D: Appl. Phys., 21, pp. 838-840, 1988.
- [2] J. R. Roth, M. Laroussi, and C. Liu, "Experimental Generation of a Steady-State Glow Discharge at Atmospheric Pressure", in Proc. 1992 IEEE Int. Conf. Plasma Sci., pp. 170-171.

4P14

Plasma diagnostics in ECRIN- a prototype microwave plasma reac tor for thin film deposition Carmen Ciubotariu, University of Lethbridge, Lethbridge (AB) T4K3MY, Canada

Plasma diagnostics in ECRIN - a prototype microwave plasma reactor* for thin film deposition

Carmen Ciubotariu Physics Department University of Lethbridge (AB), Canada

Plasma parameters values and profiles determined from probe and multi-grid electron/ion energy analyser measurements show that the microwave plasma reactor called ECRIN (Electron Cyclotron Resonance Ions Negatifs) can be considered as a small volume (1.7 I) prototype of a plasma deposition reactor for polymer photoresist stripping following microlithography.

The set-up comprises the microwave (mw) applicator (2.45 Ghz, TE10 waveguide, 240 V/cm electric field intensity peal value at 500 W incident mw power), permanent magnets at mw entrance (primary ECR zone) and the cylindrical plasma chamber (multimode mw cavity) with a picket-fence magnetic field (secondary ECR zone) and an exit through which vacuum (order of mtorr) and diagnostics are installed.

Langmuir probes and ion/electron retarding field energy analyzers were used to determine H2 and Ar plasma parameters. Two electron (bulk and fast) and bimodal ion populations and very complicated radial and axial profile patterns were found. A secondary plasma chamber in the extraction region of ECRIN (where the plasma potential is higher than 22 V) could be adapted to suit deposition requirements on a RF polarised substrate.

The plasma source characterization has shown that the discharge impedance varies dynamically as the incident power is matched into the discharge or as operating conditions (gas pressure or nature, forward mw power and plasma-mw coupling) are changed.

Optimal discharge conditions can be created so that the plasma parameters are suitable for uniform ion implantation in samples placed in the upper part, while under controlled operating regime, the axial plasma potential profile has maximum values in the lower part of the reactor, thus providing the ion beams for plasma deposition at its bottom.

^{*}Work supported in part by AFOSR Grant F49620-95-1-0277 in cooperation with DDR&E Air Plasma Ramparts MURI program.

^{*} Experiments were performed at Laboratoire de Physique des Milieux Ionises de l'Ecole Polytechnique de Palaiseau, in France.

High Voltage Ionization during Plasma Immersion Ion Implantation

X.B. Tian, Z. M. Zeng, T. K. Kwok, B.Y. Tang and P.K. Chu, City University of Hong Kong, Hong Kong, SAR, China

High Voltage Ionization during Plasma Immersion Ion Implantation

X. B. Tian^{1,2}, Z. M. Zeng^{1,2}, T. K. Kwok¹, B. Y. Tang^{1,2}, and P. K. Chu¹

Department of Physics and Materials Science, City University of Hong Kong, 83 Tat Chee Avenue, Kowloon, Hong Kong.
 Advanced Welding Production & Technology National Key Laboratory, Harbin Institute of Technology, Harbin, China

During the plasma immersion ion implantation (PIII) process, ions are typically created by an external plasma source, such as electron impact glow discharge using hot filaments, radio frequency, electron cyclotron resonance, metal arc, and so on. There is, however, a less obvious ion formation mechanism by the high voltage itself, especially for a long pulse duration or at high working pressure, as shown by the implantation current not decreasing monotonically as predicted by the Child-Langmuir law. A proof of this secondary phenomenon is that the measured total current sometimes increases dramatically in a low vacuum sustained by RF glow discharge. Another example is that the current can gradually rise after a short delay during long pulse, hot filament glow discharge PIII. These phenomena can be attributed to high voltage ionization during the PIII process and are related to the gas pressure, high voltage pulse duration, target size, target materials, and so on. In this paper, we will present supporting experimental data in addition to a theoretical analysis.

4P16

Influence of Sample Placement on Dose Uniformity in Plasma Immersion Ion Implantation of Industrial Bearings

Z.M Zeng, X.B. Tian, T.K. Kwok, B.Y. Tank and P.K. Chu, City University of Hong Kong, Hong Kong, SAR, China

Influence of Sample Placement on Dose Uniformity in Plasma Immersion Ion Implantation of Industrial Bearings

Z. M. Zeng^{1,2}, X. B. Tian^{1,2}, T. K. Kwok¹, B. Y. Tang^{1,2}, and P. K. Chu¹

Department of Physics and Materials Science, City University of Hong Kong, 83 Tat Chee Avenue, Kowloon, Hong Kong.
 Advanced Welding Production & Technology National Key Laboratory, Harbin Institute of Technology, Harbin, China

Plasma immersion ion implantation (PIII) is an effective technique to enhance the surface properties of industrial components possessing an irregular shape such as ball bearings. However, it is difficult to achieve uniform implantation along the groove surface on such a bearing and our previous work indicates that the angle of incidence is the primary factor affecting the lateral uniformity. As the incident angle is more glancing toward the edge of the bearing, it is possible to change the sample placement to attain better dose uniformity. In this work, three practical sample stage configurations are investigated: (a) direct placement on the sample stage platen, (b) placement on a copper shroud extension with the same diameter as the bearing resting on the sample platen, and (c) placement on a copper plate connected vertically to the sample platen by a small copper rod for electrical contact. Using a theoretical model developed from our previous work, the largest dose is achieved along the race surface for (c) whereas the best uniformity is observed for (b). Our simulation results also reveal that in (a), the highest dose is observed in the lower part of the groove (closer to sample platen) and it is verified experimentally. Hence, in order to improve the lateral dose uniformity across the groove surface, the ball bearing must be elevated from the sample platen using an extension. The diameter of the extension relative to the bearing also affects the total dose and uniformity. The right combination depends on the tolerable non-uniformity as well as the capacity of the pulsing power supply as a larger extension rod will increase the current demand.

Comparison of Hot Cathode and Inductively Coupled Discharges for Application in Plasma Immersed Ion Implantation and Deposition

G.H. Kim, S.A. Nikiforov, Y. Kan, C.H. Cho, Y.W. Choi, H.S. Lee, G.H. Lim, Korean Electrotechnology Research Institute Changwon 641-600, Korea

Comparison of Hot Cathode and Inductively Coupled Discharges for Application in Plasma Immersed Ion Implantation and Deposition

G. H. Kim, S. A. Nikiforov, Y. Kan, C. H. Cho, Y. W. Choi, H. S. Lee, G. H. Lim Korea Electrotechnology Research Institute (KERI),

P. O. Box 20, Changwon, Korea 641-600

Different kinds of gas discharges are being used for large volume steady state plasma generation. They are various glow, radio frequency, microwave, and others. PIII&D technology requires creation of dense (of order 10¹⁰-10¹¹ cm⁻³) uniform plasma of up to several m³ in volume providing high energy and gas efficiency, reliability in a presence of reactive gases and/or high metal ion/atom fluxes. To meet collisionless sheath and proper surface treatment environment conditions low-pressure plasma is preferable.

Comparative analysis of plasma parameters and performance for hot cathode DC and inductively coupled 13.56 MHz RF discharges has been carried out. Both discharges were sustained in the same 18-liter cylindrical processing chamber of the self developed 30 kV experimental PIII&D facility. High emission impregnated cathodes had been used in case of dc discharge. Inductive coupling for RF discharge had been provided using a internal two-half-turn antenna, coated with Al₂O₃. Different operating modes were tested including in situ sputter deposition with simultaneous implantation. Effects of degradation of cathode emission due to coating and contamination of deposited films with cathode impregnated materials and antenna coating have been analyzed. Results are being use in design of 120 kV, 1m³ PIII&D facility which is under developing now.

4P18

Plasma Drift and Non-Uniformity Effects in Plasma Immersion Ion Implantation

M. Keidar, O.R. Monteiro and I.G. Brown, Lawrence Berkeley National Laboratory, Berkeley, CA 94720, USA

Plasma Drift and Non-Uniformity Effects in Plasma Immersion Ion Implantation

M. Keidar*, O.R. Monteiro and I.G. Brown

Lawrence Berkeley National Laboratory University of California Berkeley, CA 94720

Plasma immersion ion implantation (piii) is a technology used to modify material surface properties. By repetitively applying negative high-voltage bias pulses to the substrate, ions are extracted from the plasma, accelerated across the high voltage sheath and implanted into the substrate. The accumulated ion implantation dose for this technique depends upon the ion current drawn by the substrate, which is determined by the sheath expansion during the pulse. We have carried out some measurements of ion saturation current in piii using a filtered vacuum arc metal plasma source. The vacuum arc plasma jet is characterized by its spatial non-uniformity and high ion drift velocity. In order to investigate these effects we have placed the substrate at various distances from the source exit plane and various angles with respect to the jet streaming direction. The bias pulse was up to -8 kV. We found that the ion saturation current increases with applied voltage. We have also measured the dependence of ion saturation current on the angular target position with respect to the plasma stream. A model was developed for the sheath expansion in a non-uniform plasma with substantial drift velocity. We find that generally the nonuniformity and high drift velocity lead to a decrease in the sheath thickness. In a non-uniform plasma, the ion saturation current increases with applied voltage. Predictions of our model were found to be in agreement with experiment.

*Present address: Cornell University, 287 Grumman Hall, Ithaca, NY 14853 (keidar@mae.cornell.edu)

This work was supported by the US DOE under Contract No. AC03-76SF-00098.

Ion Sheath Dynamics in a Plasma for Plasmabased Ion Implantation

M. Yatsuzuka, S. Miki, K. Azuma, E. Fujiwara and O. Ishihara, Himeji Institute of Technology, Himeji, Hyogo 6712201, Japan

Ion Sheath Dynamics in a Plasma for Plasma-based Ion Implantation

M. Yatsuzuka, S. Miki, K. Azuma, E. Fujiwara and O. Ishihara*
 Himeji Institute of Technology
 Himeji, Hyogo 671-2201, Japan
 *Texas Tech University
 Lubbock, TX 79409-3102

Spatial and temporal growth and collapse of ion sheath around an electrode of a negative high-voltage pulse (voltage: -10 kV, pulse duration: 10 µs) have been studied in a plasma for plasma-based ion implantation. A spherical electrode of 1.9 cm in a diameter is immersed in a nitrogen plasma with the plasma density range of 10° to 10¹0 cm³, the electron temperature of 1.4 eV and the gas pressure of 8x10¹⁴ Torr. The transient sheath dynamics was observed by the measurement of electron saturation current to a Langmuir probe, where a depletion of electron saturation current indicates the arrival time of sheath edge at the probe position.

The expanding speed of sheath edge is higher than the ion acoustic speed until the sheath length reaches the steady-state extent determined by Child-Langmuir law. In the region beyond the steady-state extent, the rarefying disturbance produced by sheath expansion continues to propagate into the plasma at the ion acoustic speed. After the pulse voltage is returned to zero (more exactly, the floating potential), the electron current begins to recover. When the pulse fall time is shorter than the plasma transit time, the electron saturation current overshoots the steady-state saturation current at once, resulting in an excess of plasma density which propagates like a tidal wave into the plasma at the ion acoustic speed.

4P20

Electron Beam Ablated Plasma Plumes and Deposited Thin Films of fused Silica

S.D. Kovaleski, R.M. Gilgenbach, L.K. Ang, Y. Y. Lau, University of Michigan, Ann Arbor, MI 48109-2104, USA

Electron Beam Ablated Plasma Plumes and Deposited Thin Films of Fused Silica¹

S.D. Kovaleski, R.M. Gilgenbach, L.K. Ang, Y.Y. Lau

Intense Energy Beam Interaction Laboratory
Department of Nuclear Engineering and Radiological Sciences
University of Michigan
Ann Arbor, MI 48109-2104

Fused silica has been ablated by a channelspark electron beam and depositied as a thin film. The channelspark is a high current, low accelerating voltage electron beam device developed at KFK². The channelspark has an e-beam current of 1.5 kA, accelerating voltage of 15-20 kV, and requires a background gas fill of 15 to 20 mTorr of either Ar or N2. Optical emission spectroscopy reveals the presence of Si I, Si II, and Si III in the ablation plume. The optical emission of these constituents is seen for up to 4 µs. Dye Laser Resonance Absorption Photography (DLRAP) has revealed expansion velocities of the channelspark ablation plumes³ ranging from 0.4 to 1.4 cm/µs. This expansion velocity is dependent both on choice of background gas and gas fill pressure. Resonant Ultra-Violet Interferometry (RUVI) has also been performed on the fused silica ablation plume to determine line integrated neutral Thin films of fused silica ablated by the channelspark have been deposited on substrates. These films are composed predominantly of particulate with diameters of 100's of nm to µm's.

¹Supported by a grant from the National Science Foundation. ²G. Muller and C. Schultheiss, Proc. of Beams 1994, Vol. II, p833.

³S.D. Kovaleski, R.M. Gilgenbach, L.K. Ang, and Y.Y. Lau, Appl. Phys. Lett., **73**, 2576 (1998).

A Steady-State One Atmosphere Uniform DC Glow Discharge Plasma

Igor Alexeff, Mounir Laroussi, Weng Lock Kang and Ali Alikafesh, University of Tennessee, Knoxville, TN 37996-2100, USA

A Steady-State One Atmosphere Uniform DC Glow Discharge Plasma

Igor Alexeff, Mounir Laroussi¹, Weng Lock Kang, and Ali Alikafesh; University of Tennessee.

We have produced a one-atmosphere DC glow discharge plasma with a density (so far) of 10¹¹ /cm³. The basic discovery is twofold: First, we have found a theorem that shows that any complex AC geometry containing materials of varying dielectric constant can be replaced by a DC system containing materials of varying electrical conductivity. The geometries of the electric field lines are identical, as long as the varying permittivity in the AC system is matched by the varying conductivity in the DC system: Second, we have found a suitable electrode material for the DC case that replaces the dielectriccoated metal electrodes for the AC case. This new electrode material is inexpensive and robust. This new material is presently proprietary (A patent is pending.), but is to be discussed at ICOPS. In addition, we intend to present photographs of the apparatus in operation, as well as samples of the new electrode material.

The advantages of a DC system over an AC system are that it is less expensive and more efficient, as no RF power supply is necessary. Actually, 60 Hz line power can also be used, and a simple neon sign transformer suffices for experimental work. This plasma can be used for chemical and biological decontamination, as well as surface modification.

1. Present address: Applied Research Center, Old Dominion University.

4P22

Effects of Non-Equilibrium Plasmas on Microorganisms

Mounir Laroussi, Igor Alexeff, Old Dominion UniversityNewport News, VA23606, USA

Effects of Non-Equilibrium Plasmas on Microorganisms

Mounir Laroussi Applied Research Center Old Dominion University 12050 Jefferson Ave. Newport News, VA 23606

Igor Alexeff
Microwave & Plasma Laboratory
The University of Tennessee
Knoxville, TN 37996-2100

Abstract

Non-equilibrium plasmas have been shown to be excellent sterilization agents [1]-[3]. Garate & Alexeff used a corona discharge, and Laroussi & Sayler used an R.F. driven glow discharge. Also, most recently Alexeff & Laroussi have been able to generate a glow discharge at atmospheric pressure using a DC power source. The use of R.F. and DC driven discharges showed that a large population (~10⁸ per ml) of harmful microorganisms can be neutralized after a few minutes exposure to the plasma. The optimum exposure time is dependent on the type of microorganism, the medium supporting the microorganism, the plasma power density, and the gas mixture used in the discharge [3]. However, the biophysical and biochemical effects leading to the death of the cells of the microorganisms are yet to be understood. In this paper, we discuss the various factors, which play an active role in the cellplasma interaction.

- [1] M. Laroussi "Sterilization of Contaminated Matter with an Atmospheric Pressure Plasma", IEEE Trans. Plasma Sci., Vol.24, No.3, pp. 1188-1191, 1996.
- [2] E. Garate et al. "Atmospheric Plasma Induced Sterilization and Chemical Neutralization", in Proc. IEEE Int. Conf. Plasma Sci., p. 183, 1998.
- [3] M. Laroussi et al. "Images of Biological Samples Undergoing Sterilization by a Glow Discharge at Atmospheric Pressure", IEEE Trans. Plasma Sci. Special Issue on Images in Plasma Sci., Vol.27, No.1, 1999.

Characteristics of a barrier discharge in monatomic gases

R. Sankaranarayanan, B. Pashaie and S. K. Dhali, Southern Illinois University, Carbondale, IL 62901, USA

Characteristics of a barrier discharge in monatomic gases

R. Sankaranarayanan, B. Pashaie, and S. K. Dhali Department of Electrical Engineering Southern Illinois University Carbondale, Illinois 62901

Experiments in a simple parallel-plate dielectric-barrier discharge show that the structure of monatomic gases is very differently from molecular gases. Time-resolved images show diffused discharge for monatomic gases and filamentary discharge for molecular gases. In addition, current waveforms also show a marked difference.

Two-dimensional streamer calculation show that in a monatomic gas the discharge is diffused compared to molecular gases. The high ionization coefficient at low reduced field, the high diffusion constant and the high secondary ionization coefficient of monatomic gases can account for these differences.

Also an empirical relationship for power and voltage is derived which shows good agreement with experimental results for both monatomic and molecular gases.

This work was partially supported by funding from ${\tt NSF}$

4P24

Diagnostic of hydroxyl radical concentration in high pulse voltage triggered dielectric barrier discharges

C. Hibert, I. Gaurand, O. Motret, M. Nikravech, R. Viladrosa and J. M. Pouvesle, University of Orleans, BP 6759 45007 Orleans Cedex 2, France

Diagnostic of hydroxyl radical concentration in high pulse voltage triggered dielectric barrier discharges

C. Hibert, I. Gaurand, O. Motret, M. Nikravech, R. Viladrosa and J.M. Pouvesle. GREMI, UMR 6606, University of Orléans BP 6759 45067 Orléans Cedex 2 - France

Dielectric barrier discharges (DBDs) are well known to be non-thermal, cold discharges which are used in the treatment of different types of pollutants such as volatile organic compounds (VOCs) or flue gases.

The hydroxyl radical (*OH) is a very efficient oxidant species and represents an important agent in the pollutant remediation. An estimation of potentialities of depollution processes involve notably a good kwnoledge of the hydroxyl concentration and its time evolution. Classically the *OH concentration measurements are realized by LIF principally in the earth atmosphere and in flames. This technique seems not to be very well adapted to filamentary DBD plasmas and represents a rather expensive investment.

We have developed a diagnostic of absolute concentration measurement based on a time resolved resonant absorption spectroscopy. The probe signal *OH($A^2\Sigma^+$ - $X^2\Pi$, $\lambda \approx 308$ nm) is generated in a high pulse voltage triggered DBD probe. The gas mixture (1 atm argon + 200 ppm water vapor) was optimized to adjust lifetime and intensity of the *OH(A-X) UV fluorescence. This signal is sent through the main DBD plasma. After absorption, the output signal is used to calculate the *OH(X) concentration in the main discharge. The delay between the onset of the main discharge and the probe pulse can be adjusted in order to probe the fondamental level *OH(X) during the whole post-discharge.

This diagnostic has been tested first in argon + water vapor mixtures. Various effects of discharge parameters like input energy or water vapor concentration on the ${}^{\bullet}OH(X)$ density have been clarified. Next more practical gas mixtures like air + water vapor + pollutant (TCE) mixtures have been investigated. The temporal decay of ${}^{\bullet}OH(X)$ radical concentration with and without TCE has been studied. The decay frequency of ${}^{\bullet}OH(X)$ is in good agreement with the literature data and allows to valid this diagnostic.

A Low Frequency Impedance Matching Circuit for a one Atmosphere Uniform Glow Discharge Plasma (OAUGDP) Reactor

Zhiyu Chen, Daniel M. Sherman, Rami B. Gadri, Fuat Karakaya and J. Reece Roth, University of Tennessee, Knoxville, TN 37996-2100, USA

A LOW FREQUENCY IMPEDANCE MATCHING CIRCUIT FOR A ONE ATMOSPHERE UNIFORM GLOW DISCHARGE PLASMA (OAUGDP) REACTOR*

Zhiyu Chen, Daniel M. Sherman, Rami B. Gadri, Fuat Karakaya and J. Reece Roth

UTK Plasma Sciences Laboratory Department of Electrical Engineering University of Tennessee Knoxville, TN 37996-2100

ABSTRACT

The One Atmosphere Uniform Glow Discharge Plasma (OAUGDP)^[1] is capable of operating at one atmosphere in air and other gases, and its active species can be used, among other things, to sterilize and decontaminate surfaces. The OAUGDP can be operated in a wide range of geometrical configurations, ranging from a slab plasma between parallel plates^[1], to a plasma layer which can cover an isolated flat or curved surface^[2]. The OAUGDP reactor requires a power supply which is capable of delivering a few kilowatts at a frequency of a few kilohertz, and an rms voltage up to 20 kilovolts.

The OAUGDP reactor with plasma on can be modeled as two or three capacitors in parallel with a resistor. The non-ideality of the transformer between the RF power supply and the plasma reactor also has an imaginary part in its impedance. Thus, the whole load of the power supply, seen by its output terminals, is highly reactive. The impedance mismatch resulting from the absence of a matching network can cause a large reflected power from the load which does not contribute to plasma formation, but requires an expensive over-rated power supply. In addition, the reactive current can deposit charge on the surface of the dielectric which does not face the plasma. This will disturb the "memory" voltage^[3], and may complicate attempts to achieve a uniform (as opposed to filamentary) discharge. In this paper, we will present the design details of a new impedance matching circuit which matches the load at the primary side of the transformer. This arrangement avoids dealing with impedance matching components at high voltage in the secondaryside matching circuit presented in our last year's paper. Some new data and improvements of plasma reactor operation will also be presented.

- *Supported in part by a DoD STTR subcontract from Environmental Elements Corporation of Baltimore, MD and a Research Agreement with March Instruments, Inc. of Concord, CA
- 1.) Roth, J. R. (1995): <u>Industrial Plasma Engineering: Volume I Principles.</u>
 Institute of Physics Press, Bristol, UK ISBN 0-7503-0318-2, Section 12.5.2.
- 2.) Roth, J. R.: Method and Apparatus for Covering Bodies with a Uniform Glow Discharge Plasma and Applications Thereof, U. S. Patent 5,669,583, Issued Sept. 23, 1997.
- 3.) Massines, F.; Rabehi, A.; Decomps, Ph.; Gadri, R. B.; Ségur, P.; Mayoux, C.: "Experimental and Theoretical Study of a glow discharge at atmospheric pressure controlled by dielectric barrier", Journal of Applied Physics, Vol. 83, N 6, pp 2950-2957, March 1998.

4P26

Atmospheric Pressure Plasma for Decontamination of Chem/Bio Warfare Agents

H.W. Herrmann, G.S. Selwyn, I. Henins, J. Park, Los Alamos National Laboratory, Los Alamos, NM 87545, USA

Atmospheric Pressure Plasma for Decontamination of Chem/Bio Warfare Agents

H.W. Herrmann, G.S. Selwyn, I. Henins, J. Park Los Alamos National Laboratory

The Atmospheric Pressure Plasma Jet (APPJ) is a unique, capacitively-coupled rf, nonthermal, uniform discharge operating at atmospheric pressure with a high flow of He/O2 feedgas. The APPJ generates highly reactive atomic and metastable species of oxygen and directs them onto a contaminated surface at high velocity. This may provide a much needed method of decontamination of CBW agents which, unlike traditional decon methods, is dry and nondestructive to sensitive equipment. The reactive effluent of the APPJ at 175°C has been shown to kill Bacillus globigii spores, a surrogate for Anthrax, with a D value (time to reduce viability by a factor of 10) of 4.5 sec at a standoff distance of 0.5 cm. This is 10 times faster than hot gas at the same temperature and requires 80% less energy input to achieve the same level of kill. This D value is also an order of magnitude better than achieved by other nonthermal plasma discharges, and unlike these other discharges, the APPJ provides a downstream process which can be applied to all accessible surfaces with no need for the contaminated object to fit within a chamber. Through active cooling of the electrodes we have also achieved a D value of 15 sec at an effluent temperature of just 75°C, making the decontamination of personnel a definite possiblity. The APPJ has also been shown to oxidize surrogates of the CW agents, Mustard and VX, and a collaborative effort is now proceeding with the actual agents at the Edgewood Chem/Bio Center (ECBC, formerly ERDEC). Efforts are now being directed towards reducing the consumption of He and increasing the working stand-off distance.

A New Electrothermal-Chemical Method for Metals Carbides and Ceramics Hard Coating: Experiment and Theory

D. Zoler, C. Bruma, S. Cuperman, Tel-Aviv University, Tel-Aviv, 69978, Israel

A NEW ELECTROTHERMAL-CHEMICAL METHOD FOR METALS CARBIDES AND CERAMICS HARD COATING. EXPERIMENT AND THEORY.

D. Zoler, C. Bruma, S. Cuperman Raymond and Beverly Sackler Faculty of Exact Sciences. School of Physics and Astronomy, Tel-Aviv University, Tel-Aviv 69978, Israel. S. Wald

Propulsion Physics Laboratory, Soreq NRC. Yavne 81800, Israel.

A new method and an experimental device for powders of metals, carbides and ceramics coating of various substrates are presented. The powder-particles are accelerated and heated by a mixture of plasma and gases resulted from the burning of an energetic (propellant). The operating prototype already allows one to obtain coatings of metals. carbides and ceramics. Some of the coatings obtained, especially those by carbides powders. indicate even at the present stage of research, properties (as hardness. porosity) which are comparable to those provided by the presently industrial methods in use. The accelerating-heating agent in our device (the plasma-gas mixture) is characterized by very high densities (up to 120 kg/m^3), temperatures (up to 20000 K) and velocities (more than 1500 m/s). Due to these characteristics, the powder particles are accelerated to velocities significantly higher than those reached in other coating devices as, for example, the detonation (D) gun. Some preliminary experimental data show that the accelerated particle can reach velocities higher than 1000 m/s. In parallel, in order to better understand the phenomena taking place inside the device and to determine the optimal process parameters leading to high quality coatings an appropriate theoretical model was developed. The model is able to describe the complex processes of plasma-gas-propellant interaction, gas flow and powder particles heating and acceleration. The model gives a detailed description of the gas, propellant and accelerated particle parameters, their spatial distribution and temporal evolution; predicts their dependence on the values of some input quntities such as: the plasma energy, propellant characteristics and accelerated particles type and geometry. The computational results we obtained show that, indeed, during the acceleration process the par-ticles are heated, melted and eventually vaporized. One of the most interesting theoretical results is that the particles exit velocity is practically independent on the particle dimensions (diameter) and mass. This result as well as the predicted values of particle exit velocity are in good agreement with some preliminary experimental data we obtained.

4P28

Constrained Evolutionary Optimization of the Signal Growth rate in an RKO with an Axially Varying Waveguide Diameter

Laurence D. Merkle and John W. Luginsland, U.S. Air Force Research Laboratory, Kirtland AFB, NM 87117, USA

Constrained Evolutionary Optimization of the Signal Growth Rate in an RKO with an Axially Varying Waveguide Diameter

Laurence D. Merkle, John W. Luginsland
Air Force Research Laboratory
Directed Energy Directorate
Center for Plasma Theory and Computation
AFRL/DEHE, Kirtland AFB, NM 87117

The relativistic klystron oscillator (RKO) is a high power microwave (HPM) source based on enhancing mature non-relativistic klystron technology, in which the kinetic energy of a population of electrons is converted into coherent microwave radiation. There is significant interest in maximizing the growth rate of the RKO's microwave signal as a function of the RKO design parameters.

A model relating the growth rate to the beam voltage, beam current, and gap separation is generalized to reflect dependence on additional device parameters. Specifically, the lumped circuit model from which resonant frequencies of the cold tube are determined is extended to allow axial variation of the waveguide diameter, and to reflect the simultaneous existence of the "zero mode" and the "pi mode." These modes have associated frequencies that are up-shifted and downshifted symmetrically (though not necessarily respectively) from the (common) resonant frequency of the driver and booster cavities. The hot tube model is also generalized to reflect the dependence of the stop current on the beam diameter and axial variation of the waveguide diameter.

The growth rate is optimized using a real-valued evolutionary algorithm (EA), which performs mutation, recombination, and selection on a population of candidate design parameters. The limiting and stop currents are treated as non-linear inequality constraints. The best designs identified by the EA are compared using particle-in-cell simulations.

Comparisons of Particle Tracking and Charge Deposition Schemes for a Finite Element Gun Code

E.M. Nelson, K.R. Eppley, J.J. Petillo and S. Humphries Jr., SAIC, Burlington, MA 01803, USA

Comparisons of Particle Tracking and Charge Deposition Schemes for a Finite Element Gun Code* E.M. Nelson, LANL; K.R. Eppley, J.J. Petillo, SAIC, and S. Humphries, Jr., Field Precision

A new finite element gun code is under development. In an effort to improve the gun code model, a concept [1] has been proposed recently that treats fields in a typical way, but includes a unique, formal approach to both particle tracking and source allocation. Being a new approach, there are concerns about the speed, accuracy, and appropriateness of this proposal for the electrostatic, steady-state particle-in-cell (PIC) gun model. In order to resolve some of these issues, a variety of particle tracking and charge deposition schemes are being evaluated with respect to accuracy, speed, robustness, and effect on the model. This includes various methods for computing the electric field at the particle locations. For this study, we are using the SAIC 3D gun code AVGUN as a testbed to incorporate and evaluate these methods. Results of a theoretical analysis of the methods will be presented, and a comparison will be made with the empirical results.

- * Work supported by DOE, contract W-7405-ENG-36, and ONR, NRL contract N00014-97-C-2076.
- [1] Eric M. Nelson and John J. Petillo, "Conceptual Description of a Novel Finite Element Gun Code," ICAP'98.

4P30

Comparison of Electrostatic Wave Energy Levels in Models of Electron Beam-Plasma Interactions D.V. Rose, J.U. Guillory, J.H. Beall, Jaycor, Alexandria, VA 22303, USA

Comparison of Electrostatic Wave Energy Levels in Models of Electron Beam-Plasma Interactions

D. V. Rose, a J. U. Guillory, and J. H. Beallb,c

Institute for Computational Sciences and Informatics
George Mason University
Fairfax, Virginia 22030

A dimensionless stability model that tracks the growth and predation of various wave populations is compared with one-dimensional particle-in-cell (PIC) simulations. The stability model uses rate equations to evaluate the coupling of longitudinal waves created by beam-plasma instabilities in order to estimate beam propagation distances. These wave energies and beam propagation distance estimates are compared with bounded one-dimensional PIC simulations. The onset and saturation of the beam-plasma instabilities are evaluated in the simulations. The simulations enable the stability model to be benchmarked and to explore the temporal evolution of background plasma energy distribution, a capability not presently included in the stability model. The scaleable, dimensionless stability model can be used in laboratory and astrophysical parameter regimes while numerical constraints limit the parameter regimes treatable in the PIC simulations.

¹W. K. Rose, J. Guillory, J. H. Beall, and S. Kainer, Ap. J. **280**, 550 (1984).

^aJaycor, Vienna, VA 22102

^bNaval Research Laboratory, Washington, DC 20375

^cSt. John's College, Annapolis, MD 21404

Implementation of the FRED 2-D Electromagnetic PIC Code on a Distributed Memory Parallel Computer with Application to the Modeling of the Long Conduction time POS

Paul Steen and Eduardo Waisman, Maxwell Technologies, San Diego, CA 92123, USA

Implementation of the FRED 2-D Electromagnetic PIC Code on a Distributed Memory Parallel Computer with Application to the Modeling of the Long Conduction Time POS

Paul Steen and Eduardo Waisman Maxwell Technologies, Inc., San Diego, CA 92123 USA

The efficient implementation of the FRED electromagnetic particle-in- cell (PIC) code on a modern distributed memory supercomputer is made difficult by the conflicting objectives of balancing the computational load and minimizing interprocessor communication. The irregular nature of the Lagrangian particle description in the FRED PIC code results in time-fluctuating data communication patterns which hinder efficient utilization of distributed memory parallel computers because of the resulting overhead for frequent data redistribution and dynamic load balancing. Some possible approaches to the resolution of these issues are presented and experience with one such approach on the LANL Blue Mountain (SGI Origin 2000) computer is discussed.

The motivation for distributed memory implementation of the FRED code is to enable practical calculation of the plasma evolution of plasma opening switches in the 10**14 electron number density, ~100 ns timescale regime for volumes of ~1000 cc. Illustrative examples will be given.

Sponsored by the Defense Threat Reduction Agency

4P32

Preliminary Implementation of Piecewise Linear Conformal Boundaries in ICEPIC

Joseph D. Blahovec, Jr., Gerald E. Sasser, John W. Luginsland, U.S. Air Force Research Laboratory, KAFB, NM 87118-5776, USA

<u>Preliminary Implementation of</u> <u>Piecewise Linear Conformal Boundaries in ICEPIC</u>

JOSEPH D. BLAHOVEC, JR., GERALD E. SASSER, JOHN W. LUGINSLAND, Air Force Research Laboratory, Directed Energy Directorate, Center for Plasma Theory and Computation, Kirtland AFB, NM, JOHN J. WATROUS, NumerEx, Albuquerque, NM. ICEPIC, developed by the Air Force Research Lab, is a 3-D Particle-In-Cell (PIC) code capable of being operated on parallel architectures using either the MPI or PVM message passing standards. ICEPIC utilizes a Cartesian coordinatebased grid system to simulate collisionless plasma physics phenomena, such as those that occur in high power microwave devices. Previous versions of ICEPIC represented curved boundaries by using 'stair-step' approximations. These Cartesian grid 'stair-steps' may cause inaccurate results in certain simulations, particularly in regions of extreme curvature. In order to increase the accuracy of the code, while retaining the computational ease of the Cartesian grid, various methods of embedded and conformal boundaries are considered. Preliminary results of tests of the accuracy and stability of these models are presented.

Progress Toward a Parallel MAGIC

M.H. Bettenhausen, L. Ludeking, D. Smithe, S. Hayes, Mission Research Corporation, Newington, VA 22122-8560, USA

Progress Toward a Parallel MAGIC

M.H. Bettenhausen, L. Ludeking, D. Smithe, S. Hayes

Mission Research Corporation Newington, VA 22122

MAGIC^a is an electromagnetic particle-in-cell code. MAGIC uses the finite-difference time-domain method to support simulations of both two- and three-dimensional geometries with a wide variety of diagnostics and models for outer boundaries, material properties and emission processes. The greater availability of parallel computing platforms has generated interest in a parallel version of MAGIC to enable larger simulations. We are proceeding with an incremental approach to parallelization of MAGIC. An incremental approach will gradually improve the efficiency of the parallel implementation while maintaining the full capability of the MAGIC code. We discuss the recent progress made in implementing loop-level parallelism in MAGIC using OpenMP^b. OpenMP has been chosen because it permits initial loop-level parallelism while also providing for tasklevel parallelism in the future. We also outline future plans for improved parallel execution using domain decomposition of the simulation grid and particles.

Acknowledgments

This research is supported by Mission Research Corporation IRAD funds.

4P34

Analysis of Self-Force Error In Relativistic PIC Simulations

K.L. Cartwright, J.P. Verboncoeur and C.K. Birdsall, University of California, Berkeley, Cory Hall, Berkeley, CA 94720, USA

Analysis of self-force error in relativistic PIC simulations ¹

K. L. Cartwright, J. P. Verboncoeur, and C. K.Birdsall Electronics Research Laboratory University of California, Berkeley, CA 94720

A mathematically and physically rigorous error analysis of Maxwell's equations coupled with Newton-Lorentz equation of motion for relativistic PIC simulations will be given. The goal of this work is an improved PIC algorithm for simulating relativistic plasmas; for example, accelerators and high power microwave tubes. The analysis shows the error of the method in term of Δt and Δx , with computational verification. First, a brief review is presented of the error in the Maxwell and Newton-Lorentz equations analyzed separately. Next, the coupled equations will be analyzed for a single particle. The coupling is accomplished through the use of weighting functions to weight the particle contribution to the source terms of the Maxwell equations, ρ and J, to the grid. The converse operation, weighting the fields back to the particle location, is also considered. Finally, the Klimontovich equation, together with Maxwell's equations, which constitutes an exact description of a plasma, is analyzed. The difference between this and the PIC algorithm de-..nes the error. Refinements and extensions to reduce the error of the classical PIC method are described. The accuracy and stability of these new algorithms, as well as their impact on performance, are examined.

^aB. Goplen, L. Ludeking, D. Smithe and G. Warren, Comp. Physics Comm. **87**(54), (1995).

^bL. Degum and R. Menon, Computational Science & Engineering, 5, No. 1, (1998).

Accurate, Finite-Volume Methods for Three Dimensional Magneto-Hydrodynamics on Lagrangian Meshes

C.L. Rousculp and D. C. Barnes, Los Alamos National Laboratories, Los Alamos, NM 87545, USA

Accurate, Finite-Volume Methods for Three Dimensional Magneto-Hydrodynamics on Lagrangian Meshes, C. L. Rousculp and D. C. Barnes, Los Alamos National Laboratory - Recently developed algorithms for ideal and resistive 3D MHD calculations on Lagrangian hexahedral meshes have been generalized to work with a Lagrangian mesh composed of arbitrary polyhedral cells. This allows for mesh refinement during a calculation to prevent the well known problem of tangling in a Lagrangian mesh. Arbitrary polyhedral cells are decomposed into tetrahedrons. The action of the magnetic vector potential, $\mathbf{A} \cdot \delta \mathbf{l}$, is centered on all face edges of this extended mesh. Thus, $\nabla \cdot \mathbf{B} = 0$ is maintained to round-off error. For ideal flow, $(\mathbf{E} = \mathbf{v} \times \mathbf{B})$, vertex forces are derived by the variation of magnetic energy with respect to vertex positions, $\mathbf{F} = -\partial W_B/\partial \mathbf{r}$. This assures symmetry as well as magnetic flux, momentum, and energy conservation. The method is local so that parallelization by domain decomposition is natural for large meshes. In addition, a simple, ideal-gas, finite pressure term has been included. The resistive diffusion, $(\mathbf{E} = -\eta \mathbf{J})$, is treated with a support operator method, to obtain an energy conservative, symmetric method on an arbitrary polyhedral mesh. The equation of motion is timestep-split. First, the ideal term is treated explicity. Next, the diffusion is solved implicitly with a preconditioned conjugate gradient method. Results of convergence tests are presented. Initial results of an annular Z-pinch implosion problem illustrate the application of these methods to multimaterial problems.

4P36

A Numerical Method for the Solution Of The Magnetic Convection- Diffusion Equation For High Magnetic Reynolds Numbers

C.A. Borghi and A. Cristofolini, University of Bologna, I-40136 Bologna, Italy

A Numerical Method for the Solution of the Magnetic Convection-Diffusion Equation for High Magnetic Reynolds Numbers

C.A. Borghi and A. Cristofolini

Department of Electrical Engineering, University of Bologna, Viale Risorgimento 2, I-40136 Bologna., Italy

In plasma technological applications with high electrical conductivity, magnetic convection can become comparable to or even exceed magnetic diffusion. The physical formulation, derived from the Maxwell equations and Ohm's law, yields the convection-diffusion equation of the magnetic flux density. For high magnetic Reynolds numbers, the first order space derivatives dominate over the second order derivatives. Under these circumstances, special attention must be paid to the numerical solution of the problem.

When utilizing standard methods based on finite difference and finite element formulations to solve convection-diffusion equations, numerical stability is not always reached when the mesh size becomes too large. In the solution of the magnetic field convection-diffusion equation, the mesh size critical value for stability is strongly related to the magnetic Reynolds number. Thus, for increasing values of the conductivity and of the flow velocity, an acceptable solution can be obtained by a reduction of the element size. In order to overcome this problem, upwinding techniques or exponential fitting has been adopted in finite difference methods [1].

A numerical method based on a finite element formulation for the solution of the magnetic convection-diffusion equation has been developed. The method proposed utilizes an upwinding technique as in the finite difference methods mentioned above. A first order set of shape functions has been utilized to approximate the unknown function. In applying the weighted residual method, a second order weighting function has been adopted. An optimal value of the convexity of the weighting function is chosen to obtain an oscillation free solution with a good accuracy.

The method has been utilized to solve the electrodynamics of a discharge in SF₆ at a pressure of 10 MPa and a current of 2 kA.

 C.A. Borghi, A. Cristofolini, G. Minak, "Numerical Methods for the Solution of the Electrodynamics in Magnetohydrodynamic Flows", *IEEE Transactions on Magnetics*, vol. 32, n. 3, pp. 1010-1013, May 1996.

This work sponsored in part by the Accelerated Strategic Computing Initiative (ASCI).

A Fully Implicit Method for the Numerical Solution of the MGD Problem in an SF6 Discharge

C.A. Borghi and A. Cristofolini, University of Bologna, I-40146 Bologna, Italy

A Fully Implicit Method for the Numerical Solution of the MHD Problem in an SF₆ Discharge

C.A. Borghi and A. Cristofolini

Department of Electrical Engineering, University of Bologna, Viale Risorgimento 2, I-40136 Bologna., Italy

A fully implicit method for the numerical solution of the model for the analysis of the discharge in an SF₆ circuit breakers is presented. The numerical model developed is an essential tool for the understanding of the operation of the device, to improve its efficiency and reliability during nominal operation and during faults. The physical formulation of the model [1] is constituted by the continuity equation of mass, momentum and energy, by the state equations of gas and by the convection-diffusion equation of the magnetic flux density, derived from the Maxwell equations and Ohm's law. The main difficulties to deal with, are the presence of a moving boundary between hot gas and the surrounding cold gas, and the strong dependency of plasma conductivity and transport coefficients on temperature. When solving numerically the discharge model, due to the mentioned feature, attempts to explicitly perform the time integration, result in an excessively restricted stability condition on time step. An implicit method, which calculates at each time step the fluid dynamics and the electrodynamics, is needed to overcome the stability problem of the time integration.

A two dimensional time dependent fully implicit method is proposed for the solution of the magneto-plasmadynamic equations. It separately performs the integration in space and in time. The space discretization for the fluid dynamics is carried out by means of a cell vertex scheme based on a unstructured triangular mesh. The same mesh is utilized for the space discretization of the magnetic convection-diffusion equation, which is solved through a finite element scheme. An optimized weighting function is utilized to avoid numerical instabilities. A multi-step technique has been adopted for the time integration. The discretization procedure yields a non-linear system at each time step. The unknowns of the system are the pressure, the density and the velocity components of the gas, and the azimuthal component of the magnetic flux density. The system is solved by means of a inexact Newton method. Convergence is iteratively reached through a GMRES algorithm.

The high current phase of a discharge occurring during the opening of the contact in an SF_6 circuit breakers are considered. The magneto-plasmadynamic regime of the discharge is analyzed. The effect of the magnetic convection and the time derivative of the magnetic flux density are discussed.

[1] C.A. Borghi, A. Cristofolini and P.L. Ribani, "Analysis of Magneto-Plasma Dynamic Transients in a Combustion Gas MHD Generator", Physics of Plasmas, vol. 4, n. 8, pp. 3082-3090, August 1997.

4P38

Trace Hazardous Metals Detection with an Atmospheric Microwave- Generated Plasma Kamal Hadidi, Paul Woskov, Karyn Green, Guadalupe Flores III and Paul Thomas, Massachusetts Institute of Technology, Cambridge, MA 02139, USA

Trace Hazardous Metals Detection with an Atmospheric Microwave-Generated Plasma*

Kamal Hadidi, Paul Woskov, Karyn Green, Gaudalupe Flores III, and Paul Thomas Plasma Science and Fusion Center Massachusetts Institute of Technology Cambridge, MA 02139

A 1.5 kW atmospheric microwave plasma at 2.45 GHz is being developed as an excitation source for real-time detection of hazardous metals in smokestack exhaust. There is currently an important need for metals continuous emissions monitors (CEMs) to meet current and future clean air regulations. A number of plasma generation methods for metals atomic emission spectroscopy are being tested for this application including inductively coupled plasmas (ICPs), laser sparks, dc electrode sparks, and microwave discharges. The microwave plasma has a significant advantage to continuously operate robustly in large volumes of fast flowing (≥ 14 l/minute) air or undiluted stack exhaust. Good performance has been achieved on an incinerator to sensitively ($\sim 1 \mu g/m^3$) and accurately (< 45% relative to EPA method-29) detect lead, chromium, and beryllium. However, it has been found that the excitation of other hazardous metals such as mercury, cadmium, and arsenic is very dependent on the oxygen content of the gas matrix. In a pure nitrogen or noble gas plasma the detection of mercury 253.65 nm, cadmium 228.89 nm, and arsenic 193.73 nm can approach that of Pb, Cr, and Be. However, the intensity of these lines is significantly reduced as oxygen is added. Less than 1% addition of oxygen can dramatically reduce the detection limit of these metals while not effecting other metals such as lead. In addition, the 228.89 nm cadmium line reverses to an absorption feature for a certain range of oxygen content. Experimental measurements will be presented of the performance of this microwave plasma with Hg, Cd, and As as a function of oxygen additive. An attempt will be made to explain the behavior in terms of the possible UV absorption and atomic excitation mechanisms in the plasma.

Radiation Power of Ar Torch Short Plasma as Function of Length near 100A

Toru lwao, Takayuki Ishida, Tatsuya Hayashi, Takahiro Hirano, Masao Endo and Tsuginori Inaba, Chuo University, Tokyo 112-8551, Japan

Radiation Power of Ar Torch Short Plasma as Function of Length near 100A

Toru Iwao, Takayuki Ishida, Tatsuya Hayashi, Takahiro Hirano, Masao Endo and Tsuginori Inaba

When reduction of waste and dissolution of iron are carried out by using arc plasma, we need to put down the arc radiation power, because there are some cases of damaging the furnace wall due to the radiation. On the other hand, we can use it as a clean source for heating materials at new viewpoint. In this case, it's expected that radiation becomes greater. In both cases the radiation power from plasmas has to be precisely controlled.

We measured the radiation power from torch. The radiation power increased in proportion to the 1.8-1.0th power of the current. The radiation power in a unit length increases with the appearance plasma length.

4P40

The Effect of Carbonaceous Deposit for NOx Dissociation by Barrier Discharge

Kazue Fujiwara, Kagehiro Itoyama, Takeshi Yanobe, Nagasaki University, Nagasaki 852-8521, Japan

The Effect of Carbonaceous Deposit for NOx Dissociation by Barrier Discharge

Kazue FUJIWARA*, Kagehiro ITOYAMA*, Takeshi YANOBE**

- *Faculty of Education, Nagasaki University, Nagasaki, 852-8521 Japan.
- **Hokushin Industries Inc., 2-3-6 Shitte, Tsurumi-ku, Yokohama, 230-0003 Japan.

A carbonaceous deposit was formed on the dielectric and the surface of electrodes, when the barrier discharge is generated in the mixed gas of CH₄ and N₂+NO. Authors have done this pre-treatment with changing 60% to 80% for the ratio of CH₄ and N₂+NO gases under the condition of 500 to 700 Torr in pressure. After this pre-treatment was carried out, we introduced N₂+NO gas into chamber. NOx dissociation was done with keeping 700 Torr of pressure in chamber and 300 ml/min of flow rate. Authors investigated the effect of carbonaceous deposit and barrier discharge for NOx dissociation. We measured mass-spectra on NOx by Q-mass. The dielectric is hard glass of 0.15mm in thickness. The length of gap is 0.8mm. An applied potential between electrodes was about ac 4,000 volts (peak value) and its frequency is 4.7 kHz.

In comparison with reduction of NO in present data and the data reported previously[1], which had been used a short gap discharge, the former is 49.3% and the latter is 16.4%. From this result, we concluded that the barrier discharge is more effective. Because a carbonaceous deposit was formed widely on the surface of electrodes in barrier discharge than in short gap discharge.

Reduction of NO with carbonaceous deposit is larger than that without one for NOx dissociation. In the case without carbonaceous deposit, the ratio of the rate of increase of O_2 to the rate of decrease of NO is about 2: 1. The following reaction is considered from mentioned above.

$$2NO \rightarrow N_2 + O_2 \tag{1}$$

In case that the carbonaceous deposit was formed, a ratio of the rate of increase of O_2 to the rate of decrease of NO is 1.1. From the result, authors discussed on the different reaction from the above reaction.

In case of short gap discharge, authors had concluded that C_2H_2 is generated by the decomposition of carbonaceous deposit and increases in momentary at a beginning of discharge. The carbonaceous deposit formed in pre-treatment was composed of double or triple combination of carbon and hydrogen from results of FT-IR analysis. However, we can not find the change of C_2H_2 in barrier discharge. From this result authors regard as the different composition of carbonaceous deposit on the electrode and the dielectric surfaces.

Reduction of NO by barrier discharge is larger than that by short gap discharge.

Reduction of NO with carbonaceous deposit is larger than that without one for NOx dissociation.

[1]K.Itoyama, K.Fujiwara, H.Eguchi, T.Yanobe: The effect of carbonaceous deposit for NOx dissociation, Bulletin of the American Physical Society, GEC-51/ICRP-4, vol.43, No.5, p.1489, 1998.

Study of pulsed HF discharge in N2/O2/NO for gas cleaning

M. Baeva, H. Gier, A. Pott, J. Uhlenbusch, University of Dusseldorf, Dusseldorf, Germany

Study of pulsed HF discharge in N2/O2/NO for gas cleaning

M. Baeva, H. Gier, A. Pott, J. Uhlenbusch

Institute of Laser and Plasma Physics, University of Düsseldorf, Universitätsstr. 1, D-40225 Düsseldorf, Germany

The aim of the study is the reduction of NO_x components in exhaust gases by means of a pulsed microwave discharge. The discharge is operated in $N_2/O_2/NO$ mixtures under atmospheric pressure. Contrary to cw operated microwave discharges, pulsed systems show strong non-thermal behavior. Discharge chambers have been developed with resonance frequencies near 2.45 and 3 GHz. Pulse duration of several of microseconds up to 50 μs and repetition frequencies of 50Hz-25kHz are typical for these experiments.

The spatial and temporal resolved rotational and vibrational excitation of N_2 molecules has been investigated using coherent anti-Stokes Raman scattering (CARS) technique. The concentration of NO_x compounds produced during the discharge has been detected by means of FTIR measurements.

A model has been developed to describe the chemical and vibrational kinetics in the discharge. A large number of chemical processes between neutral and charged particles is taken into account. The excitation of vibrational levels of the ground electronic states of N_2 , O_2 and NO molecules as well as the metastable states of N_2 and O_2 have been considered. The rates of the processes with electrons are calculated by solving the Boltzmann equation for the electrons. Published data for the other processes are used. A global energy balance is applied to determine the electric field. The model delivers the temporal behavior of the concentrations of all species under consideration. The vibrational temperature of N_2 and O_2 molecules follow from the population densities of the vibrationally excited levels.

De Anza Ballroom 8:30 AM, Wednesday, June 23, 1999

Plenary Talk

Plasma Science and Applications Committee Award Address

Simple models on some nasty problems in beams and plasmas

Prof. Y.Y. Lau
University of Michigan

Chairperson

Dr Virginia Ayres

Michigan State University,

Oral Session 5A Plasma, Ion and Electron Sources

Chairperson
Paul Chu
City University of Hong Kong

5A01-2

Invited -

Large-Area Plasma Processing System

R.F. Fernsler, W.M. Manheimer, R.A. Meger, D.P. Murphy, D. Leonhardt, R.E. Pechacek, S.G. Walton and M. Lampe, U.S. Naval Research Laboratory, Washington, DC 20375-5346, USA

Large-Area Plasma Processing System*

R. F. Fernsler, W. M. Manheimer, R. A. Meger, D. P. Murphy, D. Leonhardt, R. E. Pechacek, S. G. Walton and M. Lampe Plasma Physics Division, Naval Research Laboratory, Washington, DC 20375-5346

The Naval Research Laboratory has developed a new type of plasma processing reactor called the Large-Area Plasma Processing System (LAPPS). This device uses a magnetically confined, sheet electron beam to produce planar plasmas with densities up to 5×10^{12} cm⁻³, area ~ 1 m², and thickness ~ 1 cm. Other LAPPS attributes include: high uniformity; operation over a wide range of gas type and pressure; independent control of the ionization rate; efficient production of ions and free radicals; low metastable density; modest gas heating; a low and partially adjustable electron temperature; and independent bias control. Disadvantages of LAPPS include: the need for an energetic electron beam (a few keV and 10's mA/cm²); the need for a longitudinal magnetic field (~ 200 G) to confine the beam; cross-field restrictions on the plasma flow; beam-plasma instabilities; and energy losses to the beam dump. This talk will present the theory underlying LAPPS, while the experimental results and future plans will be presented elsewhere [1].

*Work supported by the Office of Naval Research.

†SFA Inc., Landover, MD 20785

[1] D. Leonhardt, et al., this conference.

Development of Hollow-Cathode Plasma Electron Gun for Operation at Forepump Gas Pressure

Viktor Burdovitsin, Alexey Mytnikov and Efim Oks, State University of Control Systems and Radioelectronics, TUSUR, Tomsk 634055, Russia

DEVELOPMENT OF HOLLOW-CATHODE PLASMA ELECTRON GUN FOR OPERATION AT FOREPUMP GAS PRESSURE

Viktor Burdovitsin, Alexey Mytnikov and Efim Oks

State University of Control Systems and Radioelectronics, 40 Lenin Ave., Tomsk, 634050, Russia

The characteristics, performance and design feature of a new version of a filamentless plasma-cathode electron gun for beam generation in the forepump gas pressure range are presented. The plasma cathode is based on a hollow cathode dc discharge. Using the method of "grid stabilization" it was possible to generate an ebeam at a background gas pressure as high as about 10⁻¹ Torr. This pressure can be easily obtained by using mechanical pump only.

The electrode configuration of the plasma-cathode e-gun consists of a 50 mm diameter, 100 mm length hollow cathode, plane anode, and electron extractor. The hollow cathode bottom has a centric hole; its diameter was either $d_{\rm c}=16$ mm or 25 mm. Electrons are extracted from the plasma surface through the anode hole of $d_{\rm a}=16$ mm. The extractor hole has the same diameter ($d_{\rm c}=d_{\rm a}$), and distance of the accelerating gap is 10 mm. The hollow cathode was made from stainless steel, and anode and extractor were made from copper. There are also ceramic insulators and an air cooling system. To produce an axial magnetic field (up to 0.1 T) both in discharge and accelerating regions a solenoid coil was used.

The operation of the gun with a magnetic field up to 0.1 T was investigated. The presence of a magnetic field (*B*-field) is often required, for instance in plasma chemistry and surface treatment processes. The effect of the *B*-field both on discharge and emission parameters of the gun observed. The results obtained can be explained based on the concept of electron confinement by a magnetic field and their motion across the *B*-field.

With the accelerating voltage up to 8 kV, the gun is able to generate of about 0.7 A dc electron beam. Our previous publication concerning the first version of the hollow cathode plasma e-gun as well as about general properties of plasma e-guns one can find in [1] and [2] correspondingly.

1. A. Mytnikov, E. Oks, A. Chagin, Instruments and Experimental Technique, 41, 234 (1998).

2. E.M. Oks, Plasma Sources SCI. Technol. 1, 249 (1992).

5A04

Carbon Shunting Arc and Its Induced Plasma and DLC Film Deposition

Ken Yukimura, Ryoto Isono and Kenji Yoshioka, Doshisha University, Kyotanabe Kyoto, Japan

Carbon Shunting Arc and Its Induced Plasma and DLC Film Deposition

Ken Yukimura, Payoto Isono and Kenji Yoshioka Department of Electrical Engineering Faculty of Engineering, Doshisha University Pelectronic mail: kyukimur@mail.doshisha.ac.jp

Plasma Based Ion Implantation PPBII) technology is a promising method for realizing uniform ion implantation into materials with three dimensional topologies. Recently, a conformal implantation has become possible using a combination of a pulsed discharge with a pulsed bias of the materials. Non-gaseous plasmas such as carbon and tungsten with a high melting point are desirable as they can be produced without any external trigger devices. We think that a shunting arc is a promising method for creating a pulsed arc using the above materials without any trigger sources. This report is concerned with the production of DLC using shunting arcs as well as the formation of the shunting arc and its induced gaseous plasma. In addition, the possibility of a hybrid PBII system including gaseous and non-gaseous ions will be discussed. A shunting arc is a pulsed arc discharge, self-ignited in a low pressure gas without external trigger source and its current is easily attained to 1000A with a sinusoidal waveform. The shunting arc is created using a carbon rod at an air pressure of 0.1 Pa and expands at about 20km/s. Due to the grounding of the positive side of the charged capacitor bank, the arc is negatively biased to the grounded vacuum chamber. This causes a newly developed plasma to form in the chamber which has a gaseous content of nitrogen, whereas the shunting arc has carbon abundant plasma. Thus, there are two kinds of plasma existing in one process of the arcing. This is clarified by the temporal behavior of the spectra emitted from the plasma. During the shunting arcs. carbon and nitrogen spectra appear, whereas only nitrogen spectra are observed after the shunting arcs. The induced plasma from the shunting arc lasts more than 100 µs because the plasma has a high impedance due to a low density gaseous plasma formation. Several methods of ion implantation and deposition are possible using this process which features a new type of a hybrid PBII facility that includes non-gaseous and gaseous species.

Recent Advances in Plasma-based Ion Sources for Commercial Ion Implantation of Semiconductors

T.N. Horsky and B.H. Vanderberg, Eaton Corporation SEO, Beverly, MA 01915, USA

Recent Advances in Plasma-Based Ion Sources for Commercial Ion Implantation of Semiconductors

T. N. Horsky and B.H. Vanderberg
Eaton Corporation Semiconductor Equipment Operations, Beverly,
MA, 01915

Commercial Ion Implanters have always used plasma sources to generate the dopant ions which form the implanter ion beam. This variable-energy beam is used to modify the electrical properties of silicon wafer substrates. We will describe some of the source technologies which have recently been developed specifically for ion implant. The standard technology in the industry is the Enhanced Bernas hot cathode arc discharge source¹, but more recently an indirectly-heated cathode version has been developed which yields more attractive production performance and reliability². Both of these design configurations have been further customized by OEM's, for example by implementing dual emitter configurations. The implant application of RF ion sources will also be discussed and a historical context will be established, focusing on the advantages of the relatively cold plasma provided by the RF source technology originally developed for neutral beam injection in fusion research³.

Certain of these developments have become enabling technologies for new semiconductor processes. The required applications space of CMOS processing, for example, has been expanded to require the production of high perveance ion beams of a few hundred eV, and also low perveance beams of several MeV. The results of these recent design innovations has resulted in customized source designs for specific regions of the required applications space.

- D.R. Swensen, A. Renau, S.R. Walther and M.E. Mack, IEEE Proc. 11th Int. Conf. on Ion Implantation Technol., Austin, TX, 1(1) 283-286, June 16-21, 1996.
- 2. T.N. Horsky, Rev. Sci. Instrum. 62(2) 840-843 (1998).
- I.G. Brown, The Physics and Technology of Ion Sources, Chap. 17 (Wiley & Sons, New York, 1989).

5A06

TiN coating to Three Dimensional Materials by PBII Using Vacuum Titanium Arc Plasma

Masanori Sano and Ken Yukimura, Toshiro Maruyama, Akiyoshi Chayahara and Yuji Horino, Doshisha University, Kyotamake, Kyoto, Japan

TiN Coating to Three-Dimensional Materials by PBII Using Vacuum Titanium Arc Plasma

Masanori Sano and Ken Yukimura^a
Department of Electrical Engineering, Doshisha University
^{a)}e-mail: kyukimur@mail.doshisha.ac.jp

Toshiro Maruyama
Department of Chemical Engineering, Kyoto University
e-mail: maruyama@cheme.kyoto-u.ac.jp

Akiyoshi Chayahara and Yuji Horino^b Osaka National Research Institute ^{b)}e-mail: horino@onri.gp.jp

Plasma-based ion implantation (PBII) is a promising method for modifying the surface properties of materials in order to improve wear resistance and hardness in engineering fields. Our PBII facility for obtaining metal ions consists of a metal plasma source in the same vacuum chamber with a substrate and has an advantage that the thin film preparation and the ion implantation are simultaneously carried out. A water-cooled titanium cathode was mounted with a trigger electrode. The vacuum chamber was grounded to make an anode. A trigger discharge was ignited by disconnecting the trigger electrode from the cathode to generate a DC metal-arc of 70A between cathode and grounded chamber. For suppressing the trigger-discharge current after the main arc ignition, a resistance of 1 ohm is provided in the trigger discharge circuit. In Plasma Based Ion Implantation (PBII) using a titanium vacuum arc of DC 70A with a pulse voltage of -40kV/20 μ s, titanium nitride (TiN) films were coated on a silicon substrate (p-type, (111)). The shapes of substrate holders were trench, sphere (40mm in diameter) and triangle (angles of 30, 45 and 60°). Titanium nitride (TiN) thin films have been prepared using nitrogen ions reacting with titanium atoms by the process time of 2min. For the substrate distance from the arc source are 150mm and 400, number of Ti atoms are about 2040 × 10¹⁵ and 320 × 1015 atoms/cm2, respectively for pulsed voltage of $-30kV/20 \mu$ s. This result indicates that there is a divergent flow of Ti particles to the substrate from the arc source. The XPS results indicate that the Ti ions are implanted inside the silicon substrate. The thickness of the implanted layer is independent of the tilt angle ϕ of the substrate, whereas TiN deposition thickness depends on $\sin \phi$ for ϕ from 0° to 90°. Ti atoms was also recognized on the back wall ($\phi = 0^{\circ}$ to -60°) of the substrate holder. When the Ti ions were implanted into the walls of the trench-shaped substrate holder, the implantation depth in the inner side wall was shorter than those in the outer side and bottom wall of the trench.

High Current Vacuum Arc Ion Source for Heavy Ion Fusion

N.Qi, J. Schein, S. Gensler, R. R. Prasad, M. Krishnan, I. Brown, Alameda Applied Sciences Corporation, San Leandro, CA 94577, USA

High Current Vacuum Arc Ion Source for Heavy Ion Fusion

N. Qi, J. Schein, S. Gensler, R. R. Prasad and M. Krishnan Alameda Applied Sciences Corporation, San Leandro, CA 94577

Ian Brown

Lawrence Berkeley National Laboratory, Berkeley, CA 94720

Heavy Ion Fusion (HIF) is one of the approaches for the controlled thermonuclear power production. A source of heavy ions with charge states 1+ to 2+, in ≈0.5 A current beams with ≈20 µs pulse widths and ~10 Hz repetition rates are required. Thermionic sources have been the workhorse for the HIF program to date, but suffer from slow turn-on, heating problems for large areas, are limited to low (contact) ionization potential elements and offer relatively low ion fluxes with a charge state limited to 1+. Gas injection sources suffer from partial ionization and deleterious neutral gas effects.

The above shortcomings of the thermionic ion sources can be overcome by a vacuum arc ion source. The vacuum arc ion source[1] is a good candidate for HIF applications. It is capable of providing ions of various elements and different charge states, in short and long pulse bursts, with low emittance and high beam currents.

Under a Phase-I STTR from DoE, the feasibility of the vacuum arc ion source for the HIF applications is investigated. An existing ion source at LBNL was modified to produce ≈0.5 A, ≈60 keV Gd (A≈158) ion beams. The experimental effort concentrated on beam noise reduction, pulse-to-pulse reproducibility and achieving low beam emittance at 0.5 A ion current level. Details of the source development will be reported.

- * Supported by DoE-STTR, Contract # DE-FG03-98ER86071.
- I. G. Brown, "Vacuum arc ion sources", Rev. Sci. Instrum. 65, 3061 (1994).

5A08

Hydrogen and Hydrogegn-Argon Discharge Measurements and Models of a Compact Microwave ECR Plasma Source

M.H. Tsai and T. A. Grotjohn, Michigan State University, East Lansing, MI 48824, USA

Hydrogen and Hydrogen-Argon Discharge Measurements and Models of a Compact Microwave ECR Plasma Source

M.-H. Tsai and T. A. Grotjohn Electrical and Computer Engineering Michigan State University East Lansing, MI 48824

Hydrogen discharges and hydrogen-argon discharges are created and studied in a compact microwave ECR plasma source operating in the 0.4-5 mTorr pressure range. The source[1] has a discharge region of 3.6 cm in diameter and an excitation volume of 50 cm³. The plasma species diffuse out of the source into a larger materials processing region. The discharge is excited at a frequency of 2.45 GHz with input power levels of 50-90 watts. Measurements of the ion density, electron temperature, and absolute atomic hydrogen concentration are performed using Langmuir probes, OES and actinometry. Measurements are performed in both the source/excitation region and in the downstream processing region. A global model for the discharges in this plasma source and a downstream charge particle diffusion model are also developed. The features of these plasma discharges determined by the combined measurements and models include a source region ion density in the 10¹¹ cm⁻³ range, which corresponds to an ionization ratio of 0.001 to 0.01. The dominant ion species in the pure hydrogen discharge was ${\rm H_2}^+$. Also, it was found for the hydrogen discharge that the electron temperature was in the range 5-14 eV, the atomic hydrogen molar fraction was measured as 8-25% with an increasing fraction at higher pressures, and the surface recombination coefficient of atomic hydrogen was determined to be approximately 0.001. The global model developed includes a term to account for magnetic confinement/electron heating enhancement by the ECR magnets in the source. The global model is also compared to a two-dimensional self-consistent microwave field and plasma simulation model[2] at selected operating points.

[1] J. Asmussen, R. Fritz, L. Mahoney, G. Fournier, and G. Demaggio, Rev. Sci. Instrum., 61, 282, 1990
[2] T. A. Grotjohn, Rev. Sci. Instrum., 67, 921, 1996.

De Anza II 10 AM, Wednesday, June 23, 1999

Oral Session 5B Fast Wave Devices and Intense Beams

Chairperson
Steve Gold
Naval Research Laboratory

5B01-2

Invited -

Analytical Theory of Multi-State Gyro-Amplifiers G.S. Nusinovich and B. Levush, University of Maryland, College Park, MD 20742-3511, USAA

Large-Area Plasma Processing System*

R. F. Fernsler, W. M. Manheimer, R. A. Meger, D. P. Murphy, D. Leonhardt, R. E. Pechacek, S. G. Walton and M. Lampe Plasma Physics Division, Naval Research Laboratory, Washington, DC 20375-5346

The Naval Research Laboratory has developed a new type of plasma processing reactor called the Large-Area Plasma Processing System (LAPPS). This device uses a magnetically confined, sheet electron beam to produce planar plasmas with densities up to 5×10^{12} cm⁻³, area ~ 1 m², and thickness ~ 1 cm. Other LAPPS attributes include: high uniformity; operation over a wide range of gas type and pressure; independent control of the ionization rate; efficient production of ions and free radicals; low metastable density; modest gas heating; a low and partially adjustable electron temperature, and independent bias control. Disadvantages of LAPPS include: the need for an energetic electron beam (a few keV and 10's mA/cm2); the need for a longitudinal magnetic field (~ 200 G) to confine the beam; cross-field restrictions on the plasma flow; beam-plasma instabilities; and energy losses to the beam dump. This talk will present the theory underlying LAPPS, while the experimental results and future plans will be presented elsewhere [1].

*Work supported by the Office of Naval Research. †SFA Inc., Landover, MD 20785

[1] D. Leonhardt, et al., this conference.

Dynamic Simulation of Mode Selective Extended Interaction Cavity for Wideband, High Power Gyrotron Applications

A.T. Lin, H. Guo and V. Granatstein, University of California, Department of Physics, Los Angeles, CA 90095-1547, USA

DEVELOPMENT OF HOLLOW-CATHODE PLASMA ELECTRON GUN FOR OPERATION AT FOREPUMP GAS PRESSURE

Viktor Burdovitsin, Alexey Mytnikov and Efim Oks

State University of Control Systems and Radioelectronics, 40 Lenin Ave., Tomsk, 634050, Russia

The characteristics, performance and design feature of a new version of a filamentless plasma-cathode electron gun for beam generation in the forepump gas pressure range are presented. The plasma cathode is based on a hollow cathode dc discharge. Using the method of "grid stabilization" it was possible to generate an ebeam at a background gas pressure as high as about 10⁻¹ Torr. This pressure can be easily obtained by using mechanical pump only.

The electrode configuration of the plasma-cathode e-gun consists of a 50 mm diameter, 100 mm length hollow cathode, plane anode, and electron extractor. The hollow cathode bottom has a centric hole; its diameter was either $d_{\rm c}=16$ mm or 25 mm. Electrons are extracted from the plasma surface through the anode hole of $d_{\rm a}=16$ mm. The extractor hole has the same diameter ($d_{\rm c}=d_{\rm a}$), and distance of the accelerating gap is 10 mm. The hollow cathode was made from stainless steel, and anode and extractor were made from copper. There are also ceramic insulators and an air cooling system. To produce an axial magnetic field (up to 0.1 T) both in discharge and accelerating regions a solenoid coil was used.

The operation of the gun with a magnetic field up to 0.1 T was investigated. The presence of a magnetic field (*B*-field) is often required, for instance in plasma chemistry and surface treatment processes. The effect of the *B*-field both on discharge and emission parameters of the gun observed. The results obtained can be explained based on the concept of electron confinement by a magnetic field and their motion across the *B*-field.

With the accelerating voltage up to 8 kV, the gun is able to generate of about 0.7 A dc electron beam. Our previous publication concerning the first version of the hollow cathode plasma e-gun as well as about general properties of plasma e-guns one can find in [1] and [2] correspondingly.

- 1. A. Mytnikov, E. Oks, A. Chagin, Instruments and Experimental Technique, 41, 234 (1998).
- 2. E.M. Oks, Plasma Sources SCI. Technol. 1, 249 (1992).

5B04

A Smith-Purcell Free Electron Laser Based on an X-Band Photoinjector

E. Schamiloglu, S.R.J. Brueck and F. Hegeler, R.V. Hartemann, E.C. Landahl, A.L. Troha, C.H. Ho, J.P. Heritage, H.A. Baldis and N.C. Luhmann Jr., University of New Mexico, Albuquerque, NM 87131,

A SMITH-PURCELL FREE ELECTRON LASER BASED ON AN X-BAND PHOTOINJECTOR

E. Schamiloglu, S.R.J. Brueck,* and F. Hegeler Department of Electrical and Computer Engineering University of New Mexico, Albuquerque, NM 87131

F.V. Hartemann, E.C. Landahl, A.L. Troha, C.H. Ho,**
J.P. Heritage,*** H.A. Baldis, and N.C. Luhmann, Jr.***

Department of Applied Science
University of California at Davis, Davis, CA 95616

A Smith-Purcell free electron laser (SPFEL) involves the interaction of an electromagnetic (EM) wave, a periodic grating structure, an electron beam propagating parallel to the plane of the grating and normal to the grating rulings, and an optical cavity. The scattering of the EM wave from the grating leads to a number of diffracted waves, both propagating and evanescent. For effective coupling with the beam, one of these evanescent modes should have a longitudinal propagation velocity along the grating direction approximately equal to the beam velocity. SPFEL's have clear antecedents in classical traveling wave tubes (TWT's) and millimeter (mm) wave devices such as orotrons. A major difference is in the unconfined nature of the EM mode in which external feedback is required in order to have stimulated emission. In contrast, the EM mode in a TWT propagates in a bounded slow wave structure (SWS). This SWS provides feedback of the radiation into the beam and hence, results in stimulated emission. Similarly, in planar orotrons, the EM mode propagates in a waveguide structure in a direction parallel to the beam, which provides the feedback process. Orotrons have also been operated in open geometries analogous to the SPFEL's. Most of this work has focused on relatively long wavelengths. We are interested in the extension of these technologies into the mm, sub-mm, and then ultimately into the infrared where tunable coherent radiation sources would be of particular interest.

In this presentation we describe plans for a detailed experimental and theoretical study of a SPFEL The source of the electron beam will be the X-band photoinjector under development at LLNL [1]. This source was originally designed for the optimum production of coherent radiation at frequencies up to 1 THz; the device produces relativistic (5 MeV) electron bunches with sub-ps duration. Therefore, the X-band rf gun would be ideally suited to generate high power (MW) pulses of coherent mm-wave radiation, via the coherent SPFEL interaction mechanism. Details of both the experimental hardware and theoretical motivations will be provided.

[1] E.C. Landahl, F.V. Hartemann, G.P. Le Sage, W.E. White, H.A. Baldis, C.V. Bennett, J.P. Heritage, N.C. Luhmann, Jr., and C.H. Ho, IEEE Trans. Plasma Sci., vol. 26, pp. 814-824 (1998).

Work supported in part by an AFOSR/DOD MURI grant.

Initial Operation of a High Power Cusp Gun

D. Gallagher, M. Barsanti, J. Richards, F. Scafuri, C. Armstrong, Northrop Grumman ESSS-DSD, Rolling Meadows, IL 60008, USA

Initial Operation of a High Power Cusp Gun*

D. Gallagher, M. Barsanti, J. Richards, F. Scafuri, C. Armstrong

Northrop Grumman Corporation Electronics Sensors & Systems Sector Defensive Systems Division 600 Hicks Road, M/S H6402 Rolling Meadows, IL 60008-1098 Tel (847) 259-9600 Fax (847) 590-3177

A cusp gun, designed to generate an axis encircling beam with low velocity spread for high harmonic, high power (70 kV, 3.5 A) operation in gyrotrons and peniotrons, has been successfully fabricated and hot tested at reduced voltage, in a beam tester designed to measure beam perveance, size, thickness, velocity ratio (beam alpha), and later, beam ripple and velocity spread. The correct beam perveance was observed, and a relatively thin, round, hollow beam, with approximately the correct dimensions, was imaged on the Cerium glass witness plate. The data indicated, however, that there was substantial current intercepted on the anode and excessively high beam alpha measured through the capacitive probes. Maxwell magnetic field simulations and EGUN rajectory simulations showed these results to be consistent with a substantial fraction of the electrons incident on the glass probe generating reflecting secondaries and/or re-reflected primaries, which back-stream through the capacitive probes and then are intercepted at the anode.

The design of the beam tester was therefore modified so that back-streaming from the glass probe would be removed. Beam transmission through the anode could then be accurately determined, and capacitive probe data could provide an accurate determination of the beam alpha. The modification was completed and hot testing continued. At normal operation of the gun at 10 kV, the beam transmission was as high as 98.5%. Furthermore, the beam alpha, calculated from the capacitive probes, was 1.42 to 1.48, compared to the EGUN prediction of 1.37 to 1.41 at the probes (and 1.49 to 1.53 in the circuit region). In another test, the polarity of the heater coil was reversed, and the measured drop in beam alpha was found to range between 0.07 and 0.14, compared to 0.14 in the EGUN simulation. In other tests, the beam transmission and beam alpha were measured and plotted over a full range of gun coil current and focus electrode voltage. In the next iteration, the beam tester will be modified to make it possible to measure beam ripple and velocity spread.

Many exciting opportunities exist for fast wave devices employing an axis encircling electron beam including slow wave cyclotron masers, broadband frequency multipliers and high harmonic gyrotrons and peniotrons. Two Cusp guns are currently being fabricated for the University of California - Davis for joint experiments with Northrop Grumman on fourth harmonic, 50 kW, gyrotrons and peniotrons operating at 94 GHz. Development of a higher perveance Cusp gun has also been proposed for use on an eighth harmonic 25 kW, 94 GHz gyrotron. The eighth harmonic W-Band gyrotron would be compatible with the use of a permanent magnet focusing structure, thereby offering the potential for small size and light weight.

5**B**06

Linear Theory of the Multi-Stage Gyro-TWTG. Nusinovich, M. Walter, University of Maryland IPR, College Park, MD 20742, USA

Linear Theory of the Multi-Stage Gyro-TWT G. Nusinovich, M. Walter, IPR, University of Maryland College Park, MD 20742

Abstract:

The Gyro-TWT is a promising candidate for applications requiring high power mm wave amplifiers with large bandwidth. Single stage devices are limited in their operation by backward wave instabilities. Multistage gyro-TWT's may be used to reduce interaction lengths of each section below minimum startup requirements for the parasitic backward wave. Such a two stage device is comprised of an input section, a cutoff drift region, and an output section. However analysis of such devices is complicated because of a large number of free parameters involved.

We have developed the formalism for operation of the multi-stage gyro-TWT amplifier in the linear regime. Such operation can be characterized by the normalized length, detuning, and electron beam current. Two distinct operating conditions are examined. The first is operation near cutoff, while the second is operation far from cutoff.

Results of gain and bandwidth calculations will be presented for both near and far from cutoff operation for a two stage gyro-TWT at arbitrary detunings of the input and output sections.

This work was supported by the DoD MURI program under grant F49620-95-I-0358 and by the Naval Research Laboratories under grant N00173981G000.

^{*}Work supported in part by the DoD/AFOSR MURI program on High Energy Microwave Sources.

Experimental Studies of a Four-Cavity, 35 GHz Gyroklystron Amplifier

M. Garven, J.P. Calame, B.G. Danly, B. Levush and F. Wood, U.S. Naval Research Laboratory, Code 6843, Washington, DC 20375, USA

Experimental Studies of a Four-Cavity, 35 GHz Gyroklystron Amplifier *

M. Garven[§], J. P. Calame, B. G. Danly, B. Levush and F. Wood[†] Naval Research Laboratory Washington, DC 20375

At the Naval Research Laboratory gyroklystron amplifiers are being investigated as high power sources for the next generation of millimeter wave radars^{1,2}. A fourcavity, 35 GHz gyroklystron amplifier experiment has recently demonstrated a peak output power of 203 kW at 34.90 GHz, with a -3 dB bandwidth of 0.6%, a saturated gain of 52.5 dB and an electronic efficiency of 30%. These values were obtained in the TE01 mode with a beam voltage of 70 kV, a beam current of 9.8 A and a pulse width of 2µs. The nominal magnetic field for these results was 13.08 kG. Recent experimental results, along with comparisons to theory, will be presented which show that variations in magnetic field and voltage affect the trade-offs between power, bandwidth and efficiency. Future experiments will with broader bandwidth investigate gyro-devices capabilities and these design studies will be discussed.

References

5B08

Experiments on a 28 GHz, 200 kW Gyroklystron Amplifier for Plasma Heating

J.J. Choi, S.W. Baik, W.K. Han, D.M. Park, J.H. Oh, S.H. Lee, J.G. Yang, and S.M. Hwang, Kwangwoonn University, Seoul, Korea

Experiments on a 28GHz, 200kW Gyroklystron Amplifier for Plasma Heating#

J. J. Choi, S. W. Baik, W. K. Han, D. M. Park, J. H. Oh, S. H. Lee, J. G. Yang*, and S. M. Hwang*

Kwangwoon University, Department of Radio Engineering, Seoul, Korea 139-701

Korea Basic Science Institute, Daejeon, Korea 305-333

Experiments are underway to demonstrate an amplified radiation power of 200kW operating at 28GHz. A long pulse operation of up to 500msec is required for plasma heating experiments of Hanbit. A five-cavity interaction circuit is designed by the use of small signal and large signal non-linear simulation codes. Simulations predict a saturated gain of 54dB and an electronic efficiency of 35%. An input drive cavity designed by the use of HFSS consists of a WR-28 waveguide, a TE311 single-ridged coaxial cavity, and a circular TE011 central cavity. In this high gain amplifier, an input power of less than 1 W is enough to saturate the amplifier, which is the power level available from a high power solid state power amplifier. Three penultimate cavities are loaded by lossy ceramic rings. A water cooled beam collector is designed to spread the beam over a wide surface by carefully tapering an external magnetic field. An input window which is a typical pillbox configuration is designed. Simulations predicts a bandwidth of more 7% with a center frequency of 28GHz at -20dB return loss. An half wavelength thick BeO window is designed for extracting the amplified radiation power of 200kW with a pulselength of 500msec. Thermal analyses on ceramic loaded cavities, rf vacuum windows, beam collector performed by ANSYS are currently underway to design the tube to be operated at a duty of 50%. Cold-tests of the interaction circuits are presented.

Work supported by KBSI and KOSEF

^{*}Work supported by the Office of Naval Research.

[§]Institute for Plasma Research, University of Maryland, College Park, MD 20742.

[†]DynCorp, Rockville, MD 20850.

J. J. Choi, A.H. McCurdy, F. Wood, R.H. Kyser, J.P. Calame, K. Nguyen, B.G. Danly, T. Antonsen, B. Levush and R.K. Parker, IEEE Trans. Plasma Sci. 26(3), 416, 1998.
 J. P. Calame, M. Garven, J. J. Choi, K. Nguyen, F. Wood, M. Blank, B. G. Danly and B. Levush, Phys. Plasmas 6, 285, 1999.

Spontaneous Emission of an Electron Beam in a Quasiperiodic Wiggler Magnet Configuration

M.G. Kong and A. Voudras, University of Liverpool, Liverpool, UK

Spontaneous Emission of an Electron Beam in a Quasiperiodic Wiggler Magnet Configuration

M. G. Kong and A. Vourdas

Department of Electrical Engineering and Electronics, University of Liverpool, Liverpool L69 3GJ, UK

For many electron beam devices, electron interaction with a single frequency electromagnetic field is relatively well understood. New interaction mechanisms may be produced when the electron beam is strongly coupled to an electromganetic field at different frequencies. In the case of free electron lasers (FEL's), such new interactions are often enhanced for their exploration by altering the characteristics of the wiggler magnet. For instance, it has been suggested to use an auxiliary harmonic wiggler to enhance radiation at higher harmonics when the field strength of the main wiggler is only modest[1]. A different harmonic wiggler configuration has also been shown to be capable of enhancing the gain of optical klystron devices at the fundamental frequency[2]. For high gain Compton FEL's, however, it has been found useful to employ a magnet system comprising two wigglers of similar periods to control the generation of sidebands[3].

In a recent paper, we have studied an unusual FEL interaction mechanism in which the electron beam is premodulated at two different frequencies[4]. We have shown that if the two modulation frequencies are not integrally but irrationally related then considerable radiation is generated at frequencies that are irrational multiples of the fundamental FEL radiation frequency. The generation of these irrationally related harmonics modifies the basic FEL mechanism and as such they may be ultilized to manipulate the FEL spectrum. In this contribution, we extend our previous results and consider the realization of electron beam modulation at two irrationally related frequencies by means of a quasiperiodic wiggler configuration consisting of two conventional periodic wigglers. In order to understand the characteristics of this quasiperiodic wiggler configuration, spontaneous emission of a general dual-wiggler structure is formulated. Number theory arguments are then used to derive the resonant condition for an FEL interaction in an infinitively long quasiperiodic wiggler. Subsequently numerical examples are used to demonstrate that significant radiations can be generated simuyltaneously at both the usual FEL harmonics, which are integer multiples of the fundamental FEL radiation frequency, and the irrationally related harmonics. When the interfernece between the two constituent wigglers of the quasiperiodic wiggler configuration is appropriately adjsuted and enhanced, the integrally related harmonics are suppressed considerably. This may be used to relieve the problem of mirror degradation for some FEL's operated at ultraviolet and x-ray wavelengths.

References:

- [1] M. J. Schmitt and C. J. Elliott, *IEEE J. Quantum Electron.*, 23 (1987) 1552.
- [2] M. G. Kong, Phys. Rev. E, 52 (1995) 3060.
- [3] D. Iracane and P. Bamas, Phys. Rev. Lett. 67 (1991) 3086.
- [4] M. G. Kong and A. Vourdas, Europhys. Lett. 38 (1997) 25.

5B10

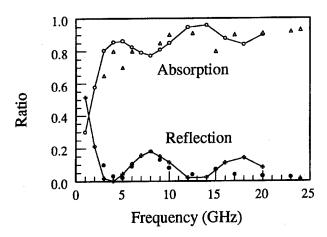
A broad band (4-25 GHz) calorimeter for diagnosing high power microwave sourcesa

A. Shkvarunets, S. Kobayashi, Y.Carmel, J. Rodgers, T. Antonsen, Jr. and V.Granatstein Institute for Plasma Research, University of Maryland, College Park, MD 20742-3511 USA

A broad band (4-25 GHz) calorimeter for diagnosing high power microwave sources

A. Shkvarunets, S. Kobayashi, Y. Carmel, J. Rodgers,
 T. Antonsen, Jr. and V. Granatstein
 Institute for Plasma Research, University of Maryland
 College Park, MD 20742-3511 USA

The measurement of microwave output energy is critical for reliable evaluation of the properties of high power, single pulse microwave sources. We describe the design, calibration and use of a broad band (4-25 GHz) calorimeter with resolution of +/- 0.05 J. The calorimeter absorbs the microwave energy across the entire output of an antenna cross-section. Thus the measurement is insensitive to the output radiation pattern and the operating RF mode. The calorimeter is composed of a microwave absorber, a measurement instrumentation and a thermal stabilization system. An ethanol layer (15 mm thick) sandwiched between two planar acrylic plates acts as an absorber. The calculated (solid line) and measured (dots) power absorption ratio (over 80%) is shown in the figure as a function of frequency. A fine wire is immersed in the ethanol and heated by a computer-controlled current supply programmed to thermally stabilize the ethanol. This system also functions to calibrate each energy measurement by generating a reference energy pulse of 1 or 5 Joule. The results of measuring the output energy of a tunable, plasma loaded backward wave oscillator will be presented.



^{*} Work supported by AFOSR, MURI Program on High Power Microwaves.

Influence of the Microwave Magnetic Field on High Power Microwave Window Breakdown

D. Hemmert, A. Neuber, J. Dickens, H. Krompholz, L.L. Hatfield and M. Kristiansen, Texas Tech University, Lubbock, TX 79409-3102, USA

Influence of the Microwave Magnetic Field on High Power Microwave Window Breakdown

D. Hemmert, A. Neuber, J. Dickens, H. Krompholz, L.L. Hatfield, and M. Kristiansen Departments of Electrical Engineering and Physics Texas Tech University, Lubbock, TX 79409-3102

Effects of the microwave magnetic field on window breakdown are investigated at the upstream and downstream side of a dielectric interface. Simple trajectory calculations of secondary electrons in an rf field show significant forward motion of electrons parallel to the microwave direction of propagation. The Lorentz-force due to the microwave magnetic field on highenergy secondary electrons might substantially influence the standard multipactor mechanism. As a result, the breakdown power level for the downstream side of a window would be higher than for the upstream side. This hypothesis was tested utilizing an S-band traveling wave resonant ring, powered by a 3 MW magnetron at 2.85 GHz, leading to a total power greater than 60 MW. Breakdown was studied on an interface geometry consisting of a thin alumina slab in the waveguide, oriented normal to the microwave propagation direction. Two field enhancement tips are placed in the middle of the broad waveguide wall on the slab surface, either in downstream or in upstream direction. This ensures an almost purely tangential electric field at the interface surface and a localized breakdown. Diagnostics include local field probes, forward and reverse power probes, high speed (5 ns exposure time) imaging, and xray imaging. Preliminary results show an increase in the breakdown field amplitude on the downstream surface as compared to the upstream surface. X-ray imaging shows a distributed x-ray source located between the field enhancement tips, with several keV quantum energy of the emitted x-rays. The intensity and spatial resolution of these preliminary measurements, however, is not sufficient to reveal differences for the upstream and downstream direction. Still, the observed higher necessary power for downstream breakdown, and the existence of high energy electrons, confirm the hypothesis of the influence of the microwave Lorentz-force on breakdown and multipactoring.

This work was solely funded by the High Energy Microwave Device MURI program funded by the Director of Defense Research & Engineering (DDR&E) and managed by the Air Force Office of Scientific Research (AFOSR).

5B12

A Long Pulse (>1 µsec) Field Emission Electron Gun With Stable Cross Secrion for HPM Sources

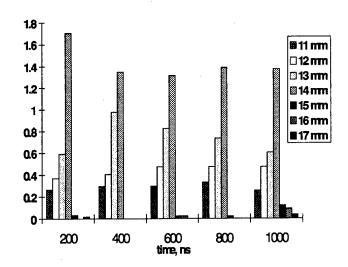
O. Loza, P. Strelkov, I. Ivanov, Y. Carmel, J. Rodgers, T. Antonsen, Jr, V.L. Granatstein, University of Maryland, Institute for Plasma Research, College Park, MD 20742-3511, USA

A LONG PULSE (>1 μsec) FIELD EMISSION ELECTRON GUN WITH STABLE CROSS SECTION FOR HPM SOURCES *

- O. Loza, P. Strelkov, I. Ivanov, General Physics Inst., Moscow, Russia,
- Y. Carmel, J. Rodgers, T. Antonsen, Jr., V. L. Granatstein, University of Maryland, College park, MD 20742.

Field emission guns, such as those used in many HPM devices, are effected by the plasma formed on both the cathode and anode surfaces by the high voltage pulse. Both the gun impedance and the electron beam cross-section change during the pulse because the plasma rapidly expands (>2mm/µsec). This may reduces the beam-wave interaction efficiency since the beam is no longer at the correct position for optimum rf interaction, and may lead to beam interception and early termination of the microwave pulse. Intense, relativistic, long pulse electron guns designed to minimize these effects is therefore a major issue in the development of long pulse HPM sources. We report the results of a foil-less, long pulse (1µsec), relativistic field emission gun with a stable beam cross section. The gun is immersed in a magnetic field of unique geometry. The figure demonstrates the temporal stability of the beam cross section by showing the radial distribution of the electron beam current density J(r) [kA/cm²] vs. time [nsec].

*Work supported by AFOSR, MURI program on HPM sources, through a DURIP grant number F496209610391.



De Anza II 10 AM, Wednesday, June 23, 1999

Session 5C Fast Z-pinches and X-ray Lasers

Chairperson

Bruno Bauer

University of Nevada, Reno

5C01-2

Invited -

Long Implosion experiments and simulations on the Saturn and Z machines

M.R. Douglas, C. Deeney, R.B. Spielman, N. Roderick, & M.G. Haines, Sandia National Laboratories, Albuquerque, NM 87185-1194, USA

Long implosion experiments and simulations on the Saturn and Z machines

Melissa Douglas, Christopher Deeney, Rick Spielman Sandia National Laboratories, Albuquerque, NM, 87185*

Norm Roderick
University of New Mexico, Albuquerque, NM, 87131

Malcolm Haines Blackett Laboratory, Imperial College, London, SWZ 2BZ, UK

By increasing the implosion time for Z-pinches from the canonical 100 ns to 200-300 ns, the complexity and power flow risks can be reduced for future higher current generators, assuming that the implosions still produce high energies and powers. The recent success of high wire number arrays and nested configurations have permitted load designs to be considered that could provide the necessary performance at the longer implosion times, i.e. can we challenge the conventional wisdom?

At Sandia National Laboratory, two experimental campaigns (on Saturn and Z) plus two-dimensional MHD modeling have been performed to investigate the scaling of tungsten wire arrays to 150 to 250 ns implosion times. For the Saturn experiments 25 mm diameter, 240 tungsten wire arrays of increasing mass were used. A comparison with short pulse data shows similar powers, risetimes, final pinch diameters, and instability mode structure. For the same final implosion velocity, measured risetimes were faster than the equivalent short pulse. Fall times were much longer and correlated to late time on-axis dynamics. Simulations using the Mach2 code incorporated a cell-to-cell random density to initiate a Rayleigh-Taylor instability, believed to dominate the implosion dynamics. The results of these simulations show that the risetime of the x-ray power correlates to the FWHM of the sheath and has a strong dependence on perturbation level. The mode evolution is similar to the short pulse simulation and experimental results are reproduced. Both simulations and theory suggest that in the long pulse mode, the wires have time to merge and form a more uniform shell prior to acceleration. Modeling of the long pulse Z data is in progress. The Z experiments were carried out using 40 mm diameter, 480 wire tungsten arrays of increasing mass. Initial analysis indicates broader pulses, lower powers (100-120 TW) and larger pinch diameters compared to the corresponding short pulse data. By employing a nested array configuration, the pinch diameter was reduced by 50% with a corresponding increase in power of > 30%. For the parameters being considered here, merger no longer plays a strong role and both experimental evidence and preliminary simulations suggest opacity may be the dominant effect. This is opposed short pulse, suggesting that another mechanism besides RT broadens the pulse.

5C03-4

Invited -

New X-ray Backlighting Results on Small-Scale Structure Formation, Including Liquid-vapor Foam-like Appearance, in Exploding wire Zpinches and X-pinches

S.A. Pikuz, T.A. Shelkovenko, D.A. Hammer, D.B. Sinars, Y.S. Dimant and J.B. Greenly, Cornell University, Ithaca, NY 14853, USA

New X-ray Backlighting Results on Small-Scale Structure Formation, Including Liquid-vapor Foam-like Appearance, in Exploding Wire Z-pinches and X-pinches

S.A. Pikuz**, T.A. Shelkovenko**, D. A. Hammer, D.B. Sinars, Y.S. Dimant and J.B. Greenly

Laboratory of Plasma Studies, Cornell University Ithaca, NY 14853

Exploding wire and wire array experiments have been carried out in Z-pinch and X-pinch geometry using low current (4.5kA amplitude, 1.4 µs period damped sinusoid) and high current (up to 225 kA, 100 ns) drivers. X-ray backlighter images have been obtained using Mg, Al, Ti, Fe, Ni, NiCr, Cu, brass, Mo, Pd, Ag, Ta, W, Pt, Au, and Ni-coated Ti wires with initial diameters ranging from 7.5 µm (W) to 46 µm (Mg). There were typically two Mo X-pinch x-ray backlighters which generated pulses of <0.5 ns duration from sources small enough to allow resolution of ~1 um scale structure in the resulting images. In the high current experiments, images of dense cores within coronal plasmas are obtained with higher Z materials including Ni, Cu, Mo. Pd. Ta. W. Pt and Au; with lower Z materials, only the dense cores are visible in the backlighter images. In all cases a fine structure in the interior of the dense cores, and/or surface instabilities are observed. Some of the dense cores show a shock-wave-like structure and others show gaps that open up more rapidly than the wire cores are expanding. The wire interiors develop a foam-like liquid-vapor mix, with some of the bubbles breaching the surface and spewing vapor out of the dense core. The low current experiments follow the same general behavior but require several us to complete the process instead of 50-100ns. With W and Al wire explosions, step wedges have been used to permit calibrated density measurements to be made of the core (W and Al) and coronal (W) plasmas. The two X-pinches have also been used to radiograph each other, yielding high resolution images of the on-axis collapsing z-pinch and minidiode formation at the Xpinch cross point very close to the time of x-ray burst emission.

Additional information on all of these topics will be presented in 5 papers presented in a poster session later in this conference by the above authors.

5C05

Dynamic Hohlraum and ICF Pellet Implosion Experiments on Z

T.J. Nash, M.S. Derzon, G.A. Chandler, R. Leeper, D. Fehl, J. Lash, C. Ruiz, S. Slutz, G. Cooper J.F. Seaman, J. McGurn, S. Lazier, J. Torres, D. Jobe, T. Gilliland, R. Mock, P. Ryan, D. Nielsen, J. Armijo, J. McKenney, R. Hawn and D. Hebron, D. Petersen, R. Bowers and W. Matuska, Sandia National Laboratories, Albuquerque, NM 87185-1196, USA

Dynamic Hohlraum and ICF Pellet Implosion Experiments on Z*

T.J. Nash, M.S. Derzon, G. A Chandler, R. Leeper, D. Fehl, J. Lash, C. Ruiz, S. Slutz, G. Cooper, J.F. Seaman, J. McGurn, S. Lazier, J. Torres, D. Jobe, T. Gilliland, R. Mock, P. Ryan, D. Nielsen, J. Armijo, J. McKenney, R. Hawn, and D. Hebron

Sandia National Laboratories

D. Petersen, R. Bowers, and W. Matuska

Los Alamos National Laboratory

By stabilizing an imploding z-pinch on Z (20 MA, 100 ns) with a solid current return can and a nested wire array we have achieved dynamic hohlraum radiation temperatures over 200 eV at a diameter of approximately 1 mm. yielding configuration temperature is a nested tungsten wire array of 240 and 120 wires at 4 and 2 cm diameters weighing 2 and 1 mg, 1 cm long, imploding onto a 5 mm diameter, 14 mg/cc cylindrical CH foam, weighing We have used the a single 4 cm 3 mg. diameter tungsten wire array to drive a 1.6 mm diameter ICF capsule mounted in a 6 mg/cc foam inside a 3 mg copper annulus at 5 mm diameter, and measured x-ray emissions indicative of the pellet implosion. Mounting the pellet in foam may have caused the hohlraum to become equator-hot. present results from upcoming pellet experiments in which the pellet is mounted by thread and driven by a larger diameter, 6 or 7 mm, copper mounted by annulus to improve radiation drive We will also discuss symmetry. foam annular designs for tapered targets that distort a cylindrical pinch into a quasi-sphere that will wrap around an ICF pellet to further improve drive symmetry.

^{*}Research supported by DOE contracts DE-FG03-98DP00712 and DE-FG02-98ER54496, and Sandia National Laboratories, Albuquerque, contract BD-9356.

^{**}Permanent address: Lebedev Physical Institute, Moscow, Russia

¹T.A. Shelkovenko, S.A. Pikuz, A.R. Mingaleev and D.A. Hammer, Rev. Sci. Instrum. **69**, in press (1999).

^{*}Sandia is a multiprogram laboratory operated by Sandia Corporation, a Lockheed Martin Company, for the United States Department of Energy under Contract DE-AC04-94AL85000.

Issues in the 2-D Simulation Physics of High-Performance Z-Pinch Experiments

D.L. Peterson, J. Aubrey, R.L. Bowers, W. Matuska, K.D. McLenithan, G. Chandler, C. Deeney, M. Derzon, M. Douglas, T. Nash, M.K. Matzen, R.B. Spielman, Los Alamos National Laboratory, Los Alamos, NM 87545, USA

Issues in the 2-D Simulation Physics of High-Performance Z-Pinch Experiments

D. L. Peterson, J. Aubrey, R. L. Bowers, W. Matuska, K. D. McLenithan

Los Alamos National Laboratory, MS-B259

Los Alamos NM 87545,

G. Chandler, C. Deeney, M. Derzon, M. Douglas, T. Nash, M. K. Matzen, R. B. Spielman Sandia National Laboratories, Albuquerque, MS-1194 Albuquerque NM 87185-1194,

> N. F. Roderick University of New Mexico Albuquerque NM 87131

Recent experiments conducted on the Sandia Z accelerator have continued the progress which began with the Saturn large-wire-number array implosions. Included in this progress was the discovery that total radiated energy is roughly independent of pinch length leading to improved power/length performance for short length pinches; the use of "nested" arrays to reduce instability effects, increase power and decrease pulsewidth; and the employment of on-axis cylindrical foam targets to create high-temperature (>200 eV) "dynamic hohlraums".

Two-dimensional simulations have confirmed and provided an explanation for the results from short length pinches and produced good matches to measured currents, radiation powers and energies for a variety of experimental configurations. Simulations of nested array implosions and dynamic hohlraum experiments have also reproduced important results and in some cases were able to provide accurate predictions of experimental results. In other cases, the experimental performance has not matched the simulation results, at times with better experimental performance than expected. In this presentation, we will review the successful match which has been achieved of 2-D simulations to experimental data and examine the underlying physical mechanisms which appear to be important. In addition. comparisons will be made with experiments which have not been as well matched, and examine possibilities for the underlying physical mechanisms which may be responsible.

Work supported by DOE.

5C07

Long Implosion Wire Array Implosions on the Saturn and Z Accelerators

C. Deeney, M.R. Douglas, C.A. Coverdale, R.B. Spielman, K. Struve, D.L. Peterson and M.G. Haines, Sandia National Laboratories, Albuquerque, NM 87185, USA

Long Implosion Wire Array Experiments on the 8-MA Saturn and 20-MA Z Accelerators

C. Deeney, M.R. Douglas, C.A. Coverdale, R.B. Spielman, D.L. Peterson, N. Roderick, M.G. Haines, T.J. Nash, M. Derzon, J. McGurn, D. Jobe, T. Gilliland, S. Breeze, J. Torres and J.F. Seamen
Sandia National Laboratories
P.O. Box 5800
Albuquerque, NM 87185-1194

The quest to reduce the complexity, cost and risk of higher current accelerators drives the need for implosion times that are longer than the canonical 100 ns of present waterline Experiments have been generators. performed at 100 to 200 ns implosion times on the 10-MA Saturn and the 20 MA Z accelerators. These experiments have shown that 7 to 10 ns FWHM pulses can be produced even at the longest implosion times. The experimental data will be presented along with calculations which indicate that stability, uniformity and plasma opacity are critical to determining the radiation efficiency of these implosions.

Two Dimensional and Three Dimensional MHD Simulations of Wire Array Z-pinch Experiments J.P. Chittenden, S.V. Lebedev, R. Aliaga-Rossel, A.R. Bell, S.N. Bland, S.G. Lucek and M.G. Haines, Imperial College, London SW72BZ, UK

Two Dimensional and Three Dimensional MHD Simulations of Wire Array Z-pinch Experiments.

J.P. Chittenden, S.V. Lebedev, R. Aliaga-Rossel, A.R. Bell, S.N. Bland, S.G. Lucek and M.G. Haines

Blackett Laboratory, Imperial College, London, SW7 2BZ, U.K.

Recent experiments on the MAGPIE generator at Imperial College (see S.V. Lebedev et. al., at this meeting) have demonstrated the complex three dimensional nature of wire array Z-pinch implosions. We have developed a 3D resistive MHD code, in order to model these experiments. Running the code in 2D(x,y) geometry with high spatial resolution, reproduces the collapse dynamics, radial plasma streaming and precursor formation observed experimentally. The persistence of cold, unionized, wire cores dominates the collapse dynamics. Lower resolution 3D runs illustrate the differences in the behavior of the Rayleigh-Taylor instability in wire arrays compared to uniform shell implosions. Results of simulations of single and nested wire array experiments at Sandia National Laboratories will also be presented.

5C09

A study of Rayleigh-Taylor instability growth in wire array z-pinch experiments

S.V. Lebedev.R. Aliaga-Rossel, S.N. Bland, J.P. Chittenden, A.E. Dangor, M.G. Haines and O. Willi, Imperial College, London SW72BZ, UK

A study of Rayleigh-Taylor instability growth in wire array z-pinch experiments.

S.V. Lebedev, R. Aliaga-Rossel, S.N. Bland, J. P. Chittenden, A.E. Dangor, M.G.Haines and O. Willi

Blackett Laboratory, Imperial College, Prince Consort Road, London SW7 2BZ, U. K.

Wire array z-pinches are extremely efficient sources of high power soft x-ray pulses (up to 280 TW [1]) for energising hohlraums for inertial confinement fusion and other high energy density physics applications. The main processe affecting quality of the implosion and x-ray power at stagnation is development of the Rayleigh-Taylor instability in a plasma accelerated by the magnetic pressure.

In this paper we present experimental results on Rayleigh-Taylor instability growth in wire array z-pinches driven by a 1.4 MA, 240 ns current pulse. Al, W and Ti wire arrays of 16 mm diameter with between 8 and 64 wires were studied. Comparison of the instability development for different wire material and wire number with be presented. The radial structure of the instability was observed by laser probing and soft x-ray imaging in implosions of arrays consisting of four groups of four closely spaced wires (4x4 wire array). Experiments to study the instability development in nested-wire arrays and effect of the B_z magnetic field induced by wires twisting will be presented.

C. Deeney, M.R. Douglas, R.B. Spielman et al., Phys. Rev. Lett. 81, 4883 (1998).

Time-resolved optical spectroscopy measurements of pre-pulse plasma formation on Z J.E. Bailey, A.L. Carlson, M.E. Cuneo, C. Deeney, P. Lake, R.B. Spielman,K.W. Struve and W.A. Stygar, Sandia National Laboratories, Albuquerque, NM 87185-1196, USA

Time-resolved optical spectroscopy measurements of pre-pulse plasma formation on Z

J.E. Bailey, A.L. Carlson, M.E. Cuneo, C. Deeney, P. Lake, R.B. Spielman, K.W. Struve, and W.A. Stygar Sandia National Laboratories, Albuquerque, N.M., 87185-1196 and Y. Maron

Weizmann Institute of Science, Rehovot, Israel, 76100

The compression of annular wire arrays in z-pinch experiments produces large radiation pulses which are useful for high energy density research. The initial transformation of the wire array into a plasma shell impacts the subsequent implosion of the shell because it affects the current distribution, possibly seeding instabilities. On the Z accelerator the initial plasma is created when a ~300 kA prepulse current flows through the 240-300 wire array during a ~50 nsec period prior to the arrival of the main power pulse, approximately 100 nsec prior to the pinch. Ideally, we would like to measure the pre-pulse plasma density and temperature with nsec time resolution and sub ~100 micron two-dimensional spatial resolution. Such measurements are difficult at large accelerators, such as Z, because of limited line of sight access and low experiment rates. Nevertheless, the unique conditions produced on Z discharges imply that it is important to measure the plasma formation characteristics on Z. Our strategy is to perform an initial set of limited measurements at Z and interpret the results with the aid of models based on more detailed benchtop experiments performed elsewhere. Subsequent more-detailed measurements at Z can then be pursued.

The principle diagnostic for the pre-pulse plasma is time-resolved optical spectroscopy. Light is collected from ~1 mm diameter lines of sight aimed at the wire array through a slot in the cylindrical return current case. The light is transported using fiber optics to two streaked spectrographs operating in the 2300-4300 Å and 4000-7000 Å regimes. Data has been obtained on discharges using Al and W wires. Spectral lines are observed beginning about 150 nsec before the pinch and they persist until the main power pulse arrives. At this time a rapidly growing continuum swamps any optical line emission. In Al wire experiments bright emission is observed from Al III 3d-4p, 4s-4p, and 4p-4d transitions. In W wire experiments emission is observed from C IV 3s-3p and 5f-6g, possibly blended with C III 3s-3p. The C IV emission is presumably from carbon contamination of the W wires, although it is difficult to rule out contributions from the return current case. Both experiments are valuable; the Al because there is no doubt that the emission arises from the wires and a more complete set of lines is observed, and the W because W wire implosions produce the largest radiation pulses. Work is in progress to evaluate using the relative line intensities and line widths to determine the plasma temperature and density,

Sandia is a multiprogram laboratory operated by Sandia Corporation, a Lockheed Martin Company, for the U.S. Dept. of Energy under contract #DE-AC04-94AL85000.

5D

Bonsai I/II 10 AM, Wednesday, June 23, 1999

Oral Session 5D
Plasma Opening Switches

Chairperson
Ralph Schneider
Defense Threat Reduction Agency

5D01

Spectroscopic Characterization of Impurity Ions on the Hawk POS

J.J. Moschella, C.C. Klepper , C. Viodoli, R.C. Commisso, D.C. Black, B. Moosmann, Y. Maron, HY-Tech Research Corporation, Radford, VA 24141, USA

Spectroscopic Characterization of Impurity Ions on the Hawk POS.¹

J.J. Moschella, C.C Klepper, and C. Vidoli HY-Tech Research Corp., Radford VA

R.C. Commisso, D.C. Black, and B. Moosmann Plasma Physics Branch Naval Research Laboratory, Washington DC

Y. Maron Weizmann Institute of Science, Rehovot Israel

The intensities of several optical emission lines of C II, C III and C IV were measured on the Hawk plasma opening switch (POS) in order to determine the role of contamination from plasma-surface interactions during the conduction phase. To operate the switch, the inverse pinch (IP) plasma source was used with hydrogen gas. This source injects a pure hydrogen plasma from inside the inner conductor (cathode) into the POS gap. Therefore, detection of carbon is direct evidence that impurities from material surfaces have been incorporated in to the switch plasma. In fact, previous experimental results with the IP suggested that impurities dominate the conduction scaling. ²

A visible and UV range monochromator was used simultaneously to monitor sets of lines from carbon in each spectral range. Both monochromators were set to view the switch plasma using an axial line-of-sight at the same radial position, but at different azimuths. Data was taken at three radial positions, near the anode, near the cathode, and in the radial center of the switch. Each system was calibrated for absolute intensity using two traceable standards: a tungsten filament spectral radiance lamp and an UV deuterium spectral irradiance lamp. Initial analysis showed that the impurity emission was significantly higher near the anode, which is reasonable, because the anode is solid and the cathode semitransparent using the IP source. The data analysis is being performed with input from a time-dependent collisionalradiative model. The absolute intensities together with electron temperatures from line ratios (and from the time-histories), will be used to quantitatively determine impurity concentrations. Results from this analysis will be presented and the significance of these results to the future of POS development will be discussed.

1. Work supported by DTRA.

5D02-3

Invited --

Magnetic Field and Electron Density evolutions in a POS

R. Arad, K. Tsigutkin and Y. Maron, A. Fruchtman, Weizmann Institute of Science, 78100 Rehovot, Israel

Magnetic Field and Electron Density evolutions in a POS

R. Arad, K. Tsigutkin, and Y. Maron
Physics Faculty, Weizmann Institute of Science, Rehovot Israel
A. Fruchtman
Center for Technological Education, Holon, Israel

We study the operation of a planar microsecond plasma opening switch (POS) in which a current of 140 kA is conducted by the plasma for a duration of 400 ns before opening into an inductive load within 90 ns. Spectroscopic measurements, local in 3D, are made by doping the plasma with various species and observing the characteristic emission of the doped particles. The electron density and temperature and the plasma composition of the prefilled flashboard plasma are studied spectroscopically. The electron density and temperature are found to be (5±2)×10¹⁴ cm⁻³ and 6±0.5 eV, respectively. The plasma is found to consist mainly of protons with a significant fraction of CIV and CV ions only near the anode. During the POS operation, measurements of the magnetic field evolution from Zeeman splitting, the electron density and temperature from line intensities and collisionalradiative calculations, and the ion velocities from Doppler shifts are made. The magnetic field is seen to penetrate into the POS region in the form of a broad current channel (>1.5 cm) at an average velocity of 3.5×10⁷ cm/s. The electron density at each location is found to rise by 20-40% at the time when the magnetic field reaches 50% of its peak value. This is followed by a drop in the electron density to a value that is ≈5 times lower than the initial value. The 2-D map of the electron density indicates that significant plasma flow towards the electrodes is responsible for the density drop. The proton velocity is measured by observing the H_n spectral profile, which is affected by charge-exchange of protons with hydrogen. This velocity is compared to the axial velocities of CIV and doped HeII, that are found to be 2.5 times than the field propagation velocity. Currently, measurements of the ion velocities towards the electrodes are being made. We attempt to understand these results by modeling the magnetization and drifts under the effects of the electric and magnetic fields assuming a low-collisionality plasma. Possible mechanisms that may explain the broad current channel in the plasma, the fast magnetic field penetration into the plasma, and the differences in the velocities of the different-mass ions will be discussed.

^{2.} Moschella et al., in Proc. 12th Inter. Conf. on High-Power Particle Beams, to be published.

5D04

Effect of Plasma Flow Direction on the Performance of Microsecond Plasma Opening Switch

I.V. Lisitsyn, S. Kohno, Y. Teramoto, S. Katsuki, H. Akiyama, Kumamoto University, Kumamoto 860-8555, Japan

EFFECT OF PLASMA FLOW DIRECTION ON THE PERFORMANCE OF MICROSECOND PLASMA OPENING SWITCH

I.V. Lisitsyn, S. Kohno, Y. Teramoto, S. Katsuki and H. Akiyama

Department of Electrical and Computer Engineering, Kumamoto University, 2-39-1 Kurokami, Kumamoto 860, Japan.

The scaling of the microsecond plasma opening switch operation in a wide range of currents and plasma densities allowed to suggest the importance of the snow-plow plasma displacement model for long-conduction-time switches. The model does not require the magnetic field penetration into the bulk plasma and it is free of assumptions like anomalous plasma resistivity and shock-like field penetration. The plasma ahead the current-conducting layer is displaced by hydrodynamic pressure of the magnetic piston.

Assuming this model to be true, a significant modification of the plasma displacement parameters can be achieved by changing the initial shape of the plasma fill. The characteristics of a microsecond plasma opening switch have been improved by the modification of the plasma source. The nozzles were arranged to provide the plasma flow, which gets out of gun axis. The plasma flow directed 30° downstream the inductive load resulted in 50% improvement of the load current risetime and switch impedance.

5D05

Electron Angular Distribution in an Opening Switch Driven Coaxial Diode

V.J. Harper-Slaboszewicz and C. Martinez, Sandia National Laboratories, Albuquerque, NM 87185-1159, USA

Electron Angular Distribution in an Opening-Switch-Driven Coaxial Diode

V. J. Harper-Slaboszewicz and C. Martinez Sandia National Laboratories, Albuquerque, NM

Characterization of the angular distribution of electrons produced in a coaxial high-current relativistic electron beam diode may be important in evaluating the applications of these diodes. This angular distribution has not previously been measured for an opening-switch-driven low impedance coaxial diode. Because the opening switch may have plasma in the vicinity of the diode, it is expected that the angular distribution may differ from that found in a closing-switch driven system.

On the DECADE Module 1, the distribution was measured using a multiple-aperture shadowbox imaging system, using radiochromic film to record the distribution. Nominal DM1 electron beam parameters are 1.7 MV peak voltage, 700 kA peak current, and 40 ns FWHM produced with a 6 inch diameter cathode. Twenty-one 0.332 cm diameter apertures on a grid pattern with a center-to-center spacing of 4.45 cm are distributed over the the central 8 inch diameter of the anode.

Usable information was obtained on two shots, and the gross features of the distribution was similar for the two shots. There was no indication of local shorting of the diode, which produces a characteristic damage pattern. The beam is not strongly pinched, and covers approximately one-half of the ten inch diameter of the anode. In each of the apertures that sample the beam area, the electron beam appears to be concentrated in one direction, with an angle of incidence greater than 45 degrees. The directions of the electrons at each of the apertures appear to be random or weakly correlated. The beam does appear to be concentrated over an area covering one to three of the apertures.

These results differ significantly from those obtained in measurements on closing-switch driven coaxial high current relativistic electron beam diodes. They suggest that the opening switch plasma plays an important role in the electron dynamics in these diodes.

This work was supported by the Defense Threat Reduction Agency.

Sandia is a multi-program laboratory operated by Sandia Corporation, a Lockheed Martin Company, for the United States Department of Energy under Contract DE-AC04-94AL85000.

5D06

High Energy Electron Production in Plasma Opening Switches

John R. Goyer, David Kortbawi, John E. Rauch, William Rix and John R. Thompson, Mark A. Babineau, Maxwell Technologies, San Diego, CA 92123, USA

High Energy Electron Production in Plasma Opening Switches

John R. Goyer, David Kortbawi*, John E. Rauch, William Rix, and John R. Thompson Maxwell Technologies, Inc., San Diego, CA 92123-1506 USA

Mark A. Babineau SVERDRUP Technology, Inc., Arnold AFB, TN 37389-6700 USA

One of the practical difficulties of coupling a plasma opening switch to a bremsstrahlung diode, is the production of a small population of anomalously high energy electrons. These electrons are accelerated through a potential noticeably higher than that of the inferred opening switch voltage, and force an increase in the thickness of material used for the vacuum barrier in the system over that otherwise needed; thus reducing the radiation output through absorption of lower energy photons. We will present spatial and temporal measurements of these high energy electrons, and summarize our attempts to understand where and how they are produced and how they may be eliminated.

*Maxwell Physics International, 2700 Merced Street, San Leandro, CA 94577-0599

Sponsored by the Defense Threat Reduction Agency

5D07

MACH2 Simulations of the DECADE Plasma Opening Switch

Dennis Keefer and Robert Rhodes, University of Tennessee Space Institute, Tullahoma, TN 37388, USA

MACH2 Simulations of the DECADE Plasma Opening Switch

Dennis Keefer and Robert Rhodes

University of Tennessee Space Institute Tullahoma, TN 37388

The DECADE nuclear effects simulator at the Arnold Engineering Development Center (AEDC) uses a plasma opening switch (POS) to create a high voltage pulse used for a bremsstrahlung x-ray diode. AEDC has supported a modeling effort for the past several years at the University of Tennessee Space Institute (UTSI) in which the MACH2 computer code has been used to make numerical simulations of the POS and the cableguns used to initiate the switch. It was found that the Hall effect played an important role in the opening of the switch, but simulations predicted that current progressed along the cathode prior to the anode, in contrast to measurements Some interferometer obtained with B-dot probes. measurements presented at a DECADE review meeting in 1998 indicated that a higher density plasma layer approximately one millimeter thick formed on the electrode surfaces.

For axisymmetric geometry and no axial or radial components of the magnetic field the equation for Hall propagation is:

 $\frac{\partial B_{\theta}}{\partial t} = B_{\theta} / (m_0 e N_e) [(2/r + \partial \ln N_e / \partial r) \partial B_{\theta} / \partial z - 2/r \partial \ln N_e / \partial z \partial (r B_{\theta}) / \partial r]$

A density gradient at the electrode surfaces where the electron concentration decreases with distance from the wall will enhance propagation along the anode and retard propagation along the cathode. New MACH2 numerical simulations of the DECADE switch have been made that include the Hall effect and a model for gas desorption from the surface of the electrodes. A plasma layer occurs on the electrode surfaces and the current propagates first along the anode. This removes a point of disagreement between the experiments and simulations that we have previously shown. The simulations indicate that much less than a monolayer of adsorbed gas is required to produce this effect.

5D08-9

Invited -

POS-Load Coupling Performance On Ace 4

J.R. Thompson, P.L. Coleman, R.J. Crumley, P.J. Goodrich, J.R. Goyer and J.E. Rauch, Maxwell Technologies Inc., San Diego, CA 92123, USA

POS-Load Coupling Performance On Ace 4

J.R. Thompson, P.L. Coleman, R.J. Crumley, P.J. Goodrich, J.R. Goyer, and J.E. Rauch
Maxwell Technologies, Inc., San Diego, CA 92123-1506 USA

The ACE 4 POS is being developed as a monolithic switch option for DTRA's DECADE Quad. Although the ACE 4 POS performance in terms of conduction time, 1 µs, conduction current, 3.5 MA, and POS voltage generation, 2.5 MV, has been sufficient, a demonstration of efficient coupling to a bremsstrahlung diode load has not been demonstrated. The POS-load coupling issue appears to be dominated by plasma flow between the POS and the load. Increasing the POS to load distance has partly solved this problem on other pulsed power machines such as DM1 and HAWK, but does not appear to be a practical solution on ACE 4. Results from load coupling studies on ACE 4 will be presented which address the issues and potential ways of eliminating plasma downstream of the POS.

Sponsored by the Defense Threat Reduction Agency

5D10

Electron Energy Balance and MHD Modeling of the Conduction Phase in a Plasma Opening Switch

J.W. Schumer, D. Mosher, S.B. Swanekamp, P.F. Ottinger, R.J. Commisso, U.S. Naval Research Laboratory, Washington, DC 20375, USA

Electron Energy Balance and MHD Modeling of the Conduction Phase in a Plasma Opening Switch*

J.W. Schumer^{a)}, D. Mosher, S.B. Swanekamp^{b)}, P.F. Ottinger, R.J. Commisso

Plasma Physics Division, Naval Research Laboratory, Washington, DC 20375

Inductive energy storage devices, utilizing the fast opening of a plasma opening switch (POS), may generate high power (>1 TW) and short duration (<0.1 μ s) pulses, ideal for driving intense beam diodes or z-pinches. The use of high-density plasma switches (10^{15} to 10^{16} cm⁻³) has allowed an extension of the conduction time to above 1 μ s while still allowing a rapid opening time (few tens of ns).

Understanding of the POS plasma redistribution and thinning (in preparation for opening) during the conduction phase can be acquired via magneto-hydrodynamic (MHD) modeling and simulation. In an effort to extend the validity of MHD methods into low-density regimes (switch opening) where space-charge separation and kinetic effects are expected to play a key role, we are required to incorporate the Hall and thermoelectric effects into generalized Ohm's Law.

Including the Hall term into Ohm's Law extends the applicability of MHD methods to plasmas with density gradient scale lengths in the range $c/\omega_{pe} < L_n < c/\omega_{pi}$. However, in low-density plasmas, these spatial scale lengths approach c/ω_{pe} (electron inertia becomes important) and the Hall-MHD assumption is violated, a failure characterized by superluminal Hall speeds. Thermoelectric effects counteract some of the Hall effects in regions with large electron pressure gradients, such as the POS current channel, and have been included in simulations for this purpose. In addition, resistive diffusion of magnetic fields broadens the current channel, thereby smoothing the density gradients and reducing the Hall effect.

Electron temperatures and temperature gradients determine the magnitude of Spitzer resistivity, pressure gradients, and local ionization states of the fluid. On the other hand, heating and cooling rates are strongly influenced by current channel widths and thermally-generated fields.

We will discuss the subtle non-linear coupling between MHD, Hall, thermoelectric, and resistively diffusive processes in POS plasmas during the conduction phase. Specifically, the dependence and influence of these processes on electron temperature profiles in the plasma requires a detailed electron energy balance before accurate MHD simulations of POS plasmas can be performed. Improved methods for thermal conduction in a strong magnetic field, electron energy convection in current channels, and radiation cooling in POS plasmas will be presented, including some preliminary MHD simulation results.

^{*}Work supported by the Defense Threat Reduction Agency.

a) NRL-National Research Council, Research Associate

b) JAYCOR, McLean, VA 22102

Serra I, Conference Centre 10 AM, Wednesday, June 23, 1999

Poster Session 5P

5P01

Cathode Fall Measurements in a High Pressure Low Current Argon Arc Using Langmuir Probes

Jens Luhmann, Daniel Nandelstadt, Jurgen Mentel, Ruhr University Bochum, 44780 Bochum, Germany

CATHODE FALL MEASUREMENTS IN A HIGH PRESSURE LOW CURRENT ARGON ARC USING LANGMUIR PROBES

Jens Luhmann, Daniel Nandelstädt, and Jürgen Mentel
Department of Electrical Engineering
Ruhr University Bochum, 44780 Bochum, Germany

This work is part of investigations aiming at a "Fundamental Characterization of Thermionic Cathodes". In order to verify and further develop models of the cathode boundary layer, measured values of the cathode fall are of great importance. In this paper a method is introduced with which the cathode fall can be determined from measurements of the local plasma potential in an argon model lamp by a Langmuir probe. Typical conditions are $I_{DC} = 1$ to 10 amps and p = 1 to $6 \times 10^5 \, Pa$.

The Langmuir probe is a diagnostic tool for measuring the local plasma potential by means of the current-voltage-characteristic of the probe. Two independent probes are used. Both probes are inserted into the same cross section of the tube. The probes consist of cylindrically bent pure tungsten wires, 0.5 mm in diameter. It is possible to get a good contact between the cold probes and the hot discharge by using two half circular probes. Only one of the probes is connected to an increasing voltage ramp supply ranging from 0 to 80 V, however. The probecurrent is measured as a function of its potential. In this case the cathode is used as the reference potential. Inspite of the high pressure the shape of the current-voltage-characteristic of the probe correspondes to that from the low pressure plasmas. To determine the cathode voltage drop, the plasma potential UPP is taken with different distances Lprobe-cathode between the probe and the cathode. Assuming that the cathode voltage layer is very small, the cathode voltage fall is determined by plotting the plasma potential UPP as a function of the distance Lprobe-cathode: The cathode voltage drop can be read off at the Y-axial section of this plot. Results are presented for cylindrical electrodes with different materials and diameters ranging from 0.6 to 2.0 mm. The results indicate that the cathode voltage fall decreases in the investigated current range. Typical values for a pure tungsten electrode lie between 15 and 40 volts. In addition, results are presented, which demonstrate the dependence on parameters like pressure, gas types, electrode diameter and the attached mode of the arc to the cathode. The results are in good agreement with the cathode fall voltage, determined from caloric measurement at the same lamp as well as with the theoretical data calculated by M. Benilov [1]. The caloric method to determine the cathode voltage drop and the results are presented in another paper submitted to ICOPS99.

REFERENCES

[1] "Nonlinear Surface Heating of a Plane Sample And Modes of Current Transfer to Hot Arc Cathodes", M S Benilov, Phys. Rev. E, volume 58, page 6480-6494,1998

Determination of the Cathode Fall in a High Pressure Argon Model Using Pyrometric and Temperature Measurements

Daniel Nandelstadt, Jens Luhmann, Jurgen Mentel, Ruhr University Bochum, 44780 Bochum, Germany

CATHUDE FALL MEASUREMENTS IN A HIGH PRESSURE LOW CURRENT ARGON ARC USING LANGMUIR PROBES

Jens Luhmann, Daniel Nandelstädt, and Jürgen Mentel
Department of Electrical Engineering
Ruhr University Bochum, 44780 Bochum, Germany

This work is part of investigations aiming at a "Fundamental Characterization of Thermionic Cathodes". In order to verify and further develop models of the cathode boundary layer, measured values of the cathode fall are of great importance. In this paper a method is introduced with which the cathode fall can be determined from measurements of the local plasma potential in an argon model lamp by a Langmuir probe. Typical conditions are $I_{DC} = 1$ to 10 amps and p = 1 to $6 \times 10^5 \, Pa$.

The Langmuir probe is a diagnostic tool for measuring the local plasma potential by means of the current-voltage-characteristic of the probe. Two independent probes are used. Both probes are inserted into the same cross section of the tube. The probes consist of cylindrically bent pure tungsten wires, 0.5 mm in diameter. It is possible to get a good contact between the cold probes and the hot discharge by using two half circular probes. Only one of the probes is connected to an increasing voltage ramp supply ranging from 0 to 80 V, however. The probecurrent is measured as a function of its potential. In this case the cathode is used as the reference potential. Inspite of the high pressure the shape of the current-voltage-characteristic of the probe correspondes to that from the low pressure plasmas. To determine the cathode voltage drop, the plasma potential U_{PP} is taken with different distances Lprobe-cathode between the probe and the cathode. Assuming that the cathode voltage layer is very small, the cathode voltage fall is determined by plotting the plasma potential UPP as a function of the distance Lprobe-cathode: The cathode voltage drop can be read off at the Y-axial section of this plot. Results are presented for cylindrical electrodes with different materials and diameters ranging from 0.6 to 2.0 mm. The results indicate that the cathode voltage fall decreases in the investigated current range. Typical values for a pure tungsten electrode lie between 15 and 40 volts. In addition, results are presented, which demonstrate the dependence on parameters like pressure, gas types, electrode diameter and the attached mode of the arc to the cathode. The results are in good agreement with the cathode fall voltage, determined from caloric measurement at the same lamp as well as with the theoretical data calculated by M. Benilov [1]. The caloric method to determine the cathode voltage drop and the results are presented in another paper submitted to ICOPS99.

REFERENCES

[1] "Nonlinear Surface Heating of a Plane Sample And Modes of Current Transfer to Hot Arc Cathodes", M S Benilov, Phys. Rev. E, volume 58, page 6480-6494,1998

5P03

Two-temperature, two-dimensional modeling of cathode hot spot formation including sheath effects application to high pressure xenon arc lamps

J. Wendelstorf, H. Wohlfahrt and G. Simon, Technische Universitat Braunschweig, D-38023 Braunschweig, Germany

Two-temperature, two-dimensional modeling of cathode hot spot formation including sheath effects - application to high pressure xenon arc lamps

J. Wendelstorf*, H. Wohlfahrt and G. Simon

Technische Universität Braunschweig, Postfach 3329, D-38023 Braunschweig, Germany

One of the fundamental problems in high pressure gas discharges is the prediction of plasma/cathode interaction. The cathode hot spot temperature determines electron emission and plasma formation. The critical physical processes in the cathode/plasma system are electron emission, heat conduction and the formation of the cathodic boundary layers and the thermal plasma expansion zone. The nonlinear interaction of these phenomena is decisive for important technological parameters like electrode erosion and peak plasma temperature, e.g. in HID-lamps.

The self consistent single temperature model [1] is extended to allow for deviations of electron temperature T_e from heavy particles temperature T_h. Modeling of the cathode-plasma region now includes the following physical processes self consistently:

- heat conduction within the cathode body (2-D).
- electron emission of the surface (T, TF,...).
- space charge layer formation (sheath).
- diffusion and ionizational non-equilibrium within a thin skin layer (presheath).
- current and heat transport in the cathodic plasma, without the LTE assumption (2-D).

Assuming a stationary discharge in cylindrical symmetry, the model is applied to high pressure xenon short arc lamps with operating pressures of 1-4 MPa and currents of several ampere. The temperature split region is found to extend over 200µm in front of the cathode surface. Sheath effects critically influence the hot spot temperature of the cathode.

This modeling approach can be regarded as an important step in the development of predictive models of thermal plasma gas discharges like high pressure (arc) lamps.

Financial support by the BMBF (Germany) under Contract No.13N7105 is gratefully acknowledged.

[1] J Wendelstorf *et.al.*, 8th Int. Symposium Science & Techn. Light Sources (LS-8), Greifwald, 1998, M01, p.382 *E-Mail: jens@wendelstorf.de

Modeling and Measurements of Tungsten
Sputtering in High Intensity Discharge Lamps
During Starting

Alan Lenef, Osram Sylvania, Beverly, MA 01915, USA

Modeling and Measurements of Tungsten Sputtering in High Intensity Discharge Lamps during Starting

Alan Lenef
OSRAM SYLVANIA
Lighting Research Center, Beverly, MA 01915

Electrode sputtering during starting and subsequent tungsten deposition on the wall reduces life of high intensity discharge lamps. Using differential time-dependent ultra-violet absorption spectroscopy, we have previously measured relative tungsten densities during starting as a function of starting current [1].

We present new results on tungsten linewidths to calibrate the absorption data in [1] and new modeling results to estimate tungsten flux to the wall. Tungsten linewidths were measured using a two-meter spectrometer in second order. As in [1], lamps contained mixtures of Ar and Hg to simulate starting conditions in metal halide lamps. Measured linewidths on the 287.94 nm tungsten resonance transition were on the order of 0.25 cm⁻¹ during the glow to arc transition, increasing to about 0.45 cm⁻¹ during the initial thermionic phase. Neutral and ionic tungsten fluxes to the wall were then estimated from absorption and linewidth data as a function of starting current. Calculations were performed using a 1-D numerical model that incorporated both neutral particle and tungsten ion transport. The numerical results revealed a strong dependence of tungsten ion fluxes with Hg pressure during starting also observed in [1]. Unusual features in the measured lineshapes will also be discussed.

[1]. A. Lenef, W. Moskowitz, and J. Olsen, in Proc. Of the 50th Gaseous Electronics Conference, Madison, WI, 1996.

5**P**05

Measurement of barium emitted from thermionic electrodes in steady-state Hg-rare gas discharges R.C. Garner, Osram Sylvania, Beverly, MA, 01915, USA

Measurement of barium emitted from thermionic electrodes in steady-state Hg-rare gas discharges

R. C. Garner OSRAM SYLVANIA 71 Cherry Hill Dr, Beverly, MA 01915

Using atomic absorption we measure the densities of neutral and ionic barium in the vicinity of the barium oxide coated electrodes in low pressure Hg-rare gas discharges. The technique is sensitive to the small amount of barium that evaporates from the electrode during a steady state discharge. It uses a current modulated barium hollow cathode lamp light source and a phase sensitive detector.

Several researchers previously have detected barium using spectroscopic techniques. Two researchers have used simple atomic absorption as described here. 1,2 One researcher has employed frequency modulated laser atomic absorption. A variety of laser induced fluorescence experiments also have been performed. 4,5

In the present work we concentrate on comparing barium densities with electrode temperature. Spatially resolved electrode temperature is measured with a thermal emission based diagnostic developed previously. Comparisons are made with respect to variations of key discharge parameters, such as current and rare gas pressure. As such, we investigate in detail the connection between the electrode temperature and the presence of free barium in the discharge.

J. Shi, Ph.D. thesis, Penn. State Univ. 1993.

² S. Drawert, M. Riemann, W. Jordanov, *Contrib. Plasma Phys.* **31** (4), 1991.

³ Y.M. Li, P.M. Moskowitz, ICOPS 1994, Santa Fe.

⁴ A.K. Bhattacharya, P.G. Hlahol, Proceedings of the 4th International Symposium on the Science and Technology of Light Sources, Karlsruhe, Germany, 1986. ⁵ P.M. Moskowitz, Proceedings of the 6th International Symposium on the Science and Technology of Light Sources, Budapest, Hungary, 1992.

⁶ R. C. Garner, Proceedings of the 8th International Symposium on the Science and Technology of Light Sources, Greifswald, Germany, 1998.

Ionization Wave Propagation In Long Tube Discharges

R. Kenneth Hutcherson, Osram Sylvania, Beverly, MA 01915, USA

Ionization Wave Propagation In Long Tube Discharges

R. Kenneth Hutcherson OSRAM SYLVANIA 71 Cherry Hill Dr, Beverly, MA 01915

We describe observations of ionization wave propagation during the starting of long tube, rare gas discharges. Particular emphasis is placed on how the discharge tube internal surface conditions and wall curvature influence wave propagation velocity.

The starting of a discharge with large length to diameter ratio occurs in several steps. A free electron must be generated which then initiates an avalanche, typically near the cathode. The resulting avalanche produces a conductive plasma which charges up the long tube's insulating wall in the electrode region. The localized wall charging launches an ionization wave which bridges cathode to anode with a conductive path, after which the discharge starts. Wall properties influence charge production and loss and thus affect wave propagation.

We infer the existence of ionization waves from discharge current and voltage waveforms and from the time dependence of spectroscopically resolved optical emission at various positions along the discharge tube. These waveforms also provide a measure of ionization wave properties (velocity, intensity...). Results will be described for 1 to 100 Torr rare gas discharges in 5 mm ID insulating tubes. The relation between discharge tube properties and ionization wave propagation will be described and compared to a simple model.

5P07

Atomic transition probabilities for Dy I and Dy II G. Nave, M.E. Wichliffe and J.E. Lawler, NIST, Gaithersburg, MD 20899-8421, USA

Atomic transition probabilities for Dy I and Dy II

G. Nave*
National Institute of Standards and Technology,
Gaithersburg, MD 20899
and Harvard- Smithsonian Center for Astrophysics,
Cambridge, MA 02138

M. E. Wickliffe and J. E. Lawler Department of Physics, University of Wisconsin, Madison, WI 53706

Abstract

Atomic transition probabilities for 915 spectral lines of neutral and singly ionized dysprosium are reported. Typical uncertainties are 10%. Branching fractions, measured using the 1.0 m Fourier transform spectrometer (FTS) at the National Solar Observatory and the 2.0 m FTS at the National Institute of Standards and Technology (NIST), are combined with recently published radiative lifetimes, measured using time-resolved laser induced fluorescence on a slow atomic/ionic beam, to determine these transition probabilities. Reference sets of Ar I and Ar II branching ratios are used in most of the work reported here to establish a radiometric calibration for the Fourier transform spectra from the National Solar Observatory. A subset of the lines are also measured using the NIST FTS. Most importantly, an independent radiometric calibration based on standard lamps is used with the NIST FTS. The generally good agreement between these independent measurements provides additional confidence in the radiometric calibration and the accuracy of the measurements.

*Research performed as participant in the EPRI ALITE program

The geometry effects of the ditched dielectric in AC-PDP cell

Y.K. Shin, C.H. Shon, W. Kim and J.K. Lee, Pohang University of Science and Technology, Pohang, Kyoungbuk 790-784, S. Korea

The geometry effects of the ditched dielectric in AC-PDP cell

Y.K. Shin, C.H. Shon, W. Kim, and J.K. Lee
Dept. of Phys., Pohang University of Science and
Technology,
Pohang 790-784, S. Korea

We present the cell-geometry effects with a fluid code in AC-PDP cell. The fluid code ^{1,2}consists of the continuity equation and Poisson equation, and an equation for dielectric charging. The coplanar-electrode geometry is widely used because of the easiness of manufacturing and driving circuit. The luminance efficiency in the coplanar geometry is low because the dielectric layer deposited above the electrodes reduces the electric fields between the adjacent electrodes. Because the strong electric fields exist inside the dielectric layer, the reduced electric field does not generate effectively the plasma particles. We present the cell geometry with a ditched dielectric between the adjacent electrodes. This geometry uses the strong electric field in the ditched region. The plasma densities are increased and the discharge ignition time is decreased due to the strong electric field. The area and shape of the ditched region are discussed.

[1] Y.K. Shin, J.K. Lee, and C.H. Shon, IEEE Trans. Plasma Sci. (to appear in Feb. 1999).

[2] J.K. Lee, L. Meng, Y.K. Shin, H.J. Lee, and T.H. Chung, Jpn. J. Appl. Phys. 36 5714 (1997).

5P09

Simulation of Magnetron Sputter with Three-Dimensional Magnetic Field

C.H. Shon, J.S. Park and J.K. Lee, Pohang University of Science and Technology, Pohang, Kyoungbuk 790-784, S Korea

Simulation of Magnetron Sputter with Three-Dimensional Magnetic Field

C. H. Shon, J. S. Park, and J. K. Lee

Dept. of Phys., Pohang University of Science and

Technology,

Pohang 790-784, S. Korea.

Various properties of planar magnetron system are obtained with a kinetic code[1] in a magnetic field in two dimension and three dimension. We simulate the magnetron system to obtain various plasma characteristics and erosion profiles of target material with these magnetic fields[2]. The steady-state properties are calculated from the scaling formulas to save computing time. Various geometries and magnetic fields are used to optimize the erosion profiles and plasma characteristics. The calculated erosion profile is compared with experimental one. The maximum erosion point of calculation coincides well with the experimental one. The discrepancy of erosion width between calculation and experiment originates from the changes of electric field and magnetic field in the eroded target region. This is verified from the simulation with a pre-eroded target geometry.

 J.P. Verboncoeur, A. B. Langdon, and N.T. Gladd, Comp. Phys. Com. 87 (199) 1995.

[2] C.H. Chon, J.K. Lee, H.J. Lee, Y.K. Shin, Y. Yang, and T. H. Chung, IEEE Trans. Plasma Sci., vol. 26 (No. 6) 1998.

Computer Simulation of Field Emission Devices with Focusing Structure

Y.C. Lan, S.H. Chen, J.H. Tsai, T.L. Lin, Y.Hu, J.T. Lai, C.M. Lin, C.H. Wan, W.C. Wang, National Center for High-Performance Computing, Hsinchu, Taiwan 300, ROC

Computer Simulation of Field Emission Devices with Focusing Structure

Y. C. Lan, S. H. Chen, J. H. Tsai
National Center for High-Performance Computing,
Hsinchu, Taiwan, ROC
T. L. Lin, Y. Hu
ESS Dept., National Tsing Hua University,
Hsinchu, Taiwan, ROC
J. T. Lai, C. M. Lin, C. H. Wan, W. C. Wang
Vacuum Microelectronics Development Dept., ERSO/ITRI,
Chutung, Hsinchu, Taiwan, ROC

Beam focusing is a crucial technique for promoting the resolution of the field-emission displays. Various focusing structures for the Spindt-type field emission device have been proposed and applied on previous works, e.g. coaxial-type focusing, coplanar-type focusing [1], ridge-type focusing [2], and mesh-electrode focusing [3]. The diamond-film coating provides another possibility to design new types of field emission devices with inherently smaller beam size. The planar-type and concave-lens-type cathodes are examples.

In this study, diamond-film-coated field emitters with different emitting shapes are proposed and simulated by the MAGIC particle-in-cell code [4]. The focusing effect inherent in the emitting shape will be characterized and analyzed. The traditional Spindt-type devices with various focusing structures are also studied for comparisons. The electron trajectories, the spot sizes of beams, and the I-V curves are investigated systematically for each device.

- [1] W. D. Kesling and C. E. hunt, IEEE Trans. Electron Devices, 42(2), 340, 1995.
- [2] U. S. Patent No. 5528103 (1996).
- [3] U. S. Patent No. 5508584 (1995).
- [4] B. Goplen, L. Ludeking, D. Smithe, and G. Warren, MAGIC User's Manual, Mission Research Corp., MRC/WDC-R-409, 1997.

5P11

Measurement of plasma parameters by electric probes in a simulated PDP

K.S. Chung, Y.S. Choi, D.H. Chang, Y.H. Jung, K.C. Ko, G.H. Kim, Hanyang University, Seoul, Korea

Measurement of plasma parameters by electric probes in a simulated PDP

K.-S. Chung, Y.-S. Choi, D.-H. Chang, Y.-H. Jung, K.-C. Ko, G.-H. Kim

Applied Plasma Laboratory

Hanyang University

Seoul, Korea

Spatial and temporal variations of plasma density, temperature and potential are measured in a simulated Plasma Display Panel(PDP) cell by using a fast-scanning electric probe system. A PDP simulator are made 200 times bigger than the actual cell. Effect of collisionality on the probe analysis is discussed and change of plasma parameters due to different gases(Ar, He, Xe) are shown. Thermalization of electrons are analyzed by comparing the data of single probe with those of triple probe. Time dependent plasma properties are also measured at 5 points within one period(20kHz) using a single probe with sub harmonic sweep frequency (200Hz) of applied AC power supply and 100kHz sampling rate.

Study of High Power, Two-Stage, TWT X-Band Amplifier

P.Wang, Cz. Golkowski, Y. Hayashi, J.D. Ivers, J.A. Nation, Cornell University, Ithaca, NY 14853, USA

Study of High Power, Two-Stage, TWT X-Band Amplifier *

P. Wang, Cz. Golkowski, Y. Hayashi, J. D. Ivers, J.A. Nation, School of Electrical Engineering, Cornell University, Ithaca, NY 14853, USA

and L. Schachter,

Department of Electrical Engineering, Technion- IIT, Haifa 32000, ISRAEL

A disk loaded slow wave structure with a cold wave phase (without electron beam) velocity of the TM_{01} wave greater than the speed of light (1.05c) is used as the electron bunching stage of a two stage X-band amplifier. The high phase velocity section produces well defined electron bunches. The second section, where the cold wave phase velocity is (0.84c), i.e. less than beam velocity of 0.91c, is used to generate the high output power microwave radiation. The tightly bunched beam from the high phase velocity section enhances the beam energy conversion into microwave radiation compared to that obtained with a synchronous electron-wave buncher.

The amplifier is driven by a 7mm diameter 750 kV, 500A pencil electron beam. The structure, which has a 4 GHz bandwidth, produces an amplified output with a power in the range of 20-60 MW. At higher output powers (>60MW) pulse shortening develops. We suspect that the pulse shortening is a result of excitation of the hybrid mode, HEM_{11} , which overlaps (about 0.5 GHz separation) with the frequency domain of the desired TM_{01} mode.

A new amplifier with similar phase velocity characteristics but with a 1 GHz bandwidth and an HEM₁₁, TM₀₁ mode frequency separation of 3.3 GHz has been designed and constructed. The interaction frequency for the HEM mode is above the passband of the TM mode. Testing is in progress. The performance of the new amplifier will be compared with results obtained using the earlier configuration.

* Work supported by the AFOSR under the MURI High Power Microwave Program, and by the USDOE.

5P13

High Power Microwave Generation using a Repetitive Electron gun with a Ferroelectric Cathode

Y. Hayashi, J.D. Ivers, J.A. Nation, P. Wang, Cz. Golkowski, D. Flechtner, Cornell University, Ithaca, NY 14850, USA

High Power Microwave Generation using a Repetitive Electron Gun with a Ferroelectric Cathode *

Y. Hayashi, J. D. Ivers, J.A. Nation, P. Wang, Cz. Golkowski, D. Flechtner,

School of Electrical Engineering, Cornell University, Ithaca, NY 14853, USA

and L. Schächter,

Department of Electrical Engineering, Technion- IIT, Haifa 32000, ISRAEL

An electron gun using a ferroelectric cathode driven by a ferrite core transformer-pulse line system produces a 500kV, 50-200A, 250ns long beam. The beam is used to drive an X-band amplifier. The amplifier consists of a single stage disk loaded type structure. At the end of the amplifier, a coaxial mode converter is used to decouple the beam from the microwave radiation. The amplifier operates at a repetition rate of 0.1Hz. The beam emission is controlled by a voltage pulse applied to the back of the ferroelectric.

Results will be reported on the amplifier performance characteristics with a 50A beam and the results compared with simulation data. An improved gun design, which gives a uniform cross section 200A beam is being built, and early results obtained, using the high current gun, will also be presented

* Work supported by the AFOSR under the MURI High Power Microwave Program, and by the USDOE.

High Power Ka band TWT Amplifier

Cz. Golkowski, J. D. Ivers, J.A. Nation, P. Wang, Cornell University, Ithaca, NY 14850, USA

High Power Ka Band TWT Amplifier *

Cz. Golkowski, J. D. Ivers, J.A. Nation, P. Wang,
School of Electrical Engineering, Cornell University, Ithaca, NY
14853, USA
and L. Schachter,
Department of Electrical Engineering, Technion- IIT, Haifa
32000, ISRAEL

Two high power 35 GHz TWT amplifiers driven by a relativistic pencil, 850 kV, 200A electron beam have been assembled and tested. The first had a dielectric slow wave structure and was primarily used to develop diagnostics, and to gain experience in working with high power systems in Ka band. The source of the input power for the amplifier was a magnetron producing a 40 kW, 200ns long pulse of which 10 kW was delivered to the experiment. The 30 cm long dielectric (Teflon) amplifier produced output power levels of about 1 MW with a gain of about 23 dB. These results are consistent with expectations from PIC code simulations for this arrangement.

The second amplifier, which is a single stage disk loaded slow wave structure, has been designed. It consists of one hundred uniform cells with two sets of ten tapered cells at the ends to lower the reflection coefficient. The phase advance per cell is $\pi/2$. The amplifier passband extends from 28 to 40 GHz. It is designed to increase the output power to about 20 MW. The amplifier is in construction and will be tested in the near future. Details of the design of both systems will be provided and initial results from the new amplifier presented.

* Work supported by the AFOSR under the MURI High Power Microwave Program, and by the USDOE.

De Anza Ballroom 1:30 PM, Wednesday, June 23, 1999

Plenary Talk

The Future of High-Power Microwaves

James N. Benford
Microwave Sciences, Inc., Lafayette, CA USA
and
John A. Swegle
Lawrence Livermore National Laboratory,
Livermore CA USA

The field of High-Power Microwaves [>100 MW] has matured considerably in the quarter century since the initial development of relativistic backward wave oscillators and other source types by researchers in Russia and in the US. In this talk, we discuss the future in relation to the general development of electromagnetic technology, review some of the signs of the maturity of the field, including changes such as an observed narrowing in the number of source types under development, an increase in commercial suppliers, and a growing internationalization of the research field. In addition, within the context of historical trends in the field, we discuss the development of high peak power systems and the abandonment of the pursuit of ever-higher power in favor of the development of gigawatt-level systems with manageable weight and volume, repetitive operation, and tunability. Such systems offer scientific and engineering users flexibility for a range of applications.

Chairperson

Dr Jack Agee

Air Force Office of Science and Research

De Anza I 3 PM, Wednesday, June 23 1999

Oral Session 6A Plasmas for Lighting

Chairperson

Ken Hutcherson
Osram Sylvania

6A01

Microhollow Cathode Discharge Excimer Light Sources A.El-Habachi, M. Moselhy, A. El-Dakroury and K.H. Schoenbach, Old Dominion University, Norfolk, VA 23529, USA

Microhollow Cathode Discharge Excimer Light Sources

A. El-Habachi, M. Moselhy, A. El-Dakroury and K. H. Schoenbach

Electrical and Computer Engineering Department Physical Electronics Research Institute Old Dominion University, Norfolk, VA 23529

Microhollow Cathode discharges are non-equilibrium, high pressure, direct current discharges. By reducing the diameter of the cathode opening in a hollow cathode discharge geometry to values in the sub millimeter range we were able to operate discharges in argon and xenon in a direct current mode up to atmospheric pressure [1]. We have shown that these discharges are intense source of xenon and argon excimer radiation peaking at wavelengths of 172 nm and 130 nm, respectively [2].

Spatially resolved measurements of the excimer source in xenon have been performed. The source was found to be cylindrical along the axis of the electrodes. Its radius increases with current and decreases with pressure.

Stacking the discharges, operating them in series, holds the promise for the generation of a laser medium with sufficient length to provide the required threshold gain for a dc excimer laser. Experimental studies of the gain of the plasma column in microhollow cathode discharges are underway.

Excimer efficiencies, defined as the ratio of optical to electrical power, of 6% to 9% have been achieved [3]. Further increase of the efficiency seems to be possible; according to our modeling results, efficiencies of 30% to 40% may be obtainable. The effect of various parameters such as electrode geometry, gas flow and pulsed versus cw operation on the excimer efficiency is being studied with the goal to optimize the discharge.

This work is supported by the U.S. Department of Energy (DoE), Advanced Energy Division, and the National Science Foundation (NSF).

- [1] K. H. Schoenbach, A. El-Habachi, W. Shi, and M. Ciocca, Plasma Sources Sci. Technol. 6, 468 (1997).
- [2] A. El-Habachi and K. H. Schoenbach, Appl. Phys. Lett. 72, 22 (1998).
- [3] A. El-Habachi and K. H. Schoenbach, Appl. Phys. Lett. 73, 885 (1998).

Investigation of a Moly-Oxide Electrodeless Discharge For Lighting Applications

J.L. Giuliani, R.A. Meger, R.E. Pechacek and D.D. Hinshelwood, V. Shamamian and J.E. Butler, U.S. Naval Research Laboratory, Washington, DC 20375-5346, USA

INVESTIGATION OF A MOLY-OXIDE ELECTRODELESS DISCHARGE FOR LIGHTING APPLICATIONS*

J.L. Giuliani, R.A. Meger, R.E. Pechacek[†], and D.D. Hinshelwood Plasma Physics Division, Naval Research Laboratory Washington, DC 20375

V. Shamamian, and J.E. Butler Chemistry Division, Naval Research Laboratory Washington, DC 20375

Due to the hazardous material designation of spent fluorescent bulbs on board naval vessels, the Naval Research Laboratory has been investigating alternative lighting concepts which are free of mercury. The ideal goal is an efficient, large volume source, which provides white light directly without the use of a phosphor coating. Experiments with a μ wave plasma reactor normally used for diamond growth at ~40 Torr revealed that a combination of O_2 , N_2 , and a heated molybdenum puck led to intense plasma emission in the visible domain. As the reactor was not designed for lighting studies, we have been investigating the process in glass tubes with a re-entry geometry and RF driven coils. Results will be presented on the initial discovery, the role of moly-oxide in surface evaporation, and the favorable emission spectrum of atomic molybdenum for visible light. Initial studies of the RF system, including coil design, measured electron density, B-dot measurements, E-to-H transitions, and spectroscopic analysis of various compositions will also be discussed. Finally, the essential problem of a recycling process for the moly emitters from the glass walls back to the moderate pressure plasma using chlorine will be addressed.

6A03-4

Invited -

Atomic physics in plasma modeling for lighting R.E.H. Clark, G. Csanak and J. Abdallah, Los Alamos National Laboratory, Los Alamos, NM 87545, USA

Atomic physics in plasma modeling for lighting

R. E. H. Clark, G. Csanak, and J. Abdallah Los Alamos National Laboratory

In this talk we discuss the effects of various approximations in atomic physics calculations on plasma modeling. We summarize the procedures we have developed to produce a consistent and complete set of atomic physics data for use in a plasma model. We discuss several approximations used in the atomic data calculations such as distorted wave, first order many body theory, and plane wave Born approaches to cross section calculations. We present some comparisons between experiment and theory for cross sections for electron impact excitation of mercury. We then present model calculations of emission spectra for low temperature mercury plasmas to illustrate the effect of various approximations on an actual plasma model. We also present some similar comparisons for barium.

This work was supported by the United States Department of Energy and the EPRI-ALITE Research Program.

^{*} Work supported by ONR. † SFA, Inc., Largo, MD 20774

Modeling of Ba low pressure discharges

G.G. Lister, Osram Sylvania Inc., Beverly, MA 01915, USA

Modeling of Ba low pressure discharges

G.G. Lister

OSRAM SYLVANIA Development Inc., 71 Cherry Hill Dr., Beverly, MA 01915

The use of barium as a radiative emitter in low pressure discharge lamps has created considerable interest recently. Such lamps operate in a similar fashion to low pressure sodium or mercury lamps, in which the emitter is present as a low (a few to a few tens of micron) vapor pressure component in a rare buffer gas at several torr filling pressure. Mercury emits principally in UV, sodium in the visible, predominantly yellow, and neutral barium in the green, near the peak of the eye sensitivity curve. Discharges in Na and Ba can be highly ionized, leading to strong depletion of the emitting species at the discharge axis. This effect need not be as detrimental in Ba as with Na, since Ba has a number of strong ionic lines in the visible spectrum, which may assist in the production of white light. Detailed models of low pressure Na and Cs lamps have reproduced many of the experimental observations [1] and a similar approach can be used to model Ba discharges. Further, the inelastic electron excitation processes in Ba are better documented than for most other elements. Results of a numerical model will be presented, using the best available atomic data, showing the predicted influence of discharge parameters on electrical characteristics, cataphoresis and radiation output in barium discharges.

[1] H. van Tongeren, Philips Res. Repts. Suppl., 1975, No 3 Co-sponsored by the EPRI-ALITE Research Program

6A06

Modelling the Spectrum of a S2 High Pressure Discharge

Achim Korber, Philips Research Laboratories, D52085 Aachen, Germany

MODELLING THE SPECTRUM OF A S₂ HIGH PRESSURE DISCHARGE

Achim Körber

Philips Research Laboratories, Weisshausstr. 2, D 52066 Aachen, Germany

High power microwave discharges in S_2 vapour at pressures of several bars have been discovered as a highly efficient white light source several years ago [1]. The discharge spectrum is originating mainly from bound-bound transitions in the S_2 B $^3\Sigma_u^-$ – X $^3\Sigma_g^-$ band system. At such high S_2 pressures re-absorption is an essential mechanism shifting the spectral maximum from the UV into the visible region [2].

Assuming spherical symmetry, local thermal equilibrium and a cubic temperature profile the onedimensional radiation transport equation is solved for each of the 330 vibronic bands connecting the niveaus v' = 0...9and v" = 0...32 yielding a quantitative description of the spectrum with only two free parameters: the maximum discharge temperature T_{max} and the mean width δv_{vib} of a vibronic band. The response of the spectrum to variations of experimental conditions (S2 pressure, input power, ...) may be expressed by very reasonable changes of these model parameters: The input power determines the total amount of radiation (via the value of T_{max}) and the S₂ pressure influences the position of the spectral maximum (reflected by the value of $\delta\nu_{vib}).$ In the red and IR the experimental spectrum is higher than the simulation indicating contributions of continuum radiation or other molecular transitions which are not included in the model.

References:

- [1] J.T. Dolan, M.G. Ury and C.H.Wood, 6th Int. Symp. on the Science and Technology of Light Sources, Budapest (1992).
- [2] B.P. Turner, M.G. Ury, Y. Leng and W.G. Love,J. Illum. Eng. Soc. 26 (1), 10 (1997).

Application of Vane-type Resonator to Microwave Powered Electrodeless HID Lamp

Akira Hochi, and Mamoru Takeda, Matsushita Electric Industrial Co. Ltd, Soraku, Kyoto 619-0237, Japan

Application of Vane-type Resonator to Microwave Powered Electrodeless HID Lamp

Akira Hochi, Mamoru Takeda Matsushita Electric Industrial Co., Ltd. 3-4, Hikaridai, Seika, Soraku, Kyoto, 619-0237, Japan

A cavity resonator has been generally used as microwave applicator for an electrodeless high intensity discharge (HID) lamp. The size of a cavity resonator is determined by the wavelength of a microwave applied. For example, for a microwave of 2.45 GHz, a inner diameter of more than about 76 mm is necessary for obtaining a microwave resonant field, and then the size of a plasma arc capable of maintaining a stable discharge is experimentally limited at about 15 mm and above. Accordingly the microwave powered electrodeless HID lamp device using cavity resonator is inappropriate in applications where a point light source is required.

A vane-type resonator is generally known as an anode of a magnetron, which decides the oscillation frequency of the magnetron. The vane-type resonator, made of aluminum and so on, forms a structure in which vanes protrude toward the center of a cylinder. A microwave resonant electric field is generated inside of a space formed by the vane protuberant portions, where an electrodeless HID lamp provided. An inner diameter of the resonant space can be 10 mm and below at 2.45 GHz. Compared with the cavity resonator, resonant electric field generated at the center of vane-type resonator can be concentrated in a very small space. Therefore, a much smaller plasma arc can be maintained by using the vane-type resonator.

We used 3-D finite element method simulation for a design of a vane-type resonator with parabolic reflector to obtain a desired resonant frequency. According to the results of the simulation, the sizes of a 4-vanes resonator with the parabolic reflector were decided, and the resonator made of aluminum and copper was prepared. An electrodeless lamp with InBr and Ar gas enclosed in a spherical quartz glass tube having an inner diameter of about 4 mm was also prepared, and was set at center portion of the resonator. The total luminous flux was about 2150 lm at microwave input of 27 W. Incidentally, the CRI and Tc for this lamp were 93 and 10200 K, respectively.

Thus, it becomes possible to efficiently couple microwave energy with a smaller-sized electrodeless HID lamp than conventional.

6A08

High Luminance Metal Halide Lamp Containing ScBr3 for LCD Projectors

Kiyoski Takahashi, Makoto Horiuchi, Mamoru Takeda, Matsushita Electric Industrial Co., Soraku, Kyoto 619-0237, Japan

High Luminance Metal Halide Lamp Containing ScBr₃ for LCD Projectors

Kiyoshi TAKAHASHI, Makoto HORIUCHI, and Mamoru TAKEDA Matsushita Electric Industrial Co.,Ltd. 3-4, Hikaridai, Seika, Soraku, Kyoto 619-0237, JAPAN

Recently needs of high luminance and good color rendering light sources for LCD projectors have increased. Metal halide lamps are widely used for LCD projectors because of their good color rendering and high efficacy. Their luminance, however, are so low that it is difficult to achieve bright screen with projectors in which the metal halide lamps are used.

This study reports excellent characteristics of the new 250W metal halide lamp with 2.0mm arc length which have higher luminance. Our new metal halide lamp contains ScBr₃.

The ScBr₃ lamp achieves more than 2 times as high luminance as the priory metal halide lamp which contains InI and HoI₃[1]. This result is due to high ionization potential of Sc and high vapor pressure of ScBr₃. Ionization potential of Sc(6.7eV). is higher than that of In (5.8eV). Also vapor pressure of ScBr₃ (7000pa at 1100K) is higher than that of HoI₃(80pa at 1100K). Higher ionization potential makes an arc thinner. Higher vapor pressure makes more amounts of radiation. Therefore higher luminance is achieved. Luminance of the ScBr₃ lamp is approximately the same as that of ultra high pressure mercury lamps.

In addition the ScBr₃ lamp has strong line emission around the wavelength of 630nm. So the color rendering of the ScBr₃ lamp is better than that of ultra high pressure mercury lamps.

We confirm that by use of ScBr₃ metal halide lamps are closer to the ideal light source for LCD projectors, especially small scale portable TV projection systems.

[1]M.Horiuchi et al;LS8 Greifswald C19(1998) p228

Non-equilibrium plasma formation as a lighting source

Dr. Pankova M., State Research Institute for Aviation Systems, 121248 Moscow, Russia

Non-equilibrium plasma formation as a lighting source

Dr. Pankova M. State Research Institute for Aviation Systems Russia

The problem of high effective energy transformer source searching brought the need of applied properties investigation of serial and perspective plasma generators, which have the well known effectivity of primary energy transformation into different kinds of energy: gasdynamics, heat, light, irradiation, electricity. Erosive plasma generators of supersonic plasma jets [1] are characterized by the jet selffocusing, high parameters of effectivity transfer into irradiation (10-20%) and the possible controllability of spectral constitution allow to recommend them as impulse powerful lighting source in visible spectrum range.We chose for our investigative research the electrodischarge erosive pasma accelerator and modified it to get optimal total discharge energy (up to 1 kJ). Its generated highpower plasma jet (specific energy up to 10J/cm³, electron density up to 10⁻¹⁷cm⁻³, decay time up to 0.5s) is characterized by the spatial structure along with some applied properties in each of them it reveals the high effectivity of primary electric power transfer [2]. There are several construction schemes of this generator at our institute with the solid and liquid working substances of organic and polymeric origin [3]. In all visible spectral range and near UV the proposed plasma formation has the specific intensity of lighting 10³ times higher than that of the analogous of nitrogen electrodischarge. As it is measured in our experiments the irradiation part in UV range for solide erosion polymer is up to 40%, for liquid organics up to 55%. The primary power transfer effectivity for the mentioned above erosive materials consists 10% and 25% relatively. The first experimental results allow to consider the construction of bench scale model of high specific power UV-source in impulse and quasicontinuous regimes as a good perspective. The application fields may be different : medicine(oftalmology, dermatology, surgery), chemical industry of organic materials production, agriculture(stored grain processing) and some others of social interest.

1.KamrukovA.S.,ProtasovYu.S.,J.Tech.Phys.,v55,N5,1985,p5

2.PankovaM.,LeonovS.Ball Lightning at the Laboratory.Composition of articles.Moscow.Chemistry.1994,p.95.
3.Bocharovv.,PankovaM.,Samolet, 1995, 1,p15.

6B

De Anza II 3 PM, Wednesday, June 23, 1999

Oral Session 6B
Intense Beams and MURI

Chairperson
Tom spencer
AFRL/DEHE

Characterization of the Power Handling Capability of an S-Band and Double Disc Gas Cooled Microwave Window

A. Neuber, P. Ferguson, K. Hendricks, D. Hemmert, H. Krompholz, L.L. Hatfield, M. Kristiansen, Texas Tech University, Lubbock, TX 79409-3102, USA

Characterization of the Power Handling Capability of an S-band Double Disc Gas Cooled Microwave Window

A. Neuber, P. Ferguson*, K. Hendricks**,
D. Hemmert, H. Krompholz, L.L. Hatfield, M. Kristiansen
Departments of Electrical Engineering and Physics,
Texas Tech University, Lubbock, TX 79409-3102

*MDS Company, Union City, CA

**AFRL at Kirtland AFB, NM

The S-Band double disc microwave window comprises a rectangular waveguide to circular pillbox transition with two separate high purity, TiN coated Alumina discs brazed into the pillbox. The geometrical dimensions are optimized for minimum electromagnetic wave reflection at a microwave frequency of 2.85 GHz in TE₁₀ mode. The window is designed for power levels up to a few 100 MW with several microseconds pulse duration. Crucial for the power handling capability is the gas species and pressure of the gas flow applied for cooling the Alumina discs.

The window has been incorporated in a resonant S-Band ring that provides a maximum power of about 100 MW for several microseconds [1]. Since only about 2 J are stored in the ring at any time, a window failure will not result in catastrophic destruction of the window by a single shot. This makes it possible to find the maximum power the window will transmit as a function of pressure and gas species without destroying the window when coming close to or moving into the breakdown regime. Diagnostics include upstream end-on observation of the window with an intensified CCD camera, downstream end-on observation with a nanosecond resolution photodiode and side-on observation of the space between the Alumina discs with a photomultiplier. Also, time resolved forward and reflected microwave power has been measured.

[1] A. Neuber, J. Dickens, D. Hemmert, H. Krompholz, L. L. Hatfield, M. Kristiansen: Window Breakdown caused by High Power Microwaves. IEEE Trans. Plasma Sci. 26, 296-303 (1998)

This work was primarily funded by the High Energy Microwave Device MURI program funded by the Director of Defense Research & Engineering (DDR&E) and managed by the Air Force Office of Scientific Research (AFOSR).

6B02-3

Invited -

3D PIC Simulation Study of a Relativistic, Rising Sun Magnetron

R.W. Lemke, T.C. Genoini and T.A. Spencer, Sandia National Laboratories, Albuquerque, NM 87185-1186, USA

3D PIC Simulation Study of a Relativistic, Rising Sun Magnetron

R. W. Lemke^a, T. C. Genoni^b, and T. A. Spencer^c

^aSandia National Laboratories, Albuquerque, NM 87185

^bMission Research Corporation, Albuquerque, NM 87106

^cAir Force Research Laboratory, Kirtland AFB, NM 87117

The magnetron oscillator can be a highly efficient device for generating microwaves. When operated at low voltage (V < 100 kV) efficiencies greater than 50% can be achieved. At relativistic voltages (V~500 kV), however, the peak efficiency is generally much less than 30%. Results of a recent numerical study 1 of the A6 magnetron suggest that the low efficiencies realized in previous relativistic magnetron experiments were due more to using an inappropriate tube configuration than to relativistic effects. In particular, it was suggested that efficient high power operation at relativistic voltages would require a significant increase in tube dimensions relative to the free-space wavelength of the desired mode.

To test this hypothesis we have performed a numerical study of a 14 cavity magnetron oscillator using 3D particle-in-cell (PIC) simulation. The magnetron has an anode diameter to free-space wavelength ratio of about 1:1, and its oscillation frequency is 1.1 GHz. Because of the large number of cavities a rising sun configuration is required to achieve oscillation in the π -mode (n=7). Power is extracted from every deep cavity. We investigated the performance of this tube in the range of operating voltages 300 < V < 650 kV, and corresponding applied magnetic field in the range $1.3 < B_z < 1.95$ kG. In our numerical experiments this tube vielded maximum power and efficiency at the high end of the voltage range; approximately 4 GW power at 25% efficiency at 600 kV. This efficiency is similar to that achieved in earlier work with rising suns operated at low voltage². Overall our results suggest that this efficiency is not limited by effects associated with high voltage, but by inherent shortcomings of a rising sun configuration (e.g., contamination by the zero-harmonic of the π -mode). In addition, we find that the rising sun configuration can shift mode competition from the n=6 to the n=3 or n=4 modes depend ing on the ratio of cavity depths.

1. R. W. Lemke, T. C. Genoni, and T. A. Spencer, "Three-dimensional particle-in-cell simulation study of a relativistic magnetron," to be published, Physics of Plasmas, February, 1999.

2. A. G. Smith, in *Microwave Magnetrons*, ed. G. B. Collins (McGraw Hill, New York, 1988) pp. 784-794.

This work was supported in part by the USAF Research Laboratory and Sandia National Laboratories. Sandia is a multiprogram laboratory operated by Sandia Corporation, a Lockheed Martin Company, for the US Department of Energy under Contract DEACO4-94AL8500.

Development of a High Power Klystron For the Spallation Neutron Source

T.A. Hargreaves, M.F. Kirshner, R. J. Hansen, Y. Misaki, R.B. True, G.R. Good, Litton Electron Devices, San Carlos, CA 94070, USA

Development of a High Power Klystron For the Spallation Neutron Source*

T.A. Hargreaves, M.F. Kirshner, R.J. Hansen, Y. Misaki, R.B. True, G.R. Good Litton Electron Devices Division San Carlos, CA 94070

> P.J. Tallerico and W. A. Reass Los Alamos National Laboratory Los Alamos, NM 87545

The Spallation Neutron Source (SNS) provides an intense beam of neutrons for scattering experiments. The SNS is comprised of an ion source, a 1 GeV H linear accelerator, an accumulator ring, a target for neutron production, and an area for the scattering experiments. The linear accelerator is driven by 52 klystrons operating at 805 MHz, and 3 klystrons operating at 402.5 MHz.

A prototype of the 805 MHz klystron is being developed at Litton and is the subject of this paper. The klystron will produce 2.5 MW of peak power at 10% duty. The pulse width is 1.7 msec and the efficiency is specified at a minimum of 55%. Testing is scheduled to begin in April, with delivery to Los Alamos in June. The design of the klystron and available test results will be presented.

*This work was performed under the auspices of the US Department of Energy.

6**B**05

Electrodynamic Pulse Shortening Mechanism Due to a Novel Beam/Cavity Interaction

J.W. Luginsland, K. J. Hendricks, D.A. Shiffler and Y.Y. Lau, U.S. Air Force Research Laboratory, Kirtland AFB, NM 87117, USA

Electrodynamic Pulse Shortening Mechanism Due to a Novel Beam/Cavity Interaction

J.W. Luginsland, K.J. Hendricks, D.A. Shiffler, and Y.Y. Lau¹

U.S. Air Force Research Laboratory
Directed Energy Directorate
Kirtland AFB, NM 87117-5776

Abstract

Beam/Cavity interactions are fundamental to the understanding and production of High Power Microwaves (HPM), especially in klystron-type devices. Relativistic Klystron Oscillators and Amplifiers (RKO/A) using Intense Relativistic Electron Beams (IREB) are an active area of research and development to produce HPM at the Gigawatt level. We report on a novel beam/cavity interaction, unique to these intense space charge beams, wherein the electromagnetic field energy is reflected back into the cavity if the beam density is sufficiently high. This effectively raises the Q of the cavity, and potentially destroys coupled cavity modes. This novel mechanism can explain pulse shortening in the Air Force Research Laboratory's RKO and features of RKA research performed at the Naval Research Laboratory in the late 1980's. Results include simulations in the time and frequency domain, as well as an analytic scaling law for this phenomenon. These results are compared with experimental data.

1. With The University of Michigan, Ann Arbor.

Halo Formation In High-Power Klystrons

Renato Pakter & Chiping Chen, MIT Plasma Science & Fusion Center PSFC/NW16-164, Cambridge, MA 02139, USA

HALO FORMATION IN HIGH-POWER KLYSTRONS*

Renato Pakter and Chiping Chen Plasma Science and Fusion Center Massachusetts Institute of Technology Cambridge, MA 02139

Beam losses and radio-frequency (rf) pulse shortening are important issues in the development of high-power microwave (HPM) sources [1] such as high-power klystrons and relativistic magnetrons. In this paper, we explore the formation and characteristics of halos around intense relativistic electron beams in a Periodic Permanent Magnet focusing klystron [2] as well as in a uniform solenoidal focusing klystron. A self-consistent electrostatic model is used to investigate intense relativistic electron beam transport as an rf field induced mismatch between the electron beam and the focusing field develops. To model the effect of such mismatch in the PPM klystron experiment [3], we initialize the beam with an envelope mismatch. For zero canonical angular momentum and an initial mismatch of 100 percent, for example, our preliminary results show halo particles with a maximum radius extending up to several core radii at the rf output section. Transient effects and the influence of finite canonical angular momentum are being studied.

*This work was supported by AFOSR and DOE.

- 1. A. J. Agee, et al., Proc. SPIE 3158, 21 (1997).
- 2. R. Pakter and C. Chen, "Nonlinear Dynamics of Intense Relativistic Electron Beams in Periodic Permanent Magnet (PPM) Focusing Systems," to appear in Proc. UHF-99.
- 3. D. Sprehn, et al., to appear in Proc. LINAC'98.

6**B**07

High Efficiency Milo

M. Joseph Arman, Air Force Research Lab, Kirland AFB, NM 87117-5776, USA

HIGH EFFICIENCY MILO

M. Joseph Arman

AIR FORCE RESEARCH LABORATORY

Directed Energy Directorate

Kirtland AFB, NM

ABSTRACT

The Magnetically Insulated Line Oscillator (MILO) is a low impedance, highly powerful source of coherent RF radiation. It is also compact and relatively simple. MILO's rms efficiency however is not very high. This is due to the fact that a large fraction of the dc input current goes into the generation of the azimuthal magnetic field needed to guide the initially radial beam into an axial flow. It has been shown that providing the azimuthal magnetic field through an external means, will not interfere with the MILO operation¹. This can be achieved through an independent circuit flowing an axial current near the cathode. Building upon this finding, we have designed a new MILO that operates with a significantly less input power while producing the same output as the conventional MILO. The new design has a higher impedance and provides no particle current for self-insulation. Results of the numerical simulations, carried out using the PIC code MAGIC will be presented.

1. "Externally Magnetized MILO" by Arman etal, presented at the 40th Annual Meeting Of the American Physical Society, Plasma Division, in New Orlean, Louisiana, 16-20 Nov. 1998

Initial Studies of an Annular Cesium Iodide Cathode

R. Umstadtt, M. Lacour, K. Hendricks, D. Shiffler, T. Spencer and D. Voss, U.S. Air Force Research Laboratory, AFRL/DEHE, Kirtland, NM 87117, USA

Initial Studies of an Annular Cesium Iodide Cathode

R. Umstadtt, M. Lacour*, K. Hendricks, D. Shiffler, T. Spencer and D. Voss**

AFRL, DEHE Kirtland AFB, NM 87117-5776

Abstract:

Cesium iodide (CsI) cathodes have been a topic of research in recent years as efforts have mounted to find a material that has the benefits, without the drawbacks, of explosive field emission cathodes. In particular, when typical explosive field emission cathodes are utilized for high power microwave tubes, microwave pulse shortening can occur due to motion of the cathode plasma across the anode-cathode (A-K) gap. Ultimately, this gap closure can sufficiently change the diode impedance such that the tube can no longer operate under the desired conditions. CsI cathodes have offered one solution to this problem. These cathodes have demonstrated low A-K gap closure times with applied fields in the range of a few tens of kV/cm to several hundred kV/cm with currents into the several kiloampere range. This poster reviews the results of experiments on the Cathode Test Bed at the Air Force Research Laboratory/Phillips Laboratory site. We review experiments on a cathode produced by Voss Scientific, with emphasis on conditioning effects and gas evolution from the cathode.

D. Shiffler, K. Hendricks, R. Umstattd, and T. Spencer are with the Air Force Research Laboratory/Phillips Laboratory, Kirtland AFB, NM 87117.

M. Lacour is with Maxwell Laboratories, Inc., Albuquerque, NM 87119.

D. Voss is with Voss Scientific, Inc., Albuquerque, NM 87108

6C

De Anza III 3 PM, Wednesday, June 23, 1999

Session 6C Fast Z-pinches and X-ray Lasers

Chairperson
Bruno Bauer
University of Nevada, Reno

6C01-2

Invited -

Review of Electrical Resistivity Measurements of Dense Aluminum

John F. Benage Jr., William R. Shanahan, Michael S. Murillo,

Los Alamos National Laboratory, Los Alamos, NM 87545, USA

Review of Electrical Resistivity Measurements of Dense Aluminum.*

John F. Benage, Jr., William R. Shanahan, Michael S. Murillo Los Alamos National Laboratory, Los Alamos, N.M. 87545

We have completed an analysis of recent experiments that were done at Los Alamos and other laboratories that measured the electrical resistivity of aluminum at conditions where the aluminum is in a dense, strongly coupled, plasma state. A plasma is strongly coupled when the parameter Γ , defined as the ratio of the average potential energy between ions to their temperature, is > 1. These plasmas occur naturally in the interiors of giant planets and brown dwarfs and on the surfaces of white dwarfs and neutron stars. They also occur in laboratory systems of high energy density whenever solid material is rapidly heated to plasma conditions, such as laser heated plasmas and ohmically heated metals. The properties of these plasmas cannot be treated using standard plasma theory, which treats the correlations among particles as a small effect. Many theories have been developed which predict the properties of such plasmas, but their is little data from experiments with which to compare. These experiments provide data for a comprehensive comparison of resistivity data with dense plasma theories. The experiments provide data under a wide range of conditions, from temperatures < 1 e.V. up to 25 e.V. and densities from nearly solid to < 1% solid. In all cases $\Gamma > 1$ for these experiments. In this presentation, we will present a comparison of the data with various theoretical predictions. From this comparison we will draw some conclusions concerning under what conditions some of the theories are adequate and other conditions where none of the theories appear to be accurate. Possible reasons for this continued discrepancy will be discussed.

6C03

Examination of Resistivity Issues In Solid Liner Z-Pinches

W.L. Atchison, R.J. Faehl and R.E. Reinovsky, Los Alamos National Laboratory, Los Alamos, NM 87545, USA

EXAMINATION OF RESISTIVITY ISSUES IN SOLID LINER Z-PINCHES

W.L. Atchison, R.J. Faehl, and R. E.
Reinovsky,
Plasma Applications Group and Pulsed
Power Program Office,
Los Alamos National Laboratory, Los
Alamos New Mexico 87545.

Experiments being conducted at the Los Alamos National Lab Pegasus facility are examining driving an aluminum liner with a pulsed magnetic field. The Pegasus facility provides a current of 5 to 8 Mega-amps to compress a cylindrical liner. Liners of various size and thickness are used. depending on the specific experimental objectives. In several of these experiments, a B-dot probe has been used to measure the field diffused through the liners. This data has been compared to predictions of field penetrations using numerical simulations. These predictions were made with a 2D Eulerian and a 1D Lagrangian MHD code. The simulations were made with a wide variety of resistivity models including both SESAME tabular values and analytic The results of these comparisons models. show that the behavior of aluminum in the region from a few tenths of an eV to leV and densities from about .2 to 3.0 g/cc is not this While is reproduced well. understandable base on the lack conclusive data in region, the experiments confirm the in-applicability of extrapolating existing models into this region where phase changes are drastically changing the behavior.

^{*}Work performed under the auspices of the Department of Energy.

Radius Scaling of Titanium Wire Arrays on the Z Accelerator

C.A. Coverdale, C. Deeney, R.B. Spielman, M.R. Douglas, T.J. Nash, K.G. Whitney, J.W. Thornhill, J. P. Apruzeses, R.C. Clark, J. Davis, D.L. Peterson, F.N. Beg, J. Ruiz-Comacho, R.Schneider, Sandia National Laboratories, Albuquerque, NM 87185-1159, USA

Radius Scaling of Titanium Wire Arrays on the Z Accelerator

C.A. Coverdale, C. Deeney, R.B. Spielman, M.R. Douglas, T.J. Nash Sandia National Laboratories, Albuquerque, NM

K.G. Whitney, J.W. Thornhill, J.P. Apruzese, R.C. Clark, J. Davis Naval Research Lab, Washington D.C.

D.L. Peterson
Los Alamos National Laboratory, Los Alamos, NM

F.N. Beg, J. Ruiz-Camacho Imperial College, U.K.

R. Schneider Defense Threat Reduction Agency, Alexandria, VA

The 20 MA Z accelerator has made possible the generation of substantial radiation (> 100 kJ) at higher photon energies (4.8 keV) through the use of titanium wire arrays. In this paper, the results of experiments designed to study the effects of initial load radius variations of nickel-clad titanium wire arrays will be presented. The load radius was varied from 17.5 mm to 25 mm and titanium K-shell (4.8 keV) yields of greater than 100 kJ were measured. The inclusion of the nickel cladding on the titanium wires allows for higher wire number loads and increases the spectral broadness of the source; kilovolt emissions (nickel plus titanium L-shell) of 400 kJ were measured in these experiments. Comparisons of the data to calculations will be made to estimate pinched plasma parameters such as temperature and participating mass fraction. These results will also be compared with previous pure titanium wire array results.

This work was supported by the Defense Threat Reduction Agency and DOE. Sandia is a multi-program laboratory operated by Sandia Corporation, a Lockheed Martin Company, for the United States Department of Energy under contract DE-AC04-94AL85000.

6C05

Long Implosion PRS Experiments On Double Eagle

J.S. Levine, P.L. Coleman, B.H. Failor, J.C. Riordan, Y. Song, H.M. Sze, E.M. Waisman, C.Deeney, J.S. McGurn, J.P. Apruzese, J.Davis, A. Fisher, B. Moosman, S. Stephanakis, J.W. Thornhill, B.V.Weber, K.G. Whitney, S. Gensler, N.Qi and R.F. Schneider, Maxwell Physics International, San Leandro, CA 94577, USA

LONG-IMPLOSION PRS EXPERIMENTS ON DOUBLE-EAGLE*

J. S. Levine, P. L. Coleman, B. H. Failor, J. C Riordan, Y. Song, H. M. Sze, E. M. Waisman, C. Deeney¹,
 J. S. McGurn¹, J. P. Apruzese², J. Davis², A. Fisher²,
 B. Moosman², S. Stephanakis²
 J. W. Thornhill², B. V. Weber², K. G. Whitney²,
 S. Gensler³, N. Qi³ and R. F. Schneider⁴

Maxwell Physics International 2700 Merced Street P.O. Box 5010 San Leandro, CA 94577-0599

Previous research on the high-power generators DM2, at Maxwell Physics International, and Saturn, at Sandia National Laboratories, has demonstrated that long-implosion (200-300 ns) PRS sources, both gas puff and wire load, can be sufficiently stable to produce well-assembled pinches and high-power radiation pulses of soft x-rays (1-4 keV). This has substantial implications for reducing the cost and risk of future higher current facilities (e.g. Decade Quad).

To extend our knowledge and understanding of long-implosion sources, we are conducting a well-diagnosed series of experiments on long-pulse Double-EAGLE (4 MA at 200 ns). Results from Ar gas puffs, with various nozzles and valves, and Al wire arrays will be presented. Where possible, comparison with short-pulse results will be discussed.

*This work supported by Defense Threat Reduction Agency.

¹Sandia National Laboratories

²Naval Research Laboratory

³Alameda Applied Sciences Corp

⁴Defense Threat Reduction Agency

X-Ray Spectroscopy on Double Eagle and DM-2

E.J. Yadlowsky, E.P. Carlson, J. Niemel, F. Barakat, R.C. Hazelton, C.C. Klepper, J. Riordan, B. Failor, P. Coleman, J. Levine, Y. Song, B. Whitton, J. Apruzese, J. Davis, F. Cochran, K. Whitney, HY-Tech Research Corporation, Radford, VA 24141, USA

X-RAY SPECTROSCOPY ON DOUBLE EAGLE AND DM-2

E. J. Yadlowsky, E. P. Carlson, J. Niemel, F. Barakat R. C. Hazelton and C. C. Klepper HY-Tech Research Corporation 104 Centre Court, Radford, VA 24141

J. Riordan, B. Failor, P. Coleman, J. Levine, Y. Song, and B. Whitton Maxwell Physics International San Leandro, CA

J. Apruzese, J. Davis, F. Cochran, and K. Whitney Radiation Hydrodynamics Branch Naval Research Laboratory, Washington, DC

The radial distribution of the ion density and electron temperature in a z-pinch has been inferred by comparing the measured values of the x-ray power and the ratio of optically thick spectral line intensities with calculated ones for a range of assumed radial distributions. This procedure provided evidence for an on-axis dip in the ion density. A complementary procedure is described to analyze spectra obtained on the DM-2 and Double Eagle accelerators at Maxwell Physics International. In this case, the radially resolved intensities of optically thin dopants added to the pinch were measured using a high resolution Johann spectrometer. The line intensities were Abel inverted and the radial distribution of two line ratios [La/(Hea+IC) and IC/Heal were obtained from which the localized electron temperature and density were inferred. Here IC is the intercombination line of the He-like stage. The ion temperature distribution was obtained by Abel inverting each wavelength interval of the ion line profile and determining the Doppler width at each radial position. The density profile inferred for Ar gas puff pinches on DM-2 with 4% Cl and Al wire loads coated with 5% Si on Double Eagle indicated a density dip on-axis similar to that deduced in refs. 1 and 2. The imploded linear mass density was inferred to be about 47% of the initial mass density. Similar on-axis local minima were observed for the ion temperature on both machines. Since different ion temperatures were inferred from the He, line than from the intercombination line of Cl, opacity and gradients may be affecting these results. These results demonstrate the details of the internal structure of the stagnated pinch that can be inferred from the radially resolved spectral intensities of optically thin dopants.

- 1 J. P. Apruzese, et al, Phys. Plasmas <u>5</u>. 4476 (1998).
- 2 K. G. Whitney, et al, Phys. Rev. E <u>5</u>, 3540 (1997).

6C07

72-pixel, diamond soft x-ray camera

R.R. Prasad, A.C. Crisman, N.Qi, S.W. Gensler and M. Krishnan, Alameda Applied Sciences Corp., San Leandro, CA 94577, USA

72-pixel, diamond soft x-ray camera*

R. R. Prasad, A. C. Crisman, N. Qi, S. W. Gensler, and M. Krishnan

Alameda Applied Sciences Corporation San Leandro, CA 94577

Rayleigh-Taylor instabilities in imploding plasma z-pinches are thought to limit the pulse-width, compression ratio, power coupling from driver to pinch and radiation efficiency, for z-pinches at 4 MA (Double-EAGLE), 8 MA (Saturn) and 18 MA (Z). A new metrology tool that can provide sufficient details of the evolution of "spikes" and "bubbles" in z-pinches, so that 2-D codes that model them may be anchored to experiments and eventually lead to better load designs such as structured and multi-shell loads is required.

This paper describes a camera that can provide 200 ps snap shots of the evolution of z-pinch radiation, in the soft x-ray and vacuum ultraviolet, with spatial resolution <0.5 mm (with 2:1 magnification). The camera uses a 12 x 6 array of diamond detectors with 1 mm x 1 mm pixels with 85% total open area. This detector has been fabricated and the absolute sensitivity of all the pixels has been determined on the laser plasma source at Sandia National Laboratory (courtesy R. B. Spielman, SNL). The camera was subsequently used to image the x-ray and VUV emissions from Ar long implosions on Double-EAGLE, capturing 400 ps snap shots of a z-pinch. These images show the limitations of existing instruments used to image z-pinch emissions. They also show evidence of "spike" and "bubble" formation in the pinch. These data will be presented.

*Work supported by the Defense Threat Reduction Agency under contract DSWA01-96-C-0171.

Model of enhanced energy deposition in a RT unstable strongly radiating Z-pinch plasma due to fast penetration of magnetic bubbles to the axis

L. I. Rudakov, J. Davis and A. L. Velikovich, Advanced Power Techologies, Springfield, VA 22150, USA

Model of enhanced energy deposition in a RT unstable strongly radiating Z-pinch plasma due to fast penetration of magnetic bubbles to the axis

L. I. Rudakov, J. Davis, and A. L. Velikovich Advanced Power Technologies, Inc.
Plasma Physics Division, Naval Research Laboratory
Berkeley Research Associates, Inc.

A model of a strongly radiating Z-pinch plasma saturated with "magnetic bubbles", or toroidal tubes carrying magnetic flux is developed. This model is an advanced extension of the earlier "bubble model" suggested by Rudakov and Sudan [1]. It describes, in a self-consistent way, the most relevant physical effects like fast penetration of magnetic flux in the imploding and stagnating plasma, additional energy supply due to the pdV work associated with the "magnetic bubble" penetration, and dissipation of this induced turbulent motion due to ion viscosity. The goal of this development is to provide the rigorous framework for an averaged onedimensional simulation of Z-pinch plasma radiation sources (PRS). This approach, in particular, would allow us to simulate magnetic energy coupling into the pinch plasma associated with the development of Rayleigh-Taylor (RT) instability [2] without sacrificing the accuracy of the radiation transport modeling.

As demonstrated in recent experiments and 2D simulations, the radiated energy is supplied to the plasma through the variety of physical mechanisms, and the conventional thermalization of kinetic energy is not necessarily the dominant one [2]. These results will be discussed in the context of search for some new, more efficient regimes of PRS operation, where the energy is delivered to the radiating plasma primarily through the described above turbulent heating mechanism. It could allow starting Z-pinch implosions from smaller radii, to stagnate near the axis before the current pulse reached its peak amplitude. In such a regime, it would be easier to get the soft component of radiation trapped, thus minimizing the losses to the soft radiation in a PRS and increasing the efficiency of magnetic energy conversion into the K-shell emission.

- [1] L. I. Rudakov and R. N. Sudan, Phys. Reports 283, 253 (1997).
- [2] C. Deeney, D. L. Peterson et al., 5, 2605 (1998);
 D. L. Peterson, C. Deeney et al., Phys. Plasmas 5, 3302 (1998).

6C09

Time Resolved Detection of the XUV-Laser Activity in a Fast Z-Pinch Plasma

B. Bayerlein, A. Tauschwitz and R. Presura, Universitat Erlangen-Nurnberg, GSI, 64294 Darmstadt, Germany

Time Resolved Detection of the XUV-Laser Activity in a Fast Z-Pinch Plasma

B. Bayerlein, A. Tauschwitz¹, R. Presura²

Physikalisches Institut der Universität Erlangen-Nürnberg
Erlangen, Germany

¹Gesellschaft für Schwerionenforschung GSI
Darmstadt, Germany

²National Institute for Lasers, Plasma, and Radiation Physics
Bucharest, Romania

Measurements with time and spectral resolution were carried out on the XUV emission of an argon Z-pinch plasma potentially presenting amplification. The time evolution of several line intensities was recorded by means of a grating monochromator equipped with a microsphere plate. The time resolution was less than 0.3 ns and the spectral resolution about 0.11 nm. The discharges were performed in aluminum oxide tubes 7 mm in diameter filled with 10 Pa argon. Typical values of the maximum discharge current intensity and current rise-time were 38 kA and 35 ns, respectively.

The spectral range around the laser line of the Ne-like Ar ions at 46.88 nm was scanned in steps of 0.037 nm. An analysis of the intensity signals evidenced sub-structures during the pinch phase. For all investigated lines, the intensity displays a first maximum at $t \approx 55$ ns from the discharge initiation. After this point the signals either interrupt suddenly for $3 \div 5$ ns or drops sharply. Later on, while the Ar VI and the Ar VII lines intensities continue to decrease, the intensities of the Ar IX lines show a second, much higher maximum around $t \approx 65$ ns. Computer simulations of the dynamics of fast Z-pinch discharges in argon explain the occurrence of the first maximum observed at $t \approx 55$ ns in terms of sudden plasma overheating by a shock wave, leading to the fast ionization of the plasma ions. When the Ar X to Ar XII ions are formed, the populations of the lower ionization stages, including Ar IX, decrease for a short while.

The laser activity was studied in more detail by measuring the Ar IX line intensity at 46.88 nm for five discharge lengths between 3 and 16 cm. Two other lines were used as intensity reference, namely the Ar VII line at 47.95 nm and the Ar IX line at 48.49 nm. In the case of longer tubes, the data were affected by alignment problems. For the shorter lengths, $3 \div 9$ cm, an over-proportional increase of the second intensity maximum of the Ar IX line at 46.88 nm was observed. By fitting the data with the Linford formula, an absolute gain coefficient $g \approx 0.16$ cm⁻¹ was inferred, corresponding to a gain-length product $g \cdot l \approx 1.4$. A calculated compensation of the misalignment effect indicated that the actual values could reach up to $g \approx 0.29$ cm⁻¹ and $g \cdot l \approx 2.6$, respectively. There are indications that the discharge length affects also the pinch dynamics. An estimation of the absolute intensity of the laser line gives a value of about 10 mW.

Rayleigh-Taylor Stability Criteria for Magnetically Imploded Solid Liners

Edward L. Ruden, Air Force Research Laboratory, KAFB, NM 87117, USA

Rayleigh-Taylor Stability Criteria for Magnetically Imploded Solid Liners

Edward L. Ruden Air Force Research Laboratory Directed Energy Directorate

Approximate analytic Rayleigh-Taylor stability criteria for elastic-plastic solid liners, where convergence imposes a background strain rate tensor [1], is reviewed and compared to other work. It is shown that in the incompressible twodimensional planar limit, with constant yield strength and shear modulus, the dynamics of a liner driven by a massless fluid vs. a magnetic field orthogonal to the perturbation are equivalent. This holds regardless of the form or magnitude of the perturbation or degree of magnetic diffusion. The proposition that a redistribution of the magnetic pressure due to diffusion has no effect on the material dynamics has proven to be counterintuitive to many, so will be discussed in depth. Beyond the above limit, however, thermal softening and phase transitions due to Ohmic heating, compressibility, threedimensional flow, and cylindrical geometry can be issues. The conditions where these effects can be expected to significantly effect the dynamics are discussed.

[1] E.L. Ruden and D.E. Bell, J. Appl. Phys. 82, 163-170 (1997)

6D

Bonsai I/II 3 PM, Wednesday, June 23, 1999

Oral Session 6
Vacuum Microwaves (Microelectronics)

Chairperson
Capp Spindt
SRI

6D01-2

Invited -

PPM Focused TWT Using a Field Emitter Array Cold Cathode

D.R. Whaley, C.M. Armstrong, B. Gammon, Northrop Grumman Corporation, Rolling Meadows, IL 60008, USA

PPM Focused TWT Using a Field Emitter Array Cold Cathode

D. R. Whaley, C. M. Armstrong, B. Gannon Northrop Grumman Corporation, 600 Hicks Rd., M/S H6402, Rolling Meadows, IL 60008-1098

P. Mukhopadhyay-Phillips, C. A. Spindt, C. E. Holland SRI International, 333 Ravenswood Ave., Menlo Park, CA 94025

With the recent advances in field emitter array (FEA) technology, current densities as well as total currents from planar arrays have reached values meeting or exceeding many moderate power TWT beam requirements. The development of a robust high current density (>10 A/cm²) cold cathode source, such as the FEA, would open new vistas in the power-bandwidth performance of microwave devices, particularly those operating at millimeter wavelengths. Extremely compact, lightweight, low frequency designs may also result with the advent of FEA gated emission cathodes. Before the development of such technologies, however, the challenges of FEA beam generation, focusing and confinement in a TWT PPM configuration must be solved. This experimental program is designed to address these issues.

Several SRI field emitter arrays (known as Spindt cathodes) have been fabricated and tested for incorporation into a PPM-focused C-Band TWT. The emitting portion of the arrays has a 1 mm diameter and is comprised of 50,000 tips, each tip having a 200 Å radius. The 0.5 μm aperture and 4 μm tip-to-tip spacing reduce the probability of failure of an entire array due to neighboring tip arcing. The 0.146 A beam of the C-Band TWT will require a tip loading of 3 μA per tip. SRI International has routinely demonstrated 10 μA per tip from small arrays. One goal of this project is to demonstrate such current densities on larger arrays with larger total currents. The cathodes fabricated for this project incorporate a resistive base of approximately 2500 Ω , important for arc protection in the initial stages of testing. The cathodes have been tested independently of the electron gun up to .010 A and show no indication of current limits.

The electron gun which will incorporate the FEA cathodes has been fabricated. The gun structure is a modified Einzel lens and uses a series of shaped electrostatic lenses to overcome the problems associated with inherent defocusing of high current density FEA electron beams. In TWT geometry, confinement and focusing of the FEA beam is complicated by the low magnetic field at the cathode surface, the nonconvergent nature of the emitted beam, high emittance, and high preacceleration current density. The electron gun and PPM magnetic field structure have been designed to overcome these difficulties for all modes of operation. Unlike space-charge limited thermionic cathodes, FEA emitters can be operated at any current below the operating current. The electron gun and magnetic field structure accommodates all modes of operation by producing laminar, non-scalloping, electron beams for low current as well as full current operation. The first FEA electron gun fabricated was sectioned to verify build tolerances and insure proper lens placement. High voltage standoff tests show the gun can withstand ~2x operating voltage on each of the individual lenses without arcing. A second FEA gun has been fabricated incorporating several small changes from analysis of the first gun. An FEA test station has also been built at Northrop Grumman to test FEA emission and transmission as well as TWT RF performance. Results of these tests will be presented.

6D03-4

Invited -

Performance of Field Emission Cathodes in Xenon Environments

C.M. Marrese, J.E. Polk, K.L. Jensen, A.D. Gallimore, C. Spindt, R.L. Fink and Z.L. Tolt W.D. Palmer, U.S. Naval Research Laboratory, Washington, DC

Performance of Field Emission Cathodes in Xenon Environments

C. M. Marrese¹, J. E. Polk², K. L. Jensen³, A. D. Gallimore¹, C. Spindt⁴, R. L Fink and Z. L. Tolt⁵, W. D. Palmer⁶

¹ University of Michigan/ JPL, Ann Arbor, MI 48109

² Jet Propulsion Laboratory, Pasadena, CA 91109

³ Naval Research Laboratory, Washington, DC 20375

⁴ SRI International, Menlo Park, CA 94025

⁵ FEPET, Austin, TX 78758

⁷ MCNC, Research Triangle Park, NC 27709

Field emission (FE) cathodes are currently being considered to supply electrons in electric propulsion systems for propellant ionization and ion beam neutralization. Hollow cathodes with thermionic electron emitters typically used with Hall and ion thrusters require propellant and heaters for operation. Therefore there are lower limits on their size and power. Because FE cathodes do not require propellant or heaters they can be used with small and micropropulsion systems. The primary concern with integrating these two technologies is cathode lifetime. An FE cathode must be capable of operation in a plasma environment where xenon pressures exceed 2x10⁻⁶ Torr. Experiments were conducted at the Jet Propulsion Laboratory to evaluate the performance of silicon and molybdenum microtip field emission array cathodes, and carbon film cathodes in xenon pressures up to 2x10⁻⁵ Torr. Experimental and modeling results were used to determine energy thresholds for sputtering silicon and molybdenum by xenon ions. Experiments and theoretical results are presented for performance degradation in xenon environments.

6D05

High Current dc and Pulsed Field Emission From Single Cyrstal ZrC(100) emitters mounted in apertures

W.A. Mackie, Tianbao Xie, Kristin Lee, and P.R. Davis, Linfield Research Institute, McMinnville, OR 97128, USA

High current dc and pulsed field emission from single crystal ZrC(100) emitters mounted in apertures

W. A. Mackie, Tianbao Xie, Kristin Lee, and P.R. Davis Linfield Research Institute McMinnville, OR 97128-6894

Abstract

We have been working for several years on field emission from transition metal carbides. These studies have covered emission from solid carbide field emitters as well as thin film carbide overcoatings on single tip field emitters and field emitter arrays. These carbide materials have emission properties making them attractive candidates for uses requiring high currents, small spot sizes, and cold cathodes for operation in poor vacuum. Uses might include microwave devices, electron accelerators, free-electron lasers, and other high current applications.

Two main requirements for these types of applications are high total current and high beam brightness. Historically, materials that have been used require ultra-high vacuum for stable operation. The method we have been investigating uses gated, cold field emission. We feel that this approach coupled with cathodes fabricated from transition metal carbides have the potential of delivering the required currents, either dc or in pulsed operation, even in less than ideal vacuum conditions.

We report on field emission studies using (100) oriented ZrC field emitters configured in an extraction or gate aperture. This geometry can allow for efficient confinement and a high brightness beams. Stable high-current emission has been obtained in the 2 mA range dc and pulsed currents as high as 50 mA are demonstrated.

6D06

Migration and Escape of Barium Atoms in a Thermionic Cathode and Their Contribution to Noise

K.L. Jensen, Y.Y. Lau, B. Levush, Naval Research Laboratory, Washington, DC 20375-5347, USA

Migration and Escape of Barium Atoms in a Thermionic Cathode and Their Contribution to Noise

K. L. Jensen, Y. Y. Lau*, B. Levush Naval Research Laboratory, Washington, DC 20375

An understanding of the noise mechanisms inherent in thermionic cathodes is necessary insofar as flicker noise from the cathode can degrade amplifier performance. The noise is generally attributed to the fluctuations of the barium sites ("islands") on the cathode surface [1], from which the electron current is mostly drawn. Cathode lifetime likewise is dependent upon the migration of barium atoms to the surface of the cathode, and their subsequent sputtering off by ion bombardment and evaporation due to high cathodic temperature.

To investigate the noise processes associated with these phenomena, we have developed a model of barium migration to the surface and its subsequent removal by bulk and monolayer evaporation and ion sputtering. The diffusion constant, which governs the migration, is determined from the product of the (thermally dependent) probability for transition multiplied by the probability that the target site is vacant. Similarly, the removal rates are governed by tube environmental parameters by barium bulk and monolayer evaporation rates, and by ion back-bombardment on the cathode.

We have endeavored to provide coverage estimates, adsorbate work function values, lifetime estimates, and current density predictions, which are in qualitative agreement with experiment [2]. The numerical approach is based on a hopping model of barium diffusion to determine barium concentration within the cathode as a function of time, as well as the surface coverage ratio. Differential equations governing the barium evolution are constructed from the discrete model, from which an analytical model is proposed that allows for estimates of lifetime and total current from the cathode. Insofar as possible, all parameters are determined from simple models of the underlying physical processes, though a limited number of parameters are obtained from the literature.

We shall describe both the numerical and analytic models, and describe the parametric dependence of barium evolution obtained. We shall then provide estimates of various characteristics, e.g., cathode lifetime, surface coverage, current density and its fluctuations, etc.

Funding provided by Office of Naval Research
*On sabbatical leave from U. Michigan, Ann Arbor, MI
[1] A. van der Zeil, Noise, (Prentice-Hall, New York, 1954) p224-232.
[2] See, e.g., M. C. Green, Tech. Digest of the IEDM (1987) p925; R. T. Longo, E. A. Adler, and L. R. Falce, ibid, (1984) p318; R. Forman, J. Appl. Phys. 47, 5272 (1976).

6D07

Electron Migration Across Transverse Kicker Magnet In Beam Collector/RF Waveguide SystemK.T. Nguyen, N.J. Dionne, M. Blank, B.D. Danly and B. Levush, Naval Research Laboratory, Washington, DC 20375, USA

ELECTRON MIGRATION ACROSS TRANSVERSE KICKER MAGNET IN BEAM COLLECTOR / RF WAVEGUIDE SYSTEM

K.T. Nguyen^a, N..J. Dionne^b, M. Blank, B.D. Danly, and B. Levush

Naval Research Laboratory, Washington, D.C. 20375

For gyro-amplifiers, the collector often also serves as the RF output waveguide. The axial magnetic field in such collectors is tapered so that most of the beam electrons can be collected on the collector. Transverse kicker magnets are used as a barrier to prevent stray electrons from being intercepted by the dielectric RF window. This is to reduce the possibility of electron-induced damages for the RF windows. This procedure has been implemented in the collector of the recently developed NRL/Litton/CPI high-power, W-band gyro-amplifier [1-3].

Using the gun code UGUN, it is shown that electron interception by the window is a possibility, even when the transverse kicker magnet is sufficient to deflect all the primary beam electrons away from the window. UGUN, which includes models for scattered primaries and true lowenergy secondary electrons, was modified to treat the 3-D nature of the kicker magnet. It is found that the electron migration across the transverse magnetic field barrier is due to multiple bounces, forward-scattered primaries. Consequently, it is necessary for the kicker magnet design to take into account this effect to minimize the possibility of window damage. Detailed simulation results using the collector of the high-power, W-band gyro-amplifier [3] as an example will be presented.

*This work was supported by the Office of Naval Research.

- [1] K. Nguyen, et al., *IEEE Trans. on Plasma Science* 26, 799 (1998).
- [2] B. Danly, et al., Digest 23rd Int. Conf. Infrared & mm Wave, Colchester, England, 1998, p32
- [3] M. Blank, et al., "Demonstration of a High Power W-band Gyroklystron Amplifier for Radar Application," this conference.

6P

Serra I, Conference Center 3 PM, Wednesday, June 23, 1999

Poster Session 6P

a) KN Research, Silver Spring, MD 20905

b) Raytheon Systems Company, Tewksbury, MA 01876

Diagnostics and Experiments on LAPPS

D. Leonhardt, D.P. Murphy, S.G. Walton, R.A. Meger, R.F. Fernsler and R.E. Pechacek, U.S. Naval Research Laboratory, Washington, DC 20375, USA

Diagnostics and Experiments on LAPPS*

D. Leonhardt, D. P. Murphy, S. G. Walton, R. A. Meger, R. F. Fernsler, R. E. Pechacek Plasma Physics Division, U.S. Naval Research Laboratory, Washington, DC 20375-5346

NRL is developing a new plasma processing reactor called the 'Large Area Plasma Processing System' with applications to semiconductor processing and other forms of surface The system consists of a planar plasma distribution generated by a magnetically collimated sheet of 2-5kV, 10 mA/cm² electrons injected into a neutral gas background. This beam ionization process is both efficient at plasma production and readily scalable to large (square meters) area. The use of a beam ionization source largely decouples the plasma production from the reactor chamber. Ion densities (oxygen, nitrogen, argon, helium) of up to 5x10¹² cm⁻³ in a volume of 2 cm x 60 cm x 60 cm have been produced in the laboratory. Typical operating pressures range from 20-200 mtorr with beam collimating magnetic fields strengths of 10-Thus far the system has been operated with a 300 Gauss. pulsed (10-2000 µs pulse length, <10 kHz pulse repetition Temporally frequency) hollow cathode. measurements of the plasma sheet using Langmuir probes, spectrally resolved optical emission, microwave interferometry, and cyclotron harmonic microwave emission will be presented. Results of initial processing tests using an oxygen plasma showing isotropic ashing of a photoresist will be shown. Progress in the development of a dc hot filament cathode will be presented along with the status of the 1 m² UHV chamber for future processing tests. An overview of the LAPPS process along with theoretical treatments and issues will also be presented by co-authors1.

6P02

Generation of High Density Plasma with Large Volume Using Pulsed Glow Discharge

K. Takaki, D. Kitamura and T. Fujiwara, Iwate University, Morioka/Iwate 020-8551, Japan

Generation of High Density Plasma with Large Volume Using Pulsed Glow Discharge

K. Takaki, D. Kitamura, and T. Fujiwara
Department of Electrical and Electronics Engineering
Iwate University, Ueda 4-3-5
Morioka, Iwate, 020-8551, Japan

A new technique, Plasma Source Ion Implantation (PSII) for the surface modification of materials, was proposed by J. R. Conrad in 1989. Recently, this technique has been studied all over the world as Plasma Based Ion Implantation (PBII), Plasma Immersion Ion Implantation (PIII, PI3), IONCLAD (called by General Motors), PLAD (by Varian). In PBII, it is necessary to generate high density plasma with large volume. Pulsed glow discharge is one of the candidates for the ion source plasma because it can easily generate large volume plasma, although for a short time. This paper describes the characteristics of high current pulsed glow discharge generated using a low impedance circuit. A low inductance capacitor of 1.89 µF was used in this experiment. The inductance of the device was calculated to be 444 nH from its geometry. The discharge current was measured using PEARSON C.T varying a circuit resistance in the range of 1 Ω and several tens ohm. The gap voltage and consumed energy were obtained from a circuit equation and the measured values of discharge currents and breakdown voltage (i.e. initial charging voltage). The gas used is dry air. As the results, the pulsed glow discharge with high current above one hundred ampere was generated for several microseconds. The current density on the cathode reached to 3.7 A/cm² for a 2 cm gap at 12 Torr. This current density is one or two order of magnitude larger than the calculated value of a normal glow current density for a copper cathode and air. For the calculation, a formula j $[\mu A/cm^2] = 240*P^2$ where P is gas pressure in Torr. When the circuit resistance become larger, the current density of the pulsed glow discharge is gradually approaching the value of the normal glow discharge.

^{*}Work supported by the Office of Naval Research †SFA Inc., Landover, MD 20785

¹R. F. Fernsler, et al., this conference.

On the Theory of a Low Pressure Magnetron Glow Discharge

L.Pekker, S.I. Krasheninnikov, DSI, Santa Rosa, CA, 95401, USA

On the Theory of a Low Pressure Magnetron Glow Discharge

L. Pekker

Deposition Sciences Incorporation, Santa Rosa, CA 95401

S. I. Krasheninnikov

Plasma Science and Fusion Center, MIT, Cambridge, MA 02139

A one-dimensional analytical model of a magnetron glow discharge is considered assuming classical electron and ion transport across magnetic field lines. In our derivation of the model we assume slab geometry where the transverse magnetic field H is parallel to the electrode, and the electric field E is directed along the z-axis, perpendicular to the electrode. We assume that the ion cyclotron radius, and the ion mean free path are greater than the anode-cathode distance, L. Unlike ions, the electrons are assumed to be significantly magnetized: their cyclotron radius is assumed to be much smaller than L. We neglect in the model electron escape in the directions parallel to the electrode, assuming that the system is infinite in the ExB direction, and the electrons are electrostaticaly confined by the walls in B direction. Thus, all parameters of the glow discharge are dependent on the z coordinate, directed along the electric field. This geometry is similar to the geometry of the cylindrical magnetron [1] when R_c - R_a << R_c, where R_c is the cathode radius and Ra is the anode radius.

In this model we consider the regimes where E is greater than zero in all of the anode-electrode gap. This case corresponds to the absence of an electrostatic trap for charged particles.

Under these assumptions the theoretical volt-ampere characteristic of the discharge is obtained. The shape of this characteristic is similar to that found in the experiments. However, the available experimental current densities exceed the theoretical ones calculated with present model.

The discrepancy between theoretical calculations and experimental data can be explained in the following way. In the present model we have assumed classical electron diffusion. This assumption is apparently correct only for small current densities. When the current density is increased the discharge becomes unstable and electron scattering by plasma oscillations prevails over classical diffusion. We believe that experimental measurements correspond to this non-classical situation. Our model can be easily transformed for the case of non-classical electron diffusion by introducing the electron - plasma oscillations collision frequency instead of the classical electron neutral atom collision frequency.

[1] Wasa K, and Hayakava S, Handbook of sputter Deposition Technology: Principal, Technology, and Applications, Park Ridges, NJ: Noyes, 1992.

6P04

Discharge Regimes and Density Jumps in a Helicon Plasma Source

S. Shinohara and K. Yonekura, Kyushu University, Kasuga, Fukuoka 816-8580, Japan

Discharge Regimes and Density Jumps in a Helicon Plasma Source

S. Shinohara and K. Yonekura

Interdisciplinary Graduate School of Engineering Sciences, Kyushu University, Kasuga, Fukuoka 816-8580, Japan

A high density plasma source using a helicon wave is becoming very attractive in plasma processing and confinement devices. In the previous work [1-5], the characteristics of this wave and plasma performance with diameters of 5 and 45 cm have been studied, and the helicon wave was only observed after the density jump. Recently, density jumps from the low to high electron densities with a level of 10^{13} cm⁻³ were investigated by changing the antenna wavenumber spectrum [6], and the obtained results were compared with the inductively coupled plasma (ICP).

However, the mechanisms of density jumps and plasma production are still open questions to be answered. Here, we try to investigate the discharge regimes and density jumps in a helicon plasma source, by changing the antenna wavenumber spectrum (two-loop antenna with the same or opposite current directions), Ar filling pressure (P = 6 and 51 mTorr) and the external magnetic field ($B \le 1$ kG). The plasma was produced in a Pyrex tube with a diameter of 5 cm by RF with a frequency of 7 MHz.

For the case of the parallel current directions in the antenna, where the low wavenumber spectrum part is large, the density jump was observed with the low RF input power of $P_{\rm in} < 300$ W regardless of the magnetic field. On the other hand, for the case of the opposite directions, where the low wavenumber spectrum part is small, the threshold power to obtain the jump became high with the increase in the magnetic field. This can be understood from the dispersion relation of the helicon wave. The wave structures and the dispersion relations in the discharge modes will be also shown.

References

- [1] S. Shinohara, Y. Miyauchi and Y. Kawai, Plasma Phys. Control. Fusion 37 (1995) 1015.
- [2] S. Shinohara, Y. Miyauchi and Y. Kawai, Jpn. J. Appl. Phys. 35 (1996) L731.
- [3] S. Shinohara, S. Takechi and Y. Kawai, Jpn. J. Appl. Phys. 35 (1996) 4503.
- [4] S. Shinohara, Jpn. J. Appl. Phys. 36 (1997) 4695.
- [5] S. Shinohara, S. Takechi, N. Kaneda and Y. Kawai, Plasma Phys. Control. Fusion 39 (1997) 1479.
- [6] S. Shinohara, N. Kaneda and Y. Kawai, Thin Solid Films 316 (1998) 139.

RF Wave Propagation in Large Diameter Plasma under the Various Magnetic Field Configurations

S. Shinohara, S. Takechi and A. Fukuyama, Kysushu University, Kasuga, Fukuoka 816-8580, Japan

Diagnostics and Experiments on LAPPS*

D. Leonhardt, D. P. Murphy, S. G. Walton, [†] R. A. Meger, R. F. Fernsler, R. E. Pechacek [†] Plasma Physics Division, U.S. Naval Research Laboratory, Washington, DC 20375-5346

NRL is developing a new plasma processing reactor called the 'Large Area Plasma Processing System' with applications to semiconductor processing and other forms of surface The system consists of a planar plasma modification. distribution generated by a magnetically collimated sheet of 2-5kV, 10 mA/cm² electrons injected into a neutral gas background. This beam ionization process is both efficient at plasma production and readily scalable to large (square meters) area. The use of a beam ionization source largely decouples the plasma production from the reactor chamber. Ion densities (oxygen, nitrogen, argon, helium) of up to 5x10¹² cm⁻³ in a volume of 2 cm x 60 cm x 60 cm have been produced in the laboratory. Typical operating pressures range from 20-200 mtorr with beam collimating magnetic fields strengths of 10-300 Gauss. Thus far the system has been operated with a pulsed (10-2000 µs pulse length, <10 kHz pulse repetition frequency) hollow cathode. Temporally resolved measurements of the plasma sheet using Langmuir probes, spectrally resolved optical emission, microwave interferometry, and cyclotron harmonic microwave emission will be presented. Results of initial processing tests using an oxygen plasma showing isotropic ashing of a photoresist will be shown. Progress in the development of a dc hot filament cathode will be presented along with the status of the 1 m² UHV chamber for future processing tests. An overview of the LAPPS process along with theoretical treatments and issues will also be presented by co-authors¹.

6P06

Evanescent Electromagnetic Field Structures in Inductively Coupled Plasma

S. Shinohara and S. Takechi, Kyushu University, Kasuga, Fukuoka 816-8580, Japan

Evanescent Electromagnetic Field Structures in Inductively Coupled Plasma

S. Shinohara and S. Takechi

Interdisciplinary Graduate School of Engineering Sciences, Kyushu University, Kasuga, Fukuoka 816-8580, Japan

Inductively coupled plasma (ICP) has been recognized as a high-density plasma source in the radio frequency (RF) range for plasma application fields. Although the characterization and optimum plasma production have been actively tried, the role of the electron thermal motion especially in the low pressure regime has not been elucidated yet. In our previous study [1,2], this motion was investigated by measuring the skin depth of the evanescent wave and antennaplasma resistance in a wide range of collision frequencies: For the ICP production, the dominant role of the collisionless (collisional) heating mechanism in the low (high) collisionality was demonstrated.

Here, we present the effect of the electron thermal motion [3] based on the non-local, collisionless model on the evanescent electromagnetic field structures in the ICP with a large diameter of 45 cm produced by a planar, spiral antenna. The axial profiles of the amplitude and phase of the evanescent electromagnetic fields by the magnetic probes and also the antenna-plasma loading resistance were measured, and they were compared with the theoretical models.

The point of the minimum wave amplitude (axial profile of the non-monotonic wave decay) shifted by changing the boundary condition with the use of the metal end plate (effective axial length of the chamber: 5 - 60 cm), Ar filling pressure (0.65 - 26 mTorr) and the RF frequency (3 - 15 MHz), i.e., varying the ratio of the contribution of the electron thermal motion. These results were consistent with the calculation results based on the collisionless, non-local model (one dimension) [4] but not on the conventional classical, local model. The observed peak antenna-plasma resistance in the low collisionality also showed the existence of a resonant coupling between the electromagnetic field and the electron bounce motion.

References

- [1] S. Shinohara, S. Takechi and Y. Kawai, Jpn. J. Appl. Phys. 35 (1996) 4503.
- [2] S. Takechi, S. Shinohara and Y. Kawai, Jpn. J. Appl. Phys. 36 (1997) 4558.
- [3] S. Takechi and S. Shinohara, Jpn. J. Appl. Phys., in press.
- [4] N. S. Yoon, S. S. Kim, C. S. Chang and Duk-In Choi, Phys. Rev. E 54 (1996) 757.

^{*}Work supported by the Office of Naval Research †SFA Inc., Landover, MD 20785

¹R. F. Fernsler, et al., this conference.

Electrostatic probe measurements of electron temperature and number density in helium ICP-MS interface region

Hironobu Yabuta, Akitoshi Okino and Eiki Hotta, Tokyo University of Technology, Yokohama 226-8502, Japan

Electrostatic probe measurements of electron temperature and number density in helium ICP-MS interface region

Hironobu Yabuta, Akitoshi Okino* and Eiki Hotta
Department of Energy Sciences,
Tokyo Institute of Technology,
4259 Nagatsuta, Midori-ku, Yokohama 226-8502, JAPAN.
*Department of Electrical and Electronic Engineering,
Tokyo Institute of Technology,
2-12-1 O-okayama, Meguro-ku, Tokyo 152-8552, JAPAN.

Argon inductively coupled plasma mass spectrometry (Ar ICP-MS) has become the most powerful technique for elemental analysis, and spread quickly all over the world. However, it is considered that the efficient detection capabilities of Ar ICP offered for most metals are not realized for elements such as halogens. If helium ICP is used, it is possible to ionize all the elements except neon because helium has the larger metastable excitation energy (19.81eV) than argon and the largest ionization energy among all elements.

We successfully generated stable helium plasma at the atmospheric pressure using the enhanced vortex flow torch for practical He ICP-MS use. However, mass analysis device for Ar ICP-MS is not appropriate for He ICP-MS, since the properties (ionization energy, coefficient of kinematic viscosity and etc.) of helium and argon are quite different and a secondary discharge is remarkable in the interface region. A secondary discharge was overcome for Ar ICP by applying several control methods. However, these methods were not effective for He ICP. Therefore, to find other method for controlling the secondary discharge, it is necessary to clarify characteristics of the secondary discharge.

We measured the plasma characteristics (electron temperature, electron number density and etc.) with electrostatic probes in He ICP-MS interface region. We used a probe such that a tip was a few mm in diameter and a few mm long. Using this probe, reasonable I-V characteristics could not be obtained. It is considered that this result was due to an effect of the ion beam. Threrefore, we made another two types of probe. One has an electrode of 1mm in diameter and 0mm long. In this case the ion beam strikes only against the cross section of the tip, and we obtain linear I-V characteristics. These results are due to the beam effect. Another has an electrode of 1mm in diameter, 1mm long and its surface faced to the beam is covered with ceramics. In this case the ion beam effect was not observed and it is found that the latter probe is adequate to measure the secondary discharge characteristics in the interface region. The results of several measurements using this probe will be reported at the conference.

6P08

Experimental and Simulation Study of Spherically Convergent Beam Fusion

Yasushi Takeuchi, Kunihito Yamauchi, Yutaka Ogina, Masato Watanabe, Akitoshi Okino, Kwang-cheol Ko and Eiki Hotta, Tokyo Institute of Technology, Yokohama 226-8502, Japan

Experimental and Simulation Study of Spherically Convergent Beam Fusion

Yasushi TAKEUCHI, Kunihito YAMAUCHI, *Yutaka OGINO, Masato WATANABE, *Akitoshi OKINO, **Kwang-cheol Ko and Eiki HOTTA

Department of Energy Sciences, Tokyo Institute of Technology,
Nagatsuta, Midori-ku, Yokohama, 226-8502, Japan.

*Department of Electrical and Electronic Engineering,
Tokyo Institute of Technology,
O-okayama, Meguro-ku, Tokyo, 152-8552, Japan.

**Department of Electrical and Computer Engineering,
Hanyang University,
Seongdong-ku, Seoul, 133-791, Korea.

The experimental and simulation results of spherical glow discharge will be presented. The device is made of 50-cm diameter, 30-cm high stainless steel cylindrical chamber, in which a spherical anode of 30-cm diameter is set. The grid cathode is made of 1.9-mm diameter stainless steel wire, which is made into an open-spherical-grids of 5-cm diameter. The system is maintained at a constant pressure of 1-15 mTorr by bleeding hydrogen or deuterium gas into the chamber through a leak valve. A 0-60 kV, 0-20 mA constant current dc power supply was used to power the device. Using deuterium, the neutron production was observed. The basic discharge characteristics such as the breakdown voltage versus pressure, the operating voltage versus current with changing the gas pressure were measured. The motions of ions and electrons in the device were simulated using a particle code, which is onedimensional in coordinate system and two-dimensional in velocity space. The simulation shows that a shallow potential well for ions is formed in the central part inside the grid cathode. However, the well is observed to be very unstable.

Particle-in-cell modeling of electron oscillation inside a vacuum arc plasma source duct

T.K. Kwok, T.Zhang, P.K. Chu, M.M.M. Bilek and I.G. Brown, City University of Hong Kong, Hong Kong SAR, China

Particle-in-cell modeling of electron oscillation inside a vacuum arc plasma source duct

T. K. Kwok¹, T. Zhang¹, P. K. Chu¹, M. M. M. Bilek², and I. G. Brown³

Department of Physics and Materials Science, City University of Hong Kong, 83 Tat Chee Avenue, Kowloon, Hong Kong.

Department of Engineering, University of Cambridge,

Cambridge CB2 1PZ, UK.

Lawrence Berkeley National Laboratory, University of California, Berkeley CA 94720, USA.

Vacuum arc or cathodic arc metal plasma sources can deposit high quality thin metal films and metallurgical coatings. A metal plasma consisting of positive metal ions and electrons is created when an arc discharge is triggered between two metal electrodes in vacuum. Metal plasma immersion ion implantation can improve the wear and corrosion resistance of the treated surface. A three-dimensional particle-in-cell (PIC) numerical model has been developed to simulate the motion of electrons inside the duct of a vacuum arc metal plasma source. It is found that electrons will travel back and forth inside the duct tube. This new phenomenon can be explained by the combined effects of the electric and magnetic fields. The electron oscillation will increase the charged state of the positive ions and the ions will consequently gain more energy. Due to the influence of electron oscillation, the plasma throughput of the duct will be different from that of a duct under the influence of only the magnetic field. This novel finding should be taken into account when designing metal arc sources and optimizing their performance.

6P10

Generation of High Charge State Ions in Vacuum Arc Ion Sources by a "Current Jump" Method A.S. Bugaev, E.M. Oks, G. Yu. Yushkov and I.G. Brown, High Current Electronics Institute, Tomsk 634055, Russia

GENERATION OF HIGH CHARGE STATE IONS IN VACUUM ARC ION SOURCES BY A "CURRENT JUMP" **METHOD**

A.S. Bugaev^{1,2}, E.M.Oks^{1,2}, G.Yu. Yushkov¹ and I.G. Brown³

¹High Current Electronics Institute, Tomsk, 6340055, Russia ²State University of Control Systems and Radioelectronics, Tomsk, 634050, Russia ³Lawrence Berkeley National Laboratory, Berkeley, CA, 94720,

In our investigation of ion charge state distributions (CSD) in vacuum arc plasmas, good correlation between increase in arc operating voltage and mean ion charge state has been established [1]. Therefore, to increase the mean charge state of a vacuum arc plasma, it is necessary to find ways to increase the arc operating voltage. The voltage can be increased via transients associated with the arc current by means of which a rather high operation voltage can be established across the discharge gap.

Experiments were performed both in Tomsk and Berkeley with the discharge system of a vacuum arc ion source. To effect a step current rise an additional power supply was connected to the usual vacuum arc supply. This power supply made it possible to increase the vacuum arc current up to 1 kA for several µs. As a rule the current jump was produced after $100-200~\mu s$ into the main discharge pulse when all principal parameters of the vacuum arc were already established. To measure the CSD a time-of-flight method was used.

As followed from experiments, superposition of a short, high current pulse to the vacuum arc current pulse is accompanied by a jump in arc operation voltage. Subsequently during the current step the voltage falls exponentially to one hundred volts after the completion of the current jump, and the arc voltage takes its conventional value (20-40V). Because of this increase in arc operation voltage, an enhancement of high charge state ion fractions was observed. For example, with a Ti-cathode with conventional arc parameters there is only very small value of Ti4+ ion fraction in the vacuum arc plasma. Applying strong magnetic field increases the fraction of these ions up to 20% of the total beam current. The current jump enhanced this value up to 40%.

1. E.M. Oks, A. Anders, I.G. Brown, M.R. Dickinson, R.A. Mac-Gill. IEEE Trans. Plasma Sci. 24, 1174 (1996).

Importance of repeller voltage on ion current generation in an arc ion source

B.H. Vanderberg and T.N. Horsky, Eaton Corporation SEO, Beverly, MA 01915, USA

Importance of repeller voltage on ion current generation in an arc ion source

B. H. Vanderberg and T. N. Horsky
Eaton Corporation
Semiconductor Equipment Operations
108 Cherry Hill Drive
Beverly, MA 01915

In most arc ion sources, electrons emitted by a cathode are confined in an arc column by an axial magnetic field and by a repeller electrode biased at cathode potential. The Eaton ELS ion source uses this electron confinement principle with an indirectly heated cylindrical cathode facing a cylindrical repeller electrode. The repeller electrode can consist of a refractory metal or materials of interest in semiconductor processing.

In an earlier study, we evaluated the importance of varying the magnetic field profile in the ELS source [1]. Here, we study the influence of the repeller voltage. A floating repeller will acquire a steady-state voltage close to the cathode voltage. A more careful investigation shows that the floating voltage depends on the magnetic field such that higher magnetic fields yield higher repeller voltages. Using a free boundary arc model [2], we find that this can be explained by electron losses to the arc chamber. Thus, ion source operation at low magnetic fields, while being beneficial to source stability, results in less electron confinement. Biasing the repeller voltage positively and negatively with respect to the floating voltage affects arc current and the current extraction properties of the ion source. We find that a negative bias has little influence on the arc plasma properties, while a positive bias strongly modifies the mass spectral content of the ion source. As a consequence, a biased repeller source can have improved ion generation performance for semiconductor applications.

[1] B. Vanderberg and T. Horsky, ICOPS 98, Session 7PD61[2] M. Keidar et al., J. Appl. Phys. Vol. 84, Number 11, p. 5956, Dec. 98

6P12

Laser Heated LaB6 Thermionic Cathode on a MV Electron Beam Accelerator

R.M. Gilgenbach, D. Vollers, R. Jaynes, J. Rintamaki, M. Johnston, W. Cohen, W.D. Getty, Y.Y. Lau and T.A. Spencer, University of Michigan, Ann Arbor, MI 48109-2104, USA

Laser Heated LaB₆ Thermionic Cathode on a MV Electron Beam Accelerator *

R.M. Gilgenbach, D. Vollers, R. Jaynes, J. Rintamaki, M. Johnston, W. Cohen, W.D. Getty, Y.Y. Lau and T.A. Spencer † Nuclear Eng. & Radiological Sciences Dept. University of Michigan Ann Arbor, MI 48109-2104

One of the major problems in high voltage/current and long pulse e-beam generation is plasma diode closure. LaB₆ thermionic cathodes can eliminate plasma and are more robust from poisoning than oxide cathodes. To heat the LaB₆ disk on the MELBA cathode stalk at -1 MV we employ a 100-650 W CW Nd:YAG laser. Depending upon the LaB₆ disk diameter (1 cm or 2.2 cm), temperature, and cathode shape, preliminary analysis of experiments suggests three e-beam modes:

- 1) Thermionic mode at electron beam current density of 100-150 A/cm², with current shape which matches the voltage flatness,
- 2) Plasma mode in which 2-6 kA of current is drawn with rapid current ramping, and
- 3) Combined thermionic and plasma mode with initial thermionic current turnon which is later overtaken by plasma current.

It is believed that the plasma modes may involve explosive edge emission or outgassing from a graphite cathode mounting structure.

* Research supported by AFOSR-MURI program for high power microwaves funded through a subcontract from Texas Tech University. Support also received from AFOSR-DURIP program and Northrop Grumman Industrial Affiliates program.

† Air Force Research Lab, Phillips Site

Electron Emission from Photo-cathodes for FEL

T.Inoue, S. Miyamoto, M. Yatsuzuka and T. Mochizuki, Himeji Institute of Technology, Himeji Hyogo 6712201, Japan

*T. Inoue, S. Miyamoto, *M. Yatsuzuka, and T. Mochizuki

*Faculty of Engineering
Laboratory of Advanced Science and Technology
for Industry (LASTI)
Himeji Institute of Technology (HIT)
Japan

Development of high-bright photo-cathodes for a compact infrared free electron laser operated on LEENA (Laser Emitted ElectroN Accelerator) with a plane LaB6 cathode and a third harmonics of mode-lock Nd;YLF laser (micropulse width: 10 psec, jitter: < 1 psec) at LASTI/HIT was studied to enhance laser output. Photo-emission from the plane photo-cathodes of different materials such as LaB₆, W, DLC-W, Al, and AlN was measured with an aid of a focused Hg-lamp light and a band-pass filter. Before the measurement of electron emission the cathode was annealed for about 1 hour in the vacuum of $< 1.2 \times 10^{-9}$ Torr. The power P of light on the cathode was measured with a power-meter (wavelength range: 200-1100 nm), where the light was filtered by the band-pass filter (range : 330 ± 100 nm). The electron emission current I, was measured by a pico-ammeter. The cathode was biased at 2500 V. A gap between the cathode and the anode was 2 mm. The quantum efficiency was evaluated by dividing the emitted electron number per second N_e by irradiated photon number per second N_p , where N_e was calculated from I_e and N_p was determined from P, a spectrum distribution of the Hg-lamp, a transmittance of the low-pass filter, and a sensitivity of power-meter.

The quantum efficiencies of the different cathode materials were shown in Table 1.

Table 1. The quantum efficiencies of different cathode materials

Materials	Quantum efficiency	
W	:	5.6×10 ⁴
*DLC-W	:	2.1×10 ⁴
Al	:	8.7×10 ⁻⁵
*AIN(1/50)	:	2.1×10 ⁻⁴
*AIN(1/10)	:	1.6×10 ⁴
*AIN(1/1)	:	1.5×10 ⁴

The DLC film was prepared by CVD. An AlN film was prepared by ion implantation of N^+ ion to an Al plane cathode, where the ratio N^+ ion to Al density was 1/50, 1/10 and 1/1.

* DLC-W film and AlN film are polycrystalline.

6P14

The Effect of the surface microstructures on the Emission Characteristics of Ferroelectric Cathode Koichi Yasuoka, Kenji Suzuki, Masatoshi Miyake and Shozo Ishii, Tokyo Institute of Technology, Tokyo 152-8552, Japan

The Effect of the surface microstructures on the Emission Characteristics of Ferroelectric Cathode

Koichi YASUOKA, Kenji SUZUKI, Masatoshi MIYAKE and Shozo ISHII

Department of Electrical and Electronic Engineering, Faculty of Engineering, Tokyo Institute of Technology

The pulsed electron source using a ferroelectric cathode can easily produce an electron beam of high current density with relatively low driving voltage. The originally proposed mechanism in which the screening electrons captured on the surface of the ferroelectric cathode were pulled away by coulomb potential of spontaneous polarization is not adequate to explain the experimental data. It has been shown that the surface plasma triggered by a reversal of spontaneous polarization is crucial for the electron emission [1]. Microscopic studies have been conducted from a point of view on the mechanism of ferroelectric electron emission (FEE) under the influence of surface microstructures [2,3].

Commercially available disk shaped PZT ceramics of $500~\mu m$ thickness are used as cathodes. The gold electrodes were deposited; fully solid on the bottom surface and grid electrode of $100~\mu m$ width and $300~\mu m$ separations on the top surface. Negative pulsed voltage with the rise time of 100~n is applied to the bottom surface. The luminescence is always observed whenever the electron emission occurs. The luminescence points are mostly found not on the edge of the grid electrode but on the cutoff points of grid electrode. After the several shots, many micro cracks are formed near the cutoff points.

In case of both of the cathode surfaces are covered with solid electrodes, no electron and light emission occurred. By polishing of the surface of PZT cathode, however, both the electron emission and light emission were observed. The data showed above implies that the surface microstructure is one of the important factors for triggering the surface plasma and FEE.

- [1] D. Shur, et al., Appl. Phys. Lett. 70, 574 (1997)
- [2]M. Miyake, et al., Jan. J. Appl. Phys. 36 (1997) 6004.
- [3] W. Zhang and W. Huebner, J. Appl. Phys. 83 (1998) 6034.

Electron Emission from Ferroelectric Thin Film Cathodes

F.Liu and C.B. Fleddermann, University of New Mexico, Albuquerque, NM 87131, USA

Electron Emission From Ferroelectric Thin Film Cathodes

F. Liu and C. B. Fleddermann

Department of Electrical and Computer Engineering,
University of New Mexico,
Albuquerque, NM 87131

Thin film ferroelectric cathodes have been proposed for several applications, such as flat panel displays. For this application, electron emission currents of 10s of mA/cm² will be required. Strong pulsed electron emission from bulk ferroelectric cathodes has been widely reported (100s of A/cm²), but reports on thin film ferroelectric cathodes have shown that only relatively small currents (~0.1 μ A/cm²) are obtainable when the thickness is reduced to a few microns. Because of the attractive advantages of thin film cathodes in flexibility and low switching voltage, we are systematically studying ways to improve the emission performance.

Three kinds of ferroelectric thin film cathodes have been fabricated: PLZT 2/95/5 (0.15 μm thick), PNZT 4/20/80 (0.8 μm), and PLZT 25/10/90 (0.15 μm). Standard microelectronic techniques were used to make the devices. The top electrodes were patterned into strips that have equal width and spacing between strips. For comparison, three patterns of different electrode strip width, 1.5 μm , 3.0 μm , and 10 μm , were made for each material. The electrode strip widths used here are much smaller than those reported by others (200-300 μm) and are a close match to the thickness of the film. This has been suggested in the literature to produce higher emission.

The cathode top electrode was grounded and negative pulses were applied to the cathode bottom electrode with a typical rise time of 50 ns. A pre-bias voltage up to 4.5 volts was added across the ferroelectric thin film during pulsed switching. The anode was biased to positive 2KV and was used both for electron extraction and emission measurement. The sensitivity of the emission current measurement was about $10~\mu A$.

Emission currents higher than 10mA/cm² have been measured for applied voltage between 20 and 30 volts. However, the emission reproducibility was not good. Also, the ferroelectric cathodes normally did not survive when pulsed to voltages between 35 and 45 volts. Reasons for the inconsistent emission and potential failure mechanisms will be discussed.

This work is supported through a High Energy Microwave Devices Consortium funded by an AFOSR/DOD MURI grant and administrated through Texas Tech University.

6P16

Penetration of a Plasma by a Beam in Multipulse Radiography

A.G. Sgro and T.J.T. Dwan, Los Alamos National Laboratory, Los Alamos, NM 87545, USA

Penetration of a Plasma by a Beam in Multipulse Radiography

A. G. Sgro and T. J. T. Kwan, Los Alamos National Laboatory

In multipulse radiography, electron beam pulses will encounter a background plasma consisting of low atomic weight elements such as water vapor and hydrocarbons, and also vaporized target material, generated by previous pulses. This is important because subsequent pulses penetrating the plasma plumes may suffer spot size increase and misalignment with the radiographic axis if the beam propagation is unstable. The region of this material that is farthest from the target will have a low density and will be collisionless. The beam will collisionlessly penetrate this intervening plasma, rather than pushing a hole through it as would happen in the high density fluid regime. The particle in cell code MERLIN is used to simulate this interaction.

When the beam density is much higher that the background density, the space charge field of the impinging beam rapidly blows away the low density electron background. The ions, being much heavier, take longer to move. In the heavy (i.e., immobile) ion limit, a steady state develops in which the beam undergoes a betaton oscillation along its axial length. When the background density is much higher than the beam density, the background electrons are pushed axially as well as radially. The space charge of the background ions prevents these electrons from being blown too far away. In the heavy ion limit, the system settles into an approximate equilibrium qualitatively similar to the previously mentioned one.

When the beam impinges on a background with a density ramp, the low density region of the background is blown away just as in the first case, while the high density region of the background behaves as in the second case for the same reasons.

In the heavy ion limit, the background plasma does not appear to disrupt the beam. A light ion background is more complicated and can negatively affect the beam propagation in some cases.

Focusing Methods for Drifting Relativistic Electron Beams for Radiography at AWE

C.L. Olson, S.E. Rosenthal, B.V. Oliver and D.R. Welch, A. Birrell, R. Edwards, D. Forster, T.J. Goldsack and M. Sinclair, Sandia National Laboratories, Albuquerque, NM 87185, USA

Focusing Methods for Drifting Relativistic Electron Beams for Radiography at AWE*

C.L. Olson and S.E. Rosenthal
Sandia National Laboratories, Albuquerque, NM 87185, USA

B.V. Oliver and D.R. Welch Mission Research Corporation, Albuquerque, NM 87106, USA

A. Birrell, R. Edwards, D. Forster, T.J. Goldsack and M. Sinclair Atomic Weapons Establishment, Aldermaston Reading, Berkshire RG7 4PR, England

Minimization of the radiographic spot size is a continuing long-range goal for development of pulsed-power x-ray radiography sources. In these devices, a high current (10's of kA's), high voltage (multi-MV) electron beam is created in a vacuum diode. X-ray radiation is produced when the electron beam impinges on a high-Z target. The target may be located directly on the anode, or the anode may be a thin metallic foil through which the beam passes; in the latter case, the beam enters into a transport/focus region, is focused, and then impinges on a target assembly. It is the purpose of this paper to investigate several transport/focus methods and compare them with experimental data obtained with a paraxial diode on the E-Minor Blumlein machine at AWE.

Transport/focus methods assessed here include: (1) ballistic focusing in a gas cell (with essentially complete charge and current neutralization), (2) $\lambda/4$ focusing in a gas cell with only partial current neutralization, (3) cone focusing in a gas-filled tapered metallic cone¹, (4) pressure-gradient focusing in a gas-filled drift tube with an axial pressure gradient², (5) foil focusing, in which one or more foils in vacuum are used to short out the beam's radial electric field, and (6) a tapered z-discharge, in which a preformed current-carrying axial discharge produces a focusing effect. Each method is analyzed and assessed for radiographic spot size optimization.

Analysis of experimental data from spot-size reduction and electron-beam propagation experiments on E-minor is presented. Analytical results, and computational results using the IPROP computer code, are presented for various experimental configurations including ballistic focusing, $\lambda/4$ focusing, and cone focusing. In addition, possible methods for improving the spot size are proposed, in relation to all six transport/focus methods discussed above.

*Supported by Atomic Weapons Establishment, England, and United States Department of Energy.

¹C.L. Olson, Physics of Fluids <u>16</u>, 529 (1973); <u>16</u>, 539 (1973).

²C.L. Olson, Physics of Fluids <u>16</u>, 2224 (1973).

6P18

Theory and Simulation of Electron Beam Dynamics in the AWE Superswarf Magnetically Immersed Diode

B.V. Oliver, D.R. Welch, C.L. Olson, S.E. Rosenthal and D.C. Rovang, Mission Research Corporation, Albuquerque, NM 87106, USA

Theory and Simulation of Electron Beam Dynamics in the AWE Superswarf Magnetically Immersed Diode*

B.V. Oliver and D.R. Welch Mission Research Corp., Albuquerque, NM 87106

C.L. Olson, S.E. Rosenthal, and D.C. Rovang Sandia National Laboratories, Albuquerque, NM 87185

Results from numerical simulation and analytic theory of magnetically immersed diode behavior on the United Kingdom's Atomic Weapons Establishment (AWE) Superswarf accelerator are presented. The immersed diode consists of a cylindrical needle point cathode immersed in a strong ~10-20 T solenoidal magnetic field. The anode-cathode (A-K) accelerating gap is held at vacuum and is ~ 5-10 cm in length, with the anode/target located at the mid-plane of the solenoid. Typical accelerator parameters are 5-6 MeV and 40 kA.

Ions emitted from the anode target stream toward the cathode and interact strongly with the electron beam. Collective oscillations between the beam electrons and counter-streaming ions are driven unstable and result in a corkscrew rotation of the beam, yielding a time-integrated spot size substantially larger than that expected from single particle motion. This magnetized ion-hose instability is three dimensional. On the other hand, beam transverse temperature variations, although slightly enhanced in 3D, are primarily due to changes in the effective potential at the cathode (a combination of both the electrostatic and vector potential) and are manifest in 2D.

Simulation studies examining spot and dose variation with varying cathode diameter and A-K gap distance are presented and confirm the above mentioned trends. Conclusions are that the diode current is determined by standard bi-polar space-charge limited emission, the minimum beam spot-size is limited by the ion-hose instability saturation amplitude, and the beam transverse temperature at the target is a function of the initial conditions on the cathode. Comparison to existing data will also be presented.

*In collaboration with D. Forster and P. Carpenter at AWE. Work supported by Sandia National Labs.

Experimental Study of Ion-Beam Self Pinched Transport for MeV Protons

J.M Neri, F.C. Young, S.J. Stephanakis, P.F. Ottinger, D.V. Rose, D.D. Hinshelwood and B.V. Weber, U.S. Naval Research Laboratory, Washington, DC 20375, USA

Experimental Study of Ion-Beam Self-Pinched-Transport for MeV Protons*

J.M. Neri, F.C. Young^a, S.J. Stephanakis, P.F. Ottinger, D.V. Rose^a, D.D. Hinshelwood, and B.V. Weber

Plasma Physics Division, Naval Research Laboratory Washington DC, 20375-5346

A 100-kA, 1.2-MeV proton beam from a pinch-reflex ion diode on the Gamble II accelerator is used to test the concept of self-pinched ion transport. Self-pinched transport (SPT) uses the self-generated magnetic field from the ion beam to radially confine the ion beam. A proton beam is injected through a 3-cm radius aperture covered with a 2-μm thick polycarbonate foil into a 10-cm radius transport region. The transport region is filled with helium at pressures of 30-250 mTorr, vacuum (10⁻⁴ Torr), or 1-Torr air. The beam is diagnosed with witness plates, multiple-pinhole-camera imaging onto radiachromic film, time- and space-resolved proton-scattering, and with prompt-γ and nuclear-activation from LiF targets.

Witness-plates and the multiple-pinhole-camera are used to determine the size, location, and uniformity of the beam at different distances from the injection aperture. A beam global divergence of 200 mrad is measured at 15 cm. At 50 cm, the beam fills the transport region. At 110 cm and 100- to 200-mTorr helium, there is evidence of beam filamentation.

At 50 cm from the injection aperture, evidence for SPT is observed with the proton-scattering and Li(Cu) nuclear-activation diagnostics in the pressure range of 35-80 mTorr helium. In this range, both measurements show a substantial increase in the total proton content within a 10-cm diameter on axis compared to results at higher and lower pressures or with 1-Torr air. Across the 10-cm diameter, measured radial beam profiles are flat and proton time-histories have similar shapes. The increases in proton content are up to $2.8\times$ for proton-scattering and $1.5\times$ for nuclear-activation, compared with ballistic transport (1-Torr air). These increases are attributed to the self-generated magnetic field that confines the protons to small radius. Timing of the highest energy protons, determined from fluorine prompt- γ signals, is consistent with the kinetic energy expected from the measured diode voltage.

The measured increase in protons is consistent with the physical picture for SPT, and comparisons with IPROP simulations are in qualitative agreement with the measurements.

- * Work supported by DOE.
- a. JAYCOR, Vienna, VA.

6P20

Electron Density Measurements During Ion Beam Transport on Gamble II

B.V. Weber, D. D. Hinshelwood, J.M. Neri, P.F. Ottinger, D.V. Rose, S.J. Stephanankis and F.C. Young, U.S. Naval Research Laboratory, Washington, DC 20375, USA

Electron Density Measurements During Ion Beam Transport on Gamble II*

B. V. Weber, D. D. Hinshelwood, J. M. Neri, P. F. Ottinger, D. V. Rose, *S. J. Stephanakis, and F. C. Young*

Plasma Physics Division, Naval Research Laboratory
Washington, DC 20375

High-sensitivity laser interferometry was used to measure the electron density created when an intense proton beam (100 kA, 1 MeV, 50 ns) from the Gamble II generator was transported through low-pressure gas as part of a project investigating Self-Pinched Transport (SPT) of intense ion beams. This measurement is non-perturbing and sufficiently quantitative to allow benchmarking of codes (particularly IPROP) used to model beam-gas interaction and ion-beam transport. Very high phase sensitivity is required for this measurement. For example, a 100-kA, 1-MeV, 10-cm-radius proton beam with uniform current density has a line-integrated proton density equal to $n_b L = 3 \times 10^{13} \text{ cm}^{-2}$. An equal electron line-density, $n_e L = n_b L$, (expected for transport in vacuum) will be detected as a phase shift of the $1.064\,\mu m$ laser beam of only 0.05° , or an optical path change of 1.4×10^{-4} waves (about the size of a hydrogen atom!). The time-history of the line-integrated electron density, measured across a diameter of the transport chamber at 43 cm from the input aperture, starts with the proton arrival time and decays differently depending on the gas pressure. The gas conditions included vacuum (10⁻⁴ Torr air), 30 to 220 mTorr He, and 1 Torr air. The measured densities vary by three orders of magnitude, from 1013 to 1016 cm2 for the range of gas pressures investigated. In vacuum, the measured electron densities indicate only co-moving electrons $(nL \sim nL)$. In He, when the gas pressure is sufficient for ionization by beam particles and SPT is observed, n.L increases to about 10 n.L. At even higher pressures where electrons contribute to ionization, even higher electron densities are observed with an ionization fraction of about 2%. diagnostic technique as used on the SPT experiment will be described and a summary of the results will be given. The measurements are in reasonable agreement with theoretical predictions from the IPROP code.

- * Work supported by US DOE.
- ⁺ Jaycor, McLean, VA 22102.
- 1. B. V. Weber and S. F. Fulghum, Rev. Sci. Instrum. 68, 1227 (1997).

Advanced Diagnostics and Applications of Pulsed Ion Beams and Lasers

K.Kasuya, T. Yamashita, Y. Kishi, S. Tamamura, C.Wu, T. Kamiya, M.Funatsu, S. Saitoh, H. Koinuma T. Renk, D. Hanson, K. Lamppa, J. Torres, B.Turman, T. Mehrhorn, R. Leeper, J.Quintenz and M. Thompson, Tokyo Institute of Technology, Midori-ku Yokohama 226-8502, Japan

ADVANCED DIAGNOSTICS AND APPLICATIONS OF PULSED ION BEAMS AND LASERS¹

K.Kasuya, T.Yamashita, Y.Kishi, S.Tamamura, C.Wu, T.Kamiya, M.Funatsu, S.Saitoh, H.Koinuma, Department of Energy Sciences, Interdisciplinary Graduate School of Science and Engineering, Tokyo Institute of Technology, Nagatsuta 4259, Midori-ku, Yokohama, Japan 226 T.Renk, D.Hanson, K.Lamppa, G.Torres, B.Turman, T.Mehrhorn, R.Leeper, J.Quintenz and M.Thompson²
 Sandia National Laboratories, PO Box 5800, Albuquerque, NM, USA 87185

Several kinds of experiments are shown concerning the generation, diagnostics and applications of pulsed ion beams and lasers. We are interested in a few research fields of ICF, material and space sciences. Several high voltage machines both at Yokohama and Albuquerque were used to produce ion beams and laser lights.

Proton beams of a few hundred kV energy were produced with a conventional magnetically insulated diode. The beams were measured with the following two methods. One was a track detector with a CCD element, and the other was a conventional plastic track detector, Baryotrak-P(CR). The beam tracks were counted with a particle counter, and the both results were compared.

A cryogenic anode with N_2O ice as the candidate ion source was operated with the same kind of high voltage apparatuse, and the beam species and divergence were measured with the Baryotrak. The purpose of this experiment was to check the possibility of medium mass ion beams as the ICF energy driver in the near future.

Various species of ion beams were focused on to a few kinds of targets, and the ablation processes were observed. Two of the aims of these experiments were (1) to clarify the basic processes and (2) to apply the beams to material processing. One of the methods was to make thin films of YBCO or C_3N_4 as examples.

Two kinds of KrF and a CO₂ laser were planned to be applied to targets ablation. We use targets at cryogenic and room temperature, and substrates at cryogenic and high temperature. We also made some numerical simulations of target ablation processes with these lasers. The results will be presented, if we shall have enough minutes during the conference session.

We also want to use our beams to simulate wall materials for the future advanced ICF reactors with lasers and Z pinches..

² Permanent address, Cornell University, Ithaca, NY USA

6P22

SABRE Extraction Ion Diode Results and the Prospects for Light Ion Inertial Fusion Energy Drivers

M.E. Cuneo, R.G. Adams, J.E. Bailey, M.P. Desjarlais, A.B. Filuk, W.E. Fowler, D.L. Hanson, D.J. Johnson, T.A. Mehlhorn, P.R. Menge, C.L. Olson, T.D. Pointon, S.A. Slutz, R.A. Vesey, D.F. Wenger and D.R. Welch, Sandia National Laboratories, Albuquerque, NM 87185-1193, USA

SABRE Extraction Ion Diode Results and the Prospects for Light Ion Inertial Fusion Energy Drivers*

M. E. Cuneo, R, G. Adams, J. E. Bailey, M. P. Desjarlais, A. B. Filuk, W. E. Fowler, D. L. Hanson, D. J. Johnson, T. A. Mehlhorn, P. R. Menge, C. L. Olson, T. D.Pointon, S. A. Slutz, R. A. Vesey, D. F. Wenger, D. R. Welch Sandia National Laboratories

Experimental and theoretical work over the last 6 years shows that high-brightness ion beams meeting the requirements for an IFE-injector could be possible with control of electrode plasma and electron sheath, uniformity and stability. This control is achieved by establishing [1]: 1) diode alignment, 2) appropriate B-field uniformity, profiles, and intensity, 3) clean surfaces for minimal plasma formation at high electric fields, and 4) pure, preformed, uniform, non-protonic anode plasmas. We have not achieved the integration of these issues required prior to ion program suspension, and yet partial integration has resulted in significant improvements. Successively improved integration of these issues has produced non-protonic beams on the SABRE accelerator with a FOM = $J\tau/\theta^2$ that has increased by about an order of magnitude since the first lithium beam experiments in 1993 [2]. The remaining factor of 3 necessary to meet IFE injector requirements (FOM = 20 @ 4 MeV) would be achieved with a further 30% reduction in ion beam divergence to 20 mrad, to levels that have already been achieved under some conditions.

We have found that the ion source has a profound impact on ion diode performance. The production of pre-formed lithium ion sources required for fusion has been more difficult than anyone ever imagined under typical pulsed-power conditions. We have used a laser at 40 to 80 MW/cm² to pre-form, for the first time, non-protonic plasmas from a LiAg anode film, and in-situ deposited Li films. Ion beams have also been generated from carbon surfaces with this laser. We observe a 20 ns earlier turn on of current, at a Child-Langmuir level, and the best impedance history that we have ever produced with an enhancement below 4, and no impedance collapse for up to 45 ns. This impedance history may be acceptable to drive the 2nd stage of a two-stage system. Divergence in these experiments may have been dominated by laser and source non-uniformity. Also, the ion beams produced were either dominated by contaminant ions for the case of Li, or by a charge-state spread in the case of carbon. We have discovered nothing however, to indicate that simultaneously achieving the requisite divergence current density, and impedance history is fundamentally impossible. Recommendations are given for further work on these systems.

[1] M. E. Cuneo, Bull. Amer. Phys. Society, 42, 1948(1997).
[2] M. E. Cuneo, et al., IAEA-CN-69/IFP/14 in Proceedings of the 17th IAEA Fusion Energy Conference (Yokohama, Japan), 1998.
*Sandia is a multi-program laboratory operated by Sandia Corporation, a Lockheed Martin Company, for the U.S. Department of Energy under Contract No. DE-AC04-94AL85000.

¹ Supported by the Ministry of Education, Science, Culture and Sports in Japan, and Sandia National Laboratories.

Effects of RF Plasma Processing on the Impedance and Electron Emission Characteristics of a MV Beam Diode

J.I. Rintamaki, R.M. Gilgenbach, W.E. Cohen, R.L. Jaynes, L.K. Ang, Y.Y. Lau, M.E. Cuneo and P.R. Menge, University of Michigan, Ann Arbor, MI 48109-2104, USA

Effects of RF Plasma Processing on the Impedance and Electron Emission Characteristics of a MV Beam Diode*

J.I.Rintamaki^a, R.M. Gilgenbach, W.E.Cohen, R.L. Jaynes, L.K.Ang, Y.Y.Lau, M.E. Cuneo^b, P.R. Menge^b

Intense Energy Beam Interaction Laboratory Nuclear Engineering and Radiological Sciences Department University of Michigan, Ann Arbor, MI 48109-2104

Experiments have proven that both the surface contaminants and microstructure topography on the cathode of an electron beam diode influence impedance collapse and electron emission current. Experiments have characterized effective RF plasma processing protocols for high voltage A-K gaps using argon and argon/oxygen gas mixtures. RF processing time, feed gas pressure, and RF power were adjusted. Time resolved optical emission spectroscopy measured contaminant (hydrogen) and bulk cathode (aluminum) plasma emission versus transported axial electron beam current. Experiments utilize the Michigan Electron Long Beam Accelerator (MELBA) at parameters: V = -0.7 to -1.0 MV, I(diode) = 3-30 kA, and pulselength = 0.4 to 1.0 microseconds. Microscopic and macroscopic E-fields on the cathode were varied to characterize the scaling of breakdown conditions for contaminants versus the bulk material of the cathode after plasma processing. Electron emission was suppressed for an aluminum cathode in a high voltage A-K gap after RF plasma processing. Experiments using a two-stage low power (100W) argon/oxygen RF discharge followed by a higher power (200W) pure argon RF discharge yielded an increase in turn-on voltage required for axial current emission from 662 ± 174 kV to 981 + 97 kV. After two-stage RF plasma processing axial current emission turn-on time was increased from 100 \pm 22 nanoseconds to 175 ± 42 nanoseconds. Aluminum optical emission was delayed > 150 nanoseconds after the overshoot in voltage after two-stage RF plasma processing. Removal of hydrogen contamination on the cathode surface was observed by optical spectroscopy during the MELBA pulse. Axial and diode current were reduced 40-100% after RF plasma processing. SEM analysis suggests the aluminum cathode surface is being modified by the RF plasma discharge

6P24

Ultra-Violet Triggered Vacuum Flashover of a Water-Vacuum Interface as a Low-Inductance Closing Switch

L. Courtois, B. Cassany, G. Avrillaud, L. Frescaline, SCA ITHPP, Thegra 46500, France

Ultra-Violet Triggered Vacuum Flashover of a Water-Vacuum Interface as a Low-Inductance Closing Switch

L. Courtois, B. Cassany, G. Avrillaud, L. Frescaline I.T.H.P.P. Hameau de Drèle, 46500 Thégra, France

F. Lassale C.E.G. 46500 Gramat, France

GSI is one of the two-prototype candidates for driving the future MAG3 Z-pinch load. It is a 640 kJ inductive generator, made of 4 fast Marxes in parallel, a water transmission line, a vacuum storage line and a plasmaopening switch.

The plastic interface between the water transmission line and the vacuum storage inductor is used as a crowbar to avoid Marx damage due to reverse voltage. The large-area discharge at large radius provides a very low-inductance closing switch element. Also, the low current density can lower erosion rates of the electrodes.

The arrangement of the system will be shown. The flashboard system which provides the triggering illumination will also be described. Equivalent interface circuit and UV triggering abilities will be presented as a function of the electric and magnetic fields.

^{*}Research supported by DoE Contract #DE-AC04-94AL85000 to Sandia National Labs and Sandia Contract No. AL-7553 to the University of Michigan

^{*}FES Graduate Fellowship

^bSandia National Laboratories, Albuquerque, NM, MS-1193

Evaluating the Residual Inductance of a Ranchero Coaxial Flux-Compression Generator as Storage Inductance for Powering Imploding Hydrodynamic Liner Loads

J.H. Goforth, W.L. Atchison, C.M. Fowler, E.A. Lopex, H. Oona, R.E.Reinovsky, J.L. Stokes, D.G. Tasker, I.R. Lindemuth, J.V. Parker, Los Alamos National Laboratory, Los Alamos, NM 87545, USA

Evaluating the Residual Inductance of a Ranchero Coaxial Flux-Compression Generator as Storage Inductance for Powering Imploding Hydrodynamic Liner Loads.

J.H. Goforth, W.L. Atchison, C.M. Fowler, E.A. Lopez, H. Oona, R.E. Reinovsky, J.L. Stokes, D.G. Tasker, I.R. Lindemuth, J. V. Parker, Los Alamos National Laboratory

The Ranchero coaxial flux-compression generator system is an explosive-driven generator designed for high current (up to 100 MA per module) applications. A single module consists of a 15.2 cm diameter armature that is detonated simultaneously along its axis, to expand a factor of two out to the coaxial stator. Most, but not all, tests have used a taper on the stator to minimize flux trapping as the armature closes the generator volume. We have experimentally evaluated the residual inductance for a variety of stator insulation thicknesses, and reported some of these results in previous work. For a 1.4 m-long module, the residual inductance is ~3.6 nH using 0.5 mm thick polyethylene insulation along the stator. Thicker insulation increases the residual inductance. Since some of that residual inductance is due to flux that has diffused into the generator conductors, not all of it can be considered storage inductance for driving short time scale experiments. In addition, the armature is shocked by the explosive, extruded to half its original thickness, then shocked on impact with the stator, all while carrying a large current. These factors lead to increased diffusion, further reducing the amount of flux available for microsecond time scale experiments. Experimental data and MHD calculations are compared to evaluate the usefulness of flux in the residual inductance for transfer to loads of interest.

6P26

Operation of a Heated POS IN DM1

N.R. Pereira, J.R. Goyer, D. Kortbawi, J.R. Thompson and S.E. Davis, Ecopulse, Springfield, VA 22150, USA

Operation of a Heated POS IN DM1 N. R. Pereira*

J.R. Goyer, D. Kortbawi, J.R. Thompson, and S.E. Davis, *
(Ecopulse, Inc., PO Box 528, Springfield, VA 22150 USA)

*(Maxwell Technologies, Inc., 8888 Balboa Ave, San Diego, CA 92123)

DM1, located at Maxwell Physics International (MPI), is DTRA's test bed for its innovative flash x-ray simulator DECADE. One quarter of this is presently being delivered by MPI to the Arnold Engineering and Development Center (AEDC). DM1's low cost design has a water transfer capacitor followed by a plasma opening switch that shortens the microsecond Marx discharge into the desired 40 ns wide hard x-ray pulse.

A detailed assessment of DM1 operation has indicated current loss between the POS and load. The losses could include parasitic ion currents from plasma in the diode, and unintended POS plasma generated from the electrode surfaces in the switch. These plasmas could come from the electrode surfaces: hot electrodes are intended to minimize plasma evolution from the electrodes.

We are presently designing an experiment with electrodes heated to a temperature exceeding 800 K in a way that is consistent with discharge cleaning. We expect to present results from shots with hot electrodes. We anticipate improvements similar to the delayed impedance collapse in the bremsstrahlung diode heated by Pereira and Fisher at NRL [1], and the lower jitter in a heated high power magnetron observed by Price et al. at MPI [2]. Attacking the surface plasma problem has also been very successful in suppressing parasitic current in ion diodes. [3]

- [1] N. R. Pereira and A. Fisher, IEEE Trans. Plasma Sci. (1999?).
- [2] D. Price et al., IEEE Trans. Plasma Sci 26, 325 (1998).
- [3] M. E. Cuneo et al., IEEE Trans. Plasma Sci, 25, 229, 1997.

A POS with a Two-Ion-Species Plasma

N. Chakrabarti, A. Fruchtman, Weizmann Institute of Science, 76100 Rehovot, Israel

A POS with a Two-Ion-Species Plasma

N. Chakrabarti
Physics Faculty, Weizmann Institute of Science, Rehovot Israel
A. Fruchtman
Center for Technological Education Holon, 52 Golomb St.,
Holon 58102, Israel

In many Plasma Opening Switches (POS) the plasmas are composed of more than one ion species. Often these are Carbon ions and protons. We assume that the magnetic field has penetrated into the plasma and examine the dynamics of the ions in the magnetized plasma. We employ a simple one-dimensional model in which the ion equations of motion are linearized. It is shown that different ions are pushed differently by the magnetic field pressure. The role of various drifts that determine the ion motion, the crossed electric and magnetic fields drift and the polarization drift, is discussed. It is further shown that while in a one-ion-species the current is carried only by electrons, in a two-ion-species a significant fraction of the current is carried by the ions. Possible implications for the POS performance are discussed.

6P28

Mass Separation in a 100-ns Plasma Opening Switch

A. Weingarten, C. Grabowski, N. Chakrabarti, and Y. Maron, A. Fruchtman, Weizmann Institute of Science, Rehovot 76100, Israel

Mass Separation in a 100-ns Plasma Opening Switch

A. Weingarten, C. Grabowski, N. Chakrabarti, and Y. Maron Weizmann Institute of Science, Rehovot, Israel
A. Fruchtman

Center for Technological Education, Holon, Israel

The behavior of the different ion species that make up multicomponent plasmas can affect the results of various laboratory experiments and is important for understanding phenomena in space plasmas. We study the motion of various plasma ions in a 100-ns, 170-kA Plasma Opening Switch (POS) by observing the time dependence of the electron density and the ion velocity distribution. The prefilled-plasma composition is determined from absolute line intensities and collisional-radiative calculations. Close to the inner electrode, most of the plasma ions are protons (as high as 90%) with the rest being mainly CIV. Near the outer electrode, there is a much larger fraction (\approx 50%) of non-protonic species. The prefilled-plasma density and temperature are almost constant at all radii, where $n_e = (2.2\pm0.5) \times 10^{14} \, \text{cm}^{-3}$ and $T_e = 5.5\pm1 \, \text{eV}$.

During the current pulse the velocities of non-protonic ions, which are studied locally from Doppler shifts of ions doped into the plasma using laser evaporation, are observed to be much lower than the proton Alfven velocity. The 3-D resolved electron density, studied from the line intensities of doped Mg ions, is observed to increase and then to drop sharply to 10-50 % from the initial value within 10-30 ns. Magnetic field intensities, determined from Zeeman splitting, indicate that plasma is pushed by the magnetic piston. The diagonal piston propagates from the generator towards the load at about half the proton Alfven velocity. The data suggest that protons are specularly reflected by the magnetic pressure at the piston front. The heavy ions, however, are seen to cross the potential hill in the piston, acquiring a lower velocity.

The magnetic field distribution is now being studied using chordal observation, thus reducing the Doppler broadening prevalent along axial lines of sight. A mapping of these data throughout the POS plasma region will be presented. Also presented are a theoretical analysis of n_e and the magnetic field evolution.

Compact Pulsed Power Generator Using a Marx Circuit and a Exploding Wire

Naoyuki Shimomura, Masayoshi Nagata, Hidenori Akiyama, University of Tokushima, Tokushima 770-8506, Japan

Compact Pulsed Power Generator Using a Marx Circuit and a Exploding Wire

Naoyuki Shimomura, Masayoshi Nagata

The University of Tokushima,
Minami-josanjima 2-1, Tokushima 770-8506, Japan

Hidenori Akiyama

Kumamoto University, Kurokami 2-39-1, Kumamoto 860, Japan

A compact pulsed power generator with an inductive energy storage system is investigated. The energy transfer ratio into the load is considered by generic calculations, which confirmed the need of a high fuse opening resistance. Long and thin wires are suitable to generate the high voltage as a fuse opening switch. The generator circuit parameters are optimized by numerical analysis, taking into account the stored energy in the inductor at the beginning of wire vaporization and energy consumed during wire vaporization. The generator is designed for high voltage applications. Although the output current is low because of the low initial charging energy, the voltage multiplication factor is, accordingly, high. The inductive pulsed power generator consists of a Marx circuit, an inductor, and a thin and long exploding copper wire. An output voltage up to 800 kV and voltage risetimes of 15 to 40 ns are experimentally obtained.

6P30

Spectroscopic Observations of Optical Emission on the ACE Multi-Megamp Plasma Opening Switch

Philip Coleman, Phillip Goodrich, and John Thompson, Maxwell Technologies, San Diego, CA 92123, USA

Spectroscopic Observations of Optical Emission on the ACE Multi-Megamp Plasma Opening Switch

Philip Coleman, Phillip Goodrich, and John Thompson Maxwell Technologies, San Diego, CA, USA

The ACE 4 high current (>3 megamp) plasma opening switch (POS) uses a high density (>10¹⁵/cc) plasma to achieve microsecond conduction periods. During the conduction phase, a MHD snowplow process is dominant. During the opening phase, less-well-understood processes (Hall, erosion, etc.) seem to be operative. We report here on new measurements meant to help diagnose the opening phase.

Emission spectroscopy can give data on plasma composition, ionization state, and temperature, all properties that influence POS performance. Coleman et al. (1996) showed some initial results using POS spectroscopy to probe the plasma conditions prior to and during the conduction interval. Line radiation was very strong for carbon, fluorine and hydrogen ions located within the POS. Here we present new data on spectral intensities and time histories for plasmas downstream of the switch during the opening phase. Very strong emission is seen from cathode and anode surfaces. A much lower level of emission is due to low density plasma in the A-K gap. With only a few exceptions, this downstream emission is only continuum. These results have implications for the density and temperature of the opening phase plasma.

(1) Coleman, P., P.Melcher and J.Thompson, Paper 6E05, IEEE International Conference on Plasma Science, June, 1996

Sponsored by the Defense Threat Reduction Agency

Modeling of Ion Currents Upstream of POS on ACE 4 and DMI

Don Parks, Maxwell Technologies, San Diego, CA 92123, USA

Modeling of Ion Currents Upstream of POS on ACE 4 and DMI

Don Parks Maxwell Technologies, Inc., San Diego, CA

Faraday cups have been used to measure ion currents at distances ranging from a few centimeters to a few tens of centimeters upstream of the nominal region of injection of opening switch plasmas on ACE 4 and DM1. The purpose of this paper is to explain the magnitude and time dependence of these currents in terms of the initial plasma conditions and physical mechanisms leading to the observed behavior.

In the case of plasma injection through a rodded anode structure on ACE 4, the measured ion currents rise to a peak value of about 150 amps/sq cm at about 400 ns following the onset of conduction by a one-microsecond plasma opening switch. The ion current profile decays from the peak in about 100 ns to a level of a few tens of amperes through the remainder of the conduction phase. Following this the measured currents rise again as the POS passes through its opening phase and higher voltages are present. On DM1 and on ACE 4 with a mesh anode the measured current during conduction are within noise levels, amounting to less than a few tens of amps/sq cm and indicating ion populations substantially lower than for ACE 4 with a rodded anode.

The conduction phase results are analyzed in terms of the ion motion in the crossed magnetic and inductive electric fields arising from a linearly increasing generator current and motion of the POS plasma. In this dynamic environment the square root of the time derivative of the cyclotron frequency of a plasma ion is an important determinant of the main body of the ion current waveform. Other factors, such as polarization current and ionization may affect the late time dependence of the current in the conduction phase.

During opening, voltages upstream of the POS reach the megavolt level and ion current densities range from several hundred amps/sq cm to one kiloamp/sq cm. In this environment the velocity of the cross field drift of electrons exceeds that corresponding to ionization thresholds. Much of the data appear to support the expected threshold behavior, and in general indicate that ionization phenomena as well as ion transit time effects are important in the determination of the ion current pulse shape. The ion current density levels, if extrapolated to cathode areas equal to those subtended by the plasma injection region, are a substantial fraction of the total load and generator currents.

Sponsored by Defense Threat Reduction Agency

7

De Anza Baliroom 8: 30 AM, Thursday, June 24, 1999

Plenary Talk

Z-Pinches: Past, Present and Future

Prof. Malcom Haines Imperial College

Chairperson

Dr Keith Matzen Sandia National Laboratories

De Anza III 10 AM, Thursday, June 24, 1999

Oral Session 7A

Plasmas for Lighting Lighting Consortium (EPRI/ALITE) Overview

> Chairperson Voitek Byszewski Osram Sylvania

7A01-2

Invited -

Radiation Trapping of the Hg 185 nm Resonance Line

J.E. Lawler, J.J. Curry, K.L.Mennigen, Madison, University of Wisconsin - Madison, Madison, WI 53706, USA

Radiation Trapping of the Hg 185 nm Resonance Line¹
J. E. Lawler, J. J. Curry, University of Wisconsin –
Madison, K. L. Mennigen, University of Wisconsin –
Whitewater

The trapped decay rate of the 6¹P₁ level at 185 nm was measured as a function of cold spot temperature (Hg density) and buffer gas pressure in cylindrical sealed fused silica cells. The decay rates were obtained using timeresolved, laser induced flourescence after multi step laser excitation at 253.7 nm and 312.6 nm. Cold spot temperatures from 25°C to 100°C were studied. The Hg densities for this temperature range with no buffer gas yield the lowest possible trapped decay rates due to partial frequency redistribution. Argon buffer gas pressures of 3 and 30 Torr were also studied. The results are in agreement with the afterglow data of Post² for zero buffer gas pressure. Monte Carlo simulations of radiation transport in the cell, including the effects of hyperfine and isotope structure and the effects of foreign gas broadening, agree well with the experimental data.

¹Supported by EPRI and OSRAM-SYLVANIA INC. ²Post, H.A., Phys. Rev. A 33, 2003 (1986)

On The Radiation Trapping Calculation on Discharge Lamps

Hasnaa Sarroukh, Michel Aubes, Georges Zissis and Jean Jacques Damelincourt, CAPAT Univ. P. Sabatier, Toulouse 31062, France

ON THE RADIATION TRAPPING CALCULATION IN DISCHARGE LAMPS

Hasnaa Sarroukh*, Michel Aubes, Georges Zissis and Jean-Jacques Damelincourt

Centre de Physique des Plasmas et de Leurs Applications de Toulouse 118, Route de Narbonne. F-31062 Toulouse Cedex (France) *H. Sarroukh Faculté des sciences de Tétouan, BP 2121, Tétouan, Morocco

The energy balance of discharge lamps strongly depends on radiation trapping. Hence, the radiative flux is a fundamental quantity in radiation source research and development. Radiative transfer has been studied for several decades [1] and different formalisms have been introduced. They lead to more or less interesting solutions depending on the particular objective to be achieved.

The purpose of this paper is to present and to discuss specific interest of some approaches achieved in our laboratory in the study of discharge lamps radiation.

Direct computation of the radiative flux is time consuming especially when a good description line profile is needed. Several attempts have been made in order to minimise the computation time. We shall describe a particular method (OPT model) [2] based on the localization of the more effective contribution areas relative to each one of the integrated functions.

Bartels [3] and Multiple parameters formalisms [4] enable to follow, without too much computing, the effect of the parameters (temperature, partial pressures, optical thicknesses) on the discharge emission outside the discharge tube. They also lead to simple expressions of the total radiance and flux of spectral lines.

As an exemple of intermediate method, we also present a detailed calculation of the 254nm line resonance radiation trapping in the discharge Hg-Ar low pressure plasma taking into account Hg-Hg and Hg-Ar collisions.

Roughly, these formulations may give either a local balance or net emission of the radiative term inside the discharge either only the radiative flux outside the discharge. Most of these formalisms also lead to the emission photometry.

[1]: Church, C. H., Schlecht, R. G., Liberman, I. and Swanson, B. W., AlAA 4, 1966 (1947).

[2]: Simonet, F., Aubes, A., Elloumi, H. and Sarroukh, H., J. Quant. Spectrosc. Radiat. Transfer., No. 2, PP. 197-207, (1999).

[3]: Bartels, H., Teil. Zeit. Physik, 125, 597, (1949).

[4]: Karabourniotis, D., " Radiative Processes in Discharge Plasmas", ed. J.M. Proud and L. H. Luessen, Plenum Press, 171, (1986).

7A04

Chemi-ionization of Excited Mercury

R.L. Martin, J.S. Cohen and L.A. Collins,
Alamos National Laboratory, Los Alamos, NM 87545,
USA

Chemi-ionization of Excited Mercury

R.L. Martin, J.S. Cohen, and L.A. Collins Los Alamos National Laboratory, Los Alamos, NM 87544

We report calculations of the chemi-ionization for the collisions of Mercury (Hg) atoms in the excited singlet and triplet P states (1,3P), examining both the Penning and Associative Ionization mechanisms. The doubly-excited mercury dimer presents an intricate situation for chemi-ionization. For example, with only one of the atoms excited, chemi-ionization is not energetically possible. Some of the asymptotes correlating to two excited ³P atoms still lie just below the energy of the atomic ion. so that only associative ionization can occur. On the other hand, others lie just above it, enabling both associative and Penning ionization.

Potential energy curves for the excited neutral(Hg2**) and the ion(Hg2⁺) molecular states are generated using relativistic effective core potentials and full four-electron configuration interaction, based upon the orbitals of the ground state at each internuclear distance. We have examined the influence of core-valence correlation and the errors associated with the interaction curves will be discussed. For such heavy atomic systems, the spin-orbit interaction plays an important role, and its inclusion follows from an effective hamiltonian based on the atomic splittings. Finally, we shall present the cross sections for both Penning and associative ionization.

Research performed as a participant in the EPRI ALITE program and under the auspices of the U.S. Department of Energy through the Los Alamos National Laboratory.

Chemi-ionization in mercury and neon discharges

Valery Sheverev, Lorcan Folan, Vadim Stephaniuk, Polytechnic University, Brooklyn, NY 11201, USA

Chemi-ionization in mercury and neon discharges.

Valery Sheverev, Lorcan Folan, Vadim Stepaniuk
Polytechnic University, Brooklyn, New York, and
Graeme Lister

OSRAM SYLVANIA Development Inc.

Modeling of discharge light sources is becoming increasingly important in predicting device performance and determination of optimal regimes for their operation. A good knowledge of the elementary processes occurring under non-equilibrium conditions is a prerequisite for any model. Chemi- ionization processes involving collisions of excited atoms play a crucial role in many lighting discharges, both for low (a few torr) and higher (>10 torr) gas pressures. The understanding of such processes and their role in discharge power balance is scant, and quantitative data on the rate coefficients is inadequate. Experimental studies of chemi-ionization in collisions of metastable neon and mercury atoms were recently initiated at Brooklyn Polytechnic University. Rate coefficients for collisions between two p⁵3s¹³P₂ and between 2p⁵3s¹³P₂ and ³P₁ excited neon atoms were measured using plasma electron spectroscopy. Investigation of chemi-ionization in collisions of 6³P_{0.1.2} mercury states is under way and the intermediate results will be reported. Results of quantitative evaluation of the importance of the chemiionization for neon and mercury lamp modeling will also be presented.

Research performed as participant in the EPRI ALITE program

7A06

Chemo-Ionization in Decaying Neon Plasma

D. Loffhagen, S. Pfau and R. Winkler, INP Greifswald, 17489 Greifswald, Germany

Chemo-Ionization in Decaying Neon Plasmas

D. Loffhagen¹, S. Pfau² and R. Winkler¹

- ¹ Institut für Niedertemperatur-Plasmaphysik, 17489 Greifswald, Germany
- ² Institut f\u00fcr Physik, Universit\u00e4t Greifswald, 17489 Greifswald, Germany

Theoretical and experimental results obtained for the afterglow in the positive column plasma of a neon glow discharge are reported. In these investigations a significant impact of the chemo-ionization processes on the temporal behaviour of the decaying plasma is found.

The self-consistent model for the discharge plasma consists of the time-dependent electron Boltzmann equation for the decermination of the electron kinetics, the rate equations for the mainly populated two lowest excited states Ne[1s₅] and Ne[1s₄] in the cylindrical, axially uniform column plasma and an appropriate description of the decaying electric field. To determine the temporal evolution of the kinetics of the electrons and excited neon atoms a radially averaged treatment of the column plasma has been used. Following the relevant literature the inscattering of the electrons produced by chemo-ionization has been assumed to take place at kinetic energies below 11.7 eV and with a width of the energetic spectrum of less than 1 eV. The studies of the afterglow decay have been performed for a column plasma with a tube radius of 1.7 cm at a pressure of 75 Pa, starting from steady-state conditions in a dc glow discharge at currents around 20 mA. The results obtained by the model calculations are compared with probe measurements of the electron velocity distribution function, the electron density and the mean electron energy. Large structural changes of the distribution function are found in about the first 40 us of the decay as a results of the change from an active, electricfield-driven discharge plasma to a state that is strongly determined by the action of the chemo-ionization processes, especially by collisions between two Ne[1s₅] atoms. These collision processes are mainly responsible for a slight increase of the electron density within a period of about 150 µs and represent a power reservoir for the decaying plasma. The comparison between theoretical and experimental results at various instants of the afterglow shows satisfactory agreement in about the first 10 μ s, while increasing differences arise in the further afterglow. The analysis indicates that these discrepancies basically come from the impact of the chemo-ionization processes, in particular from the assumption made in the model with respect to the in-scattering of the electrons produced by chemo-ionization. To evaluate the influence of the in-scattering probability of the electrons several model calculations assuming different shapes and widths of the in-scattering probability have been performed. The corresponding results are discussed.

Modeling of Highly Loaded Fluorescent Lamps

G.G. Lister, J.E. Lawler and J.J. Curry, Osram Sylvania, Inc., Beverly, MA 01915, USA

Modeling of Highly Loaded Fluorescent Lamps

G. G. Lister

OSRAM SYLVANIA Development Inc., 71 Cherry Hill Dr., Beverly, MA 01915

J. E. Lawler and J J Curry

Department of Physics, University of Wisconsin, Madison, WI 53706

Numerical modeling of the positive column of fluorescent lamps under conditions of high current density are of current interest, particularly in view of recent developments in electrodeless lamps. Current models tend to overestimate radiation output, and consequently the maintenance electric field in these discharges [1]. Under highly loaded conditions, mercury-rare gas fluorescent lamps exhibit strong mercury depletion on axis (cataphoresis), and an understanding of resonance radiation transport under these conditions is therefore vital to the development of models with a predictive capability.

We have explored the effect of radial cataphoresis on resonance radiation trapping for situations in which the radiation transport is dominated by foreign gas broadening, Doppler broadening, or resonance collisional broadening of the spectral line. Several different production rates per unit volume of resonance (excited) atoms have also been studied. It is advantageous in many cases to parameterize the trapped decay rate in terms of the total number of ground state atoms in the positive column independent of their radial distribution. The results of this work have been included in a numerical model of the positive column and the predicted influence on discharge parameters will be presented for cases of interest to highly loaded lamps.

[1] G.G. Lister, in H. Schlüter and A. Shivarova, Editors, Advanced Technologies Based on Wave and Beam Generated Plasmas, NATO ASI Series; Plenum (1998), in press

Research performed as participants in the EPRI ALITE program

7B

Bonsai I 10 AM, Thursday, June 24, 1999

Oral Session 7B Magnetic Fusion Energy

Chairperson
Irv Lindermuth
Los Alamos National Laboratory

7B01-2 Invited -

Magnetic pressure driven implosion of solid liner suitable for compression of Field Reversed Configurations

J.H. Degnan, R. Bartlett, T. Cavazos, D. Clark, S.K. Coffey, R.J. Faehl, M. Frese, D. Fulton, D.Gale, T.W. Hussey, T. P. Intrator, R. Kirkpatrick, G.F. Kiuttu, F.M. Lehr, I. Lindemuth, W. McCullough, R. Moses, R.E. Perterkin, R.E. Reinovsky, N.F. Roderick, E.L. Ruden, J. Schlacter, K. Schoenbert, D.Scudder, R.E. Siemon, W. Sommars, P.J. Turchi, G. Wurden, F. Wysocki,

U.S. Air Force Research Laboratory, Albuquerque, NM 87117-5776, USA

Magnetic pressure driven implosion of solid liner suitable for compression of Field Reversed Configurations

J.H.Degnan, R.Bartlett(1), T.Cavazos(2), D.Clark(1),
S.K.Coffey(3), R.J.Faehl(1), M.Frese(3), D.Fulton(1),
D.Gale(2), T.W.Hussey, T.P.Intrator(1), R.Kirkpatrick(1),
G.F.Kiuttu, F.M.Lehr, I.Lindemuth(1), W.McCullough,
R.Moses(1), R.E.Peterkin, R.E.Reinovsky(1),
N.F.Roderick(4), E.L.Ruden, J.Schlacter(1), K.Schoenberg(1),
D.Scudder(1), R.E.Siemon(1), W.Sommars(1), P.J.Turchi
(5), G.Wurden(1), F.Wysocki(1)

Directed Energy Directorate, Air Force Research Laboratory, Kirtland AFB, NM, USA

- (1) Los Alamos National Laboratory, Los Alamos, NM
- (2) Maxwell Technologies, Inc, Albuquerque, NM
- (3) NumerEx, Albuquerque, NM
- (4) Permanent address: Department of Chemical and Nuclear Engineering, University of New Mexico, Albuquerque, NM
- (5) Permanent address: Department of Aerospace Engineering, Applied Mechanics and Aviation, Ohio State University, Columbus, OH

The initial design and performance of a magnetic pressure driven imploding solid liner with dimensions suitable for compressing a Field Reversed Configuration (FRC) is presented and discussed. The nominal liner parameters are 30 cm length, 5 cm outer radius, ~0.1 cm thickness, Al material. The liner is imploded by magnetic pressure from an axial discharge driven by a 1300 microfarad capacitor bank. Other nominal discharge parameters are ~ 80 kV initial bank voltage, ~ 44 nanohenry initial total inductance, and ~ milliohm series resistance. The discharge current exceeds 10 megamps in ~ 9 usec. Several types of calculations indicate that such a liner will implode in ~22 to 25 /µsec, and will achieve a >0.3 cm/usec implosion velocity by the time the liner has imploded to ~2.5 cm radius. This performance and these dimensions are suitable for FRC formation and compression, as discussed by K.Schoenberg, R. Siemon et al (1). The diagnostics for the initial experiments include current (via Rogowski coils and inductive magnetic probes), voltage (via capacitive divider probes), flash radiography, and diagnostic magnetic field compression. Several types of simulations, including two dimensional magnetohydrodynamic simulations, are also discussed.

7B03

Proton Ring Formation Studies on the Cornell Field-reversed Ion Ring Experiment FIREX

W.J. Podulka, J.B. Greenly, A.Gretchikha and Y. Tang, Cornell University, Ithaca, NY 14853, USA

Proton Ring Formation Studies on the Cornell Field-reversed Ion Ring Experiment FIREX*

W.J. Podulka, J.B. Greenly, A. Gretchikha, and Y. Yang Laboratory of Plasma Studies, Cornell University, Ithaca, NY 14853

The goal of FIREX is to produce a field-reversed ring of greater than 500 keV protons. The ring is formed by axial cusp injection into a solenoid of an annular beam from a magnetically-insulated ion diode driven by a 1 MV, 800 kA, 150 ns pulser. The first phase of experiments using a passive flashover proton source is now complete. At 90% charge of the FIREX pulse power, the diode produces 12 mC of protons over 120 ns, while the voltage decreases from 850 to 550 kV. These protons are injected through the cusp into a 6 kG solenoid to Diagnosis of ring formation with arrays of magnetically-insulated Faraday cups show that 6 mC are in the ring at 100 cm axial location in the solenoid, in agreement with simulations using the quasineutral FIRE code (1). However, the radial distribution of the ring protons differs significantly from the simulations, and is dependent on the pressure of the neutral hydrogen gas fill that is used in the solenoid to provide beamformed plasma for charge neutralization of the ring. The radial distribution is shifted strongly to smaller radius in the solenoid with fill pressures below 100 mTorr, indicating residual spacecharge effects in the cusp. Above 200 mTorr, no significant change in radial distribution is seen. The self-magnetic field of these rings is only about 10% of the solenoid field. To increase this to field reversal, the ring must be shortened from its present ~100 cm axial length to <20 cm, and the proton charge must be increased to 20 mC. Presently the experiment is moving into a second phase using an active proton source to increase the proton output of the diode. This source uses a thin (<1 micron) titanium foil on the anode, loaded with hydrogen gas, to produce a nearly pure proton plasma on the anode at the start of the diode voltage pulse. The aim of this change is to increase the initial rate of rise of proton current, which would both increase the total proton charge output and also load down the early diode voltage to produce less spread in the proton energy, allowing an axially shortened ring in the solenoid. Both these effects would increase the ring self-field toward reversal. Initial results will be reported.

^{*}Research supported by DOE Grant #DE-FG02-93ER54221.

7B04

Numerical Simulations of Plasma Working Fluid Compression of a Cylindrical Copper Target Liner

Norman F. Roderick and Robert E. Peterkin Jr., U.S. Air Force Research Laboratory, Kirtland AFB, NM 87117, USA

Numerical Simulations of Plasma Working Fluid Compression of a Cylindrical Copper Target Liner

Norman F. Roderick* and Robert E. Peterkin, Jr.
Air Force Research Laboratory: Directed Energy Directorate
Center for Plasma Theory and Computation
Kirtland AFB, NM 87117, USA

Experiments performed by Degnan et al. have been carried out to study the compression of a cylindrical copper target with a hydrogen working fluid. The working fluid is produced by a 350 kJ electrical discharge through a hydrogen gas that is initially at room temperature and 40 torr in a coaxial plasma gun. This discharge pushes the hydrogen gas from the plasma gun into a dynamic chamber that is formed by a quasi-spherical aluminum outer liner, a cylindrical copper inner liner, and converging electrodes at ±45° with respect to the equator of the quasi-spherical liner. The discharge heats and compresses the hydrogen gas-which we now refer to as the working fluid—as it pushes it into the chamber. A second electrical discharge of about 5 MJ from the Shiva Star capacitor bank compresses the quasi-spherical aluminum liner that is filled with the working fluid. The temperature of the working fluid is made sufficiently high by the first discharge—on the order of 1 eV—that the sound speed is faster than the implosion speed of the quasi-This allows for 'shockless' spherical liner. compression of the inner cylindrical copper target. Most previous numerical simulations of this system with the MHD code MACH2 have included only the compressing liners, and not the plasma gun. these simulations assumed Therefore, compressing working fluid to be of uniform temperature and mass density. Recent simulations have been made for the entire coupled system of plasma gun and compressing liners as illustrated in the top figure. As a consequence, the effect of non-

uniform working fluid on the system has been investigated, and results will be presented for the first time. For example, the state of the dynamic chamber for one such simulation at 20 μs is shown in the bottom figure.

7B05

Solid Liner Inner Surface Phenomena During Compression Of A Field Reversed Configuration Plasma For A Magetized Target Fusion Proof Of Principle Demonstration

G.F. Kiuttu, P.J. Turchi, R.J. Faehl, U.S. Air Force Research Laboratory, Kirtland AFB, NM 87117-5776, USA

Solid Liner Inner Surface Phenomena During Compression
Of A Field Reversed Configuration Plasma For A
Magnetized Target Fusion Proof Of Principle
Demonstration

G.F. Kiuttu, P.J. Turchi, Air Force Research Laboratory, Kirtland AFB, New Mexico, USA R.J. Faehl, Los Alamos National Laboratory, Los Alamos, New Mexico, USA

A proposed Magnetized Target Fusion (MTF) proof of principle demonstration involves compression of a field-reversedconfiguration (FRC) plasma by a cylindrical, or quasi-spherical, solid liner. Peak internal poloidal magnetic fields are anticipated to be in the range of 1 - 10 MG at radial compression factors of approximately 10. Several phenomena occurring at the solid liner inner surface affect the performance of this plasma heating and compression scheme. They include nonlinear magnetic field diffusion, phase changes and ablation due to surface and volumetric heating, and magnetohydrodynamic instability growth. Magnetic field diffusion limits the magnetic field amplification and reduces the magnetic flux buffer region between core plasma and liner. Melting and vaporization due to Joule heating alone have been shown to be likely to occur.² Evaporated liner material traveling ahead of the liner solid surface can potentially interact deleteriously with the core plasma before peak compression. We present results of studies of the various phenomena using analytic models and 1- and 2-dimensional MHD simulations.

^{*}Permanent address: Dept. of Chemical and Nuclear Engineering, University of New Mexico, Albuquerque, NM 87131.

^{*} Work sponsored by US DOE Office of Fusion Energy Sciences
* Permanent address: The Ohio State University, Columbus, Ohio, USA

¹ K.F. Schoenberg et al, "Magnetized Target Fusion, A Proof of Principle Research Proposal," LA-UR-98-2413, 1998.

² G.F. Kiuttu, "Estimate of solid liner Joule heating for an MTF proof of principle experiment," Bull. Am. Phys. Soc. **43**, 1911, 1998.

7B06

Numerical Studies of Liners for Magnetized Target Fusion (MTF)

R.J. Faehl, W.L. Atchison, P.T. Sheehey and I.R. Lindemuth, Los Alamos National Laboratory, Los Alamos, NM 87545, USA

NUMERICAL STUDIES OF LINERS FOR MAGNETIZED TARGET FUSION (MTF)

R.J. Faehl, W.L. Atchison, P. T. Sheehey and I. R. Lindemuth,
Plasma Applications Group
Los Alamos National Laboratory, Los Alamos New Mexico
87545.

Magnetized Target Fusion (MTF) requires the fast compression of hot, dense plasmas by a conducting liner. We have used two-dimensional MHD calculations to study the electromagnetic implosion of metallic liners driven by realistic current waveforms. Parametric studies have indicated that the liner should reach velocities of 3-20 km/s, depending on the magnetic field configuration, and reach convergence ratios (initial radius divided by final radius) of at least 10. These parameters are accessible with large capacitor bank power supplies such as SHIVA or ATLAS, or with magnetic flux compression generators. One issue with the high currents that are required to implode the liner is that Ohmic heating will melt or vaporize the outer part of the liner. Calculations have shown that this is a realistic concern. We are currently addressing questions of liner instability and flux diffusion under MTF conditions. Another issue is that the magnetic fields needed to inhibit thermal losses to the walls will also heat, melt, or vaporize the inner wall surfaces. For initial fields between 5-50 Tesla, the wall heating is significant but does not result in rapid melting. As the implosion evolves, flux compression leads to fields in excess of 100 Tesla. Calculations which include flux diffusion, Ohmic heating, and realistic material properties show that a significant fraction of the inner surface of an aluminum liner will have melted and vaporized in the final microsecond of implosion. It is not clear at this time that such material mixes will the hot plasma. We are conducting studies to determine the extent of wall-plasma interaction under these conditions.

7B07

Measurement of MTF Target Plasma Temperature Using Filtered Photodiodes

J.M. Taccetti, F.J. Wysocki, G. Idzorek, H. Oona, R.C. Kirkpatrick, I.R. Lindemuth, P.T. Sheehey, F.Y. Thio, Los Alamos National Laboratory, Los Alamos, NM 87545, USA

Measurement of MTF Target Plasma Temperature Using Filtered Photodiodes

J.M. Taccetti, F.J. Wysocki, G. Idzorek, H. Oona, R.C. Kirkpatrick, I.R. Lindemuth, P.T. Sheehey, F.Y. Thio[†]

Los Alamos National Laboratory, Los Alamos, New Mexico

†Massey University, Auckland, New Zealand

Magnetized Target Fusion (MTF) is an approach to fusion where a preheated and magnetized plasma is adiabatically compressed to fusion conditions. Successful MTF requires a suitable initial target plasma with a magnetic field of al least 5 T in a closed-field-line topology, a density of roughly 1018 cm⁻³, a temperature of at least 50 eV but preferably closer to 300 eV, and must be free of impurities which would raise radiation losses. The goal of these experiments is to demonstrate plasma conditions meeting the requirements for an MTF initial target plasma. The plasma is produced by driving a z-directed current of 1-2 MA through either a static gas fill or a 38 µm diameter polyethylene fiber. The data obtained from an array of filtered photodiodes is used to estimate the plasma temperature. The filter material and thickness for each diode is chosen such that the lowest absorption edge for each is at a successively higher energy, covering the range from a few eV to 5 keV. The analysis assumes a fully stripped optically thin plasma which radiates as either a blackbody, a bremsstrahlung emitter, or a group of emission lines (gaussian-like).

7B08

Analysis of Data From Z-Pinch MTF Target Plasma Experiments

F.J. Wysocki, J.M Taccetti, J.F. Benage, G. Idzorek, H. Oona, R.C. Kirkpatrick, I.R. Lindemuth and P.T. Sheehey, Los Alamos National Laboratory, Los Alamos, NM 87544, USA

Analysis of Data From Z-Pinch MTF Target Plasma Experiments

F. J. Wysocki, J. M. Taccetti, J. F. Benage, G. Idzorek, H. Oona, R. C. Kirkpatrick, I. R. Lindemuth, and P. T. Sheehey

Los Alamos National Laboratory, Los Alamos, New Mexico, USA

Magnetized Target Fusion (MTF) target plasma experiments have been performed at the Los Alamos National Laboratory Colt facility for roughly three years. 1,2 The capacitor bank has a maximum output voltage of 120 kV, maximum energy store of 0.25 MJ, and can deliver at least 2 MA of current to a load in 2.5 microseconds. The approach for MTF target plasma generation has been to drive a z-directed current through a plasma which is contained by a 2 cm radius by 2 cm high cylindrical metal wall. The initial mass for the target plasma comes from either a static uniform fill of hydrogen or deuterium gas, or from a polyethylene fiber mounted along the central axis. Polyethylene fibers were used as a substitute for the cryogenically frozen deuterium fibers that were originally planned for. The diagnostic set includes an array of 12 B-dot probes, optical framing camera, gated OMA visible spectrometer, time-resolved monochrometer, filtered silicon photodiodes, neutron yield, and a laser interferometer. The data obtained allows an assessment of the plasma temperature, density, magnetization, and decay time. With this, the suitability of these plasmas for an MTF application will be addressed.

¹ F. J. Wysocki et al., Digest of Technical Papers for the 11th IEEE International Pulsed Power Conference, Baltimore, Maryland, June 29 to July 2, 1997, G. Cooperstein and I. Vitkovitsky editors, p. 1393.

² F. J. Wysocki et al., Proceedings of the VIIIth International Conference on Megagauss Magnetic Field Generation and Related Topics, Tallahassee, Florida, October 18 to 23, 1998.

7C

Bonsai II 10 AM, Thursday, June 24, 1999

Session 7C Closing Switches and Plasma Opening Switches

Chairperson

Mark Savage

Sandia National Laboratories

7C01-2

Invited - Hobetron Current Regulating Switch Tube

R.B. True, R.J. Hansen, D.N. Deb, G.R. Good and W.A. Reass, Litton Systems Inc., San Carlos, CA 94070, USA

HOBETRON CURRENT REGULATING SWITCH TUBE*

R.B. True, R.J. Hansen, D.N. Deb, G.R. Good Litton Systems, Inc., Electron Devices Division San Carlos, CA 94070 and W.A. Reass Los Alamos National Laboratory Los Alamos, NM 87544

This paper describes a novel high power electron tube that can hold off voltages up to hundreds of kilovolts, and switch hundreds of amps of current. We call the device the "Hobetron" since it utilizes a hollow electron beam. Unlike magnetron injection gun (MIG) switch tubes, it does not require a magnet. Further, it uses nonintercepting control elements, and a dispenser cathode for long life and reliability. Finally, it features a double walled Faraday cage collector for high power dissipation capability. Current is very tightly controlled against changes in voltage across the switch (it is an almost perfect pentode), thus this tube is ideally suited for direct series switching applications.

In the paper, various Hobetron designs, and the computer codes and methods used to create them, will be described. One is the L-6026 which was designed for plasma source ion implantation (PSII) modulator use. This tube can hold off voltages up to 125 kV DC (200 kV for transients) in the off mode, then rapidly switch to a 200 amp conducting state. In this tube, at the 200 amp level, net voltage drop across the switch (cathode to collector) can be as low as 4.5 kV. This level is considerably lower than MIG switch tubes enabling overall system efficiency to be substantially higher.

Hobetrons are also ideally suited for use in high energy physics klystron power supply modulators. For example, with two minor modifications to the basic L-6026 Hobetron design, it is possible for the tube to hold off 170 kV DC and switch 120 amps of current. The paper will also present an even higher power device, the "Hobetron-Plus," which has been designed to hold off 500 kV DC and switch 500 amps.

Hobetrons utilize all metal ceramic construction and they are designed to be extremely tough and reliable. Further, they are configured for rapid turn-on and turnoff (very high switching speed). The paper will present mechanical details, and hot test data on the most recent L-6026 design.

7C03

Geometric Considerations for UltraFast Spark Gap Switching

Jane M. Lehr and Carl E. Baum, U.S. Air Force Research Laboratory, KAFB, NM 87117-5776, USA

GEOMETRIC CONSIDERATIONS FOR ULTRAFAST SPARK GAP SWITCHING

Jane M. Lehr and Carl E. Baum

Air Force Research Laboratory
Directed Energy Directorate
Kirtland, AFB, NM

In general, spark gap design is dominated by features that enhance the switch initiation mechanism and affect performance, such as over-voltages, gap inductance, delay time and switch jitter. For timescales exceeding sub-microsecond duration, many of the geometry dependent parameters, such as capacitance, can be ignored. As achievable risetimes approach the picosecond timescale, the geometry of the spark gap itself influences its performance.

A circuit model of the spark gap is introduced for an analytical solution, and bounds are placed on the circuit parameters that reflect that physical geometry of the spark gaps. A full circuit synthesis has been performed on a spark gap that is both fed and terminated in a transmission line. The transmitted waveforms are calculated from the model, and related back to the physical geometry of the system. Simple circuit models of a spark gap is used to investigate the effect of the geometric considerations on charge time, the achievable risetime, the critical damping condition, and its relation to notches in the spectrum of radiated waveforms.

^{*}The authors wish to thank the members of the NIST PSII Consortium administered by ERIM International for partial support of the L-6026 Hobetron development.

7C04

Rise Time Considerations For Photoconductive Switch Materials Used in High Power UWB Microwave Applications

N.E. Islan, E. Schamiloglu, C.B. Fleddermann, J.S. H Schoenberg, R. P. Joshi, University of New Mexico, Albuquerque, NM 87131, USA

RISE TIME CONSIDERATIONS FOR PHOTOCONDUCTIVE SWITCH MATERIALS USED IN HIGH POWER UWB MICROWAVE APPLICATIONS*

N. E. Islam, E. Schamiloglu, and C. B. Fleddermann Department of Electrical and Computer Engineering, University of New Mexico, Albuquerque NM, 87131

> J.S. H Schoenberg, Air Force Research Laboratory Directed Energy Directorate, Kirtland AFB, NM 87117-5776

R. P. Joshi

Department of Electrical and Computer Engineering Old Dominion University, Norfork VA 23529-0246

Because of its high resistivity undoped semi-insulating (SI) GaAs grown through the liquid encapsulated Czochralski technique has been used as photoconductive semiconductor switches (PCSS) in high power applications. In such cases, the device can withstand an off-state voltage in excess of 20 kV, which can then be transferred to the load during the on state.

The signal rise time is an important device parameter to consider in high power microwave (HPM) applications. Rise time depends to a large extent on the bias across the device and is also material dependent. High resistivity materials used in PCSS can be grown through different techniques. Doping levels and the methodology of compensation (e.g. deep donor shallow acceptor like EL2/C or shallow donor deep acceptor Si/Cr) are important factors that may influence rise time. The effects of trapping and de-trapping at high fields, avalanche and double injection phenomena, all contribute to this important device parameter. It is therefore important to investigate these materials and their effect on the collection mechanism and on other parameters of the PCSS.

We present results from the simulation studies of an 'opposed' contact PCSS, made from EL2/C compensation and compare it with an intrinsic GaAs material. The study presents physical conditions inside the device during the switching operation and looks into the possible effects of low doping verses high resistivity through compensation on the switch rise time. Preliminary results show that the non-compensated (intrinsic) materials behave as 'relaxation' semiconductors and the recombination mechanism tends to have an adverse effect on the rise time of the device. Effects of bias on the rise time are also investigated.

7C05

Explosively Formed Fuses for High Voltage Systems

D.G. Tasker, J.H. Goforth, C.M. Fowler, D.H. Herrera, J.C. King, E.A. Lopez, E.C. Martinez, H. Oona, S.P. Marsh, R.E. Reinovsky, J.L. Stokes, L.J. Tabaka, D.T. Torres, F.C Sena G. Kiuttu and J. Degnan, Los Alamos National Laboratory, Los Alamos, NM 87545, USA

Explosively Formed Fuses for High Voltage Systems

D.G. Tasker, J.H. Goforth, C.M. Fowler, D.H. Herrera, J.C. King, E.A. Lopez, E.C. Martinez, H. Oona, S.P. Marsh, R.E. Reinovsky, J.L. Stokes, L.J. Tabaka, D.T. Torres, and F.C. Sena University of California, Los Alamos National Laboratory

G. Kiuttu and J. Degnan
Air Force Research Laboratory, Kirtland AFB

At Los Alamos, we had previously applied Explosively Formed Fuse (EFF) techniques to large systems, where the EFF has interrupted currents from 19 to 25 MA. More recently we have been investigating the use of the EFF technique to apply high voltages to high impedance loads in compact systems, and have used 43-cm EFF systems to interrupt currents of ~3 MA and produce voltages up to 300 kV. We now report our progress towards producing up to 500 kV, 1-us duration pulses using 76-cm EFF systems. In compact explosive systems, the interactions of shock and detonation waves with conductors and insulators offers some significant challenges, especially when the local electric fields approach the breakdown strengths of the insulators. The results of computer calculations and experiments of switch performance will be presented.

7C06

Experimental Study of the Decade Cableguns

Dennis Keefer, L. Montgomery Smith and Newton Wright,

University of Tennessee Space Institute, Tullahoma, TN 37388, USA

Experimental Study of the DECADE Cableguns

Dennis Keefer, L. Montgomery Smith and Newton Wright

University of Tennessee Space Institute Tullahoma, TN 37388

The cableguns used to initiate the operation of the DECADE plasma opening switch (POS) consist of sections of Teflon insulated copper coaxial cable machined to a conical nozzle shape. An arc formed across this nozzle ablates the Teflon insulator and copper center conductor and injects the resulting plasma into the POS. Single cableguns have been tested in a laboratory facility to obtain measurements of the average mass ablated and to obtain optical emission spectra, laser time resolved interferometer measurements and The cableguns were weighed and photographs. measured before and after a sequence of 300 shots to determine the average mass of Teflon and copper lost per shot. It was found that the average mass loss of 277 micrograms per shot consisted of 61% copper and 39% Teflon when a capacitor voltage of 25 kV was used. Time integrated spectral emission data revealed mostly spectral lines of singly ionized fluorine and carbon with no copper visible. A semi-quantitative analysis of the plasma temperature spectrum suggests a approximately 2.5 eV. At this temperature most of the copper is doubly ionized and this ion has no spectrum at wavelengths above the quartz ultraviolet cutoff at 200 nm. Time resolved spectra show a rapid transition of copper through the singly ionized state at the beginning of the current pulse and then again late in the pulse when the neutral copper spectrum is observed both in absorption and emission. The measured mass loss data has been used to calibrate an ablation model used in numerical simulations of the flow using the MACH2 code.

7C07

Testing of the MITL and POS for the Decade Ouad

D. Kortbawi, F.K. Childers, H.D. Price, Maxwell Physics International, San Leandro, CA 94577, USA

Testing of the MITL and POS for the Decade Quad

<u>D. Kortbawi</u>, F.K. Childers, H.D. Price Maxwell Technologies - Physics International

The Decade Quad is a modular nuclear weapons effects simulator that uses an Inductive Energy Store (IES) and Opening Switch (OS) as the final stage of pulse compression. This simulator is presently under construction at the Amold Engineering Development Center. A variety prototype modules for this system have been in operation as the development of this system has progressed. Decade Module 2 (DM2) was used to test the final design of the Magnetically Insulated Transmission Line (MITL) and Plasma Opening Switch (POS) for this system. This test showed improved operation of the POS compared to previous experiments and demonstrated an interesting effect of current asymmetry feeding the POS.

The MITL and POS that was assembled on DM2 had several modifications from those tested previously. The MITL had a higher geometric impedance and a shorter electrical length (preserving the overall inductance). The system also incorporates a set of stepper motors and bellows to allow careful centering of the cathode with respect to the anode. The POS design was essentially a copy of the one developed previously on DM1, another prototype. There were modifications to improve serviceabilty and allow the multiple modules that make up the Decade Quad to be packed closely. The entire vacuum system was chemically cleaned before assembly.

In initial operation of the system using a thick stainless steel anode, the POS consistently reached system impedances ($Z_{\rm Sys} = V_{\rm POS}/I_{\rm upstream}$) higher than were achievable on the similar POS on DM1. During previous experiments on DM1 it had been demonstrated that discharge cleaning had a very beneficial effect on the operation of the POS. This was the reason for the chemical cleaning of the entire vacuum section. Discharge cleaning was also used on DM2 for these experiments.

When operation was shifted to the use of a tantalum anode, a problem was noticed. The POS continued to operate at high values of $Z_{\rm sys}$, but the radiation output was poor. There was significant damage to the anode hardware downstream of the POS, indicating that the electron beam was striking the MITL anode rather than the tantalum converter. In analyzing the data, it was noticed that the current feeding the POS was very asymmetric due to a misaligument of the anode and cathode. The damage to the downstream hardware was approximately aligned with the area of lowest current density feeding the POS. Once the misalignment was corrected, the current feed was symmetric and the radiation output significantly improved. There also was significantly less damage to the MITL anode. The correction of the asymmetry did not have a significant effect on the values of $Z_{\rm sys}$ that were achieved.

Sponsored by the Defense Threat Reduction Agency

7C08

Analysis of Power Flow in a Plasma Opening Swith Coupled to an Electron-Beam Diode

D.C. Black, R.J. Commisso, B.V. Weber, U.S. Naval Research Laboratory, Washington, DC 20375, USA

Analysis of Power Flow in a Plasma Opening Switch Coupled to an Electron-Beam Diode*

D. C. Black ⁺, R. J. Commisso, B. V. Weber Plasma Physics Division, Naval Research Laboratory Washington D.C. 20375, USA

Analysis is performed on data obtained from the HAWK inductive storage generator at the Naval Research Laboratory using a Plasma Opening Switch (POS) to drive an electronbeam (e-beam) diode load. The aim of this analysis is to gain new insights into the POS opening process and its effect on switch-load coupling, a phenomenon which is not currently well understood. Currents and voltages measured both at the generator and at the load are used to infer load impedance, flow impedance, load power, POS gap size, and the critical POS gap for magnetic insulation. An important finding is that, at the time of peak load power, the inferred POS gap size is equal to the critical POS gap for magnetic insulation in both switch-limited and load-limited operation. This suggests that POS-load coupling is self-regulated to maintain saturated flow in the POS. Generator current and voltage upstream of the POS are used to determine the time varying inductance upstream of the POS current channel. From this inductance calculation, the location of the current channel at the time of switch opening may be inferred and compared with the location where bremsstrahlung emission is observed to begin in side-viewing x-ray pinhole photographs of Hawk. The effect of varying the conduction time, the anode-cathode gap and the POS-to-load distance on the inferred current-channel location at the time of POS opening is studied.

- Weber, B. V., et. al., Proc. of 11th International Conf. on High Power Particle Beams, p. 121-126 (1996)
- * Work supported by the US Defense Threat Reduction Agency
- + National Research Council Research Associate

7D

Bonsai III 10 AM, Thursday, June 24, 1999

Oral Session 7D
Plasma Thrusters and Arcs

Chairperson
Mark Capelli
Stanford University

7D01-2

Invited -

Electron Transport and Electron Energy Dissipation in Hall Thruster Discharges

M.A. Cappelli, N.B. Meezan and D. Schmidt, Stanford University, Stanford, CA 94305-3032, USA

Electron Transport and Electron Energy Dissipation in Hall Thruster Discharges

M. A. Cappelli, N.B. Meezan, and D. Schmidt

Department of Mechanical Engineering Stanford University Stanford, CA 94305-3032

Due to their high thrust efficiencies and low propellant consumption, coaxial, cross-field (E x B) plasma accelerators (also called Hall thrusters) are gaining popularity as orbit-maintenance devices on commercial, scientific, and military satellites. Stanford University has constructed several laboratory Hall thruster models for investigation of the physical mechanisms, which control electron transport and electron energy dissipation. These types of plasmas are magnetized, and the mechanism for cross-field (Bfield) electron transport is poorly understood. A variety of diagnostics have been developed and applied to this type of plasma These include time-resolved optical emission discharge. measurement spectroscopy, laser-induced fluorescence, direct thrust measurements, and electrostatic probe techniques to characterize the mean fluctuations in the plasma properties within the acceleration region of the discharge. The disturbances have both "coherent" and stochastic components, the later of which ranges from the tens of kHz to MHz range, and are consistent with a Bohm-type mechanism of cross-field transport. In this paper, we present a study of some of these interesting discharge phenomenon, their variations with changes in operating conditions, and the impact that they may have in applications in satellite propulsion.

7D03

Abrupt sonic transition in the Hall thruster

A. Fruchtman, N.J. Fisch, Center for Technological Education, Holan, Holan 58102, Israel

Abrupt sonic transition in the Hall thruster*

A. Fruchtman

Center for Technological Education Holon, 52 Golomb St., Holon 58102, Israel N. J. Fisch

Princeton Plasma Physics Laboratory, P.O. Box 451, Princeton, NJ 08543, USA

Plasma acceleration to supersonic velocities occurs both in space and laboratory plasmas. For a laboratory plasma accelerator, it is desirable that the plasma flow be stable, continuous and controllable. Yet, both experiments and numerical simulations of the Hall thruster¹ exhibit in many cases an oscillatory behavior of the accelerated plasma. Steady flows rarely exist, a fact that is a serious restriction on the flexible use of the accelerator and an obstacle in the quest for an accelerator of variable thrust. Employing a simple model², we show that the acceleration of the plasma to supersonic velocities as a steady flow occurs only when certain relations between the flow parameters are satisfied. The desirable smooth steady acceleration in which the sonic transition occurs inside the accelerator is therefore an exception rather than the rule. We demonstrate that point by a comparison of the plasma acceleration to the acceleration of a gas to supersonic velocities at a Laval nozzle. We then demonstrate that by forcing an abrupt sonic transition, via the introduction of a discontinuity at the plasma flow (here by placing a floating electrode inside the channel), we enlarge the regime of parameters where a smooth sonic transition occurs. Moreover, the formation of a large electric field at the plane of the abrupt sonic transition provides a more efficient acceleration.

- * Work partially supported by AFOSR.
- A. I. Morozov, Yu. V. Esipchuk, G. N. Tilinin, A. V. Trofinov, Yu. A. Sharov, and G. Ya. Shahepkin, "Plasma acceleration with closed electron drift and extended acceleration zone", Sov. Phys. Tech. Phys. 17, 38 (1972).
- 2. A. Fruchtman and N. J. Fisch, "Modeling the Hall thruster", AIAA 98-3500, Cleveland, Ohio (1998).

7D04

LIF Measurements of a low-power Helium Arcjet

Q.E. Walker and M.A. Cappelli, Stanford University, Stanford, CA 94305, USA

LIF Measurements of a low-power Helium Arcjet
Q.E. Walker and M.A. Cappelli
High Temperature Gasdynamics Laboratory
Stanford University
Stanford, CA 94305

Arcjet thruster technology has advanced from laboratory devices to in-flight operational thrusters for northsouth station-keeping. If arcjets can deliver 1000 s of specific impulse at 35-50% efficiency, then they would also be a candidate thruster technology for orbit transfer. A better understanding of the physics controlling arcjet performance is needed in order to achieve these performance goals. Analytical modeling of arcjets is one means of understanding the factors affecting performance, however the validation of the arcjet models can only be performed by comparison with experimental measurements of operating parameters and plasma properties. These comparisons have shown discrepancies between the analytical models and experimental measurements. The models contain both flow physics and propellant chemistry, so it is difficult to determine which portion of the model is incorrect. For this study, we have chosen to operate an arcjet using helium propellant. It is the simplest propellant to model since there is no associated chemistry. This significantly eases the difficulties in modeling the arcjet flow physics.

We are interested in measuring the plasma properties of the helium arcjet flowfield. A number of different diagnostic have been developed to investigate the arcjet plasma plume. Among these diagnostics, laser-induced fluorescence (LIF) has proven to be very useful due to it

spatial resolution and species specific nature.

This paper presents the results of LIF measurements of the velocity and temperature of the arcjet flowfield. From previous studies, the arcjet flowfield is known to have electron number densities in the range of $10^{-12} \, \mathrm{cm}^3$ and electron temperatures of $0.2 - 0.5 \, \mathrm{eV}$. In the preliminary study of the helium arcjet, velocities between 9 and 15 km/s were measured 7 cm downstream of the exit plane with temperatures between 300 and 900 K. In this study, the 587.5 nm transition will be used. A dye ring laser using Rhodamine 6G pumped by a 5W argon-ion laser will be used to probe this transition. By comparing the measured linecenter position with that of a stationary reference source, the Doppler shift was measured and converted into an axial velocity. The FWHM of the lineshape will be used to determine the translational temperature.

7D05

Ablation and Erosion Measurements in an Electrothermal Plasma Gun

G.E. Dale and M.A. Bourham, North Carolina State University, Raleigh, NC, USA.

Ablation and Erosion Measurements in an Electrothermal Plasma Gun

G. E. Dale and M. A. Bourham Department of Nuclear Engineering North Carolina State University Raleigh, NC 27695-7909

The Plasma Interactions with Propellants Experiment (PIPE) is a facility designed to study the response of materials and propellants exposed to a pulsed, high-heat flux plasma produced with an Electrothermal plasma gun. PIPE produces a high-density (10^{25} to 10^{26} m⁻³), low-temperature (1 to 3 eV) plasma for pulse lengths on the order of $100~\mu s$. PIPE is powered by a single 340-uF capacitor with a maximum charging voltage of 10-kV, for a maximum discharge energy of 17-kJ. This paper discusses the results of mass loss measurements made on metallic samples, as well as erosion of gun components (the plasma gun electrode, and the capillary sleeve.) Experiments were conducted at discharge energies between 0.07 and 8.62 kJ.

These measurements were made during melt-layer erosion experiments, where metallic samples were exposed to the pulsed plasma to determine the effect of the liquid phase on erosion. In these experiments, the mass loss of the samples was measured to determine the net sample erosion. Results from aluminum (2042 Al), copper (OFHC Cu), and stainless steel (316 SS) samples are discussed.

During the course of the melt-layer experiments, many of the operational parameters of the gun were measured. One of these parameters is the mass loss of components within the plasma gun, specifically the cathode and the capillary sleeve. In this experiment, the sleeve was fabricated from Lexan, and the cathode was fabricated from HD17, a tungsten alloy.

In a capillary discharge, the ablated sleeve material is the main source of material for the formation of the high density plasma. The total ablation of the sleeve is indicative of the net plasma density.

Erosion of the cathode is an undesirable consequence of the high-current plasma arc. During these experiments, it was found that the erosion of the cathode was quite large. This caused difficulties through the redeposition of eroded cathode material on the surface of the samples.

It will be shown that much of the mass loss data can be fit to simple empirical relations. These empirical relations are shown and discussed. Also discussed are possible schemes to minimize the erosion of the cathode.

Work Supported by the US Army Research Office contract DAAH04-95-1-0214.

7PDe Anza I & II 3 PM, Wednesday, June 23, 1999

Poster Session 7P

7P01

Time correlation of plasma focus X-ray emission in various energy ranges

I. Paraschiv, V. Zoita, R. Presura, University of Nevada - Reno, Reno, NV 89557, USA

Time correlation of plasma focus X-ray emission in various energy ranges

I. Paraschiv[†], V. Zoita, R. Presura^{††}

National Institute for Lasers, Plasma and Radiation Physics, Dense Magnetized Plasma Laboratory, P.O. Box MG36, Magurele, Bucharest, R-76900, Romania [†]Currently at University of Nevada, Reno, USA ^{††}Currently at Technical University, Darmstadt, Germany

The correlation between the onset times of the X-ray emissions in three energy ranges has been studied on a plasma focus device (11 kJ at 16 kV) with various gas fillings. Soft X-ray line emission at about 1 keV photon energy (H- and He-like neon ion resonance lines) was detected by means of a crystal spectrometer. Medium energy X-ray emission (5-30 keV) was measured by filtered PIN diodes. Hard X-rays (energy above 100 keV) were detected by scintillator-photomultiplier detectors. In most of the measurements all detection devices were placed in a plane perpendicular to the electrode axis viewing a region at about 1 cm in front of the central electrode. The visible light emission from the collapsing plasma sheath was taken as the time reference in the correlation studies. It was found that the onset times of the plasma focus X-ray emission in the energy ranges specified above were highly correlated (correlation coefficients close to unity were found). This was not the case for the duration and intensity of the same emissions.

Transition in x-ray yield, mass scaling observed in the high-wire-number, plasma-shell regime

K.G. Whitney, P.E. Pulsifer, J.P. Apruzese, J.W. Thornhill and J. Davis, T.W.L. Sanford, R.C. Mock and T.J. Nash, U.S. Naval Research Laboratory, Washington, DC 20375, USA

Transition in x-ray yield, mass scaling observed in the high-wire-number, plasma-shell regime

K. G. Whitney, P. E. Pulsifer, J. P. Apruzese, J. W. Thornhill, and J. Davis Naval Research Laboratory Plasma Physics Division Washington D.C. 20375

T. W. L. Sanford, R. C. Mock, and T. J. Nash Sandia National Laboratories P. O. Box 5800 Albuquerque, N.M. 87185

Initial calculations, based on classical transport coefficients and carried out to predict the efficiency with which the implosion kinetic energy of aluminum Z pinches could be thermalized and converted into kilovolt x rays [1], predicted a sharp transition between m^2 and m yield scaling, where m is the aluminum array mass. Later, when ad hoc increases in the heat conductivity and artificial viscosity were introduced into these calculations and the densities that were achieved on axis were sharply reduced, the transition from m^2 to m scaling was found to have shifted, but was otherwise still fairly sharp and well-defined [2]. The location of these breakpoint curves defined the locus of implosion velocities at which the yields would obtain their maximum for different mass arrays. The first such mass breakpoint curve that was calculated is termed hard, while the second is termed soft.

Early 24, 30, and 42 aluminum wire experiments on the Saturn accelerator at the Sandia National Laboratories confirmed the predictions of the soft breakpoint curve calculations. In this talk, we will present results from a more recent set of aluminum experiments on Saturn, in which the array mass was varied at a fixed array radius and in which the radius was varied for a fixed mass. In both sets of experiments, the wire numbers were large: in excess of 92 and generally 136 or 192. In this high-wire-number regime, the wire plasmas are calculated to merge to form a plasma shell prior to significant radial implosion [3]. Large wire number has been found to improve the pinch compressibility [4], and the analysis of these experiments in the shell regime shows that they come very close to the original predictions of the hard breakpoint curve calculations. A discussion of these detailed comparisons will be presented.

- 1. K. G. Whitney, et. al., J. Appl. Phys. 67, 1725 (1990).
- 2. J. W. Thornhill, et. al., Phys. Plasmas 1, 321 (1994).
- 3. T. W. L. Sanford, et. al., Phys. Rev. Lett. 77, 5063 (1996).
- 4. T. W. L. Sanford, et. al., Phys. of Plasmas, to be published, (1999).

7P03

Zero Dimensional Scaling of Ar K-shell Radiation in Long Implosion Z-Pinch Experiments

Eduardo Waisman, Philip Coleman and Charlie Gilbert, Maxwell Technologies, San Diego, CA 92123, USA

Zero Dimensional Scaling of Ar K-shell Radiation in Long Implosion Z-pinch Experiments

Eduardo Waisman, Philip Coleman and Charlie Gilbert Maxwell Technologies, Inc., San Diego, CA, USA

Zero Dimensional models are useful in predicting trends and optimal experimental parameters to maximize K-shell radiation in z-pinch experiments. We apply the model of Mosher, Qi and Krishnan (MOK) to Ar K-shell radiation in the range of 2 to 10 MA and implosion times from 100 to 300 ns. In particular we analyze recent experiments on the Double Eagle machine at Maxwell Physics International going to up to 4 MA and implosion times from 100 to 200 ns. The critical step in applying the MQK model is assuming either a final radius for the implosion, or a given effective compression ratio (ratio between the initial and final radii). We derive the optimal solution for the MQK model in both cases, keeping the effective compression ratio or the final radius fixed, as the current and implosion time are varied, for the particular case of a constant I-dot "ideal machine." Two types of loads are considered: infinitely thin shells (slug model) and uniform fills (constant gas density between initial radius and axis). We next apply the model using the implosion parameters resulting from circuit calculations of various pulsed power generators. The application of the model shows clearly the trends to be expected for Ar K-shell radiation yield as current is increased, as well as the influence of implosion time, and the differences between the two type of loads considered. We show that the experimental data from DM2, Double Eagle, Saturn, and ACE 4 can be explained by reasonable choices of effective compression ratios. Finally, we use the experimental result and the 0-D scaling to show that the simple physical assumptions of the 0-D model imply that the DE results justify the expectation of obtaining 40 kJ or more of Ar K-shell radiation for DECADE QUAD, when it comes on line next year.

Sponsored by the Defense Threat Reduction Agency

Robust Gas Preionization System For Double Eagle PRS Experiments

Y.Song, P.L. Coleman, B.H. Failor, D. Kortbawi, J.S. Levine, J.C. Riordan, H.M. Sze, J.R. Thompson, R.J. Commisso, B. Moosman, S.J. Stephanakis, B.V. Weber, A. Fisher and R.F. Schneider, Maxwell Physics International, San Leandro, CA 94577-0599, USA

ROBUST GAS PREIONIZATION SYSTEM FOR DOUBLE-EAGLE PRS EXPERIMENTS*

Y. Song, P. L. Coleman, B. H. Failor, D. Kortbawi, J. S. Levine, J. C. Riordan, H. M. Sze, J. R. Thompson, R. J. Commisso¹, B. Moosman¹, S. J. Stephanakis¹, B. V. Weber¹, A. Fisher² and R. F. Schneider²

Maxwell Physics International 2700 Merced Street San Leandro, CA 94577-0599

In a previous research, an azimuthally symmetric UV source was used to preionize the argon gas puffs in the DM2 Plasma Radiation Source (PRS) experiment. It indicated that the preionization helped to improve the PRS K-shell yield and reduce shot to shot variations. It also revealed that the issues of survivability and replaceability must be addressed for such a preionization source to be used in super-power generator environments.

Based on the evaluation of the previous preionizer, a robust new preionizer has been fabricated and fielded on Double-EAGLE during the PRS experiment. Design of the new preionizer and its performance on Double-EAGLE will be presented. Comparison with the previous preionizer will also be discussed.

7P05

Correlation of the Time History of Argon Z-Pinch K-Shell Emission and Initial Gas Distribution

Philip Coleman and J. Levine, Maxwell Technologies, San Diego, CA 92123, USA

Correlation of the Time History of Argon Z-Pinch K-Shell Emission and Initial Gas Distribution

> <u>Philip Coleman</u> and J. Levine Maxwell Technologies, San Diego, CA, USA

The success of recent Z-pinch wire-array experiments on the Saturn and Z machines testifies to the importance of initial conditions to quality implosions. We report here on the correlation of the K-shell emission of a gas puff load with the initial gas distribution.

Weber and Fulghum (1997) demonstrated the use of a precision interferometer to determine the gas density profiles of z-pinch gas puff nozzles. On recent Double Eagle experiments, we have made use of a one dimensional array of x-ray-sensitive silicon diodes to measure the time history of argon K-shell emission as a function of distance across the A-K gap of the pinch. We present data from this "zipper" array and discuss the correlation of the zipper data with the measured initial gas distribution.

 Weber, B. V. and S. F. Fulghum, Rev. Sci. Instruments, 68, 1227 (1997).

Sponsored by the Defense Threat Reduction Agency

^{*}This work is supported by the Defense Threat Reduction Agency.

Naval Research Laboratory

²Defense Threat Reduction Agency

Results of structured load implosion experiments and its comparison with simulation

A.V. Shishlov, R.B. Baksht, A.V. Fedunin, B.M. Kovalchuk, V.A. Kokshenev, A. Yu. Labetsky, V.I. Oreshkin, A.G. Russkikh, High Current Electronics Institute, Tomsk 634055, Russia

Results of structured load implosion experiments and its comparison with simulation*.

A.V.Shishlov, R.B.Baksht, A.V.Fedunin, B.M.Kovalchuk, V.A.Kokshenev, A.Yu.Labetsky, V.I.Oreshkin, A.G.Russkikh

High Current Electronics Institute SB RAS, Tomsk, Russia

Loads with a structured density profile (such as double gas puffs or uniform fill loads) can be an alternative to conventional thin shells when implosions from large initial diameters with long implosion times are desired [1]. It was shown in the experiments [2] that radiative performance of thin shell decreases significantly as the initial load radius exceeds 2 cm. Structured loads are expected to be more stable due to the mechanism of snow-plow stabilization. The experiments with structured load were carried out on GIT-12 generator (2.5 MA, 2.4 MJ). Implosions of structured load were simulated with the help of quasi two-dimensional model. The experimental results and their comparison with the results of simulations are presented.

- F.L.Cochran, J.Davis, A.L.Velikovich, Phys. Plasmas 2 (7), 2765 (1995).
 R.J.Commisso et al., IEEE Trans. Plasma Sci., vol.26, No.4, 1068 (1998).
- *The work was supported in part by ISTC Project #525 and RFBR grant "198-02-16963

7P07

Simulation of imploding Z-pinch loads with quasi two-dimensional models

V.I. Oreshkin, A.V. Shishlov, High Current Electronics Institute, Tomsk 634055, Russia

Simulation of imploding Z-pinch loads with quasi two-dimensional models.

V.I.Oreshkin, A.V.Shishlov

High Current Electronics Institute SB RAS, Tomsk, Russia

Two major stages can be distinguished in the process of Z-pinch implosion: a run-in phase and a stagnation phase. The first, run-in phase, is characterised by an important role of shock waves and small radiative losses. The second stage is a phase of existence of a dense high temperature pinch. At this stage, the role of radiation is more significant than the role of shock waves. In this work, the first phase is simulated with the help of 2D snow-plow model [1] that allows taking into account the influence of the Rayleigh-Taylor instabilities and the snow-plow stabilization mechanism [2].

The simulation shows that the growth of the RT instabilities leads to the lost of the substantial part of the imploded mass during the acceleration. The fraction of the lost mass is less in case of double gas-puff implosion than in case of single gas-puff implosion due to the presence of the snow-plow stabilization mechanism.

The second phase is simulated with the help of quasi 2D model [3], where all thermodynamic quantities have a fixed radial rofile. The initial conditions for the calculations are taken from the results of the 2D snow-plow model calculations. The model allows estimation of K-shell radiation yields. The results of calculations are compared with the results obtained in the experiments on GIT-4 and GIT-12 generators.

- 1. G.Basqne, A.Jolas, I.P. Wattean, Phys. Fluids, vol.11, 1484 (1968).
- 2. S.M.Gol'berg, A.L.Velikovich, Phys. Fluids B 5, 1164 (1993).
- 3. V.S.Imshennik, S.M.Osovets, I.V.Otroschenko, Zh.Eksp.Teor.Fis. (Sov.Phys.JETF), vol.64 (1973).
- *The work was supported in part by ISTC Project #525 and RFBR grant #198-02-16963

Gas Puff Z-Pinch Plasmas driven by Inductive Voltage Adder ASO-X modified by POS

Sunao Katsuki, Koichi Murayama, Susumu Kohno, Igor V. Lisitsyn and Hidenori Akiyama, Kumamoto University, Kumamoto 860-8555, Japan

Time correlation of plasma focus X-ray emission in various energy ranges

I. Paraschiv[†], V. Zoita, R. Presura^{††}

National Institute for Lasers, Plasma and Radiation Physics, Dense Magnetized Plasma Laboratory, P.O. Box MG36, Magurele, Bucharest, R-76900, Romania [†]Currently at University of Nevada, Reno, USA ^{††}Currently at Technical University, Darmstadt, Germany

The correlation between the onset times of the X-ray emissions in three energy ranges has been studied on a plasma focus device (11 kJ at 16 kV) with various gas fillings. Soft X-ray line emission at about 1 keV photon energy (H- and He-like neon ion resonance lines) was detected by means of a crystal spectrometer. Medium energy X-ray emission (5-30 keV) was measured by filtered PIN diodes. Hard X-rays (energy above 100 keV) were detected by scintillator-photomultiplier detectors. In most of the measurements all detection devices were placed in a plane perpendicular to the electrode axis viewing a region at about 1 cm in front of the central electrode. The visible light emission from the collapsing plasma sheath was taken as the time reference in the correlation studies. It was found that the onset times of the plasma focus X-ray emission in the energy ranges specified above were highly correlated (correlation coefficients close to unity were found). This was not the case for the duration and intensity of the same emissions.

7P09

X-ray spectrometers with cylindrical, spherical and toroidal dispersive elements

E.O. Baronova, V.V. Lider, M.M. Stepanenko, V.V. Vikhrev and N.R. Pereira, Eco Pulse Inc., Springfield, VA, USA

X-ray spectrometers with cylindrical, spherical and toroidal dispersive elements.

E.O. Baronova*, V. V. Lider*, M.M. Stepanenko*, V.V. Vikhrev*, and N. R. Pereira\$

*(RRC Kurchatov Institute, Nuclear Fusion Institute , 123182 Moscow, Russia.)

⁴(Institute of Crystallography, RAS, Moscow, Russia.)

⁵(Ecopulse, Inc., PO Box 528, Springfield, VA 22150 USA)

This paper describes a series of crystal spectrometers for soft x-ray diagnostics of pulsed plasmas. Most use high quality quartz crystals with different orientations of their crystal planes, attached by optical contact to spherical and toroidal substrates. We developed special procedures to attach spherical Johansson quartz crystals with optical contact, and to mount Cauchois type (transmission) crystals. Some mica crystals can be connected to the substrate with glue.

The spectrometers cover an extended energy range, from the low end (0.7 keV) in reflection with a Johann or Johannson configuration to the high end (200 keV) with the Cauchois crystal. We use film as x-ray detector.

We pay special attention to spectral and spatial resolutions. These characteristics are modeled analytically and compared with experimental calibration. Some crystals have spectral resolution better than 9×10⁻⁵, and spatial resolution of a few microns. One of these is a uniquely large (100 mm by 40 mm) quartz crystal bent to a 3770 mm radius.

The spectrometer was used on a 500 kA plasma focus, with enough resolution to estimate temperature and density of the argon plasma from the line shapes, and the fraction of current in an electron beam from the line's polarization. Compared to a conventional spectrometer with a cylindrically bent crystal, the spectrometer with a chemically polished spherical crystal has much better resolution of the fine structure.

In the Cauchois (transmission) version we [1] measured bremsstrahlung spectra in the range 20-200 keV from a 360 kA plasma focus. The detector was an absolutely calibrated combination of intensifier (LaOBr) and film. The measured spectra showed evidence of an electron beam, bombarding the anode surface.

Future spectrometers will have their film replaced with a CCD to allow immediate readout of time-integrated measurements, and with a pulsed microchannel plate intensifier to allow time-resolved registration.

[1] E. O. Baronova, PhD Thesis (1995).

Calculations of Capillary Z-Pinch At 100 MA Scale Currents

Yu V. Afanas'ev, V.N. Shlyaptsev, A.L. Osterheld, Lebedev Physical Institute, Moscow, Russia

CALCULATIONS of CAPILLARY Z-PINCH AT 100 MA - SCALE CURRENTS

Yu.V.Afanas'ev, P.N.Lebedev Physical Institute, Moscow,

V.N.Shlyaptsev, A.L.Osterheld,

Different capillary Z-pinch configurations from hundreds of microns to several cm in diameter have been previously investigated experimentally during last two decades for the purposes of suppression of current instabilities. They demonstrated quenching of accretion and m=1 instabilities as well as high heating rates and temperatures substantial to generate 1 keV-range X-rays [1]. Very stable and homogeneous heating and compression in fast capillary discharges were the key factors which allowed to achieve X-ray laser generation [2].

Here we report the numerical investigations of different capillary Z-pinch configurations aimed at next generation pulsed power driver currents. Several cases of interest have been examined, including 'classical' gas-filled capillary pinch, staged pinch and some others.

7P11

Study of capillary discharges for soft x-ray lasers

D. Hong, R. Dussart, W. Rosenfeld, S. Gotze, C. Cachoncinlle, R. Viladrosa, C. Fleurier and J.M. Pouvesle, Universite d'Orleans, 45067 Orleans Cedex 2, France

Study of capillary discharges for soft x-ray lasers

D. Hong, R. Dussart, W. Rosenfeld, S. Götze, C. Cachoncinlle, R. Viladrosa, C. Fleurier and J.M. Pouvesle GREMI, CNRS/Université d'Orléans, BP 6759, 45067 Orléans cedex 2, France

Since the first demonstration of a compact discharge pumped soft x-ray laser by Rocca et al¹, there is an increasing interest in the study and the development of such tabletop systems with a high energetic efficiency. At GREMI, we developped two fast capillary discharge devices based on different pulsers. In the first experiment, the discharge is driven by a Blumlein generator allowing high injected power density in low pressure argon filled, 3 to 10 cm in length, 4 mm in diameter, polyacetal capillaries. Argon timeintegrated spectra show that highly ionized argon states, up to Ar7+, are efficiently produced at rather low values of the stored energy (<20 J). Time-resolved soft x-ray spectroscopy is in progress in order to facilitate the observation, if produced, of excited states of Ar IX at the origin of the lasing transition while scaling to larger input energy is under development.

In the second experiment, we developed a low inductance system based on preionized direct discharges of a knob capacitor bank into evacuated, 0.8 to 3 cm in length, 1 mm in diameter, capillaries of polyethylene, polyacetal or teflon. The soft x-ray photons are emitted from a plasma column resulting from the capillary wall ablation. In case of polyethylene capillaries, the spectrum consists essentially of CIV, CV and CVI carbon lines. Using a constant input power density of 70 GW/cm⁻³, we observed an exponential growth of the CVI Ha at 18.2 nm and Hb at 13.5 nm line intensities as a function of the capillary length (0.8 to 1.6 cm) wich seems to indicate an amplification.

This work was supported in part by DRET/DGA and in part by the CNRS and the Région Centre.

^{1.} J.D.Sethian, K.A.Gerber, A.W.Desilva, A.E.Robson. Proc.4-th Int.Conf on Megagauss Magnetic Field Generation and Related Topics, (1986) 131-1

^{2.} J.J. Rocca, V. Shlyaptsev, F.G. Tomasel, O.D. Cortazar, D. Hartshorn, J.L.A. Chilla, Phys. Rev. Lett., 1994, V73, p.2192.

¹ J.J. Rocca et al, Phys. Rev. Lett., 73, 2192 (1994)

Characterisation of a 10 A/s Micro Capillary Discharge as an Ion and Soft X-rays Source

A. Engel, P. Choi, C. Dumitrescu, I. Krisch, J. Larour, J. Rous, T.N. Hansen, J.G. Lunney, LPMI, Palaiseau 91128, France

Characterisation of a 10¹³ A/s Micro Capillary Discharge as an Ion and Soft X-rays Source

A. Engel, P. Choi, C. Dumitrescu, I. Krisch, J. Larour, J. Rous Laboratoire de Physique des Milieux Ionisés, Ecole Polytechnique, 91128 Palaiseau, France

T. N. Hansen, J. G. Lunney Department of Physics, Trinity College, Dublin, Ireland

Capillary discharges are known to be high intensity sources for incoherent and coherent radiation of soft X-rays and VUV. These devices are very compact and therefore suited for laboratory applications.

Here we present a Micro Capillary with effective source dimension of 100 microns in diameter and in length. Due to an optimised energy transfer of 0.2 Joule from the capacitors to the capillary a peak current rise time of 10¹³ A/s is achieved and a dense plasma is observed.

Experimental investigations on its plasma parameter and the influence by different capillary material are presented. Results show that a kT = 150 eV and $Ne = 3 \cdot 10^{20}$ cm⁻³ plasma is formed, which emits 8 keV fast ions due to free expansion.

This work is supported in part by a TMR Contract ERBFMRXCT980186, FACADIX, and an INCO-Copernicus Contract ERBIC15CT970705, HEIBE, from the European Commission and a CNRS/FORBAIRT international cooperation agreement.

7P13

Dynamic Properties of Ultra-fast Pulsed Capillary Discharge Devices

I. Krisch, P. Choi, C. Dumitrescu, A. Engel, J. Larour, J. Rous, L. Juschkin, H-J. Kunze, LPMI, Palaiseau 91128, France

Dynamic Properties of Ultra-fast Pulsed Capillary Discharge Devices

I. Krisch, P. Choi, C. Dumitrescu, A. Engel, J. Larour, J. Rous, Laboratoire de Physique des Milieux Ionisés, Ecole Polytechnique, Palaiseau 91128, France

L. Juschkin, H-J. Kunze Institut für Experimentatlphysik V, Ruhr-Universität Bochum, 44780 Bochum, Germany

We report on a fast pulsed capillary discharge device, which combines the features of transient hollow cathode discharge with the inherent characteristics of the capillary discharge to guarantee radiation in the VUV and soft X-ray region with ns rise time. Various combinations of discharge parameters differing in capacitance of the cell, in the aspect ratio and in the pressure of the filling gas have been studied in order to optimize this table top source to technical and scientific backlighting applications.

After rapidly igniting the discharge by an electron beam resulting from the hollow cathode effect, the plasma emits bright radiation in the soft-X-ray and VUV region, with $\lambda \geq 3$ nm. Using Argon as the filling gas, the spectrum consists of Ar VII to Ar X lines during the period of extreme emission. Energy losses due to radial thermal conduction effect shorten the radiation pulse. A series of VUV spectra which are detected by a calibrated spectrometer covers the period of the discharge and allows a quick estimation of discharge parameters.

The spatial evolution of the radiation source is studied using a time resolved Slit-Wire camera. Two different regimes of wall and gas dominated discharges have been identified based upon the spectra obtained, under different operating pressures.

Acknowledgement: The work is supported by a TMR Contract ERBFMRXCT980186, FACADIX, from the European Commission

Scaling Calculations of Optimal Liner Performance to Determine the Voltage Design Configuration in Atlas

Huan Lee, Los Alamos National Laboratory, Los Alamos, NM, 87545, USA

Scaling Calculations of Optimal Liner Performance to Determine the Voltage Design Configuration in Atlas

Huan Lee

Los Alamos National Laboratory Los Alamos, NM 87544

Atlas is the new pulsed power facility [1] being designed at Los Alamos National Laboratory (LANL) to perform high energy-density experiments in support of weapons physics and basic research programs. At the initial design stage, Marx module "building block" of 120 kV was chosen and there were five possible voltage options, in multiples of 120 kV up to 600 kV. Since the primary mission for Atlas is to drive hydrodynamic experiments, we search for the best liner performance in the sense that it produces the highest collision shock pressure [2] with a fixed target as the figure of merit to determine the optimal voltage configuration. Although the bank capacitance and inductance satisfy some simple scaling in bank voltage, the total circuit inductance does not as it depends on the liner radius to be optimized. Furthermore, the condition on voltage reversal to protect the bank circuit also affects the current waveform significantly as we change the voltage. In this investigation we first derived an approximate scaling relation for the current waveform, through its dependence on circuit parameters, as a function of voltage. From this result we could show in general that the optimized liner performance decreases with increasing voltage. Detailed simulations using the 1-D MHD code RAVEN confirm that the optimized liner at 120 kV indeed outperforms the one at 240 kV, but merely by about 10% in shock pressure. But the 240 kV configuration is much more favorable in terms of the radiation source applications, and so it became our final design choice for Atlas. Some physical insights on the Atlas circuit design gained from this study will be discussed.

- 1. J. J. Trainer *et al.*, "Overview of The Atlas Project," Proceedings of 11th IEEE International Pulsed Power Conference, Baltimore, MD, July 1997, p.37.
- H. Lee et al., "Megabar Experiments on Pegasus II," Proceedings of 11th IEEE International Pulsed Power Conference, Baltimore, MD, July 1997, p.336.

7P15

Simulations of the Formation of Strongly Coupled Plasmas Using Pulsed Power

R.K. Keinigs, Blake Wood, Carter Munson and R.J. Trainor, Los Alamos National Laboratory, Los Alamos, NM 87545, USA

Simulations of the Formation of Strongly Coupled Plasmas Using Pulsed Power

R.K. Keinigs, Blake Wood, Carter Munson, and R.J.
Trainor
Los Alamos National Laboratory
Los Alamos, NM 87545

One experimental campaign planned for the pulse power facility, Atlas, will be devoted to the investigation of strongly-coupled plasma (SCP) effects on transport phenomena and equations-of-state in high-Z materials. Methods for forming strongly coupled plasmas using the pulsed-power facility, Atlas, are currently under investigation. For SCP experiments being planned, a metal plasma ($\rho/\rho_o \sim 0.1$, and T ~ 1-2 eV) imbedded in gas or foam ($\rho \sim .05~\rho_{metal},~T~\sim$ 0.5eV) can produce initial values of Γ (coupling parameter) between 2-20. One approach to forming a plasma with the desired properties involves using an auxiliary capacitor bank to ohmically heat a thin metal shell to vaporization. The expansion of the plasma is impeded by the imbedding gas. Both one and twodimensional magneto-hydrodynamic models are being employed to characterize the plasma and determine the tamping conditions required for its confinement. Results for a titanium plasma, the confinement dynamics for this system, and values obtained for Γ will be presented. Means for experimentally diagnosing such plasmas will also be discussed.

Computational Modeling of Z-Pinch-Driven Hohlraum Experiments on Z

R.A. Vesey, J.L Porter Jr., M.E. Cuneo, C.A. Hall, T.A.Mehlhorn, L.E. Ruggles, W.W. Simpson, M.F. Vargas, J.H. Hammer, O. Landen, J. Koch,

Computational Modeling of Z-Pinch Driven Hohlraum Experiments on Z*

R. A. Vesey, J. L. Porter, Jr., M. E. Cuneo, C. A. Hall, T. A. Mehlhorn, L. E. Ruggles, W. W. Simpson, M. F. Vargas

Sandia National Laboratories

J. H. Hammer, O. Landen, J. Koch Lawrence Livermore National Laboratory

The high-yield inertial confinement fusion concept based on a double-ended z-pinch driven hohlraum [1] tolerates the degree of spatial inhomogeneity present in z-pinch plasma radiation sources by utilizing a relatively large hohlraum wall surface to provide spatial smoothing of the radiation delivered to the fusion capsule. The z-pinch radiation sources are separated from the capsule by radial spoke arrays. Key physics issues for this concept are the behavior of the spoke array (effect on the z-pinch performance, x-ray transmission) and the uniformity of the radiation flux incident on the surface of the capsule. Experiments are underway on the Z accelerator at Sandia National Laboratories [2] to gain understanding of these issues in a single-sided drive geometry. These experiments seek to measure the radiation coupling among the z-pinch, source hohlraum, and secondary hohlraum, as well as the uniformity of the radiation flux striking a foam witness ball diagnostic positioned in the secondary hohlraum.

This paper will present the results of computational modeling of various aspects of these experiments, including:

- (a) the overall flux distribution and foam ball flux uniformity as calculated by three-dimensional radiosity ("view factor") codes, illustrating the dominance of the P₁ asymmetry inherent in single-sided drive geometry,
- (b) the results of a secondary hohlraum geometry optimization study, performed with constrained optimization techniques applied to simple hohlraum representations and refined with full 3D radiosity calculations, and
- (c) radiation-hydrodynamics simulations of z-pinch/hohlraum radiation coupling, source hohlraum to secondary hohlraum coupling, and the simulated response of various diagnostics (remote optical and in-situ shock measurements) under experimental conditions.
- [1] J. H. Hammer, et al., IAEA-F1-CN-69/IFP/18 in Proceedings of 17th IAEA Fusion Energy Conference (Yokohama, Japan, 19-24 October 1998).
- [2] R. B. Spielman, et al., *Phys. Plasmas* 5, 2105 (1998).
 *Sandia is a multiprogram laboratory operated by Sandia Corporation, a Lockheed Martin Company, for the U. S. Department of Energy under Contract No. DE-AC04-94AL85000.

7P17

Time- and Space-resolved measurements of soft x-ray emissions viewed 4x from the z axis at Z

S. Lazier, J. McKenney, D. Jobe, Ktech Corporation, M. Derzon, T. Nash, and G. Chandler, Sandia National Laboratories, Albuquerque, NM, USA.

Time- and space-resolved measurements of soft x-ray emission viewed 4° from the z axis at Z*

S. Lazier, J. McKenney, D. Jobe, Ktech Corporation, Albuquerque, NM M. Derzon, T. Nash and G. Chandler, Sandia National Laboratories, Albuquerque, NM

We have developed a near-axis time-resolved x-ray imaging capability to make measurements of the emission profile for foam targets on the Z accelerator. By slit-imaging spectrally filtered x-ray emission from the z-pinch target to an array of scintillator coupled fiber-optics, we obtain an emission profile as a function of time sampling every 260 μm viewing 4° from the z axis. The plasma run in and reexpansion are observed. Implosion velocities, and compressed sizes for annular and foam targets have been measured. We describe the diagnostics, results from the instrument and instrument characterization. *Sandia is a multiprogram laboratory operated by Sandia Corporation, Lockheed Martin Company, for the United States Department of Energy under Contract DE-AC04-94AL85000.

Investigating Differences between Calculated and Observed X-ray Images of Z-pinches,

W. Matuska, R. Bowers, D. Peterson,Los Alamos National Laboratory,C. Deeney and M. Derzon,Sandia National Laboratories, NM, USA 87185, USA

Investigating Differences between Calculated and Observed X-ray Images of Z-pinches

W. Matuska, R. Bowers, D. Peterson Los Alamos National Laboratory

> C. Deeney, M. Derzon Sandia National Laboratory

Abstract

Recent two-dimensional radiation magnetohydrodynamic (2D RMHD) calculations of radiating z-pinches agree well with integral data (current wave form, yield and power). The agreement between these calculations and detailed data, such as time-resolved x-ray images, is generally not as good. Here we look specifically at calculated and observed images of the pinch for Saturn and the Z-machine. Areas of investigation include temporal blurring over the duration of the exposure and non-symmetric implosion affects as calculated in (x,y)-coordinates.

7P19

Optimization of the inner array in a nested array Z-Pinch

Kyle Cochrane, Melissa Douglas, Norman F. Roderick, Sandia National Laboratories, Albuquerque, NM 87185-1106, USA

Optimization of the inner array in a nested array Z-Pinch by
Kyle Cochrane
Melissa Douglas
Norman F. Roderick

Nested wire arrays have been used to improved pinch quality and an in x-ray power. Numerical simulations suggest that the inner array acts to reduce the growth of the MHD Rayleigh-Taylor (RT) instability present in the outer array prior to impact. This instability develops during the implosion phase and can significantly broaden the pinch at stagnation unless mitigated.

Using a standard 40 mm diameter single array, a numerical parameter study was performed to investigate the mass and location of the additional inner array which would best mitigate the RT instability. The implosion performance was characterized by the peak radial plasma kinetic energy. Initially, a 1-D slug model was used to determine the optimal configuration. This model suggested minimal loss in peak kinetic energy if the inner shell was located between 16 and 22 mm. This information was then used to model the instability effects with a 2-D MHD code, MACH2. In these simulations, the outer array was approximated by a 1 mm thick shell, 10 mm high, at a diameter of 40 mm. The mass was kept constant at 4 mg and the instability was seeded with a 1% cell-to-cell random density perturbation. The mass and location of the inner array was then varied from

A fourier transform of the mass density was used to examine the instability mitigation in detail. Based on the 2D MHD simulations, two configurations provided equally optimal pinch performance: an inner array at 18mm with 1.5mg of mass, an inner array at 20 mm with 2 mg of mass.

0.5mg to 2mg, and 16mm to 22mm.

305

7P20-21

Multi-Dimensional Z-Pinch Calculations With Alegra

Allen C. Robinson, Chris J. Garasi, Thomas A. Haill, Richard L. Morse, Peter H. Stolz, Sandia National Laboratories, Albuquerque, NM 87185-0819, USA

MULTI-DIMENSIONAL Z-PINCH CALCULATIONS WITH ALEGRA

Allen C. Robinson
Chris J. Garasi
Thomas A. Haill
Richard L. Morse
Peter H. Stoltz
Sandia National Laboratories

Two and three-dimensional modeling of exploding z-pinch wires as well as the imploding z-pinch wire array is important to provide insight into the relevant issues for designing high-power z-pinch configurations. We present several calculations done with the MHD modeling capability available within the ALEGRA framework for parallel shock-physics computations. A set of wire explosion calculations illustrates the extreme sensitivity of these configurations to mesh resolution. Use of the ALE capability in ALEGRA will be illustrated. An additional set of calculations investigating the run in and stagnation of an initial merged-wire sheath configuration will be compared with previous calculations and experimental results.

Sandia is a multiprogram laboratory operated by Sandia Corporation, a Lockheed Martin Company, for the United States Department of Energy under contract DE-AC04-94AL85000.

7P22

Dense Z-Pinch Research at the Nevada Terawatt Facility

B. Bauer et al, University of Nevada ñ Reno, USA

Dense Z-Pinch Research at the Nevada Terawatt Facility*

B.S. Bauer, V.L. Kantsyrev, N. Le Galloudec,
R.C. Mancini, G.S. Sarkisov, A.S. Shlyaptseva,
F. Winterberg, S. Batie, W. Brinsmead, H. Faretto,
B. Le Galloudec, A. Oxner, M. Al-Shorman, D.A. Fedin,
I. Golovkin, I. Paraschiv, M. Sherrill, N. Ammons,
S. Hansen, D. McCrorey, Dept. of Physics, UNR;
J.W. Farley, Dept of Physics, UNLV; and
J.S. De Groot, Dept. of Applied Science, UC Davis

A high-repetition-rate, 2-terawatt z-pinch (HDZP-II from LANL: 2 MV, 1 MA, 100 ns, 200 kJ, 1.9 ohm) has been reassembled to investigate the early-time evolution of a current-driven wire, the plasma turbulence around and between wires, the acceleration of a plasma current sheet by a magnetic field, and the suppression or reduction of plasma instabilities. The heating, expansion, and dynamics of wires driven by current prepulses similar to those at SNL-Z is being examined first. Optical, laser, and radiographic measurements of prepulse-driven exploding wires will be compared with the modeling results of D. Reisman et al. (LLNL). SNL-Z wires are exploded by an independent pulse generator (100 kV, 2 kA, 50 ns). Plasma laser-schlieren, laser-absorption. self-emission, interferometric images (10 micron, 0.1 ns resolution) are obtained with streak cameras (S-1 and S-20) and an Nd:glass laser (30 ns, 1064 or 532 nm). Multiframe pointprojection radiography (few-micron, sub-ns resolution) is acheived by driving several x-pinch backlighters with HDZP-II. In addition, laser-induced-fluorescence imaging and x-ray absorption spectroscopy are being developed for this prepulse experiment, while laser polarimetry and collective Thomson scattering, and a suite of x-ray diagnostics (see next poster), are being developed for future high-current experiments.

*Work supported by DOE, UNR, SNL, NSF, and DOD.

X-ray and EUV Diagnostics for the Nevada Terawatt Facility: Plasma Imaging, Spectroscopy and Polarimetry

V.L. Kantsyre, B.S. Bauer, R.C. Mancini, A.S. Shlyaptseva, D.A. Fedin, A. Golovkin, P. Hakel, I. Paraschiv, N. Ammons, S. Hansen, University of Nevada - Reno, Reno, NV 89557-0058, USA

X-ray and EUV Diagnostics for the Nevada Terawatt Facility: Plasma Imaging, Spectroscopy, and Polarimetry*

V.L. Kantsyrev, B.S. Bauer, R.C. Mancini, A.S. Shlyaptseva, D.A. Fedin, A. Golovkin, P. Hakel, I. Paraschiv, N. Ammons, S. Hansen, Department of Physics, University of Nevada, Reno

A wide variety of advanced extreme ultraviolet (EUV) and x-ray diagnostics are being developed for the Nevada Terawatt Facility (NTF) at the University of Nevada, Time-resolved short-wavelength imaging, backlighting, imaging spectroscopy, and polarization spectroscopy will be employed to measure profiles of plasma temperature, density, flow, charge state, and magnetic field. These diagnostics will be used to examine the early-time evolution of a current-driven wire, the formation of a plasma sheet from the explosion and merging of wires, etc. (see previous poster). materials will include Al, Ti, W, and various coatings (e.g., Mg, Ni, Cu). Doping of local regions of wires is planned, for additional spatial resolution of the plasma profiles. The instruments are state-of-the-art applications of glass capillary converters (GCC), multilayer mirrors (MLM), and crystals. The devices include: a prototype of a new glass-capillary-based two-dimensional imaging spectrometer, a pinhole camera with 6 MCP imagers, a 5-channel crystal/MLM spectrometer ("Polychromator") with fast x-ray diodes and an added transmission grating spectrometer; a convex-crystal x-ray survey spectrometer; a prototype of an x-ray polarimeter/spectrometer; and a multiframe x-pinch backlighter yielding point-projection sub-ns resolution. few-micron. microscopy with Spectroscopic data will be interpreted with state-of-the-art spectral calculations that take into account line intensity, plasma broadening, opacity, and polarization effects, for both resonance and satellite lines. Emission spectroscopy will be used to measure plasma density and temperature in the hot plasma around exploding wires, with polarization measurements helping to determine the electron distribution function and the magnetic field in this region. The density and temperature of the high-density, lowtemperature plasma inside exploding Al wires will be measured with absorption spectroscopy.

*Work supported by DOE, UNR, SNL, NSF, and DOD.

7P24

Studies of the Initial Phases of Exploding W and Al Wire and Wire-array Plasma Formation Using X-ray Backlighting

D.B. Sinars, J.B. Greenly, S.A. Pikuz, T.A. Shelkovenko, D.A. Hammer and B.R. Kusse, Cornell University Ithaca, NY?14853, USA

Studies of the Initial Phases of Exploding W and Al Wire and Wire-array Plasma Formation Using X-ray Backlighting*

D.B. Sinars, J.B. Greenly, S.A. Pikuz**, T.A. Shelkovenko**, D.A. Hammer and B.R. Kusse

Laboratory of Plasma Studies, Cornell University Ithaca, NY 14853

Exploding W and Al wires and wire arrays have been investigated using direct (point-projection) x-ray backlighting as the principal diagnostic method. A 4.5kA amplitude, 350 ns quarter-period rise time sinusoidal current source which damps in about 5 µs is delivered to one or more fine W (7.5, 10 or 13.5 μ m) or Al (13.5 or 25 μ m) wires approximately 6 cm away from one or two Mo X-pinch x-ray backlighter sources. The X-pinches are placed in parallel between the output electrodes of the 450 kA, 100 ns XP pulser at Cornell University, each thereby producing a sub-nanosecond x-ray pulse. The source size is small enough to permit micron-scale spatial resolution images of the exploding wires on x-ray film1. By varying the relative timing between pulsing the current source for the W or Al wire or wires and the XP pulser, images of the initial explosion phase of W and Al wires have been obtained at times ranging upwards from about 100 ns after the start of the 4.5 kA current source. Al wires expand substantially with the linear current rise for 100 ns to 1 kA in a single wire. By the time (350ns) of peak current in a single Al wire, the Al has expanded sufficiently to be undetectable using our 3-4.8 keV x-ray backlighter source. However, two Al wires with 2 kA per wire expand more slowly and are still visible up at least 450 ns. By contrast, W wires do not expand significantly during the first ~ 1 µs. A laser schlieren imaging system to image the coronal plasma around the wire cores has been synchronized with the x-ray backlighter sources in order to see the tenuous outer coronal plasma which is invisible in the x-rays images. Comparisons of schlieren and x-ray backlighting images will be presented. The implications of these results to cylindrical plasma formation in exploding wire arrays by the prepulse on the Z accelerator, and to 2 and 3D MHD code validation will be discussed.

^{*}Research supported by Sandia National Laboratories, Albuquerque, Contract #BD-9356.

^{**}Permanent address: Lebedev Physical Institute, Moscow, Russia

¹T.A. Shelkovenko, S.A. Pikuz, A.R. Mingaleev and D.A. Hammer, Rev. Sci. Instrum. **69**, in press (1999).

Studies of Late Time Behavior of Exploding Wires Using X-ray Backlighting

J.B. Greenly, T.A. Shelkovenko, S.A. Pikuz, D.B. Sinars and D.A. Hammer,

Cornell University, Ithaca, NY?14853, USA

Studies of the Late Time Behavior of Exploding Wires Using X-ray Backlighting*

J.B. Greenly, T.A. Shelkovenko**, S.A. Pikuz**, D.B. Sinars and D.A. Hammer

Laboratory of Plasma Studies, Cornell University Ithaca, NY 14853

Fine W, Mo, Al, NiCr, Au, Ag, Ti, and other wires, exploded by a 4.5kA amplitude, 1.4 µs full period sinusoidal current pulse which damps in about 5 µs, have been imaged using direct (point-projection) x-ray backlighting as late as 12 µs after the start of the current pulse. The exploded wires, which ranged from 7.5 W to 13.5 µm W, Au, Al and Mo to 25 µm Ti and NiCr, were located about 6 cm away from two Mo X-pinch xray backlighter sources. The X-pinches are placed in parallel between the output electrodes of the 450 kA, 100 ns XP pulser at Cornell, each thereby producing a sub-nanosecond x-ray pulse. The source size is small enough to permit micron-scale spatial resolution images of the exploding wires on x-ray film¹. Changing the relative timing between the 4.5 kA current source and the XP pulser varied the image time. Wires were typically pulsed in pairs, reducing the peak current per wire accordingly. The behavior of the exploded wires on the microsecond time scale depends upon the material. For example, the W wires initially expand slowly (for ~ 1 µs), and then quickly develop a fine structure in their interior. A more rapid expansion phase follows for a few µs leading to a few hundred µm diameter exploded wire by the time the current damps away. After that, the remnant wire core appears to break up into droplets. Mo and NiCr wires behave similarly. By contrast, high initial conductivity wires, such as Au and Ag, pass through a highly structured phase very quickly and form a rapidly expanding, radially symmetric vapor/plasma cloud in just a few hundred nanoseconds with a peak current of 2 kA per wire. By 2 µs after current initiation, Au wires have formed a several hundred um diameter vapor/plasma which is reasonably axially uniform over the length of the wires except near the ends. The implications of these results to experiments on 10-20 MA pulsers and to code validation will be discussed.

7P26

Formation of Highly Structured Dense Cores from Exploding Wires with 1-5 kAper Wire

Y.S. Dimant, S.A. Pikuz, T.A. Shelkovenko, D. B. Sinars, J.B. Greenly and D. A. Hammer, Cornell University, Ithaca, NY 14853, USA

Formation of Highly Structured Dense Cores from Exploding
Wires with 1-5 kA per Wire*

Y.S. Dimant, S.A. Pikuz**, T.A. Shelkovenko**, D.B. Sinars, J.B. Greenly and D.A. Hammer

Laboratory of Plasma Studies, Cornell University Ithaca, NY 14853

The dynamics of the current-induced explosion of fine (7.5-40 µm diameter) metal wires has been studied experimentally for times up to 12 µs at 1-5 kA/wire. The main diagnostic technique is direct x-ray backlighting imaging of the exploding wires with 1 µm scale spatial resolution, obtained by using very short-time (<0.5 ns) x-ray bursts from a collapsing X-pinch1. By varying the parameters of the X-pinch and the starting time of the discharge it is possible to obtain the backlighting images at different moments of time after the discharge onset. In the high-current regime (> 30 kA per wire), exploding wires typically show fast evaporation and ionization of the wire surface forming an unstable coronal plasma around a dense core. However, in the low-current regime (<5 kA per wire), studies of wire explosions reveal very different behavior for most wire materials. It has been observed that a substantial portion of the wire material is not evaporated and ionized but remains in a condensed state for a very long time. The clear structure shown in the x-ray backlighting images of 7.5 - 13.5 um W wires as a function of time allows one to interpret different stages of the explosion as (1) efficient initial melting of the wire metal followed by (2) sudden volume boiling and (3) slow formation of a foam-like medium that consists of a liquid film "sponge" with vapor bubbles inside. If there is a vapor surrounding the wire, it is not detectable with the 2.5-4.8 keV xray backlighter (<10¹⁷/cm² areal density). During the foam formation, the wire remnant typically expands ten times in diameter, keeping the cylindrical form of the original wire. In the final stage (4) of the discharge (>5 µs), when the current through the wire remnant is negligible, the slow cooling of the "sponge" leads to a tree-like structure with gradual condensation of the remaining liquid phase material into separate drops. No typical plasma phenomena such as pinching and collapse of the plasma column are observed in these low current experiments. This behavior is typical for metals with high melting and boiling temperatures, W, Mo, NiCr and Ti, which also have relatively high resistivity, but not for Au, which vaporizes rapidly and with little structure.

^{*}Research supported by DOE contract DE-FG03-98DP00712

^{**}Permanent address: Lebedev Physical Institute, Moscow, Russia

¹T.A. Shelkovenko, S.A. Pikuz, A.R. Mingaleev and D.A. Hammer, Rev. Sci. Instrum. **69**, in press (1999).

^{*}Research supported by Sandia National Laboratories, Contract #BD-9356 and DOE Grant #DE-FG03-98DP00712.

^{**}Permanent address: Lebedev Physical Institute, Moscow, Russia

¹T.A. Shelkovenko, S.A. Pikuz, A.R. Mingaleev and D.A. Hammer, Rev. Sci. Instrum. **69**, in press (1999).

X-ray Backlighting Density Measurements of Tungsten and Aluminum Wire and Wire Array Zpinches,

D.A. Hammer, S.A. Pikuz, T.A. Shelkovenko, J.B. Greenly, D.B. Sinars and A.R. Mingaleev, Cornell University, Ithaca, NY 14853, USA

X-ray Backlighting Density Measurements of Tungsten and Aluminum Wire and Wire Array Z-pinches*

D.A. Hammer, S.A. Pikuz**, T.A. Shelkovenko**, J.B. Greenly, D.B. Sinars, and A.R. Mingaleev**

Laboratory of Plasma Studies, Cornell University Ithaca, NY 14853

Calibrated density measurements in both the coronal plasmas and dense cores of exploding W wire and wire array Z-pinches, powered by the ~450 kA, 100 ns XP-pulser at Cornell University, have been made using two-frame x-ray backlighting in conjunction with known thickness W step wedges1. The backlighting images are made by Mo wire X-pinch radiation filtered by 12.5 μm Ti impinging upon a "sandwich" of films (Micrat VR, Kodak GWL, Kodak DEF) which have different sensitivities to increase the dynamic range of the method. A W step wedge filter is placed in front of the films, giving absolute line density calibration of each exposure with estimated errors ranging from 20 to 50%. Assuming x-ray absorption by the W plasma is the same as for the solid material, we are able to measure W areal densities from 3.2×10¹⁹ to 2×10¹⁷/cm². These can be converted to number density assuming azimuthal symmetry. For example, for an exploded 7.5 µm wire with a 15-20 um diameter dense core and a 1 mm corona diameter, the implied W volume density ranges from 2×10¹⁸ to over 10²²/cm³. Integration of the line density gives an estimate of the fraction of the wire mass in the corona and core. For example, with 100 kA peak current in a single 7.5 µm W wire, ~70% (>90%) of the W mass is in the corona after 53 ns (61 ns). We also observe that the corona has large, roughly axisymmetric axial nonuniformity both in radius and in mass density. In addition, the coronal plasma contains more of the W mass, expands faster and is more uniform when the wire is surface-cleaned by preheating.

In arrays of 2-8 wires with the same 100 kA total current, detectable coronal plasma appears after 25-35 ns, and much of it is swept toward the center of the array, forming a dense channel. The portion of the initial wire mass in the coronal plasma increases with smaller wire diameter and decreases with greater wire number: 15% for $4\times13.5~\mu m$, 35% for $4\times7.5~\mu m$, and 25% for $8\times7.5~\mu m$, at 46-48 ns (unheated). Similar measurements are now being made with Al wires and an Al step wedge. Results will be presented.

7P28

X-pinch Dynamics Close to the Time of X-ray Burst Emission and X-pinch Bright Spot Location Using X-ray Backlighting

T.A.Shelkovenko, S.A. Pikuz, D.B. Sinars, D.A. Hammer, V. Serlin, Cornell University, Ithaca, NY 14853, USA

X-pinch Dynamics Close to the Time of X-ray Burst Emission, and X-pinch Bright Spot Location Using X-ray Backlighting*

T.A. Shelkovenko**, S.A. Pikuz**, D. B. Sinars, D.A. Hammer,

J.B. Greenly, Y.S. Dimant

Laboratory of Plasma Studies, Cornell University Ithaca, NY 14853

V. Serlin

Code 6730, Plasma Physics Division, Naval Research Laboratory, Washington, DC 20375

In the final few ns before the moment of the x-ray burst emission near the cross point of the two wires in an X-pinch, an on-axis z-pinch forms, the dynamics of which have been studied using direct (point projection) x-ray backlighting. The rapid collapse of the z-pinch results in a gap in the observable mass distribution, which we refer to as a minidiode. Two Mo Xpinches were placed in parallel between the output electrodes of the 450 kA, 100 ns XP pulser at Cornell University. The < 0.5 ns radiation burst from each of the two X-pinches was used to generate a magnified x-ray backlighter image on film of the other one¹. The size of the x-ray source is sufficiently small that the spatial resolution in the images is close to 1 µm. Using different wire sizes in the two X-pinches yields images separated in time by 4-20 ns; using the same wire size yields images separated in time by 0.5-2ns. Therefore, the dynamics of the rapid collapse of the on-axis z-pinch in conjunction with minidiode formation, and the break-up of that z-pinch just as the bright x-ray spots develop can be studied using the successive images from 4 ns before x-ray burst emission, through the moment of burst emission, to a few ns after burst emission. By superimposing images generated by both x-pinches of a grid of fine wires on the same films as the X-pinch images, it has been possible to locate the position of the bright x-ray emission point(s) in the z-pinch/minidiode region to within 10 µm. The emission points are usually within 100 µm of the original cross point of the two wires, near the ends of the collapsing z-pinch. Calibrated density measurements have been made with W Xpinches by including a W step wedge in the film pack. Results from these experiments will also be presented.

^{*}Research supported by Sandia National Laboratories, Albuquerque, Contract BD-9356.

^{**}Permanent address: Lebedev Physical Institute, Moscow, Russia

^{1.} The W step wedge was prepared by Dr. H.P. Neves at the Cornell Nanofabrication Facility.

^{*}Research supported by DOE Grant #DE-FG02-98ER54496.

^{**}Permanent address: Lebedev Physical Institute, Moscow, Russia

¹T.A. Shelkovenko, S.A. Pikuz, A.R. Mingaleev and D.A. Hammer, Rev. Sci. Instrum. **69**, in press (1999).

The effect of wire material on plasma formation in wire array z-pinches

S.V. Lebedev, R. Aliaga-Rossel, S.N. Bland, J.P. Chittenden, A.E. Dangor and M.G. Haines, Imperial College, London, SW72BZ, UK

The effect of wire material on plasma formation in wire array z-pinches.

S.V. Lebedev, R. Aliaga-Rossel, S.N. Bland, J. P. Chittenden, A.E. Dangor and M.G.Haines

Blackett Laboratory, Imperial College, Prince Consort Road, London SW7 2BZ, U. K.

Plasma formation in wire array z-pinches was studied in experiments with 16-mm diameter arrays of between 8 and 64 aluminium, tungsten or titanium wires, imploded in 200 to 260 ns by a 1.4 MA current pulse. Side-on (r-z plane) diagnostics included laser probing with interferometer, schlieren and shadow channels, gated 4-frame soft x-ray imaging and radial and axial optical streak photography. End-on $(r-\theta)$ plane) laser probing gave information about the azimuthal structure of the implosion. The x-ray radiation at stagnation and during the implosion phase was measured with filtered PCD and XRD detectors.

A comparison of plasma formation for different wire material will be presented, including measurements of the expansion velocities of the coronal plasma in the radial and azimutal directions, the wavelength of instabilities and the parameters of the precursor pinch.

7P30

Investigation of magnetic field effects on the mitigation of the magneto hydrodynamic Raleigh-Taylor instability in fast z-pinch implosions

Melissa Douglas, Christopher Deeney, Norm Roderick, Sandia National Laboratories, Albuquerque, NM 87185-1194, USA

Investigation of magnetic field effects on the mitigation of the magnetohydrodynamic Rayleigh-Taylor instability in fast z-pinch implosions

Melissa Douglas, Christopher Deeney Sandia National Laboratories, Albuquerque, NM, 87185*

Norm Roderick
University of New Mexico, Albuquerque, NM, 87131

Numerical simulations have been carried out to investigate the role that magnetic field diffusion and ohmic heating have on the magnetohydrodynamic Rayleigh-Taylor (RT) development in fast z-pinch implosions. Previous work has indicated these terms can strongly influence the evolution of RT growth, leading to a reduction in RT amplitude, and an improvement in pinch performance. Indeed, Roderick et al have suggested that "magnetic smoothing" is an important mechanism in linear RT growth. To examine this in more detail, simulations are presented for a 1.4 mg, 25.0 mm diameter tungsten wire array imploded in the Saturn long pulse mode. The 130 ns implosion time of this calculation should enhance any mitigating effects that may be attributed to nonideal MHD.

Calculations were performed using the 2D MHD code Mach2. The wire array was approximated by a right cylindrical slab of 1.0 mm width. Both a random density perturbation and single mode density perturbations were incorporated to initiate the instability. In the former case, a 5% cell-to-cell random perturbation was used. This allowed a range of modes to be initially present. In the single mode case, a 1.25 mm wavelength, on the order of the shell thickness, was defined. To isolate the contributions due to field diffusion, joule heating, and equation of state, simulations were run with and without ohmic heating using both constant and material-dependent spitzer resistivities. This analysis was then extended to look at the effect of such parameters on the nested shell load configuration. Detailed analysis of the simulations will be presented.

¹M.R.Douglas et al, 1997 IEEE Conference Record-Abstracts, p.49 (1997)

²N.F. Roderick and T.W. Hussey, J. Appl. Phys., 50 (2), 665 (1986)

*Sandia is a multiprogram laboratory operated by Sandia Corporation, a Lockheed Martin Company, for the United States Department of Energy under Contract DE-AC04-94AL85000.

Material Field Strength Studies at Microsecond Pulsed Voltages

D. Shiffler, M. Lacour, K. Hendricks, R. Umstattd, T. Spencer, M. Haworth, D. Vozz and A. Lovesee, U.S. Air Force Research Laboratory, AFRL/DEHE, Kirtland AFB, NM 87117, USA

Material Field Strength Studies at Microsecond Pulsed Voltages

D. Shiffler, M. Lacour*, K. Hendricks, R. Umstattd, T. Spencer, M. Haworth, D. Voss**, and A. Lovesee**

AFRL, Phillips Research Site
DEHE, Directed Energy Directorate
Kirtland AFB, NM 87117-5776

Abstract:

High power microwave tubes typically all share the same characteristic in that large electric field stresses, both pulsed and rf, can be present in the tube. These large field stresses can cause problems leading to pulse shortening. This poster reviews experiments to explore the behavior of various materials with a high voltage pulse of 1 microsecond and field stresses greater than 50 kV/cm. The voltage source used for the testing is the Cathode Test Bed, a pulse forming network based pulser with a 100 Ohm impedance. We review the results of tests with several different materials and show the field stresses at which breakdown of the material occurred.

D. Shiffler, K. Hendricks, R. Umstattd, T. Spencer, and M. Haworth are with the Air Force Research Laboratory/Phillips Research Site, Kirtland AFB, NM 87117.

M. Lacour is with Maxwell Laboratories, Inc., Albuquerque, NM 87119.

D. Voss and A. Lovesee are with Voss Scientific, Inc., Albuquerque, NM 87108

7P32

Progress In The Control of a Smart Tube High Power Backward Wave Oscillator

G.T. Park, V.S. Soualian, C.T. Abdallah, E. Schamiloglu and F. Hegeler,

University of New Mexico, Albuquerque NM?87131, USA

PROGRESS IN THE CONTROL OF A "SMART TUBE" HIGH POWER BACKWARD WAVE OSCILLATOR

G. T. Park, V. S. Soualian,* C. T. Abdallah, E. Schamiloglu, and F. Hegeler

Department of Electrical and Computer Engineering University of New Mexico, Albuquerque, NM 87131

Previous results from our studies of the control of various parameters of an intense beam-driven relativistic backward wave oscillator (BWO) include maintaining a specified or desired output power over a determined frequency bandwidth, and maintaining a constant frequency over a wide range of power [1]. This was accomplished using an iterative learning control (ILC) algorithm that yielded the appropriate input variables for the electron beam, as well as the appropriate displacement of the slow wave structure from the cutoff neck.

A problem of much greater complexity is the simultaneous control of both frequency and power, involving the independent mapping of both power and frequency dependence on the two input variables: cathode voltage and slow wave structure displacement. The resultant two-variable system is implemented and tested for convergence with minimal iterations. The experimental results are presented, along with the theoretical background and hardware description.

Work supported by an AFOSR/DOD MURI grant on high energy microwaves, administered through Texas Tech University.

[1] C. T. Abdallah, V. S. Soualian, and E. Schamiloglu, "Toward "Smart Tubes" Using Iterative Learning Control," IEEE Trans. Plasma Sci., vol. 26, pp. 905-911, 1998, and references therein.

*Present address, University of Minnesota, Department of Electrical Engineering.

Progress on Pulse Lengthening of a Realativistic Backward Wave Oscillator

F. Hegeler & E. Schamiloglu, S.D. Korovin and V.V. Rostov, University of New Mexico, Albuquerque, NM 87131, USA

PROGRESS ON PULSE LENGTHENING OF A RELATIVISTIC BACKWARD WAVE OSCILLATOR

F. Hegeler and E. Schamiloglu
Department of Electrical and Computer Engineering
University of New Mexico, Albuquerque, NM, 87131, USA

S.D. Korovin and V.V. Rostov Institute of High Current Electronics Siberian Branch, Russian Academy of Sciences Tomsk, 634055, Russia

Laser interferometry has been used to diagnose plasma formation and evolution in the slow wave structure (SWS) of a relativistic backward wave oscillator (BWO) during the course of microwave generation [1]. The results indicated that plasma from the cutoff neck inlet contributed to the termination of the high power microwave pulse. In an effort to mitigate this pulse shortening effect we have replaced the cutoff neck with a Bragg reflector [2]. As part of these studies we have observed the cross-excitation instability [3] because of the particularly shallow-ripple SWS used. We will present results from recent experiments performed with the long pulse relativistic BWO, including the implementation of a hybrid-hard tube BWO.

- [1] F. Hegeler, C. Grabowski, and E. Schamiloglu, IEEE Trans. Plasma Sci., vol. 26, p. 275 (1998).
- [2] A.V. Gunin et al., IEEE Trans. Plasma Sci., vol. 26, p. 326 (1998).
- [3] C. Grabowski, E. Schamiloglu, C.T. Abdallah, and F. Hegeler, Physics of Plasma, vol. 5, p. 3490 (1998).

This work is supported through a High Energy Microwave Devices Consortium funded by an AFOSR/DOD MURI grant and administered through Texas Tech University. The acquisition of laser and optical components was funded by an FY'96 AFOSR DURIP grant.

7P34

Comparison of Theory and Simulation for a Radially Symmetric Transit-Time Oscillator,

Robert L. Wright, Edl Schamiloglu, John W. Luginsland, M. Joseph Arman, University of New Mexico, Albuquerque, NM 87131, USA

Comparison of Theory and Simulation for a Radially Symmetric Transit-Time Oscillator¹

Robert L. Wright²; Edl Schamiloglu²; John W. Luginsland³; M. Joseph Arman³

The transit-time effect in a coaxial structure has been used by Arman⁴ to design low impedance high power microwave devices that use no externally-generated magnetic fields and have no confining foils. Luginsland et al⁵ have developed simple onedimensional (1-D) non-linear circuit equations that are solved numerically to estimate key device characteristics. This paper extends this approach to analytically estimate the values of the free parameters used in the circuit equations, compares the analytical values to similar values derived from two-dimensional (2-D) particle-in-cell simulations, and compares the results of numerical solutions of the 1-D circuit equations and 2-D simulations. It is shown that the non-linear relationship between voltage and current emission in a space charge limited diode drives an RF oscillation whose frequency is determined by the resonant characteristics of the annular diode cavity; damping and electromagnetic field saturation results from a combination of transit time effects and electron bunching due to the non-linear electron emission characteristics of the space charge limited diode. The results from the 1-D analysis and 2-D particle-in-cell simulation are shown to be in excellent agreement.

- Research supported in part by AFOSR/AASERT Grant No. F49620-96-1-0192
- University of New Mexico, Dept of Electrical and Computer Engineering; Albuquerque NM
- 3. Air Force Research Laboratory (Phillips Site); Kirtland AFB NM
- M. J. Arman; "Radial acceletron, a new low-impedance HPM source"; IEEE Trans. Plasma Sci.; Vol. 24, No. 3 (1996)
- J. W. Luginsland, M.J. Arman, Y. Y. Lau; "High-power transittime oscillator: onset of oscillation and saturation"; Phys. Plasmas Vol. 4 No. 12 (1997)

Comparison of Simulation and Experimental Results for a Radially Symmetric Transit-Time Oscillator

Robert L. Wright, Edl Schamiloglu, M. Joseph Arman, Walter R. Fayne, Kyle J. Hendricks, Diana L. Loree, John W. Luginsland, Thomas A. Spencer, Thomas C. Cavazos, Kenneth E. Golby, University of New Mexico, Albuquerque, NM 87131, USA

Comparison of Simulation and Experimental Results for a Radially Symmetric Transit-Time Oscillator¹

Robert L. Wright², Edi Schamiloglu², M. Joseph Arman³, Walter R. Fayne³, Kyle J. Hendricks³, Diana L. Loree³, John W. Luginsland³, Thomas A. Spencer³,Thomas C. Cavazos⁴, Kenneth E. Golby⁴

The transit-time effect in a coaxial structure has been proposed by Aman⁵ as a mechanism to develop low impedance high power microwave devices using no externally-generated magnetic fields and having no confining foils. The major advantages seen for this type of device include: 1) a low device impedance due to the radial geometry: 2) reduced x-ray emission and associated shielding due to the low operating voltage; 3) elimination of magnets normally used in RF oscillators to stabilize the electron beam; and, 4) simplified coupling of the device output to the RF extraction structure (waveguide or antennas). The twodimensional particle-in-cell code MAGIC has been used to design a prototype device; the radial acceletron. In the prototype device, an electron beam propagates radially within an annular anodecathode (A-K) gap. Interaction between the electron beam selfgenerated electric and magnetic fields, non-linear (with gap voltage) cathode current emission, and electron transit time across the A-K gap generates a self-sustaining RF oscillation. Due to the complex internal geometry of the prototype device, simulation is not straightforward. The prototype design has been fabricated and tested; a comparison between simulation and initial experimental data is presented.

- Research supported in part by AFOSR/AASERT Grant No. F49620-96-1-0192
- University of New Mexico, Dept. of Electrical and Computer Engineering, Albuquerque NM
- 3. Air Force Research Laboratory (Phillips Site); Kirtland AFB
- 4. Maxwell Technologies, Inc.; Albuquerque NM
- M. J. Arman; "Radial acceletron, a new low-impedance HPM source"; IEEE Trans. Plasma Sci.; Vol. 24, No. 3 (1996)

7P36

Development and Application of a Parallel Two-Dimensional Particle-in-Cell code Based on an Existing Three-Dimensional Parallel PIC Code

John J. Watrous, Gerald E. Sasser, John W. Luginsland, Shari C. Collela, Numer Ex, Albuquerque, NM 87106, USA

Development and Application of a Parallel Two-Dimensional Particle-in-Cell code Based on an Existing Three-Dimensional Parallel PIC Code¹ JOHN J. WATROUS, GERALD E. SASSER, JOHN W. LUGINS-LAND, SHARI C. COLLELA, Air Force Research Laboratory, Directed Energy Directorate, Center for Plasma Theory and Computation, Kirtland Air Force Base, NM 87117 — ICEPIC (Improved Concurrent Electromagnetic Particle-in-Cell) is a parallel, three-dimensional PIC code being used and developed at the Air Force Research Laboratory. Its principal application is to high-power microwave devices. Such devices as have been studied recently are largely two-dimensional in character, with three-dimensional aspects of arguably small influence. While three-dimensional design calculations of these devices are an essential part of the Air Force's goal virtual design, dealing with three-dimensional calculations in the early, scoping-out phase of the design sequence can limit a researcher's effectiveness. This has prompted frequent use of two-dimensional PIC codes. This, too, can limit a researcher's effectiveness, as currently available two- dimensional PIC codes are predominantly serial, and the very few efforts at parallelization are still in the development stage. ICEPIC was designed from the beginning as a parallel code, and does make efficient use of a wide range of available parallel resources. A desirable middle ground is thus to enable ICEPIC to deal with two-dimensional problems, thereby thereby giving the researcher an integrated parallel computing framework in which all aspects of the design sequence can be performed, from initial scoping calculations to final design validations. Comparisons of two-dimensional ICEPIC calculations to other two-dimensional PIC codes, as well as to three- dimensional ICEPIC calculations will be made for a variety of HPM devices. Studies of the effectiveness of parallelization in two-dimensional calculations will also be pre-

¹Authors JW and SC are with NumerEx, 2309 Renard Pl., SE, Albuquerque NM 87106

3-D PIC Investigation of an Output Circuit for the Relativistic Klystron Oscillator

L.A. Bowers, J.W. Luginsland, G.E. Sasser, J.J. Watrous, K.J. Hendricks and M.J. Arman, U.S. Air Force Research Laboratory, Albuquerque, NM 87117, USA

3-D PIC Investigation of an Output Circuit for the Relativistic Klystron Oscillator.

L.A. Bowers, J.W. Luginsland, G.E. Sasser, J.J. Watrous¹, K.J. Hendricks, and M.J. Arman

U.S. Air Force Research Laboratory
Directed Energy Directorate
Kirtland AFB, NM 87117-5776

Abstract

The Relativistic Klystron has been a promising HPM source for many years, and is currently under active research as a GW class tube. While considerable effort has been spent on understanding the bunching mechanism in both the amplifier and oscillator regimes, the issues for extracting HPM from a bunched intense relativistic electron beam (IREB) has received much less attention. In this research, we take advantage of the fact that we can isolate the output circuit from the rest of the source and concentrate on the physics of the IREB's interaction with a low-Q extractor gap. Using a prescribed beam based on profiles consistent with experimental data and simulations of the modulator circuit, we investigate the relative importance of the modulation depth, harmonic content, distribution of kinetic and potential energy, and extractor impedance on the efficiency of power extraction. With this information, we identify features for successful extractor design for AFRL's RKO.

1. NumerEx. 1400 Central Ave. SE, STE1400, Albuquerque, NM 87106

7P38

Magnetron Structure Design Using 2-and 3-D EM Codes

Thomas A. Spencer, John W. Luginsland, and Ray W. Lemke, U.S. Air Force Research Laboratory, Kirtland AFB, NM 87117, USA

Magnetron Structure Design Using 2- and 3-D EM Codes

Thomas A. Spencer, John W. Luginsland, and Ray W. Lemke[#]

Air Force Research Laboratory, Directed Energy Directorate, 3550 Aberdeen Ave SE, Kirtland AFB, NM 87117-5776

*Sandia National Laboratories, Albuquerque, NM 87185

Magnetrons, with efficiencies greater than 70% when operated at low voltages, are of great interest to the high power microwave (HPM) community. However, when operated at higher voltages (>100 kV), relativistic magnetrons suffer from short output rf pulses, as well as large decreases in efficiencies (typically less than 30%). Recent 3-D computer simulations have addressed the issue of efficiency limitations1. Short rf pulses could be caused by the large electric fields that exist in the vane structures. Using a large slot to vane ratio may lead to the reduction of the electric field stresses, however doing so leads to severe mode competition. The Air Force Research Lab has laid out a method using 2- and 3-D electromagnetic codes to investigate different magnetron structures, which may lend themselves to 'large' mode separation between the Pi-mode and its nearest adjacent modes, while minimizing the electric field stress.

1) '3D PIC Simulation Study of a Relativistic Magnetron,' Ray W. Lemke, T. C. Genoni, and T. A. Spencer, accepted in Phys. Plasmas, to be published in Feb 1999.

This work is supported in part by the Air Force Office of Scientific Research.

Optical Spectroscopy of Plasma and Plasma Processing in High Power Microwave Pulse Shortening Experiments

W.E. Cohen, R.M. Gilgenbach, R.L. Jaynes, J.I. Rintamaki, C.W. Peters, Y.Y. Lau, T.A. Spencer, G.P. Scheitrum and L.L. Laurent, University of Michigan, Ann Arbor, MI 48109-2104, USA

Optical Spectroscopy of Plasma and Plasma Processing in High Power Microwave Pulse Shortening Experiments*

W.E. Cohen, R.M. Gilgenbach, R.L. Jaynes, J.I. Rintamaki #, C.W. Peters, Y.Y. Lau, T.A. Spencer^a, G.P. Scheitrum^b, and L.L. Laurent^c

Intense Energy Beam Interaction Laboratory Nuclear Engineering and Radiological Sciences Department University of Michigan, Ann Arbor, MI 48109-2104

Spectroscopic measurements have been performed to characterize the undesired plasma in a multi-megawatt coaxial gyrotron. This gyrotron is driven by the Michigan Electron Long Beam Accelerator (MELBA) at parameters: V= -800 kV, I_{tube} =0.3 kA, and pulselengths of 0.5-1 μ s. Pulse shortening typically limits the highest (~40 MW) microwave power pulselength to 50-100 ns. Potential explanations of pulse shortening are being investigated, particularly plasma production inside the cavity and at the ebeam collector. The source of this plasma is believed to be due to water vapor. Plasma H-α line radiation has been characterized and correlated with microwave power and microwave cutoff. Experiments are underway to determine the effects of RF plasma processing of the coaxial cavity and A collaborative effort is underway with the collector. Stanford Linear Accelerator Center/ U.C. Davis to study RF cavity breakdown. A SEM is being used to examine the surface effects of RF processing cavity parts.

7P40

Microwave Production and Beam Transport in a Multi-MW Large-Orbit, Axis Encircling, Coaxial Gyrotron Oscillator

R.L. Jaynes, R.M. Gilgenbach, C.W. Peters, W.E. Cohen, J.I. Rintamaki, J.M. Hochman, Y.Y. Lau and T.A. Spencer, University of Michigan, Ann Arbor, MI 48109-2104, USA

Microwave Production and Beam Transport in a Multi-MW Large-Orbit, Axis Encircling, Coaxial Gyrotron Oscillator*

R.L. Jaynes, R.M. Gilgenbach, C.W. Peters, W.E. Cohen, J.I. Rintamaki #, J.M. Hochman, Y.Y. Lau, and T.A. Spencer^a

Intense Energy Beam Interaction Laboratory Nuclear Engineering and Radiological Sciences Department University of Michigan, Ann Arbor, MI 48109-2104

Large orbit, coaxial gyrotrons are currently under investigation with microwave power up to 40 MW. The electron beam is produced by MELBA (Michigan Electron Beam Accelerator) with the following parameters: 0.75-1.0 MV, 1-10 kA diode current, 0.2-1.5 kA tube current, 0.5-1.0 microsecond pulselength. The axis encircling electron beam is generated by a cusp magnetic field. Electron beam current transport through the magnetic cusp and through the microwave cavity are measured. The frequency of the fundamental coaxial mode, TE111, is observed to be 2.34 GHz. A novel method of Time-(TF) using reduced interference frequency analysis distributions is used to analyze heterodyne mixer data. TF analysis shows microwave frequency modulation with e-beam voltage modulation. Mode competition and mode hopping between TE111 and TE112 modes are also observed by TF analysis. Microwave cold test data are compared to operating modes of the gyrotron.

^{*}Research supported by AFOSR-MURI program contracted through Texas Tech University and by AFRL Phillips Site and Northrop Grumman Corp.

[#] DOE FES Graduate Fellowship

^aAir Force Research Lab; Kirtland AFB, NM

bSLAC; PO BOX 4349; Stanford, CA

^cUniversity of California-Davis; Davis, CA

^{*}Research supported by AFOSR-MURI program contracted through Texas Tech University and by AFRL Phillips Site and Northrop Grumman Corp.

[#] DOE MFET Graduate Fellowship

^aAir Force Research Lab; Kirtland AFB, NM

Modeling of Space Charge Effects in Intense Electron Beams Using Two and Three Dimensional Green's Functions

M. Hess, R. Pakter, C. Chen, MIT-Plasma Science & Fusion Center PSFC/NW16-168, Cambridge, MA 02139-4294, USA

Modeling of Space Charge Effects in Intense Electron Beams Using Two- and Three-Dimensional Green's Functions¹

M. Hess, R. Pakter, C. Chen MIT Plasma Science and Fusion Center

Green's functions for Maxwell equations can provide a powerful technique for the modeling of high-intensity microwave sources and high-intensity particle accelerators. We present both, two- and three-dimensional models of space charge in intense charged particle beams. Specifically, we compute the Green's function for a point charge located inside of a perfectly conducting drift tube with periodic boundary conditions. As an application of the two-dimensional Green's function, we study the effect of current oscillations and associated envelope oscillations on inducing beam halos in intense relativistic electron beams in periodic permanent magnet focusing and uniform solenoidal focusing klystrons. For system parameters corresponding to the SLAC PPM Klystron experiment, we find that a sizeable initial envelope mismatch produces halo particles with a maximum radius extending to several core radii at the output section. An eigenfunction expansion technique is utilized for the computation of the threedimensional Green's function. We show the agreement of the function with electrostatic potentials that can be computed exactly, i.e. potential due to an on axis distribution with infinite conductor radius. Results from multi-particle simulations obtained from this function are presented.

¹Research supported by the Air Force Office of Scientific Research and the Department of Energy.

7P42

3-D PIC Simulations of the Convolute and inner MITL on the Z Accelerator,

T.D. Pointon, Sandia National Laboratories, Albuquerque, NM 87185-1186, USA

3-D PIC Simulations of the Convolute and inner MITL on the Z Accelerator*

T.D. Pointon

Sandia National Laboratories Albuquerque, NM 87185-1192

The Z accelerator at Sandia National Laboratories delivers current pulses rising up to ~20 MA in ~100 ns to a Z-pinch load. The accelerator is cylindrical, with power flowing radially inward through a water pulse-forming section to the insulator stack at r ~ 2 m. Inside the stack, power flows along four conical, vacuum, magnetically-insulated transmission lines (MITL's) to the convolute, at r ~ 10 cm. The convolute couples the feed MITL currents, in parallel, into the inner MITL that drives the load. The convolute is a critical area of the vacuum power flow, because it necessarily has magnetic field nulls, which could potentially result in large electron losses.

We have been using the 3-D, electromagnetic particle-in-cell (PIC) code QUICKSILVER to simulate the convolute and inner MITL region of Z. The simulations are done in cylindrical coordinates and accurately model the Z geometry (to "stair-step" accuracy). The azimuthal extent of the simulation is π/N_p , where N_p is the number of posts (typically 12), with mirror boundaries applied on each boundary. The fairly coarse zoning used still requires ~520,000 cells for a 12-post geometry. The complex cathode structure has ~11,400 particle-emitting cells.

In addition to their large scale, these simulations encountered other new challenges. First, we need very small time steps to resolve the electron orbits in magnetic fields up to 200 T. The Courant limit for the field solver time step is $\Delta t_f \sim 0.5$ ps, but the limit on the particle time step Δt_p can be much smaller. We have experimented with a new subcycling model, pushing each particle n_s times with $\Delta t_p = \Delta t_f/n_s$ for each field solve, with n_s dynamically computed at each time step. The second challenge is modeling a low impedance load. We use a conductivity region, with special handling of particles entering this region.

Several convolute simulations have been done, using a fixed load impedance and a 20 ns rise time on the drive pulse. They study different convolute geometries: 6-post versus 12-post, and changing post diameters. We have very detailed information on electron losses to the anode, both current and energy. Although we cannot yet simulate realistic pulse lengths and time-dependent load impedances, qualitative comparisons with features of some Z shots have been instructive.

* Funding has been provided by the U.S. DOE under contract DE-AC04-94-AL85000.

Proton and Neutron Irradiation Effects of Ti: Sapphires

Guangean Wang, Jin Zhang and Jingjing Yang, Yunnan University, Kumming Yunnan 655091, China

PROTON AND NEUTRON IRRADIATION EFFECTS OF Ti: SAPPHIRES

Guangcan Wang, Jin Zhang + and Jingjing Yang++

Experiment Center, Yunnan University, Kunming 650091, China +Department of Physics, Yunnan University, Kunming 650091, China ++Hangzhou Electronic Industry College, Hangzhou 310037, China

sapphires were studied. Proton irradiation induced F, F⁺ and V centers in Ti: sapphires and 3310 cm⁻¹ infrared absorption, and made ultraviolet absorption edge shift to short wave. Neutron irradiation produced a number of F, F⁺ and F₂ centers and larger defects in Ti: sapphires, and changed Ti⁴⁺ into Ti³⁺ ions. Such valence state variation enhanced characteristic luminescence of Ti: sapphires, and no singular variances of intrinsic fluorescence spectra of Ti: sapphires took place with neutron flux of $1 \times 10^{17} \text{n/cm}^2$, but the fluorescence vanished with neutron flux of $1 \times 10^{18} \text{n/cm}^2$ which means the threshold for the concentration of improving Ti³⁺ ions by neutron irradiation.

Various effects of proton and neutron irradiated Ti:

7P44

Fluorescence Increasing Effects In Electron and Proton Irradiated BaF2:Sr Crystals

Jin Zhang, Guangcan Wang and Jingjing Yang, Yunan University, Kumming, Yunnan 650091, China

FLUORESCENCE INCREASING EFFECTS IN ELECTRON AND PROTON IRRADIATED BaF₂:Sr CRYSTALS

Jin Zhang, Guangcan Wang+ and Jingjing Yang++

Dept. of Physics, Yunnan University, Kunming 650091, China +Experiment Center, Yunnan University, Kunming 650091, China ++Hangzhou Electronic Industry College, Hangzhou 310037, China

In this paper, we summarize experimental and theoretical data on optical properties (absorption/luminescence) and fluorescence increasing effects of BaF₂: Sr crystals irradiated by fast electrons and protons.

Measurements of the emission spectra showed that fluorescence increasing effects responded in both cases. A strong luminescence with a broad spectral range from 300 to 500nm and its peak value at 353nm presented in electron irradiated BaF₂:Sr crystals, and the luminescence after electron irradiation were about ten times more intense than that before irradiation, and the similar effect appeared in proton irradiated specimen as well, but with a strong sharp peak at 346nm.

We analyze results of energy state calculations by discrete variation means (HFS-DVM-X_a) for Ba⁺, Sr⁺, Sr²⁺ ions and irradiation-induced interstitial Sr²⁺ ions in BaF₂:Sr crystals. It is shown that the emission band of electron irradiated samples comes from the overlapping of Ba⁺, Sr⁺ ions and BaF₂ intrinsic emission, and the sharp peak of proton irradiated specimen is the fluorescence emission of interstitial Sr²⁺ ions, and the mechanisms of the fluorescence increasing effects were valence state or position changes of Ba and Sr ions in BaF₂:Sr crystals during electron or proton bombardments.

The Missing Maxwell equation in magnetohydrodynamics.

JE.A. Witalis

The missing Maxwell equation in magnetohydrodynamics. E.A. Witalis

Indexing terms: Magnetohydrodynamics, Hall effect, Plasmas, Magnetic fusion

Abstract: It is shown that since its inception magnetohydrodynamics theory, MHD, has paid insufficient attention to that Maxwell equation which relates the electric field to excess charge. With reference to a recent review article on magnetic astrophysical plasmas the diffusive character and the validity region of the MHD theory are presented. The information contained in the missing Maxwell equation is exploited in an analysis of the distribution between plasma ions and electrons of angular momentum transferred by the total electromechanical torque tensor. In case of Hall effect, i.e. when the plasma electrons are free to gyrate magnetically, a strongly differing, whirlforming plasma description, the Hall effect MHD replaces MHD. The poor results of magnetic confinement fusion research are explained, and arguments given for the existence of longlived plasma structures, plasmolds or ball lightnings, in atmospheric air.

7P46

A bi-dimensional model of a Cu-HBr laser plasma

F.Girard and E. Le Guyadec

A bi-dimensional model of a Cu-HBr laser plasma.

F. Girard and E. Le Guyadec

C.E.A. Valrho DCC/DTE/SLC 26700 Pierrelatte Cedex France

Tel: 04.75.50.40.00 Fax: 04.75.50.49.62

e-mail: frederic.girard@cea.fr and erick.leguyadec@cea.fr

A two dimensional (radial and longitudinal) model is developed in order to simulate the behaviour of the plasma column constituting the active medium of a CuHBr laser. Species taken into account by the code are Cu, Ne, Br, H atoms and H_2 , HBr and CuBr molecules. We take all this species and Cu_3Br_3 to assess their densities at the thermal equilibrium.

The molecules may be dissociated by collision with an electron or thermally. The thermal dissociations are assisted by neon atoms. For association, atom-atom reactions or atomconsidered molecule reactions $H+Br+Ne \Leftrightarrow HBr+Ne \text{ or } H_2+Br+Ne \Leftrightarrow HBr+H+Ne$. Moreover, HBr can be involved in the electron dissociative attachment process: HBr + e⁻ ⇔ H + Br⁻ which has got a maximum reaction rate value of 2.5 10^{-15} m³.s⁻¹ at an electronic temperature of 0.2 eV. It may be excited toward vibrational levels v=1,2,3,4 which have higher dissociative attachment rates than v=0. The electron density is reduced by dissociative attachment process during post-discharge much more than by three bodies recombination. Within the central zone. HBr can be thermally dissociated and electron recombination is slowed down. Excitation of HBr(v=0) creates an important amount of HBr_(v=1) at the half radius of the tube. There are then many Br and few electrons there. Negative ions Br density is reduced by charge neutralisation with copper ions in the afterglow. This leads to an important electron density gradient.

In conclusion, creation of $HBr_{(v=1)}$ is favoured at the middle of the radius and causes a fast electron reduction. Hence, the recombination processes produce a confinement of the plasma column at the centre of the tube and the heat deposition is then not uniform. The laser emission only occurs in the inner zone of the tube.

REF: J. Maury, P Lemaire, JP Goossens, E Le Guyadec and JM Borgard,
"Physical consequences of the rapid drop of electronic temperature in CVL", Pulsed Metal Vap. Laser, Nato Series, n°1, vol 5, (1996)
M.J. Kushner and B.E. Warner, "Large bore copper-vaper-laser: kinetics and scalling issues", J. Appl. Phys. 54 (6), (1983)

Steam Plasma ARC Cutting

H. Pauser, J. Laimer, H. Stori, Fronius Schweissmaschinen, Wels A-4600, Austria

STEAM PLASMA ARC CUTTING

H. Pauser, J. Laimer *, H. Störi *

Fronius Schweissmaschinen Günter Fronius Str. 1, A-4600 Wels, Austria

* Institut für Allgemeine Physik, TU Wien Wiedner Hauptstr. 8-10, A-1040 Wien, Austria

Plasma arc cutting is a widely used method for cutting metals. The availability of small portable units using compressed air as plasma gas makes these devices suitable for the use in job shops. However, the need for compressed air means less flexibility in field applications.

Possible solution strategies to overcome this disadvantage are the integration of the air supply on board or the production of plasma gas in situ. A plasma cutting device using the later concept will be presented.

In order to achieve good cutting quality the plasma jet needs high enthalpy to melt the workpiece and high momentum to blow away the liquid metal. The nozzle which confines the plasmajet is usually either cooled by air or at higher power levels by water. This excess of heat, however, can be used to produce the necessary plasma gas within the plasma torch by vaporization of a fluid (e. g. water). This kind of cooling is also known as regenerative cooling.

The main aspect of the process is the thermal management of the torch. The fluid is supplied by an external pump located in the power supply. Entering the torch the fluid is heated up to its boiling point followed by its full vaporization. Leaving this zone the vapour flows into the plasma chamber acting as plasma gas. The heat balance between the heat flowing back from the nozzle and the heat needed to vaporize the fluid is important for the stability of the process and points out the importance of precise process control. Due to the high volumetric ratio of gas and fluid a few grammes fluid per minute are enough to operate the plasma torch. Proper design of the vaporization channels ensure that the operation of the plasma torch is independent of its orientation.

The concept is not limited to the commonly used transferred arc operation mode (direct plasmatron). The effectiveness of nozzle cooling makes it possible to use either the direct or indirect plasma mode. Each cutting mode, however, needs a special adaptation of the heat management since the amount of heat available is not the same in both cases due to the difference in anode arc attachment. Some modes of operation may need additional heat in order to fully vaporize the fluid. This demand could be accomplished by an additional heating element.

Most ignition methods, which are state of the art in cutting and welding, e. g. high-frequency ignition, are applicable to ignite the plasma.

Cutting experiments show that cutting speeds are comparable to air plasma torches. First results of the characterization and performance of the plasma torch will be presented.

7P48

Density and Velocity Measurements of a Sheath Plasma from MPD Thruster

J.J. Ko, T.S. Cho, M.C. Choi, E. H. Choi, G.S. Cho, Kwangwoon University, Ajou University, Paidal-Gu Suwon 448-749, Korea

Density and Velocity Measurements of a Sheath Plasma from MPD Thruster

 J. J. Ko, T. S. Cho, M. C. Choi, E. H. Choi, G. S. Cho Charged Particle Beam and Plasma Laboratory
 Department of Electrophysics, Kwangwoon University Seoul 139-701, Korea

H. S. Uhm
Department of Physics, Ajou University
Suwon 442-749, Korea

Magnetoplasma is the plasma that the electron and ion orbits are strongly confined by intense magnetic field. Recently, magnetoplasma dynamics(MPD) has been investigated in connection with applications to the rocket thruster in USA, Germany, etc. It can be widely applicable, including modification of satellite position and propulsion of the interplanetary space shuttle. A travel for a long distance journey is possible because a little amount of neutral gases is needed for the plasma source. Besides, this will provide a pollution free engine for future generations. MPD thruster is not a chemical engine. We have built a Mather type MPD thruster, which has 1 kV max charging, 10 kA max current flows, and has about 1 ms characteristic operation time. The Paschen curve of this thruster is measured and its minimum breakdown voltage occurs in the pressure range of 0.1 to 1 Torr. Langmuir and double probes are fabricated to diagnose the sheath plasma from the thruster. The temperature and density are calculated to be 2.5 eV and 1015 cm⁻³, respectively, from the probe data. Making use of photo diode, an optical probe is fabricated to measure propagation velocity of the sheath plasma. The sheath plasma from the MPD thruster in our experiment propagates with the velocity of 1 cm/µs.

X-Ray Spot Measurement and Modulation Transfer Function for the 12MeV LIA

Shi Jinshui, Li Jing, Li Qing, Luo Dashi, CAEP, Institite of Fluid Physics, Chengdu 610003, ROC

X-ray Spot
Measurement and
Modulation Transfer
Function for the
12MeV LIA

Shi Jinshui Li Jing Li Qing Luo Dashi Institute of Fluid Physics, CAEP. P. O. Box 523-56, Chengdu, 610003

This paper is intended to experimental present system measuring the x-ray spot size for the 12MeV LIA. means of one-time By discharge, the system adopts the sharpness-edge method and big-aperture imaging thereby simultaneously, acquiring the size of the x-ray spot. Further on, by numerical calculation with the predesigned program, and on the basis of the characteristics of axial approximate the symmetry of the X-ray source and the density distribution of space image, the the distribution of spot intensity is simulated. At the same time, the system can determine the modulation transfer function of the space resolution of the xray imaging for the 12MeV LIA.

7P50

High Power Microwave Generation from the Axially-Extracted Virtual Cathode Oscillator

E.H. Choi, G.S. Cho, J.J. Ko, Y. Jung, M.C. Choi, Kwangwoon University, Dept. of Physics, Ajou University, Suwon 442-749, Korea

High Power Microwave Generation from the Axially-Extracted Virtual Cathode Oscillator

E. H. Choi, G. S. Cho, J. J. Ko, Y. Jung, M. C. Choi Charged Particle Beam and Plasma Laboratory Department of Electrophysics, Kwangwoon University Seoul 139-701, Korea

> H. S. Uhm Department of Physics, Ajou University Suwon 442-749, Korea

It has been reported that the virtual cathode is formed when the electron beam current in the drift region exceeds the space charge limiting current. In this experiment, we have fabricated the axially-extracted virtual cathode oscillator (Vircator), which is the new conceptual device and the ultra-high power microwave generator. This Vircator experiment has been conducted by Chungdoong intense relativistic electron beam pulser (Max. 600 kV, 70 kA, 60 ns). The maximum power of extracted microwave has been measured to be 200 MW at the frequency range of 7.25 GHz ($\Delta f = 0.25$ GHz). The power conversion efficiency was calculated to be 3.3 % with the diode voltage of 300 kV and the A-K gap of 5 mm. The microwave propagating mode was found to be TM01 from the gas discharge experiment. Formation of the virtual cathode has been simulated with 2-dimensional PIC code "MAGIC", from which the dominant frequency and the extracted power have been evaluated and these simulation results are in good agreement of the experimental data.

Plasma Surface Modification of Aluminum Alloy Samples Treated with Argon Discharge Conditioning

S.J. Karandikar, Chetan C. Samant, S.V. Gogawale, University of Mumbai, Vidyanagari Mumbai 400098, India

Plasma Surface Modification of Aluminium Alloy Samples Treated with Argon Discharge Conditioning

S.J. Karandikar, Chetan C.Samant, S.V.Gogawale Department of Physics, University of Mumbai Mumbai 400 098. INDIA

The study of change in surface properties of metals & their alloys under Plasma Processing has a wide range of applications. It affords range, flexibility, ease and accuracy of process control at low cost as compared to other techniques. All the applications of non-equilibrium plasmas involve processes like sputtering, etching, polymerization, surface modification, etc. It is expected for industries to get a final product with specific properties with high reliability and repeatability.

Stainless steel is used to construct UHV chambers. Comparative study of outgassing rates show that SS can be replaced by Aluminium alloy for UHV chambers. Turbomoleculer Pumping Unit evacuates a cylindrical discharge chamber of SS304 with various ports on it. A hollow cathode DC glow discharge in argon for different discharge pressures and for different discharge current densities respectively, is used for treating chemically cleaned ASA6063 Aluminium alloy samples keeping all other parameters constant. TMP unit evacuates SS304 chamber to a base pressure 3x10-7 mbar. The processing gas Argon is introduced through a leak valve and with the help of throttling valve the pressure in the discharge chamber is adjusted to the operating pressure10-2mbar. The wall temperature and discharge time were the same in all treatments.

The Scanning Electron Microscope (SEM) is used to examine processed surfaces and to study topographical features. The Energy Dispersive Microanalysis by X-rays (EDX) is used to determine the elemental composition of the samples.

The results indicate that physical sputtering takes place in Argon GDC, the pits are formed due to etching of the surface by ions, the bombarding ions erode the surface. SEM micrographs show decrease in size of pits with increase in pressure. As pressure increases, molecular density increases but the number of ionising collisions decreases and their energy may not be enough to etch the surface.

The EDX spectrum shows peaks corresponding to elements Al, Mg, Ge, Fe & Mn. Absence of any other peak indicates no contamination of the sample surface and no trace of Argon is observed on the sample. Due to non-uniform etching, there is inconsistent increase or decrease in the weight percentage of various elements of Aluminium alloy.

7P52

Dynamics of Plasma Bunch in Weakly Inhomogeneous Magnetic Field

D.S. Dorozhkina, V.E. Semenov, Institute of Applied Physics RA S, Nizhny Novgorod 603600, Russia

Dynamics of Plasma Bunch in Weakly Inhomogeneous Magnetic Field

D.S. Dorozhkina, V.E. Semenov

Institute of Applied Physics RA S

Uljanova 46, Nizhny Novgorod, 603600, Russia

The initially confined plasma bunch in vacuum in the absence of magnetic field is unlimitedly expands and cools with time. It occurs that a certain configuration of external magnetic field allows the bunch to accelerate and compress as a whole. Using the exact solution of a system of two 3D Vlasov kinetic equations with a self-consistent electric field and external potential forces [1,2], it is possible to predict the dynamics of a two-component plasma bunch in nonstationary weakly inhomogeneous magnetic field in the mirror configuration:

$$\mathcal{B}(r,t) = B_0(z,t)e_z + B_r(x^2 + y^2, z, t)e_r.$$

The dynamics of the plasma in transverse direction is described in adiabatic approximation, which implies the conservation of magnetic momentum of a charged particle. Consequently, the integral distribution functions $F_{\alpha}(t,z,\nu_z)$ satisfy the one-dimensional kinetic equations with an effective external potential $U_{\alpha}^{eff} \propto B_0(z,t)$. It is demonstrated that the motion of the center of mass of the plasma bunch is governed by the value of the first derivative $\partial B_0/\partial z$ at the point $z=R_z(t)\equiv \iint zF_{\alpha}dzd\nu_z$. Therefore choosing the relevant magnetic field configuration one can obtain acceleration of the bunch as a whole. At the same time it is shown that the plasma can be confined within a certain region of space provided that the $\partial^2 B_0/\partial z^2\Big|_{z=R_z(t)}>0$. So,

the plasma will not expand unlimitedly with time and the values of the average thermal longitudinal and transverse energies will stay finite during the process of acceleration, while the full kinetic energy can unlimitedly increase. It is remarkable, that there exists a stable regime of plasma bunch acceleration with the constant longitudinal scale length. Another interesting example of the obtained solution is the compression of the plasma bunch in inhomogeneous magnetic field increasing with time.

[1] D.S. Dorozhkina, and V.E. Semenov, Physical Review Letters **81** (1998), 2691.

[2] D.S. Dorozhkina, and V.E. Semenov, Proc. 1998 ICPP & 25th EPS Conf. on Contr. Fusion and Plasma Physics, ECA, 22C, (1998), 285-288.

Initial Experimental Results of a 35 GHz Efficient Harmonic Amplifier

Jose E. Velazco, Peter H. Ceperley & Doug M. Menz, Microwave Technologies Inc., Fairfax, VA 22030, USA

INITIAL EXPERIMENTAL RESULTS OF A 35 GHz EFFICIENT HARMONIC AMPLIFIER

Jose E. Velazco, Peter H. Ceperley¹ and Doug M. Menz¹

Microwave Technologies Incorporated, Fairfax, VA 22030

George Mason University, Fairfax, VA 22030-4444

We present initial experimental results of a very compact, high efficiency harmonic amplifier (HARA) prototype [1]. In this experiment, a 6 kV 200 mA pencil electron beam is modulated by a short microwave resonator operating in circular polarization at 5.85 GHz. A 35 GHz output cavity operating at the 6th harmonic of the drive frequency is employed to efficiently extract energy from the modulated beam. This device is expected to deliver 600 watts of output power at 35 GHz with 50% efficiency. Initial experimental results of the beam-wave interactions in the output cavity of the HARA prototype will be presented. The fact that the HARA does not require a beam focusing system makes for a very compact and lightweight system which is well suited for applications where size, weight and efficiency are critical.

[1] J. E. Velazco and P. H. Ceperley, Proc.1997 Int. Conf. on IRMM, M4.6, 69, July, 1997.

Work supported by the Ballistic Missile Defense Organization and by Virginia's Center for Innovative Technology.

7P54

Improved Transition Probabilities for MnII

Rainer Kling and Ulf Greismann, National Institute of Standards and Technology, Gaithersburg, MD 20899, USA

Improved Transition Probabilities for Mn II

Rainer Kling and Ulf Griesmann

National Institute of Standards and Technology, Gaithersburg, Maryland 20899

Accurate transition probabilities are of fundamental importance for plasma diagnostics. However the knowledge of atomic data is still unsatisfactory for many elements. Especially for Mn II experimental f-values, determined from arc [1],[2] and spark [3] discharges, show big discrepancies with calculations.

Therefore we started a new project for an independent measurement of transition probabilities. Fourier Transform spectroscopy has shown to be advantageous for the evaluation of complex spectra. The high resolution, limited by the doppler width of the emission lines, helps avoiding blends whereas the simultaneous recording of all spectral contributions eliminates effects of source drifts. The signal-to-noise ratio for the strongest lines is in the order of 10000 which ensures a precise determination of line intensities. The efficiency of the instrument was calibrated using an argon miniarc and a tungsten strip lamp as radiance standards.

Resonance lines, which are affected by self absorption, have to be treated with great care. Self absorption is the biggest source of systematic errors when not thoroughly checked. The braching fractions are then brought to an absolute scale by means of lifetime measurements. The uncertainty of prensent lifetime experiments using laser-induced fluorescence (LIF) is in the range of 1%-3% [4]. Thus accurate absolute transition probabilities are obtained by this method provided that all branches of an upper level are included. The total uncertainty of the presented transition probabilities is below 10%.

References:

- [1] C.H. Corliss and W.R. Bozman, Nat. Bur. Stand., Monogr. 53 (1962).
- [2] B. Warner, Comm. Univ. London Obs. 67, 16 (1964).
- [3] B. Woodgate, Mon. Not. R. Astron. Soc. 134, 287 (1966).
- [4] E. H. Pinnington, B. Gou, Q. Ji, R.W.Berends, W. Ansbacher and E. Biemont, J. Phys. B 25, L475 (1992).

Self-oscillations of positive corona current in nitrogen

Y.S. Akishev, M.E. Grushin, A. A. Deryugin, A.P. Napartovich, M.V. Pan'kin, N.I. Trushkin, Troitsk Institute for Innovation & Fusion Research, Triniti, Russia

Self-oscillations of positive corona current in nitrogen

Y. S. Akishev, M. E. Grushin, A. A. Deryugin, <u>A. P. Napartovich</u>, M. V. Pan'kin, N. I. Trushkin

Troitsk Institute for Innovation and Fusion Research

As it was observed in a number of studies, positive corona in nitrogen is quite unstable against sparking. As a result, some researchers (see for example [1]) believe that glow mode of positive corona does not exist in nitrogen, and even in any electropositive gas.

This paper reports about conditions when the glow mode of positive corona in nitrogen exists. For the first time, an auto-oscillating regime is observed. Detailed studies on characteristics of corona pulsation in an electrode system of wire (anode) and cylinder (cathode) were done. Waveforms for oscillations of current and glow intensity were measured. Voltage-Current characteristics, amplitude and repetition frequency for oscillations were measured for a wide range of pressure 10-765 Torr. The repetition frequency of pulses varies in the range 200-500 kHz. An earlier discussed mechanisms for development of oscillations are critically analyzed and a new one is proposed. A new interpretation of old measurements of preionized electron density in nitrogen and air [2] produced by a positive corona is given. According to [2], electrons in gas are produced by UV photons created in positive corona in a small region close to a pin. Direct measurements for conditions of [2] performed by us evidenced that the positive corona generates soft X-rays which we refer to the process of bremsstrahlung at the anode surface following collisions of fast electrons appearing in the close vicinity of the pin. We believe that exactly these X-rays produced electrons in gas observed earlier [2]. Some arguments against traditional interpretation are also given.

A mathematical model was developed which is able to predict with a reasonable accuracy all characteristics of self-oscillations and of averaged in time voltage and current, as well. The model includes continuity equations for electrons and positive ions, Poisson equation, electric circuit equations and equations describing X-ray transfer. Comparison between theoretical calculations and experimental measurements will be presented in the paper.

[1] R. Morrow, J. Phys. D: Appl. Phys., 30, 3099, 1997

[2] G. W. Penny, G. T. Hummert, J. Appl. Phys., 41, 572, 1970

7P56

Nonlinear Interaction of Microwave and Magnetoactive Plasma: Hysteresis Phenomena and Application

Dr. Andrei B. Petrin, Russian Academy of Sciences, Moscow 127412, Russia

NONLINEAR INTERACTION OF MICROWAVE AND MAGNETOACTIVE HYSTERESIS PHENOMENA AND APPLICATION

Dr. Andrei B. Petrin, Member, IEEE
MHD Research Center,
Institute of High Temperatures of Russian Academy of Sciences,
Izhorskaya 13/19, IVTAN, Moscow, 127412 Russia.
Tel. (7-095) 484-2638, (7-095) 484-2844; FAX (7-095) 485-9922
E-mail: petrin@mgul.ac.ru AND bit@termo.msk.su

1999 ICOPS International Conference on Plasma Science June 20-24, 1999 Montery, California

Topic 2.6 Microwave Plasmas

Abstract - A method for calculating the interaction of a microwave with a plane layer of magnetoactive low-pressure plasma is presented. In this paper, the plasma layer is situated between a plane dielectric layer and a plane metal screen. The calculation model contains the microwave energy balance, particle balance and electron energy balance. The numerical calculations of the nonlinear interaction of the incident plane microwave and the plane plasma layer show that there are hysteresis phenomena when the external magnetic field and intensity of the incident microwave are changed. The cause of these hysteresis phenomena is considered. As a result of this investigation, the estimations for conditions of the plasma uniformity near the surface being worked in a real microwave plasmatron for giant integrated circuits and printed technology have been considered.

Modelling the Spectrum of a S2 High Pressure Discharge

Achim Korber, Philips Research Laboratory, D-52085 Aachen, Germany

MODELLING THE SPECTRUM OF A S₂ HIGH PRESSURE DISCHARGE

Achim Körber

Philips Research Laboratories, Weisshausstr. 2, D 52066 Aachen, Germany

High power microwave discharges in S_2 vapour at pressures of several bars have been discovered as a highly efficient white light source several years ago [1]. The discharge spectrum is originating mainly from bound-bound transitions in the S_2 B $^3\Sigma_u^--X$ $^3\Sigma_g^-$ band system. At such high S_2 pressures re-absorption is an essential mechanism shifting the spectral maximum from the UV into the visible region [2].

Assuming spherical symmetry, local equilibrium and a cubic temperature profile the onedimensional radiation transport equation is solved for each of the 330 vibronic bands connecting the niveaus v' = 0...9and v'' = 0...32 yielding a quantitative description of the spectrum with only two free parameters: the maximum discharge temperature T_{max} and the mean width δv_{vib} of a vibronic band. The response of the spectrum to variations of experimental conditions (S2 pressure, input power, ...) may be expressed by very reasonable changes of these model parameters: The input power determines the total amount of radiation (via the value of T_{max}) and the S_2 pressure influences the position of the spectral maximum (reflected by the value of δv_{vib}). In the red and IR the experimental spectrum is higher than the simulation indicating contributions of continuum radiation or other molecular transitions which are not included in the model.

References:

- [1] J.T. Dolan, M.G. Ury and C.H. Wood, 6th Int. Symp. on the Science and Technology of Light Sources, Budapest (1992).
- [2] B.P. Turner, M.G. Ury, Y. Leng and W.G. Love,J. Illum. Eng. Soc. 26 (1), 10 (1997).

7P58

Experimental and Theoretical Researches of Energy Exhcange Between the Electrical Circuits, Containing Plasma Active Elements and Environment

R.F. Avramenko, V.A. Grishin, V. I. Nikolaeva, A.S. Paschina, L.P. Poskacheeva, International Institute of

Experimental Research of Energy Balance During the Formation of High Energy Plasma Objects (EPO).

R.F.Avramenko, V.I.Nikolaeva, L.P.Poskacheeva. International Institute of Experimental Physics, Moscow e-mail: root@poska.msk.ru

This work devotes to the investigation of energetic characteristics of EPO and to the researches of energy balance in order to choose the optimum regime. EPO generators work in the energetic range 20 - 150 J.

Plasma formations are obtained with the help of the erosional discharge in the cylindrical channel with dielectric walls. The

discharger was set in a germetic gas calorimeter.

Ten energetic components in the equation of energy balance were measured or estimated: the energy of discharge, the energy, which translated to heat of the calorimeter's gas, the energy of a heat of graphite electrode, the energy of heat of the dielectric channel, radiant energy, chemical energy of a burning of known quantities of dielectric, copper and carbon, etc.

It was been shown, that optimum regime of EPO generators work with efficiency 138%(+28%) corresponds to the energy equal

30 T

Cathode Development for the Hard-Tube MILO

M. Haworth, K.Hendricks, D. Vozz, R. Guarnieri, M. Sena, M. LaCour, D. Ralph and T. Cavazos, Air Force Research Laboratory, Kirtland AFB, NM 87117, USA

Cathode Development for the Hard-Tube MILO

M. Haworth, K. Hendricks, D. Voss[†], R. Guarnieri[†], M. Sena[‡], M. LaCour[‡], D. Ralph[‡], and T. Cavazos[‡]

Air Force Research Laboratory, Kirtland AFB, NM 87117

The Hard-Tube MILO (Magnetically Insulated transmission Line Oscillator) is a multigigawatt cross-field microwave tube powered by a 500-kV, 60-kA electron beam. During the initial experiments with a 300-ns beam pulse, a simple velvet cathode configuration was used [1]. However, after extending the beam pulse to 600 ns, problems mainly involving cathode flares compelled cathode design changes to be made. Here we report on modifications made to the velvet cathode as well as on recent results using a CsI-coated, graphite-fiber cathode [2]. The performance characteristics and relative merits of each cathode are presented.

- [1] M. Haworth et al., "Significant pulse-lengthening in a multigigawatt magnetically insulated transmission line oscillator," *IEEE Trans. Plasma Sci.*, vol. 26, pp.312-319, 1998.
- [2] E. Garate et al., "Novel cathode for field-emission applications," Rev. Sci. Instrum., vol. 66, pp. 2528-2532, 1995.

[†]Voss Scientific, Albuquerque, NM 87108 [‡]Maxwell Technologies, Inc., Albuquerque, NM 87119

7P60

Plasma Coaxial Discharge Efficiency

E. A. Mehanna, Military Technical College, Nasr City, Cairo, Egypt

Plasma Coaxial Discharge Efficiency

E.A. Mehanna Military Technical College Cairo, Egypt

Abstract:

A coaxial discharge system with negative central electrode has been used to study the plasma current sheath and the ejected plasma parameters. Results showed that the plasma sheath velocity reached 10^7 cm/s at the muzzle. The ejected plasma velocity in the expansion chamber decreased according to the relation $V = k z^{-0.8}$, while the temperature and the density changed by $T = t z^{-1.8}$ & $N = n z^{-1.2}$ respectively. It has been detected that the plasma current sheath and the ejected plasma are accompanied with an induced axial magnetic field, which indicate that the plasma rotated within its propagation.

The input energy from the capacitor bank to the coaxial discharge system was 196 J, Joule, the energy gained by the plasma as kinetic energy was 17 J, while the plasma internal energy was 5.6 J. Hence 3% of the energy was gained as kinetic drift of the plasma.

The Generation and Application of Micro Discharge Plasmas

Masatoshi Miyake, Hikaru Takahaski, Koichi Yasuoka and Shozo Ishii, Tokyo Institute of Technology, Ookayama, Meguro-k 152-8552, Tokyo Japan

The Generation and Application of Micro Discharge Plasmas

Masatoshi MIYAKE, Hikaru TAKAHASHI, Koichi YASUOKA and Shozo ISHII

Department of Electrical and Electronic Engineering, Faculty of Engineering, Tokyo Institute of Technology

The dielectric barrier discharge lamp has been developed and commercially supplied as a tunable UV light source. However, a high-voltage over several tens of kilovolt is required to drive the device. We have attempted to reduce the driving voltages without reducing the light intensity by using new types of micro discharge plasmas, such as, microhollow cathode discharge (MHCD) [1] and surface plasma produced by a ferroelectric electron emission (FEE) [2]. [3]. These plasmas can be driven with a relatively low voltage pulses at atmospheric pressure. We have studied how to generate and operate theses micro discharge plasmas as UV excimer light source.

The MHCD has simple electrode configuration and has high potential as intense excimer light source. The operationg pD (p: gas pressure, D: cathode hole diameter) values, however, is limited below 5 Torr \cdot cm by the growth of instability. The microscopic study showed that the filamentary plasma spread over the cathode hole triggered the plasma instability. By introducing the hollow insulating plate over the cathode hole, the spread part of the plasma was successfully diminished and a limiting pD value increased twice. More over, the characteristics of V-I curves changed into positive slope that enables the parallel operation MHCD.

Another type of low driving voltage device is a ferroelectric ceramic cathode developed as an electron beam source. The peak-emitted current from a PZT cathode was several A/cm² in a vacuum condition. The operation in an atmospheric pressure was demonstrated using the PZT cathode. Many blight spots were observed by application of 500 V pulsed voltages. The reversal of a spontaneous polarization of PZT seems to be crucial for producing the surface plasma with relatively low driving voltage. The microscopic observation was made to understand the mechanism of micro plasma production.

- [1] K. H. Schoenbach, A. EL-Habachi, W. She and M. Ciocca, Plasma Sources Sci. Technol. 6, 468 (1997).
- [2] G. Rosenman, D. Shur, Kh. Garb and R. Cohen, J. Appl. Phys. 82, 772 (1997).
- [3] M. Miyake, S. Ibuka, K. Yasuoka and S. Ishii, Jpn. J. Appl. Phys. 36, 6004 (1997).

7P62

A Capsule Review of Three Years of Progress in the Sandia Z-Pinch Program,

M.A. Sweeney, Sandia National Laboratories, Albuquerque, NM 87185-1186, USA

> A Capsule Review of Three Years of Progress in the Sandia Z-Pinch Program

> > M. A. Sweeney Sandia National Laboratories* Albuquerque, NM 87185-1186

In May 1996 modifications began to the PBFA II accelerator at Sandia National Laboratories to produce fast (submicrosecond) plasma implosions, called z pinches, that are driven by intense magnetic fields (~ 1000 Tesla) associated with the large (~20 MA) axial currents. The modifications to the water lines, the insulator stack, and the self-magnetically-insulated transmission lines were completed in September 1996, and the first z-pinch-driven x-ray radiation source shot on the new facility occurred on October 2. Today the facility, renamed Z, is the most energetic source of laboratory x rays and has led to what some have termed a "renaissance" in z pinches for inertial confinement fusion (ICF) and defense applications.

The first six months of Z operation were devoted to adding and testing new diagnostics and to evaluating and optimizing the xray source. X-ray energies approaching 2 MJ, x-ray powers in excess of 200 TW, and radiation pulse lengths as short as 4 ns have been achieved. Since then, application experiments have been done in the areas of shock physics, radiation flow, equations of state, astrophysics, ICF, weapon physics, and radiation effects on Z. In addition, the early-time dynamics of the z-pinch source has been investigated via experiments on lower-current accelerators at Imperial College, the Naval Research Laboratory, Cornell University, TRINITI, and the University of Reno. In tandem with the experimental and diagnostic progress, simulations and analytic theory are being used to develop a deeper understanding of the physics of zpinch sources and to design radiation cavities (hohlraums) that are driven by the intense x rays that the multiple-wire sources on Z generate.

In these endeavors we have benefited directly from collaborations with scientists from LANL, LLNL, the Defense Threat Reduction Agency, the Atomic Weapons Establishment, Imperial College, NRL, C.E.A./DGA in France, TRINITI and the Institute of High Current Electronics in Russia, U. C. Irvine, the University of New Mexico, Cornell University, the University of Reno, the Tokyo Institute of Technology, and Osaka University, among others.

In this poster presentation, the three years of progress in our z-pinch program are summarized.

^{*}Sandia is a multiprogram laboratory operated by Sandia Corporation, a Lockheed Martin Company, for the Department of Energy under Contract DE-AC04-94AL85000.

Lagrangian Approach in the Analysis of Plasmafilled Diodes

X. Chen, P.A. Lindsay, J. Watkins and J. Zhang, King's College London, Strand, London, WC2R 2LS, UK

Lagrangian Approach in the Analysis of Plasma-filled Diodes X. Chen, P.A. Lindsay, J. Watkins and J. Zhang Dept. of Electronic Engineering, King's College London, UK

So far our detailed analysis of a plasma-filled diode was largely based on the work of Brendan Godfrey published in a seminal paper of 1987 [1]. Having extended Godfrey's analysis from $\alpha = 1$ to $\alpha \neq 1$, where $\alpha = n_{i0} / n_{e0}$ is the ion/electron number densities ratio at the entrance electrode, we have been able to show that the diode can operate in four distinct regimes: stable, oscillatory, chaotic and unstable [2]. The oscillatory regime, which is of importance in such microwave devices as vircators, was so far limited to a hydrodynamic model [3]. However we know that in the case of a vircator in particular, oscillations may occur by reversal in the direction of the electron flow, a new regime of operation which lies outside the hydrodynamic model. This regime can be handled only either by using a large number electron sheets in place of an electron beam of by employing a powerful PIC code, in our case MAGIC2D/3D. In the past we have limited ourselves to the analysis of beam/plasma interaction in the space between the entrance and exit electrodes, leaving the process of beam generation and its injection severely alone. In real life such a simplified system is physically unrealisable - clearly some kind of emission surface has to precede the entrance electrode (i.e. grid) of a plasma filled diode. Having considered the matter further, we have come to the conclusion that if we wish to include in our model the appearance of a virtual cathode and the possibility of double-stream flow in a plasma-filled diode, then for reasons of consistency we must include in our analysis the cathode/grid region. This is of particular importance if we choose to treat the diode as a model for the interaction space of a virtual cathode oscillator (vircator) since, as we know, the strongest oscillations in such a tube are generated precisely by the process of virtualcathode formation and annihilation. It is then essential to know what happens to the beam when it goes back into the cathode/grid region, assuming, as usual, that the grid is ideally permeable, its sole purpose being the establishment of a fixed potential at the entrance to the plasma-filled diode. In our contribution we propose to present the analysis of our enlarged system together with the results of some early computations, in particular the range of system parameters for which virtual-cathode type of oscillations are likely to occur.

References

- B. B. Godfrey, Oscillatory nonlinear electron flow in a Pierce diode, Phys. Fluids, vol. 30, 1987, pp.1553-1560.
- X. Chen and P.A. Lindsay, Oscillations and chaos in plasmafilled diode, IEEE Trans. Plasma Science, vol. 24, 1996, pp. 1005-1014.
- 3. X.Chen and P.A.Lindasy, Physical interpretation of oscillations and chaos in a plasma-filled diode, 39th Annunal Meeting, American Physical Society, Division of Plasma Physics, Pittsburgh PA. 1997.

7P64

Laser-Cooled Non-Neutral Plasma Experiments at NIST

L.B. King, J.J. Bollinger, B.M. Jelenkovic, T.B. Mitchell, W. M. Itano, D.J. Wineland, NIST, Boulder, CO 80303, USA

LASER-COOLED NON-NEUTRAL PLASMA EXPERIMENTS AT NIST¹

L.B. King, J.J. Bollinger, B.M. Jelenkovic, T.B. Mitchell, W.M. Itano, D.J. Wineland, NIST, 325 Broadway, Boulder, CO 80303

We summarize the status of two laser-cooled ion plasma experiments at NIST. Both experiments use Penning traps (B=4.46 T, 6.0 T) and a rotating electric-field perturbation to confine up to 106 9Be+ ions. Recent measurements of the ion correlations2, plasma modes³, and solid-state ion mobility from the first experiment will be given. Progress in the 2nd experiment on using laser-cooled 9Be+ ions to trap and sympathetically cool positrons will be discussed. We have been able to trap 0.5-mm-long, 1010 cm-3 Be+ ion plasmas which we think will be useful for trapping positrons. In this experiment we have also observed non-spheroidal plasma shapes due to deviations from These deviations a quadratic trapping potential. become pronounced at low rotation frequencies where the plasma is shaped like a disk.4

¹Work supported by the Office of Naval Research

²T.B. Mitchell, J.J. Bollinger, D.H.E. Dubin, X.-P. Huang, W.M. Itano, and R.H. Baughman, *Science* 282, 1291-1293 (1998)

³T.B. Mitchell, J.J. Bollinger, X.-P. Huang, and W.M. Itano, Optics Express 2, No. 8, 314-322 (1998)

⁴D.L. Paulson and R.L. Spencer, Phys. Plasmas 5, 345 (1998)

Optimization of Microwave Generation by Coaxial Vircator

W. Jiang, K. Woolverton, J. Dickens and M. Kristiansen, Texas Tech University, Lubbock, TX 79409-3102, USA

Optimization of Microwave Generation by Coaxial Vircator

W. Jiang*, K. Woolverton, J. Dickens, and M. Kristiansen Pulsed Power Laboratory, Departments of Electrical Engineering and Physics, Texas Tech University, Lubbock, TX 79409-3102

The coaxial virtual cathode oscillator (vircator) developed by Texas Tech University was studied in order to improve the efficiency of microwave generation. The microwave frequency and mode were diagnosed. The results were used to design a microwave reflector that enhances the microwave fields in the vircator area. The experimental results with the microwave reflector have shown that both the microwave output power and the direction of microwave field polarization strongly depend on the configuration of the microwave reflector. These results indicate that the microwave reflector could be used as a control of the beam-field interaction in the vircator. objective of this experiment is to improve the vircator performance by means of this control.

With electron beam parameters of 400 kV, 40 kA, and 30 ns, the typical output is TE_{11} mode microwaves at 2 GHz with the peak power of 800 MW. The microwave efficiency is 5% which was approximately twice as large as that obtained without the microwave reflector. These experimental results were compared with numerical simulation results to understand the effect of field enhancement by the microwave reflector.

This work was solely funded by the High-Power Microwave MURI program funded by the Director of Defense Research & Engineering (DDR&E) and managed by the Air Force Office of Scientific Research (AFOSR).

7P66

3D PIC simulations of the Relativistic Klystron Oscillator

G.E. Sasser, L. Bowers, J.W. Luginsland, J.J. Watrous, Air Force Research Laboratory, AFRL, Kirtland AFB, NN 87117, USA

3D PIC simulations of the Relativistic Klystron Oscillator, G. E. Sasser, L. Bowers, J. W. Luginsland, J. J. Watrous*, Air Force Research Laboratory, Directed Energy Directorate, Kirtland AFB, NM, 87117, *NumerEx, Albuquerque, NM, 87106. The Relativistic Klystron Oscillator (RKO) is a gigawatt class microwave source that is being investigated within the Air Force Research Laboratory (AFRL). In this talk, results of 3D simulations of the AFRL RKO using the particle-in-cell software ICEPIC (Improved Concurrent Electromagnetic Particle-In-Cell) are presented. Full 3D simulations of the RKO are challenging for a number of reasons, not the least of which is the sheer size of the problem. ICEPIC is unique in its ability to perform very large simulations and is an appropriate tool for solving problems related to the RKO. Other challenges include the correct treatment of emission from the knife-edge cathode and proper modeling of the Q of the RKO cavities.

^{*} Permanent address: Laboratory of Beam Technology, Nagaoka University of Technology, Nagaoka, Niigata 940-2188, Japan.

Control of Mechanisms for Pulse Shortening in the Reltron

J. Golden, Berkeley Research Associates, Springfield, VA 22150, USA

Control of Mechanisms for Pulse Shortening in the Reltron J. Golden Berkeley Research Associates, Inc.

Pulse shortening in the Reltron has been correlated with the interaction of the electron beam with screens used in the output cavities.[1] It appears that electron stimulated desorption (ESD) of gas from the screens leads to a high density gas cloud that is subsequently ionized by the beam and the high electric fields of the cavity. Although pulse shortening can be avoided by operation without screens in the output cavities at frequencies near 1 GHz, at higher frequencies, it is expected that the higher fields present in the modulation cavity will also lead to pulse shortening. Because elimination of the screen in the modulation cavity is not desirable, measures to reduce the gas loading in the screens are necessary. A conventional approach uses high temperature vacuum bakeout. However, high power Reltrons typically employ textile fiber cathodes, which have limited lifetime. Thus, tubes with demountable vacuum joints are necessary, and extensive bakeout and hard tube processing techniques are not practical in this case.

To avoid pulse shortening, alternative processing techniques are being developed and the mechanisms associated with the initiation of electron emission, ESD, and plasma formation are being investigated. Models have been developed and are being tested experimentally. The processing techniques include pulsed thermal desorption of screen, ESD cleaning of the fiber cathode, UV desorption of critical tube components, and a novel beam collector. These techniques can lead to improved vacuum conditions and reduced gas loading in tube components.

A full scale demonstration of these techniques in a high power Reltron is in preparation. A PFN-Marx testbed with a 2 μ s pulse duration will power a Reltron that features demountable output cavities.[2]

 R.B. Miller, Observations Related to Pulse Shortening in Reltron High Peak Power Microwave Tubes. TRT-A462, Titan Corporation/Research and Technology Division, Albuquerque, NM, 5 Feb 1998.

 Work performed as part of a Small Business Innovative Research Project supported by the Air Force Research Laboratory.

7P68

Photocell Enhanced Technique For Measuring Electrode Starting Temperature In Fluorescent Lamps

E.E. Hammer, FIEEE, FIES.LC, FIEEE, FIES, LC *Abstract not available.*

Hydrogen Plasma Diffusion Treatment of Layers Prepared by Plasma Nitridation

V. Hruby, J.Kadlec and J. Stodola Dept. of Materials and Technology of Special Production, Military Academy, Brno, Czech Republic

Hydrogen Plasma Diffusion Treatment of Layers Prepared by Plasma Nitridation

V. Hruby, J. Kadlec and J. Stodola Depth. of Materials and Technology of Special Production, Military Academy, Brno, Czech Republic

Abstract

As to at present time an annealing after nitridation process is applied. The parameters of nitridation process are chosen according to practical experiences of equipment operator only, without kow-how of passing off plots correlations among process parameters.

The main aim of this paper is experimental and theoretical explanation of diffusion and structure processes occuring in plasma nitrided layers during their subsequent isothermal annealing, included into the work cycle immediately after finishing proper plasma nitridation. The substance of experimental part is first of all quantitative determination of redistribution of interstitial elements - nitrogen and carbon in the layer - and structure and phase analysis of changes of isothermally annealed plasma nitrided layers. The results of these analyses is completed with parallelly performed hardness measurement.

On the basis of thus measured redistribution of interstitial and substitutional elements in the layer, then diffusion and phase characteristics of both groups of elements is determined, confronted with the data according to literature and thermodinamic and diffusion model of elements redistribution in plasma nitrided layer of finite thickness is elaborated.

Further, following properties of thin surface layers were measured: layer thickness, microhardness, roughness, wear resistance and surface morphology.

Abdallsh, C T	•		10 10 14 1	2P13, 2P15
Abdallah, J.				-
Abe, D. K. Adams, R. G. Advani, R. Advani, R. 3P04 Advani, R. 3P04 Afanasey, Y.V. 7P10 Afanasey, Y.V. 7P10 Aglitskiy, Y. 3P20 Akishev, Y.S. Akishev, Y.S. Akishev, Y.S. Akishawa, H. 2C07, 5D04, 6P29, 7P08 Al-Shorman, M. Alexandrovich, BM Beale, FX Beale	Abdallah, C T			
Adams, R G Adams, C G Adams, R G	Abdallah, J		1	
Advani, R	Abe, D K	2P14		
Advani, R. 3P04 Bayerlein, B. 6CC9 Adinskey, Y. 7P10 Adjitskiy, Y. 3P20 Akishev, Y. 5 Benck, E. 3P26 Bendib, A. 2P03 Benck, E. 3P26 Benck, E. 3P26 Benck, E. 3P26 Bendib, A. 2P03 Benck, E. 3P26 Benck, E. 3P28 Benck, E. 3P28 Benc	Adams, R G	6P22	Baum, C E	
Afanasey, YV 7P10 Aglitskiy, Y 3P20 Akishev, Y S 7P55 Akishev, Y S 7P56 Becker, K 2P28 Benchia, A 2P03 Berford, J N Pferalpy Talk Berthauseva, R H Berthauseva, R Bertalot, L Berthauseva, R Bertalot, L Berthauseva, R Berthauseva, R Berthauseva, R Berthauseva, R Berthauseva, R Berthausev		3P04	Bayerlein, B	6C09
Aglitsky, Y S P52		7P10	Beall, J H	4P30
Akishev, Y. S Akishev, Y. S Akishev, Y. S Akishama, H Akishoran, M Akishoran, M TP22 Alexandrovich, BM Alexeff, I Alexandrovich, BM Berland, I Berland, I Berland, I Berland, I Berland, I Berland, I Berlandrov, I Berland, I Berlandrov, I B			Becker, K	2P28
Akiyama, H 2CO7, 5D04, 6P29, 7P08 Al-Shorman, M 7P22 Al-Shorman, M 7P22 Al-Shorman, M 7P22 Alexandroxich, BM 2A03 Alexeff, I 2B10, 4P10, 4P13, 4P21, 4P22 Aliaga-Rossel, R 5C08, 5C09, 7P29 Bendib, A 2P03 Alkafesh, A 4P21 Ammons, N 7P22, 7P23 Anderson, I 3P31 Anderson, L 3P31 Anderson, L 1906, 1P07, 2P01, 4P20, 6P23 Annorsen, T M 1801-02, 1803, 1806, 1807, 1809, 2P11, 2P14, 3P05, 4801-02, 3P19, 5B12 Apruzese, J P 3006, 6C04, 6C05, 1804, 1801-02, 4P19, 5B12 Arman, M 3P08 Armstrong, C M 3P12, 5805, 6D01-02 Brash, D 2P30 Armstrong, C M 3P12, 5805, 6D01-02 Brash, M 3P10 Asay, J R 2C01-02 Brash, M 3P10 Asay, J R 2C01-02 Brash, M 3P08 Asay, J R 2C01-02 Brash, M 3P10 Asay, J R 2C01-02 Brash, M 3P10 Asay, J R 2C01-02 Brash, M 3P10			I S	6C04
Al-Shorman, M Al-Shorman, M Al-Shorman, M Alexarfi, I Alexardrovich, BM Alexardrovich, Alexardrovich, Alexardrovich, Alexardrovich, Alexar			1 5	1P01
Alexandrovich, BM Alexelf, I 2B10, 4P10, 4P13, 4p21, 4P22 Bendib, A 2P03 Aliaga-Rossel, R Alizafesh, A 4P21 Alimons, N AP22, 7P23 Andersson, L Ap21, 4P22 Bendib, A Bernford, J N Bernfo				
Alexeff, I 42B10, 4P10, 4P13, 4p21, 4P22 Bendib, A 2P03 Aliaga-Rossel, R 5C08, 5C09, 7P29 Benford, J N Plenary Talk Alikafesh, A 4P21 Bera, K 3A04 Ammons, N 7P22, 7P23 Beratlot, L 3P29 Anderson, L 3P31 Besen, M 3D02-03 Anderson, L 3P31 Besen, M Bettenhausen, M H 1P17 Ap20, 6P23 Bilek, M M M 6P09 Antonsen, T M 1B01-02, 1803, 1806, 1807, 1809, 2P11, 2P14, 3P05, 4801-02, 3P19, 5812 Apruzese, J P 3D06, 6C04, 6C05, 6C06, CP02 Black, D C 5D01, 7C08 Arad, R 5D02-03 Black, D C 5D01, 7C08 Arad, R 3P08 Bland, S N 5C08, 5C09, 7P29 Armillo, J 5C05 Blackwell, D D 2P30 Armistrong, C M 3P12, 5805, 6D01-02 Black, D C 5D01, 7C08 Armush, D 2P30, 2P15, 3P11, Blank, M 3P10, 4801-02, 2B02 Armush, D 2P30 Bland, S N 5C08, 5C09, 7P29 Asmussen, J 4P11 Blank, M 3P10, 4801-02, 2B03 Assay, J R 2C01-02 Bocquet, P 3D08 Assy, J R 2C01-02 Bocquet, P 3D08 Assy, J R 2C04, 2C05, 5C06 Bourham, M A 7D05 Aubes, M 7A03 Bourham, M A 7D05 Avarmenko, R F 7P58 Bourham, M A 7D05 Babineau, M A 4P41 Breeze, S 3P31 Baik, S W 3P18 Brinsmead, W 7P22 Baley, J E 5C10, 6P22 Brown, I G 4P18, 5A07, 6P09, 6P19 Balaksht, R B 7P06 Balaksht, R B 7P06 Barsanti, M 5805 Buhr, B 1A08 Brown, C M 3P20 Barres, D 3P28, 4P35 Buna, C 4P27 Barres, D 3P38, 4P35 Burnes, D 4D39 Brown, C M 3P30 Browner, C M 3P31 Brown, C M 3P30 Brown, C M 3P30 Browner, C M 3P30 Brown, C M 3P30 Browner, C				
Aliaga-Rossel, R Ap21 Ammons, N Ap21 Ammons, N Ap22, Pp23 Anderrson, L Ap393 Anderrson, L Ap393 Anderrson, L Ap393 Ang, L K Ap20, 6P23 Ang, L K Ap20, 6P23 Ang, L K Ap20, 6P23 Antonsen, T M Antonsen, T M BiB10-102, 1803, 1806, 1807, 1809, 2P11, 2P14, 3P05, 4801-02, 3P19, 5B12 Apruzese, J P Ap06, A801-02, 3P19, 5B12 Apruzese, J P Ap06, AP02 Arad, R Ap08 Ariona, M R Ap08 Arman, M J Ag07, 7P35, 7P36, 7P39 Blackwell, D D Armstrong, C M Armstrong, C M Armstrong, C M Ap12, 5805, 6D01-02 Blacky R Armush, D Asay, J R Achison, W L Arbitaga-Rossel, A Ap10-02, 2P03 Armstrong, C M Ap11 Atchison, W L Arbitaga-Rossel, A Ap10-02, Ap20 Aubes, M Aubrey, J Acounty Ap20 Avaramenko, R F Ap30 Avaramenko, R F Ap58 Avarlaud, G Ap19 Babineau, M A Baik, S W Ap18 Baik				
Aliaga-Rossel, R Bertarlot, L Beraldot, L Beraldot, L Beraldot, L Bestel, L Bestel, L Bestel, M Aliaga-Rossel, R Aliaga-Rosse	Alexeπ, I			
Alikafesh, A Ammons, N Ammons, N Ammons, N Ammons, N Amberson, L Ammons, N Amberson, L Ammons, N Amberson, L Ammons, N Amberson, L Ambonsen, T M Ambonsen, M A			l ·	
Ammons, N Ammons, M Ammons			1	-
Anderson, L Ang, L K Anderson, L Ang, L K Anderson, L Ap20, 6P23 Antonsen, T M Bol -02, 1803, 1806, Bord, 1809, 2P11, 2P14, Bros, 4801-02, 3P19, 5812 Apruzese, J P Apruzese, J P Arad, R Apruzese, J P Arad, R Aran, M J Aram, M	· · · · · · · · · · · · · · · · · · ·		1	
Ang, L K AP20, 6P23 Antonsen, T M Bettenhausen, M H Bilek, M M M GP09 Bilidsall, C K 1A04-05, 2P17, 2P18, 3P02, 4P34 Bilek, M M M Bilidsall, C K 1A04-05, 2P17, 2P18, 3P02, 4P34 Bilek, M M M Bilek, M C Bilek, D C Bilack, D C Bilack	Ammons, N	•	1	
Antonsen, T M 1801-02, 1803, 1806, 1807, 1809, 2P11, 2P14, 3P05, 4801-02, 3P19, 5B12 Apruzese, J P	Anderrson, L			
Antonsen, T M 1801-02, 1803, 1806, 1807, 1809, 2P11, 2P14, 3P05, 4801-02, 3P19, 5P12 Apruzese, J P 3D06, 6C04, 6C05, 6C06, 7P02 Black, D C 5D01, 7C08 Arad, R 5D02-03 Blackwell, D D 2P30 Armin, M J 6807, 7P35, 7P36, 7P39 Blackwell, D D 1P16 Armstrong, C M 2P08, 2P15, 3P11, 3P12, 5805, 6D01-02 Block, R 2B01-02, 2B03 Asmussen, J 4P11 Blank, M 3P10, 4801-02, 6D07 Axmussen, J 4P11 Blonger, J 7P64 Aubes, M 7A03 Borchard, P 4B01-02 Avaramenko, R F 7P58 Bowers, L 7P38, 7P39 Avaramenko, R F 4P06, 4P19 Bowers, K J 1A04-05, 2P17, 2P18, 2P19, 2P20 Babineau, M A 5D06 Brandenburg, J E 2B04 Babineau, M A 4P41 Breeze, S 3P31 Babineau, M A 4P41 Breeze, S 3P31 Bailey, J E 5C10, 6P22 Brown, I G 4P18, 5A07, 6P09, 6P10 Baldis, H A 4803, 5804 Bruce, R W 2802 Barres, D 3P28, 4P35 Bruna, C 4P27 Barona, M A 5B05 Burres, B 3P34 Burres, D 3P28, 4P35 Bruna, C 4P27 Barres, D 3P28, 4P35 Bruna, C 4P24 Burres, D 3P28, 4P35 Bruna, C 4P27 Barres, D 3P28, 4P35 Bruna, C 4P41 Barres, D 3P28, 4P35 Bruna, C 4P27 Barres, D 3P28, 4P35 Bruna,	Ang, L K	1P06, 1P07, 2P01,		
1807, 1809, 2P11, 2P14, 3P05, 4B01-02, 3P19, 5B12 Birnboim, A 3B03-04, 3B06 Birrell, A 6P17 Booker, Poz. Black, D C 5D01, 7C08 Black, D C 5C08, 5C08, 5C09, 7P29 Black, D C 5C08, 5C09, 7P29 Black, D C 5C08, 5C09, 7P29 Black, D C 5C08, 5C06, 5C09, 7P18 Black, D C 5C08, 5C06, 5C		4P20, 6P23	I The state of the	
1807, 1809, 2P11, 2P14, 3P05, 4801-02, 3P19, 5B12 Birnboim, A 3B03-04, 3B06 Birrell, A 6P17 Arad, R 5D02-03 Blackwell, D 2P30 Blackwell, D 2P30 Blackwell, D 2P30 Armino, J 5C05 Blackwell, D 2P30 Blackwell, D 2P30 Armino, J 5C05 Blackwell, D 2P30 Blanchard, P 3A01 Armino, J 5C05 Blackwell, D 3P16 Blanchard, P 3A01 Armino, J 5C05 Blackwell, D 3P16 Blanchard, P 3A01 Armino, J 5C05 Blackwell, D 3P10, 4801-02, 6D07 Blanchard, P 3A01 Armino, J 3P12, 5805, 6D01-02 Bletzinger, P 2A01-02 Bletzinger, P 2A01-02 Bletzinger, P 2A01-02 Block, R 2801-02, 2803 Bocquet, P 3D08 Asmussen, J 4P11 Atchison, W L 1P16, 6C03, 6P25, Booske, J H 2P12, 2P13 Bollinger, J J 7P64 Aubes, M 7A03 Borghi, C A 4P36, 4P37 Aubrey, J 2C04, 2C05, 5C06 Bourham, M A 7D05 Avramenko, R F 7P58 Bouzid, F 2P03 Avramenko, R F 7P58 Bowers, L 7P38, 7P39 Avramenko, R F 4P06, 4P19 Bowers, K J 1A04-05, 2P17, 2P18, 2P19, 2P20 Bowers, R L 2C03, 2C04, 2C05, 5C06, 7P18 Babineau, M A 4P41 Breeze, S 3P31 Brinsmead, W 3P20 Baley, J E 3Birly, B Birly, B	Antonsen, T M	1B01-02, 1B03, 1B06,	Birdsall, C K	*
Apruzese, J P 3006, 6C04, 6C05, 6C06, 7P02 Arad, R 5D02-03 Black, D C 5D01, 7C08 Arad, R 5D02-03 Blackwell, D D 2P30 Arjona, M R 3P08 Blahovec Jr, J D 1P16 Arman, M J 6807, 7P35, 7P36, 7P39 Blanchard, P 3A01 Armijo, J 5C05 Blackwell, D D 1P16 Armstrong, C M 2P08, 2P15, 3P11, Blank, M 3P10, 4B01-02, 6D07 Armush, D 2P30 Block, R 2B01-02, 2B03 Asay, J R 2C01-02 Bletzinger, P 3D08 Asmussen, J 4P11 Block, R 2B01-02, 2B03 Asmussen, J 4P11 Block, R 2B01-02, 2B03 Asmussen, J 4P11 Block, R 2P12, 2P13 Atchison, W L 1P16, 6C03, 6P25, Booske, J H 2P12, 2P13 Aubes, M 7A03 Bordard, P 3B00 Aubrey, J 2C04, 2C05, 5C06 Borchard, P 4B01-02 Avramenko, R F 7P58 Bourlam, M A 7D05 Avramenko, R F 7P58 Bowers, L 7P38, 7P39 Avramenko, R F 7P58 Bowers, L 7P38, 7P39 Azuma, K 4P06, 4P19 Bowers, K J 1A04-05, 2P17, 2P18, 2P19, 2P20 Babineau, M A 4P41 Breeze, S 3P31 Baik, S W 3P18 Brinsmead, W 7P22 Bowers, R L 2C03, 2C04, 2C05, 5C06, P18 Babineau, M A 4P41 Breeze, S 3P31 Baik, S W 3P18 Brinsmead, W 7P22 Baley, J E 5C10, 6P22 Brown, I G 4P18, 5A07, 6P09, 6P10 Baker, D A 4C03 Brown, C M 3P20 Baker, D A 4C03 Brown, C M 3P20 Bakers, D A 4C03 Brown, C M 3P20 Barsanti, M 5B05 Bulhr, B 1A08 Brima, C 4P27 Barnoova, E O 7P09 Bugaev, A S HA	·	1B07, 1B09, 2P11, 2P14,		•
Apruzese, J.P. 3D06, 6C04, 6C05, 6C06, 7P02 Black, D.C. 5D01, 7C08 Arad, R. 5D02-03 Blackwell, D.D. 2P30 Arjona, M.R. 3P08 Blackwell, D.D. 1P16 Arman, M.J. 6807, 7P35, 7P36, 7P39 Blanchard, P. 3A01 Armijo, J. 5C05 Black, M. 3P10, 4B01-02, 6D07 Armstrong, C.M. 2P08, 2P15, 3P11, 3P12, 5805, 6D01-02 Bletzinger, P. 2A01-02 Armstrong, D. 2P30 Block, R. 2B01-02, 2B03 Asay, J.R. 2C01-02 Bocquet, P. 3D08 Asmussen, J. 4P11 Bollinger, J.J. 7P64 Atchison, W.L. 1P16, 6C03, 6P25, Booske, J.H. 2P12, 2P13 Aubes, M. 7A03 Borghi, C.A. 4P36, 4P37 Aubrey, J. 2C04, 2C05, 5C06 Avramenko, R.F. 7P58 Avrillaud, G. 6P24 Bowers, L. 7P38, 7P39 Avurillaud, G. 6P24 Bowers, K.J. 1A04-05, 2P17, 2P18, 2P19, 2P20 Babineau, M.A. 4P06, 4P19 Browers, K.J. 1A04-05, 2P17, 2P18, 2P19, 2P20 Babineau, M.A. 4P41 Breeze, S. 3P31 Baik, S.W. 3P18 Brinsmead, W. 7P22 Bailey, J.E. Bailey, A.E. Bailey, A.E. Bailey, A.E. Bailey, A.E.		3P05, 4B01-02, 3P19, 5B12	Birnboim, A	3B03-04, 3B06
Arad, R Arjona, M R Arjona, M R Arjona, M R Arjona, M R Arman, M J Armijo, J Armijo, J Armstrong, C M Arman, D Armush, D Asay, J R Asmussen, J Aubes, M Aubrey, J Aubes, M Auramenko, R F Avrillaud, G Azuma, K Arillaud, G Azuma, K Arillaud, G Azuma, K Arillaud, G Azuma, K Babineau, M A Bailey, J E Babineau, M A Bailey, J E Bailey, V Bailey, J E Bailey, V Balaks, T Barakat, F Baland, S N Bocquet, P Blanchard, P Bocquet, P Booske, J H Bollinger, J J Booske, J H Bollinger, J J Booske, J H Borchard, P Booske, J H Borchard, P Boorhard, P Bourharm, M A Borchard, P Bourharm, M A Browers, L Browers, L Browers, R L Bowers, R L Booker, D Bowers, R L Bowers, R L Bowers, R L Bowers, R L Booker, D Bowers, R L Bowers	Anruzese I P	· · · · · · · · · · · · · · · · · · ·	Birrell, A	6P17
Arad, R 5D02-03 Blackwell, D D 2P30 Arjona, M R 3P08 Blahovec Jr, J D 1P16 Arman, M J 6B07, 7P35, 7P36, 7P39 Blanchard, P 3A01 Armistong, J 5C05 Blank, M 3P10, 4B01-02, 6D07 Armstrong, C M 2P08, 2P15, 3P11, 3P10, 4B01-02 Block, R 2B01-02, 2B03 Armush, D 2P30 Block, R 2B01-02, 2B03 Asay, J R 2C01-02 Bocquet, P 3D08 Asmussen, J 4P11 Bollinger, J J 7P64 Atchison, W L 1P16, 6C03, 6P25, 7806 Booske, J H 2P12, 2P13 Aubes, M 7A03 Bordhard, P 4801-02 Aubes, M 7A03 Borghi, C A 4P36, 4P37 Aubrey, J 2C04, 2C05, 5C06 Bourham, M A 7D05 Avramenko, R F 7P58 Bowers, L 7P38, 7P39 Avrillaud, G 6F24 Bowers, K J 1A04-05, 2P17, 2P18, 2P19, 2P20 Babineau, M A 5D06 Brandenburg, J E 2B04 Baeva, M 4P41 <	, tprazese, s .	· · · · · · · · · · · · · · · · · · ·	Black, D C	5D01, 7C08
Arjona, M R Arman, M J Armijo, J Armijo, J Armijo, J Armstrong, C M Arman, M J Armush, D Armstrong, C M Asay, J R Asay, J R Aubes, M Aubes, M Aubes, M Aubes, J Avrillaud, G Avrillaud, G Avrillaud, G Azuma, K Arman, M A Armstrong, C M Armstrong, C	Arad R		1	2P30
Arman, M J 6807, 7P35, 7P36, 7P39 Blanchard, P 3A01 Armijo, J 5C05 Armstrong, C M 2P08, 2P15, 3P11, 3P12, 5B05, 6D01-02 Bletzinger, P 2A01-02 Armush, D 2P30 Block, R 2B01-02, 2B03 Asay, J R 2C01-02 Bocquet, P 3D08 Asmussen, J 4P11 Booske, J P16, 6C03, 6P25, Booske, J H 2P12, 2P13 Aubes, M 7A03 Borchard, P 4B01-02 Avramenko, R F 7P58 Bourid, F 2P03 Avramenko, R F 7P58 Bourid, F 2P03 Avuma, K 4P06, 4P19 Bowers, L 7P38, 7P39 Babineau, M A 5D06 Brandenburg, J E 2B04 Baeva, M 4P41 Breeze, S 3P31 Baik, S W 3P18 Brinsmead, W 7P22 Bailey, J E 5C10, 6P22 Brown, I G 4P18, 5A07, 6P09, 6P10 Baksht, R B 7P06 Brownell, J H 2C03 Baldis, H A 4B03, 5B04 Bruce, R W 2B02 Barsanti, M 5B05 Bulancy, B 1A08 Bulancy, B 1A08 Bulancy, B 1A08 Bulancy, B 1A08 Breeze, S Bruma, C 4P27 Barnova, E O 7P09 Bugaev, A S 6P10 Barsanti, M 5B05 Bulancy, B 1A08 Bulancy, B 1A01 Bulancy, B 1				1P16
Armijo, J 5C05 Bland, S N 5C08, 5C09, 7P29 Armstrong, C M 2P08, 2P15, 3P11, 3P12, 5B05, 6D01-02 Bletzinger, P 2A01-02 Armush, D 2P30 Block, R 2B01-02, 2B03 Asay, J R 2C01-02 Bocquet, P 3D08 Asmussen, J 4P11 Booske, J H 2P12, 2P13 Atchison, W L 1P16, 6C03, 6P25, 7B06 Borchard, P 4B01-02 Aubes, M 7A03 Borchard, P 4B01-02 Aubrey, J 2C04, 2C05, 5C06 Borchard, P 4B01-02 Avramenko, R F 7P58 Bowers, L 7P38, 7P39 Avrillaud, G 6P24 Bowers, L 7P38, 7P39 Azuma, K 4P06, 4P19 Bowers, K J 1A04-05, 2P17, 2P18, 2P19, 2P20 Bowers, R L 2C03, 2C04, 2C05, 5C06, 7P18 Babineau, M A 5D06 Brandenburg, J E 2B04 Baeva, M 4P41 Breeze, S 3P31 Baik, S W 3P18 Brinsmead, W 7P22 Bailey, J E 5C10, 6P22 Brown, I G 4P18, 5A07, 6P09, 6P10 Baksht, R B 7P06 Brownell, J H 2C03 Baksht, R B 7P06 Brownell, J H 2C03 Barsanti, M 5B05 Buyle, B 5C10, 6P10 Barsanti, M 5B05			-	
Armstrong, C M 2P08, 2P15, 3P11, 3P12, 5805, 6D01-02 Bletzinger, P 2A01-02 Armush, D 2P30 Asay, J R 2C01-02 Asmussen, J 4P11 Bollinger, JJ 7P64 Atchison, W L 1P16, 6C03, 6P25, 7806 Aubers, M Aubrey, J 2C04, 2C05, 5C06 Avramenko, R F Avrillaud, G Azuma, K 4P06, 4P19 Babineau, M A Baeva, M Baeva, M Babineau, M A Baeva, M Bailey, J E Bailey, J E Bailey, J E Bailey, J E Bailey, J Baker, D A Baksht, R B Barnes, D Baronova, E O Basineau, M A Baronova, E O Baro			1	
Armush, D Armush, D Asay, J R Asmussen, J Atchison, W L Atthison, W L Armush, D Abelian, D Asay, J R Acthison, W L Atthison, W L Armush, D Abelian, D Asay, J R Armussen, J Atthison, W L Atthison, W L Armush, D Aubes, M Aubes, M Aubes, M Authery, J Avarianeho, R F Arrillaud, G Azuma, K Armush, D Belianger, P Bocake, J H Bollinger, J J Booske, J H Borchard, P Borchard, P Borchard, P Borchard, P Borchard, P Bouridham, M A Arbob Bowers, L Arbob Bowers, K J Bowers, K J Bowers, R L Arbob Bowers, R L Arbob Brandenburg, J E Babineau, M A Bowers, M Brandenburg, J E Babineau, M A Brandenburg, J E Babineau, M A Brandenburg, J E Brandenbur	•			
Armush, D Asay, J R Asay, J R Asmussen, J Atchison, W L Aubes, M Aubrey, J Avrillaud, G Azuma, K Babineau, M A Baeva, M Baeva, M Baik, S W Bailey, J Bailey, V Bailey, V Bailey, V Bailey, V Baldis, H A Baldis, H A Baldis, H A Baranes, D Barandan, A Barandan Block, R Bocquet, P Bocquet, P Booke, J H Bollinger, J J Booke, J H Aprillaud, G Aprillaud, G Aprillaud, G Aprillaud, G Aprillaud, G Babineau, M A Aprillaud, G Babineau, M A Bourid, F Bowers, R L Cora, 2c04, 2c05, 5c06 Brandenburg, J E Brown, I G Brown, I G Brown, C M Brown, C M Brown, C M Brownell, J H Cora Brown, C M Brownell, J H Cora Brown, C M Bruce, R W Brownell, J H Cora Brown, C M Bruce, R W Brownell, J H Brownell, J H Cora Brownell H Cora Brownell H Cora Brownell H Cora	Armstrong, C M			-
Asay, J R Asay, J R Asmussen, J Atchison, W L 1P16, 6C03, 6P25, 7806 Aubes, M Aubrey, J Avramenko, R F Avrillaud, G Azuma, K Babineau, M A Baeva, M Bailey, J E Bailey, J E Bailey, V Bailey, V Bailey, V Baker, D A Barakat, F Baldins, A Barakat, F Barnes, D Baranden Barakat, F Barnes, D Baranden Bocquet, P Bocquet, S Bocquet, P Bocquet, S Bocquet, S Bocquet, P Bocquet, S				
Asmussen, J 4P11 Bollinger, J J 7P64 Atchison, W L 1P16, 6C03, 6P25, 7B06 Borchard, P 4B01-02 Aubes, M 7A03 Borchard, P 4B01-02 Avramenko, R F 7P58 Bouzid, F 2P03 Avrillaud, G 6P24 Bowers, L 7P38, 7P39 Avrillaud, G 6P24 Bowers, K J 1A04-05, 2P17, 2P18, 2P19, 2P20 Babineau, M A 5D06 Brandenburg, J E 2B04 Baeva, M 4P41 Breeze, S 3P31 Baik, S W 3P18 Brinsmead, W 7P22 Bailey, V 4A04 Baley, V 4A04 Baker, D A 4C03 Brown, I G 4P18 Baldis, H A 4803, 5B04 Barnes, D 3P28, 4P35 Baronova, E O 7P09 Barsanti, M 5B05 Buorchard, P 4B01-02 Booke, J H 2P12, 2P13 Booker, J H 2P13, 5P13				
Atchison, W L The proof of the	- · · · · · · · · · · · · · · · · · · ·		l '	
Aubes, M 7A03 Borchard, P 4801-02 Aubes, M 7A03 Borghi, C A 4P36, 4P37 Aubrey, J 2C04, 2C05, 5C06 Bourham, M A 7D05 Avramenko, R F 7P58 Bowers, L 7P38, 7P39 Azuma, K 4P06, 4P19 Bowers, K J 1A04-05, 2P17, 2P18, 2P19, 2P20 Bowers, R L 2C03, 2C04, 2C05, 5C06, 7P18 Babineau, M A 5D06 Brandenburg, J E 2B04 Baeva, M 4P41 Breeze, S 3P31 Baik, S W 3P18 Brinsmead, W 7P22 Bailey, J E 5C10, 6P22 Brown, I G 4P18, 5A07, 6P09, 6P10 Baker, D A 4C03 Brownell, J H 2C03 Baksht, R B 7P06 Brownell, J H 2C03 Baldis, H A 4B03, 5B04 Bruce, R W 2B02 Baronova, E O 7P09 Bugaev, A S Buhr, B 1A08 Buhr, B 1A08			_	
Aubes, M 7A03	Atchison, W L		1	
Aubrey, J 2C04, 2C05, 5C06 Bourham, M A 7D05 Avramenko, R F 7P58 Bouzid, F 2P03 Avrillaud, G 6P24 Bowers, L 7P38, 7P39 Azuma, K 4P06, 4P19 Bowers, K J 1A04-05, 2P17, 2P18, 2P19, 2P20 Bowers, R L 2C03, 2C04, 2C05, 5C06, 7P18 Babineau, M A 5D06 Brandenburg, J E 2B04 Baeva, M 4P41 Breeze, S 3P31 Baik, S W 3P18 Brinsmead, W 7P22 Bailey, J E 5C10, 6P22 Brown, I G 4P18, 5A07, 6P09, Balley, V 4A04 Baker, D A 4C03 Brown, C M 3P20 Baksht, R B 7P06 Brownell, J H 2C03 Baksht, R B 7P06 Brownell, J H 2C03 Baldis, H A 4B03, 5B04 Bruce, R W 2B02 Barnes, D 3P28, 4P35 Bruma, C 4P27 Baronova, E O 7P09 Bugaev, A S 6P10 Barsanti, M 5B05 Buhr, B 1A08			-	
Avramenko, R F Avrillaud, G Azuma, K Bouzid, F Bowers, L Avrallaud, F Bowers, K J Avallaud-Os, 2P17, 2P18, 2P19, 2P20 Bowers, R L CCO3, 2C04, 2C05, 5C05, 5C06, 7P18 Breeze, S Aprillaud, G Breeze, S Aprillaud, G Aprillaud, G Avrallaud, F Breeze, S Aprillaud, G Aprillaud, G Avrallaud, F Breeze, S Aprillaud, G Avrallaud, F Avrillaud, F Avrillaud, F Avrillaud, G Avrallaud, F Avrillaud, F Avri	Aubes, M			•
Avrillaud, G Azuma, K Azuma, K Azuma, K Azuma, K Azuma, K Azuma, K Azuma, Azu	Aubrey, J	2C04, 2C05, 5C06		
Azuma, K Azuma, K 4P06, 4P19 Bowers, R L 2C03, 2C04, 2C05, 5C05, 5C06, 7P18 Babineau, M A Baeva, M Baik, S W Bailey, J E Bailey, V Baker, D A Baksht, R B Baldis, H A Baldis, H A Baresa, D Baronova, E O Baronova, E O Bowers, K J Bowers, K J 1A04-05, 2P17, 2P18, 2P19, 2P20 Bowers, R L 2C03, 2C04, 2C05, 5C05, 5C06, 7P18 Brandenburg, J E Brown, I G 4P18, 5A07, 6P09, 6P10 Brown, C M Brown, C M Brownell, J H 2C03 Brueck, S R J Brueck, S R J Bruma, C 4P27 Bugaev, A S Buhr, B 1A08	Avramenko, R F	7P58	Bouzid, F	
Azuma, K 4P06, 4P19 Bowers, K J 1A04-05, 2P17, 2P18, 2P19, 2P20 Bowers, R L 2C03, 2C04, 2C05, 5C05, 5C06, 7P18 Babineau, M A Baeva, M Baeva, M Baik, S W Bailey, J E Bailey, V Baker, D A Baksht, R B Baldis, H A Baldis, H A Baldis, H A Barakat, F Barnes, D Baronova, E O Barsanti, M Bowers, K J 1A04-05, 2P17, 2P18, 2P19, 2P20 Bowers, R L 2C03, 2C04, 2C05, 5C06, 7P18 Brandenburg, J E Brown, I G Brown, I G Brown, C M Brown, C M Brown, C M Brownell, J H Brown, C M Brownell, J H Brown, C M Brownell, J H Brandenburg, J E Brown, I G Brown, I G Brown, C M Brown, C M Brownell, J H Brownell	Avrillaud, G	6P24	Bowers, L	•
Babineau, M A 5D06 Brandenburg, J E 2B04 3P31 Brinsmead, W 7P22 Brown, I G 4P18, 5A07, 6P09, 6P10 Brownell, J H 2C03 Brownell, J Br	Azuma, K	4P06, 4P19	Bowers, K J	
Babineau, M A 5D06 Brandenburg, J E 2B04 Baeva, M 4P41 Breeze, S 3P31 Baik, S W 3P18 Brinsmead, W 7P22 Bailey, J E 5C10, 6P22 Brown, I G 4P18, 5A07, 6P09, 6P10 Baker, D A 4C03 Brown, C M 3P20 Baksht, R B 7P06 Brownell, J H 2C03 Baldis, H A 4B03, 5B04 Bruce, R W 2B02 Barakat, F 6C06 Brueck, S R J 5B04 Barnes, D 3P28, 4P35 Bruma, C 4P27 Baronova, E O 7P09 Bugaev, A S 6P10 Barsanti, M 5B05 Buhr, B 1A08				
Babineau, M A 5D06 Brandenburg, J E 2B04 Baeva, M 4P41 Breeze, S 3P31 Baik, S W 3P18 Brinsmead, W 7P22 Bailey, J E 5C10, 6P22 Brown, I G 4P18, 5A07, 6P09, 6P10 Bailey, V 4A04 Brown, C M 3P20 Baker, D A 4C03 Brownell, J H 2C03 Baldis, H A 4B03, 5B04 Bruce, R W 2B02 Barakat, F 6C06 Brueck, S R J 5B04 Barnes, D 3P28, 4P35 Bruma, C 4P27 Baronova, E O 7P09 Bugaev, A S 6P10 Barsanti, M 5B05 Buhr, B 1A08			Bowers, R L	
Babineau, M A 5D06 Brandenburg, J E 2B04 Baeva, M 4P41 Breeze, S 3P31 Baik, S W 3P18 Brinsmead, W 7P22 Bailey, J E 5C10, 6P22 Brown, I G 4P18, 5A07, 6P09, 6P10 Bailey, V 4A04 Brown, C M 3P20 Baker, D A 4C03 Brownell, J H 2C03 Baksht, R B 7P06 Brownell, J H 2C03 Baldis, H A 4B03, 5B04 Bruce, R W 2B02 Barakat, F 6C06 Brueck, S R J 5B04 Barnes, D 3P28, 4P35 Bruma, C 4P27 Baronova, E O 7P09 Bugaev, A S 6P10 Barsanti, M 5B05 Buhr, B 1A08	В			5C05, 5C06, 7P18
Baeva, M 4P41 Breeze, S 3P31 Baik, S W 3P18 Brinsmead, W 7P22 Bailey, J E 5C10, 6P22 Brown, I G 4P18, 5A07, 6P09, Bailey, V 4A04 6P10 Baker, D A 4C03 Brown, C M 3P20 Baksht, R B 7P06 Brownell, J H 2C03 Baldis, H A 4B03, 5B04 Bruce, R W 2B02 Barakat, F 6C06 Brueck, S R J 5B04 Barnes, D 3P28, 4P35 Bruma, C 4P27 Baronova, E O 7P09 Bugaev, A S 6P10 Barsanti, M 5B05 Buhr, B 1A08		5D06	Brandenburg, J E	2B04
Baik, S W 3P18 Brinsmead, W 7P22 Bailey, J E 5C10, 6P22 Brown, I G 4P18, 5A07, 6P09, 6P10 Bailey, V 4A04 Brown, C M 3P20 Baksht, R B 7P06 Brownell, J H 2C03 Baldis, H A 4B03, 5B04 Bruce, R W 2B02 Barakat, F 6C06 Brueck, S R J 5B04 Barnes, D 3P28, 4P35 Bruma, C 4P27 Baronova, E O 7P09 Bugaev, A S 6P10 Barsanti, M 5B05 Buhr, B 1A08	•		Breeze, S	3P31
Bailey, J E 5C10, 6P22 Brown, I G 4P18, 5A07, 6P09, 6P10 Bailey, V 4A04 Brown, C M 3P20 Baksht, R B 7P06 Brownell, J H 2C03 Baldis, H A 4B03, 5B04 Bruce, R W 2B02 Barakat, F 6C06 Brueck, S R J 5B04 Barnes, D 3P28, 4P35 Bruma, C 4P27 Baronova, E O 7P09 Bugaev, A S 6P10 Barsanti, M 5B05 Buhr, B 1A08				7P22
Bailey, V 4A04 6P10 Baker, D A 4C03 Brown, C M 3P20 Baksht, R B 7P06 Brownell, J H 2C03 Baldis, H A 4B03, 5B04 Bruce, R W 2B02 Barakat, F 6C06 Brueck, S R J 5B04 Barnes, D 3P28, 4P35 Bruma, C 4P27 Baronova, E O 7P09 Bugaev, A S 6P10 Barsanti, M 5B05 Buhr, B 1A08				4P18, 5A07, 6P09,
Baker, D A 4C03 Brown, C M 3P20 Baksht, R B 7P06 Brownell, J H 2C03 Baldis, H A 4B03, 5B04 Bruce, R W 2B02 Barakat, F 6C06 Brueck, S R J 5B04 Barnes, D 3P28, 4P35 Bruma, C 4P27 Baronova, E O 7P09 Bugaev, A S 6P10 Barsanti, M 5B05 Buhr, B 1A08	•			•
Baksht, R B 7P06 Brownell, J H 2C03 Baldis, H A 4B03, 5B04 Bruce, R W 2B02 Barakat, F 6C06 Brueck, S R J 5B04 Barnes, D 3P28, 4P35 Bruma, C 4P27 Baronova, E O 7P09 Bugaev, A S 6P10 Barsanti, M 5B05 Buhr, B 1A08			Brown, C M	
Baldis, H A 4B03, 5B04 Bruce, R W 2B02 Barakat, F 6C06 Brueck, S R J 5B04 Barnes, D 3P28, 4P35 Bruma, C 4P27 Baronova, E O 7P09 Bugaev, A S 6P10 Barsanti, M 5B05 Buhr, B 1A08				
Barakat, F 6C06 Brueck, S R J 5B04 Barnes, D 3P28, 4P35 Bruma, C 4P27 Baronova, E O 7P09 Bugaev, A S 6P10 Barsanti, M 5B05 Buhr, B 1A08			•	
Barnes, D 3P28, 4P35 Bruma, C 4P27 Baronova, E O 7P09 Bugaev, A S 6P10 Barsanti, M 5B05 Buhr, B 1A08				
Baronova, E O 7P09 Bugaev, A S 6P10 Barsanti, M 5B05 Buhr, B 1A08				
Barsanti, M 5B05 Buhr, B 1A08			1	
Dalisanti, W			•	
Bartlett, R 7B01-02 Burdette, J 3A01			1	
	Bartlett, R	/B01-02	Burdette, J	SAUT

Burdovitsin, V	5A03	Cho, C H	4P17
Butler, J E	6A02	Cho, T S	7P48
		Choi, E H	7P44, 7P48
		Choi, M C	7P44, 7P48
C		Choi, J J	3P18
Cachoncinlle, C	3P21, 7P11	Choi, P	7P12, 7P13
Calame, J P	3B03-04, 3B05, 3P09,	Choi, Y W	4P17
•	4B01-02, 4B07, 5B07	Choi, M C	7P44, 7P48
Cameron, J M	3P10	Choi, Y S	5P11
Caporaso, G J	4A01-02	Chong, C K	3P12
Cappelli, M A	4D03, 4D04,	Christ, C	4A01-02
cappen, w/	7D01-02, 7D04	Chu, T S	4B01-02, 4B05
Carlson, A L	5C10	Chu, K R	1B10
Carlson, E P	6C06	Chu, P K	3D07, 4P15, 4P16, 6P09
Carmel, Y	1B03, 1B09,	Chung, T H	3P23
Carrier, 1		_	
	3B03-04, 3B05,	Chung, S W	3P23
	3b06, 3P19, 5B12	Chung, K S	5P11
Cartwright, K L	4P34	Ciubotariu, C	4P14
Cassany, B	6P24	Clark, D	7B01-02
Castle, M	3P06, 3P07	Clark, R C	6C04
Catteloino, M	3A01	Clark, R E H	6A03-04
Cauffman, S	4B05	Cochran, F	6C06
Cavazos, T C	7B01-02, 7P59, 7P36	Cochrane, K	7P19
Ceperley, P H	7P53	Coffey, S K	7B01-02
Chakrabarti, N	6P27, 6P28	Cohen, W E	6P12, 6P23, 7P41, 7P42
Chan, Chung	3D07	Cohen, J S	7A04
Chandler, G A	2C01-02, 2C04,	Coleman, P	5D08-09, 6C05, 6C06,
•	2C05, 2C08, 3P32,	,	6P30, 7P03, 7P04, 7P05
-	5C05, 5C06, 7P17	Collela, S C	7P37
Chang, S S	1B10	Collins, L A	7A04
Chang, C H	1B10	Collins, G J	3P22
Chang, C W	1P04	Colombant, D	1C03-04
Chang, D H	5P11	Commisso, R J	4A06, 5D01, 5D10,
Chang, J S	4D06-07		7C08
Chayahara, A	5A06	Comtois, D	3C07
Che, Z	2B08, 2B09, 4P09, 4P25	Connor, K A	3P27
Chebotarev, A V	3P30	Cooke, S J	1B07, 2P08, 3A01,
Chen, C	4B06, 6B06, 7P43	200Kc, 3 3	3A02-03
Chen, S H	1P05, 3P14, 5P10	Cooper, G	5C05
Chen, W	3P05	Cooperstein, G	4A06
Chen, L	1B10	Cordell, J F	4P07
Chen, H Y	1B10	Cordova, S	4A04
Chen, L C	1B10	Coudert, J F	4D05
Chen, Zhiyu	2B08, 4P08, 4P09,	Courtois, L	6P24
Chen, Zhiyu	4P25	Couture, P	3C07
Chen, S H	1P05, 5P10	Coverdale, C A	3P32, 5C07, 6C04
	2P30	Crawford, E	1P14
Chen, F F			4D03
Chen, Xing	3D02-03, 7P63	Crawford, W S	
Chen, Y J	4A01-02	Crisman, A C	6C07
Chen, X	7P63	Cristofolini, A	4P36, 4P37
Chernin, D	1B01-02, 1B06,	Crowley, T P	3P27
	1B07, 2P10, 2P14	Crumley, R J	5D08-09
Chien, Y T	1P02, 1P03	Csanak, G	6A03-04
Chien, C Y	3C07	Cuneo, M E	2C01-02, 5C10,
Childers, F K	7C07		6P22, 6P23, 7P16
Chittenden, J P	5C08, 5C09, 7P29	Cuperman, S	4P27
Cho, G S	7P44, 7P48	Curry, J J	7A01-02, 7A07

			45.47
Czarnaski, M	1B07	Edwards, R	6P17
		Eichenberger, C	4A04
		El-Bandrawy, M	2B03
D		El-Dakroury, A	6A01
Dahlburg, J P	1C03-04	El-Habachi, A	2P28, 6A01
Dale, G E	7d05	Endo, M	4P39
Damelincourt, J J	7A03	Engel, A	7P12, 7P13
Dangor, A E	5C09, 7P29	Eppley, K R	3A01, 4P29
Daniel, R G	4D06-07	Ernst, U	B03, 4P01
Danly, B G	3P10, 4B01-02,	Esposito, B	3P29
	4B07, 5B07, 6D07		
Dashi, L	7P49		
Davidow, J	4D08	F	
Davies, J A	4B06	Faehl, R J	1P16, 6C03,
Davis, P R	6D05		7B01-02, 7B05, 7B06
Davis, J	6C04, 6C05, 6C06,	Failor, B H	6C05, 6C06, 7P04
Davis, 7	6C08, 7P02	Faleski, T J	3C11
Davis, S E	6P26	Faretto, H	7P22
Deb, D N	7C01-02	Farley, J W	7P22
Deeney, C	2C01-02, 3P31,	Farouk, B	3A04
Deeney, C	3P32, 5C01-02,	Fauchais, P	4D05
	5C06, 5C07, 5C10,	Fayne, W R	7P36
	6C04, 6C05, 7P18,	Fedin, D A	7P22, 7P23
	7P30	Fedosejevs, R	2P05
Dognan I H	7B01-02, 7C05	Fedunin, A V	7P06
Degnan, J H DeGroot, J S	7P22	Fehl, D L	2C04, 2C05, 2C08,
	2D01	1011, 02	3P32, 5C05
DeJoseph Jr, C A	3P27	Felch, K	4B01-02, 4B05
Demers, D R	3P04	Feldman, P L	4D09
Denison, D	7P55	Felker, B S	2A08
Deryugin, A A	2C04, 2C05, 2C08,	Ferguson, P	6B01
Derzon, M S	5C05, 5C06, 7P17,	Fernsler, R	3A05, 5A01-02,
	7P18	Terrisier, it	6P01
Deciarlais M.P.	6P22	Filuk, A B	6P22
Desjarlais, M P	3C07	Fink, R L	6D03-04
Desparois, A Dhali, S K	4P23	Fisch, N J	7D03
•	1A03, 5B11, 7P32	Fischer, R P	3B01, 3B02
Dickens, J	5C03-04, 7P26	Fisher, A	6C05, 7P04
Dimant, Y S	2B05, 2B06, 4P03,	Flechtner, D	5P13
Ding, G	4P04	Fleddermann, C B	6P15, 7C04
Dianna N I	3A01, 3P01, 6D07	Fleurier, C	7P11
Dionne, N J DiPietro, V	2B04	Fliflet, A W	3B01, 3B02, 3P16
Dirietro, v Dodson, I	2P12	Flores III, G	4P38
Dorozhkina, D S	7P52	Folan, L	7A05
Dorsey, D J	3C11	Forster, D	6P17
• •	2C06, 5C01-02, 5C06,	Forster, J	2D04-05
Douglas, M R	5C07, 6C04, 7P19, 7P30	Fowler, W E	6P22
Droomer D	4A04	Fowler, C M	6P25, 7C05
Droemer, D	4D05	Frand, K	4P01
Duan, Z	7P12, 7P13	Freeman, B L	3C11
Dumitrescu, C	3C03-04	Frescaline, L	6P24
Dunn, J		Frese, M	3A08, 7B01-02
Dussart, R	7P11	Frese, S D	3A08
Duthie, J	2P15	Freund, H P	2P11
Dwan, T J T	6P16		1B07
		Fridman, I Fruchtman, A	5D02-03, 6P27,
_		riuchunan, A	6P28, 7D03
E		1	0, 20, 7003

Fujiwara, E	4P06, 4P19	Goyer, J R	5D06, 5D08-09, 6P26
	4P40 4P40	Grabowski, C	6P28
Fujiwara, K			
Fujiwara, T	6P02	Graham, W G	1P01
Fukuyama, A	6P05	Granatstein, V	1803, 1809, 3P03, 3P05,
Fulton, D	7B01-02		3P06, 3P07, 3P09, 3P15,
Funatsu, M	6P21		4B04, 5B03, 3P19, 5B12
		Gravelle, D V	4D01-02
		Green, K	4P38
G		Greenly, J B	5C03-04, 7B03, 7P24,
Gadri, R B	2B07, 2B08, 4P08,	,	7P25, 7P26, 7P27
caan, n b	4P25	Gregoire, D J	2P16
Gale, D	7B01-02	Greismann, U	7P54
		Gretchikha, A	7B03
Gallagher, D A	3P11, 3P12, 5B05		
Gallimore, A D	6D03-04	Grishin, V A	7P58
Gammon, B	6D01-02	Grotjohn, T	4P11, 5a08
Ganguly, S	3B02	Grushin, M E	7P55
Ganguly, B N	2A01-02	Guarnieri, R	7P59
Garasi, C J	7P21	Gui, H	2B05, 2B06, 2P24, 4P05
Garate, E	4P10	Guiliani, J L	3D06
Garcia, M	2P22	Guillory, J U	4P30
Gardner, J H	1C03-04	Gundersen, M	2B09, 2P27, 4P07
Garner, M R C	5P05	Guo, H	3P05, 3P15, 4B08,
	2A01-02	- Guo, 11	5B03
Garscadden, A		Cur VAA	
Garven, M	3P03, 3P09, 4b07,	Guo, X M	2B06, 4P05
	5807	Guo, W	2D01
Gaskins, J	4P09	Gupta, D K	1A09
Gaudet, J	1A03	Gustwiller, J	4A04
Gaurand, I	4P24	Guy, T L	3C11
Genoini, T C	6B02-03	Guyadec, E Le	7P65
Gensler, S W	2D06, 5A07, 6C05, 6C07	Guzeyev, M Yu	3P30
Gershon, D	3B03-04, 3B05		
Getty, W D	6P12		
Gholap, A V	3C12	н	
Gier, H	4P41	Hadidi, K	4P38
Gilbert, C	7P03	Hafizi, B	2P02, 3C05
Gilgenbach, R M	1P06, 1P07, 2P01, 4P20,	Haill, T	7P21
dilgeribacii, k ivi			
Cilile and Til	6P12, 6P23, 7P41, 7P42	Haines, M G	5C07, 5C08, 5C09, 7P29
Gilliland, T L	2C08, 5C05	Hakel, P	7P23
Girard, F	7P65	Hala, A M	2P26, 3P24
Giulianai, J L	6A02	Hall, C A	2C01-02, 7P16
Godyak, V A	2A03	Hamatani, H	4D03
Goebel, D M	2P06	Hamilton, I S	3C11
Goforth, J H	6P25, 7C05	Hammer, J H	2C01-02, 7P16
Gogawale, S V	7 P51	Hammer, D A	5C03-04, 7P24,
Goilingo, R P	1P14		7P25, 7P26, 7P27, 7P28
Golby, K E	7P36	Hammer, E E	7P68
Gold, S H	3B02, 3P16	Hammerberg, J E	3A06-07
Golden, J	7P67	Han, W K	3P18
Goldsack, T J	6P17	Hansen, R J	3P16, 6B04, 7C01-02
Golkowski, Cz	5P12, 5P13, 5P14	Hansen, S	7P22, 7P23
Golovkin, I	7P22	Hansen, T N	7P12
Golovkin, A	7P23	Hanson, D	2C01-02, 6P21, 6P22
Good, G R	4B01-02, 6B04, 7C01-02	Hargreaves, T A	4B01-02, 6B04
Goodrich, P J	5D08-09, 6P30	Harper, M K	2D03
Gornostaeva, O	4P10	Harper-Slaboszewicz, V J	5D05
Gotze, S	7P11	Harriet, S B	3P12
Gousset, G	3D08	Hartemann, F V	4B03
_			

Hartemann, R V	5B04	Huey, H E	3P12, 3P13
	4P01	Hughes, T	4A01-02
Hartmann, W		•	4D06-07
Hartog, D J D	1P14	Huie, R F	
Hatfield, L L	1P07, 5B11, 6B01	Humphries Jr, S	3A01, 4P29
Hawn, R	5C05	Hunt, E	4A04
	7P59, 7P31	Hur, Min Sup	2P21
Haworth, M		·	3P21
Hayashi, Y	5P12, 5P13	Hure, L	
Hayashi, T	4P39	Hussey, T W	5B01-02
Hayashida, T	4P06	Hutcherson, K	5P06
	1P17	Hutchins, J	2P15
Hayes, S			
Hązelton, R C	6C06	Hwang, S M	3P18
Hebeler, F	7P34	•	4
Heberlein, J	4D05		
	2C08, 5C05		
Hebron, D E		lalera mala C	7007 7000
Hegeler, F	5B04, 7P33	Idzorek, G	7B07, 7B08
Heinen, V O	1B08	Inaba, T	4P39
Helfritch, D J	4D09	Inoue, T	6P13
•	5B11, 6B01	Intrator, T P	7B01-02
Hemmert, D			1P08
Hendricks, K	6B01, 6B05, 6B08,	Irzak, M A	
	7P59, 7P31, 7P36, 7P39	Ishida, T	4P39
Hendry, R	3D06	Ishihara, O	4P19
	3D04-05, 4P26	Ishii, S	6P14, 7P61
Henins, I			2P29
Heritage, J P	4B03, 5B04	Ishikawa, M	
Herrera, D H	7C05	Islan, N E	7C04
Herrmann, H W	3D04-05, 4P26	Isono, R	5A04
Herron, J T	4D06-07	Itano, W M	7P64
			4P40
Hershkowitz, N	1A08, 2D02, 2D03,	Itoyama, K	
	2P26, 3P24, 3P25	Ivanov, I	5B12
Hess, M	7P43	lvers, J D	5P12, 5P13, 5P14
Hibert, C	4P24	lves, L	4B04
	4A07-08,	Iwao, T	4P39
Hinschelwood, D D	•	10000, 1	71 33
	4A09, 4A10, 6A02,		
	6P19, 6P20		
Hirano, T	4P39	J	
Hirata, Y	3P12	James, B	4B01-02
	3P16	Jaworski, A	3B03-04
Hirshfield, J L			
Ho, C H	5B04	Jaynes, R L	6P12, 6P23, 7P4, 7P42
Hochi, A	6A07	Jelenkovic, B M	7P64
Hochman, J M	7P42	Jensen, K L	6D03-04, 6D06
Hodge, A	4P09	Jiang, W	7P32
		Jiang, Z	3C07
Hoffman, J R	2B09, 4P07	_	
Hogan, B	3P06, 3P07	Jing, Li	7P49
Holber, W	3D02-03	Jinshui, Shi	7P49
Holian, B L	3A06-07	Jobe, D O	2C08, 5C05, 7P17
	1P14	John, P I	1A09
Holly, D J			4A04, 6P22
Hong, D	7P11	Johnson, D J	and the second s
Horino, Y	5A06	Johnston, M	6P12
Horiuchi, M	6A08	Johnston, T W	3C07
Horsky, T N	5A05, 6P11	Jory, H	4B01-02, 4B05
		Joshi, C	2C09, 4P07
Hotta, Eiki	1P12, 2P29, 6P07,		
	6P08	Joshi, R P	7C04
Houck, T	4A01-02	Joyce, G	3A05, 3A09
Hsueh, H P	2A08	Jung, Y	7P44
	1P04, 5P10	Jung, Y H	5P11
Hu, Y			
Huang, T F	4D08	Juschkin, L	7P13
Huba, J D	3A09	·	
Hubbard, R F	2P02, 3C05, 3C06		
	•		

K		Korber, A	6A06, 7P57
Kalluri, D K	2B10, 2P23	Korovin, S D	7P34
Kamiya, T	6P21	Kortbawi, D	5D06, 6P26, 7P04, 7C07
Kan, Y	4P17	Kory, C L	1B05
Kanbe, N	2P29	Kostas, C	1B06, 1B07
Kang, J H	2P21	Kovalchuk, B M	7P06
Kang, W L	4P21	Kovaleski, S D	4P20
Kantsyre, V L	7P22, 7P23	Krainsky, I L	2P09
Karakaya, F	2B07, 2B08, 3P35,	Krasheninnikov, S f	6P03
Katakaya, I	4P08, 4P25	Krasnoperov, L N	3D01
Varandikar C I	7P51	Kreischer, K E	3P04
Karandikar, S J		I .	
Karasik, M	3P33	Krisch, I	7P12, 7P13
Kasuya, K	6P21	Krishman, M	2D06, 5A07, 6C07
Katsouleas, T	2B09, 4P07	Krishtopa, L G	3D01
Katsuki, S	2C07, 5D04, 7P08	Kristiansen, M	1A03, 5B11, 6B01, 7P32
Keefer, D	5D07, 7C06	Krompholz, H	1P07, 5B11, 6B01
Keidar, M	4P18	Krueger, W	3A01
Keinigs, R K	7P15	Kulkarni, S V	1A09
Kelly, K L	2B05, 2B06, 4P03,	Kull, Alan E	4D04
•	4P04, 4P05	Kunze, H-J	7P13
Kelly-Wintenberg, K	2B07, 2B08, 4P09	Kuo, S	2B10
Khaimovitch, M I	3P30	Kurunczi, P	2P28
Kharlov, A	2P27	Kushner, M J	1D05, 1D07
Khedr, M Atta	2P04, 3P24	Kusse, B R	7P24
	3C07	Kwan, TJT	4A03
Kieffer, J C			3D07, 4P15, 4P16,
Kikuchi, H	1A07, 4C04	Kwok, T K	
Kim, G H	2D02, 4P17, 5P11		6P09
Kim, W	5P08		
Kim, S J	4D06-07	_	
Kinder, Ron L	1D07	L	
King, J C	7C05	Labetsky, A Yu	7P06
King, L B	7P64	LaCour, M	6B08, 7P59, 7P31
Kinkead, A K	3B02, 3P16	LaFontaine, B	3C07
Kirkpatric, R	1P15, 1P16, 7B01-02,	Lai, Shu T	2A07
	7B07, 7B08,	Lai, K F	1D03-04
Kirshner, M F	6B04	1 = 1 T	
	ODO-	Lai, J T	5P10
Kishek, R A	1P07	Lai, K C	5P10 4D08
Kishek, R A Kishi, Y	1P07	Lai, K C	
Kishi, Y	1P07 6P21	Lai, K C Laimer, J	4D08 7P47
Kishi, Y Kitamura, D	1P07 6P21 6P02	Lai, K C Laimer, J Lake, P	4D08 7P47 5C10
Kishi, Y Kitamura, D Kiuttu, G F	1P07 6P21 6P02 7B01-02, 7B05, 7C06	Lai, K C Laimer, J Lake, P Lampe, M	4D08 7P47 5C10 3A05, 5A01-02
Kishi, Y Kitamura, D Kiuttu, G F Klapisch, M	1P07 6P21 6P02 7B01-02, 7B05, 7C06 1C03-04	Lai, K C Laimer, J Lake, P Lampe, M Lamppa, K	4D08 7P47 5C10 3A05, 5A01-02 6P21
Kishi, Y Kitamura, D Kiuttu, G F Klapisch, M Klepper, C C	1P07 6P21 6P02 7B01-02, 7B05, 7C06 1C03-04 5D01, 6C06	Lai, K C Laimer, J Lake, P Lampe, M Lamppa, K Lan, Y C	4D08 7P47 5C10 3A05, 5A01-02 6P21 3P14, 5P10
Kishi, Y Kitamura, D Kiuttu, G F Klapisch, M Klepper, C C Klimov, A I	1P07 6P21 6P02 7B01-02, 7B05, 7C06 1C03-04 5D01, 6C06 4C09	Lai, K C Laimer, J Lake, P Lampe, M Lamppa, K Lan, Y C Landahl, E C	4D08 7P47 5C10 3A05, 5A01-02 6P21 3P14, 5P10 4B03, 5B04
Kishi, Y Kitamura, D Kiuttu, G F Klapisch, M Klepper, C C Klimov, A I Kline, J F	1P07 6P21 6P02 7B01-02, 7B05, 7C06 1C03-04 5D01, 6C06 4C09 2B04	Lai, K C Laimer, J Lake, P Lampe, M Lamppa, K Lan, Y C Landahl, E C Landen, O	4D08 7P47 5C10 3A05, 5A01-02 6P21 3P14, 5P10 4B03, 5B04 2C01-02, 7P16
Kishi, Y Kitamura, D Kiuttu, G F Klapisch, M Klepper, C C Klimov, A I Kline, J F Kling, R	1P07 6P21 6P02 7B01-02, 7B05, 7C06 1C03-04 5D01, 6C06 4C09 2B04 7P54	Lai, K C Laimer, J Lake, P Lampe, M Lamppa, K Lan, Y C Landahl, E C Landen, O Langan, J G	4D08 7P47 5C10 3A05, 5A01-02 6P21 3P14, 5P10 4B03, 5B04 2C01-02, 7P16 2A08
Kishi, Y Kitamura, D Kiuttu, G F Klapisch, M Klepper, C C Klimov, A I Kline, J F Kling, R Ko, J J	1P07 6P21 6P02 7B01-02, 7B05, 7C06 1C03-04 5D01, 6C06 4C09 2B04 7P54 7P44, 7P48	Lai, K C Laimer, J Lake, P Lampe, M Lamppa, K Lan, Y C Landahl, E C Landen, O Langan, J G Larour, J	4D08 7P47 5C10 3A05, 5A01-02 6P21 3P14, 5P10 4B03, 5B04 2C01-02, 7P16 2A08 7P12, 7P13
Kishi, Y Kitamura, D Kiuttu, G F Klapisch, M Klepper, C C Klimov, A I Kline, J F Kling, R Ko, J J Ko, K-C	1P07 6P21 6P02 7B01-02, 7B05, 7C06 1C03-04 5D01, 6C06 4C09 2B04 7P54 7P44, 7P48 2P29, 6P08	Lai, K C Laimer, J Lake, P Lampe, M Lamppa, K Lan, Y C Landahl, E C Landen, O Langan, J G	4D08 7P47 5C10 3A05, 5A01-02 6P21 3P14, 5P10 4B03, 5B04 2C01-02, 7P16 2A08 7P12, 7P13 2B01-02, 4P12,
Kishi, Y Kitamura, D Kiuttu, G F Klapisch, M Klepper, C C Klimov, A I Kline, J F Kling, R Ko, J J Ko, K-C Ko, J J	1P07 6P21 6P02 7B01-02, 7B05, 7C06 1C03-04 5D01, 6C06 4C09 2B04 7P54 7P44, 7P48 2P29, 6P08 7P48	Lai, K C Laimer, J Lake, P Lampe, M Lamppa, K Lan, Y C Landahl, E C Landen, O Langan, J G Larour, J Laroussi, M	4D08 7P47 5C10 3A05, 5A01-02 6P21 3P14, 5P10 4B03, 5B04 2C01-02, 7P16 2A08 7P12, 7P13 2B01-02, 4P12, 4P13, 4P21, 4P22
Kishi, Y Kitamura, D Kiuttu, G F Klapisch, M Klepper, C C Klimov, A I Kline, J F Kling, R Ko, J J Ko, K-C Ko, J J Ko, K C	1P07 6P21 6P02 7B01-02, 7B05, 7C06 1C03-04 5D01, 6C06 4C09 2B04 7P54 7P44, 7P48 2P29, 6P08 7P48 5P11	Lai, K C Laimer, J Lake, P Lampe, M Lamppa, K Lan, Y C Landahl, E C Landen, O Langan, J G Larour, J Laroussi, M Lash, J S	4D08 7P47 5C10 3A05, 5A01-02 6P21 3P14, 5P10 4B03, 5B04 2C01-02, 7P16 2A08 7P12, 7P13 2B01-02, 4P12, 4P13, 4P21, 4P22 2C09, 2C08, 5C05
Kishi, Y Kitamura, D Kiuttu, G F Klapisch, M Klepper, C C Klimov, A I Kline, J F Kling, R Ko, J J Ko, K-C Ko, J J Ko, K C Kobayashi, S	1P07 6P21 6P02 7B01-02, 7B05, 7C06 1C03-04 5D01, 6C06 4C09 2B04 7P54 7P44, 7P48 2P29, 6P08 7P48 5P11 1B03, 1B09, 3P19	Lai, K C Laimer, J Lake, P Lampe, M Lamppa, K Lan, Y C Landahl, E C Landen, O Langan, J G Larour, J Laroussi, M	4D08 7P47 5C10 3A05, 5A01-02 6P21 3P14, 5P10 4B03, 5B04 2C01-02, 7P16 2A08 7P12, 7P13 2B01-02, 4P12, 4P13, 4P21, 4P22 2C09, 2C08, 5C05 1P06, 1P07, 2P01,
Kishi, Y Kitamura, D Kiuttu, G F Klapisch, M Klepper, C C Klimov, A I Kline, J F Kling, R Ko, J J Ko, K-C Ko, J J Ko, K C Kobayashi, S Koch, J	1P07 6P21 6P02 7B01-02, 7B05, 7C06 1C03-04 5D01, 6C06 4C09 2B04 7P54 7P44, 7P48 2P29, 6P08 7P48 5P11 1B03, 1B09, 3P19 2C01-02, 7P16	Lai, K C Laimer, J Lake, P Lampe, M Lamppa, K Lan, Y C Landahl, E C Landen, O Langan, J G Larour, J Laroussi, M Lash, J S	4D08 7P47 5C10 3A05, 5A01-02 6P21 3P14, 5P10 4B03, 5B04 2C01-02, 7P16 2A08 7P12, 7P13 2B01-02, 4P12, 4P13, 4P21, 4P22 2C09, 2C08, 5C05 1P06, 1P07, 2P01, 2P10, 4P20, 6D05,
Kishi, Y Kitamura, D Kiuttu, G F Klapisch, M Klepper, C C Klimov, A I Kline, J F Kling, R Ko, J J Ko, K-C Ko, J J Ko, K C Kobayashi, S Koch, J Kohno, S	1P07 6P21 6P02 7B01-02, 7B05, 7C06 1C03-04 5D01, 6C06 4C09 2B04 7P54 7P44, 7P48 2P29, 6P08 7P48 5P11 1B03, 1B09, 3P19 2C01-02, 7P16 5D04, 7P08	Lai, K C Laimer, J Lake, P Lampe, M Lamppa, K Lan, Y C Landahl, E C Landen, O Langan, J G Larour, J Laroussi, M Lash, J S Lau, Y Y	4D08 7P47 5C10 3A05, 5A01-02 6P21 3P14, 5P10 4B03, 5B04 2C01-02, 7P16 2A08 7P12, 7P13 2B01-02, 4P12, 4P13, 4P21, 4P22 2C09, 2C08, 5C05 1P06, 1P07, 2P01, 2P10, 4P20, 6D05, 6D06, 6P12, 6P23, 7P42
Kishi, Y Kitamura, D Kiuttu, G F Klapisch, M Klepper, C C Klimov, A I Kline, J F Kling, R Ko, J J Ko, K-C Ko, J J Ko, K C Kobayashi, S Koch, J Kohno, S Koinuma, H	1P07 6P21 6P02 7B01-02, 7B05, 7C06 1C03-04 5D01, 6C06 4C09 2B04 7P54 7P44, 7P48 2P29, 6P08 7P48 5P11 1B03, 1B09, 3P19 2C01-02, 7P16 5D04, 7P08 6P21	Lai, K C Laimer, J Lake, P Lampe, M Lamppa, K Lan, Y C Landahl, E C Landen, O Langan, J G Larour, J Laroussi, M Lash, J S Lau, Y Y	4D08 7P47 5C10 3A05, 5A01-02 6P21 3P14, 5P10 4B03, 5B04 2C01-02, 7P16 2A08 7P12, 7P13 2B01-02, 4P12, 4P13, 4P21, 4P22 2C09, 2C08, 5C05 1P06, 1P07, 2P01, 2P10, 4P20, 6D05, 6D06, 6P12, 6P23, 7P42 7P41
Kishi, Y Kitamura, D Kiuttu, G F Klapisch, M Klepper, C C Klimov, A I Kline, J F Kling, R Ko, J J Ko, K-C Ko, J J Ko, K C Kobayashi, S Koch, J Kohno, S Koinuma, H Kokshenev, V A	1P07 6P21 6P02 7B01-02, 7B05, 7C06 1C03-04 5D01, 6C06 4C09 2B04 7P54 7P44, 7P48 2P29, 6P08 7P48 5P11 1B03, 1B09, 3P19 2C01-02, 7P16 5D04, 7P08 6P21 7P06	Lai, K C Laimer, J Lake, P Lampe, M Lamppa, K Lan, Y C Landahl, E C Landen, O Langan, J G Larour, J Laroussi, M Lash, J S Lau, Y Y Laurent, L L Lawler, J E	4D08 7P47 5C10 3A05, 5A01-02 6P21 3P14, 5P10 4B03, 5B04 2C01-02, 7P16 2A08 7P12, 7P13 2B01-02, 4P12, 4P13, 4P21, 4P22 2C09, 2C08, 5C05 1P06, 1P07, 2P01, 2P10, 4P20, 6D05, 6D06, 6P12, 6P23, 7P42 7P41 5P07, 7A01-02, 7A07
Kishi, Y Kitamura, D Kiuttu, G F Klapisch, M Klepper, C C Klimov, A I Kline, J F Kling, R Ko, J J Ko, K-C Ko, J J Ko, K C Kobayashi, S Koch, J Kohno, S Koinuma, H	1P07 6P21 6P02 7B01-02, 7B05, 7C06 1C03-04 5D01, 6C06 4C09 2B04 7P54 7P44, 7P48 2P29, 6P08 7P48 5P11 1B03, 1B09, 3P19 2C01-02, 7P16 5D04, 7P08 6P21 7P06 4C06	Lai, K C Laimer, J Lake, P Lampe, M Lamppa, K Lan, Y C Landahl, E C Landen, O Langan, J G Larour, J Laroussi, M Lash, J S Lau, Y Y	4D08 7P47 5C10 3A05, 5A01-02 6P21 3P14, 5P10 4B03, 5B04 2C01-02, 7P16 2A08 7P12, 7P13 2B01-02, 4P12, 4P13, 4P21, 4P22 2C09, 2C08, 5C05 1P06, 1P07, 2P01, 2P10, 4P20, 6D05, 6D06, 6P12, 6P23, 7P42 7P41 5P07, 7A01-02, 7A07 3P03, 3P06, 3P07,
Kishi, Y Kitamura, D Kiuttu, G F Klapisch, M Klepper, C C Klimov, A I Kline, J F Kling, R Ko, J J Ko, K-C Ko, J J Ko, K C Kobayashi, S Koch, J Kohno, S Koinuma, H Kokshenev, V A	1P07 6P21 6P02 7B01-02, 7B05, 7C06 1C03-04 5D01, 6C06 4C09 2B04 7P54 7P44, 7P48 2P29, 6P08 7P48 5P11 1B03, 1B09, 3P19 2C01-02, 7P16 5D04, 7P08 6P21 7P06	Lai, K C Laimer, J Lake, P Lampe, M Lamppa, K Lan, Y C Landahl, E C Landen, O Langan, J G Larour, J Laroussi, M Lash, J S Lau, Y Y Laurent, L L Lawler, J E Lawson, W	4D08 7P47 5C10 3A05, 5A01-02 6P21 3P14, 5P10 4B03, 5B04 2C01-02, 7P16 2A08 7P12, 7P13 2B01-02, 4P12, 4P13, 4P21, 4P22 2C09, 2C08, 5C05 1P06, 1P07, 2P01, 2P10, 4P20, 6D05, 6D06, 6P12, 6P23, 7P42 7P41 5P07, 7A01-02, 7A07 3P03, 3P06, 3P07, 3P08, 3P09, 4B01-02
Kishi, Y Kitamura, D Kiuttu, G F Klapisch, M Klepper, C C Klimov, A I Kline, J F Kling, R Ko, J J Ko, K-C Ko, J J Ko, K C Kobayashi, S Koch, J Kohno, S Koinuma, H Kokshenev, V A Koloc, P M	1P07 6P21 6P02 7B01-02, 7B05, 7C06 1C03-04 5D01, 6C06 4C09 2B04 7P54 7P44, 7P48 2P29, 6P08 7P48 5P11 1B03, 1B09, 3P19 2C01-02, 7P16 5D04, 7P08 6P21 7P06 4C06	Lai, K C Laimer, J Lake, P Lampe, M Lamppa, K Lan, Y C Landahl, E C Landen, O Langan, J G Larour, J Laroussi, M Lash, J S Lau, Y Y Laurent, L L Lawler, J E	4D08 7P47 5C10 3A05, 5A01-02 6P21 3P14, 5P10 4B03, 5B04 2C01-02, 7P16 2A08 7P12, 7P13 2B01-02, 4P12, 4P13, 4P21, 4P22 2C09, 2C08, 5C05 1P06, 1P07, 2P01, 2P10, 4P20, 6D05, 6D06, 6P12, 6P23, 7P42 7P41 5P07, 7A01-02, 7A07 3P03, 3P06, 3P07,

Lazier, L	7P17	Lucek, S G	5C08
Lebedev, S V	5C08, 5C09, 7P21	Ludeking, L	1P17
Lee, H J	2B10, 2P21, 2P23	Luginsland, J W	4P28, 1P16, 6B05,
Lee, J K	2P21, 5P08, 5P09		7P35, 7P36, 7P37,
Lee, J H	2B10		7P38, 7P39, 7P40
Lee, S	3P18	Luhmann, J	5P01, 5P02
	2P23	Luhmann Jr, N C	3P11, 3P12, 3P13,
Lee, J H	7P14	Editination 51, IN C	4B03, 5b04
Lee, H		Lunney, J G	7P12
Lee, H S	4P17	Lunney, J G	7712
Lee, J K	5P08, 5P09		
Lee, K	6D05		
Leeper, R	2C05, 2C08, 5005, 6P21	M	2625
LeGalloudec, N	7P22	MacFarlane, J J	2C05
LeGalloudec, B	7P22	Mackie, W A	6D05
Lehecka, T	3P20	MacLeod, G	4A04
Lehr, F M	7B01-02	Madziwa, T G	2P30
Lehr, J	1A03, 7C03	Maenchen, J	4A04
Lei, J	3P27	Maeyama, M	4P28, 4P33
Lemke, R W	6B02-03, 7P40	Maly, J	1A02
Lenef, A	5P04	Mancini, R C	7P22, 7P23
Leonhardt, D	5A01-02, 6P01	Manheimer, W M	1B04, 2P10, 3A05,
Leou, K C	1P02, 1P03, 3P12	,	5A01-02
Leung, W C	1A06, 2A06	Mankowski, J	1A03
Levine, J	6C05, 6C06, 7P04,7P05	Marakhtanov, A M	2A05
Levush, B	1B01-02, 1B06, 1B07,	Mardahl, P J	3P02
Levusii, b	2P11, 2P14, 3A01,	Maron, Y	5D01, 5D02-03, 6P28
		Marrese, C M	6D03-04
	3A02-03, 4B01-02,	i e	7C05
	5B01-02, 5B07, 6D06,	Marsh, S P	
	6D07	Martin, F	3C07
Leylekian, L	3D08	Martin, P	1P13
Lho, T	2D02	Martin, R L	7A04
Li, S T	4D08	Martinez, E C	7C05
Li, Y	3C03-04	Martinez, C	5D05
Lichtenberg, A	1D08	Maruyama, T	5A06
Lider, V V	7P09	Maslennikov, S P	3P30
Lieberman, M A	2A04, 2A05	Mathuthu, M	3C12
Lim, G H	4P17	Matsumoto, T	4C05
Lin, A T	3P12, 5B03	Matuska, W	5C05, 5C06, 7P18
Lin, T L	1P02, 1P03, 1P04, 5P10	Matzen, M K	5C06
Lin, C M	5P10	Mawassi, R	3C07
Lindemuth, I R	1P15, 1P16, 6P25,	Mayo, R M	3C08
	7B01-02, 7B06,	McClure, T	3A01
	7B07, 7B08	McCrorey, D	7P22
Lindsay, P A	7P63	McCullough, W	7B01-02
Liou, R	2P06	McCurdy, A H	3P10
Lisitsyn, 1 V	2C07, 5D04, 7P08	McDermott, D B	3P11, 3P12, 3P13
Lisovskiy, V A	3P34	McGrath, R T	2A08
Lister, G G	6A05, 7A07	McGurn, J S	2C08, 3P32, 5C05, 6C05
Liu, F	6P15	McKenney, J	3P32, 5C05, 7P17
Lloyd, I	3B03-04, 3B05	McLenithan, K D	5C06
	7A06	McNeely, M J	2P13
Loffhagen, D	6P25, 7C05	Meacham, G`B K	1P11
Lopex, E A			7D01-02
Loree, D L	7P36	Meezan, N B	5A01-02, 6P01, 6A02
Lovesee, A	7P31	Meger, R A	•
Loza, O	5B12	Mehanna, E A	7P60
Lu, Q	1D03-04	Mehlhorn, T A	6P21, 6P22, 7P16
Lu, J	1D05	Melnik, A V	3P30

Menniger, R L AAOA, 6P2Z, 6P23 Nelson, B A 1P14 Menniger, K L 7A01-02 Neri, J M AAO7-08, AAO9, AAO, GP19, 6P20 Mental, J F901, 5P02 Neuber, A 1P07, 5911, 6P20 Mercure, H P 3C07 Ng. A 1C01-02 Mersenyashin, A I 4C08 Ng. A 1C01-02 Meseryashin, A I 4C08 Ng. A 2P14 Meseryashin, A I 4C08 Ng. A 1C01-02 Misaki, Y 6604 Nelson, J 4D08 Misakin, M 3P26 Nielson, J 4B04 Mishalia, M 3P26 Nielson, J 4B04 Mishalia, T 1P12 Nielson, J 4B04 Myamoto, S 6P13 Nikiforov, S A 4P17 Myasita, T 1P12 Nikolaeva, V I 7P58 Mizubara, M 4B04 Nikere, L 4P24 Mochizuki, T 6P13 Nikoflaeva, V I 7P58 Mortie, D 2C08, 5C05, 7P04 Nusia, M J 4D06-07 Mortier, D				
Mennigen, K.	Menge PR	4A04, 6P22, 6P23	Nelson, B A	1P14
Menninger, W L 2P06 Mental, J 5P01, 5P02 Mental, J 5P01, 5P02 Mental, J 5P01, 5P02 Mental, J 5P01, 5P02 Memora, J M 7P53 Mercure, H P 3C07 Mercure, H P 3C08 Mercure	•	-	I to the second	4A07-08, 4A09,
Mentel, J. Menz, D. M. Merue, H. P. More, D. M. Merue, H. P. More, D. M. Merue, H. P. M. Merue, H. P. More, M. M. Mesenyashin, A. I. M. Mesenyashin, A. M. Mesenyash			·	4A10, 6P19, 6P20
Merz, D. M. 753 Newman, J.W. 3C08 Merzure, H. P. 3C07 Ng. A. 1C01-02 Merzure, H. P. 3C07 Ng. A. 1C01-02 Meseryrashin, A.I. 4C08 Ng. M. T. 2P14 Meseryrashin, A.I. 4C08 Ng. M. T. 4P19 Misaki, Y. 6B04 Ng. M. T. 4B01-02, 6D07 Misaki, Y. 6B04 Ng. M. T. 4B04 Mischel, T. B. 7F64 Ng. M. T. 4B04 Miyamoto, S. 6P13 Nikforov, S. A. 4P17 Mizolek, A.W. 4D04 Ng. A. 17F55 Mizolek, A.W. 4B04 Nikfavech, M. 4P24 Mock, R.C. 2C08, 5C05, 7P02 Nikfavech, M. 4P24 Molock, R.C. 2C08, 5C05, 7P02 Nikfavech, M. 4P24 Montal, J. A. 4B04			Neuber, A	
Mercine, H. P. 3CO7 Ng. A 1 Co1-02 Merkle, L. D 4P28 Ngo. M T 4P14 Mesenyashin, A.1 4C08 Nguyen, K. T 4B01-02, 6D07 Mik, S. 4P19 Nguyen, K. T 4B01-02, 6D07 Misskian, M. 3P26 Nielson, J. 4B04 Misskian, M. 3P26 Nielson, J. 4B04 Mitskell, T. B 7P64 Niemann, C. 1P10 Miyaka, M. 6P14, 7P61 Niemel, J. 6C06 Miyaria, T. 1P12 Nikifrorov, S. A. 4P17 Mizolek, A.W. 4D06-07 Nikiravech, M. 4P24 Mizolak, A. W. 4B04 Nisen, J. 3C03-04 Mochizuki, T. 6P13 Nusca, M.J. 4D06-07 Mortilla, I. 4A04 Nisen, J. 3C3-04 Mortillo, T. C. 2B09 AD1, 3A02-03 AP18 Mortillo, T. C. 2B07, 2B08, 4P09 Obenschain, S. 3P20 Morse, R. 7P21 Oks, E. 2D06 Morse, R.	•			
Merkle, L. D. 4P28 Ngo, M.T. 2P14 Mesenyashin, A. I. 4C08 Nguyen, K. T. 3P03 Milki, S. 4P19 Nguyen, K. T. 3P03 Mirsaki, Y. 6B04 Nguyen, K. T. 3P03 Misaki, Y. 6B04 Nielsen, D. 5C05 Misaki, Y. 6B04 Nielsen, D. 5C05 Mischell, T. B. 7P64 Niemann, C. 1B10 Mikadian, M. 3P26 Nielsen, J. 6C06 Miyamoto, S. 6P13 Nikiforov, S. A. 4P17 Miyasita, T. 1P12 Nikiforov, S. A. 4P17 Mizolek, A. W. 4D06-07 Nikiforov, S. A. 4P17 Mizola, T. G. 4B04 Nikirova, A. 4P24 Mochic, T. G. 2C08, SC05, 7P02 Nikirova, A. 4P24 Montie, T. C. 2C08, SC05, 7P02 Nikirova, A. 4B04 Morr, W. B. 2B09 AD04-03 Nusca, M. Morri, W. B. 2B09 AD01, GC05, 7P04 On, J. H. 3P18				1C01-02
Mosenyashin, A I 4C08 Nguyen, K T 4B01-02, 6D07 Miki, S 4P19 Nguyen, K 3P03 Misakia, Y 6B04 Nielson, D 5C05 Misakian, M 3P26 Nielson, J 4B04 Mitchell, T B 7P64 Nienon, C 1P10 Mitchell, T B 7P64 Niemann, C 1P10 Miyake, M 6F14, 7P61 Niemel, J 6C06 Miyarioto, S 6F13 Nikfrorov, S A 4P17 Mysalia, T 1P12 Nikolaeva, V 1 7P58 Mizulek, A W 4D06-07 Nikravech, M 4P24 AV24 Mcchizuki, T 6F13 Nikravech, M 4P24 AV24 Mochizuki, T 6F13 Nusinovich, G 1803, 3P07, 4b08, Mortie, T C 2C08, 5C05, 7P02 Nusinovich, G 1803, 3P07, 4b08, Mortie, T C 2B07, 2B08, 4P09 Obenschain, S 3P20 Mortie, T C 2B07, 2B08, 4P09 Obenschain, S 3P20 Mortie, T C 2B07, 2B08, 4P09 Oks, E 208, 5A03, 6P10 Morse, Ri 7P21 Oks, E 2008, 5A03, 6P10 Moselby, M 6A01 Oks, E 2008,			-	2P14
Miki, S			1	
Mingaleev, A R 7P27 Nguyen, H 4D08 Misakin, M 3P26 Misakin, M 3P26 Miskin, M 3P26 Misken, D 5C05 Misakin, M 3P26 Misken, D 4804 Misken, D 5C05 Miskon, J 4804 Misken, M 6P14, 7P61 Miyamoto, S 6P13 Mikrawoto, S 6P13 Mikrawoto, S A 4P17 Miyasita, T 1P12 Mizolek, AW 4D06-07 Mizuhara, M 4B04 Mizuhara, M 4B04 Mizuhara, M 4B04 Mizuhara, M 4B04 Mindelli, A 1B07, 3A01, 3A02-03 Mortiero, O R 4P18 Mortiero	•			
Misaki, Y Misakian, M Misakian, T Misakian, M Misakian, T Misakian, M Misakian, T Misakian, M Misakian, T Misakian, M Misakian, M Misakian, T Misakian, M Mosilian, M Mosilian, M Mosilian, M Moselly,			1 -	
Misakian, M Misakian, T Misakian, T Misakian, M Misakian, T Misakian, M Mosharian, B Moosman, B Mori, W B Mossan, B Mori, W B Mossan, B Mori, W B Mori, W B Mossan, B Mori, W B Mossan, B Mori, W B Mossan, B Mori, W B Mori, W B Mossan, B Mori, W B Mori, W B Mossan, B Mori, W B Mossan, B Mori, W B Mori, W B Mossan, B Mori, W B Mori,	_		1 -	
Mitchell, T.B. 7P64 Niemann, C. 1P10 Niemaln, C. 1P10 Nijarke, M. 6P14, 7P61 Niemel, J. 6C06 Nijarmoto, S. 6P13 Nikiforov, S. A. 4P17 Nijarmoto, S. Mijarmoto, S. A. 4P17 Nijarmoto, S. Mijarmoto, S. A. 4P17 Nijarmoto, S. A. 4P24 Nijarmoto, S. A. 4P24 Nijarmoto, S. A. 4P24 Nijarmoto, S. A. 4P06-07 Nijarmoto, S. A. 4P06-07 Nijarmoto, S. A. 4P24 Nijarmoto, S. A. 4P06-07 Nijarmoto, S. A. 4P24 Nijarmoto, S. A. 4P08 Nijarmoto, S. A. 4P08 Nijarmoto, S. A. 4P08 Nijarmoto, S. A. 4P09 Nijarmoto, S. A. 4P08 Nijarmoto, S. A. 4P09 Nijarmoto, S. A. 4P08 Nijarmoto, S. A. 4P08 Nijarmoto, S. A. 4P09 Nijarmoto, S. A. 4P08 Nijar				
Miyake, M Myamoto, S 6P13 Miyaka, T Miyasita, T Mizolek, A W Myasita, T Mizolek, A W Mizuhara, M Med A Mizuhara, M Mochizuki, T Mock, R C Molina, I Mondelli, A Mondelli, C Moore, C Moore, C Moore, C Moore, R Moors, Ri Morse, Ri Moschella, JJ Moschella, JJ Moschell, JJ Moschell, JJ Moschell, JJ Moschell, JJ Moscher, D Moschell, JJ Moscher, D Moscher, O Morte, O Morte, O Morte, O Morte, O Morte, R Morte, O Morte, O			1	
Miyamoto, S Miyamoto, S Miyamoto, S Miyasita, T Miyasita, T Mizolek, A W Mozolek, T Mozolek, C Mo			1	
Miyasita, T Mizolek, A W Miyasita, T Mizolek, A W Miyasita, T Mizolek, A W Mizohara, M Mochizuki, T Mock, R C More, C Molina, I Monteiro, O R More, C Moore, C Moore, C Moosman, B More, R Moselhy, M Moselhy, M Moselhy, M Moselhy, M Mosely, D Moselhy, M Moser, D Moser, D Moser, D Moselhy, M Moser, D More, O More, O More, O More, O More, O More, O More, R Moselhy, M Moselhy, M Moselhy, M Mosely, D More, D	•		1	
Mizolek, A W Mizolek, A W Mizolek, A W Mizolara, M Mizolek, A W Mizolara, M Mochizuki, T GP13 Nusca, M J Mode, R C Molina, I Mondelli, A More, C Moosman, B Mori, W B Mose, R Mori, W B Mose, R Moschella, J Mosher, D Mosher, D Mosher, D Mosher, D Mosher, D Mondelli, A Mose, R Mullindi, A Mose, R Mosher, D Mondelli, A Mondelli, A Mondelli, A Mose, R Mondelli, A Monde				
Mizuhara, M Mochizuki, T Mock, R C Mock, R C Molina, I Monteiro, O R Mulforn, G More, C Moore, C Moore, C Mose, Ri More, Ri More, Ri More, Ri More, Ri Mose,	-			
Mochizuki, T 6P13 Nusca, M J 4D06-07 Mock, R C 2C08, 5C05, 7P02 Nusinovich, G 1803, 3P07, 4b08, Molina, I 4A04 Mondelli, A 1807, 3A01, 3A02-03 5801-02, 5806 Montie, T C 2B07, 2808, 4P09 Obenschain, S 3P20 Moorman, B 5D01, 6C05, 7P04 Oh, J H 3P18 Mori, W B 2809 Oks, E 2D08, 5A03, 6P10 Moschella, JJ 5D01 Oksuz, L 3P24, 3P25 Moselhy, M 6A01 Oliver, B V 4A01-02, 4A04, 4A05, 6P17, 6P18 Mosher, D 4A07-08, 4A09, 5D10 Olorunyolemi, T 3803-04, 3805 Motret, O 4P24 Olorunyolemi, T 3803-04, 3805 Muggli, P 2809, 4P07 Olson, R E 2C08 Muggli, P 2809, 4P07 Olson, R E 2C08 Mulrillo, M S 3A06-07, 6C01-02 Oreshkin, V J 7P06, 7P07 Murllo, M S 3A06-07, 6C01-02 Oreshkin, V J 7P06, 7P07 Myrnikov, A 5A03 Palter, R 6806, 7P43				
Mock, R C Molina, I Mondelli, A Mondelli, A Monteiro, O R Molina, I Mondelli, A Monteiro, O R Morie, T C Mosor, C Mosor, C Mosor, Ri Morse, Ri Moschella, JJ Moschella, JJ Moschella, JJ Moschella, JJ Moscher, D Motret, O Moses, R Mosser, R Moster, O Motret, O Motret, O Motret, O Motret, O Motret, O Motret, O Mulbrandon, M Mulbrandon, M Mulbrandon, M Mulson, C P Mursyama, K Moro, R Moro, R Moro, R Moro, R Moro, R Moro, R Moschella, JJ Moschella, JL Moschella, J			·	
Molina, I Mondelli, A 1807, 3A01, 3A02-03 Monteiro, O R 4P18 Montie, T C 2807, 2808, 4P09 Obenschain, S 3P20 Moore, C 3C06 Ogina, Y 6P08 Morsman, B 5D01, 6C05, 7P04 Oh, J H 3P18 Mori, W B 2809 Oks, E 2D08, 5A03, 6P10 Moschella, J J 5D01 Oksuz, L 3P24, 3P25 Moselhy, M 6A01 Oliver, B V 4A01-02, 4A04, 4A05, 6P17, 6P18 Moster, D 4A07-08, 4A09, 5D10 Motret, O 4P24 Oliver, B V 4A01-02, 4A04, 4A05, 6P17, 6P18 Mullbrandon, M 3D06 Oliver, B V 4A04, 4A05, 4A07-08, 4B09 Mullsaux, J 2P05 Mullbrandon, M 3D06 Oliver, B V 4A07-08, 4B09 Murayama, K 7P08 Oona, H 6P25, 7B07, 7B08, 7C05 Murillo, M S 3A06-07, 6C01-02 Orschkin, V I 7P06, 7P07 Murply, D P 5A01-02, 6P01 Osterheld, A L 3C03-04, 7P10 Myers, M 4A07-08, 4A09 Mytnikov, A 5A03 Nagata, M 6P29 Narayan, J 3C08 Narayan, J 3C	Mochizuki, T			
Mondelli, A Montiero, O R More, C Sacoa Moore, C Sacoa Moosman, B SD01, 6C05, 7P04 More, Ri Mori, W B Mori, W B Mori, W B Mori, W B More, Ri More, Ri Moschella, J J Moselly, M Moschella, J J Moselly, M Moses, R 7802-03 Moster, D Moster, O Motret, O Motret, O Mulliaux, J 2P05 Muggli, P Mullorandon, M Mullorandon, M Munson, C P Murayama, K Murayama, K Murayama, K Murillo, M S Murayama, K Myers, M Moythikov, A Moythikov, A Moythikov, A Nessela, M More, D Moythikov, A More, Ri Murayama, M More, Ri Murayama, M More, D More, C Murayama, M More, D More, C Murayama, M More, D Murayama, M More, D Murayama, M More, D Murayama, M More, R Murayama, M More, R Murayama, M More, R Murayama, M More, R More, R Murayama, M More, R More, R Murayama, M More, R Murayama, M More, R Murayama, M More, R More, R Murayama, M More, R M M M More, R M M M More, R M M M M M M M M M M M M M M M M M M M	Mock, R C	2C08, 5C05, 7P02	Nusinovich, G	1B03, 3P07, 4b08,
Monteiro, O R Montie, T C	Molina, I			
Montie, T C Moore, C Moore, C Moors, C Moosman, B Mori, W A Morio, A M	Mondelli, A	•		5B01-02, 5B06
Moore, C Moosman, B Mori, W B Mori, W B Mori, W B Morse, Ri Mori, W B Morse, Ri Mosella, J J Moselhy, M Moses, R Mosella, J J Moselhy, M Moses, R Mosella, J J Moselhy, M Moses, R Morit, O Moses, R Morit, O More, C Morit, O More, Ri Mosella, J J Moselhy, M Moses, R Mosella, J J Mosella, J Mosella, J Mosella, J J	Monteiro, O R	4P18	-	
Moosman, B Mori, W B Morse, Ri Morse, Ri Morse, Ri Moselhy, M Moselhy, M Moselhy, M Moselhy, M Moselhy, M Moselhy, D Morse, Ri Morse, Ri Moselhy, M Moselhy, M Moselhy, M Mosel, D Morse, Ri Moselhy, D Moselhy, M Mosel, R Moselhy, M Mosel, R Moselhy, M Mosel, R Moselhy, M Mosel, D Morse, R Moselly, M Mosel	Montie, T C	2B07, 2B08, 4P09	Obenschain, S	
Mori, W B	Moore, C	3C06	Ogina, Y	
Morse, Ri Moschella, J J Moschella, J J Moselhy, M Moses, R Mosher, D Mosher, D Moster, O Moulilaux, J Moulilaux, J Muggli, P Murayama, K Murillo, M S Mother, D Murayama, K Mores, M Mosher, D Murayama, K Mosher, D Murayama, K Mosher, D Murayama, K Monolilaux, J Murayama, K Moulilaux, J Murayama, K Murillo, M S Murayama, K Mores, M M	Moosman, B	5D01, 6C05, 7P04	Oh, J H	
Moschella, J J	Mori, W B	2B09	Okino, A	2P29, 6P07, 6P08
Moschella, J J 5D01 Oksuz, L 3P24, 3P25 Moselhy, M 6A01 Oliver, B V 4A01-02, 4A04, 4A01-02, 4A04, 4A05, 6P17, 6P18 Mosher, D 4A07-08, 4A09, 5D10 Olorunyolemi, T 3B03-04, 3B05 Motret, O 4P24 Olson, C L 4A04, 4A05, 4A07-08, 6P17, 6P18 Muggli, P 2B09, 4P07 Olson, R E 2C08 Mulbrandon, M 3D06 Olthoff, J 3P26 Munson, C P 2P25, 7P15 Onoi, M 4P06 Murrllo, M S 3A06-07, 6C01-02 Oreshkin, V I 7P06, 7P07 Murghy, D P 5A01-02, 6P01 Osterheld, A L 3C03-04, 7P10 Myers, M 4A07-08, 4A09 Ottinger, P F 4A07-08, 4A09, 4A10, 5D10, 6P19, 6P20 Mytnikov, A 5A03 Oxner, A 7P22 Nagata, M 6P29 Pakter, R 6B06, 7P43 Napartovich, A P 7P55 Paller, E 2B05, 2B06 Narayan, J 3C08 Palmer, W D 6D03-04 Nash, T J 2C05, 2C06, 2C08, 5C06, 2C08, 5C06, 2C08, 7P02, 7P17 Panarella, E 4C07 </td <td>Morse, Ri</td> <td>7P21</td> <td>Oks, E</td> <td>2D08, 5A03, 6P10</td>	Morse, Ri	7P21	Oks, E	2D08, 5A03, 6P10
Moselhy, M 6A01 Oliver, B V 4A01-02, 4A04, 4A05, 6P17, 6P18 Mosher, D 4A07-08, 4A09, 5D10 Olorunyolemi, T 3B03-04, 3B05 Motret, O 4P24 Olson, C L 4A04, 4A05, 4A07-08, 6P17, 6P18 Mouillaux, J 2P05 6P17, 6P18 Muggli, P 2B09, 4P07 Olson, R E 2C08 Mulbrandon, M 3D06 Olthoff, J 3P26 Murayama, K 7P08 Onoi, M 4P06 Murillo, M S 3A06-07, 6C01-02 Oreshkin, V I 7P06, 7P07 Murphy, D P 5A01-02, 6P01 Osterheld, A L 3C03-04, 7P10 Myers, M 4A07-08, 4A09 Ottinger, P F 4A07-08, 4A09, 4A09, 4A10, 5D10, 6P19, 6P20 Mytnikov, A 5A03 P P Nagata, M 6P29 P Napartovich, A P 7P55 Palker, R 2B05, 2B06 Narayan, J 3C08 Palmer, W D 6D03-04 Nash, T J 2C01-02, 2C04, 2C04, Pan'kin, M V Por'kin, M V 7P55 Nation, J A 5P12, 5P13, 5P14 Parko, D M		5D01	Oksuz, L	3P24, 3P25
Moses, R 7802-03 4A05, 6P17, 6P18 Mosher, D 4A07-08, 4A09, 5D10 Olorunyolemi, T 3803-04, 3805 Motret, O 4P24 Olson, C L 4A04, 4A05, 4A07-08, 6P17, 6P18 Mouillaux, J 2P05 6P17, 6P18 Muggli, P 2B09, 4P07 Olson, C L 4A04, 4A05, 4A07-08, 6P17, 6P18 Muggli, P 2B09, 4P07 Olson, R E 2C08 Mulbrandon, M 3D06 Olthoff, J 3P26 Munson, C P 2P25, 7P15 Onoi, M 4P06 Murayama, K 7P08 Oona, H 6P25, 7807, 7808, 7C05 Murillo, M S 3A06-07, 6C01-02 Oreshkin, V I 7P06, 7P07 Murphy, D P 5A01-02, 6F01 Osterheld, A L 3C03-04, 7P10 Myers, M 4A07-08, 4A09 Ottinger, P F 4A07-08, 4A09, 4A10, 5D10, 6P19, 6P20 Myrhikov, A 5A03 Pakter, R 6B06, 7P43 Napartovich, A P 7P55 Paller, E 2B05, 2B06 Naryan, J 3C08 Palmer, W D 6D03-04 Nash, T J 2C05, 2C06, 2C08, Panar		6A01	Oliver, B V	4A01-02, 4A04,
Mosher, D 4A07-08, 4A09, 5D10 Olorunyolemi, T 3B03-04, 3B05 Motret, O 4P24 Olson, C L 4A04, 4A05, 4A07-08, 6P17, 6P18 Muggli, P 2B09, 4P07 Olson, R E 2C08 Mulbrandon, M 3D06 Olthoff, J 3P26 Munson, C P 2P25, 7P15 Onoi, M 4P06 Murayama, K 7P08 Oona, H 6P25, 7B07, 7B08, 7C05 Murillo, M S 3A06-07, 6C01-02 Oreshkin, V I 7P06, 7P07 Murphy, D P 5A01-02, 6P01 Osterheld, A L 3C03-04, 7P10 Myers, M 4A07-08, 4A09 Oxner, A 4A07-08, 4A09, 4A09, 4A10, 5D10, 6P19, 6P20 Mytnikov, A 5A03 Pakter, R 6B06, 7P43 Napartovich, A P 7P55 Palker, R 2B05, 2B06 Napartovich, A P 7P55 Palmer, W D 6D03-04 Nash, T J 2C01-02, 2C04, 2C04, 2C04, 2C05, 2C06, 2C08, 5C06, 6C04, 7P02, 7P17 Pan'kin, M V 7P55 Nation, J A 5P12, 5P13, 5P14 Parks, T A 3C11 Nave, G 5P07 Park, G T 7P33 <td></td> <td>7B02-03</td> <td></td> <td>4A05, 6P17, 6P18</td>		7B02-03		4A05, 6P17, 6P18
Motret, O 4P24 Olson, C L 4A04, 4A05, 4A07-08, 6P17, 6P18 Mougli, P 2B09, 4P07 Olson, R E 2C08 Mulbrandon, M 3D06 Olthoff, J 3P26 Murson, C P 2P25, 7P15 Onoi, M 4P06 Murayama, K 7P08 Onoa, H 6P25, 7B07, 7B08, 7C05 Murillo, M S 3A06-07, 6C01-02 Oreshkin, V I 7P06, 7P07 Murphy, D P 5A01-02, 6P01 Osterheld, A L 3C03-04, 7P10 Myers, M 4A07-08, 4A09 Ottinger, P F 4A07-08, 4A09, Mytnikov, A 5A03 Oxner, A 7P22 Nagata, M 6P29 Palker, R 6B06, 7P43 Napartovich, A P 7P55 Paller, E 2805, 2806 Narayan, J 3C08 Palmer, W D 6D03-04 Nash, T J 2C01-02, 2C04, 2C04, 7P02, 7P17 Pan'kin, M V 7P55 Nation, J A 5P12, 5P13, 5P14 Parkova, D 6A09 Nation, J A 5P12, 5P13, 5P14 Park, G T 7P33 Nelson, E M 3A01, 4P29			Olorunyolemi, T	3B03-04, 3B05
Mouillaux, J 2P05 Muggli, P 2B09, 4P07 Mulbrandon, M 3D06 Munson, C P 2P25, 7P15 Murllo, M S 3A06-07, 6C01-02 Murphy, D P 5A01-02, 6P01 Myers, M 4A07-08, 4A09 Mytnikov, A 5A03 Nagata, M 6P29 Narayan, J 3C08 Nash, T J 2C01-02, 2C04, 2C05, 2C06, 6C04, 7P02, 7P17 Nation, J A 5P12, 5P13, 5P14 Naye, G 5P07 Nelson, E M 3A06 Mulbrandon, M 3D06 Olthoff, J 3P26 Olson, R E 2C08 Olthoff, J 3P26 Olthoff, J 3P26 Olthoff, J 3P26 Onoi, M 4P06 Oona, H 6P25, 7B07, 7B08, 7C05 Oreshkin, V I 7P06, 7P07 Osterheld, A L 3C03-04, 7P10 Ottinger, P F 4A07-08, 4A09, 4A10, 5D10, 6P19, 6P20 Oxner, A 7P22 P P P R R 6B06, 7P43 P Paller, E 2B05, 2B06 P Paller, E 2B05, 2B06 P Pan'kin, M V 7P55 P Parsk, D M 3P18 P Nation, J A 5P12, 5P13, 5P14 P Nake, G 5P07 P Park, D M 3P18			-	4A04, 4A05, 4A07-08,
Muggli, P Mulbrandon, M Munson, C P Murayama, K Murayama, K Murillo, M S Murphy, D P Myers, M Mytnikov, A Nagata, M Nagatath, D Napartovich, A P Narayan, J Nash, T J Nation, J A Nation, J A Nave, G Nursyama, B Murayama, K 708 Olson, R E Olthoff, J 3P26 Onoi, M Olthoff, J 3P26 Onoi, M Olthoff, J 3P26 Onoi, M Oreshkin, V I Probe, 7P07 PAkter, R Paller, F Paller, E Paller, E Paller, E Paller, E Panarella, E ACO7 Pan'kin, M V Press Panarella, E ACO7 Parskhin, M V Press Paraschiv, I Parish, T A Ave, G Sp07 Park, G T Park, D M 3P18 Olson, R E 2C08 Olthoff, J 3P26 Onoi, M 4P06 Oreshkin, M Press Paler, R 6B06, 7P43 Paler, E 2B05, 2B06 Palmer, W D 6D03-04 Pan'kin, M V Press Panarella, E 4CO7 Pan'kin, M V Press Paraschiv, I Pro1, 7P22, 7P23 Parsk, T A 3C11 Park, G T Press Park, D M 3P18				
Mulbrandon, M Mulbrandon, M Munson, C P Murayama, K Murayama, K Murillo, M S Murillo, M S Murphy, D P Myers, M Mytnikov, A Nagata, M Nandelstadt, D Napartovich, A P Narayan, J Nash, T J Nash, T J Nation, J A Nation, J A Nase, G Nelson, E M Mulbrandon, M Munson, C P 2P25, 7P15 Onoi, M Onoi, M AP06 AP00 Onoi, M AP0			Olson, R E	
Murson, C P 2P25, 7P15 Onoi, M 4P06 Murayama, K 7P08 Oona, H 6P25, 7B07, 7B08, 7C05 Murillo, M S 3A06-07, 6C01-02 Oreshkin, V I 7P06, 7P07 Murphy, D P 5A01-02, 6P01 Osterheld, A L 3C03-04, 7P10 Myers, M 4A07-08, 4A09 Ottinger, P F 4A07-08, 4A09, 4A10, 5D10, 6P19, 6P20 Oxner, A 7P22 Nagata, M 6P29 P Akter, R 6B06, 7P43 Napartovich, A P 7P55 P Aller, E 2B05, 2B06 Narayan, J 3C08 P Almer, W D 6D03-04 Nash, T J 2C01-02, 2C04, Pan'kin, M V 7P55 Narayan, J 3C08 P Almer, W D 6D03-04 Nash, T J 2C01-02, 2C04, Pan'kin, M V 7P55 Sc05, 5C06, 6C04, Pankova, D 6A09 TP02, 7P17 P Araschiv, I 7P01, 7P22, 7P23 Nation, J A 5P12, 5P13, 5P14 P Arish, T A 3C11 Nave, G 5P07 P Ark, D M 3P18 Nelson, E M 3A01, 4P29 P Ark, D M 3P18			1	
Murayama, K Murillo, M S Murillo, M S Murillo, M S Murphy, D P Myers, M Mytnikov, A Nagata, M Nandelstadt, D Napartovich, A P Narayan, J Nash, T J 2C01-02, 2C04, 2C05, 2C06, 2C08, 7P02, 7P17 Nation, J A Nave, G Nelson, E M Murillo, M S 3A06-07, 6C01-02 Dona, H Oreshkin, V I Ores			1	
Murillo, M S 3A06-07, 6C01-02 Oreshkin, V I 7P06, 7P07 Murphy, D P 5A01-02, 6P01 Osterheld, A L 3C03-04, 7P10 Ottinger, P F 4A07-08, 4A09, 4A10, 5D10, 6P19, 6P20 Oxner, A 7P22 Nagata, M 6P29 Pakter, R 6B06, 7P43 Paller, E 2B05, 2B06 Narayan, J 3C08 Palmer, W D 6D03-04 Nash, T J 2C01-02, 2C04, 2C04, 2C05, 2C06, 2C08, 5C05, 5C06, 6C04, 7P02, 7P17 Paraschiv, I 7P01, 7P22, 7P23 Nation, J A 5P12, 5P13, 5P14 Parish, T A 3C11 Nave, G 5P07 Park, D M 3P18 Nation, E M 3A01, 4P29 Park, D M		·		
Murphy, D P Myers, M Mytnikov, A Mytnikov, A Magata, M Napartovich, A P Narayan, J Nash, T J Mash, T J Mash, T J Nation, J A Nave, G Nelson, E M Murphy, D P 5A01-02, 6P01 4A07-08, 4A09 Ottinger, P F 4A07-08, 4A09, 4A10, 5D10, 6P19, 6P20 Oxner, A P Pakter, R Paller, E Paller, E Palmer, W D Paraschiv, I Paraschiv, I Paraschiv, I Parish, T A Parish, T A Parish, T A Parish, T A Nave, G Nelson, E M SA01-02, 6P01 Osterheld, A L SC03-04, 7P10 Ottinger, P F 4A07-08, 4A09, 4A10, 5D10, 6P19, 6P20 Oxner, A PP Pakter, R Paller, E Paller, E Palmer, W D Pan'kin, M V Pp55 Panarella, E 4C07 Pankova, D Paraschiv, I Parish, T A SC11 Park, G T Pp33 Nelson, E M SA01, 4P29 Park, D M SP18			1	
Myers, M 4A07-08, 4A09 Ottinger, P F 4A07-08, 4A09, 4A10, 5D10, 6P19, 6P20 Mytnikov, A 5A03 P Nagata, M 6P29 P Nandelstadt, D 5P01, 5P02 Pakter, R 6B06, 7P43 Napartovich, A P 7P55 Paller, E 2B05, 2B06 Narayan, J 3C08 Palmer, W D 6D03-04 Nash, T J 2C01-02, 2C04, 2C04, Pan'kin, M V 7P55 2C05, 2C06, 2C08, 5C06, 6C04, 702, 7P17 Panarella, E 4C07 Nation, J A 5P12, 5P13, 5P14 Parish, T A 3C11 Nave, G 5P07 Park, G T 7P33 Nelson, E M 3A01, 4P29 Park, D M 3P18				
Mytnikov, A 5A03 Oxner, A 4A10, 5D10, 6P19, 6P20 Oxner, A 7P22 Nagata, M Nagata, M Nandelstadt, D SP01, 5P02 Napartovich, A P Narayan, J Nash, T J 2C01-02, 2C04, 2C05, 2C06, 2C08, 5C05, 5C06, 6C04, 7P02, 7P17 Nation, J A Nave, G Nelson, E M A410, 5D10, 6P19, 6P20 Oxner, A 4A10, 5D10, 6P19, 6P20 Oxner, A 4A10, 5D10, 6P19, 6P20 Oxner, A 4A10, 5D10, 6P19, 6P20 P Pakter, R Pakter, R Pakter, R Pakter, R Paller, E 2B05, 2B06 Palmer, W D 6D03-04 Pp55 Panriella, E 4C07 Panriella, E 4C07 Paraschiv, I 7P01, 7P22, 7P23 Park, G T Park, G T Park, G T Park, D M 3P18			1	
Nagata, M Nagata, M Nandelstadt, D Napartovich, A P Narayan, J Nash, T J 2C01-02, 2C04,		· ·	Ottiligel, i	
Nagata, M Nandelstadt, D Napartovich, A P Narayan, J Nash, T J Nation, J A Nation, J A Nave, G Nelson, E M Nagata, M 6P29 Pakter, R Pakter, R Pakter, R Paller, E Paller, E Palmer, W D Pan'kin, M V Pan'kin, M V Pan'kin, M V Pan'kin, M V Paraschiv, I Paraschiv, I Paraschiv, I Park, G T Park, D M Park O M Pan'kin, M V Paraschiv, I Paraschiv, I Paraschiv, I Park, G T Park, D M Park O M Pan'kin, M V Paraschiv, I Park, G T Park, D M Park, D M Paraschiv, I Park, D M Park, D M Park, D M Paraschiv, I Park, D M Park, D M Park, D M Paraschiv, I Paraschiv, I Park, D M Paraschiv, I Par	Wythkov, A	5,405	Oxner A	
Nagata, M 6P29 P Nandelstadt, D 5P01, 5P02 Pakter, R 6B06, 7P43 Napartovich, A P 7P55 Paller, E 2B05, 2B06 Narayan, J 3C08 Palmer, W D 6D03-04 Nash, T J 2C01-02, 2C04, Pan'kin, M V 7P55 2C05, 2C06, 2C08, 5C06, 6C04, Pankova, D Pankova, D 6A09 7P02, 7P17 Paraschiv, I 7P01, 7P22, 7P23 Nation, J A 5P12, 5P13, 5P14 Parish, T A 3C11 Nave, G 5P07 Park, G T 7P33 Nelson, E M 3A01, 4P29 Park, D M 3P18			Oxner, A	,,,,,
Nagata, M 6P29 P Nandelstadt, D 5P01, 5P02 Pakter, R 6B06, 7P43 Napartovich, A P 7P55 Paller, E 2B05, 2B06 Narayan, J 3C08 Palmer, W D 6D03-04 Nash, T J 2C01-02, 2C04, Pan'kin, M V 7P55 2C05, 2C06, 2C08, 5C06, 6C04, Pankova, D Pankova, D 6A09 7P02, 7P17 Paraschiv, I 7P01, 7P22, 7P23 Nation, J A 5P12, 5P13, 5P14 Parish, T A 3C11 Nave, G 5P07 Park, G T 7P33 Nelson, E M 3A01, 4P29 Park, D M 3P18	RJ			
Nandelstadt, D 5P01, 5P02 Pakter, R 6B06, 7P43 Napartovich, A P 7P55 Paller, E 2B05, 2B06 Narayan, J 3C08 Palmer, W D 6D03-04 Nash, T J 2C01-02, 2C04, Pan'kin, M V 7P55 2C05, 2C06, 2C08, 5C06, 6C04, Panarella, E 4C07 5C05, 5C06, 6C04, Pankova, D 6A09 7P02, 7P17 Paraschiv, I 7P01, 7P22, 7P23 Nation, J A 5P12, 5P13, 5P14 Parish, T A 3C11 Nave, G 5P07 Park, G T 7P33 Nelson, E M 3A01, 4P29 Park, D M 3P18		6P29	D	
Napartovich, A P 7P55 Paller, E 2B05, 2B06 Narayan, J 3C08 Palmer, W D 6D03-04 Nash, T J 2C01-02, 2C04, 2C08, 2C08, 2C08, 2C08, 5C05, 5C06, 6C04, 7C02, 7P17 Panarella, E 4C07 4C07 Nation, J A 5P12, 5P13, 5P14 Parish, T A 3C11 7P01, 7P22, 7P23 Nave, G 5P07 Park, G T 7P33 Nelson, E M 3A01, 4P29 Park, D M 3P18			-	6R06 7P43
Narayan, J 3C08 Palmer, W D 6D03-04 Nash, T J 2C01-02, 2C04, Pan'kin, M V 7P55 2C05, 2C06, 2C08, Panarella, E 4C07 5C05, 5C06, 6C04, Pankova, D 6A09 7P02, 7P17 Paraschiv, I 7P01, 7P22, 7P23 Nation, J A 5P12, 5P13, 5P14 Parish, T A 3C11 Nave, G 5P07 Park, G T 7P33 Nelson, E M 3A01, 4P29 Park, D M 3P18			1	
Nash, T J 2C01-02, 2C04, Pan'kin, M V 7P55 2C05, 2C06, 2C08, Panarella, E 4C07 5C05, 5C06, 6C04, Pankova, D 6A09 7P02, 7P17 Paraschiv, I 7P01, 7P22, 7P23 Nation, J A 5P12, 5P13, 5P14 Parish, T A 3C11 Nave, G 5P07 Park, G T 7P33 Nelson, E M 3A01, 4P29 Park, D M 3P18	•			
2C05, 2C06, 2C08, Panarella, E 4C07 5C05, 5C06, 6C04, Pankova, D 6A09 7P02, 7P17 Paraschiv, I 7P01, 7P22, 7P23 Nation, J A 5P12, 5P13, 5P14 Parish, T A 3C11 Nave, G 5P07 Park, G T 7P33 Nelson, E M 3A01, 4P29 Park, D M 3P18	•		· ·	
5C05, 5C06, 6C04, Pankova, D 6A09 7P02, 7P17 Paraschiv, I 7P01, 7P22, 7P23 Nation, J A 5P12, 5P13, 5P14 Parish, T A 3C11 Nave, G 5P07 Park, G T 7P33 Nelson, E M 3A01, 4P29 Park, D M 3P18	INASII, I J		*	
7P02, 7P17 Paraschiv, I 7P01, 7P22, 7P23 Nation, J A 5P12, 5P13, 5P14 Parish, T A 3C11 Nave, G 5P07 Park, G T 7P33 Nelson, E M 3A01, 4P29 Park, D M 3P18				
Nation, J A 5P12, 5P13, 5P14 Parish, T A 3C11 Nave, G 5P07 Park, G T 7P33 Nelson, E M 3A01, 4P29 Park, D M 3P18				
Nave, G 5P07 Park, G T 7P33 Nelson, E M 3A01, 4P29 Park, D M 3P18	Niation I A	•	1	
Nelson, E M 3A01, 4P29 Park, D M 3P18				· ·
Nelson, E 3AU2-U3 Park, J 3DU4-U5, 4P26				
	Nelson, Ł	3A02-03	rark, J	3DU4-U3, 4Y20

		•	
Park, J S	5P09		
Parker, J V	6P25	R	
	6P31	,	2P07
Parks, D		Raguin, J Y	4D01-02
Paschina, A S	7P58	Rajabian, M	
Pashaie, B	4P23	Ralph, D	7P59
Paul, K C	2D07	Ranada, A F	4C01-02
Pauser, H	7P4 7	Rauch, J E	5D06, 5D08-09
Pawley, C	3P20	Rauf, S	1D01
Pechacek, R E	5A01-02, 6A02, 6P01	Raux, S	4D08
Pekker, L	6P03	Reass, W A	7C01-02
Penache, D	1P10	Redman, D G	2P05
Penano, J R	2P02	Reinovsky, R E	1P15, 6C03, 6P25,
Pepin, H	3C07	Removaky, R Z	7B01-02, 7C05
•	6P26, 7P09	Reiser, M	3P06
Pereira, N R		Renk, T	6P21
Perrin, M	4P11		
Pershing, D E	3P10, 4B01-02	Rhodes, R	5D07
Pert, E	3B03-04, 3B05	Ribe, F L	3P28
Peterkin Jr, R E	7B01-02, 7B04	Richards, J	5B05
Peters, C W	7P41, 7P42	Rintamaki, J I	6P12, 6P23, 7P41, 7P42
Petersen, D	2C05, 5C05	Riordan, J C	6C05, 6C06, 7P04
Peterson, D L	2C03, 2C04, 2C08,	Rix, W	5D06
	5c06, 5C07, 6C04, 7P18	Rizk, F A M	3C07
Petillo, J J	4B01-02, 4P29	Robert, E	3P21
Petillo, J	3A01	Roberts, J	3P26
Petrin, A B	7P56, 7P59	Robinson, AC	7P21
Pfau, S	7A06	Robson, A E	3D06
	1C03-04	Rock, J C	3C11
Phillips, L		Roderick, N F	5C01-02, 7B01-02,
Piejak, R B	2A03	Roderick, N F	
Pikuz, S A	5C03-04, 7P24,	Dadway I	7B04, 7P19
	7P25, 7P26, 7P27, 7P28	Rodger, J	1B03, 1B09, 3P05,
Podulka, W J	7B03		3P15, 4b08, 3P19, 5B12
Pointon, T D	6P22, 7P42	Rogers, H H	2C03
Polk, J E	6D03-04	Rose, D V	4A07-08, 4A09,
Porter, J L	2C01-02, 3P31, 7P16	-	4A10, 4P30, 6P19, 6P20
Poskacheeva, L P	7P58	Rosenfeld, W	7P11
Pott, A	4P41	Rosenthal, S E	4A04, 4A05, 6P17, 6P18
Potvin, C	3C07	Rosocha, L A	4D06-07
Pouvesle, J M	3P21, 4P24, 7P11	Rostov, V V	7P34
Prasad, R R	5A07, 6C07	Roth, G	2P27
Prather, W	1A03	Roth, J R	2B07, 2B08, 3P35,
Preinhaelter, J	1P08		4P08, 4P09, 4P25
Presura, R	1P10, 6C09, 7P01	Rous, J	7P12, 7P13
Price, H D	7C07	Rousculp, C L	4P35
	4D03	Rovang, D C	4A04, 6P18
Prinz, F B		Rozhkov, A A	2P07
Puchkarev, V	2P27	1	
Puerta, J	1P13	Rudakov, L I	6C08
Pulsifer, P E	7P02	Rudder, R	3D06
		Ruden, E L	6C10, 7B01-02
		Ruggles, L E	2C01-02, 2C08,
Q			3P31, 7P16
Qi, N	2D06, 5A07, 6C05,	Ruiz, C	5C05
	6C07	Ruiz-Comacho, J	6C04
Qing, Li	7P49	Russkikh, A G	7P06
Qiu, D W	1A04-05, 2P18	Ryan, P	3P32, 5c05
Quill, B J	1P11	Ryutov, DD	2C05
Quintenz, J	6P21		
Quintenz, J	· · · · · · · · · · · · · · · · · · ·		

s		Shelkovenko, T A	5c03-04, 7P24,
Sadowski, M J	3C09-10		7P25, 7P26, 7P27, 7P28
Saitoh, S	6P21	Sherbini, TH M El	2P04
Sakuta, T	2D07	Sherman, D M	2B07, 2B08, 3P35,
Samant, C C	7P51	Sterman, 2 m	4P08, 4P25
	4A01-02	Sherrill, M	7P22
Sampayan, S		Sheverev, V	7A05
Sanford, T W L	2C08, 7P02		1P05
Sankaranarayanan, R	4P23	Shiau, J H	
Sano, M	5A06	Shiffler, D	6B05, 6B08, 7P31
Saraph, G P	4805	Shimomura, N	6P29
Sarfaty, M	4D08	Shin, Y K	5P08
Sarkisov, G S	7P22	Shinohara, S	6P04, 6P05, 6P06
Sarroukh, H	7A03	Shishlov, A V	7P06, 7P07
Sasser, G E	1P16, 7P37, 7P38, 7P39	Shkrarunets, A	1B03, 1B09, 3P19
Scafuri, F	5B05	Shlyaptsev, V N	3C03-04, 7P10
Schamiloglu, E	5B04, 7C04, 7P33,	Shlyaptseva, A S	7P22, 7P23
3 ·	7P34, 7P35, 7P36	Shon, C H	5P08, 5P09
Scharer, J E	2B05, 2B06, 2P12, 2P13,	Shumlak, U	1P14
Scharci, J.E.	2P24, 4P03, 4P04, 4P05	Siemon, R E	1P15, 1P16, 7B01-02
Schatz, J G	3P27	Simon, G	5P03
	3P28	Simpson, W W	2C01-02, 2C08, 7P16
Schauer, M M		Sinards, D B	5C03-04, 7P24,
Schein, J	2D06, 5a07	Sinards, D B	7P25, 7P26, 7P27, 7P28
Scheitrum, G P	7P41	Cin alain NA	
Schlacter, J	7B01-02	Sinclair, M	6P17
Schmidt, D	7D01-02	Singh, N	1A06, 2A06
Schmitt, A J	1C03-04	Singh, A	4B04
Schneider, R F	6C05, 7P04	Slinker, S P	3A05
Schneider, R	6C04	Slutz, S A	2C06, 5C05, 6P22
Schoch, P M	3P27	Smith, H B	1A04-05, 2P17
Schoenbach, K H	2B01-02, 2B03,	Smith, I	4A04
	2P28, 4P01, 4P02,	Smith, D	3D02-03
	6A01	Smith, L M	7C06
Schoenberg, J S H	7C04	Smithe, D	1P17
Schoenbert, K	7B01-02	Snell, C M	4A03
Schrank, L S	3P28	Soler, M	4C01-02
Schumacher, R	4B04	Sommars, W	7B01-02
Schumer, J W	5D10	Song, Y	6C05, 6C06, 7P04
Scudder, D	5B01-02	Soualian, V S	7P33
Seaman, J F	2C08, 5C05	Spence, P	4A04
Selwyn, G S	3D04-05, 4P26	Spencer, T A	3P11, 6B02-03,
	7P52	Spericei, 1 A	6B08, 6P12, 7P31,
Semenov, V E	3C13		7P36, 7P40, 7P41, 7P42
Semyonov, O G		Spielman P.P.	2C01-02, 3P31,
Sena, M	7P59	Spielman, R B	
Sena, F C	7C05		3P32, 5C01-02,
Seo, D C	3P23		5C06, 5C07, 5C10, 6C04,
Serlin, V	7P28	Spindt, C	6D03-04
Sgro, A G	6P16	Sprangle, P	2P02, 3C05, 3c06
Shah, U	3P27	Stark, R H	2B03, 4P01, 4P02
Shamamiam, V	3D06, 6A02	Steen, P	4P31
Shanahan, W R	3A06-07, 6C01-02	Steer, W	2D02
Shapiro, M A	3P04	Stepanenko, M M	7P09
Sharkaway, H	2P04	Stephanakis, S J	4A07-08, 4A09,
Sharma, A	3C08		4A10, 6C05, 6P19, 7P04
Shaw, D M	3P22	Stephaniuk, V	7A05
Shcolnikov, E Y	3P30	Stokes, J L	6P25, 7C05
Sheehey, P T	1P16, 7B06, 7B07,	Stolz, Peter	7P21
	7B08	Stori, H	7P47
	- 	·	

Strelkov, P	5B12	Tsai, M H	5A08
	2C08, 5C07, 5C10	Tsao, M H	1B10
Struve, K		l .	5D02-03
Stutzman, R C	3P11	Tsigutkin, K	
Stygar, W A	2C08, 5C10	Tsui, Y Y	2P05
Suzuki, K	6P14	Turchi, P J	7B01-02, 7B05
Swanekamp, S B	4A06, 5D10	Turman, B	6P21
Sweeney, M A	7P50	Tynan, G R	1A07
Swegle, J A	Plenary Talk		
Sze, H M	6C05, 7P04		
		U	
		Uchiyama, H	3P22
T		Uhlenbusch, J	4P41
Tabaka, L J	7C05	Uhm, H S	4D10
Taccetti, J M	7B07, 7B08	Umstadter, K R	3P28
Takahashi, K	6A08	Umstadtt, R	6B08, 7P31
Takahaski, H	7P61	Urashima, K	4D06-07
Takaki, K	6P02	Grasiiina, it	.533 3.
Takechi, S	6P05, 6P06		
Takeda, M	6A07, 6A08	V	
	6P08	Va'vra, J	1A02
Takeuchi, Y			1A02
Tamamura, S	6P21	Va'vra, P M	
Tanaka, Y	2D07	Vacquie, S	4D01-02
Tang, D	1P14	Vaden, K R	1B08, 2P09
Tang, Y	7B03	Vahala, L	1P08
Tang, W	4C07	Vahala, G	1P08
Tang, B Y	4P15, 4P16	Valfells, A	1P06, 1P07
Tasker, D G	6P25, 7C05	Vanderberg, B H	5A05, 6P11
Tauschwitz, A	1P10, 6C09	Vargas, M F	2C01-02, 2C08, 7P16
Taylor, A J	2P25	Velazco, J E	7P53
Temkin, R J	3P04	Velikovich, AL	6C08
Teramoto, Y	5D04	Verboncoeur, J P	1P07, 3P02, 4P34
theiss, A J	4B01-02	Vesey, R A	2C01-02, 2C08,
Thio, F Y	7B07		6P22, 7P16
Thomas, R E	3D06	Vidal, F	3C07
Thomas, P	4P38	Vikhrev, V V	7P09
Thompson, M	6P21	Viladrosa, R	3P21, 4P24, 7P11
Thompson, J R	5D06, 5D08-09,	Viodoli, C	5D01
mompson, and	6P26, 6P30, 7P04	Vitello, P	1D06
Thornhill, J W	6C04, 6C05, 7P02	Vollers, D	6P12
Tian, X B	4P15, 4P16	Voss, D	6B08
Ting, A	3C01-02, 3C06	Vourdas, A	5B09
Tolt, Z L	6D03-04	Vozz, D	7P59, 7P31
	2C01-02	V022, D	71 33, 71 31
Toor, A	6P21		
Torres, G		w	
Torres, J A	2C08, 5C05	1	4D24 CCOE 7D02
Torres, D T	7C05	Waisman, E	4P31, 6C05, 7P03
Trainor, R J	2P25, 7P15	Walker, Q E	7D04
Troha, A L	4B03, 5B04	Walter, M	3B03-04, 3P03,
True, R B	3A01, 3P16, 4B01-		3P03, 1P16, 5B06
	02, 6B04, 7C01-02	Walton, S G	5A01-02, 6P01
Trueba, J L	4C01-02	Wan, P C	1B10
Trushkin, N I	7P55	Wan, C H	5P10
Tsai, J H	3P14	Wang, P	5P12, 5P13, 5P14
Tsai, Y C	1B10	Wang, Q S	3P12, 3P13
Tsai, P P Y	2807, 2808	Wang, G	7P45, 7P46
Tsai, C H	1P02, 1P03	Wang, Z	1D08
Tsai, J H	1P05, 5P10	Wang, W C	5P10

Wang, Y		3P26	Yamashita, T	6P21
	4 · · · · · · · · · · · · · · · · · · ·	1D02	Yamauchi, K	6P08
Want, S B				4P07
Watanabe, M		3P22, 6P08	Yampolsky, J	
Watkins, J		7 P63	Yang, T T	1B10
Watrous, J J	•	7P37, 7P38, 7P39	Yang, J G	3P18
Weber, B V		4A07-08, 4A09,	Yang, Y M	1P02
		4A10, 6C05, 6P19,	Yang, J	7P45, 7P46
		6P20, 7C08, 7P04	Yanobe, T	4P40
Weingarten, A		6P28	Yasuoka, K	6P14, 7P61
Welch, D R		4A01-02, 4a04,	Yatsuzuka, M	4P06, 4P19, 6P13
VI 5.1.7 5 1.1		4A05, 4A07-08,	Yonekura, K	6P04
•	e de	4A09, 6P17, 6P18, 6P22	Yoon, H J	3P23
Wendelstorf, J	,	5P03	Yoshioka, K	5A04
		1D02	Young, F C	4A07-08, 4A09,
Wendt, A E			Tourig, i C	4A10, 6P19, 6P20
Wenger, D F		6P22		•
Whaley, D R	•	2P08, 6D01-02	Yovchev, I	3P06, 3P07
Whitney, K G		6C04, 6C05, 6C06, 7P02	Yukimura, K	5A04, 5A06
Whitton, B		6C06	Yushkov, G Yu	6P10
Wichliffe, M E		5P07		$ \psi_{ij}\rangle = \psi_{ij}\rangle^{-1}$
Willi, O		5C09		$(A_{i,j}, A_{i,j}, $
Wilson, O		3B03-04, 3B05	Z	
Wineland, D J		7P64	Zaginaylov, G I	2P07
Winkler, R		7A06	Zakharov, L E	3P33
Winske, D		3A06-07	Zeng, Z M	4P15, 4P16
Winterberg, F		7P22	Zengeni, T G	3C12
Wirpszo, K W		4C07	Zhai, X	2P16
Wittmann, K		4D05	Zhang, Jin	7P45, 7P46
Wohlbier, J G		2P12	Zhang, T	6P09
		5P03	Zhang, J	7P63
Wohlfahrt, H		4A04	Zhang, J Zhao, J	3P15
Woo, L			ľ	2P05
Wood, F		5B07	Zhe, S	3P17
Wood, B P		2P25, 3D07, 7P15	Zhong, X H	
Wood, R F		1C05-06	Zissis, G	7A03
Woolverton, K		7P32	Zoita, V	7P01
Woskov, P	• • • • • • • • • • • • • • • • • • • •	4P38	Zoler, D	4P27
Wright, R L		7P35, 7P36	Zweben, S J	3P33
Wright, N	·	7 C06		
Wu, Yaoxi		2A04		
Wu, C		6P21		
Wu, F		4C07		
Wu, R L C		2D01		
Wurden, G	*	7B01-02		
Wysocki, F J		2P25, 7B01-02, 7B07,		
•		7B08		
X				
Xie, T		6D05		er en en la serie de la companya de
Xu, G		3B03-04		
, Au, G				
Y				
		6P07		
Yabuta, H		6P07		
Yadlowsky, E J		6C06		
Yakovin, S D		3P34		
Yamagata, Y		3C08		
Yamaguchi, T	t - t	1P17		
_				

Conference Schedule

Location	Monday AM June 21	Monday PM June 21	Tuesday AM June 22	Tuesday PM June 22	Wednesday AM June 23	Wednesday PM June 23	Thursday AM June 24
Title Speaker De Anza Ballroom	Plenary: Laboratory Astrophysics Experiments Dr. Paul Springer Lawrence Livermore National Laboratory	Plenary: The inexorable plasma processing challenges presented by Moore's law Rick Gottscho LAM Inc.	Plenary: Thermal Plasma Processes Richard Hubbard Naval Research Laboratory	Plenary: Communicating with Nonscientists & the Media Rick Borchelt Vanderbilt University	PSAC Award Address: Simple Models on Some Nasty Problems in Beams & Plasmas Prof. Y.Y. Lau University of Michigan	Plenary: The Future of High-Power Microwaves James N. Benford Microwave Sciences, Inc., & John A. Swegle Lawrence Livermore NL	Plenary: 2 Pinches: Past, Present & Future Prof. Malcom Haines Imperial College
A Orals De Anza I	1A Basic Processes in Fully & Partially Ionized Plasmas	2A Space Plasmas & Partially Ionized Gases	3A Computational Plasma Physics	4A Intense Electron & Ion Beams	5A Plasma, Ion, & Electron Sources	6A Plasmas for Lighting	7A Plasmas for Lighting
B Orals De Anza II	1B Slow Wave Devices	2B Microwave Plasmas	38 Microwave Systems	4B Fast Wave Devices	5B Fast Wave Devices & Intense Beams	6B Intense Beams	78 Magnetic Fusion Energy
C Orals De Anza III	1C Laser Produced Plasmas	2C Inertial Confinement Fusion	3C Laser Produced Plasmas & Dense Plasm Focus	4C Spherical Configurations	5C Fast Z-Pinches & X-ray Lasers	6C Fast Z-Pinches & X-ray Lasers	7C Closing Switches & Plasma Opening Switches
D Orals Bonsai I & II	1D Non-Equilibrium · Plasma Processing	2D Plasma Diagnostics	3D Non-equilibrium Plasma Processing	4D Thermal Plasma Chemistry & Processing	5D Plasma Opening Switches	6D Vacuum Microwaves (Microelectronics)	7D Plasma Thrusters & Arcs
Sierra I Conference Centre	1P Posters Space Plasmas, Partially Ionized Gases, Microwave Systems, ICF	2P Posters Laser Plasmas, Slow Wave Devices, Basic Phenomena, Computational Plasmas, Environmental Issues	3P Posters Fast Wave Devices, Diagnostics, Plasma Processing	4P Posters Microwave Plasmas, Non-equilibrium Plasma Processing, MFE	5P Posters Lighting, Flat Panels, Vacuum Microwaves	6P Posters Sources, Beams, Switches	7P Posters Plasma Focus, Z Pinches & X-ray Lasers, Beams, Postdeadline